AD-A055 637 AIR FORCE INST OF TECH WRIGHT-PATTERSON AFB OHIO SCH--ETC F/G 19/5
AN EXTENDED KALMAN FILTER FIRE CONTROL SYSTEM AGAINST AIR-TO-AI--ETC(U)
DEC 77 S J CUSUMANO, M DE PONTE

UNCLASSIFIED AFIT/GE/EE/77-13-VOL-2 NL

1 OF 4
ADA
055637

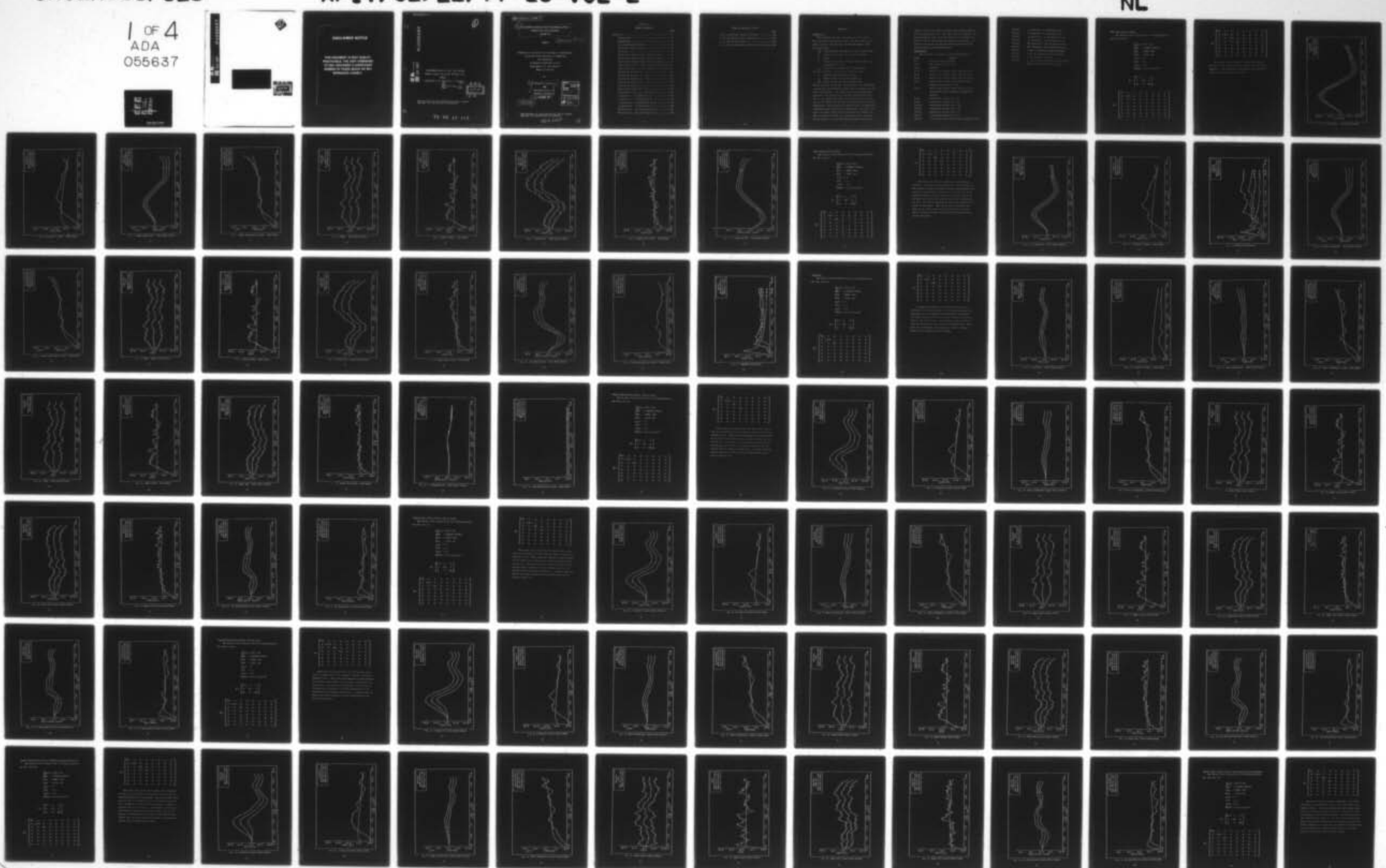

DISCLAIMER NOTICE

THIS DOCUMENT IS BEST QUALITY PRACTICABLE. THE COPY FURNISHED TO DDC CONTAINED A SIGNIFICANT NUMBER OF PAGES WHICH DO NOT REPRODUCE LEGIBLY.

AFIT/GE/EE/77-13

AN EXTENDED KALMAN FILTER FIRE CONTROL

SYSTEM AGAINST AIR-TO-AIR MISSILES (II)

THESIS

AFIT/GE/EE/77-13 Salvatore J. Cusumano
Capt USAF
and
Manuel De Ponte, Jr.
Capt USAF

(14) AFIT/GE/EE/77-13 - VOL-2

(6) AN EXTENDED KALMAN FILTER FIRE CONTROL SYSTEM

AGAINST AIR-TO-AIR MISSILES.

VOLUME II.

(9) Master's thesis,

THESIS

Presented to the Faculty of the School of Engineering

of the Air Force Institute of Technology

Air University

in Partial Fulfillment of the

Requirements for the Degree of

Master of Science

by

(10) Salvatore J. Cusumano

and

Manuel De Ponte, Jr.

Graduate Engineering

(11) December 1977

(12) 353p.

ACCESSION for		
NTIS	White Section	☒
DDC	Buff Section	☐
UNANNOUNCED		☐
JUSTIFICATION		
BY		
DISTRIBUTION/AVAILABILITY CODES		
Dist.	AVAIL. and/or SPECIAL	
A	23 EU	

012 225 LB

Volume II

Table of Contents

Table of Contents (Cont'd)

Appendix B

Introduction

This Appendix contains the graphical results of the Monte Carlo analysis of this study. The plots will be presented in sets. All sets will include the dynamic state error plots for:

V^I_{mx} - x-velocity for the missile in the inertial frame

θ_T - Line-of-sight angle as seen by the ownship

R - Range

$\dot{R}$ - Range rate (relative closing velocity where, by convention, $\dot{R} = -V_c$

a_L - Missile's developed lateral acceleration.

And when estimated, the parameter error plots for:

n - Proportional navigation constant

τ_f - Time constant of the first order lag

M/S - Ratio of mass to cross sectional area

will be included in the set. In addition to the error plots, a tuning plot (covariance matching) will be included for each state and parameter. The smooth curve on the tuning plot represents the square root of the filter-calculated covariance. The "apparently noisy" curve represents the square root of the variance of the error calculated over the twenty simulations. Also included, in various sets, are covariance convergence plots (described in Chapter IV). The box in the upper right hand corner of each plot indicates whether the plot is a mean error plot or a covariance plot. The order of the missile as well as the data set number are also in-

cluded. The data set number indicates the tuning parameters used for a particular run. The filter initial estimates, the tuning parameters and a brief description of the purpose of each set will be included at the beginning of each set. It should be noted that the high-g scenario was used for all cases except the one annotated low-g.

Organization

The sets will be arranged in the following order:

Figure	Subject
1-9	Zero order missile filter
10-21	Third order missile filter
22-31	Benchmark
32-41	Fourth order missile filter (A/P at 0 sec)
42-51	Fourth order missile filter (A/P at 3 sec)
52-61	Fourth order missile filter (A/P at 5 sec)
62-71	Fourth order missile filter (A/P at 0 sec - complete linearization of $\underline{f}$)
72-81	Fourth order missile filter (A/P at 5 sec - using fourth order Runge-Kutta integration package)
82-91	Sensitivity analysis (n = 6.)
92-101	Sensitivity analysis (n = 3.)
102-111	Sensitivity analysis (τ_2 = .8)
112-121	Sensitivity analysis (τ_2 = .1)
122-131	Sensitivity analysis (M = 2.)
132-141	Sensitivity analysis (M = 8.)
142-151	First order missile filter (τ_f set equal to .85)

152-164	n estimation - n initialized at 3.
165-178	n estimation - n initialized at 6.
179-190	τ_f estimation - τ_f initialized at 1.5
191-202	τ_f estimation - τ_f initialized at .3
203-216	M/S estimation - M/S initialized at 45.
217-230	M/S estimation - M/S initialized at 15.
231-244	n and τ_f estimation (high-g scenario)
245-258	n and τ_f estimation (low-g scenario)
259-276	n, τ_f, and M/S estimation
277-294	n, τ_f, and M/S estimation with the dynamic states initialized with some error.

Zero Order Missile Filter

The initial state estimates and the tuning parameters for this case are

$$\begin{aligned}
V^{I}_{mx}(0) &= 1225.7 \text{ fps}\\
\dot{\theta}_{T}(0) &= 4.363345 \text{ radians}\\
R(0) &= 10000. \text{ feet}\\
\dot{R}(0) &= -2122. \text{ fps}\\
a_{L}(0) &= 0.\\
n(0) &= 4.5\\
\tau_{f}(0) &= \text{N/A}\\
M/S(0) &= 29.197 \text{ slugs/ft}^2
\end{aligned}$$

$$\underline{R} = \begin{bmatrix} 4.E-5 & 0. & 0. \\ 0. & 500. & 0. \\ 0. & 0. & 100. \end{bmatrix}$$

$$\underline{P}_0 = \begin{bmatrix}
100. & 0. & 0. & 0. & 0. & 0. & 0. & 0. \\
0. & 1.E-8 & 0. & 0. & 0. & 0. & 0. & 0. \\
0. & 0. & 101. & 0. & 0. & 0. & 0. & 0. \\
0. & 0. & 0. & 4. & 0. & 0. & 0. & 0. \\
0. & 0. & 0. & 0. & 0. & 0. & 0. & 0. \\
0. & 0. & 0. & 0. & 0. & 0. & 0. & 0. \\
0. & 0. & 0. & 0. & 0. & 0. & 0. & 0. \\
0. & 0. & 0. & 0. & 0. & 0. & 0. & 0.
\end{bmatrix}$$

$$
\underline{Q} = \begin{bmatrix}
101. & 0. & 0. & 0. & 0. & 0. & 0. & 0. \\
0. & 1.E-6 & 0. & 0. & 0. & 0. & 0. & 0. \\
0. & 0. & 500. & 0. & 0. & 0. & 0. & 0. \\
0. & 0. & 0. & 100. & 0. & 0. & 0. & 0. \\
0. & 0. & 0. & 0. & 0. & 0. & 0. & 0. \\
0. & 0. & 0. & 0. & 0. & 0. & 0. & 0. \\
0. & 0. & 0. & 0. & 0. & 0. & 0. & 0. \\
0. & 0. & 0. & 0. & 0. & 0. & 0. & 0.
\end{bmatrix}
$$

These plots were generated to demonstrate the performance of this filter with the software changes noted in Appendix A. The parameters n and M/S were not estimated, but were set to their correct values.

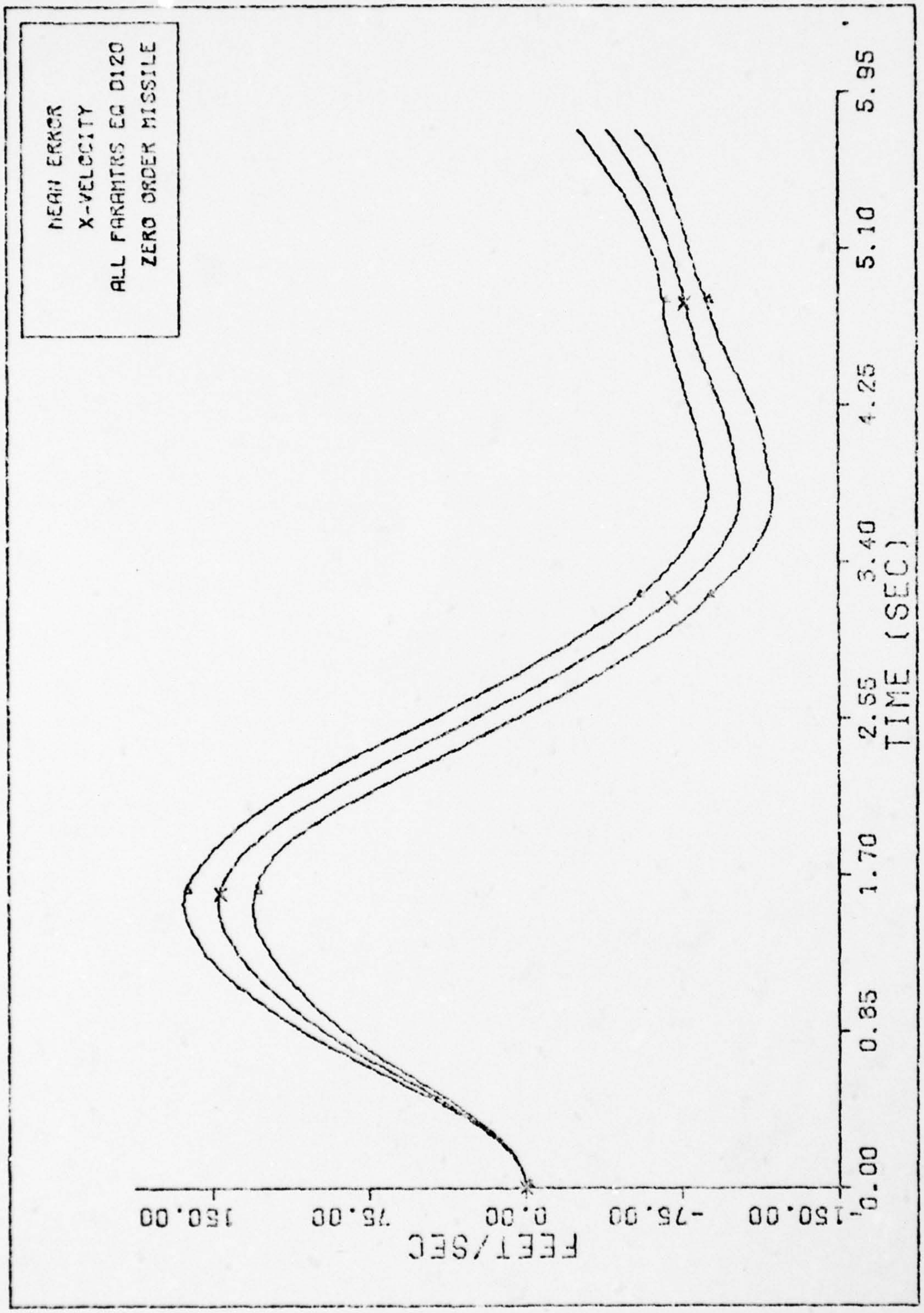

Fig. 1. X-VELOCITY ZERO ORDER MISSILE

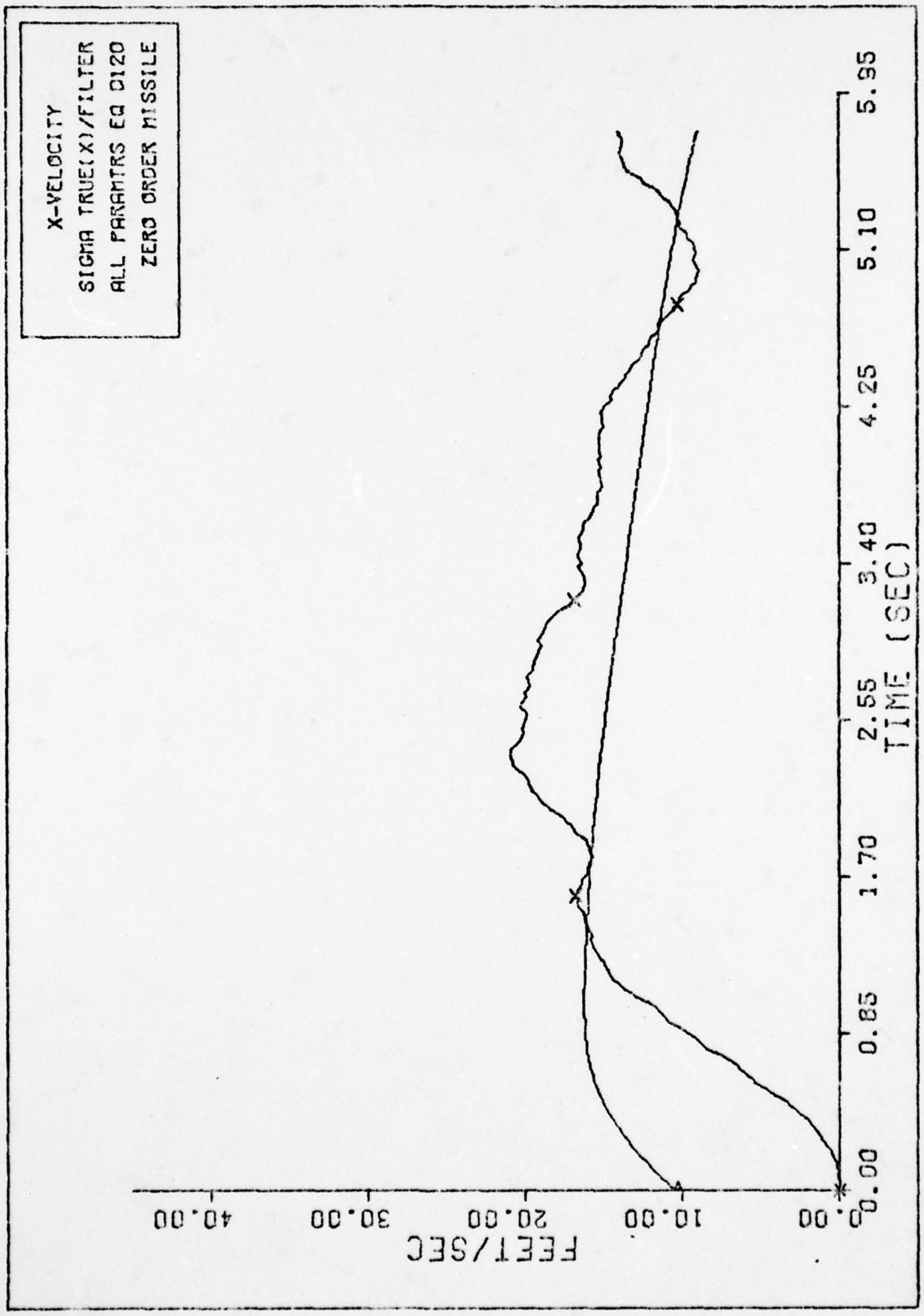

Fig. 2. X-VELOCITY SIGMAS ZERO ORDER

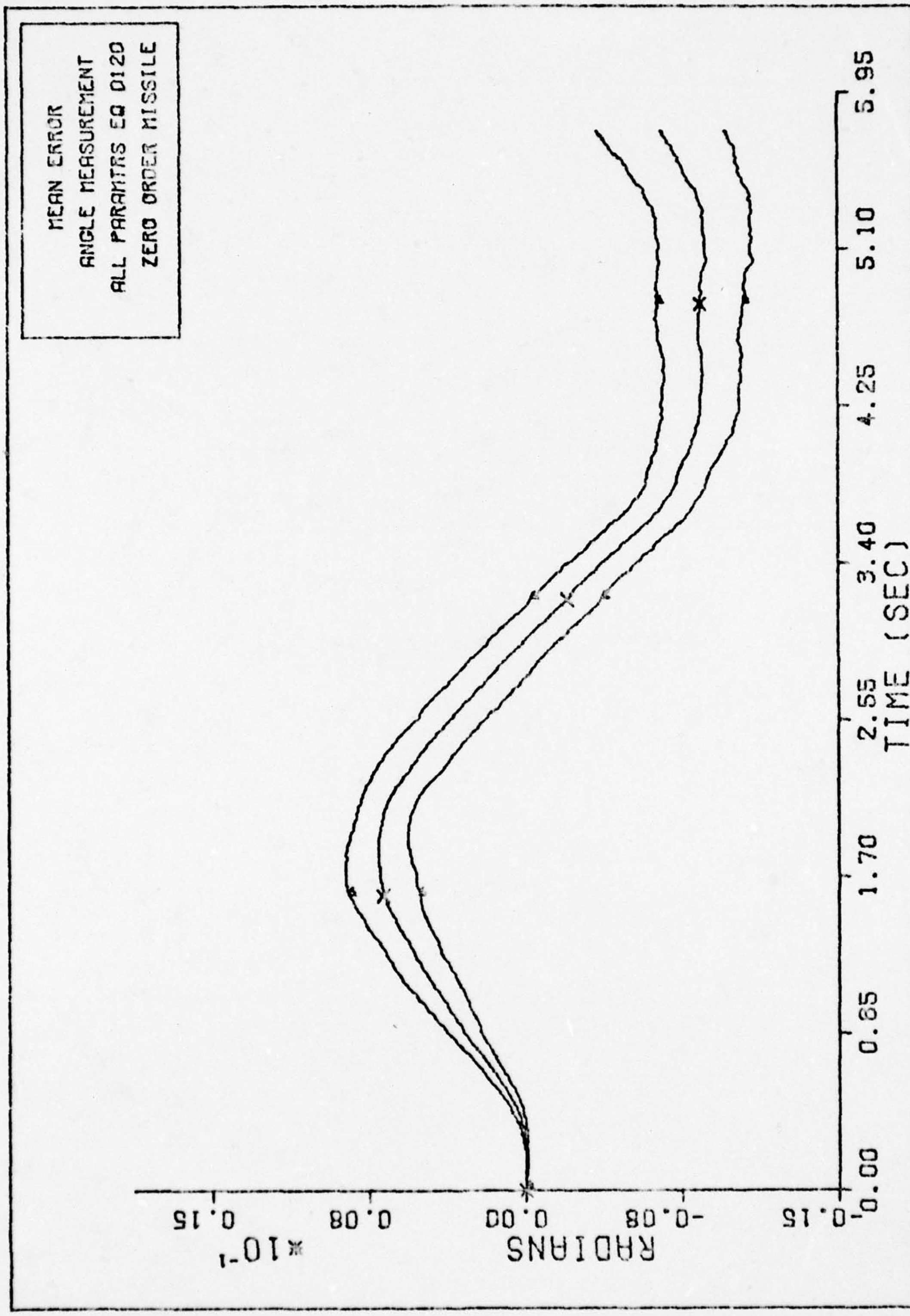

Fig. 3. ANGLE MEASUREMENT ZERO ORDER MISSILE

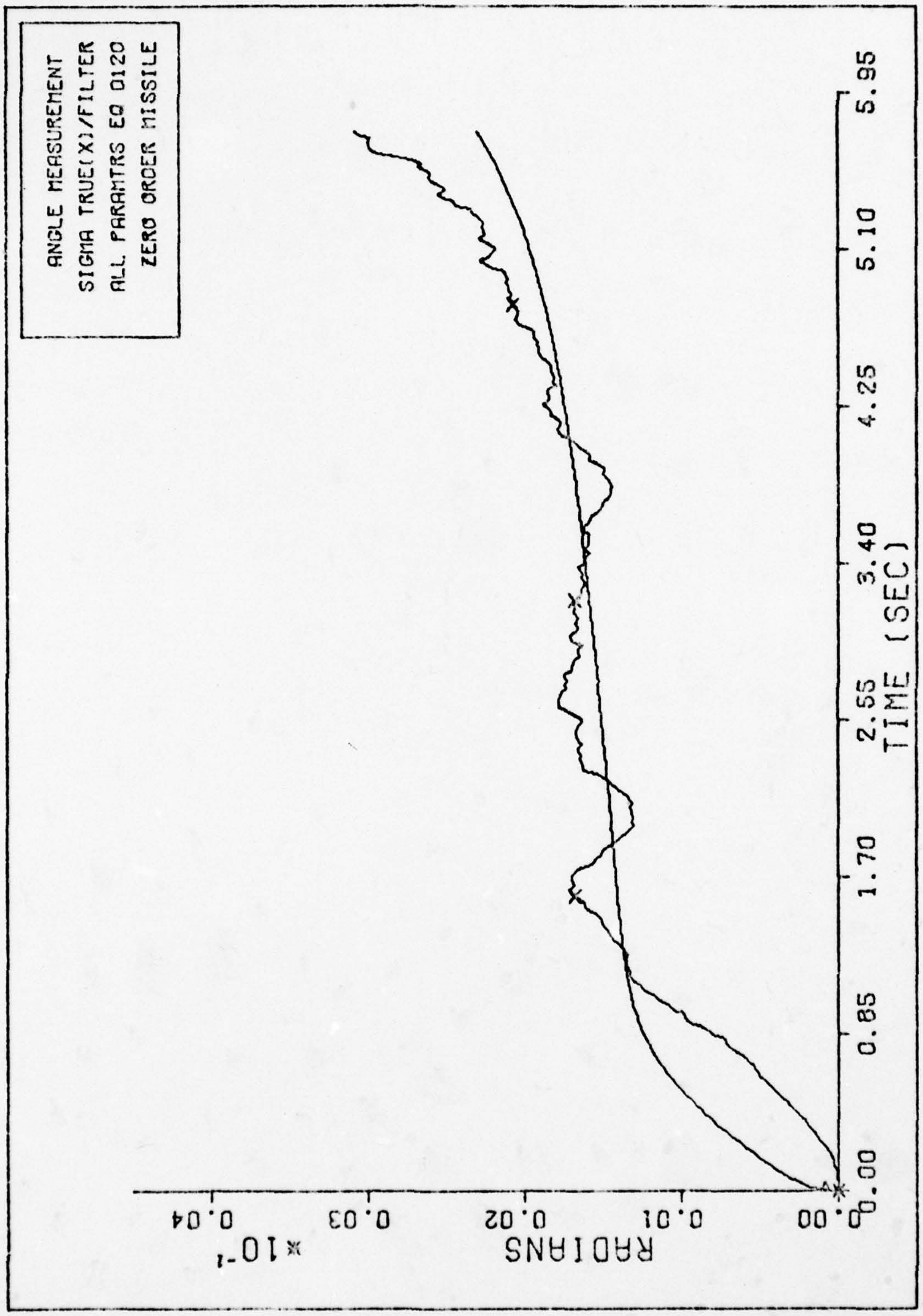

Fig. 4. ANGLE MEASUREMENT SIGMAS ZERO ORDER

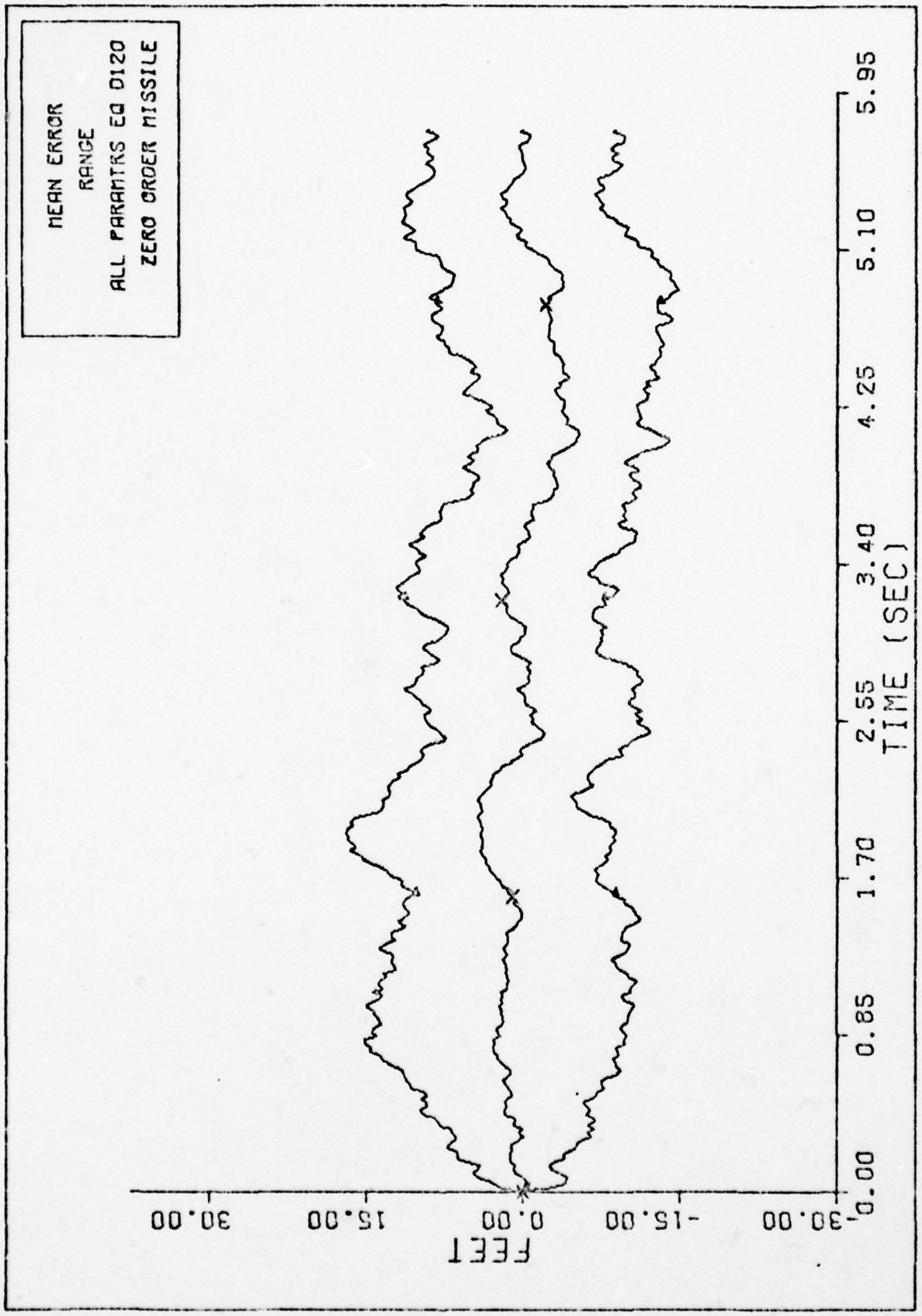

Fig. 5. RANGE ZERO ORDER MISSILE

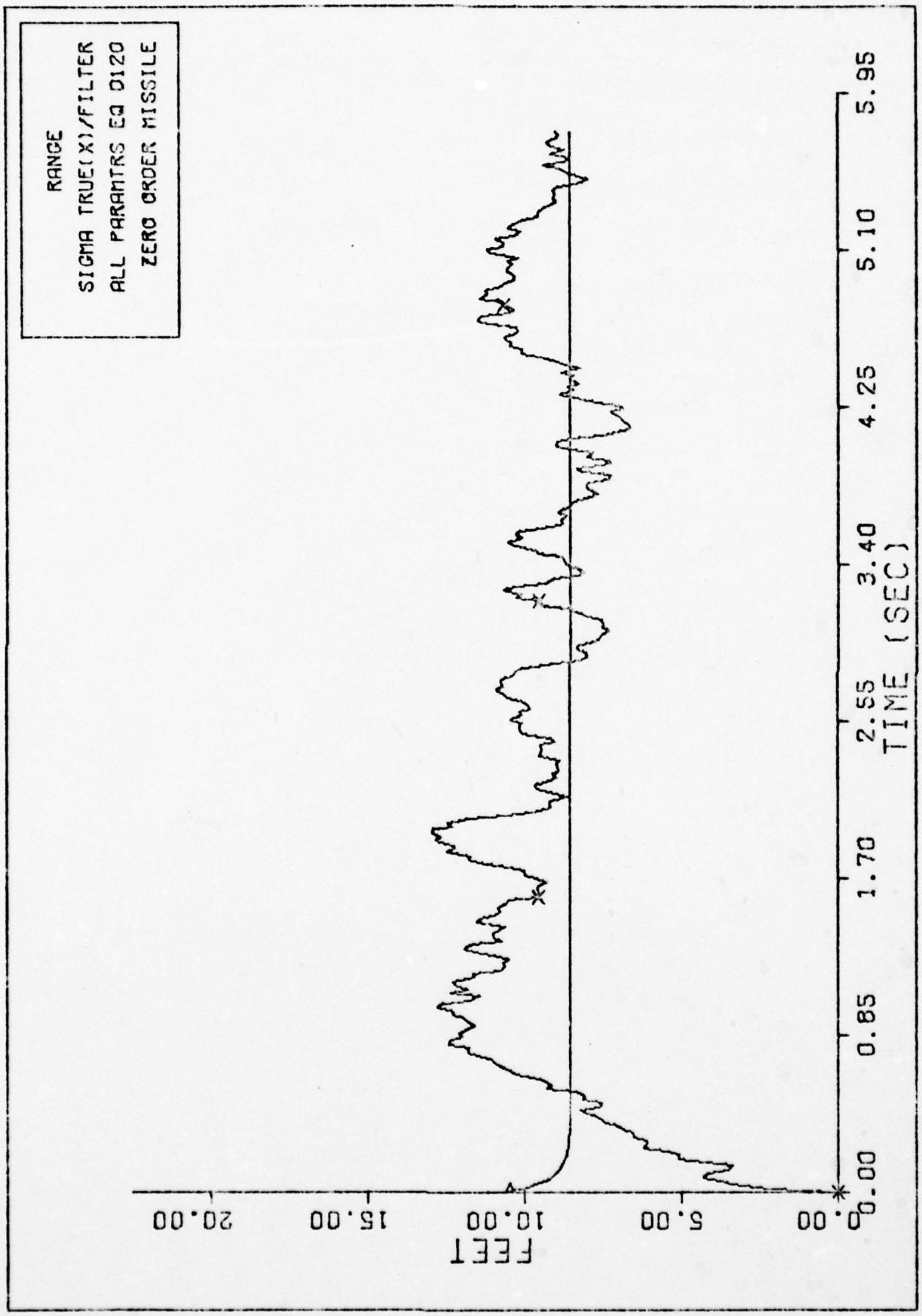

Fig. 6. RANGE SIGMAS ZERO ORDER

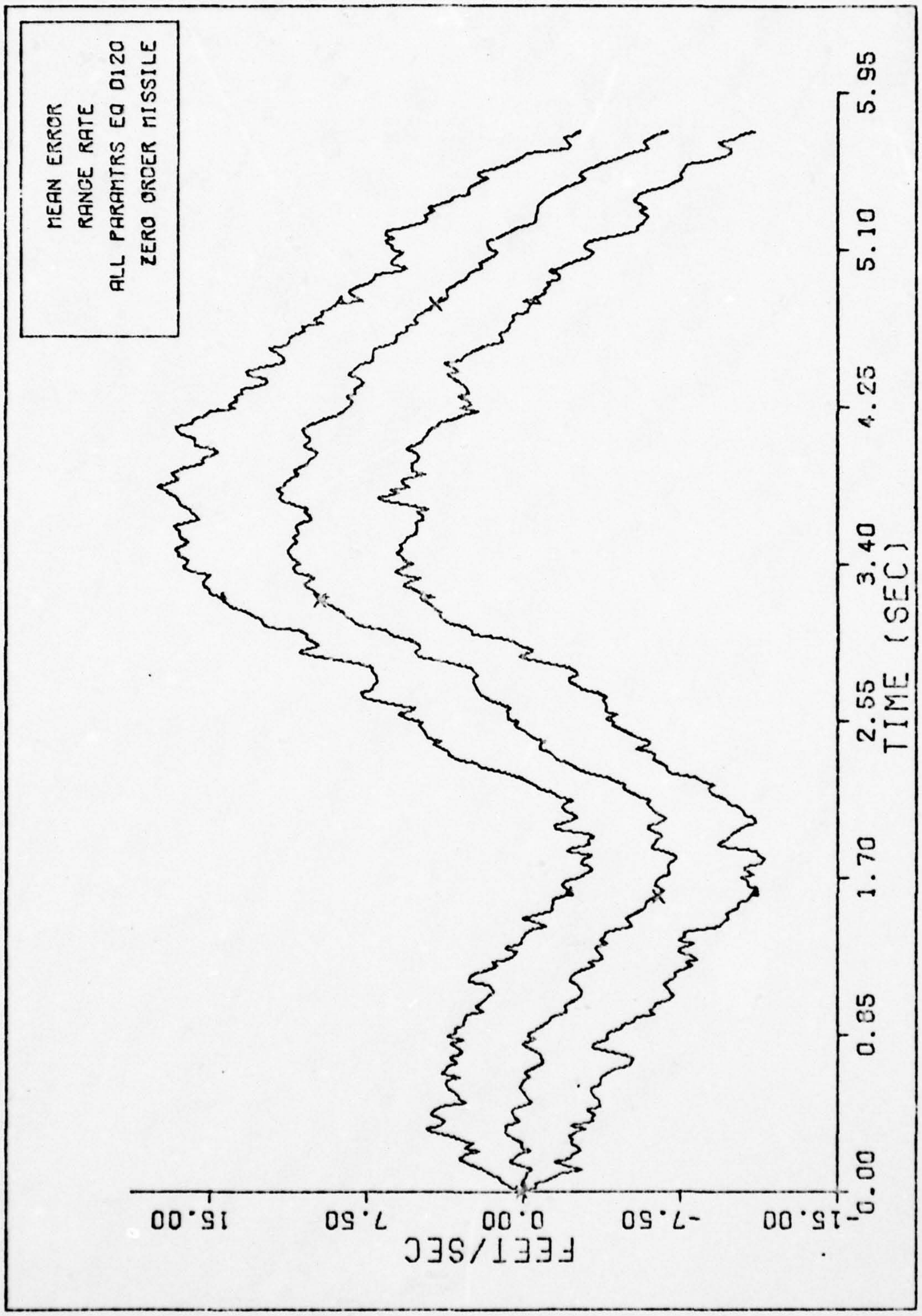

Fig. 7. RANGE RATE ZERO ORDER MISSILE

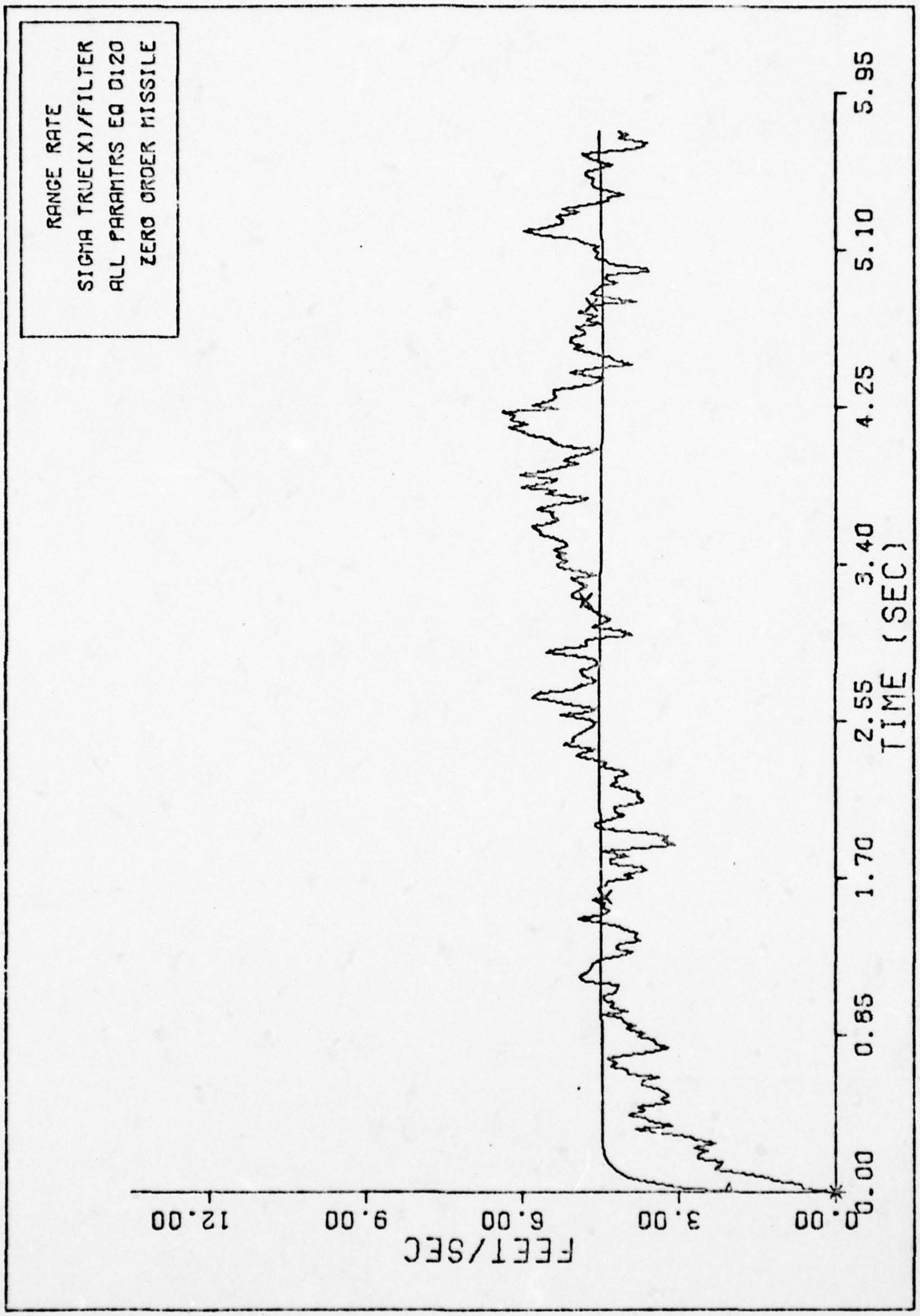

Fig. 8. RANGE RATE SIGMAS ZERO ORDER

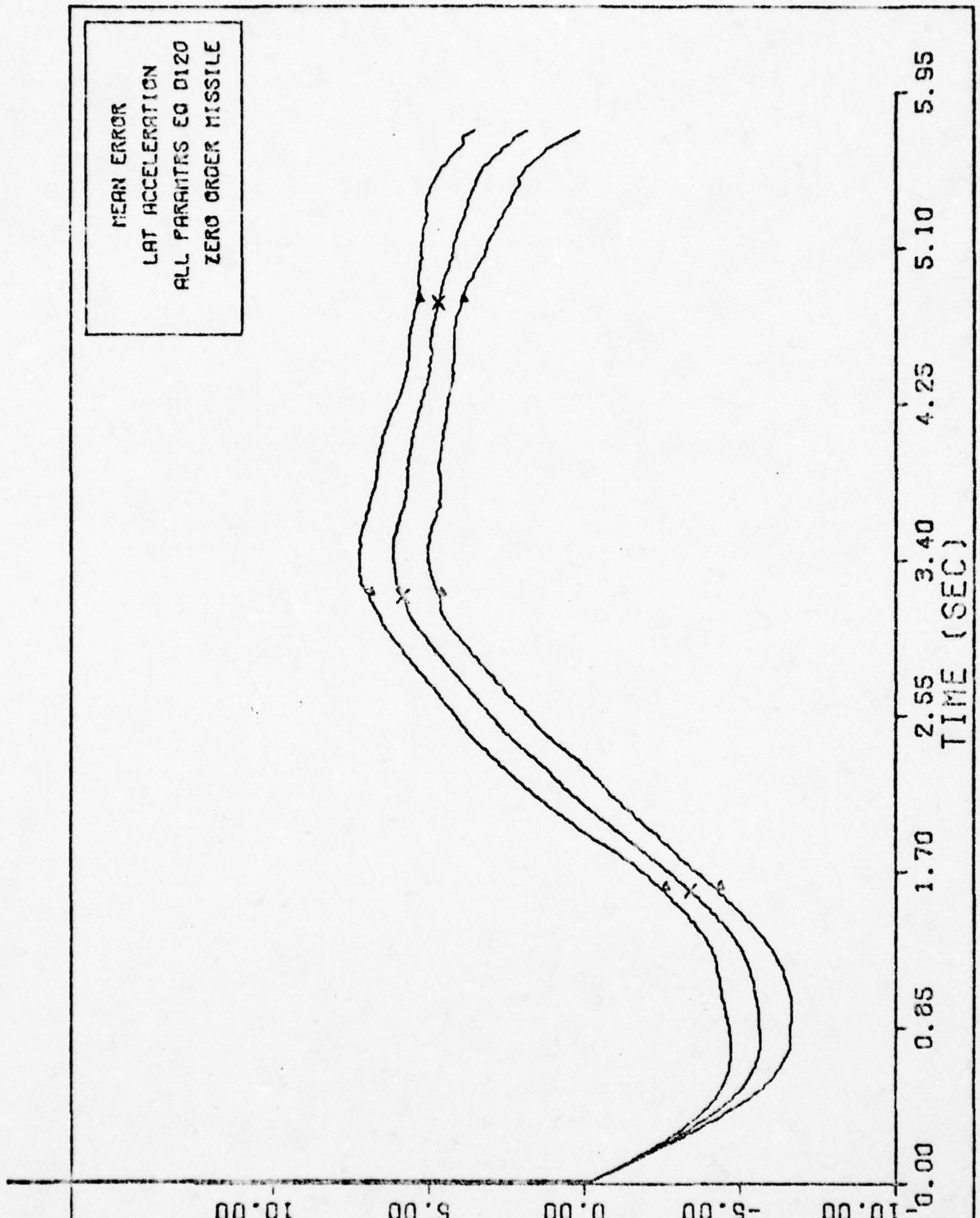

Fig. 9. LAT ACCELERATION ZERO ORDER MISSILE

Third Order Missile Filter

The initial state estimates and the tuning parameters for this case are

$$V_{mx}^{I}(0) = 1225.7 \text{ fps}$$

$$\dot{\theta}_T(0) = 4.363345 \text{ radians}$$

$$R(0) = 10000. \text{ feet}$$

$$\dot{R}(0) = -2122. \text{ fps}$$

$$a_L(0) = 0.$$

$$n(0) = 4.5$$

$$\tau_f(0) = \text{N/A}$$

$$M/S(0) = 29.197 \text{ slugs/ft}^2$$

$$\underline{R} = \begin{bmatrix} 4.E{-}5 & 0. & 0. \\ 0. & 500. & 0. \\ 0. & 0. & 100. \end{bmatrix}$$

$$\underline{P}_0 = \begin{bmatrix} 100. & 0. & 0. & 0. & 0. & 0. & 0. & 0. \\ 0. & 1.E{-}8 & 0. & 0. & 0. & 0. & 0. & 0. \\ 0. & 0. & 101. & 0. & 0. & 0. & 0. & 0. \\ 0. & 0. & 0. & 4. & 0. & 0. & 0. & 0. \\ 0. & 0. & 0. & 0. & 1. & 0. & 0. & 0. \\ 0. & 0. & 0. & 0. & 0. & 0. & 0. & 0. \\ 0. & 0. & 0. & 0. & 0. & 0. & 0. & 0. \\ 0. & 0. & 0. & 0. & 0. & 0. & 0. & 0. \end{bmatrix}$$

$$\underline{Q} = \begin{bmatrix} 101. & 0. & 0. & 0. & 0. & 0. & 0. & 0. \\ 0. & 1.E-6 & 0. & 0. & 0. & 0. & 0. & 0. \\ 0. & 0. & 500. & 0. & 0. & 0. & 0. & 0. \\ 0. & 0. & 0. & 100. & 0. & 0. & 0. & 0. \\ 0. & 0. & 0. & 0. & 1. & 0. & 0. & 0. \\ 0. & 0. & 0. & 0. & 0. & 0. & 0. & 0. \\ 0. & 0. & 0. & 0. & 0. & 0. & 0. & 0. \\ 0. & 0. & 0. & 0. & 0. & 0. & 0. & 0. \end{bmatrix}$$

This design was used as an attempt in establishing a benchmark. The filter model included the exact structure of the autopilot (found by assuming constant coefficients as described in Chapter III). Chapter III lists six sets of coefficients found at various times over the high-g scenario. The plots that follow were generated using the coefficients for t=0. This set of coefficients reduced the initial transients in the filter. This can be seen by comparing the plots of the fourth order missile filter which use three sets of autopilot transfer function coefficients to demonstrate this point.

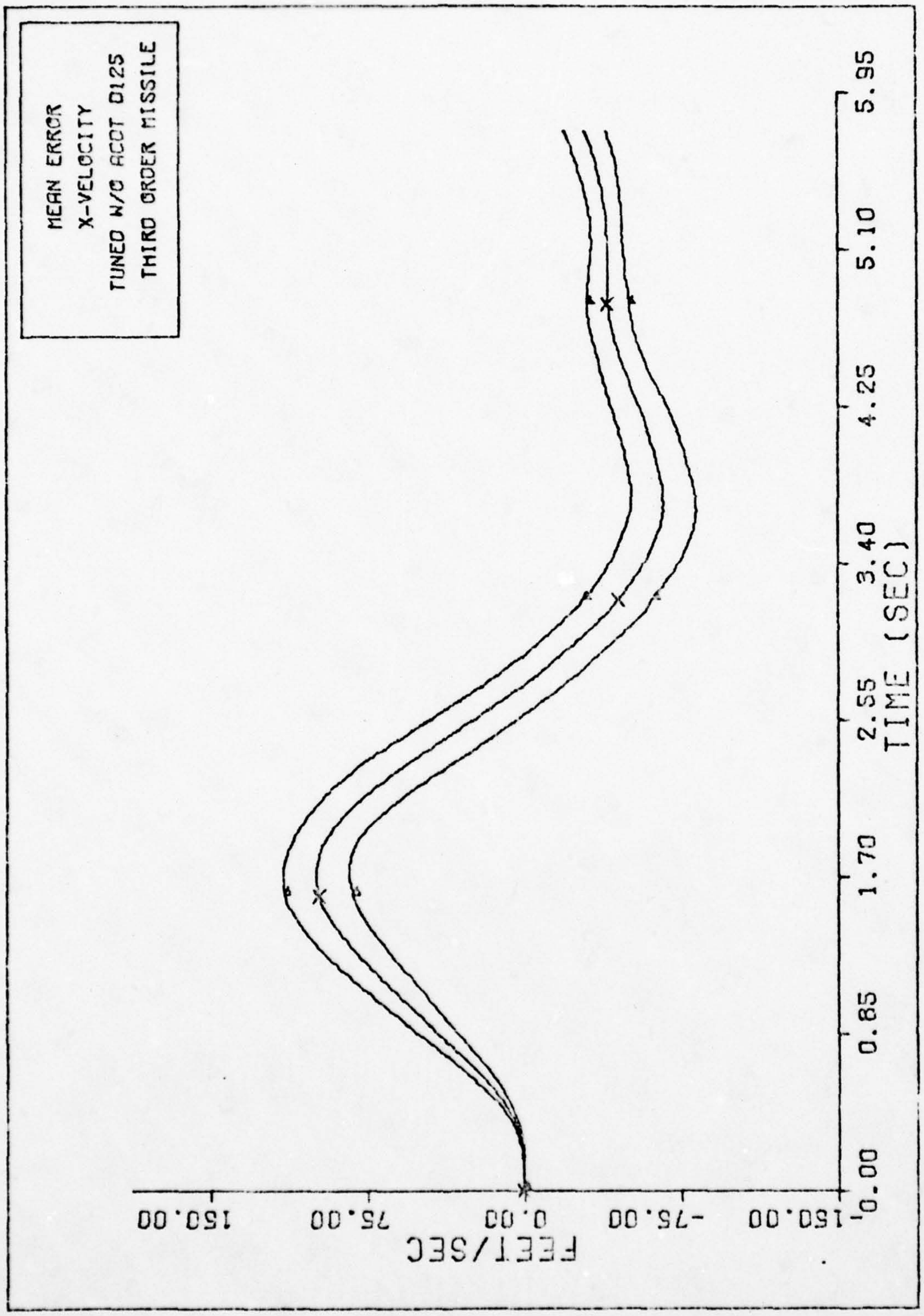

Fig. 10. X-VELOCITY THIRD ORDER MISSILE

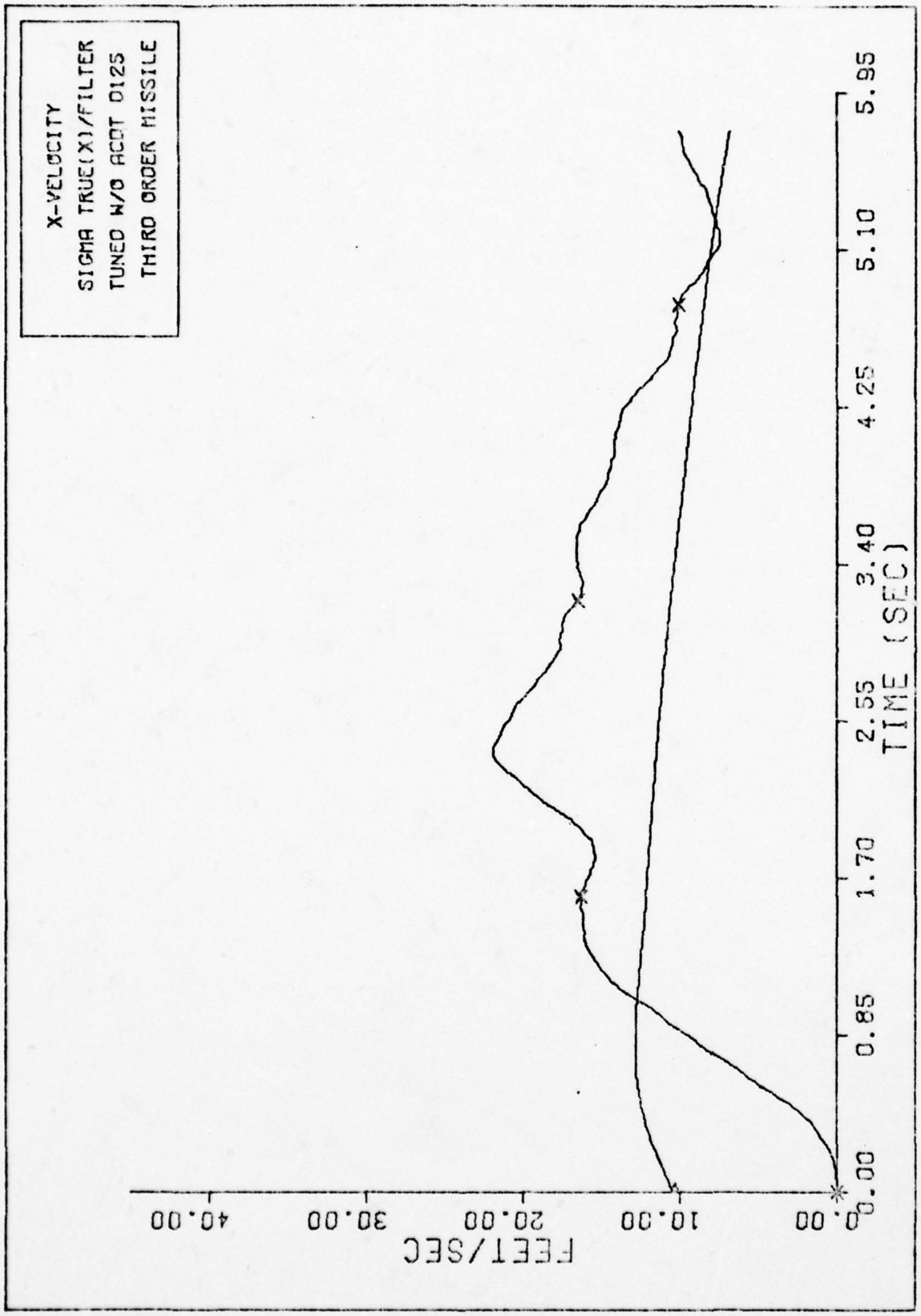

Fig. 11. X-VELOCITY SIGMAS THIRD ORDER

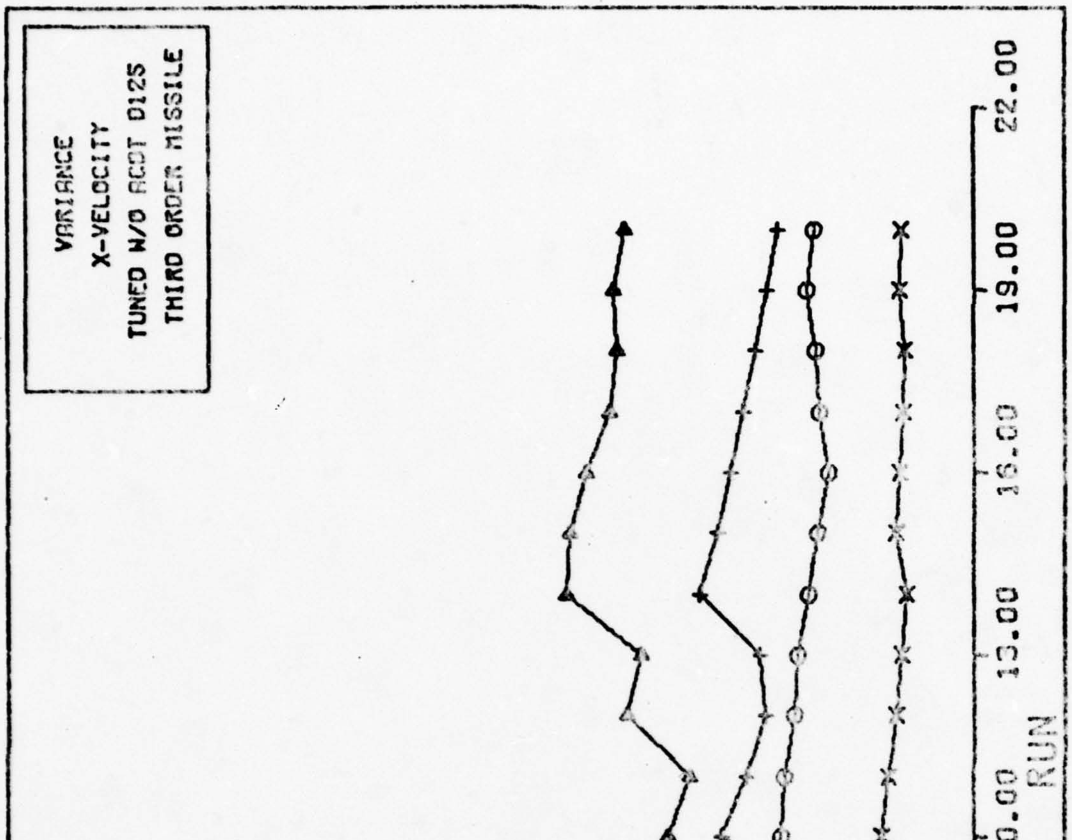

Fig. 12. VARIANCE CONVERGENCE

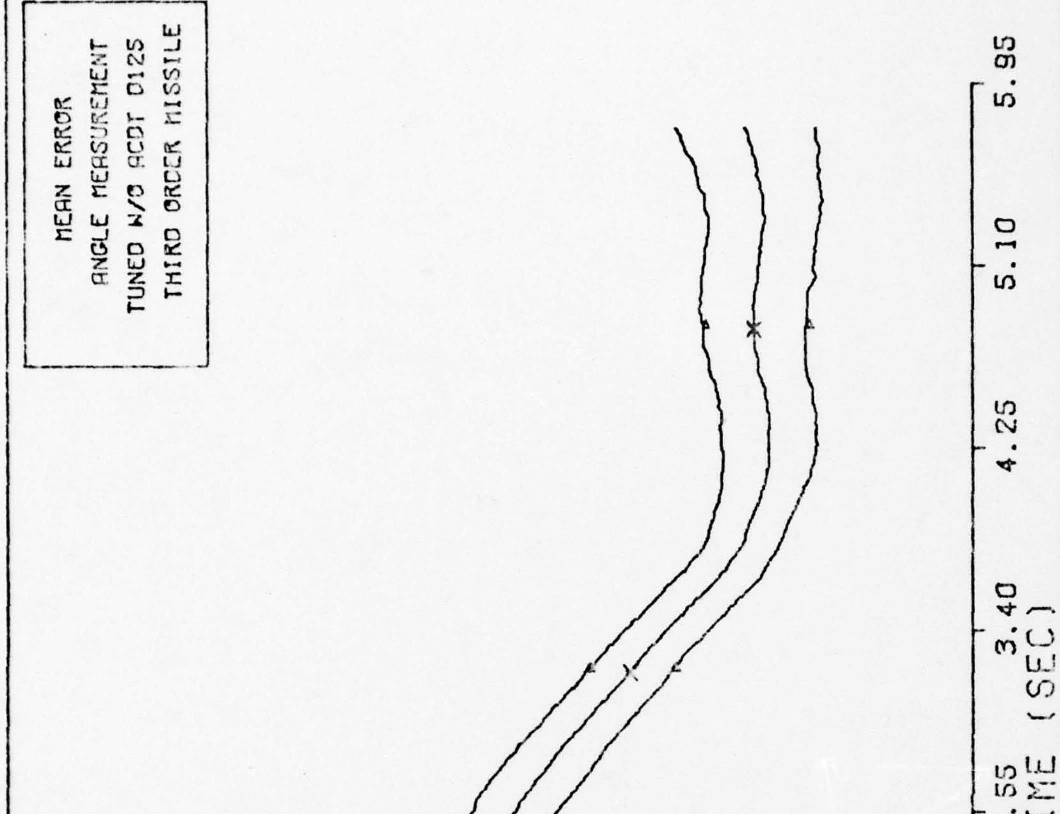

Fig. 13. ANGLE MEASUREMENT THIRD ORDER MISSILE

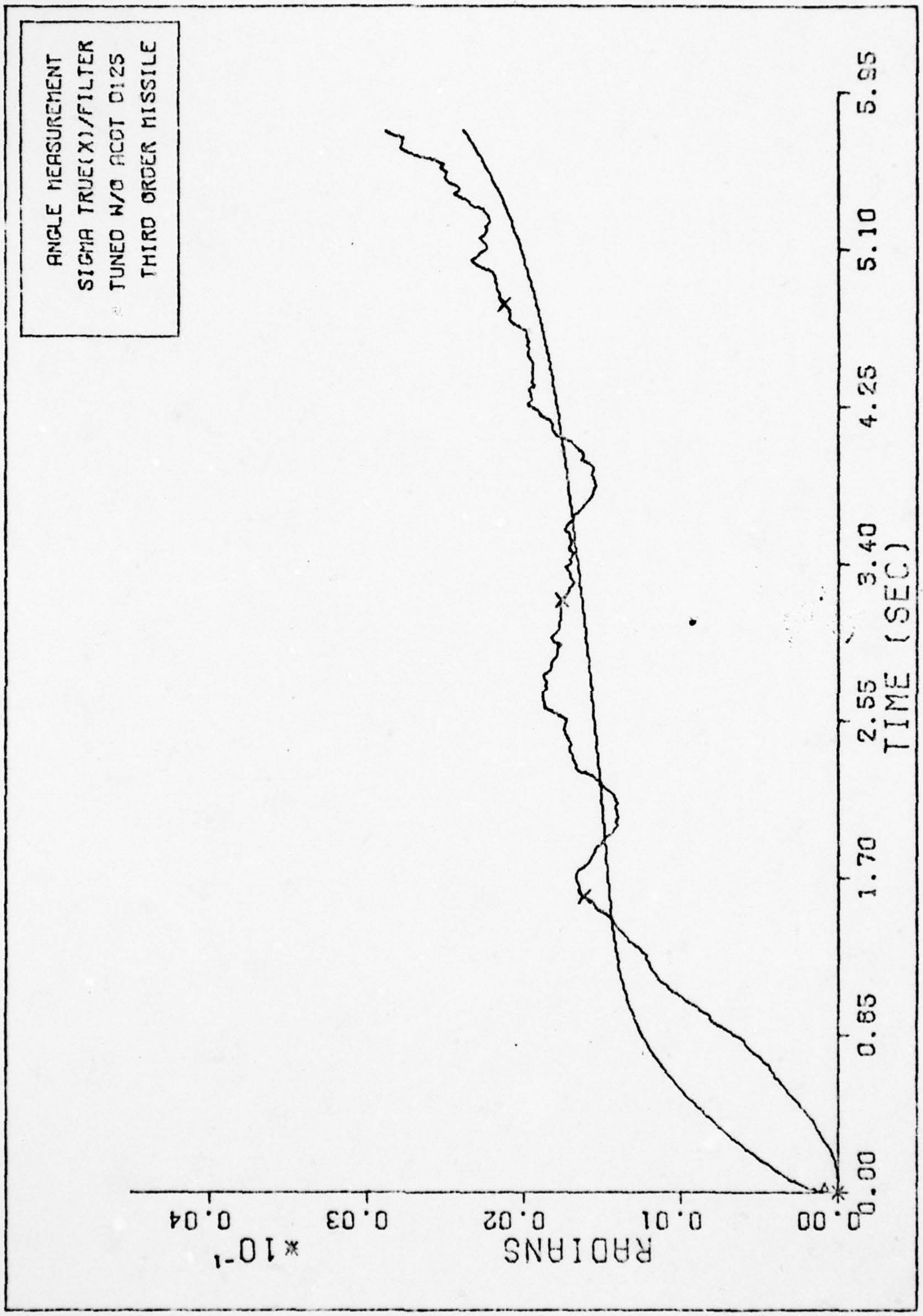

Fig. 14. ANGLE MEASUREMENT SIGMAS THIRD ORDER

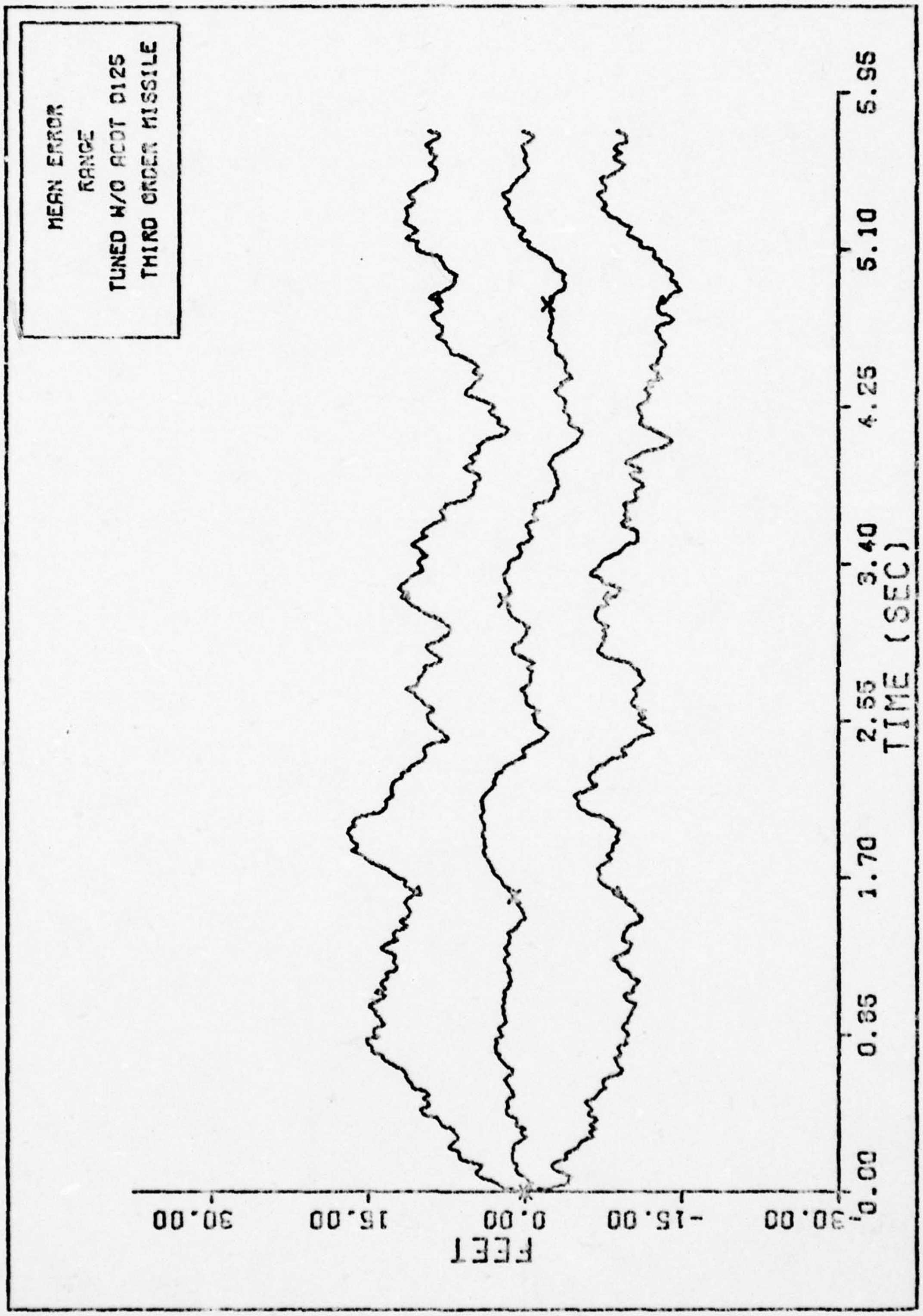

Fig. 15. RANGE THIRD ORDER MISSILE

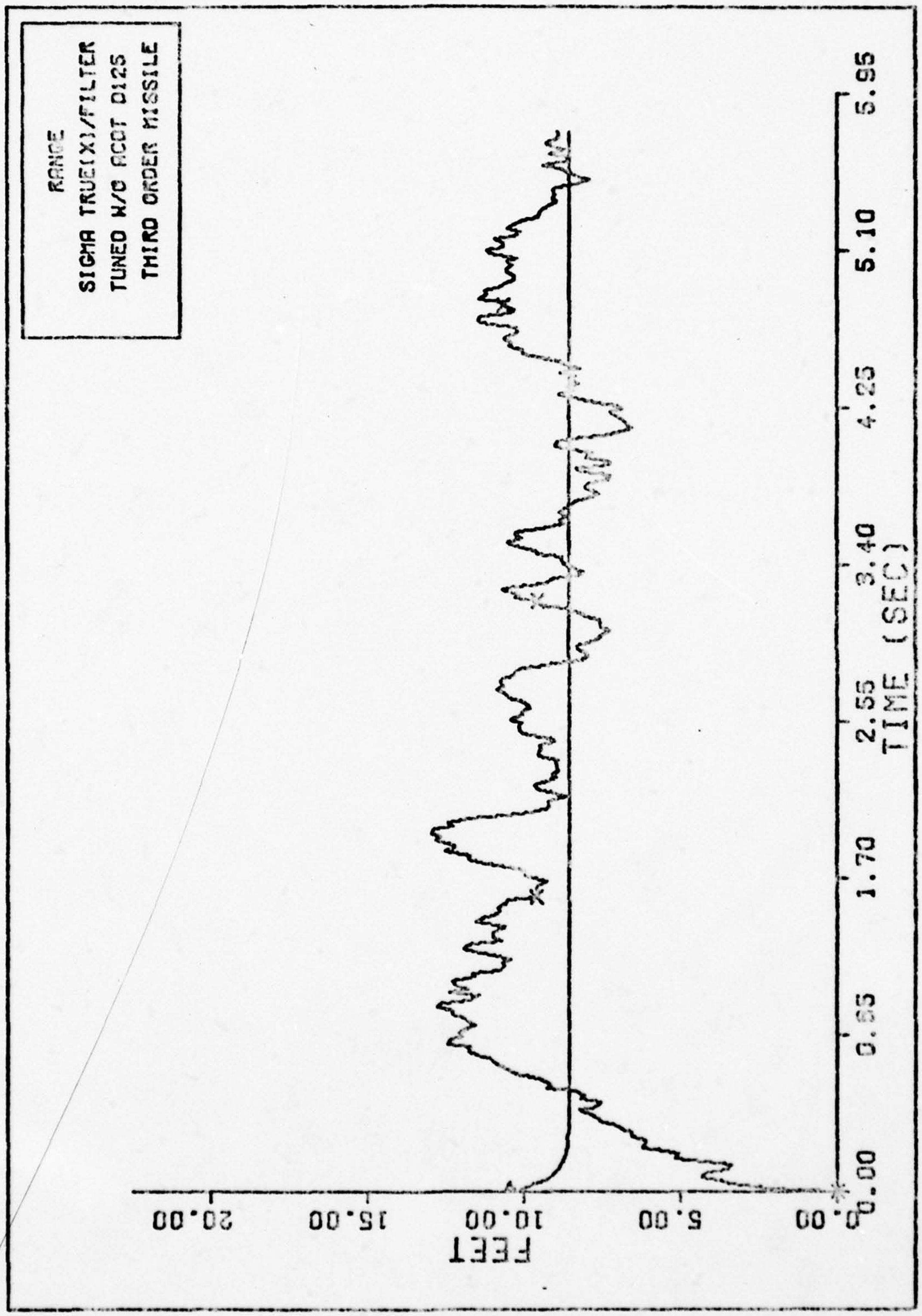

Fig. 16. RANGE SIGMAS THIRD ORDER

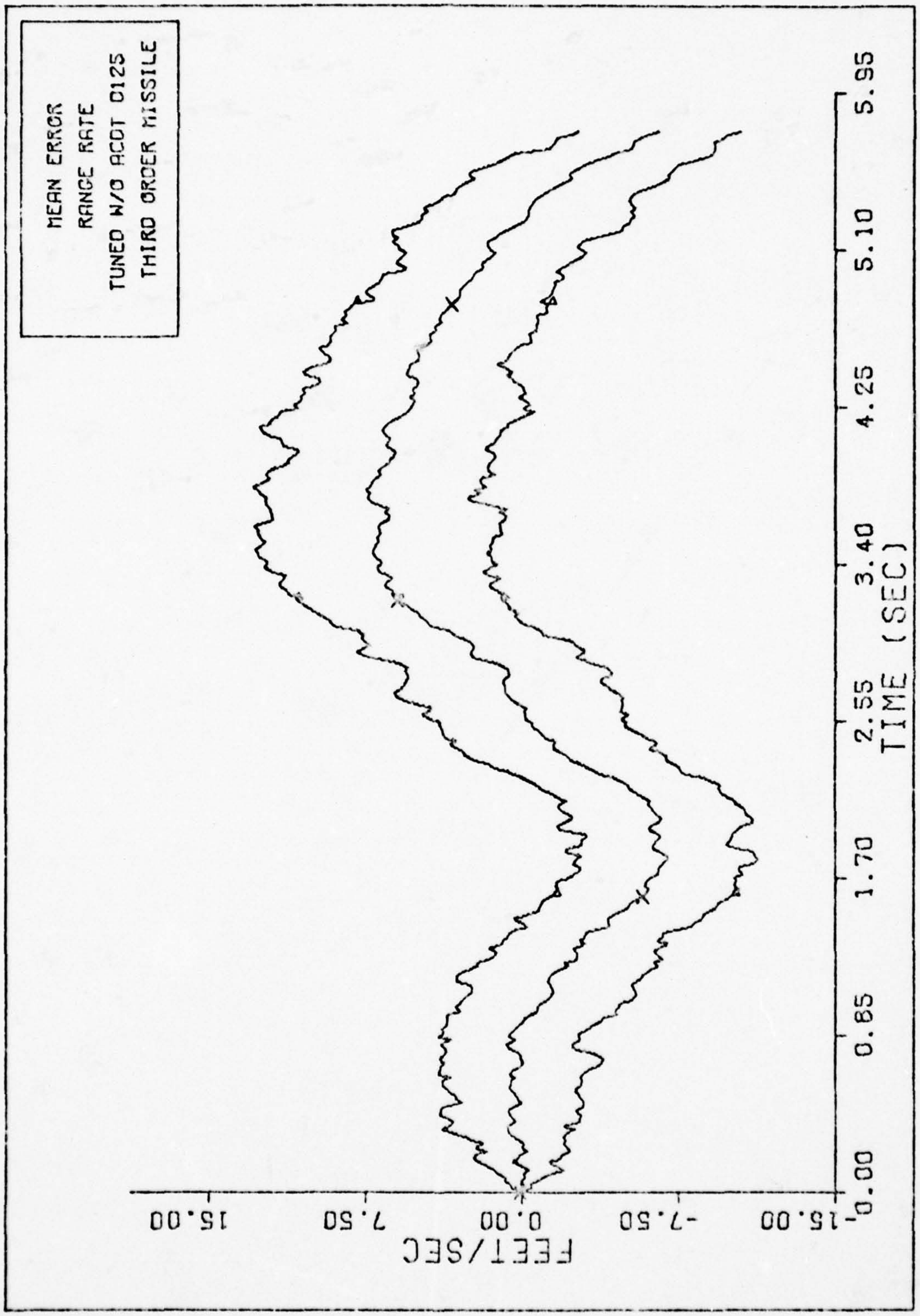

Fig. 17. RANGE RATE THIRD ORDER MISSILE

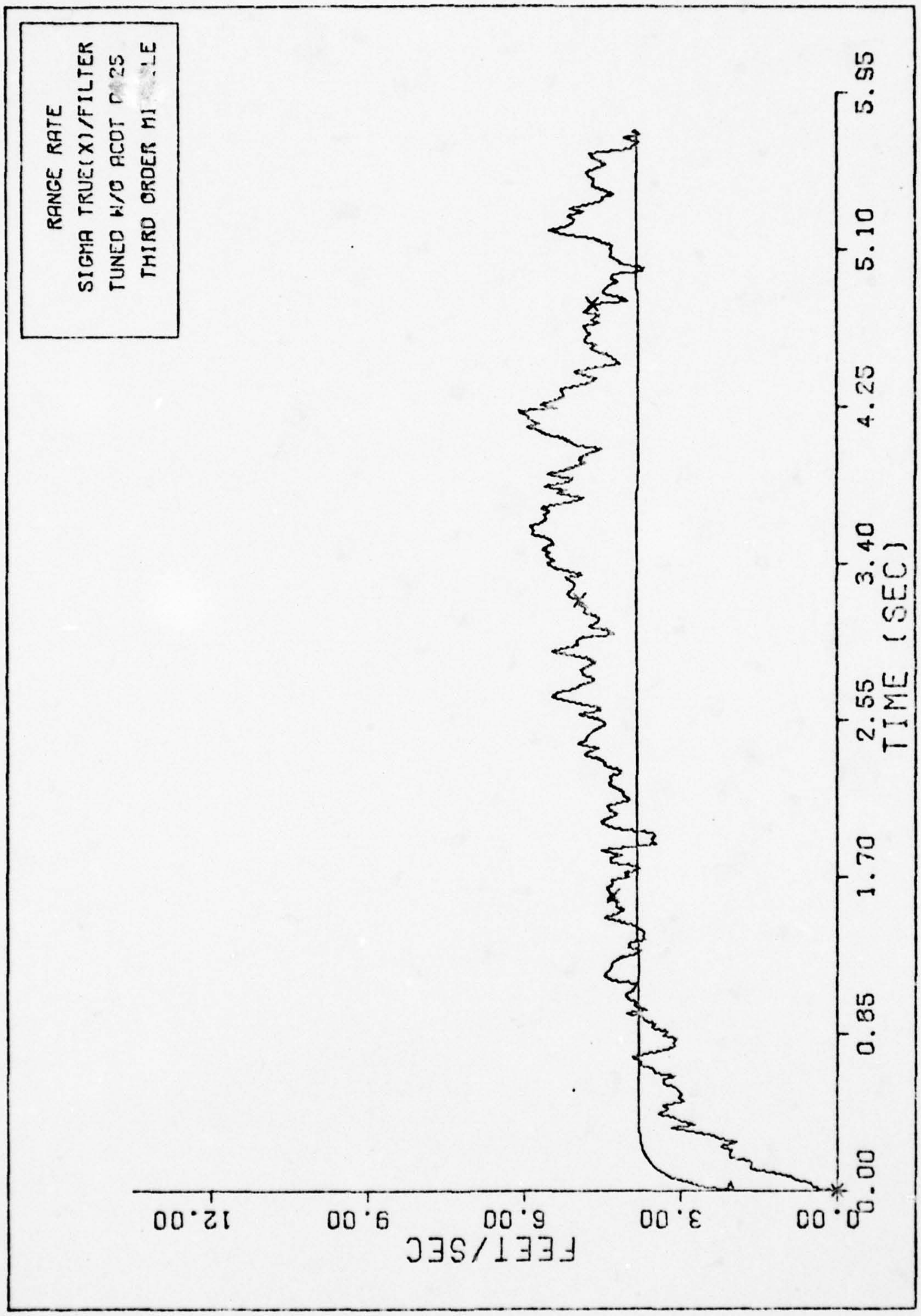

Fig. 18. RANGE RATE SIGMAS THIRD ORDER

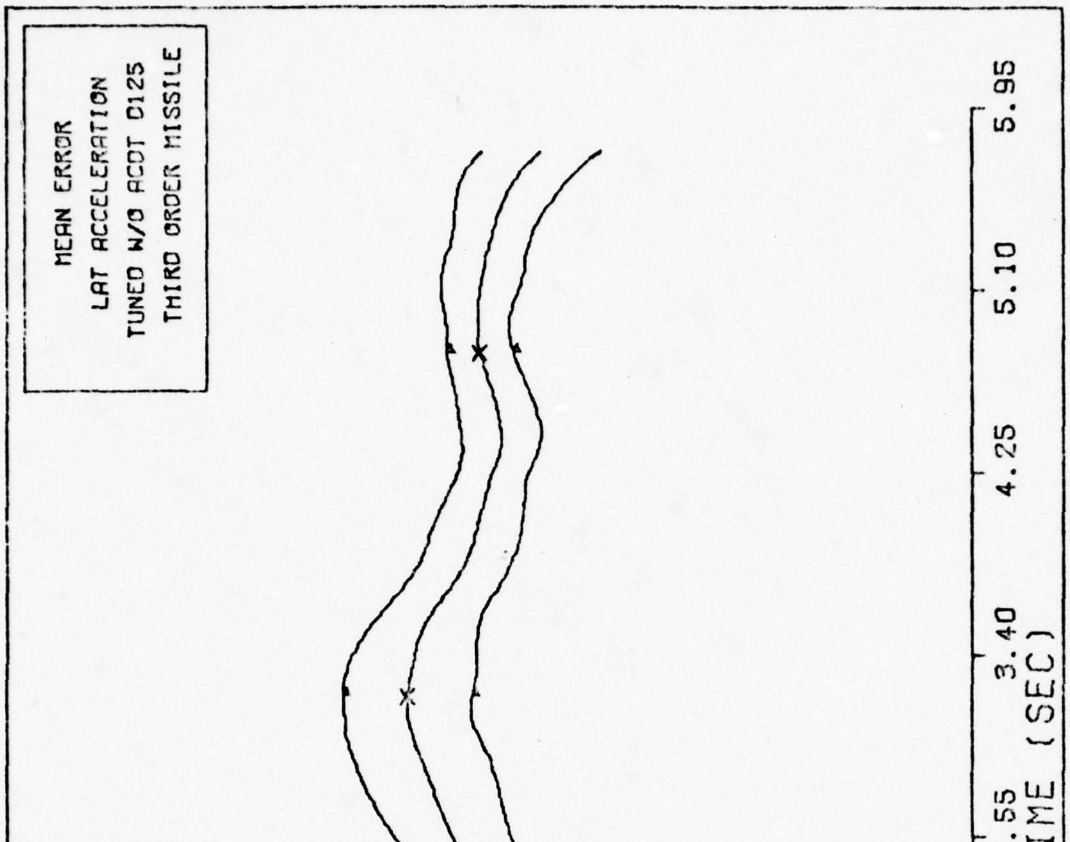

Fig. 19. LAT ACCELERATION THIRD ORDER MISSILE

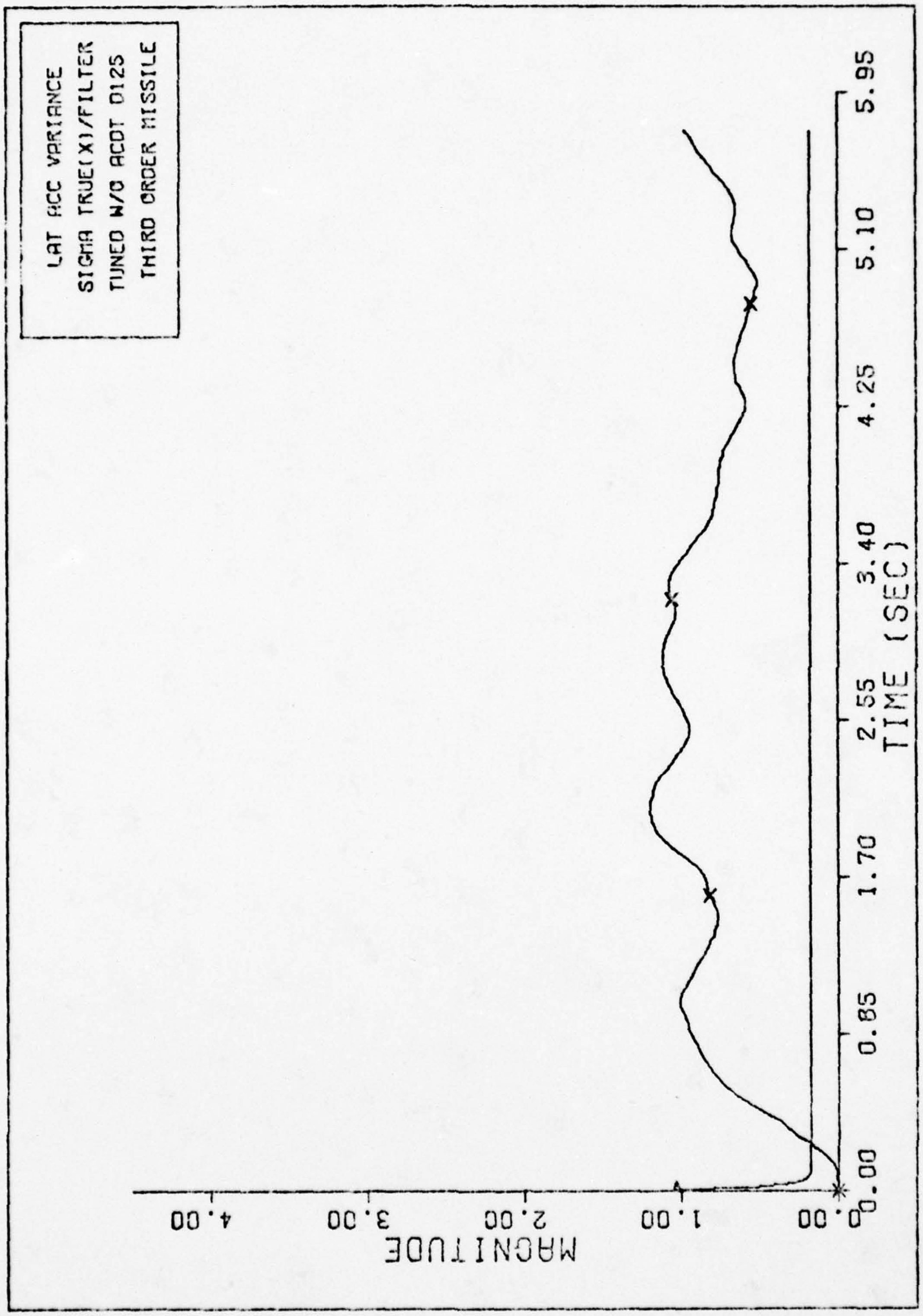

Fig. 20. LAT ACCELERATION SIGMAS THIRD ORDER

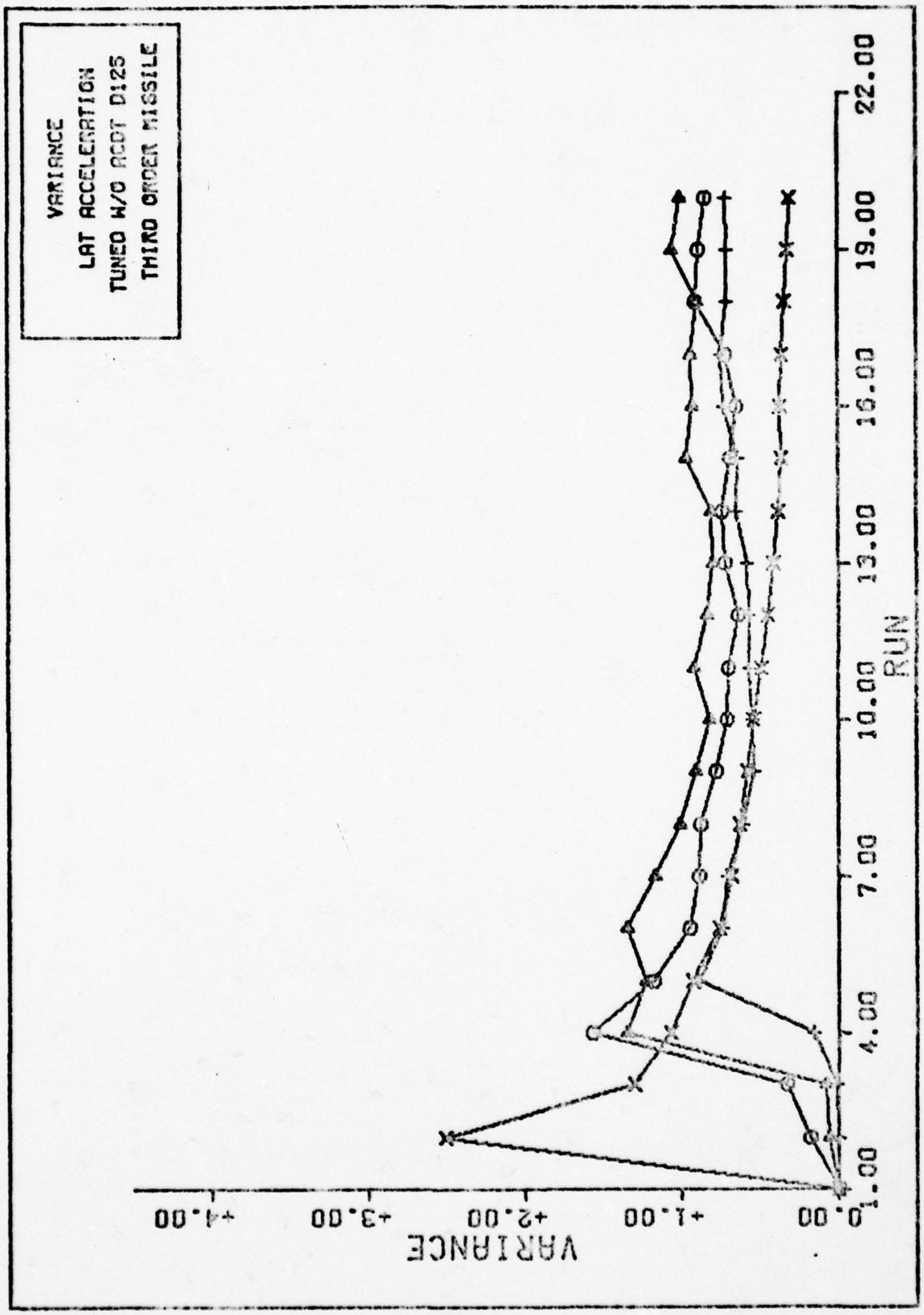

Fig. 21. VARIANCE CONVERGENCE

Benchmark

The initial state estimates and the tuning parameters for this case are

$$V^I_{mx}(0) = 1225.7 \text{ fps}$$

$$\dot{\theta}_T(0) = 4.363345 \text{ radians}$$

$$R(0) = 10000. \text{ feet}$$

$$\dot{R}(0) = -2122. \text{ fps}$$

$$a_L(0) = 0.$$

$$n(0) = 4.5$$

$$\tau_f(0) = \text{N/A}$$

$$M/S(0) = 29.197 \text{ slugs/ft}^2$$

$$\underline{R} = \begin{bmatrix} 4.E-5 & 0. & 0. \\ 0. & 500. & 0. \\ 0. & 0. & 100. \end{bmatrix}$$

$$\underline{P}_0 = \begin{bmatrix} 100. & 0. & 0. & 0. & 0. & 0. & 0. & 0. \\ 0. & 1.E-8 & 0. & 0. & 0. & 0. & 0. & 0. \\ 0. & 0. & 101. & 0. & 0. & 0. & 0. & 0. \\ 0. & 0. & 0. & 4. & 0. & 0. & 0. & 0. \\ 0. & 0. & 0. & 0. & 1. & 0. & 0. & 0. \\ 0. & 0. & 0. & 0. & 0. & 0. & 0. & 0. \\ 0. & 0. & 0. & 0. & 0. & 0. & 0. & 0. \\ 0. & 0. & 0. & 0. & 0. & 0. & 0. & 0. \end{bmatrix}$$

$$\underline{Q} = \begin{bmatrix} 101. & 0. & 0. & 0. & 0. & 0. & 0. & 0. \\ 0. & 1.E-6 & 0. & 0. & 0. & 0. & 0. & 0. \\ 0. & 0. & 500. & 0. & 0. & 0. & 0. & 0. \\ 0. & 0. & 0. & 100. & 0. & 0. & 0. & 0. \\ 0. & 0. & 0. & 0. & 1. & 0. & 0. & 0. \\ 0. & 0. & 0. & 0. & 0. & 0. & 0. & 0. \\ 0. & 0. & 0. & 0. & 0. & 0. & 0. & 0. \\ 0. & 0. & 0. & 0. & 0. & 0. & 0. & 0. \end{bmatrix}$$

A complete description of the ad hoc design, used in generating the following plots, can be found in Chapter III. Basically, the true commanded acceleration of the missile was assumed known perfectly and passed directly to the autopilot in the filter model. The autopilot transfer function used the coefficients for t=0 (refer to Chapter III). These plots were considered as benchmarks for the five dynamic states of the fundamental filter design.

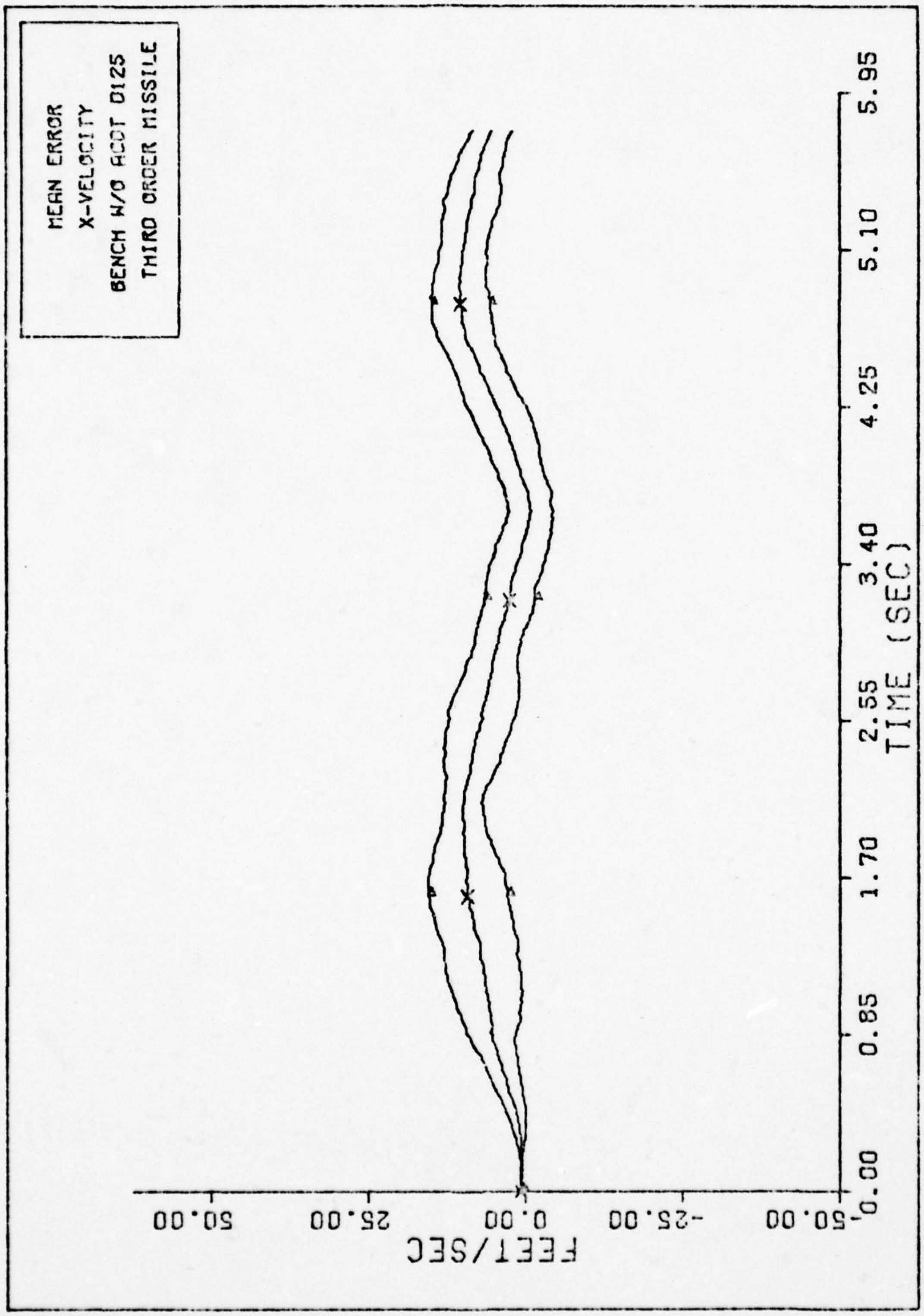

Fig. 22. X-VELOCITY THIRD ORDER MISSILE

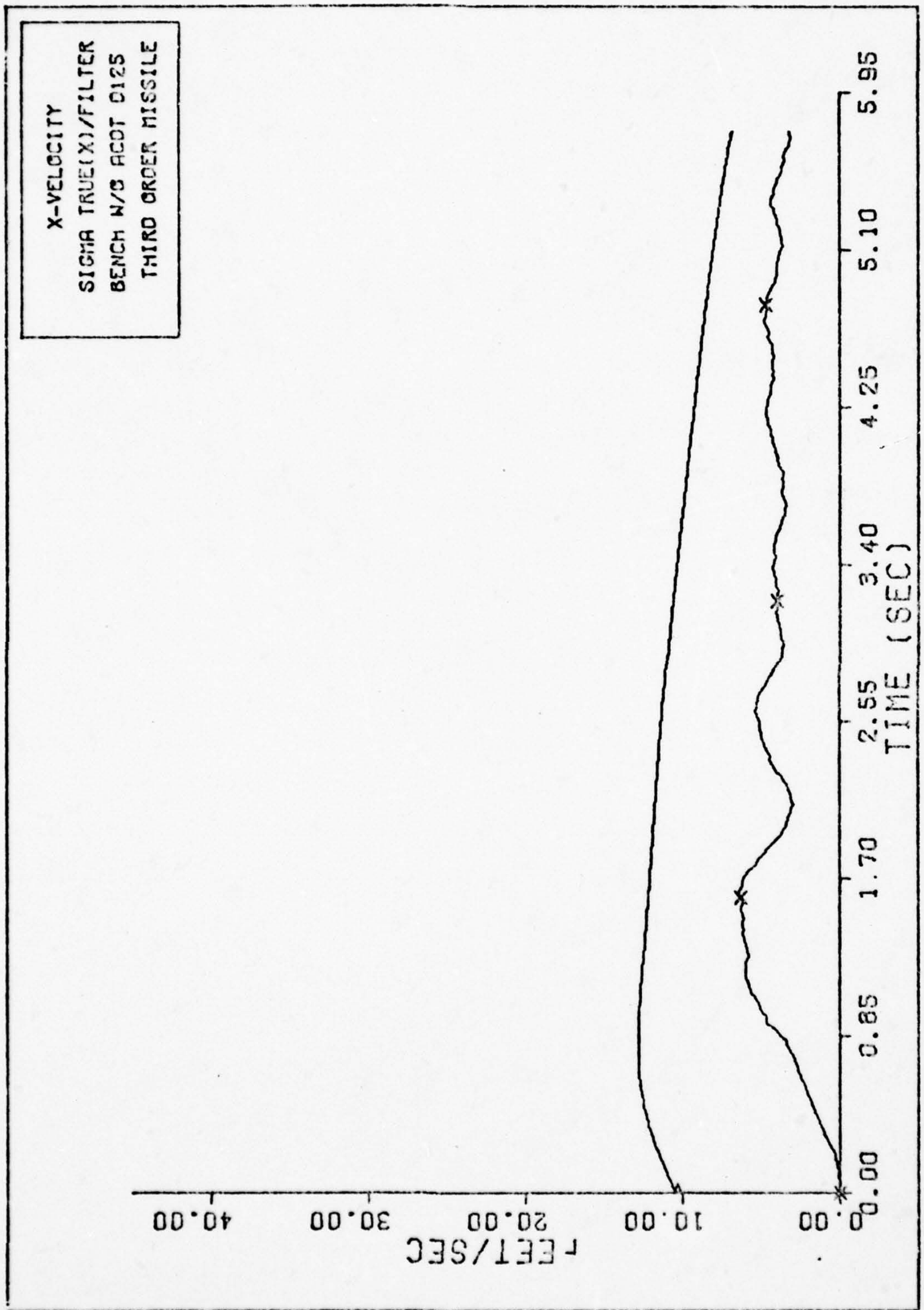

Fig. 23. X-VELOCITY SIGMAS THIRD ORDER

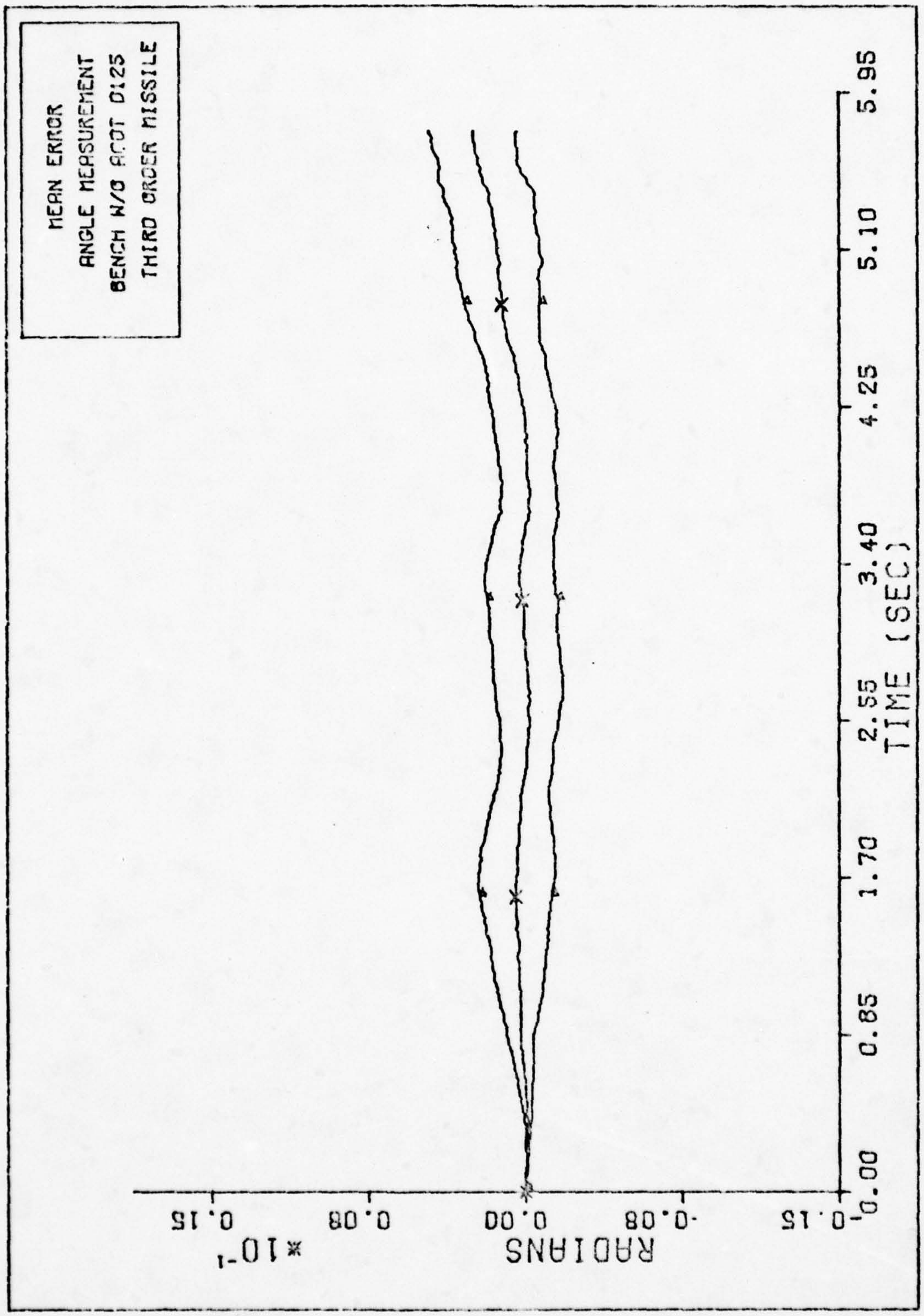

Fig. 24. ANGLE MEASUREMENT THIRD ORDER MISSILE

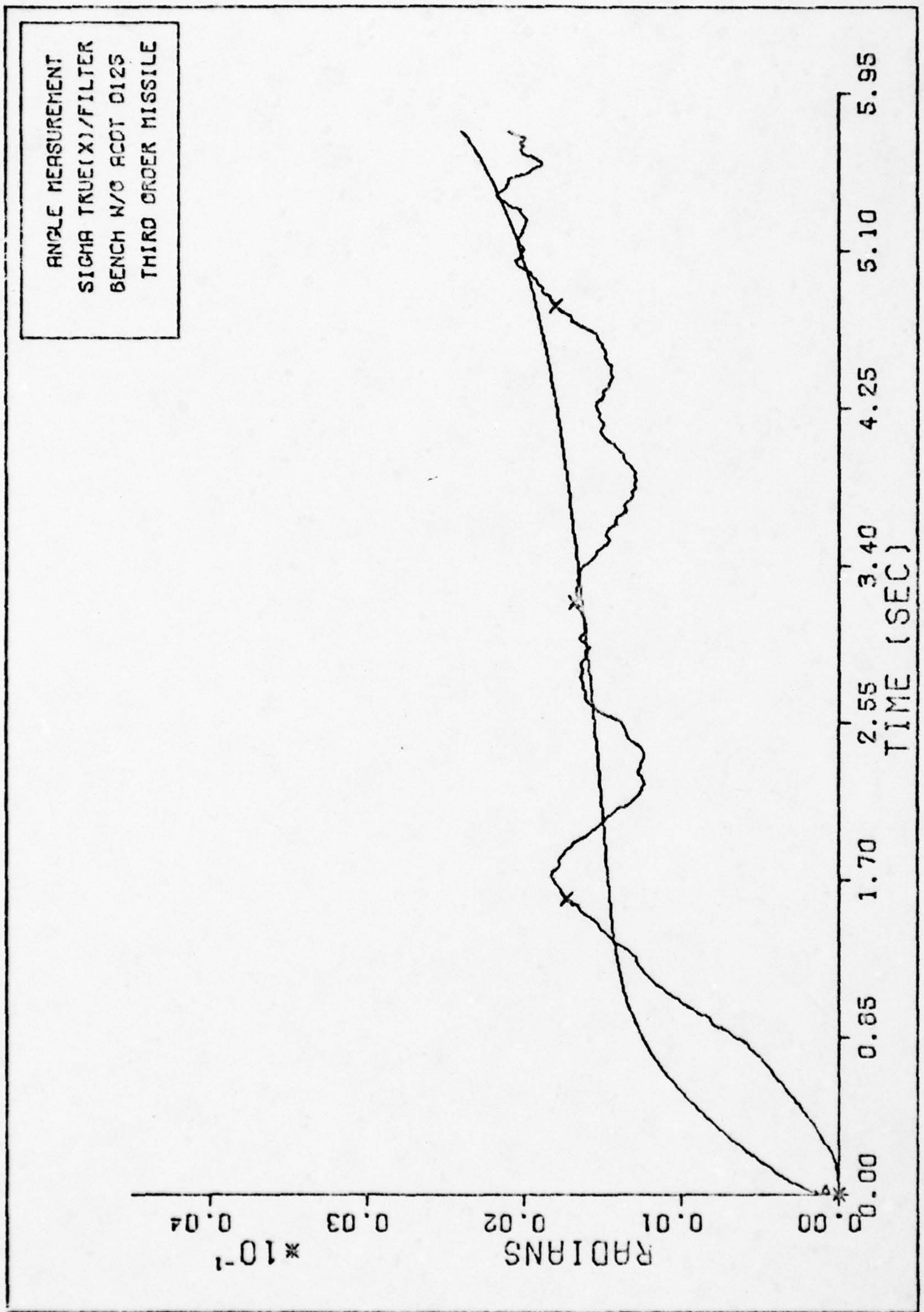

Fig. 25. ANGLE MEASUREMENT SIGMAS THIRD ORDER

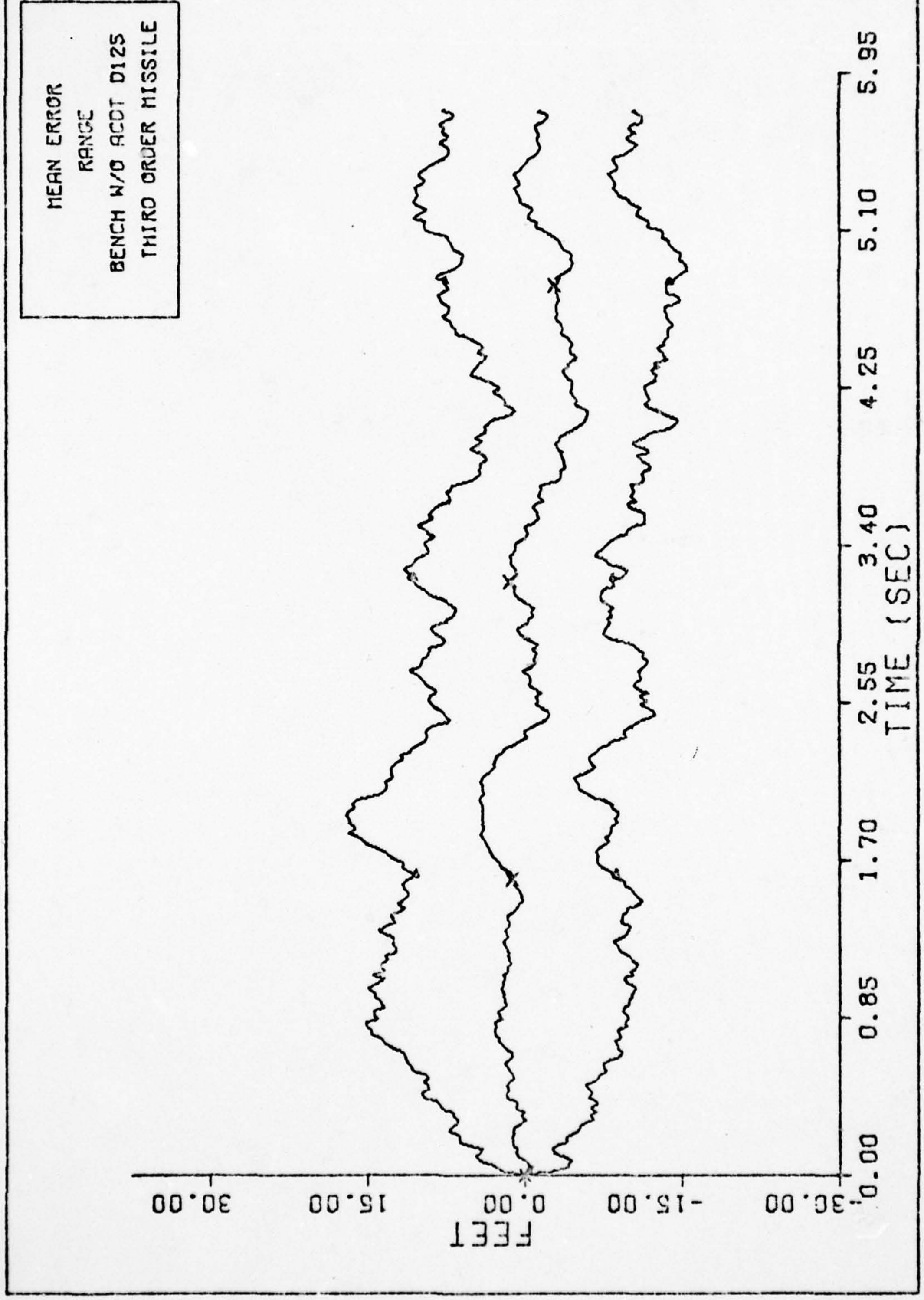

Fig. 26. RANGE THIRD ORDER MISSILE

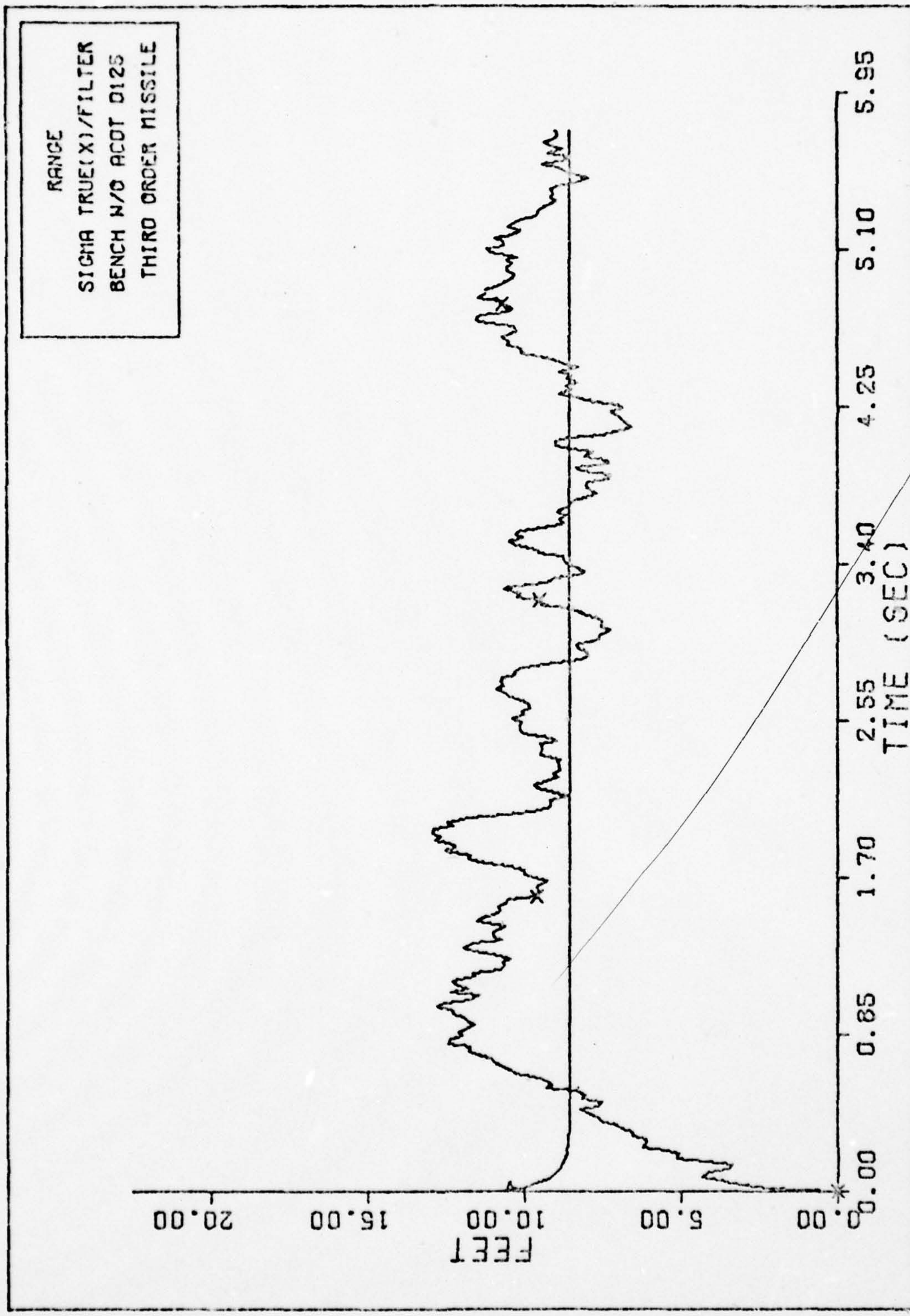

Fig. 27. RANGE SIGMAS THIRD ORDER

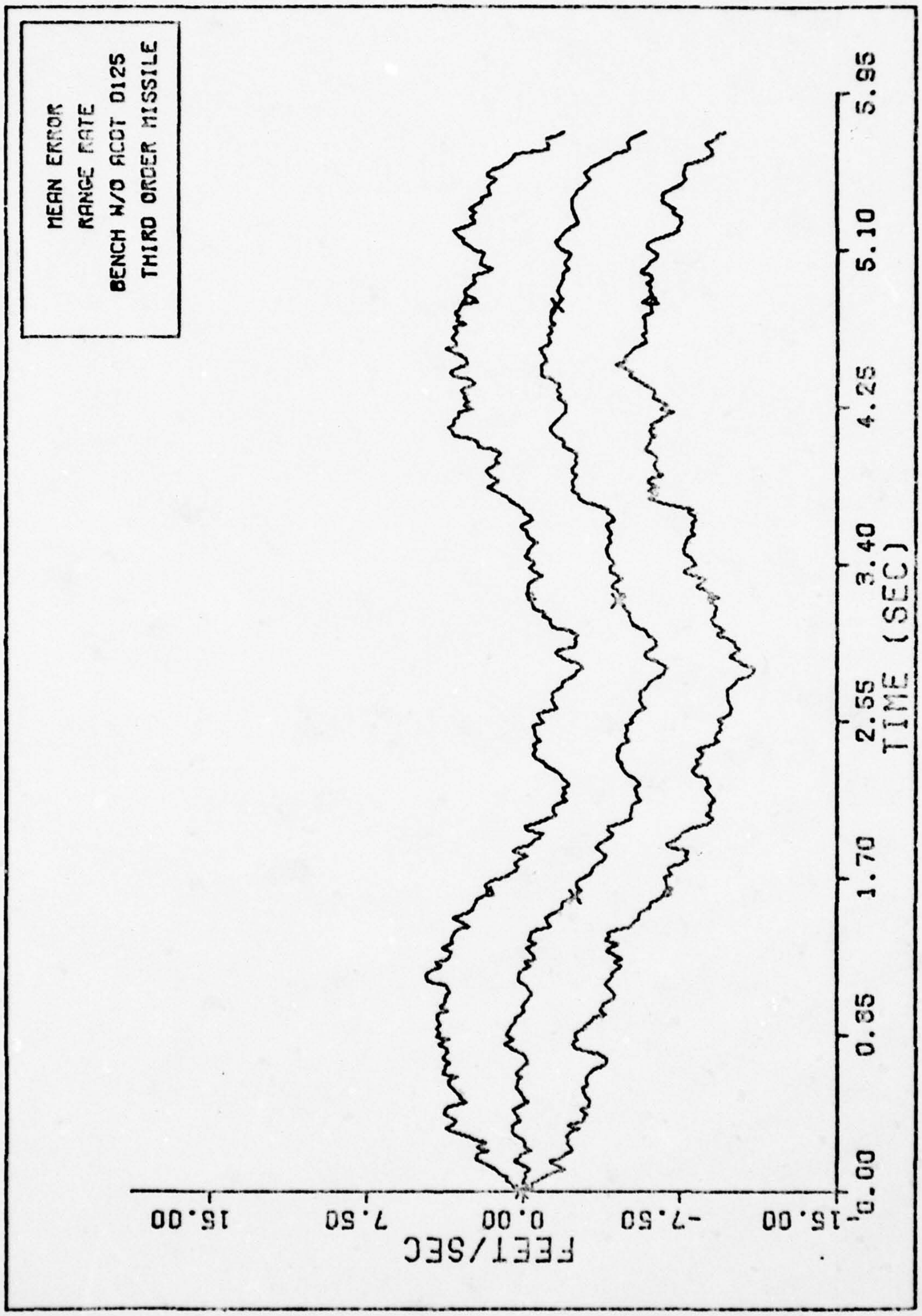

Fig. 28. RANGE RATE THIRD ORDER MISSILE

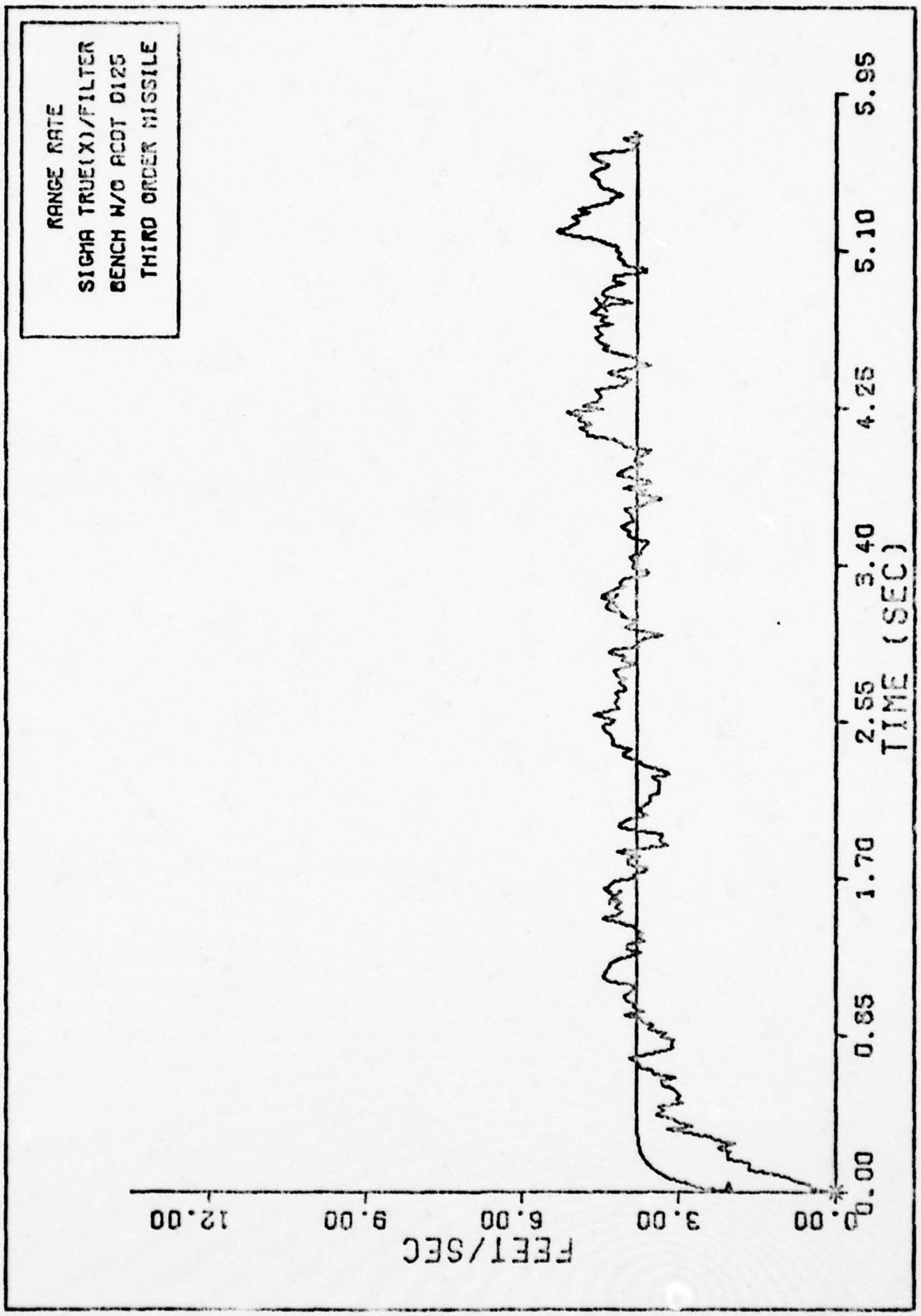

Fig. 29. RANGE RATE SIGMAS THIRD ORDER

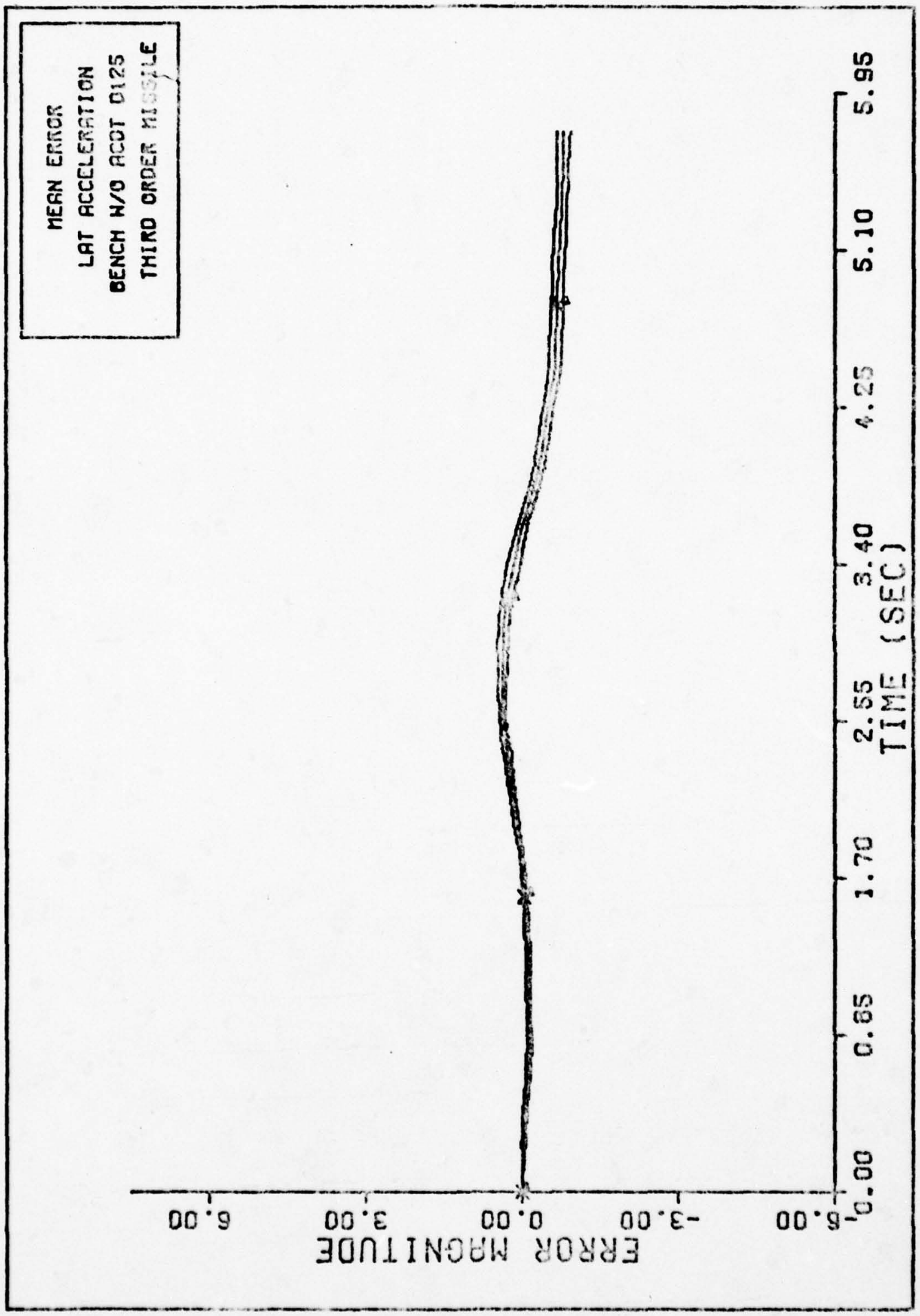

Fig. 30. LAT ACCELERATION THIRD ORDER MISSILE

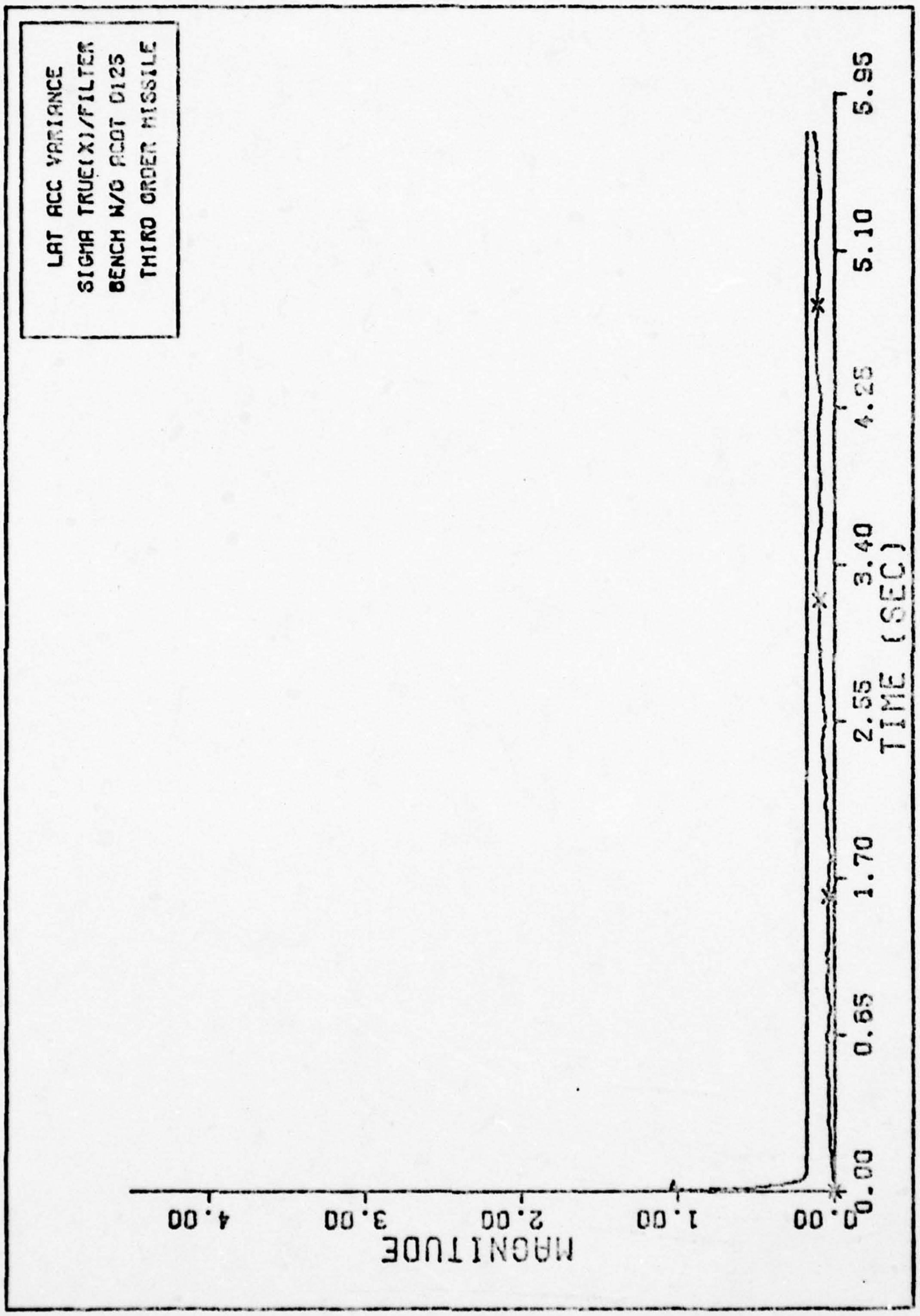

Fig. 31. LAT ACCELERATION SIGMAS THIRD ORDER

Fourth Order Missile Filter (A/P at 0 sec)

The initial state estimates and the tuning parameters for this case are

$$V^{I}_{mx}(0) = 1225.7 \text{ fps}$$
$$\dot{\theta}_T(0) = 4.363345 \text{ radians}$$
$$R(0) = 10000. \text{ feet}$$
$$\dot{R}(0) = -2122. \text{ fps}$$
$$a_L(0) = 0.$$
$$n(0) = 4.5$$
$$\tau_f(0) = \text{N/A}$$
$$M/S(0) = 29.197 \text{ slugs/ft}^2$$

$$\underline{R} = \begin{bmatrix} 4.E-5 & 0. & 0. \\ 0. & 500. & 0. \\ 0. & 0. & 100. \end{bmatrix}$$

$$\underline{P}_0 = \begin{bmatrix} 100. & 0. & 0. & 0. & 0. & 0. & 0. & 0. \\ 0. & 1.E-8 & 0. & 0. & 0. & 0. & 0. & 0. \\ 0. & 0. & 101. & 0. & 0. & 0. & 0. & 0. \\ 0. & 0. & 0. & 4. & 0. & 0. & 0. & 0. \\ 0. & 0. & 0. & 0. & 1. & 0. & 0. & 0. \\ 0. & 0. & 0. & 0. & 0. & 0. & 0. & 0. \\ 0. & 0. & 0. & 0. & 0. & 0. & 0. & 0. \\ 0. & 0. & 0. & 0. & 0. & 0. & 0. & 0. \end{bmatrix}$$

$$
\underline{Q} = \begin{bmatrix}
101. & 0. & 0. & 0. & 0. & 0. & 0. & 0. \\
0. & 1.E-6 & 0. & 0. & 0. & 0. & 0. & 0. \\
0. & 0. & 500. & 0. & 0. & 0. & 0. & 0. \\
0. & 0. & 0. & 100. & 0. & 0. & 0. & 0. \\
0. & 0. & 0. & 0. & 5. & 0. & 0. & 0. \\
0. & 0. & 0. & 0. & 0. & 0. & 0. & 0. \\
0. & 0. & 0. & 0. & 0. & 0. & 0. & 0. \\
0. & 0. & 0. & 0. & 0. & 0. & 0. & 0.
\end{bmatrix}
$$

These plots were generated by the fourth order filter with the coefficients of the autopilot transfer function determined at t=0. These plots were compared to those results of the fourth order filter using autopilot coefficients for t=3 and t=5. The intent was to determine if there was any distinguishable difference in filter performance for the various sets of autopilot coefficients. A complete description of the filter autopilot and its coefficients can be found in Chapter III.

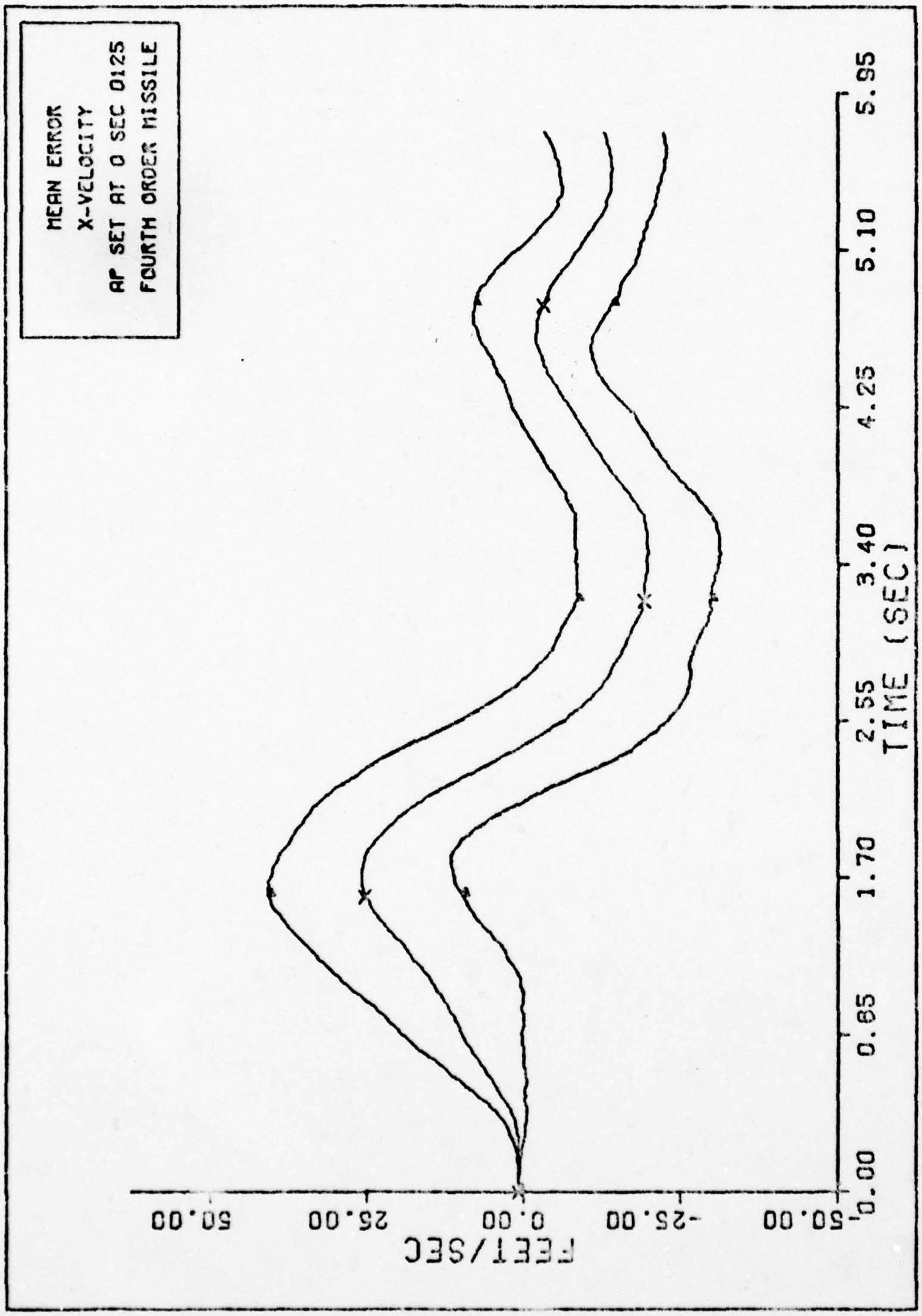

Fig. 32. X-VELOCITY FOURTH ORDER MISSILE

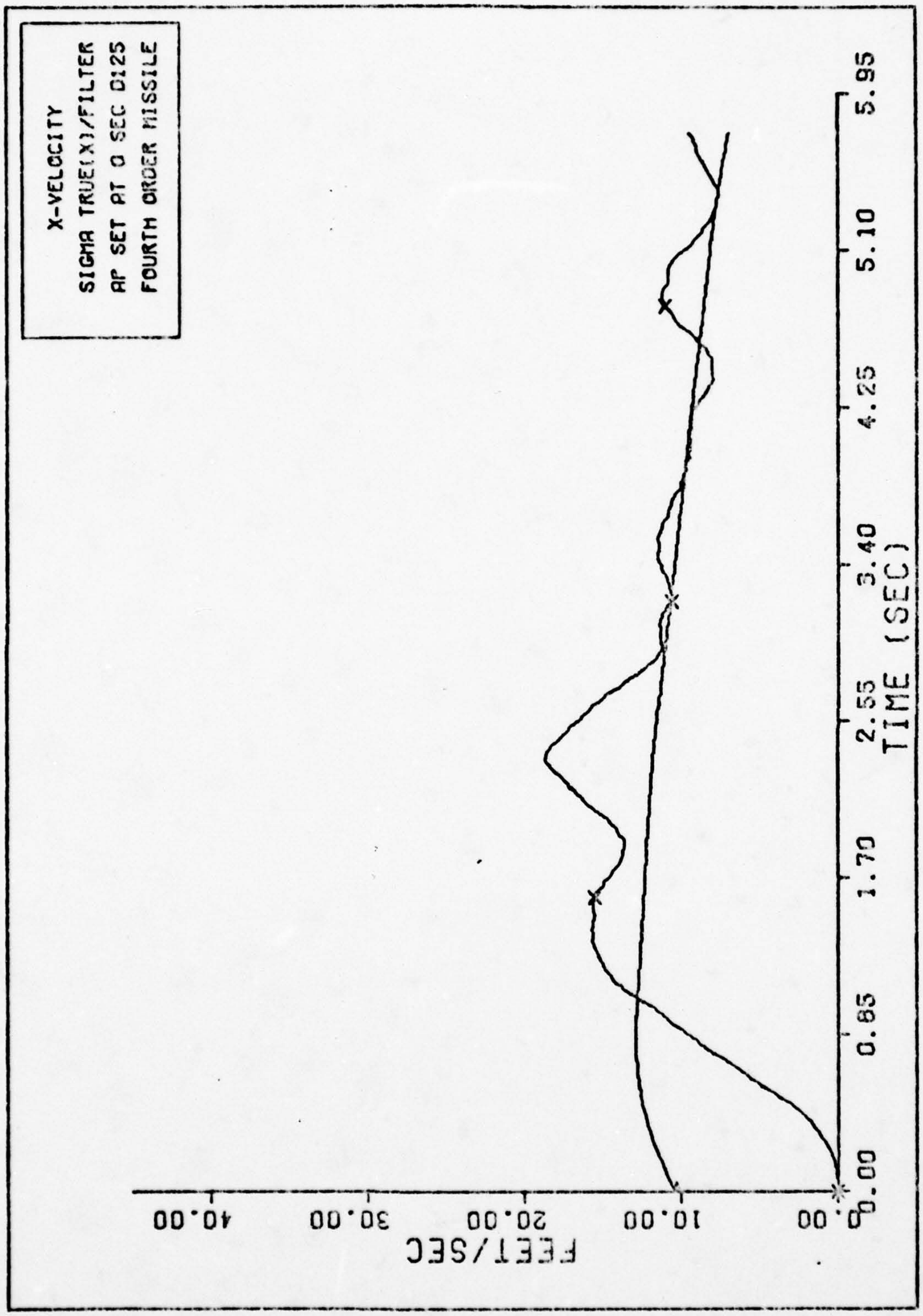

Fig. 33. X-VELOCITY SIGMAS FOURTH ORDER

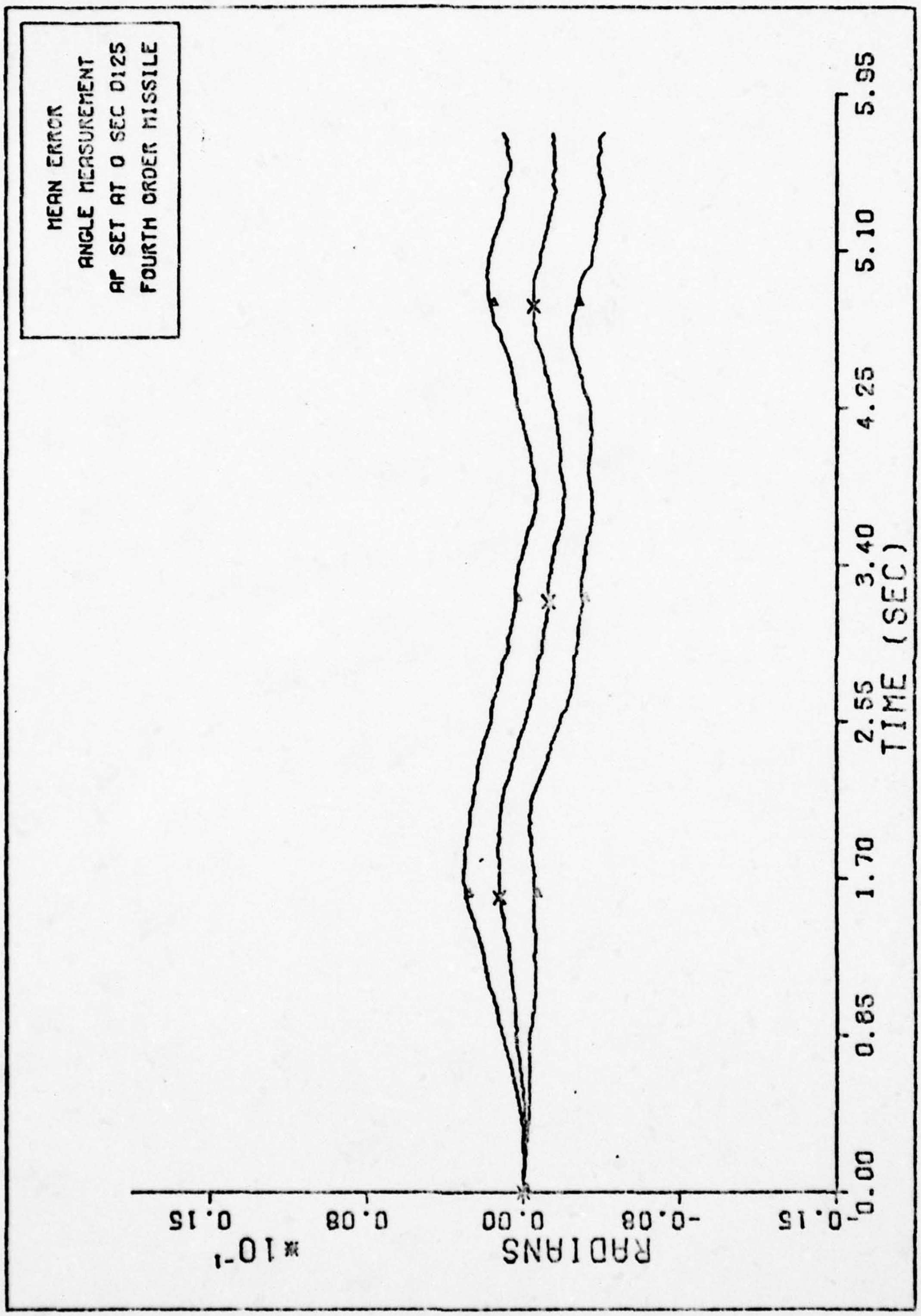

Fig. 34. ANGLE MEASUREMENT FOURTH ORDER MISSILE

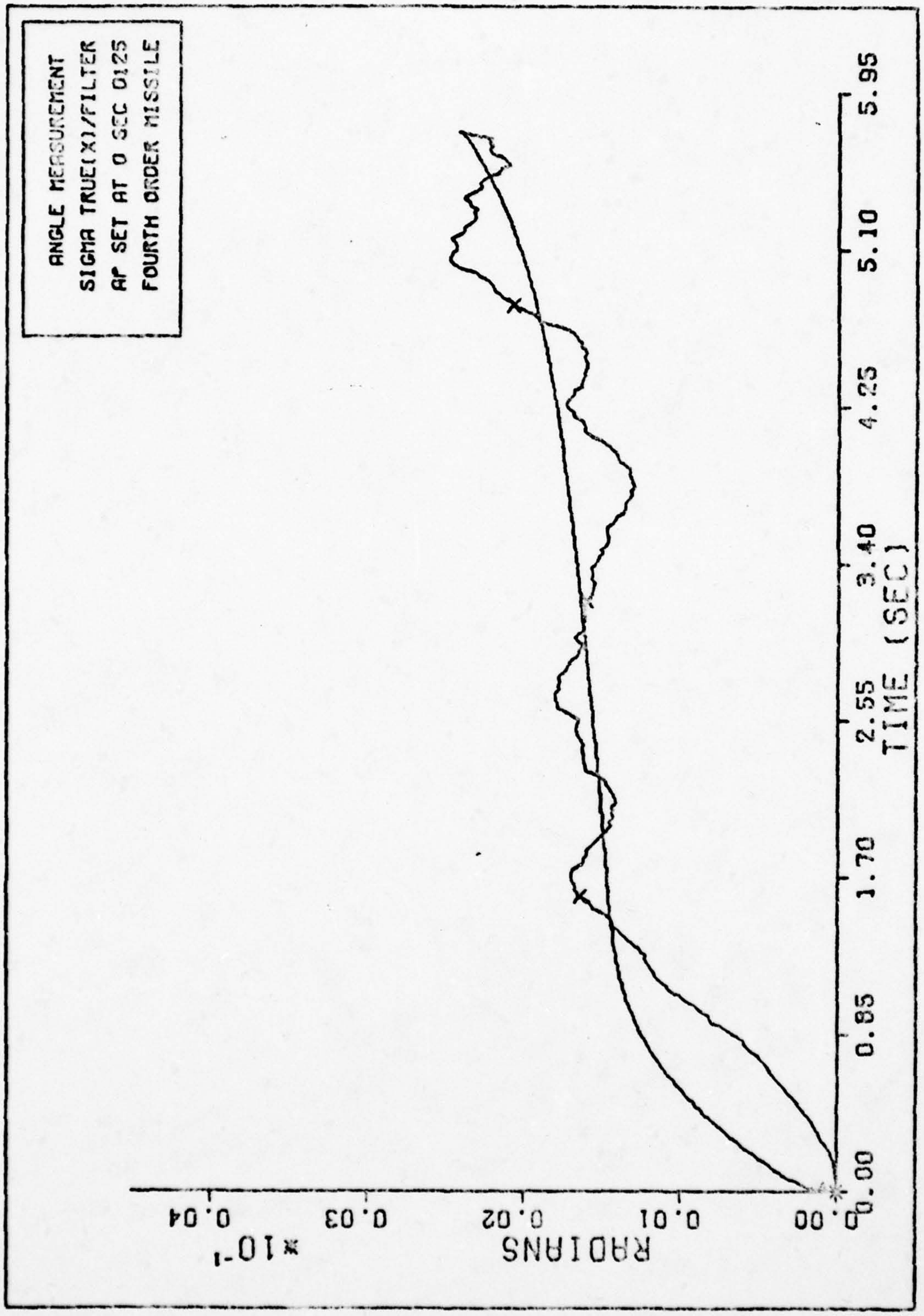

Fig. 35. ANGLE MEASUREMENT SIGMAS FOURTH ORDER

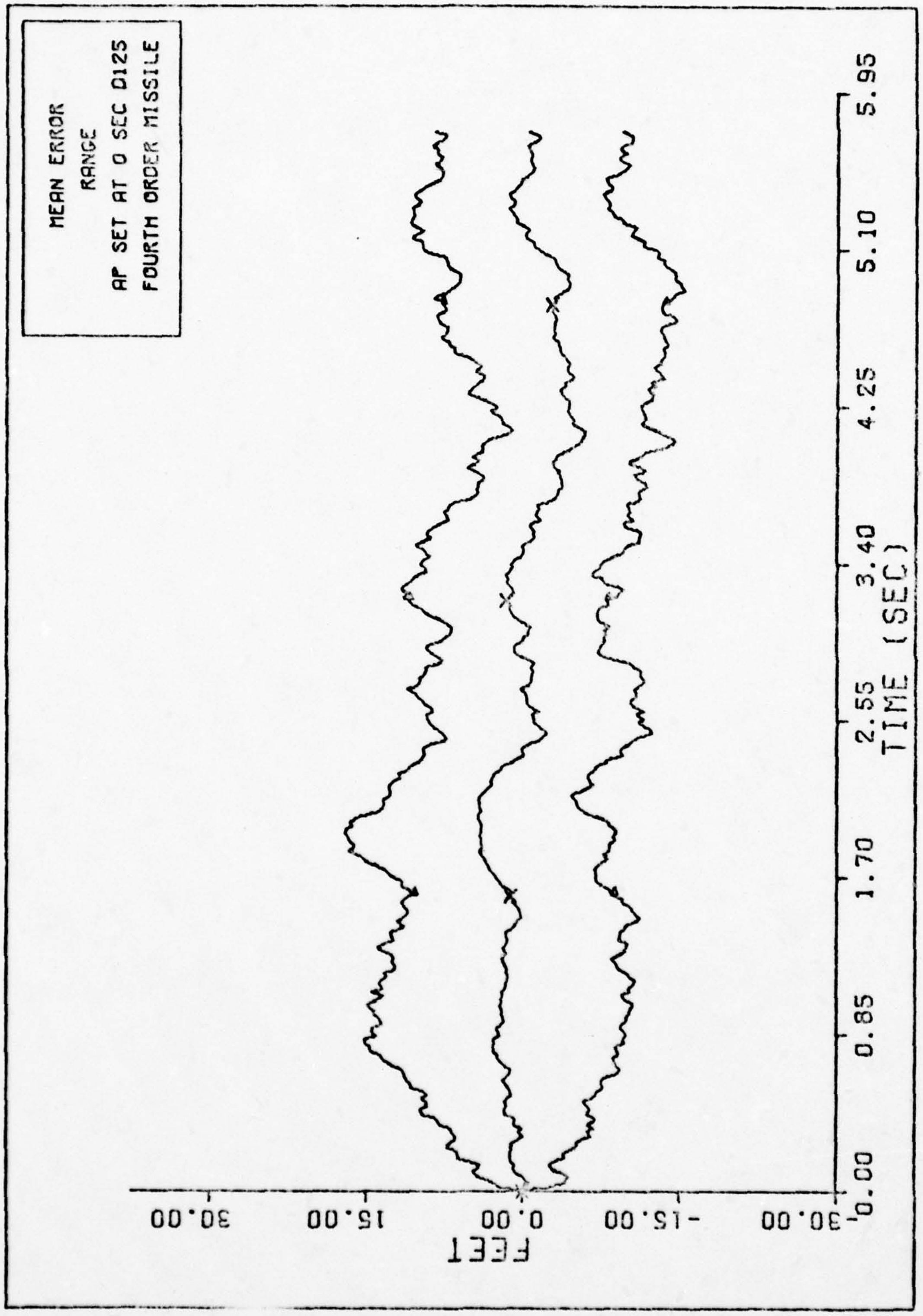

Fig. 36. RANGE FOURTH ORDER MISSILE

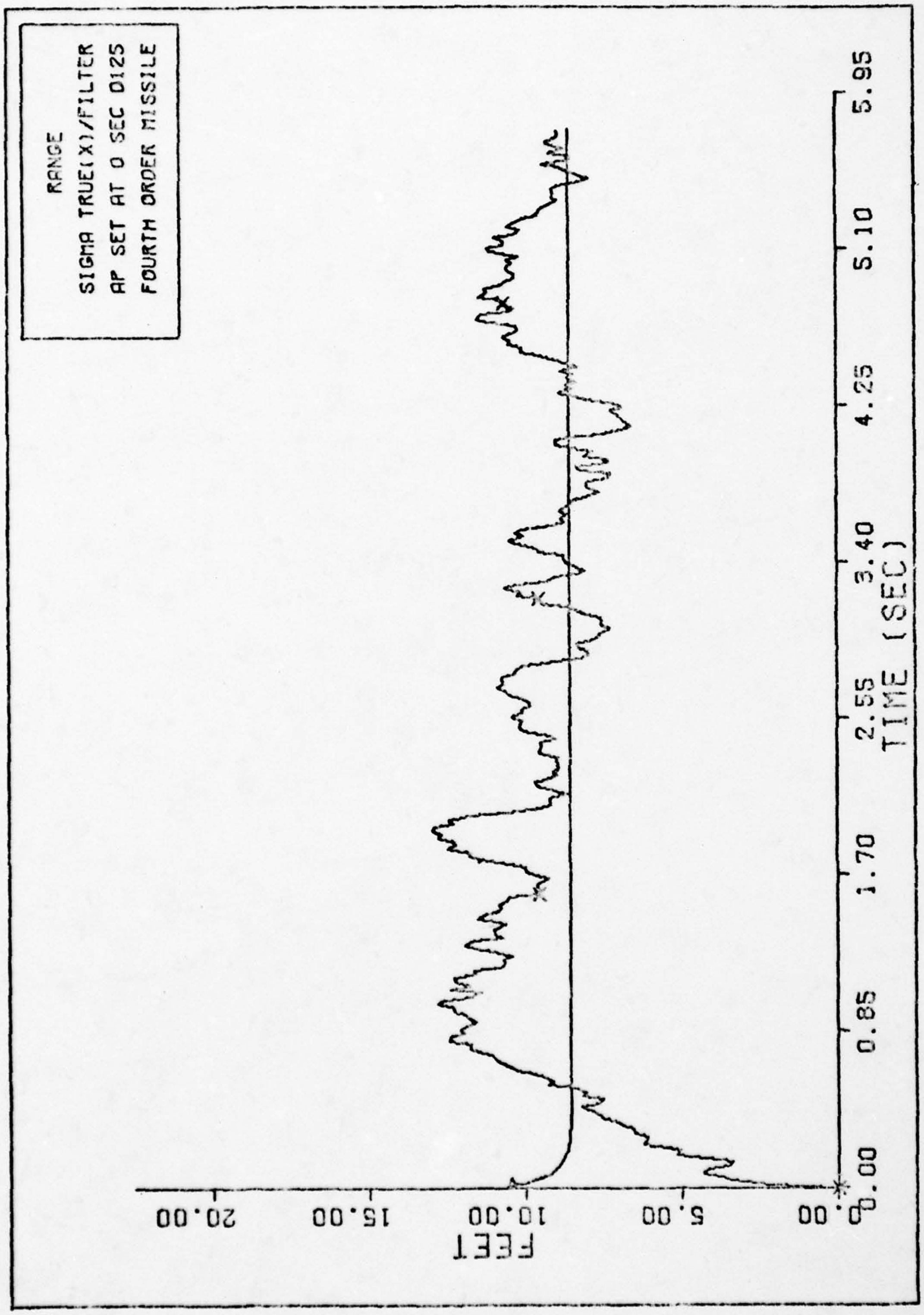

Fig. 37. RANGE SIGMAS FOURTH ORDER

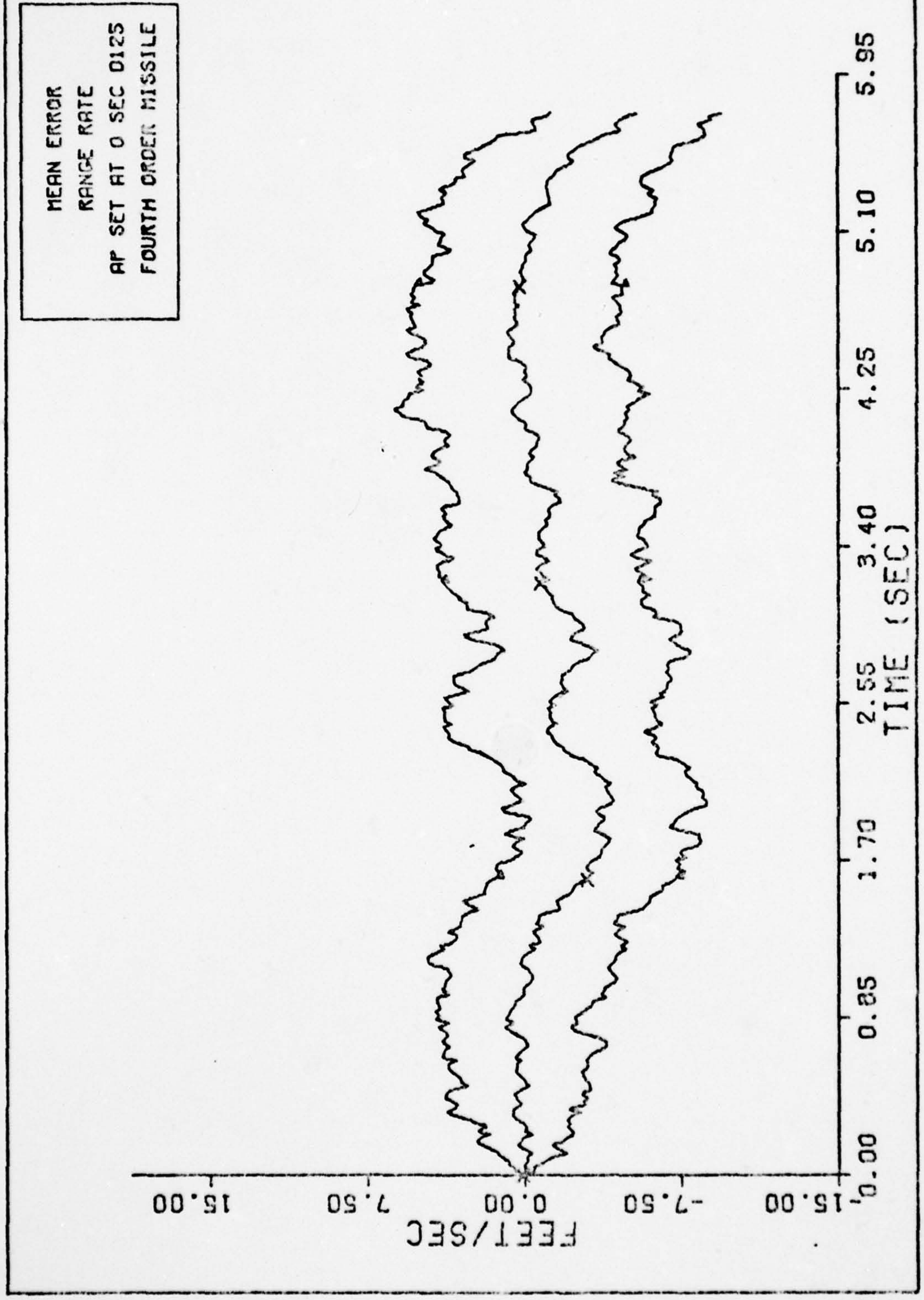

Fig. 38. RANGE RATE FOURTH ORDER MISSILE

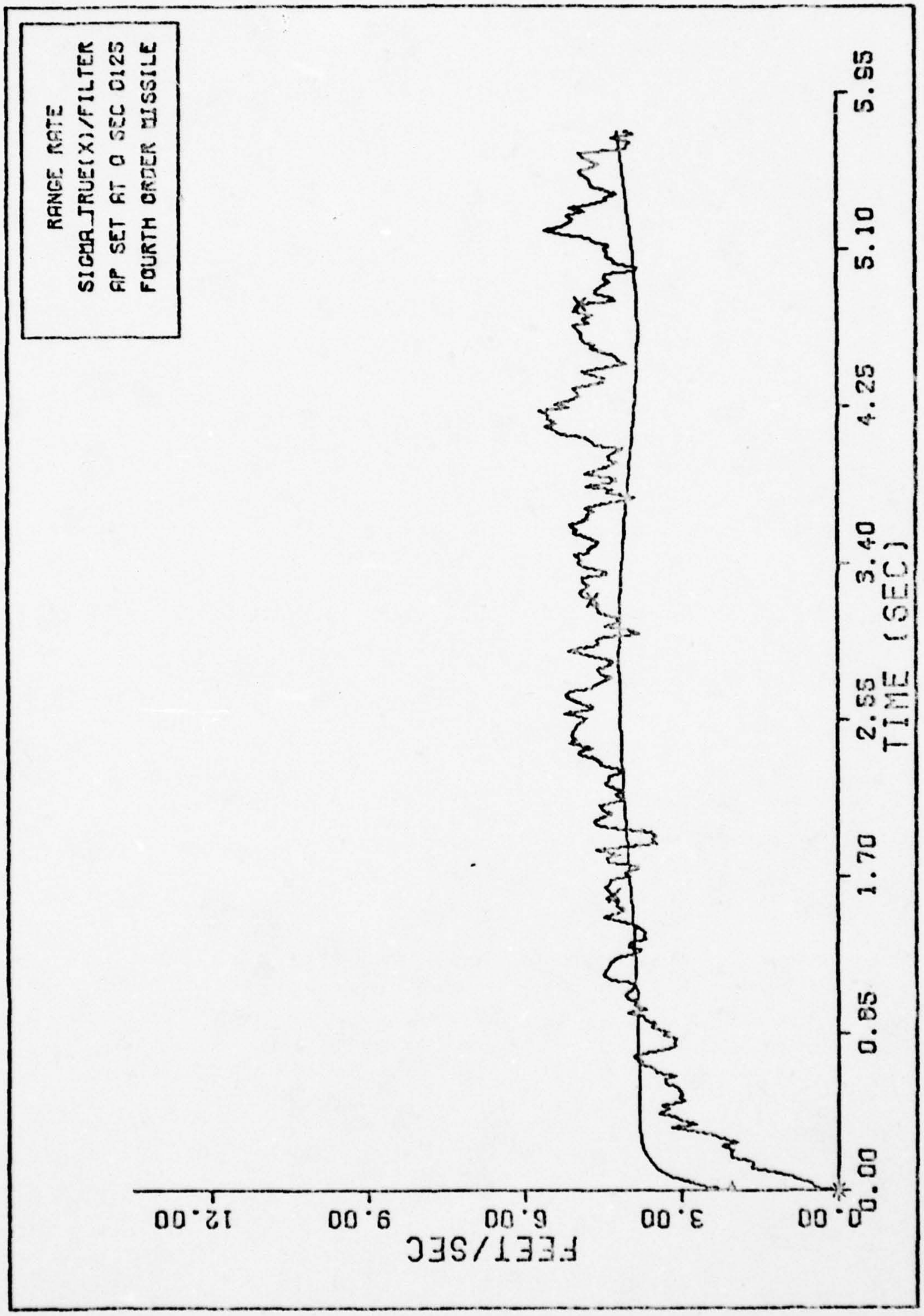

Fig. 39. RANGE RATE SIGMAS FOURTH ORDER

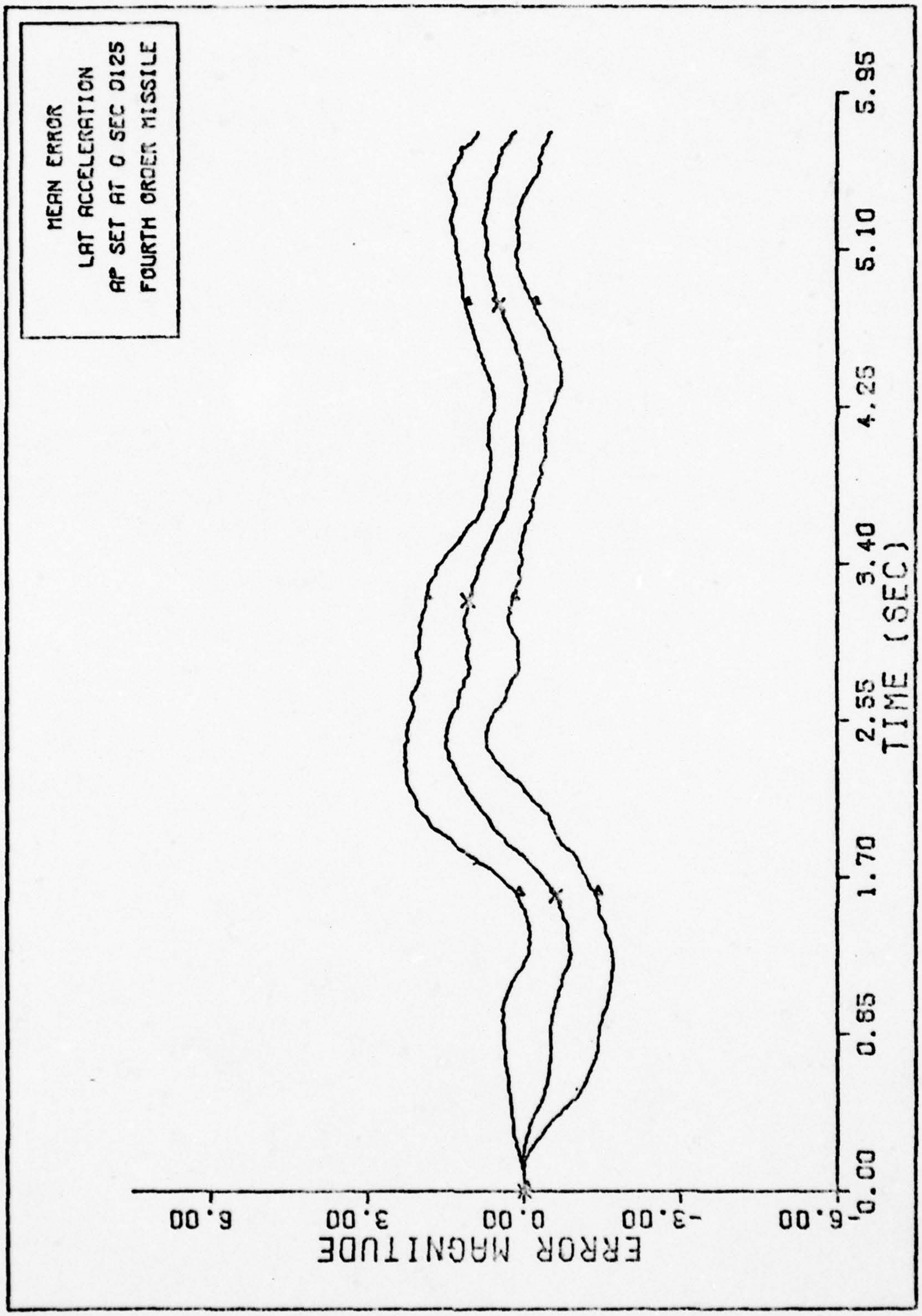

Fig. 40. LAT ACCELERATION FOURTH ORDER MISSILE

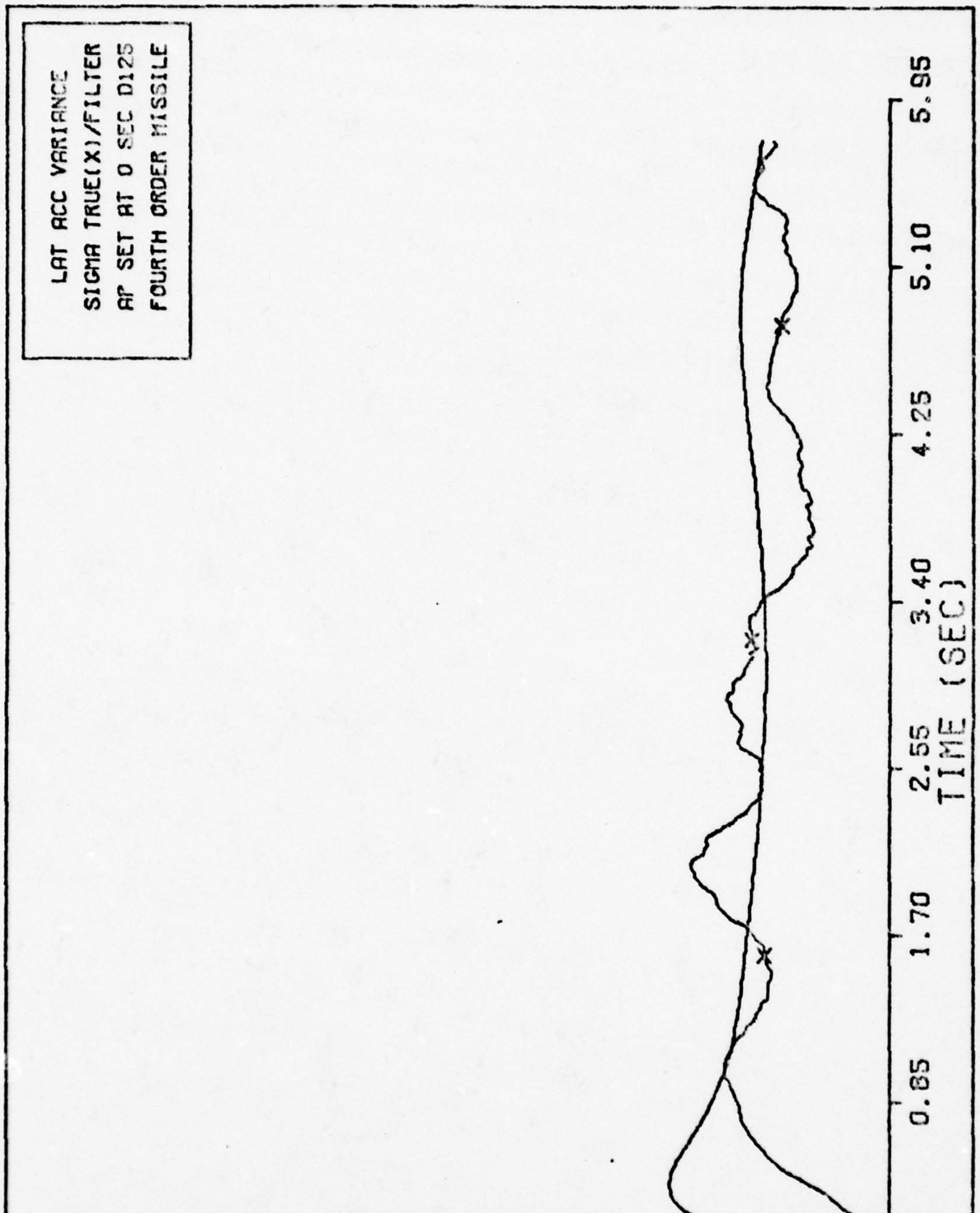

Fig. 41. LAT ACCELERATION SIGMAS FOURTH ORDER

Fourth Order Missile Filter (A/P at 3 sec)

The initial state estimates and the tuning parameters for this case are

$$V^{I}_{mx}(0) = 1225.7 \text{ fps}$$
$$\dot{\theta}_T(0) = 4.363345 \text{ radians}$$
$$R(0) = 10000. \text{ feet}$$
$$\dot{R}(0) = -2122. \text{ fps}$$
$$a_{J_L}(0) = 0.$$
$$n(0) = 4.5$$
$$\tau_f(0) = \text{N/A}$$
$$M/S(0) = 29.197 \text{ slugs/ft}^2$$

$$\underline{R} = \begin{bmatrix} 4.E-5 & 0. & 0. \\ 0. & 500. & 0. \\ 0. & 0. & 100. \end{bmatrix}$$

$$\underline{P}_0 = \begin{bmatrix} 100. & 0. & 0. & 0. & 0. & 0. & 0. & 0. \\ 0. & 1.E-8 & 0. & 0. & 0. & 0. & 0. & 0. \\ 0. & 0. & 101. & 0. & 0. & 0. & 0. & 0. \\ 0. & 0. & 0. & 4. & 0. & 0. & 0. & 0. \\ 0. & 0. & 0. & 0. & 1. & 0. & 0. & 0. \\ 0. & 0. & 0. & 0. & 0. & 0. & 0. & 0. \\ 0. & 0. & 0. & 0. & 0. & 0. & 0. & 0. \\ 0. & 0. & 0. & 0. & 0. & 0. & 0. & 0. \end{bmatrix}$$

$$\underline{Q} = \begin{bmatrix} 101. & 0. & 0. & 0. & 0. & 0. & 0. & 0. \\ 0. & 1.E-6 & 0. & 0. & 0. & 0. & 0. & 0. \\ 0. & 0. & 500. & 0. & 0. & 0. & 0. & 0. \\ 0. & 0. & 0. & 100. & 0. & 0. & 0. & 0. \\ 0. & 0. & 0. & 0. & 5. & 0. & 0. & 0. \\ 0. & 0. & 0. & 0. & 0. & 0. & 0. & 0. \\ 0. & 0. & 0. & 0. & 0. & 0. & 0. & 0. \\ 0. & 0. & 0. & 0. & 0. & 0. & 0. & 0. \end{bmatrix}$$

These plots were generated by the fourth order filter with the coefficients of the autopilot transfer function determined at t=3. These plots were compared to those results of the fourth order filter using autopilot coefficients for t=0 and t=5. The intent was to determine if there was any distinguishable difference in filter performance for the various sets of autopilot coefficients. A complete description of the filter autopilot and its coefficients can be found in Chapter III.

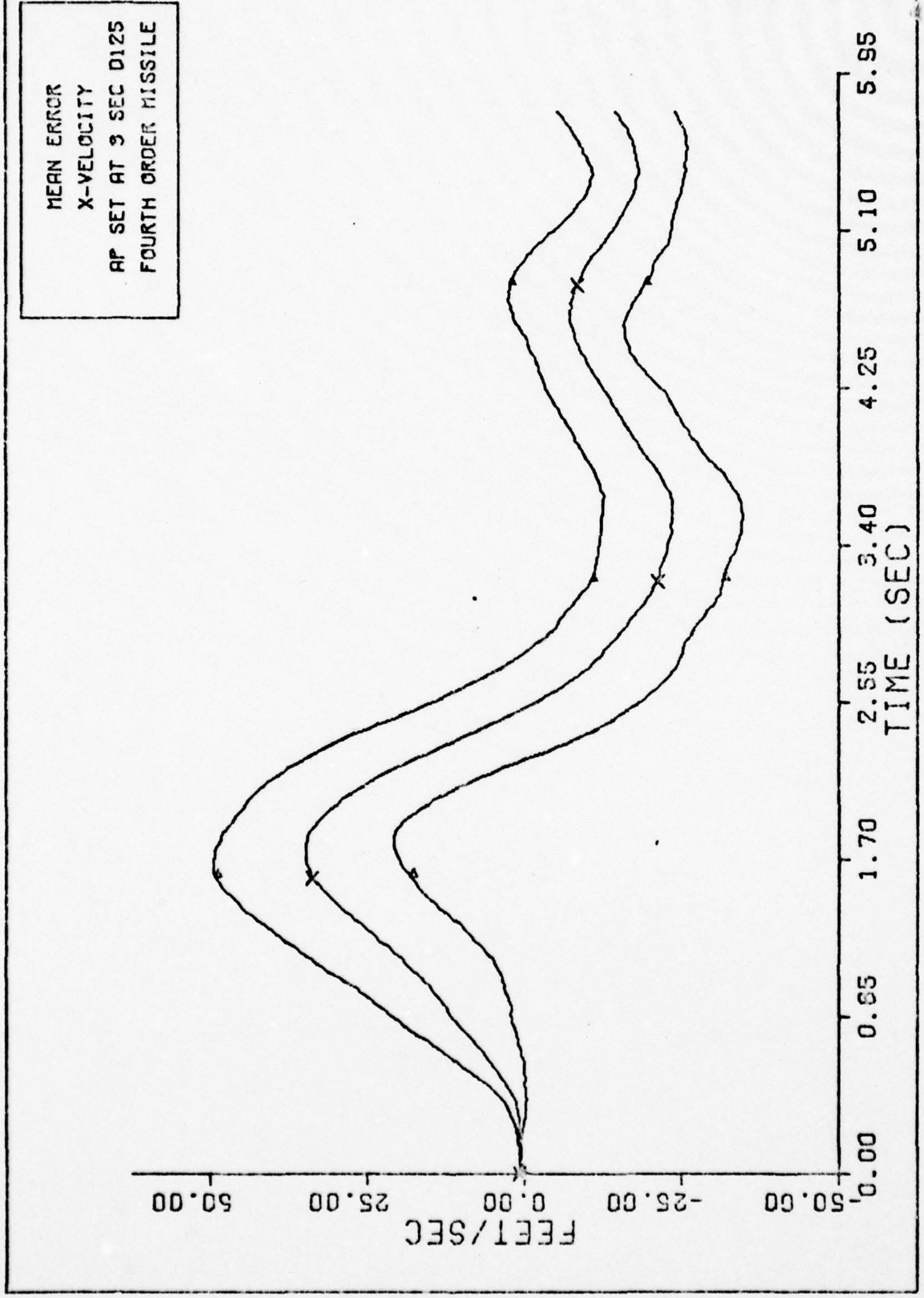

Fig. 42. X-VELOCITY FOURTH ORDER MISSILE

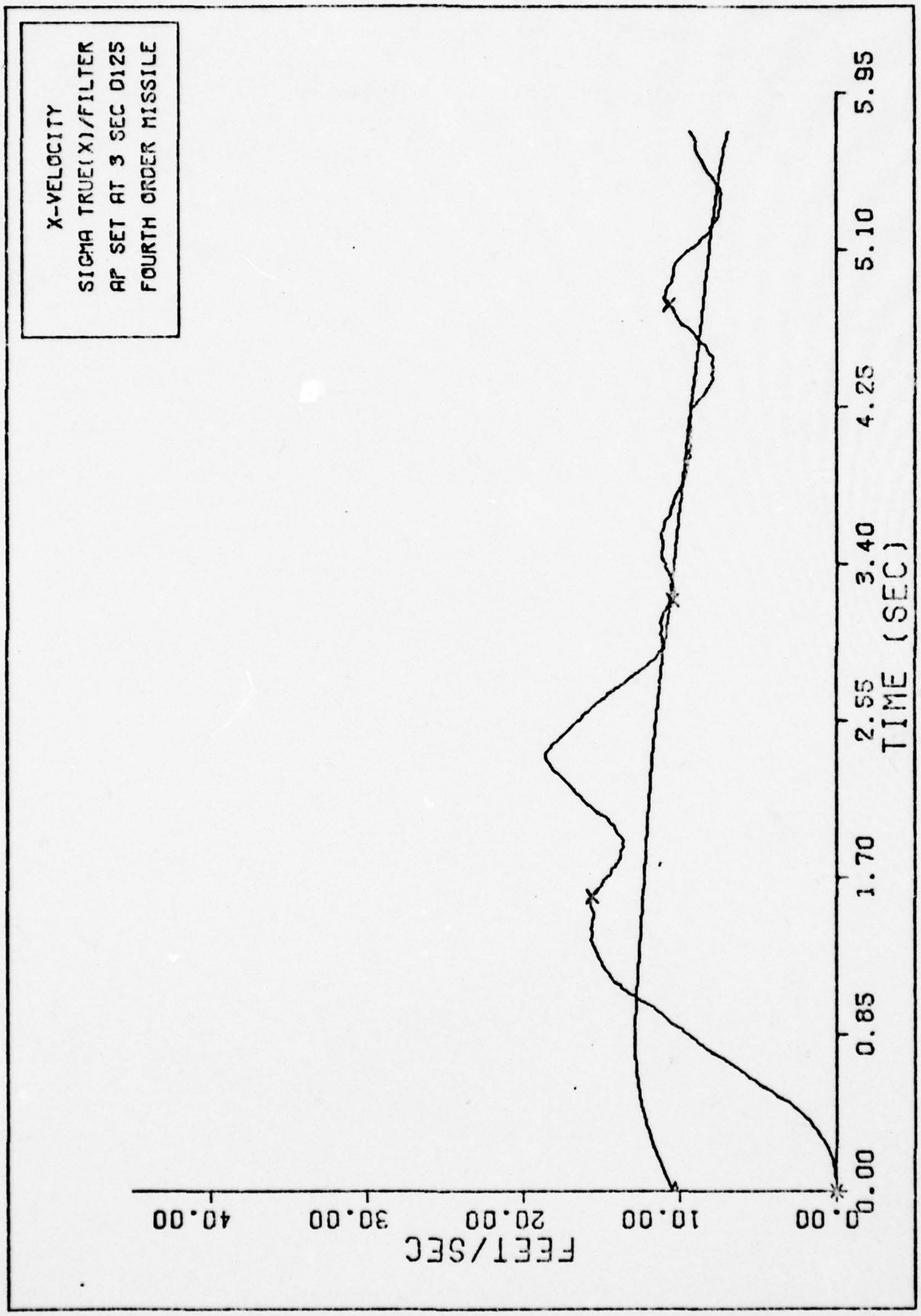

Fig. 43. X-VELOCITY SIGMAS FOURTH ORDER

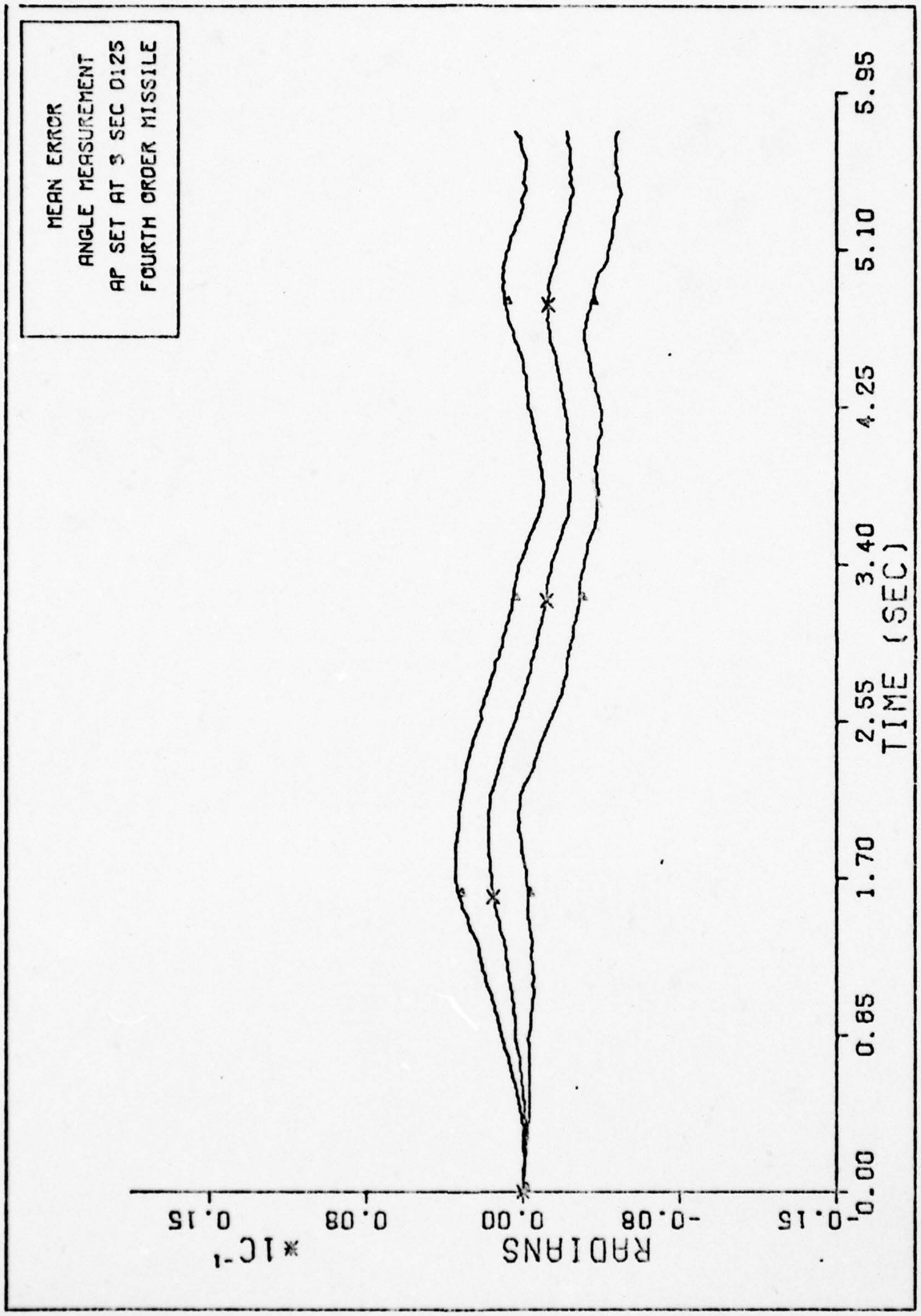

Fig. 44. ANGLE MEASUREMENT FOURTH ORDER MISSILE

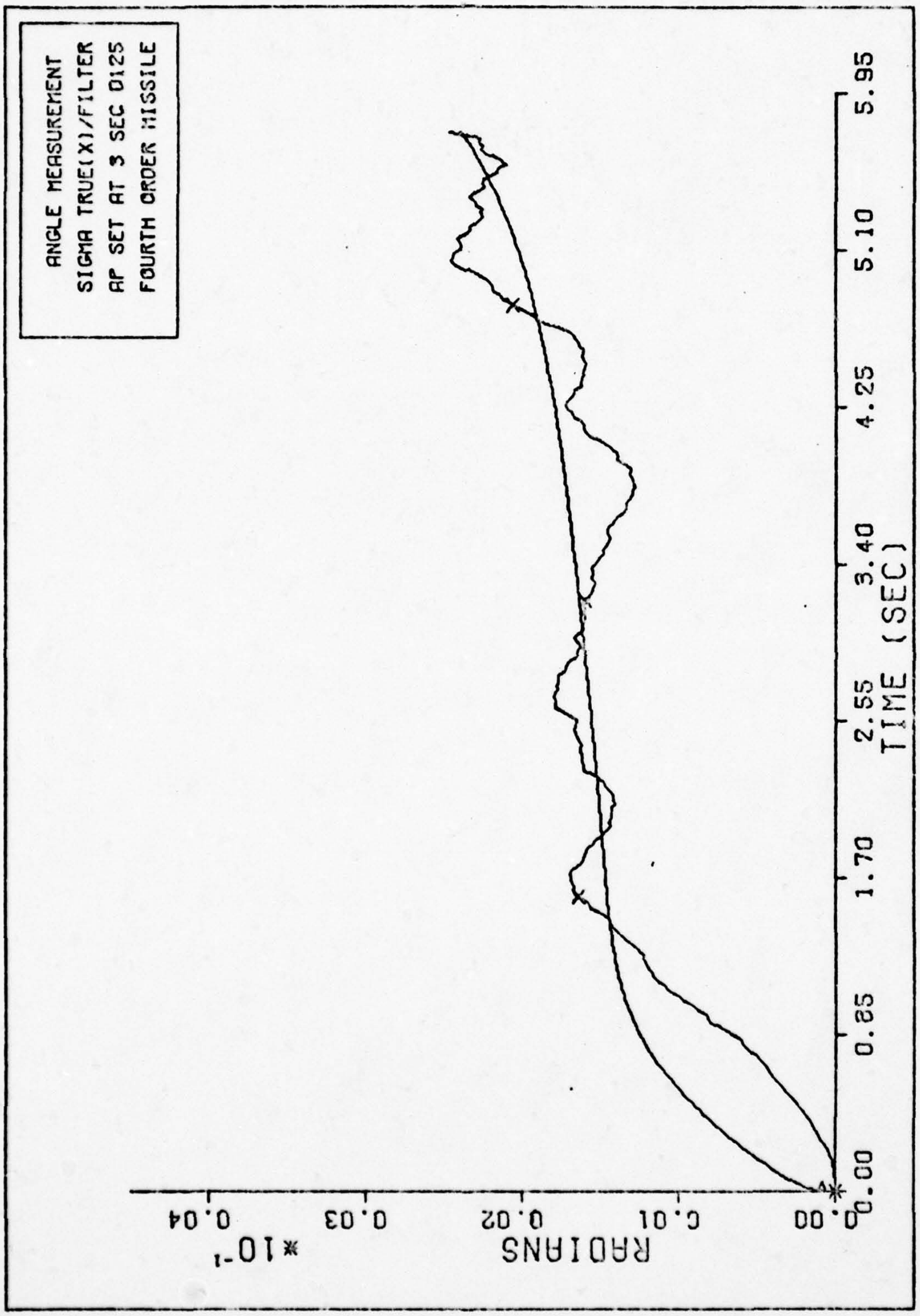

Fig. 45. ANGLE MEASUREMENT SIGMAS FOURTH ORDER

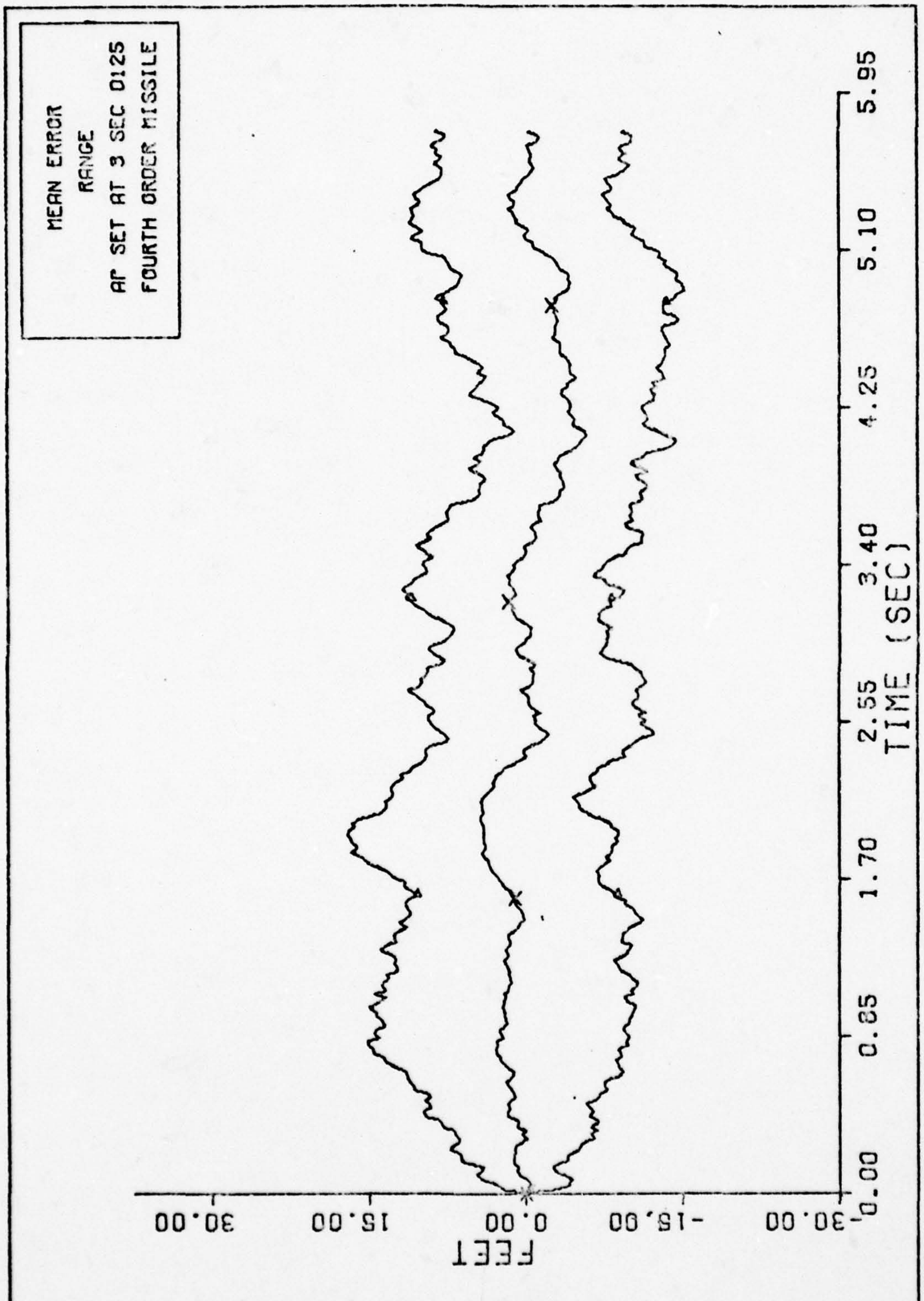

Fig. 46. RANGE FOURTH ORDER MISSILE

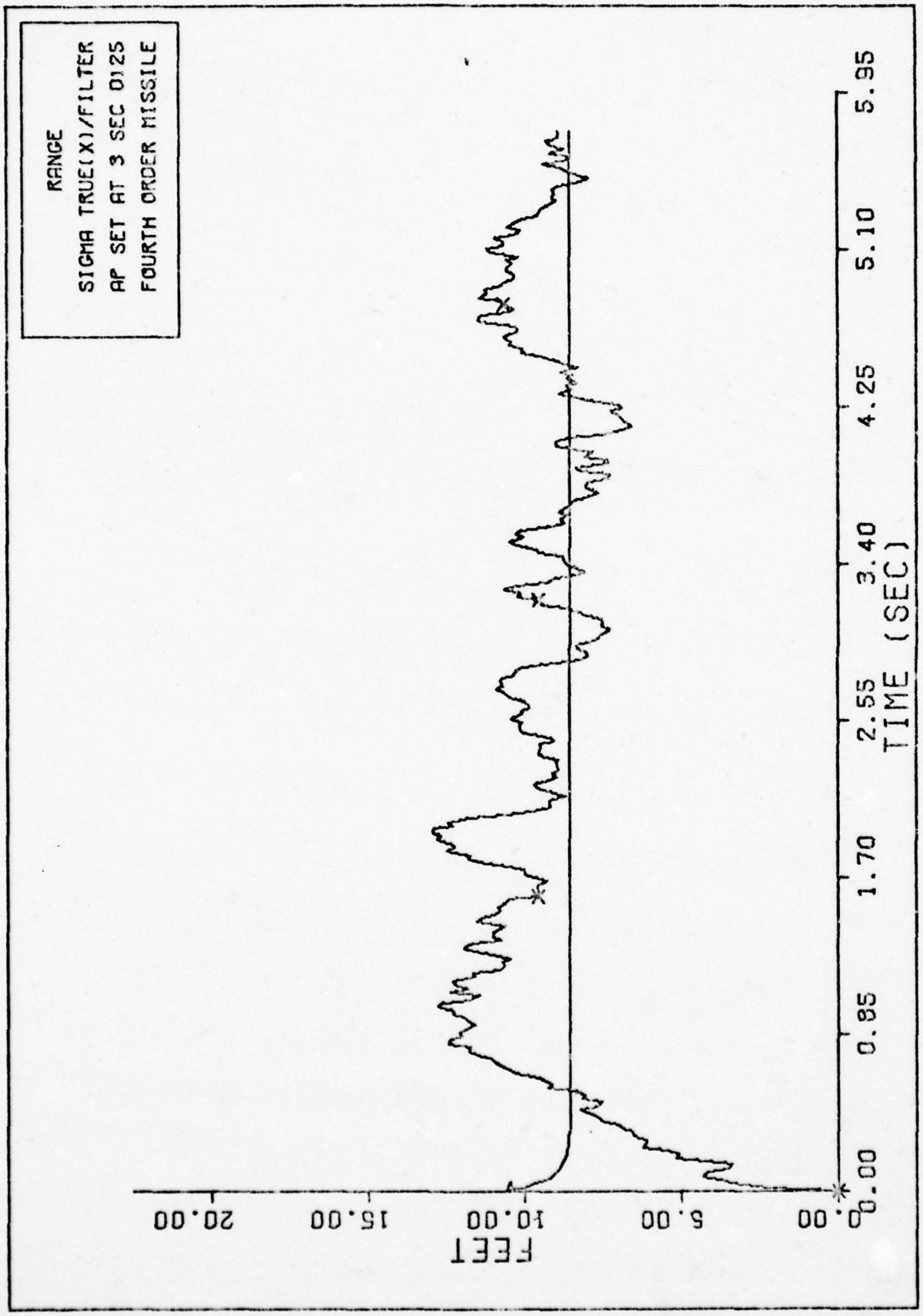

Fig. 47. RANGE SIGMAS FOURTH ORDER

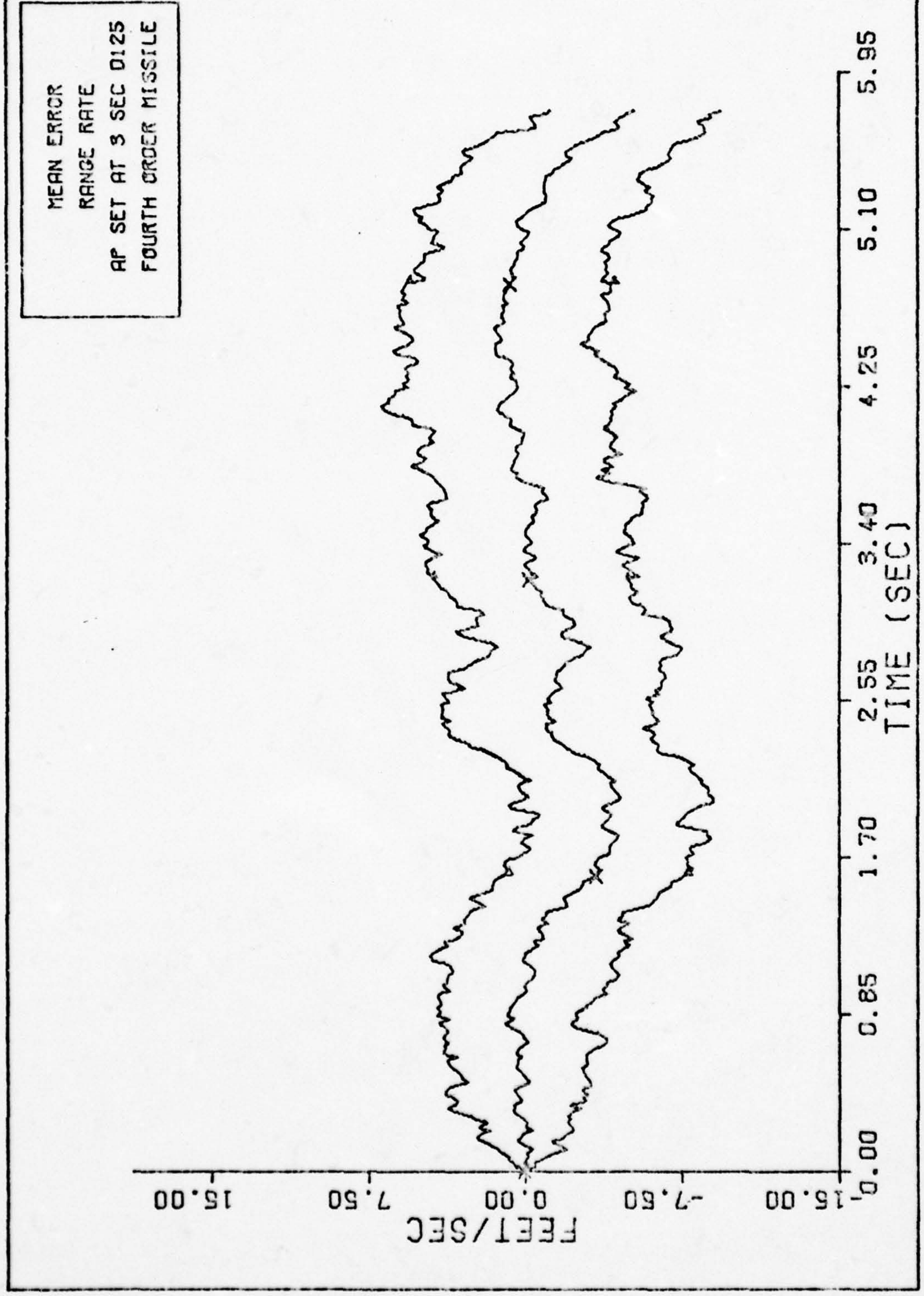

Fig. 48. RANGE RATE FOURTH ORDER MISSILE

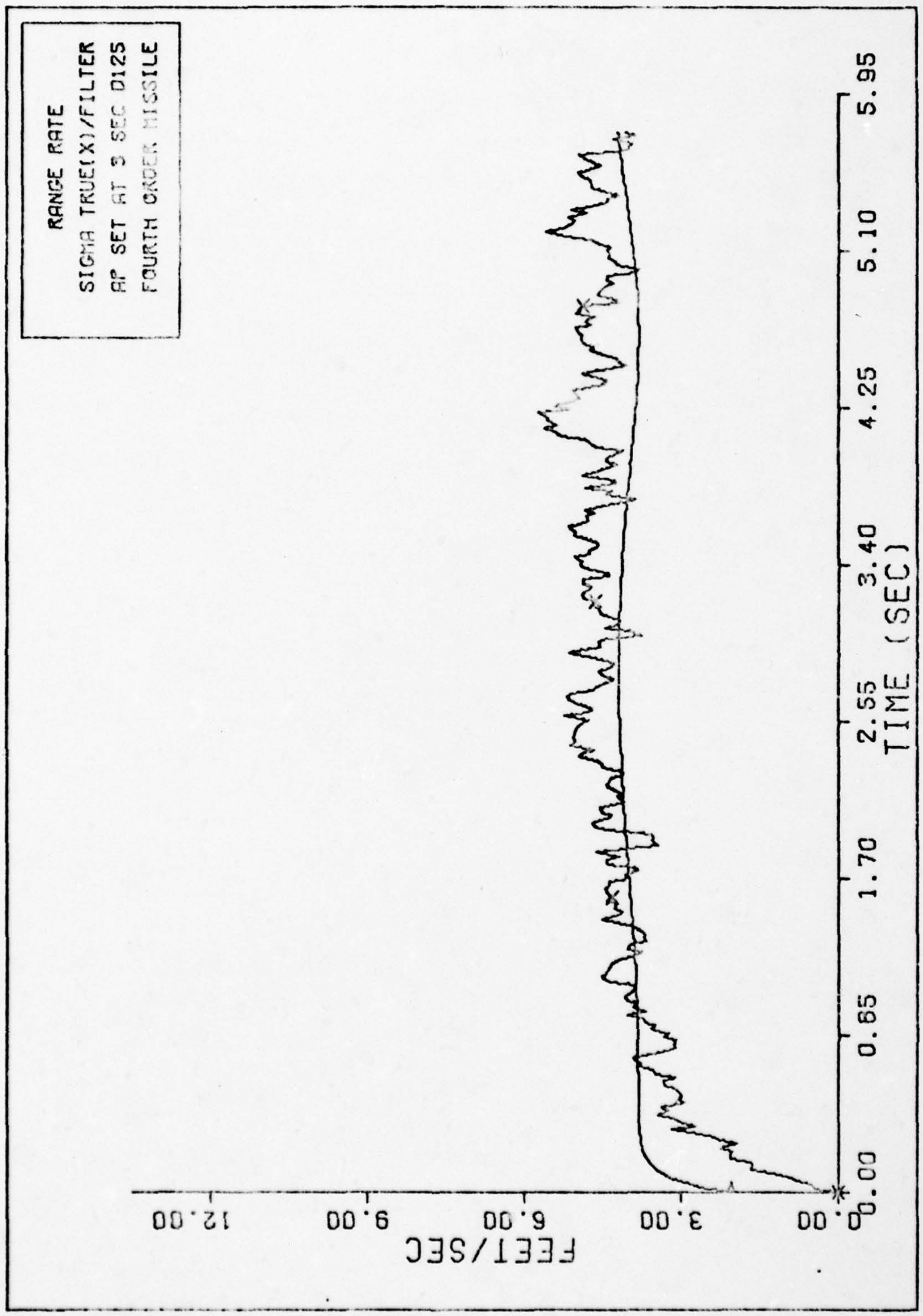

Fig. 49. RANGE RATE SIGMAS FOURTH ORDER

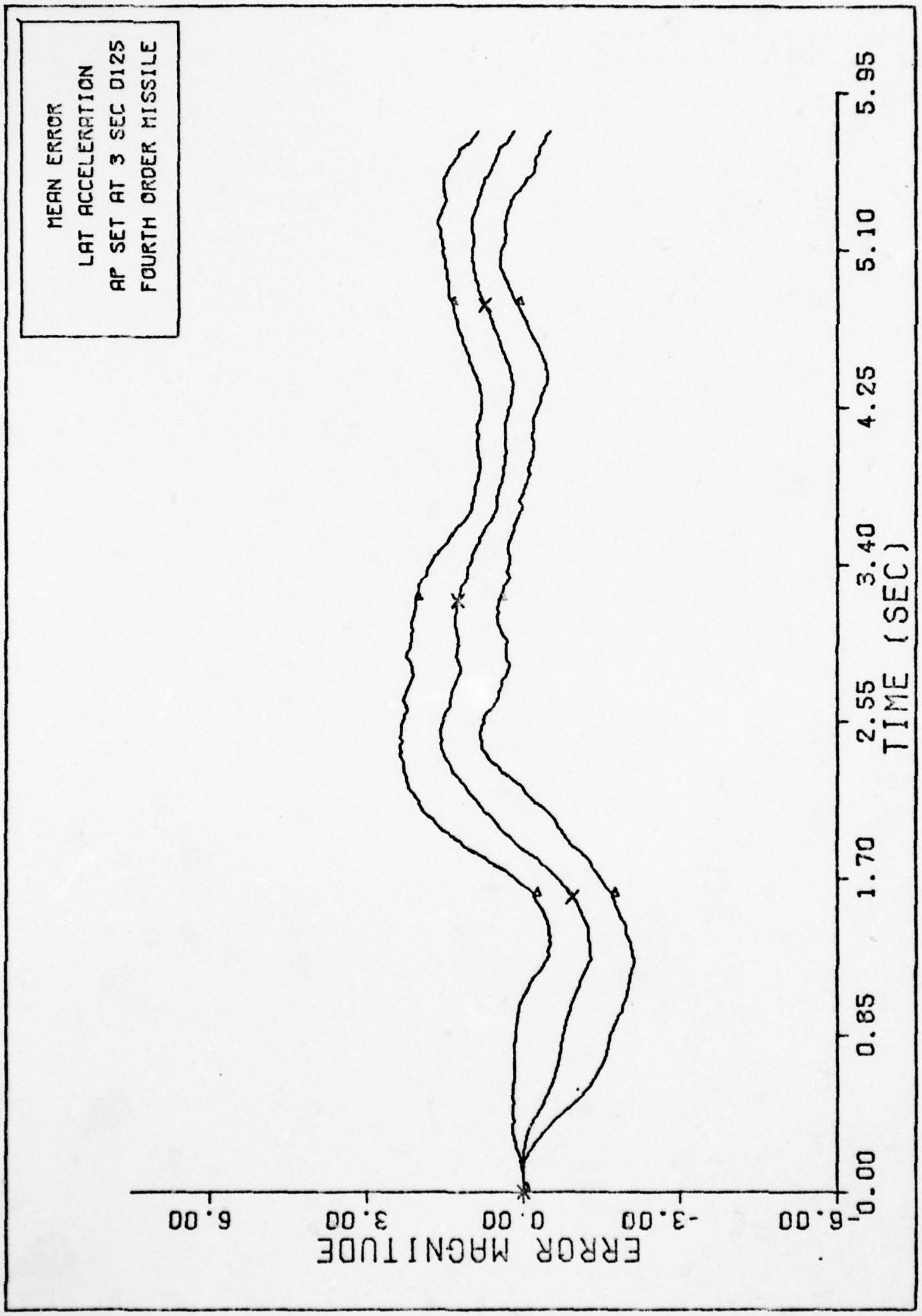

Fig. 50. LAT ACCELERATION FOURTH ORDER MISSILE

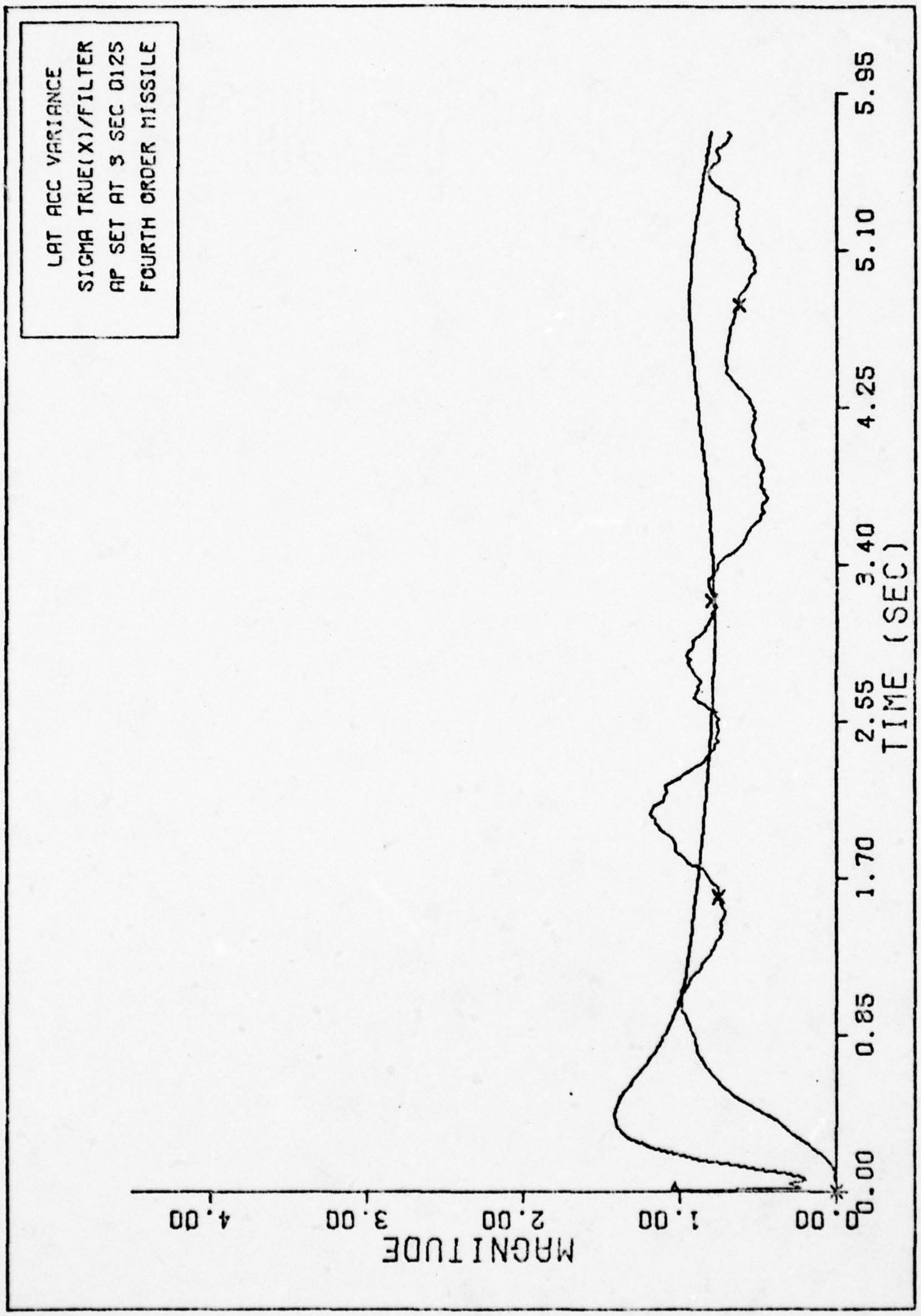

Fig. 51. LAT ACCELERATION SIGMAS FOURTH ORDER

Fourth Order Missile Filter (A/P at 5 sec)

The initial state estimates and the tuning parameters for this case are

$$
\begin{aligned}
V^{I}_{mx}(0) &= 1225.7 \text{ fps} \\
\dot{\theta}_{T}(0) &= 4.363345 \text{ radians} \\
R(0) &= 10000. \text{ feet} \\
\dot{R}(0) &= -2122. \text{ fps} \\
a_{L}(0) &= 0. \\
n(0) &= 4.5 \\
\tau_{f}(0) &= \text{N/A} \\
M/S(0) &= 29.197 \text{ slugs/ft}^2
\end{aligned}
$$

$$
\underline{R} = \begin{bmatrix} 4.E-5 & 0. & 0. \\ 0. & 500. & 0. \\ 0. & 0. & 100. \end{bmatrix}
$$

$$
\underline{P}_0 = \begin{bmatrix}
100. & 0. & 0. & 0. & 0. & 0. & 0. & 0. \\
0. & 1.E-8 & 0. & 0. & 0. & 0. & 0. & 0. \\
0. & 0. & 101. & 0. & 0. & 0. & 0. & 0. \\
0. & 0. & 0. & 4. & 0. & 0. & 0. & 0. \\
0. & 0. & 0. & 0. & 1. & 0. & 0. & 0. \\
0. & 0. & 0. & 0. & 0. & 0. & 0. & 0. \\
0. & 0. & 0. & 0. & 0. & 0. & 0. & 0. \\
0. & 0. & 0. & 0. & 0. & 0. & 0. & 0.
\end{bmatrix}
$$

$$
\underline{Q} = \begin{bmatrix}
101. & 0. & 0. & 0. & 0. & 0. & 0. & 0. \\
0. & 1.E-6 & 0. & 0. & 0. & 0. & 0. & 0. \\
0. & 0. & 500. & 0. & 0. & 0. & 0. & 0. \\
0. & 0. & 0. & 100. & 0. & 0. & 0. & 0. \\
0. & 0. & 0. & 0. & 5. & 0. & 0. & 0. \\
0. & 0. & 0. & 0. & 0. & 0. & 0. & 0. \\
0. & 0. & 0. & 0. & 0. & 0. & 0. & 0. \\
0. & 0. & 0. & 0. & 0. & 0. & 0. & 0.
\end{bmatrix}
$$

These plots were generated by the fourth order filter with the coefficients of the autopilot transfer function determined at t=5. These plots were compared to those results of the fourth order filter using autopilot coefficients for t=0 and t=3. The intent was to determine if there was any distinguishable difference in filter performance for the various sets of autopilot coefficients. A complete description of the filter autopilot and its coefficients can be found in Chapter III.

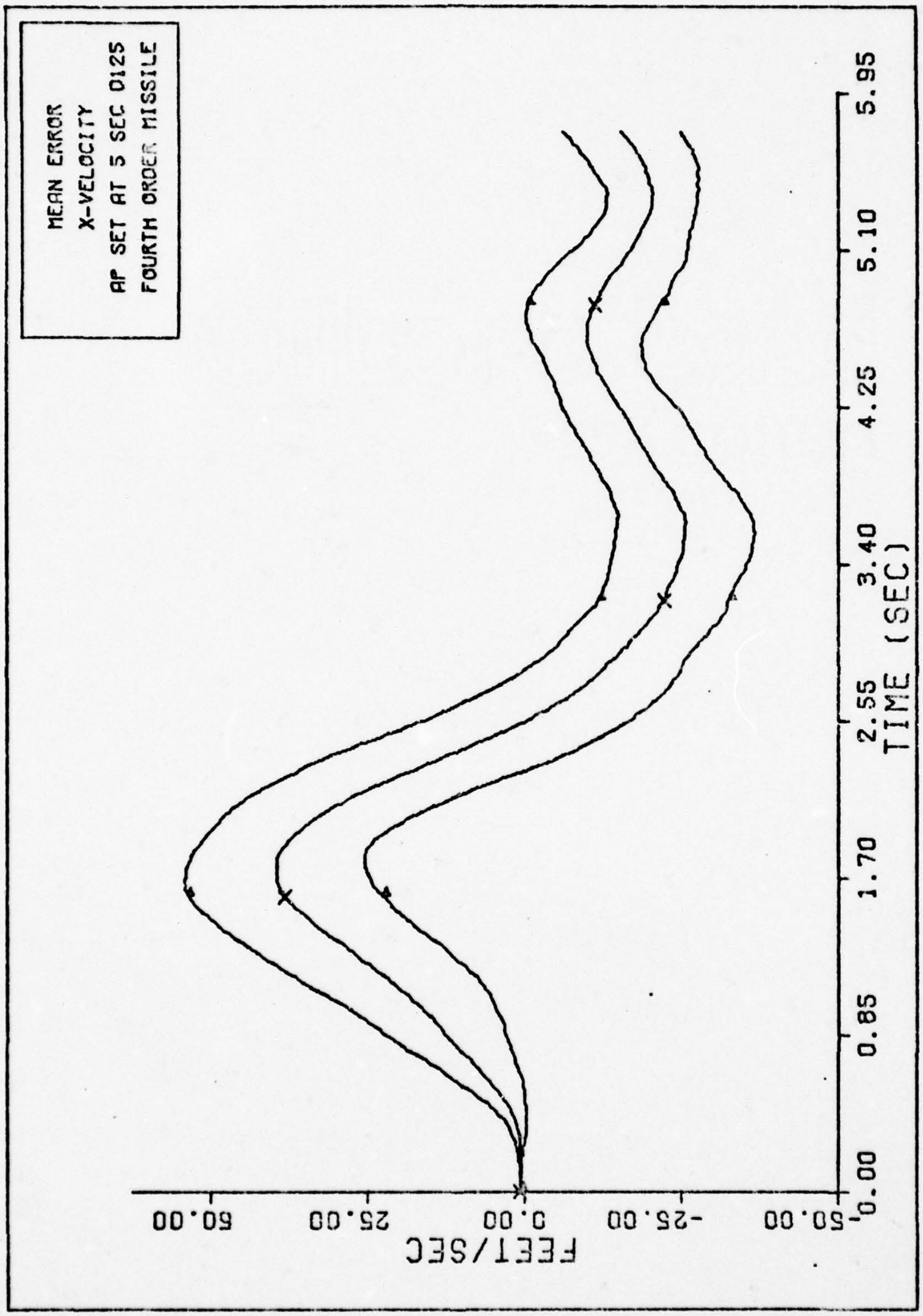

Fig. 52. X-VELOCITY FOURTH ORDER MISSILE

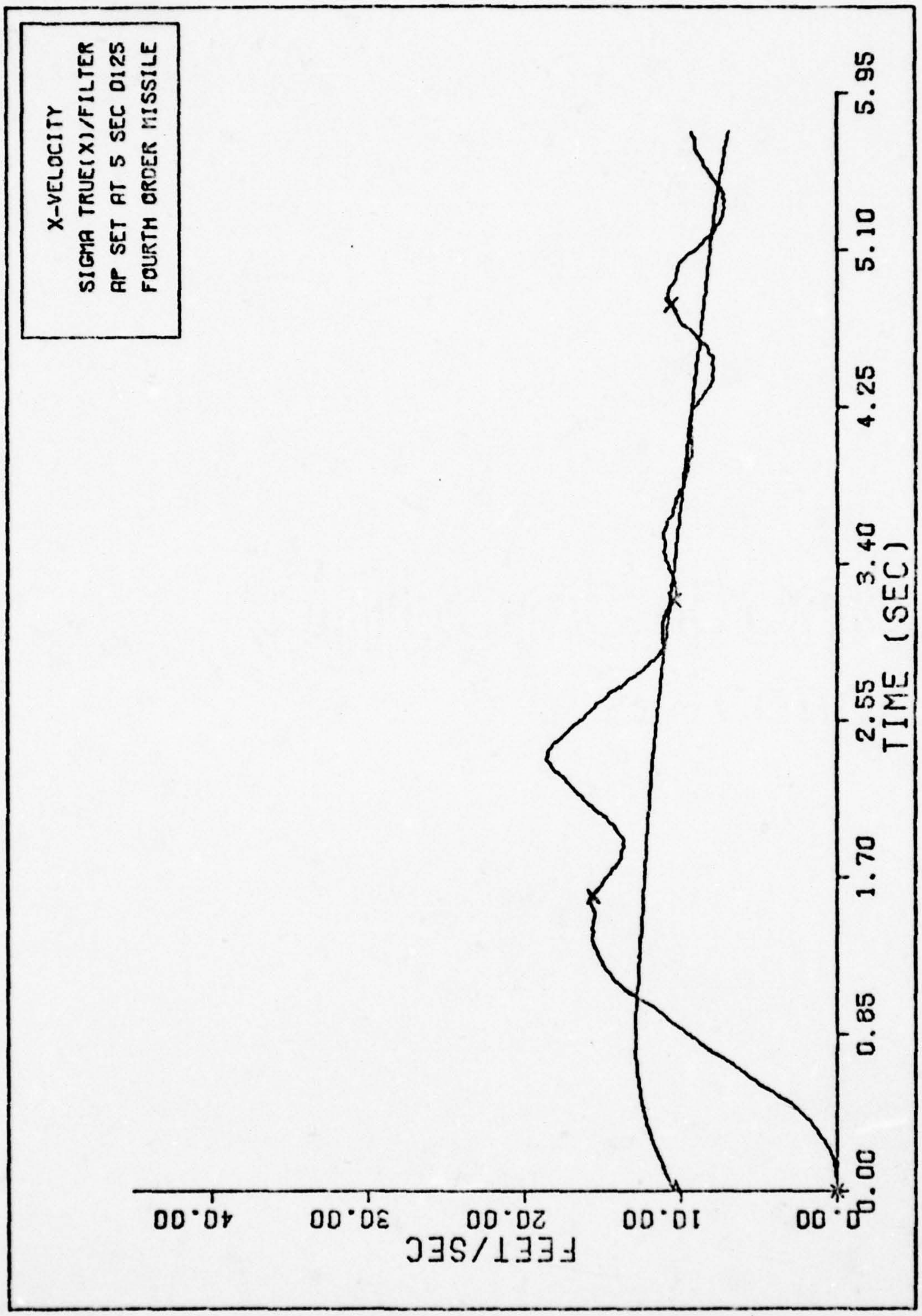

Fig. 53. X-VELOCITY SIGMAS FOURTH ORDER

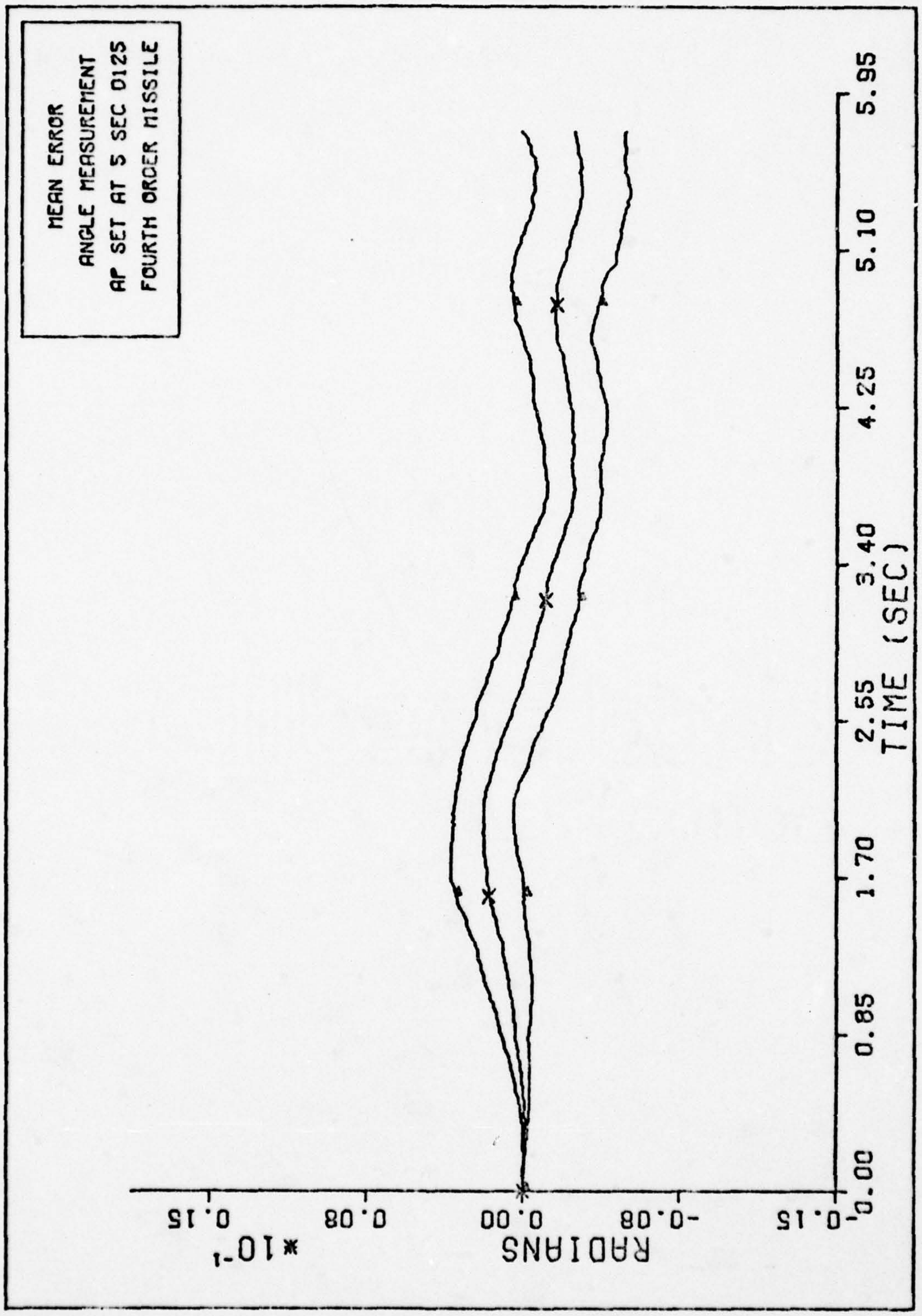

Fig. 54. ANGLE MEASUREMENT FOURTH ORDER MISSILE

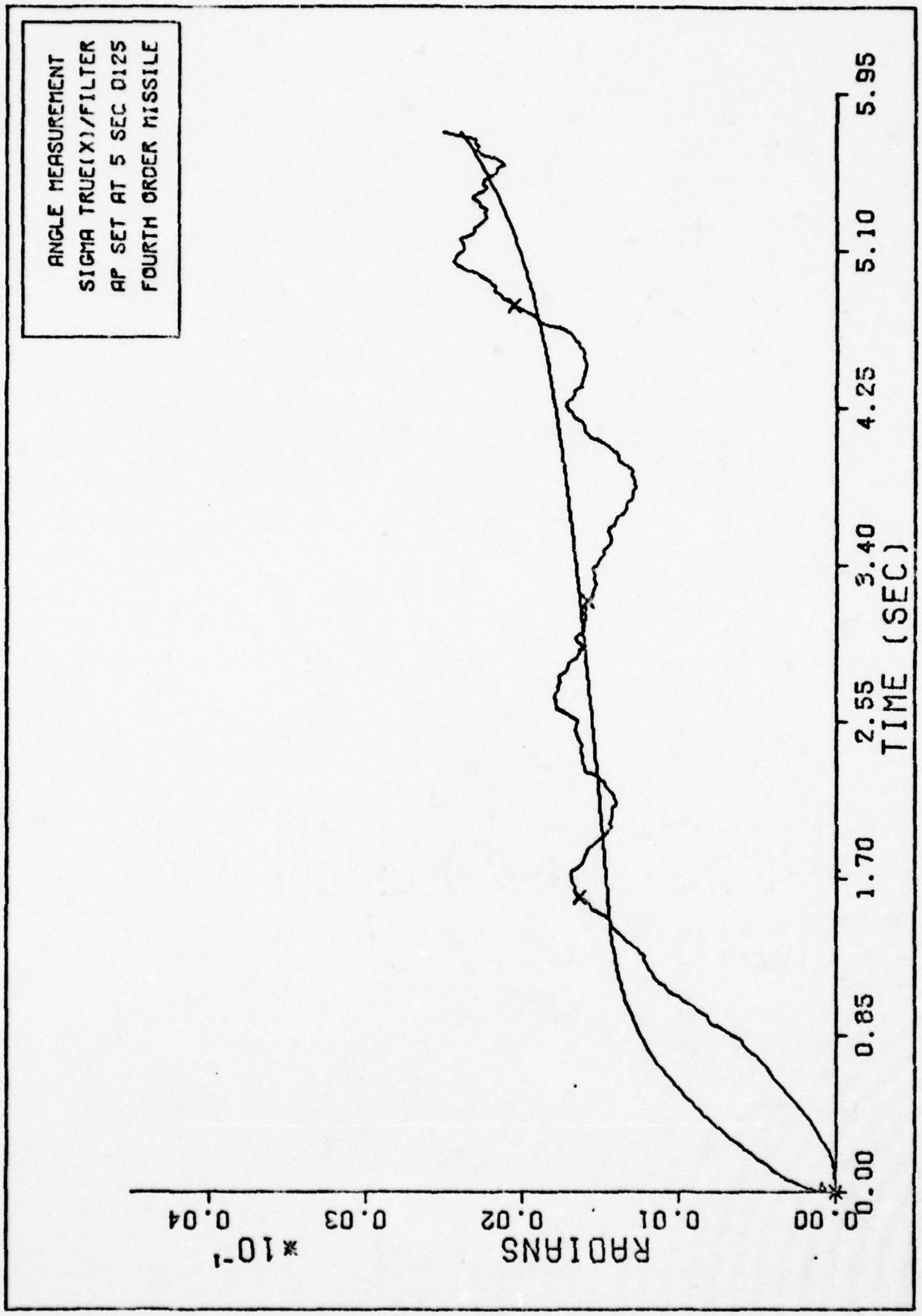

Fig. 55. ANGLE MEASUREMENT SIGMAS FOURTH ORDER

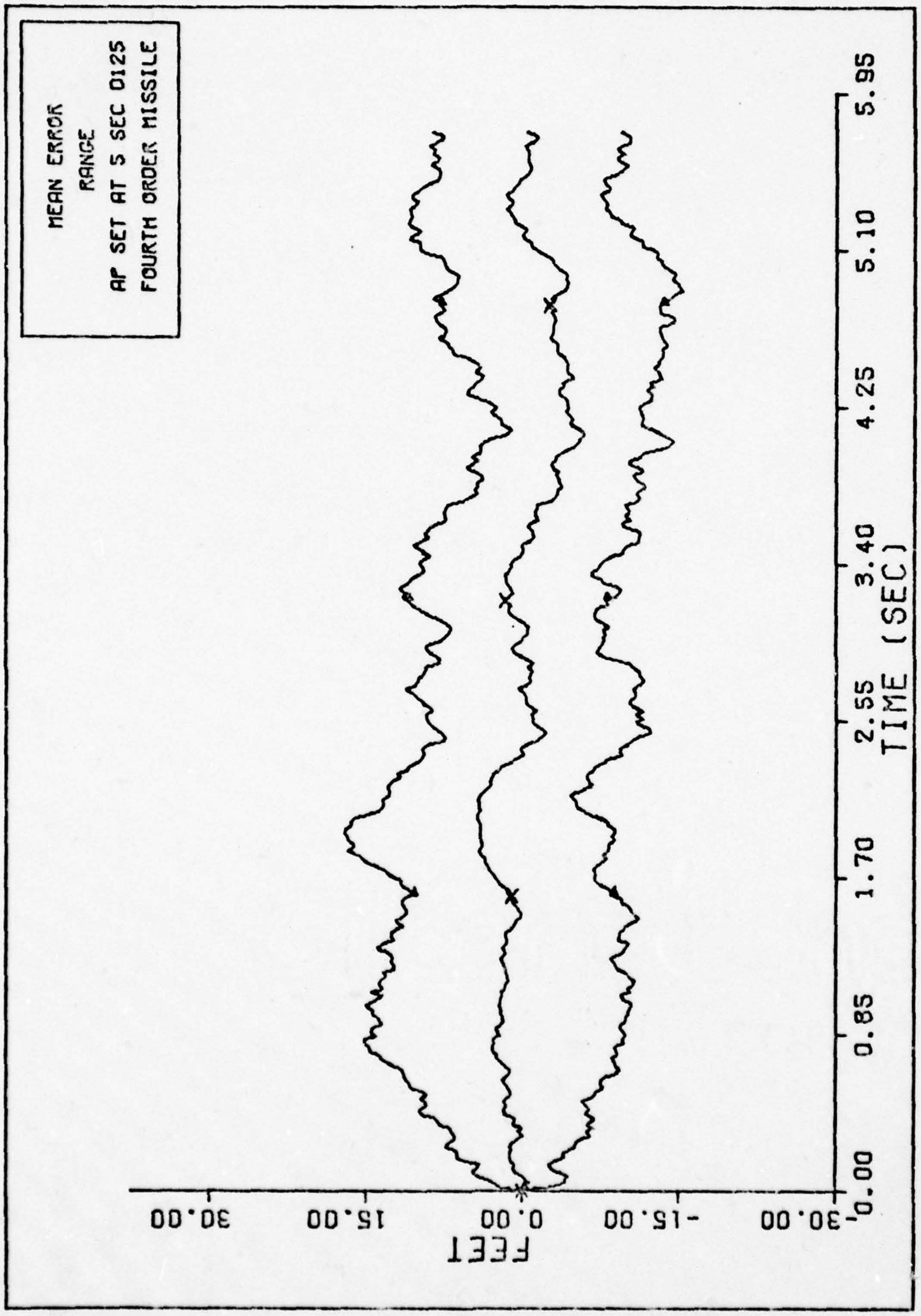

Fig. 56. RANGE FOURTH ORDER MISSILE

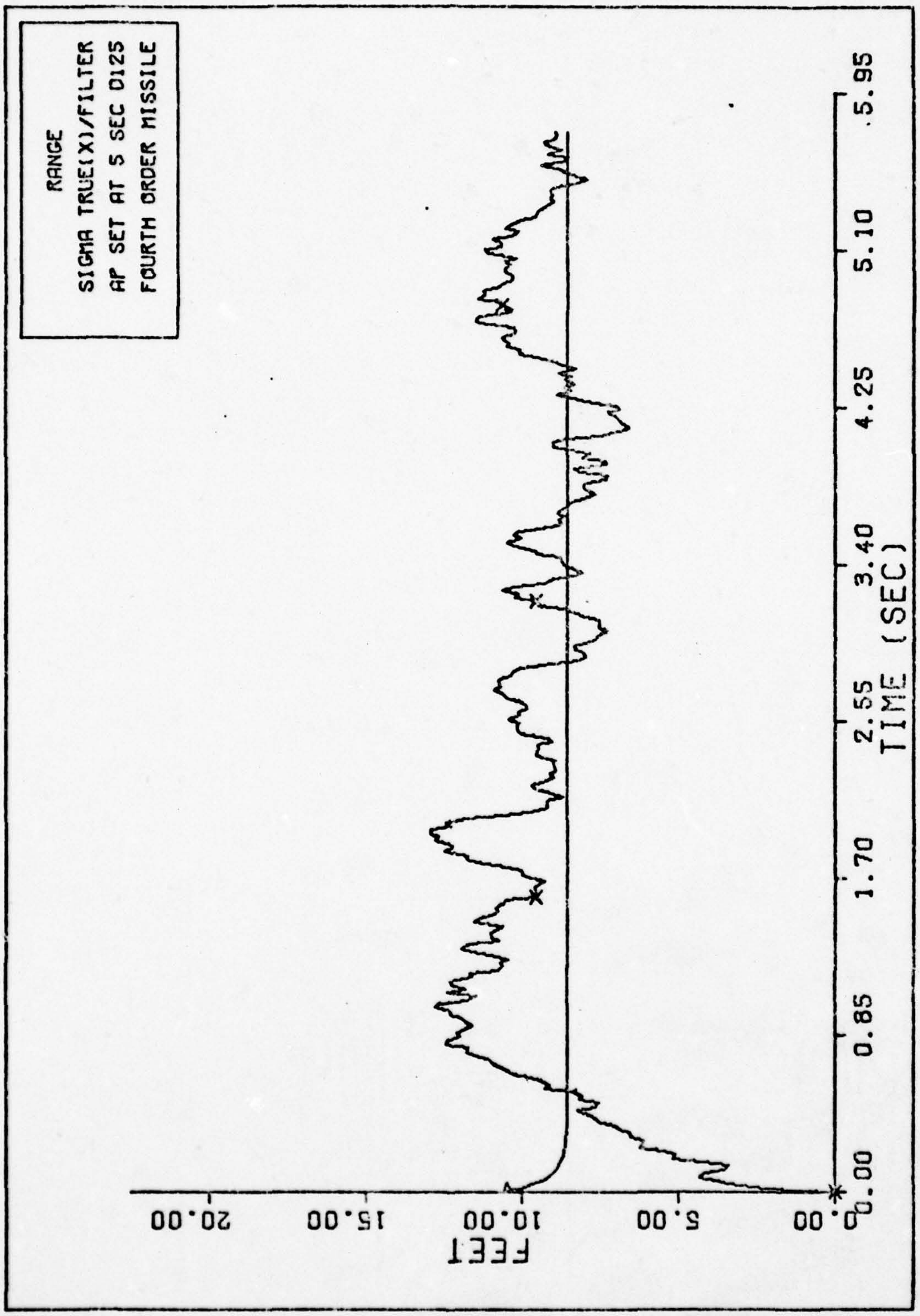

Fig. 57. RANGE SIGMAS FOURTH ORDER

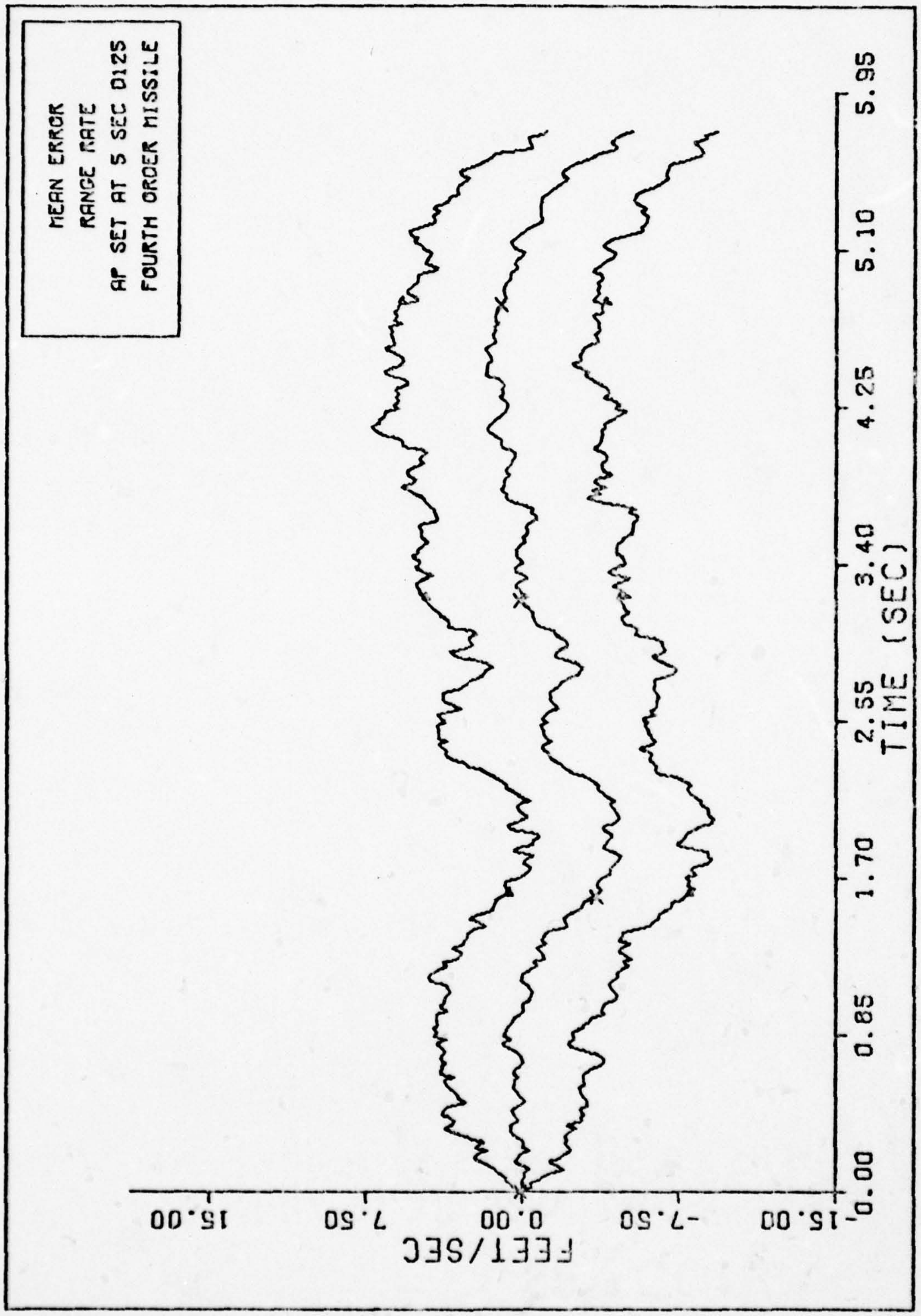

Fig. 58. RANGE RATE FOURTH ORDER MISSILE

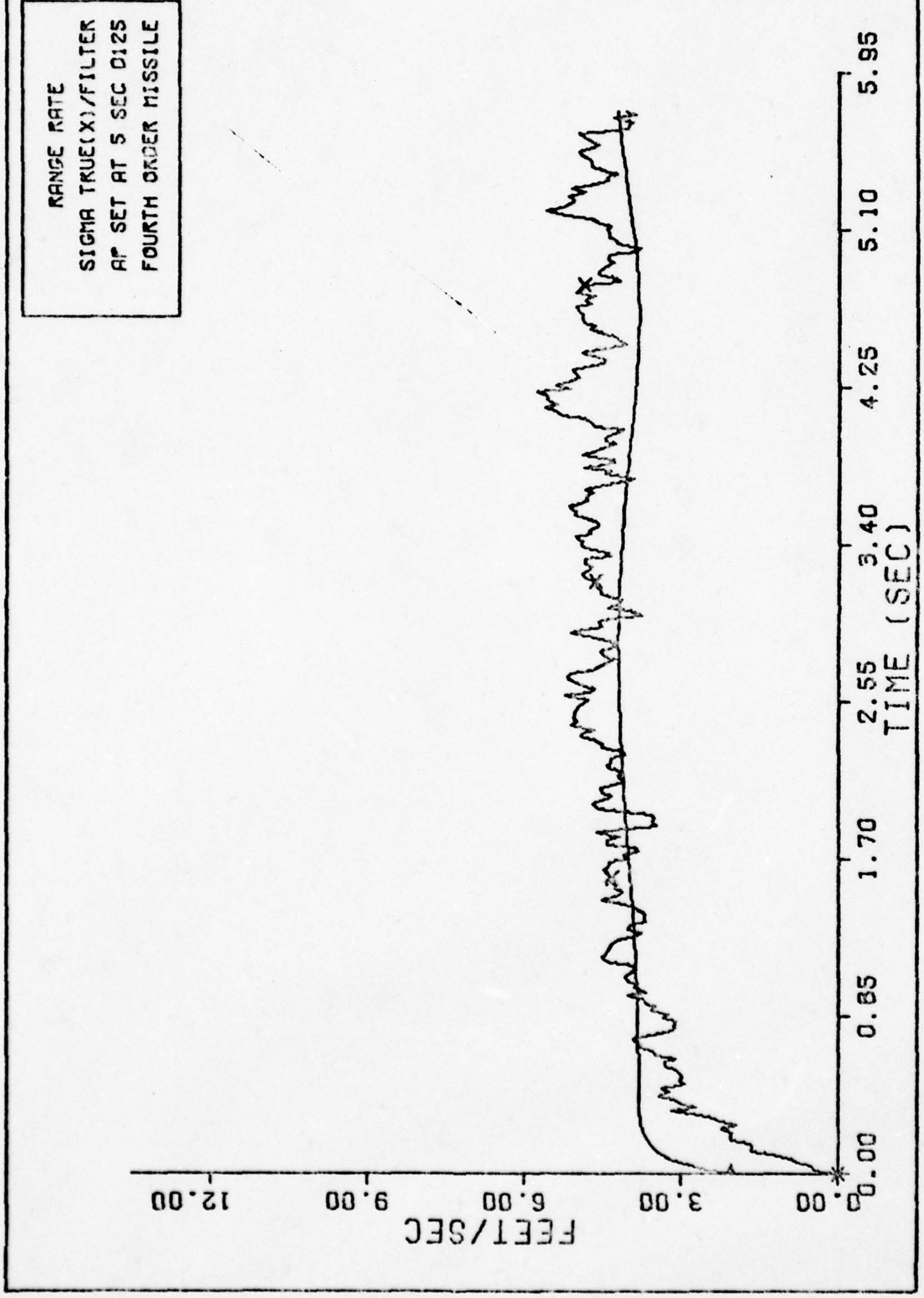

Fig. 59. RANGE RATE SIGMAS FOURTH ORDER

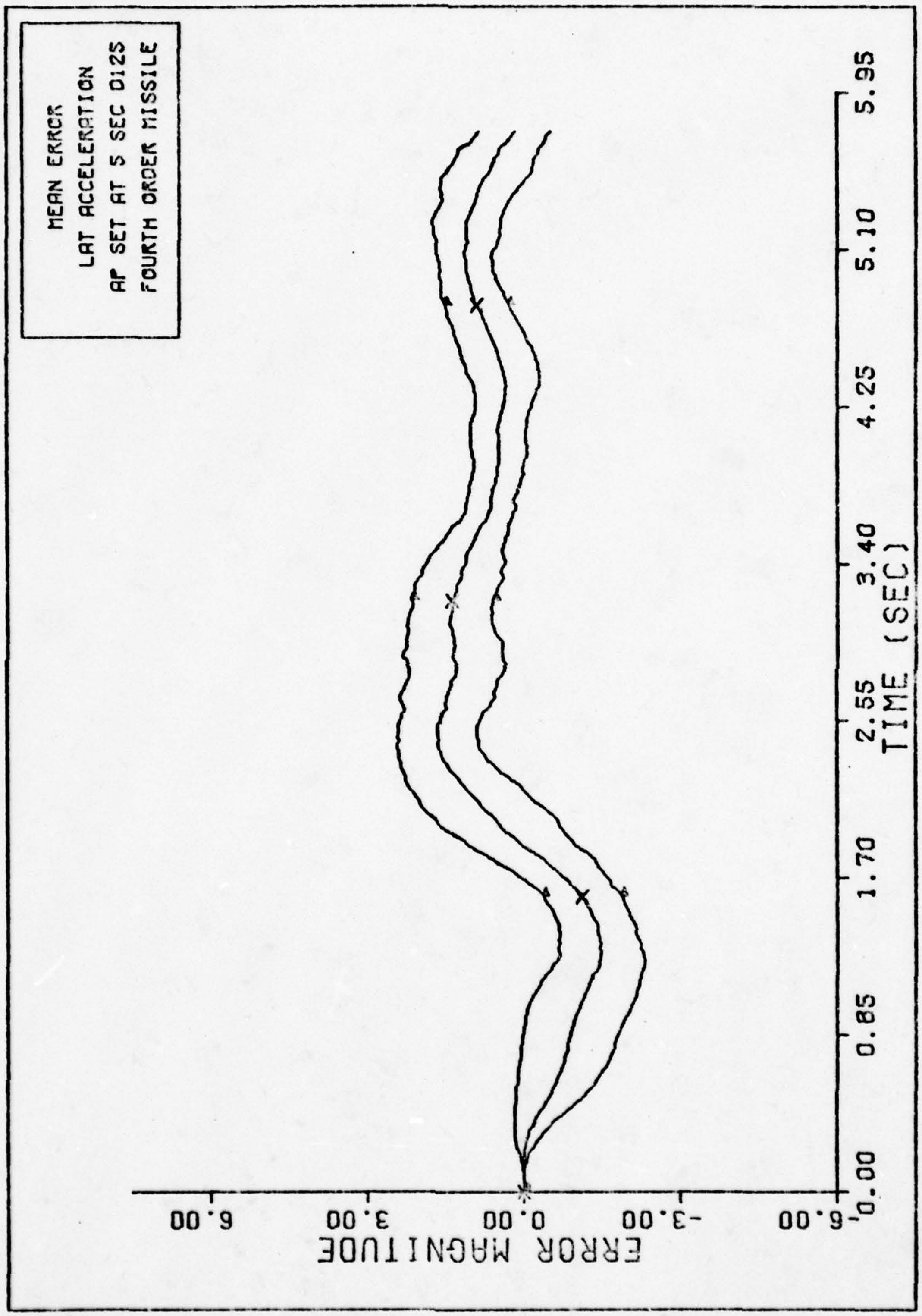

Fig. 60. LAT ACCELERATION FOURTH ORDER MISSILE

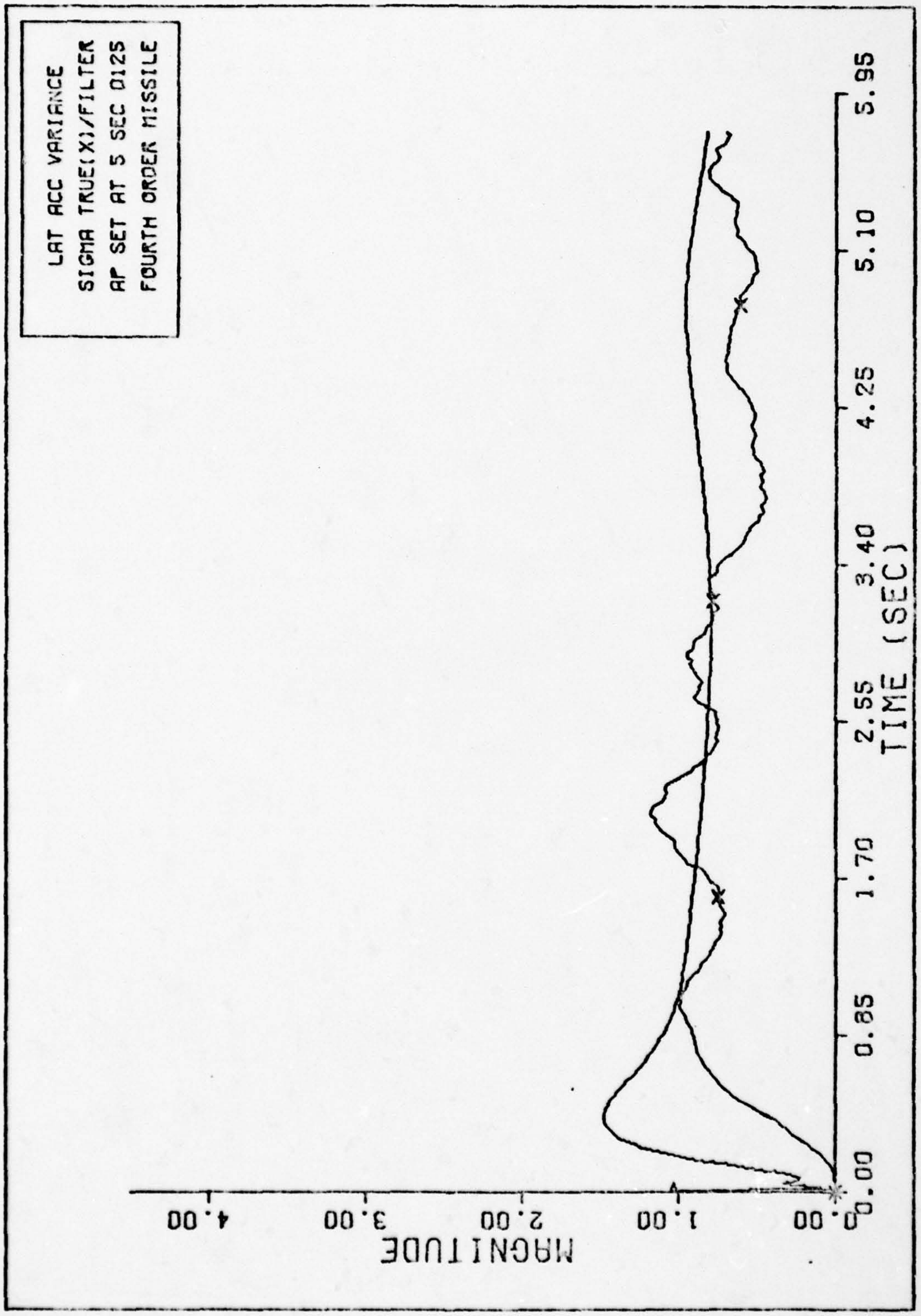

Fig. 61. LAT ACCELERATION SIGMAS FOURTH ORDER

Fourth Order Missile Filter (complete linearization of f)

The initial state estimates and the tuning parameters for this case are

$$
\begin{aligned}
V^{I}_{mx}(0) &= 1225.7 \text{ fps} \\
\dot{\theta}_T(0) &= 4.363345 \text{ radians} \\
R(0) &= 10000. \text{ feet} \\
\dot{R}(0) &= -2122. \text{ fps} \\
a_L(0) &= 0. \\
n(0) &= 4.5 \\
\tau_f(0) &= \text{N/A} \\
M/S(0) &= 29.197 \text{ slugs/ft}^2
\end{aligned}
$$

$$
\underline{R} = \begin{bmatrix} 4.E-5 & 0. & 0. \\ 0. & 500. & 0. \\ 0. & 0. & 100. \end{bmatrix}
$$

$$
\underline{P}_0 = \begin{bmatrix}
100. & 0. & 0. & 0. & 0. & 0. & 0. & 0. \\
0. & 1.E-8 & 0. & 0. & 0. & 0. & 0. & 0. \\
0. & 0. & 101. & 0. & 0. & 0. & 0. & 0. \\
0. & 0. & 0. & 4. & 0. & 0. & 0. & 0. \\
0. & 0. & 0. & 0. & 1. & 0. & 0. & 0. \\
0. & 0. & 0. & 0. & 0. & 0. & 0. & 0. \\
0. & 0. & 0. & 0. & 0. & 0. & 0. & 0. \\
0. & 0. & 0. & 0. & 0. & 0. & 0. & 0.
\end{bmatrix}
$$

$$
\underline{Q} = \begin{bmatrix}
101. & 0. & 0. & 0. & 0. & 0. & 0. & 0. \\
0. & 1.E-6 & 0. & 0. & 0. & 0. & 0. & 0. \\
0. & 0. & 500. & 0. & 0. & 0. & 0. & 0. \\
0. & 0. & 0. & 100. & 0. & 0. & 0. & 0. \\
0. & 0. & 0. & 0. & 5. & 0. & 0. & 0. \\
0. & 0. & 0. & 0. & 0. & 0. & 0. & 0. \\
0. & 0. & 0. & 0. & 0. & 0. & 0. & 0. \\
0. & 0. & 0. & 0. & 0. & 0. & 0. & 0.
\end{bmatrix}
$$

These plots were generated to justify the assumptions, that $\dot{\theta}_T$, V_m, and γ_m could be considered constant over the measurement period of 0.02 seconds. The fourth order filter was used with the coefficients of the autopilot chosen for t=0. The $\underline{F}$-matrix within the filter contains a complete linearization of the f-vector. A comparison of these plots with those for "Fourth Order Missile Filter, A/P at t=0" (Figures 32 through 41), can be made to determine the difference when the above mentioned variables are considered constant over the measurement period.

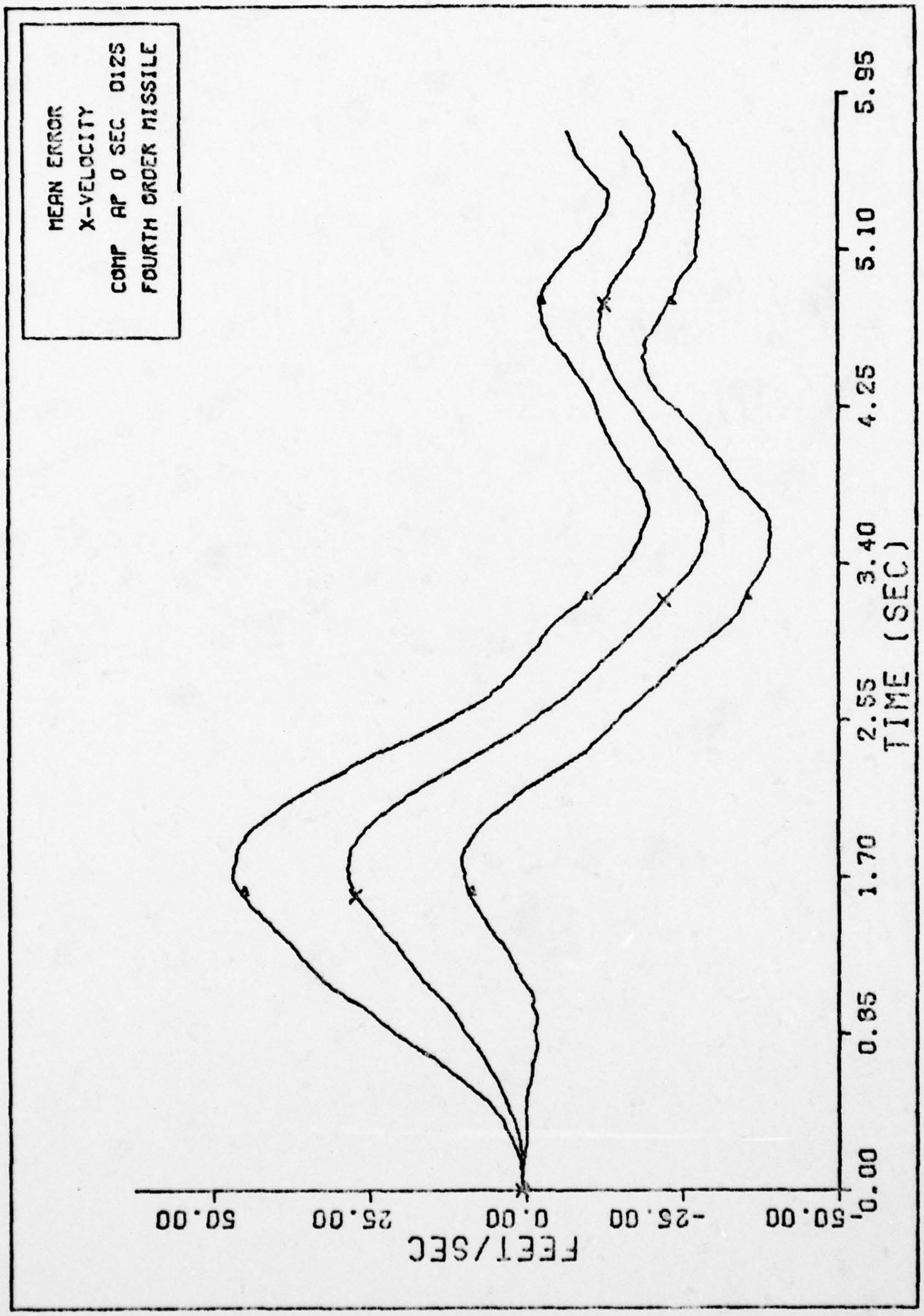

Fig. 62. X-VELOCITY FOURTH ORDER MISSILE

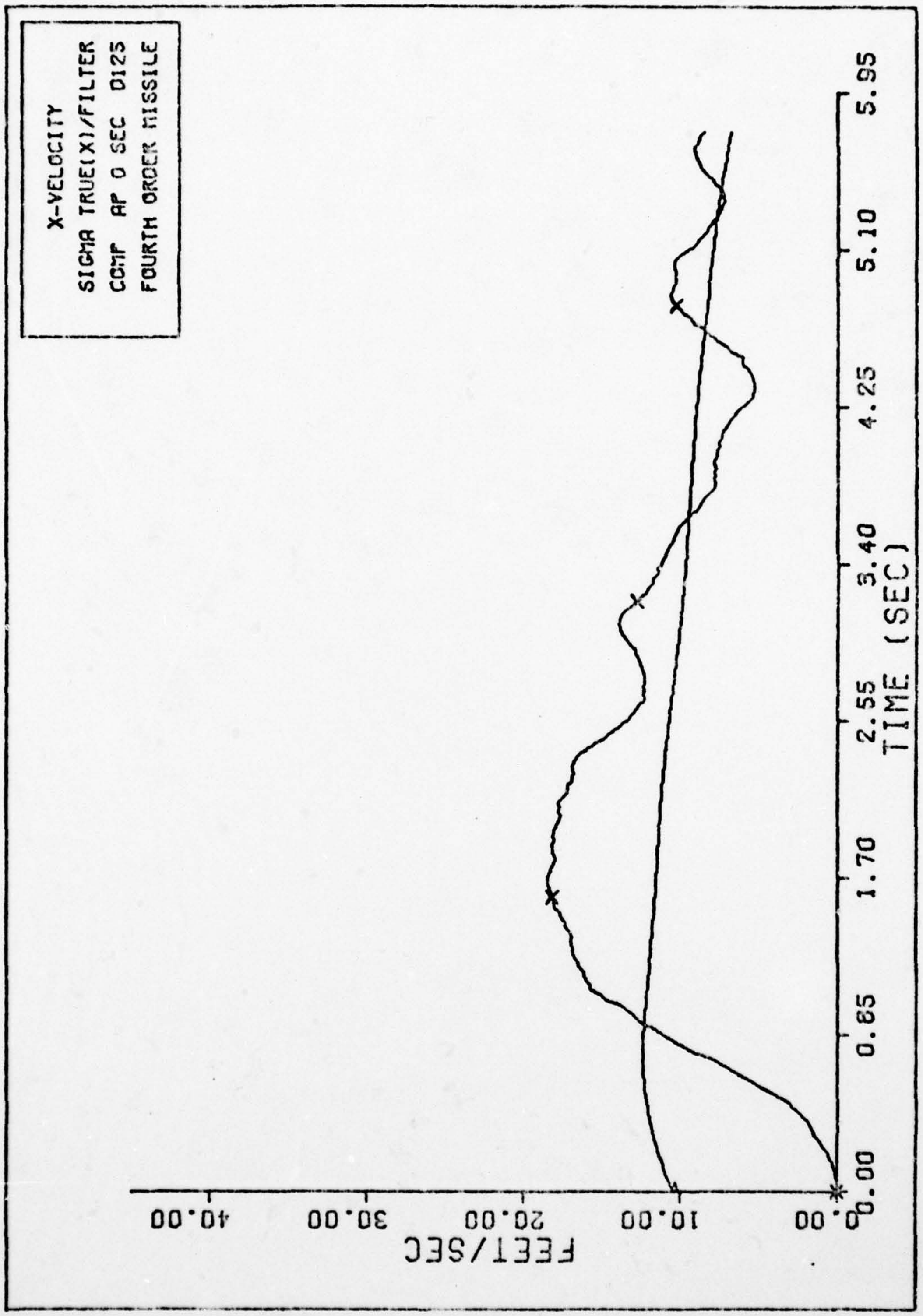

Fig. 63. X-VELOCITY SIGMAS FOURTH ORDER

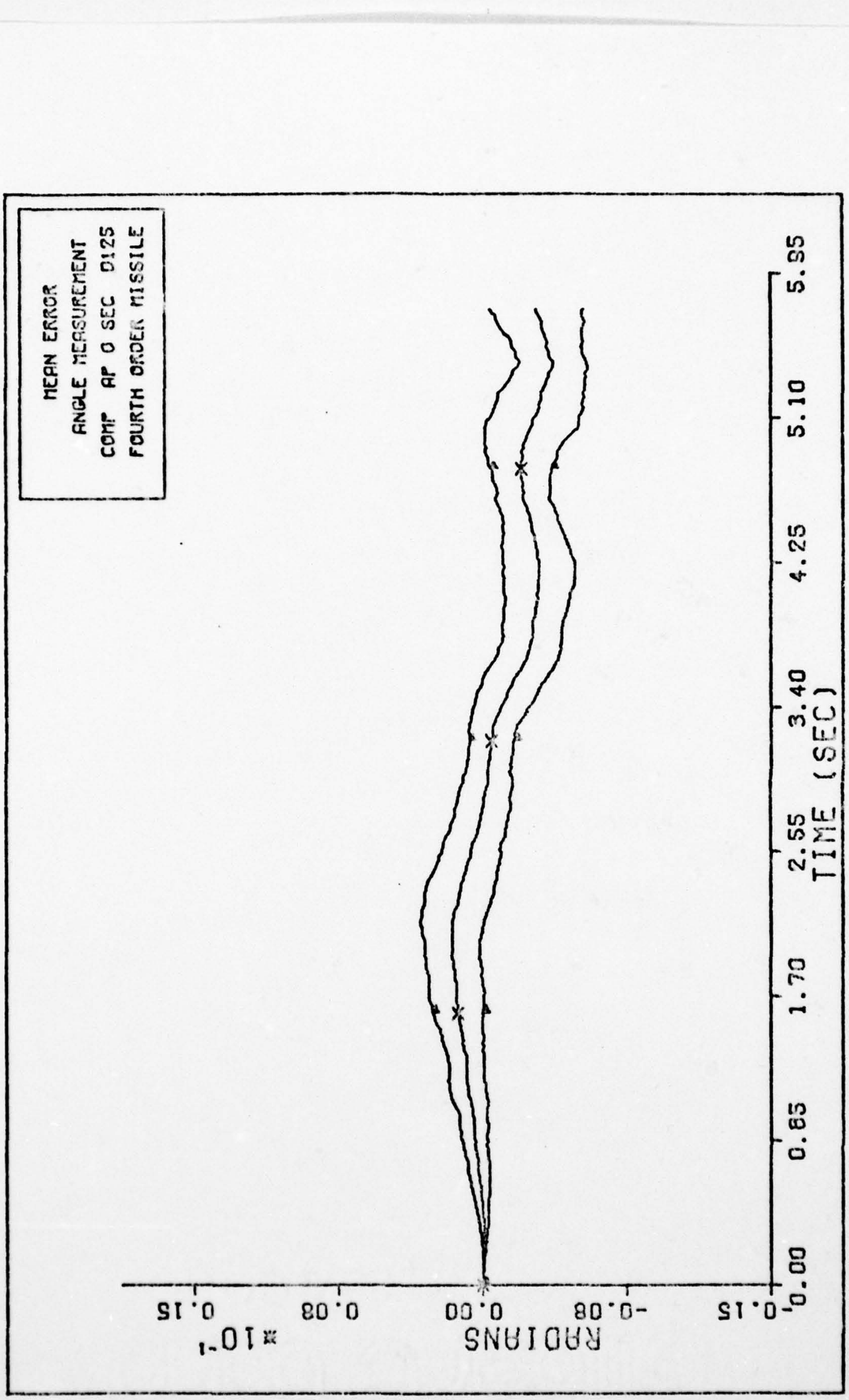

Fig. 64. ANGLE MEASUREMENT FOURTH ORDER MISSILE

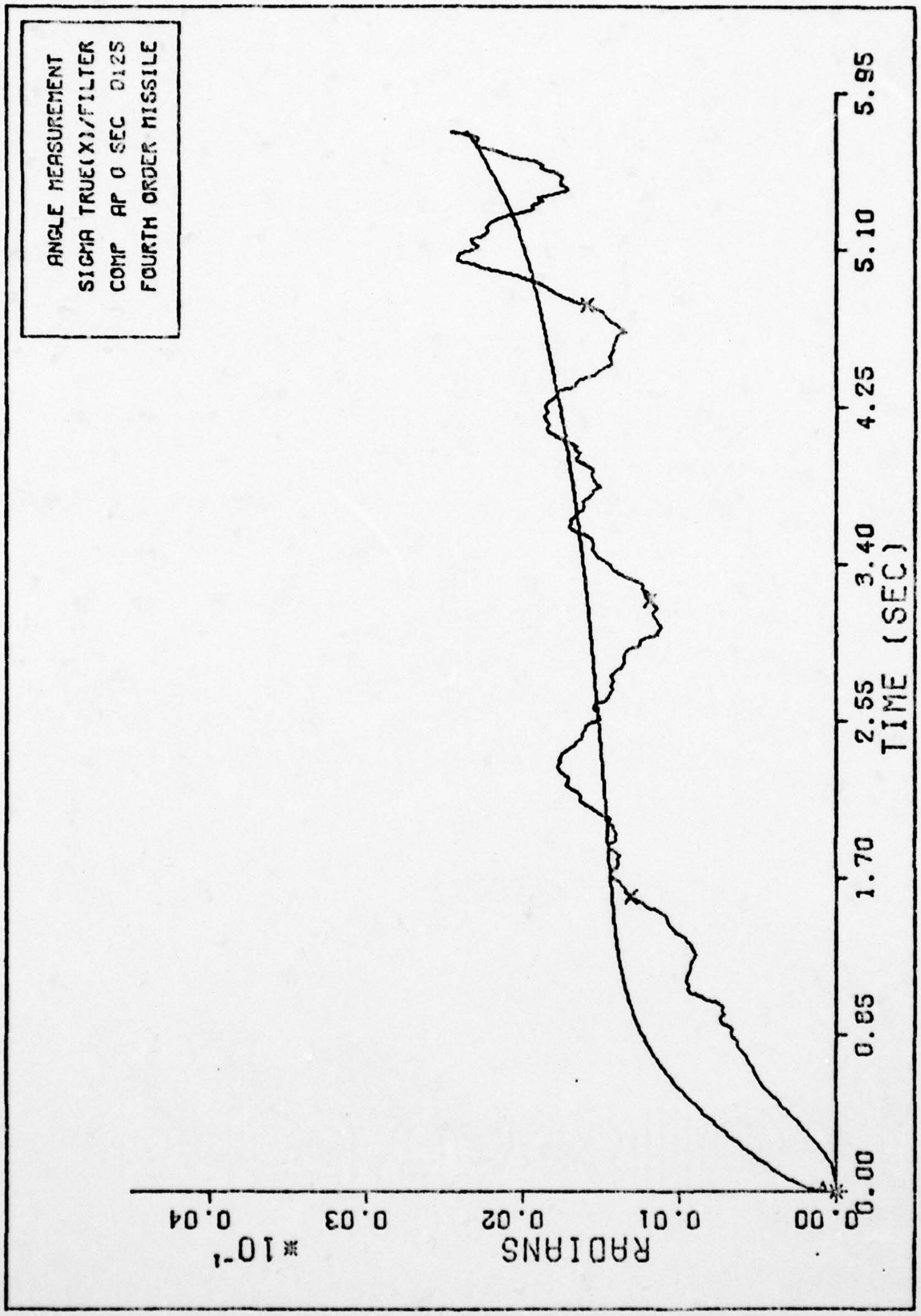

Fig. 65. ANGLE MEASUREMENT SIGMAS FOURTH ORDER

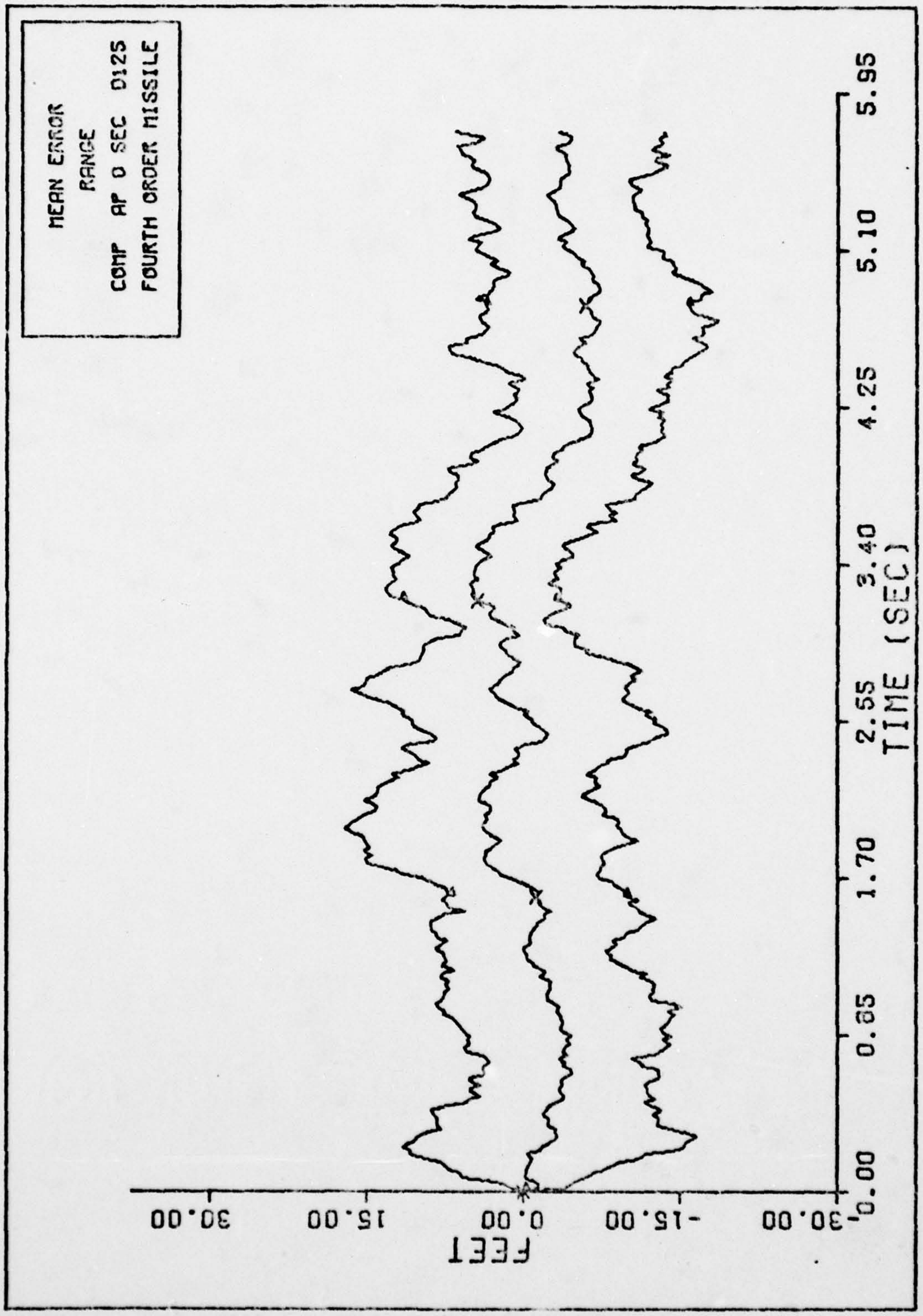

Fig. 66. RANGE FOURTH ORDER MISSILE

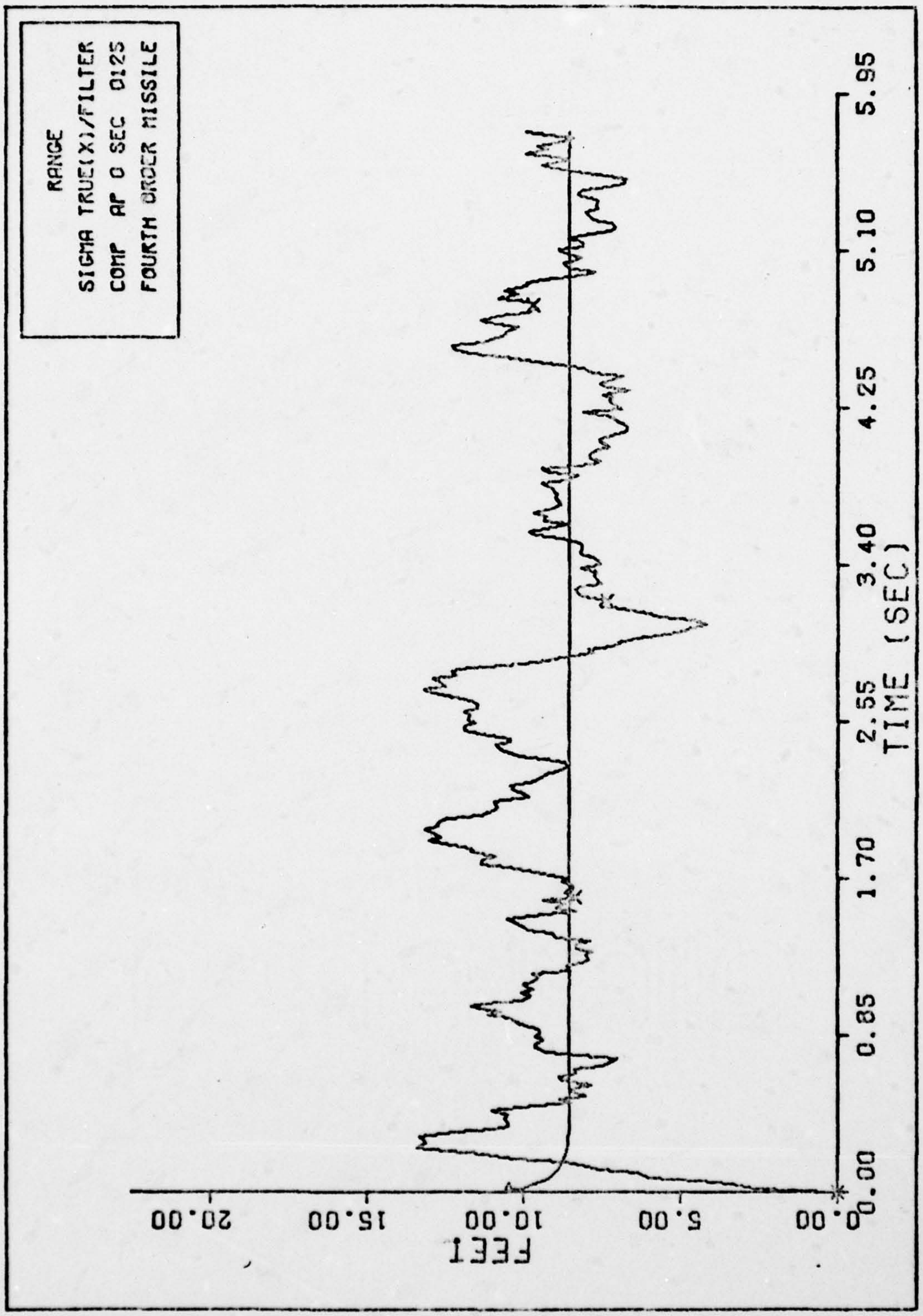

Fig. 67. RANGE SIGMAS FOURTH ORDER

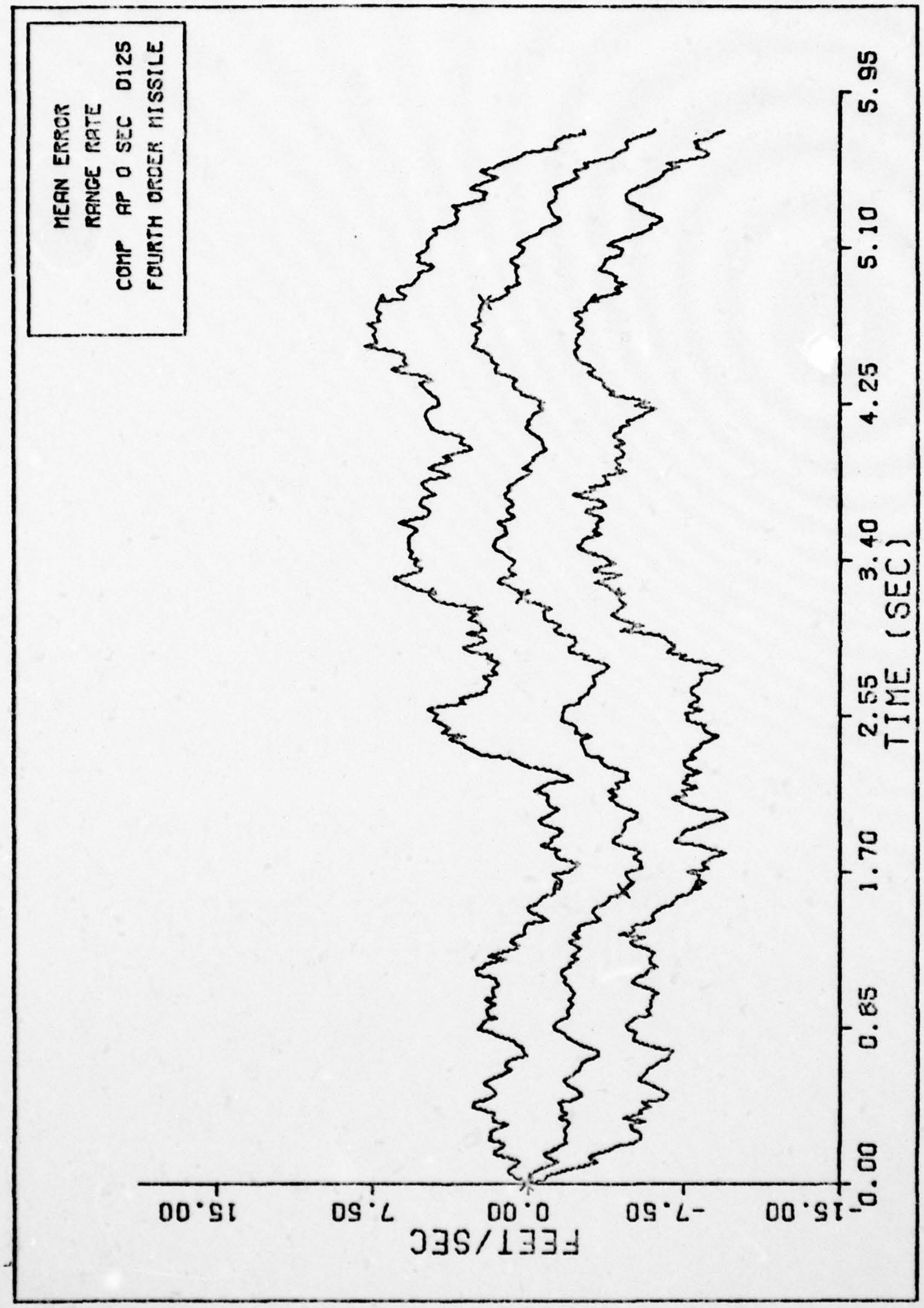

Fig. 68. RANGE RATE FOURTH ORDER MISSILE

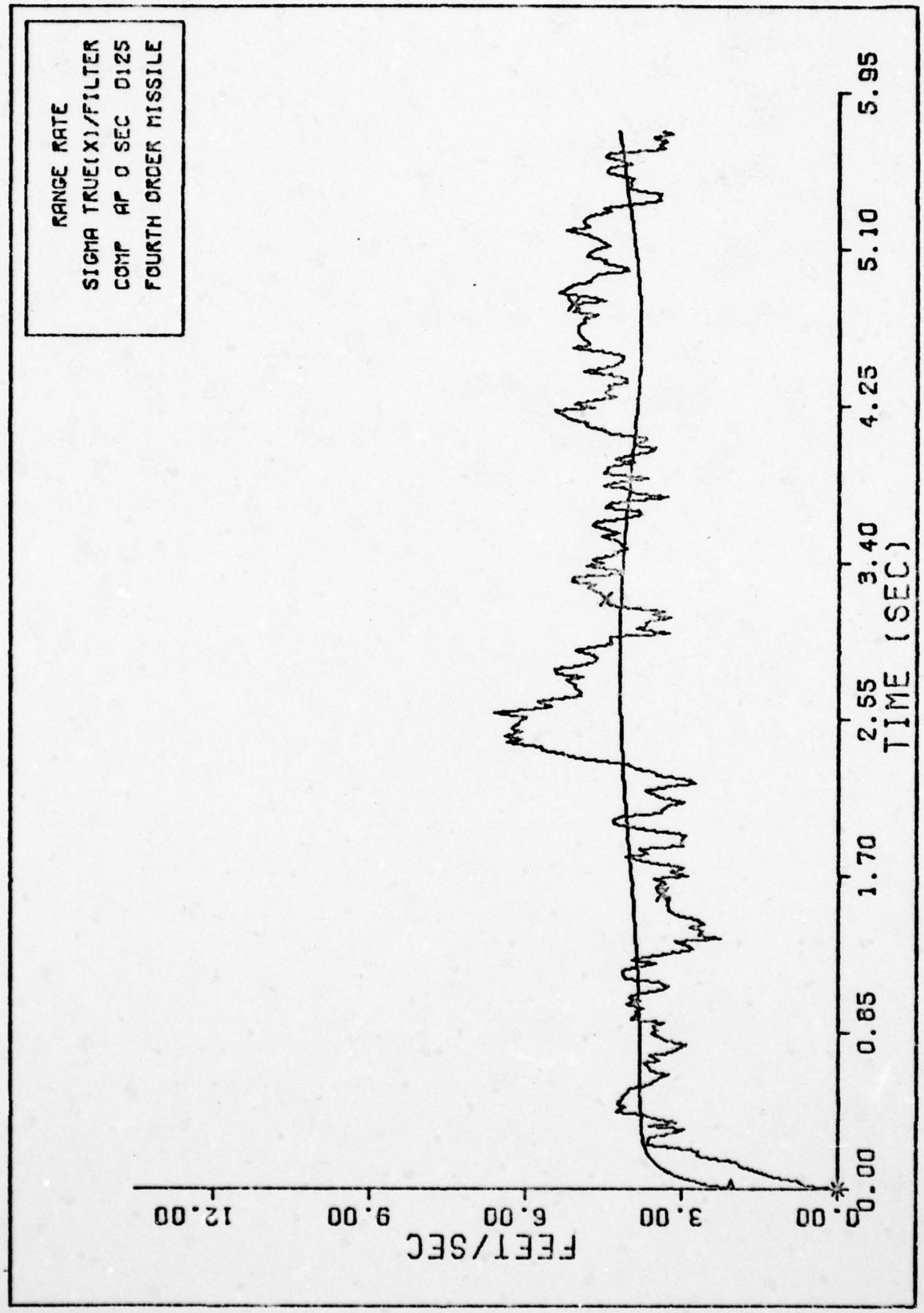

Fig. 69. RANGE RATE SIGMAS FOURTH ORDER

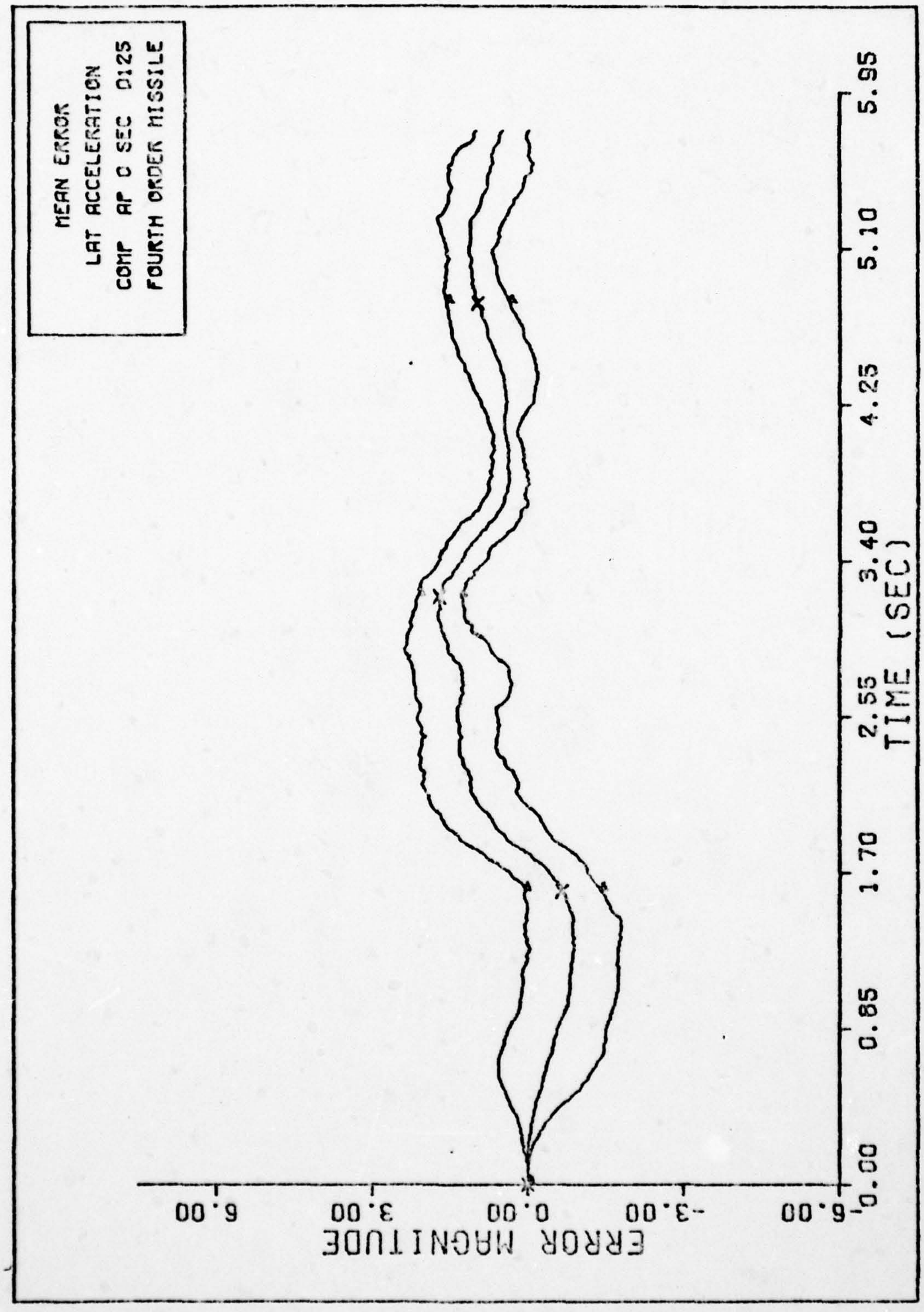

Fig. 70. LAT ACCELERATION FOURTH ORDER MISSILE

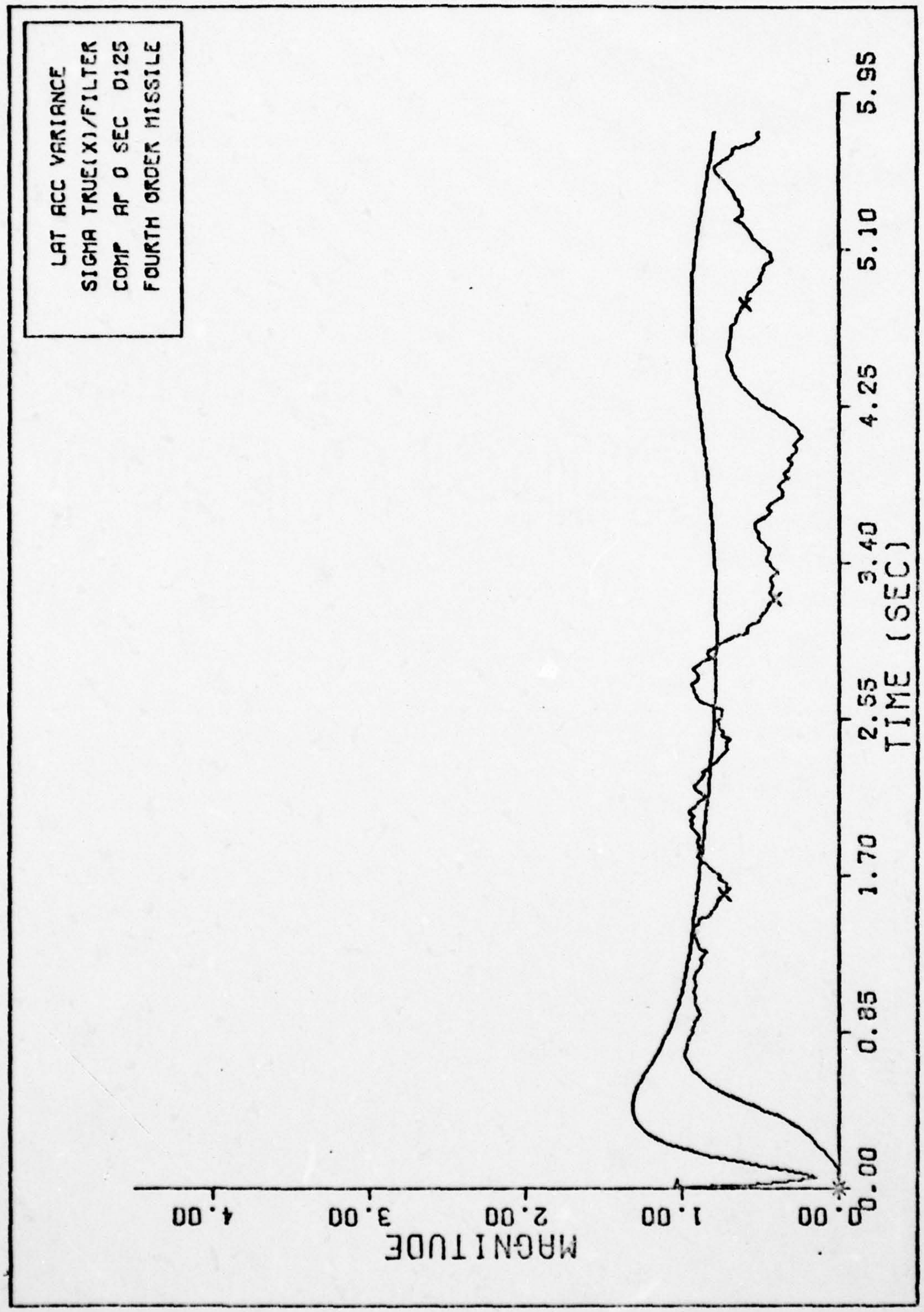

Fig. 71. LAT ACCELERATION SIGMAS FOURTH ORDER

Fourth Order Missile Filter (using Runge-Kutta integration)

The initial state estimates and the tuning parameters for this case are

$$V^I_{mx}(0) = 1225.7 \text{ fps}$$
$$\dot{\theta}_T(0) = 4.363345 \text{ radians}$$
$$R(0) = 10000. \text{ feet}$$
$$\dot{R}(0) = -2122. \text{ fps}$$
$$a_L(0) = 0.$$
$$n(0) = 4.5$$
$$\tau_f(0) = \text{N/A}$$
$$M/S(0) = 29.197 \text{ slugs/ft}^2$$

$$\underline{R} = \begin{bmatrix} 4.E-5 & 0. & 0. \\ 0. & 500. & 0. \\ 0. & 0. & 100. \end{bmatrix}$$

$$\underline{P}_0 = \begin{bmatrix} 100. & 0. & 0. & 0. & 0. & 0. & 0. & 0. \\ 0. & 1.E-8 & 0. & 0. & 0. & 0. & 0. & 0. \\ 0. & 0. & 101. & 0. & 0. & 0. & 0. & 0. \\ 0. & 0. & 0. & 4. & 0. & 0. & 0. & 0. \\ 0. & 0. & 0. & 0. & 1. & 0. & 0. & 0. \\ 0. & 0. & 0. & 0. & 0. & 0. & 0. & 0. \\ 0. & 0. & 0. & 0. & 0. & 0. & 0. & 0. \\ 0. & 0. & 0. & 0. & 0. & 0. & 0. & 0. \end{bmatrix}$$

$$
\underline{Q} = \begin{bmatrix}
101. & 0. & 0. & 0. & 0. & 0. & 0. & 0. \\
0. & 1.E-6 & 0. & 0. & 0. & 0. & 0. & 0. \\
0. & 0. & 500. & 0. & 0. & 0. & 0. & 0. \\
0. & 0. & 0. & 100. & 0. & 0. & 0. & 0. \\
0. & 0. & 0. & 0. & 5. & 0. & 0. & 0. \\
0. & 0. & 0. & 0. & 0. & 0. & 0. & 0. \\
0. & 0. & 0. & 0. & 0. & 0. & 0. & 0. \\
0. & 0. & 0. & 0. & 0. & 0. & 0. & 0.
\end{bmatrix}
$$

These plots were generated to determine if the filter performance was degraded by using a first order Euler integration routine. The results shown here used a Runge-Kutta routine and can be compared to Figures 52 through 61, which were generated with the Euler routine. The coefficients of the autopilot were chosen for t=5, since these coefficients caused the greatest transients in the dynamic states of the filter (compared to t=0 and t=3, as described in Chapter III). It was decided that a favorable comparison for this case would be the best test for the Euler routine.

AD-A055 637 AIR FORCE INST OF TECH WRIGHT-PATTERSON AFB OHIO SCH--ETC F/G 19/5
AN EXTENDED KALMAN FILTER FIRE CONTROL SYSTEM AGAINST AIR-TO-AI--ETC(U)
DEC 77 S J CUSUMANO, M DE PONTE

UNCLASSIFIED AFIT/GE/EE/77-13-VOL-2 NL

2 OF 4
ADA
055637

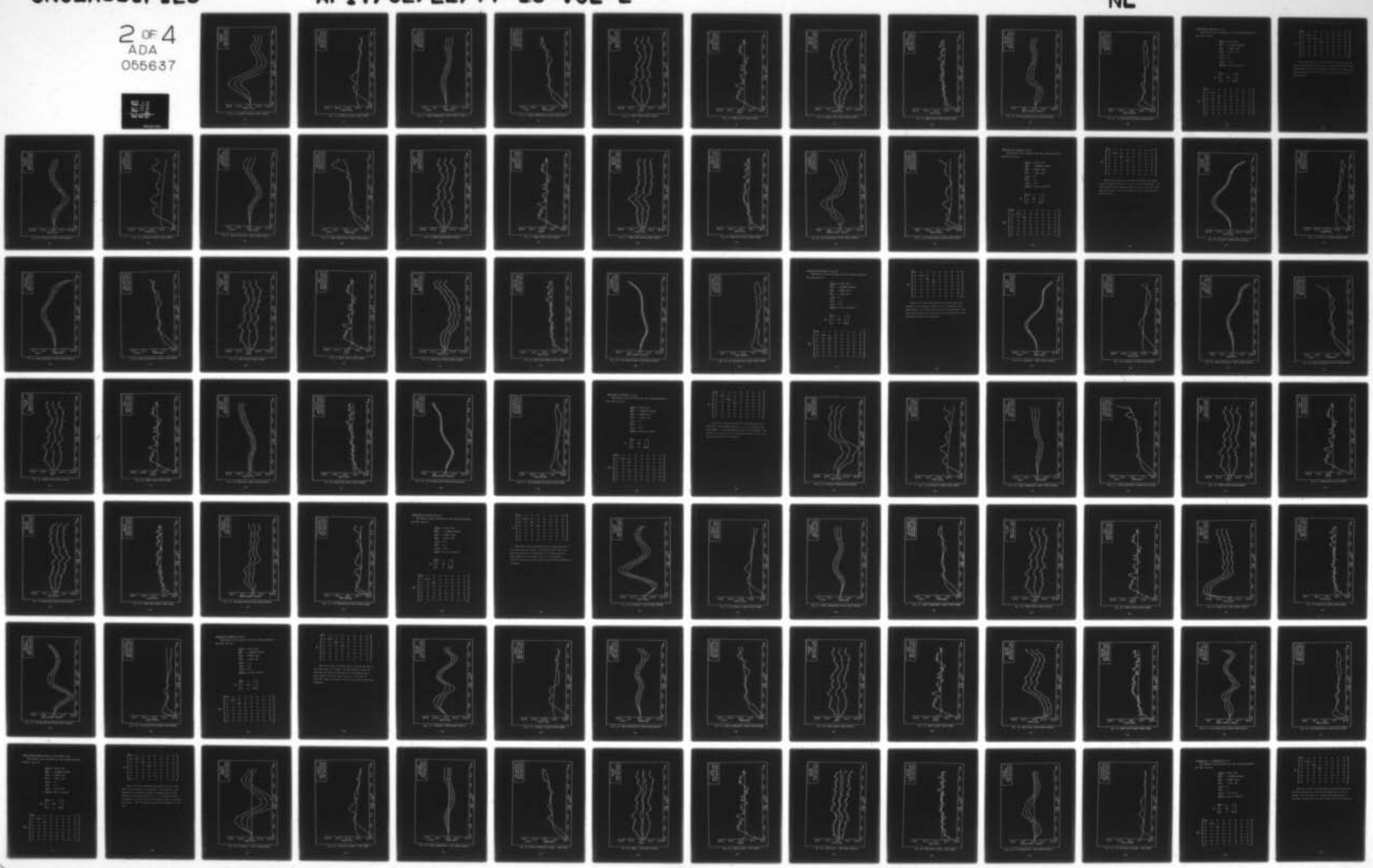

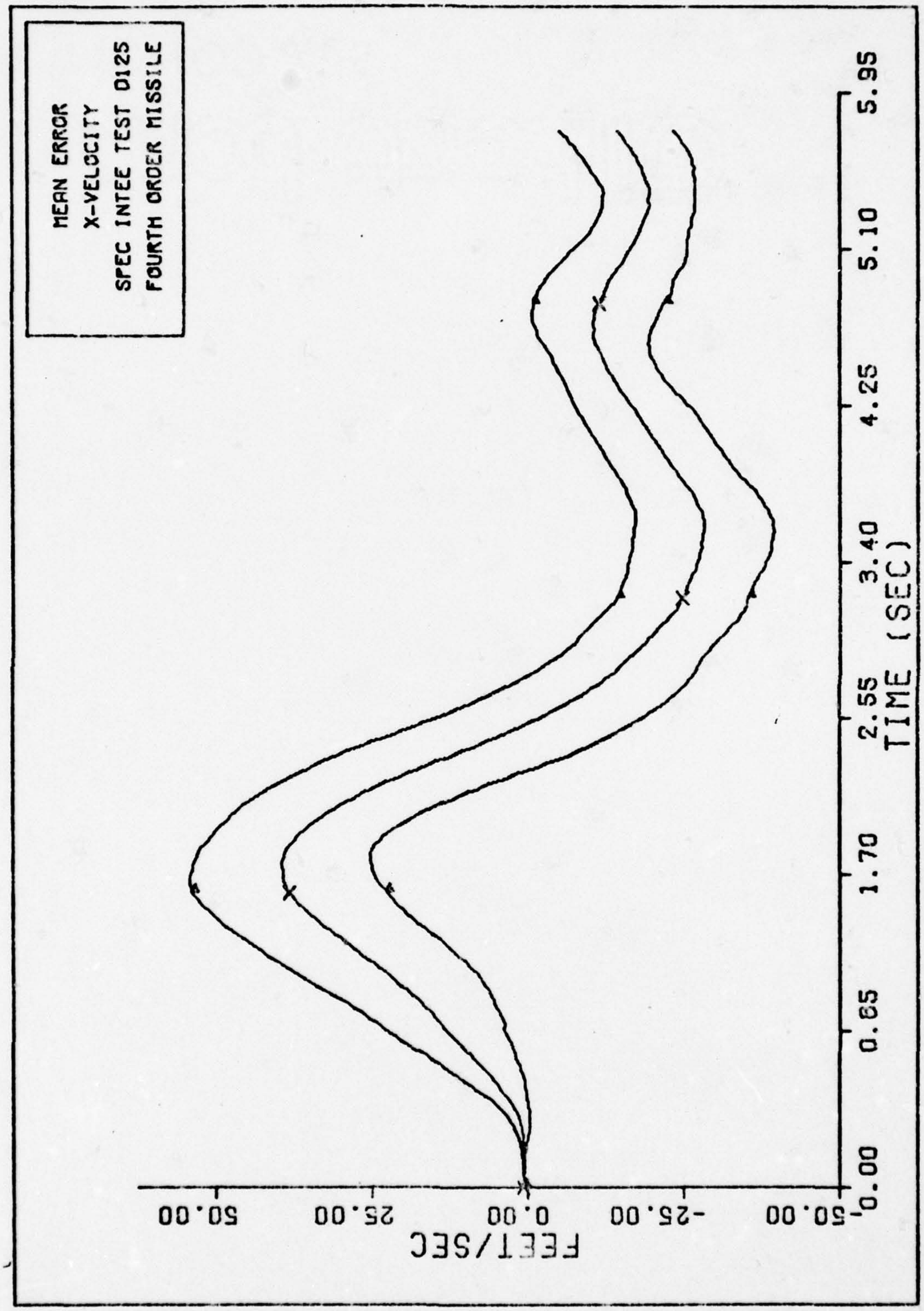

Fig. 72. X-VELOCITY FOURTH ORDER MISSILE

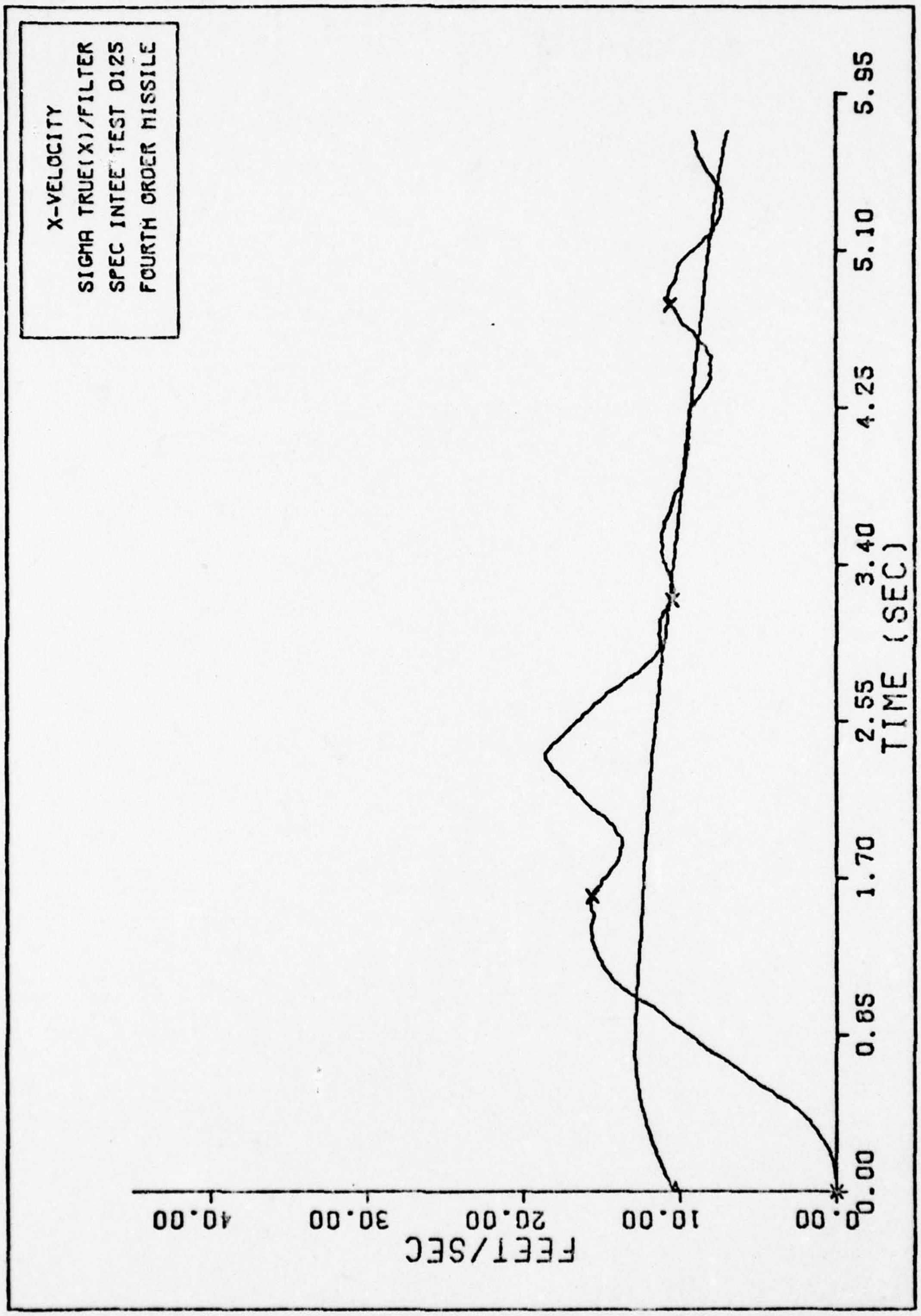

Fig. 73. X-VELOCITY SIGMAS FOURTH ORDER

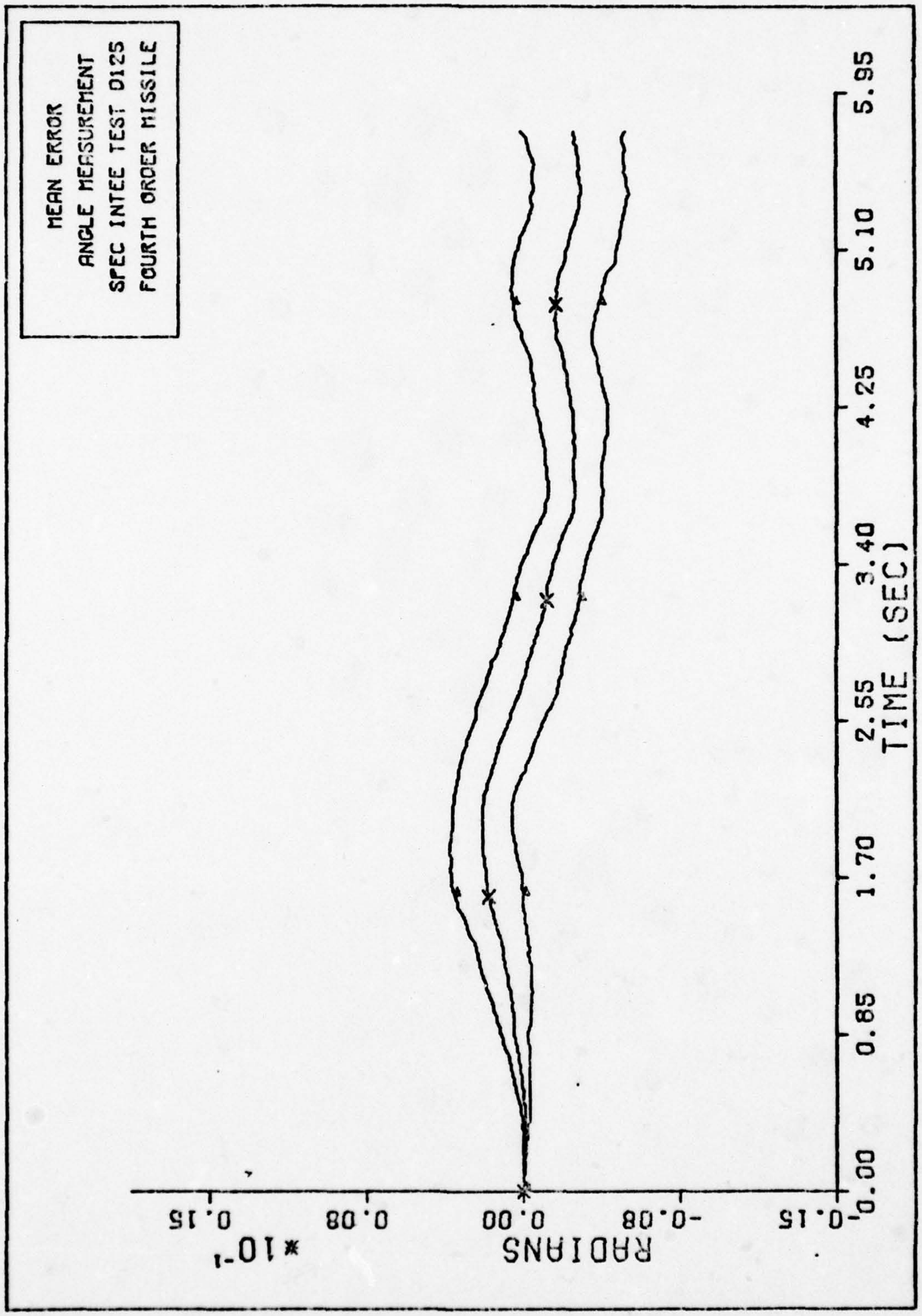

Fig. 74. ANGLE MEASUREMENT FOURTH ORDER MISSILE

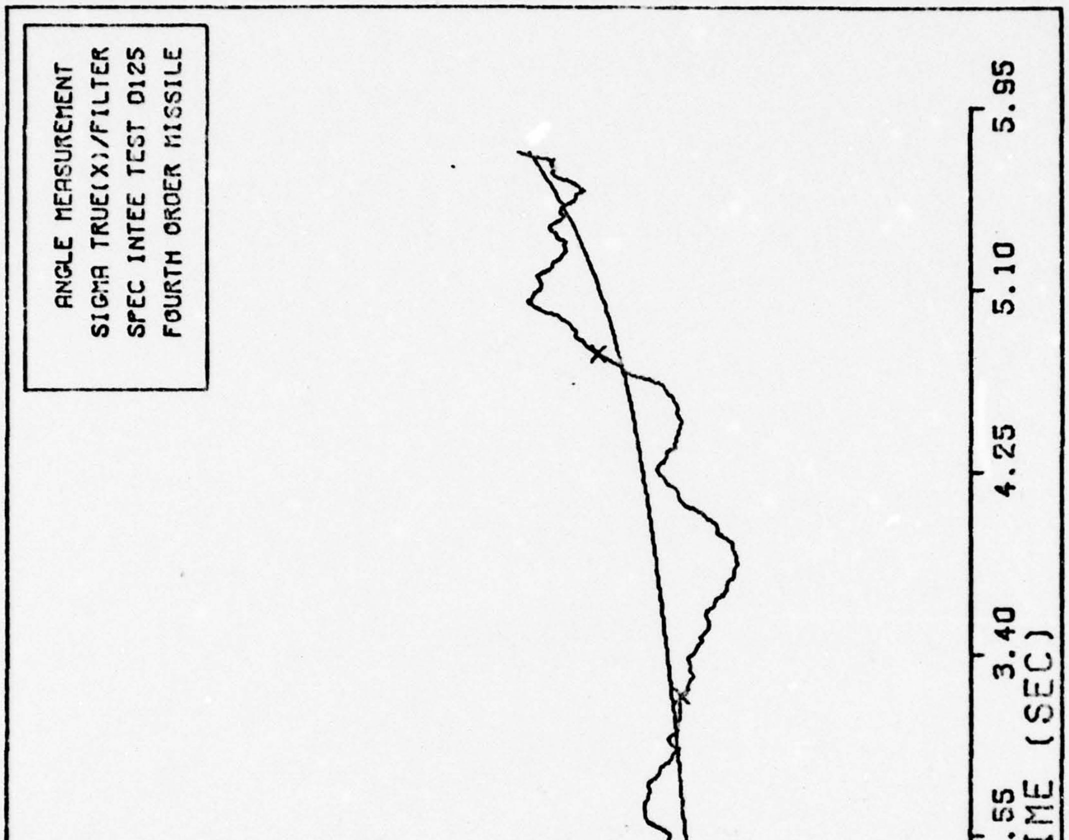

Fig. 75. ANGLE MEASUREMENT SIGMAS FOURTH ORDER

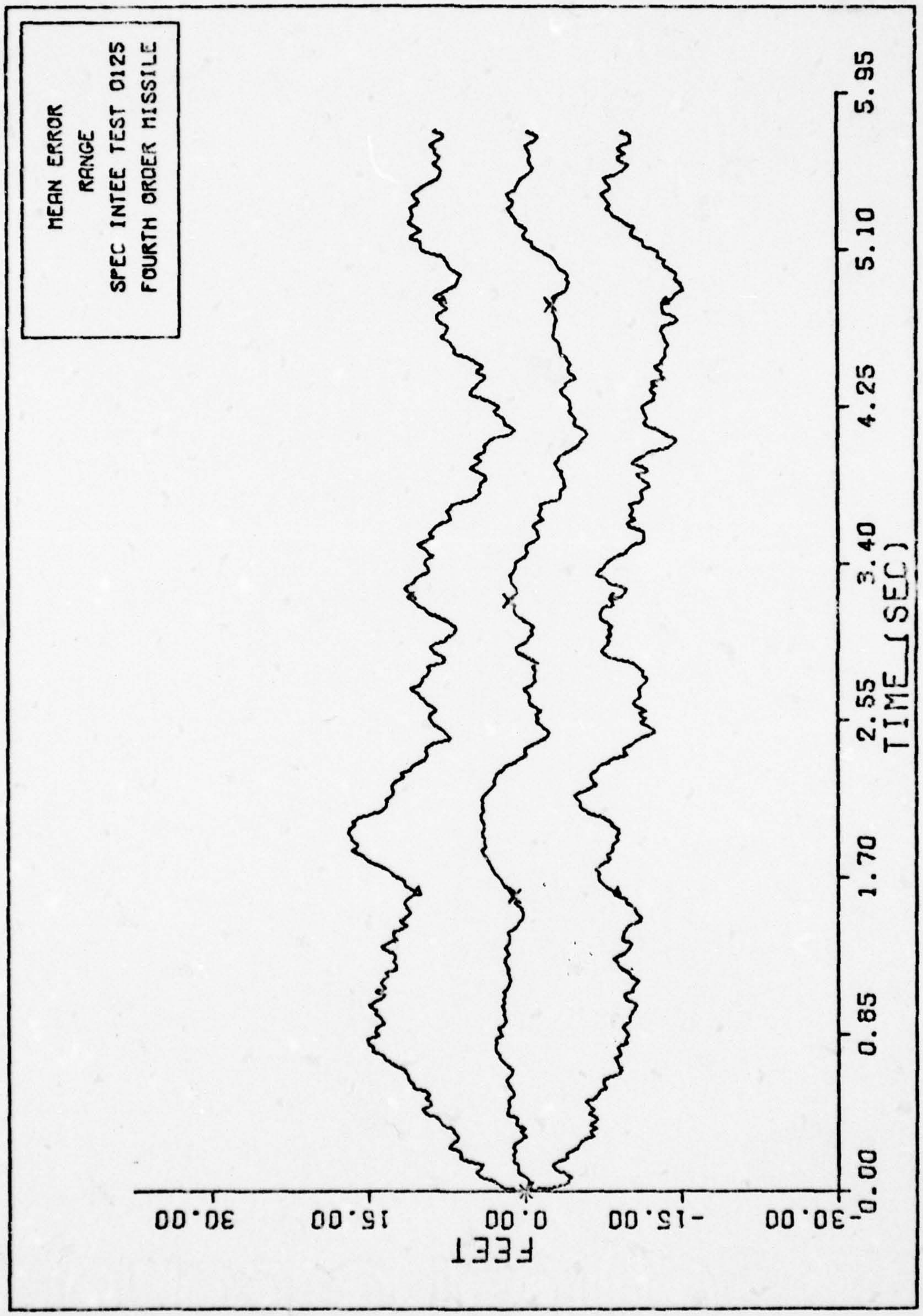

Fig. 76. RANGE FOURTH ORDER MISSILE

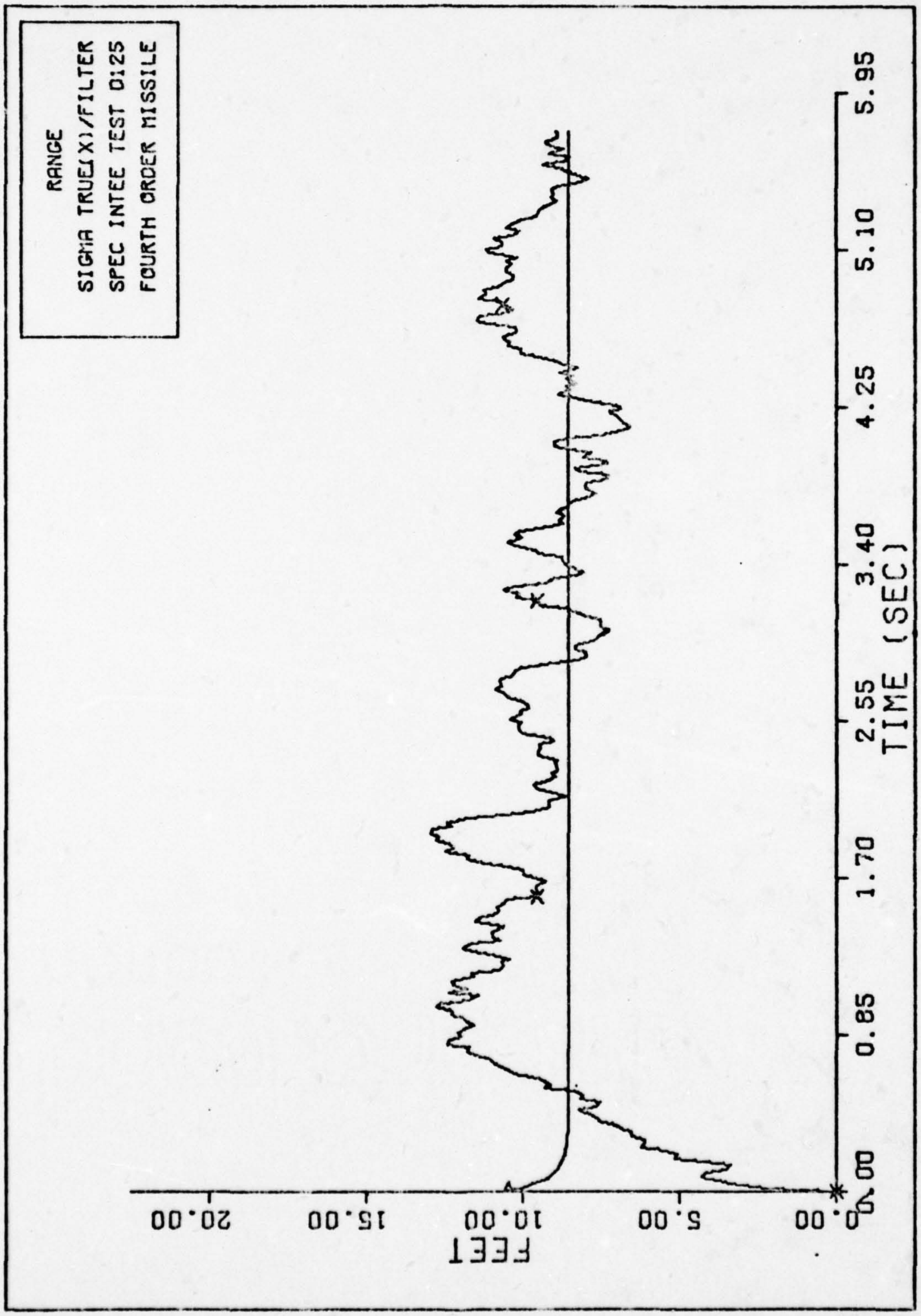

Fig. 77. RANGE SIGMAS FOURTH ORDER

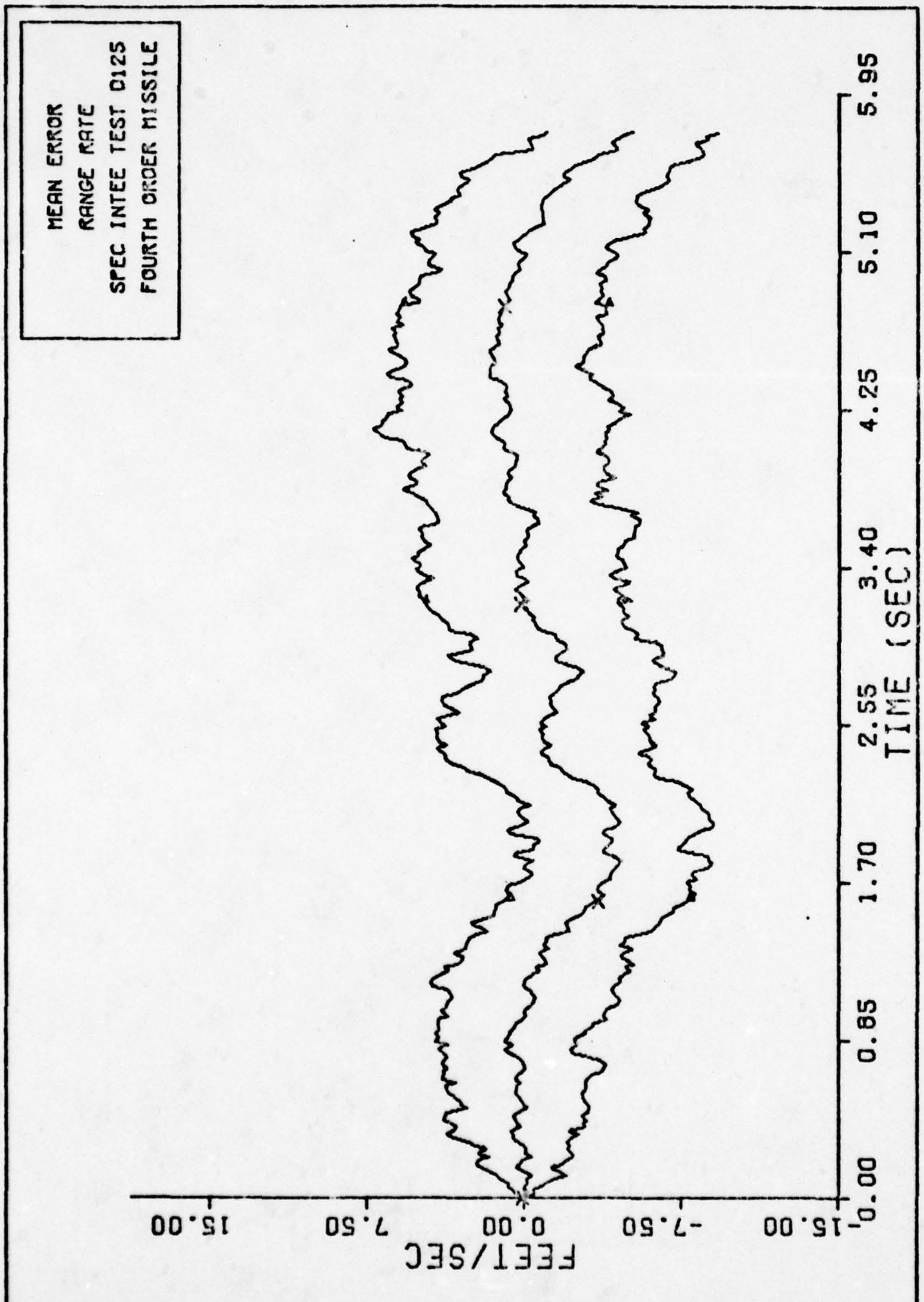

Fig. 78. RANGE RATE FOURTH ORDER MISSILE

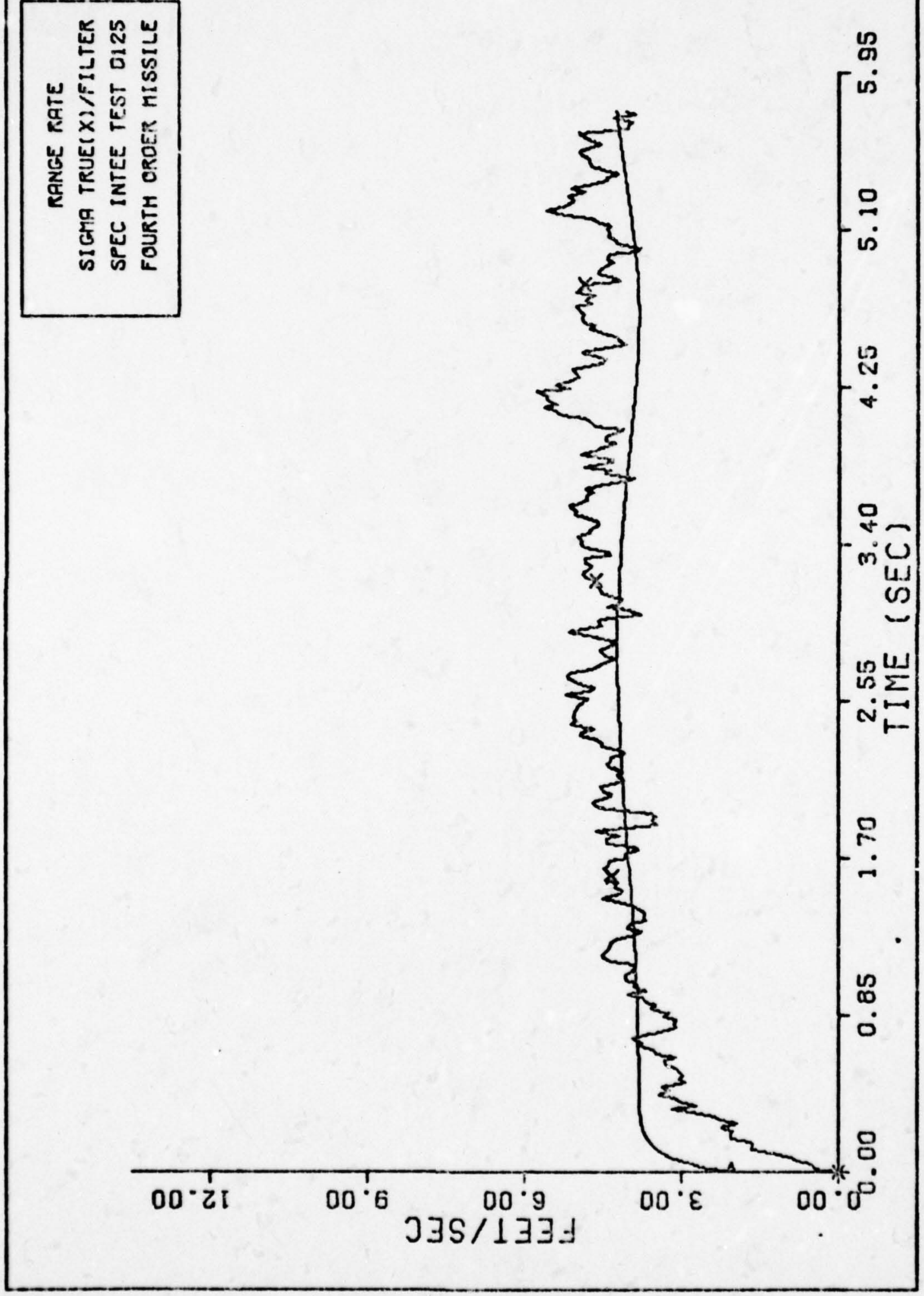

Fig. 79. RANGE RATE SIGMAS FOURTH ORDER

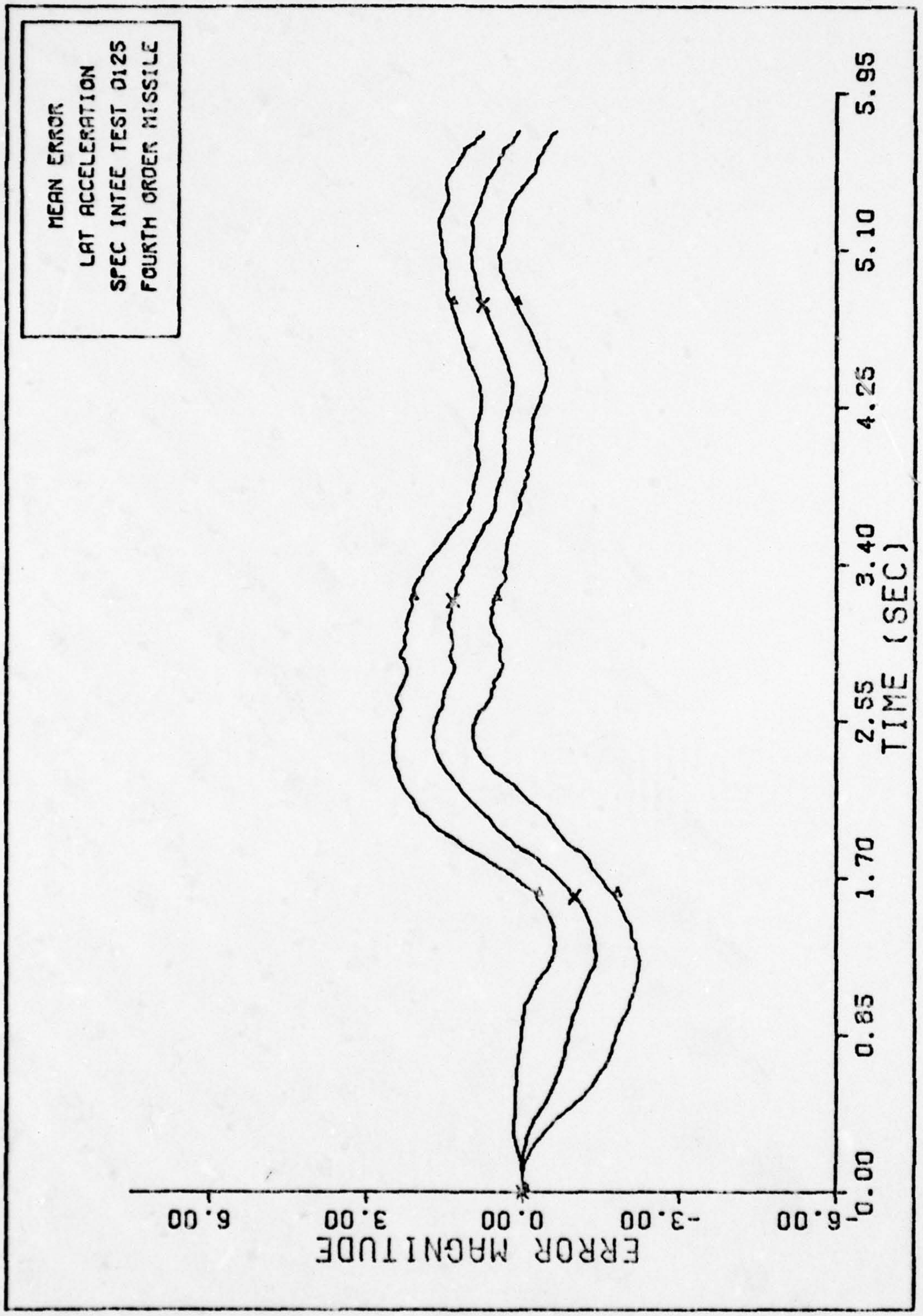

Fig. 80. LAT ACCELERATION FOURTH ORDER MISSILE

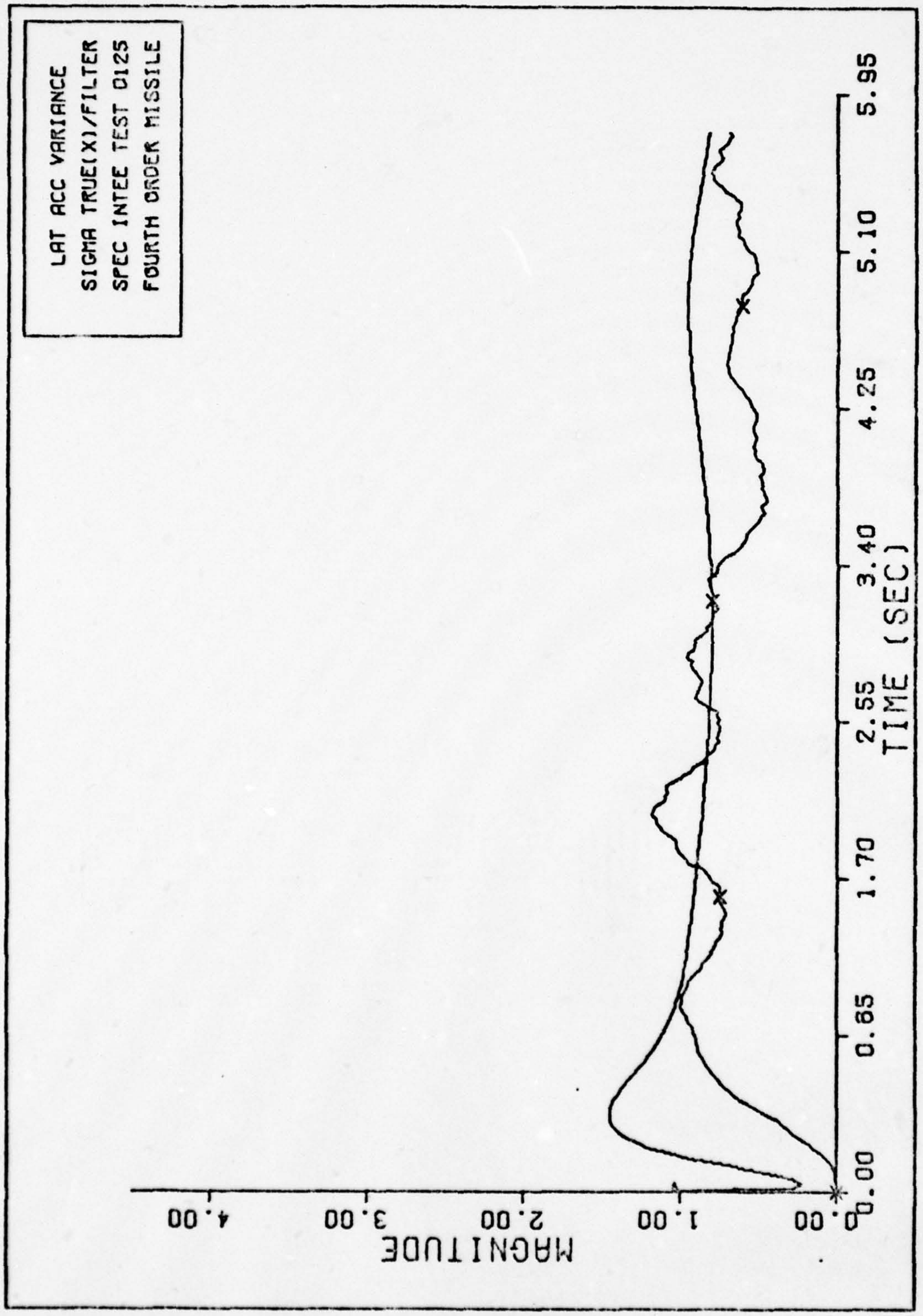

Fig. 81. LAT ACCELERATION SIGMAS FOURTH ORDER

Sensitivity Analysis (n = 6.)

The initial state estimates and the tuning parameters for this case are

$$
\begin{aligned}
V^I_{mx}(0) &= 1225.7 \text{ fps} \\
\dot{\theta}_T(0) &= 4.363345 \text{ radians} \\
R(0) &= 10000. \text{ feet} \\
\dot{R}(0) &= -2122. \text{ fps} \\
a_L(0) &= 0. \\
n(0) &= 4.5 \\
\tau_f(0) &= \text{N/A} \\
M/S(0) &= 29.197 \text{ slugs/ft}^2
\end{aligned}
$$

$$
\underline{R} = \begin{bmatrix} 4.E\text{-}5 & 0. & 0. \\ 0. & 500. & 0. \\ 0. & 0. & 100. \end{bmatrix}
$$

$$
\underline{P}_0 = \begin{bmatrix}
100. & 0. & 0. & 0. & 0. & 0. & 0. & 0. \\
0. & 1.E\text{-}8 & 0. & 0. & 0. & 0. & 0. & 0. \\
0. & 0. & 101. & 0. & 0. & 0. & 0. & 0. \\
0. & 0. & 0. & 4. & 0. & 0. & 0. & 0. \\
0. & 0. & 0. & 0. & 1. & 0. & 0. & 0. \\
0. & 0. & 0. & 0. & 0. & 0. & 0. & 0. \\
0. & 0. & 0. & 0. & 0. & 0. & 0. & 0. \\
0. & 0. & 0. & 0. & 0. & 0. & 0. & 0.
\end{bmatrix}
$$

$$\underline{Q} = \begin{bmatrix} 101. & 0. & 0. & 0. & 0. & 0. & 0. & 0. \\ 0. & 1.E{-6} & 0. & 0. & 0. & 0. & 0. & 0. \\ 0. & 0. & 500. & 0. & 0. & 0. & 0. & 0. \\ 0. & 0. & 0. & 100. & 0. & 0. & 0. & 0. \\ 0. & 0. & 0. & 0. & 5. & 0. & 0. & 0. \\ 0. & 0. & 0. & 0. & 0. & 0. & 0. & 0. \\ 0. & 0. & 0. & 0. & 0. & 0. & 0. & 0. \\ 0. & 0. & 0. & 0. & 0. & 0. & 0. & 0. \end{bmatrix}$$

This set of plots was generated by setting the proportional navigation constant, n, to 6 in the truth model. The fourth order filter was used with n set to 4.5 in the filter. Only the dynamic states of the missile model were estimated by the filter.

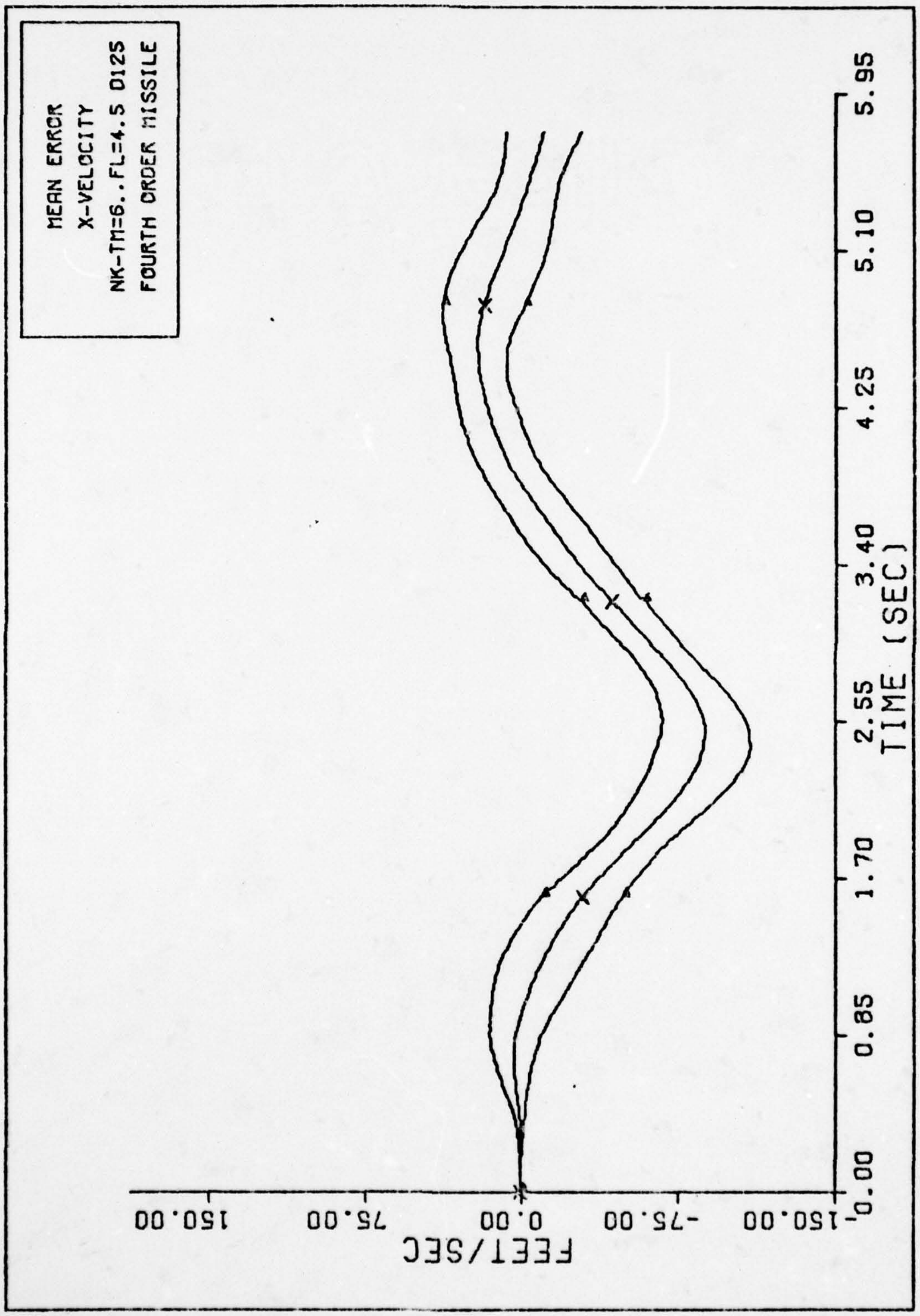

Fig. 82. X-VELOCITY FOURTH ORDER MISSILE

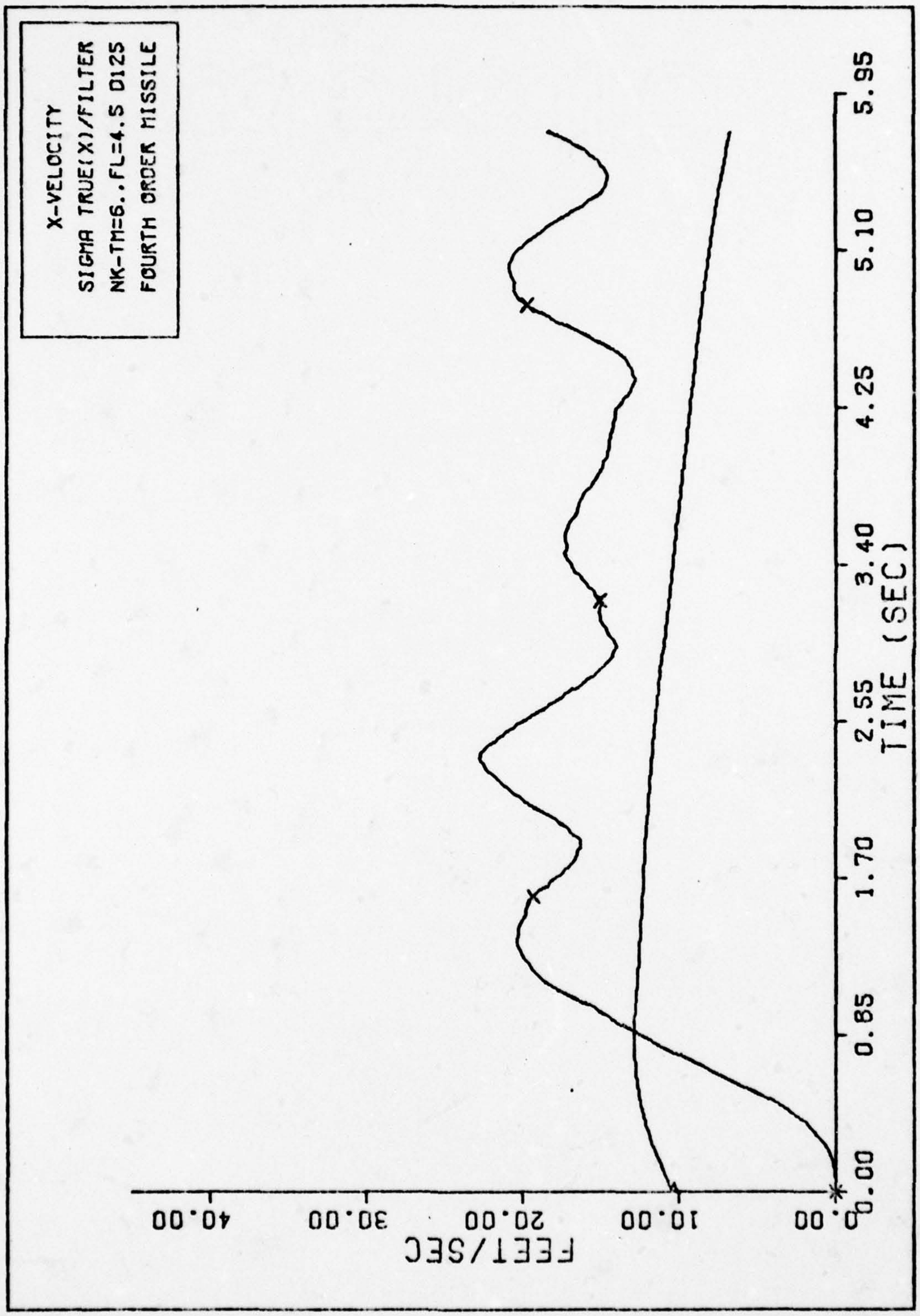

Fig. 83. X-VELOCITY SIGMAS FOURTH ORDER

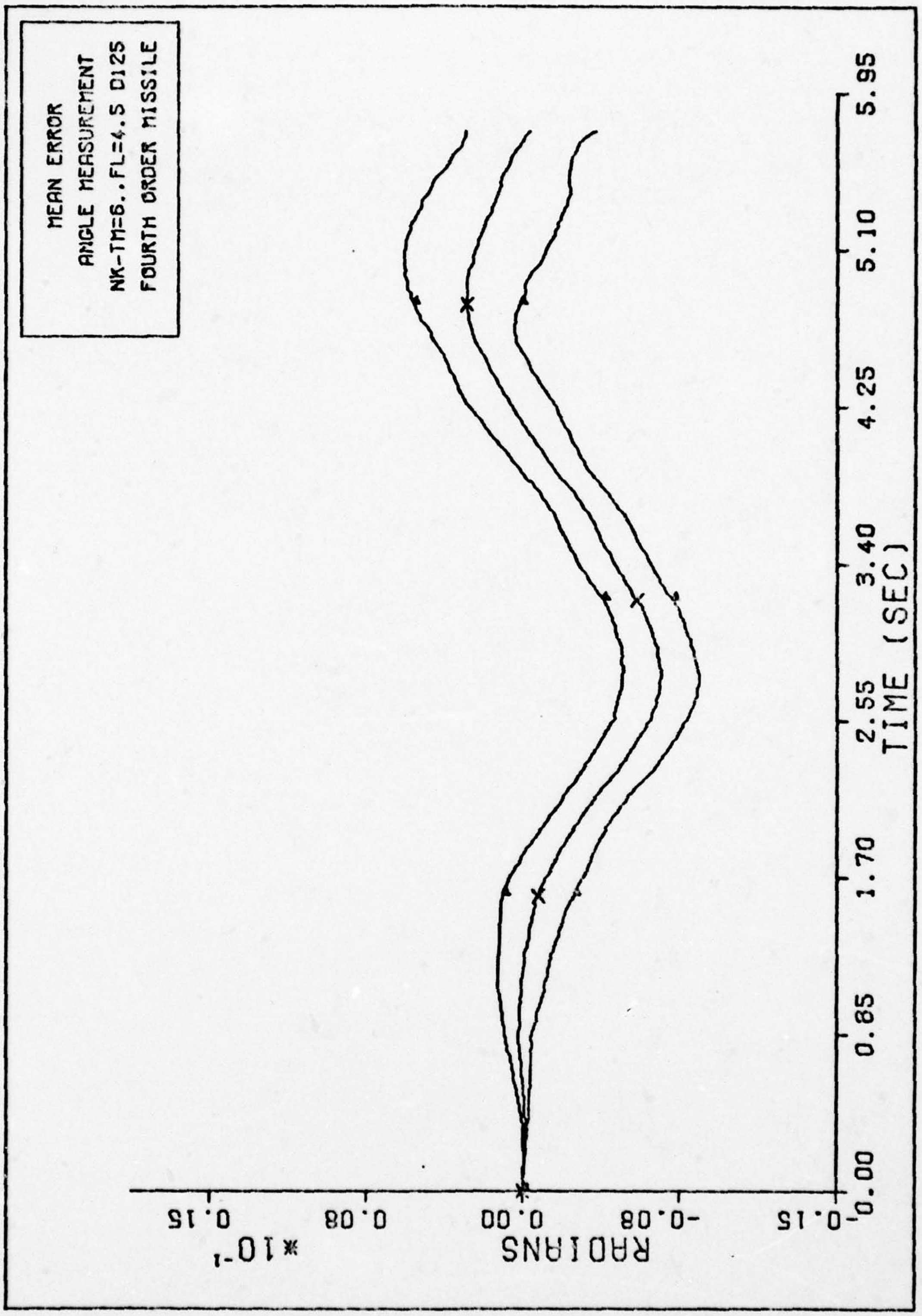

Fig. 84. ANGLE MEASUREMENT FOURTH ORDER MISSILE

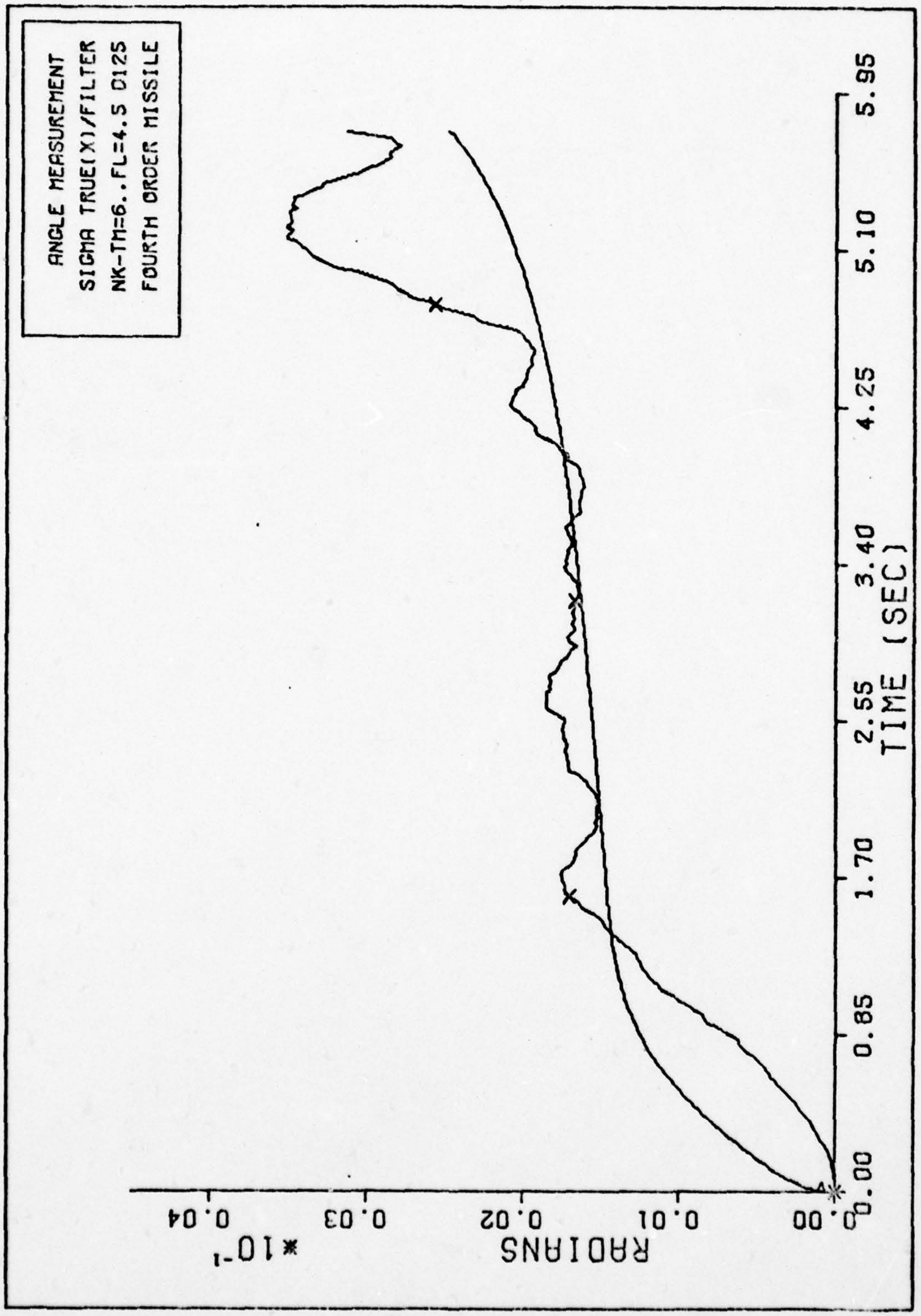

Fig. 85. ANGLE MEASUREMENT SIGMAS FOURTH ORDER

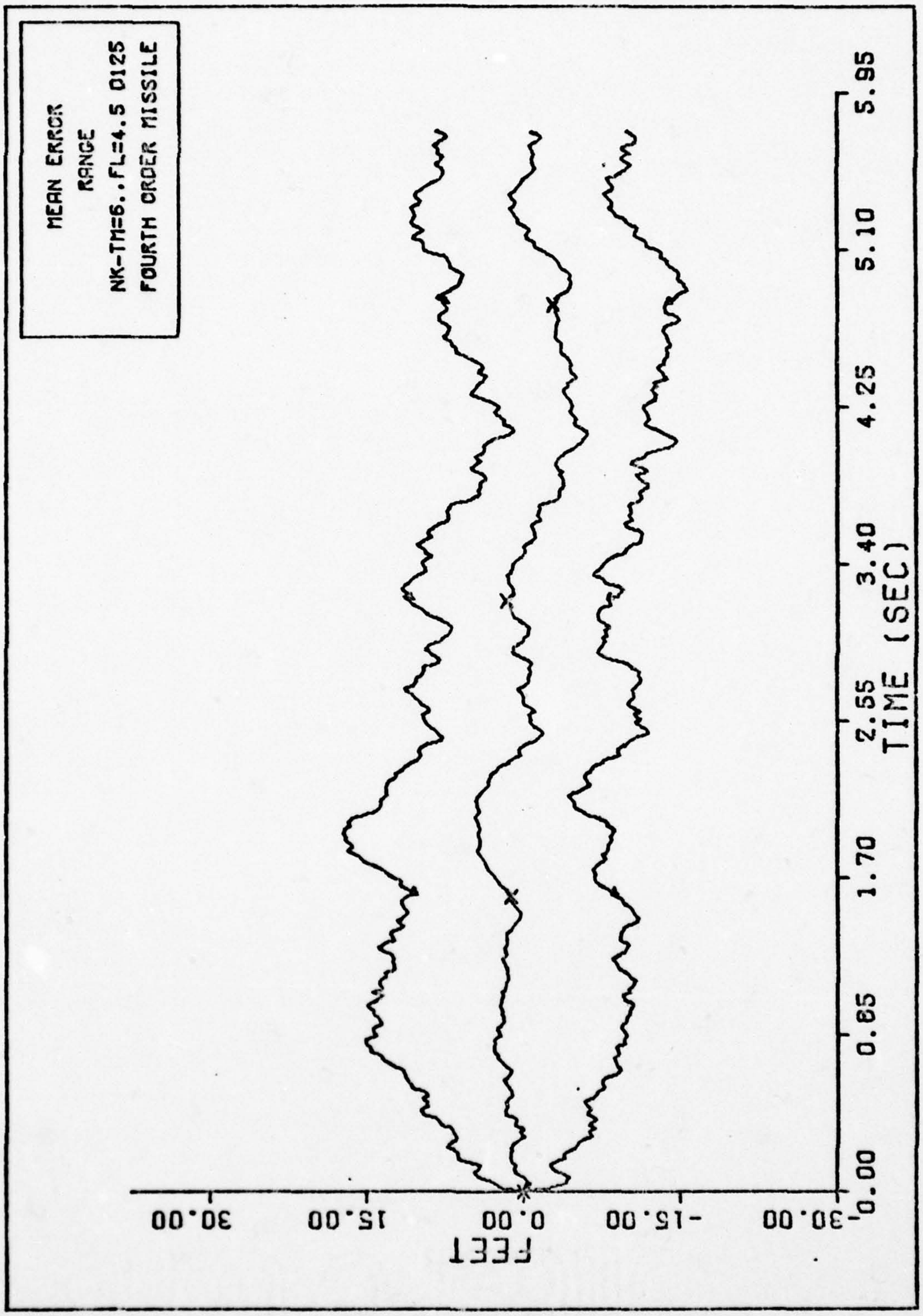

Fig. 86. RANGE FOURTH ORDER MISSILE

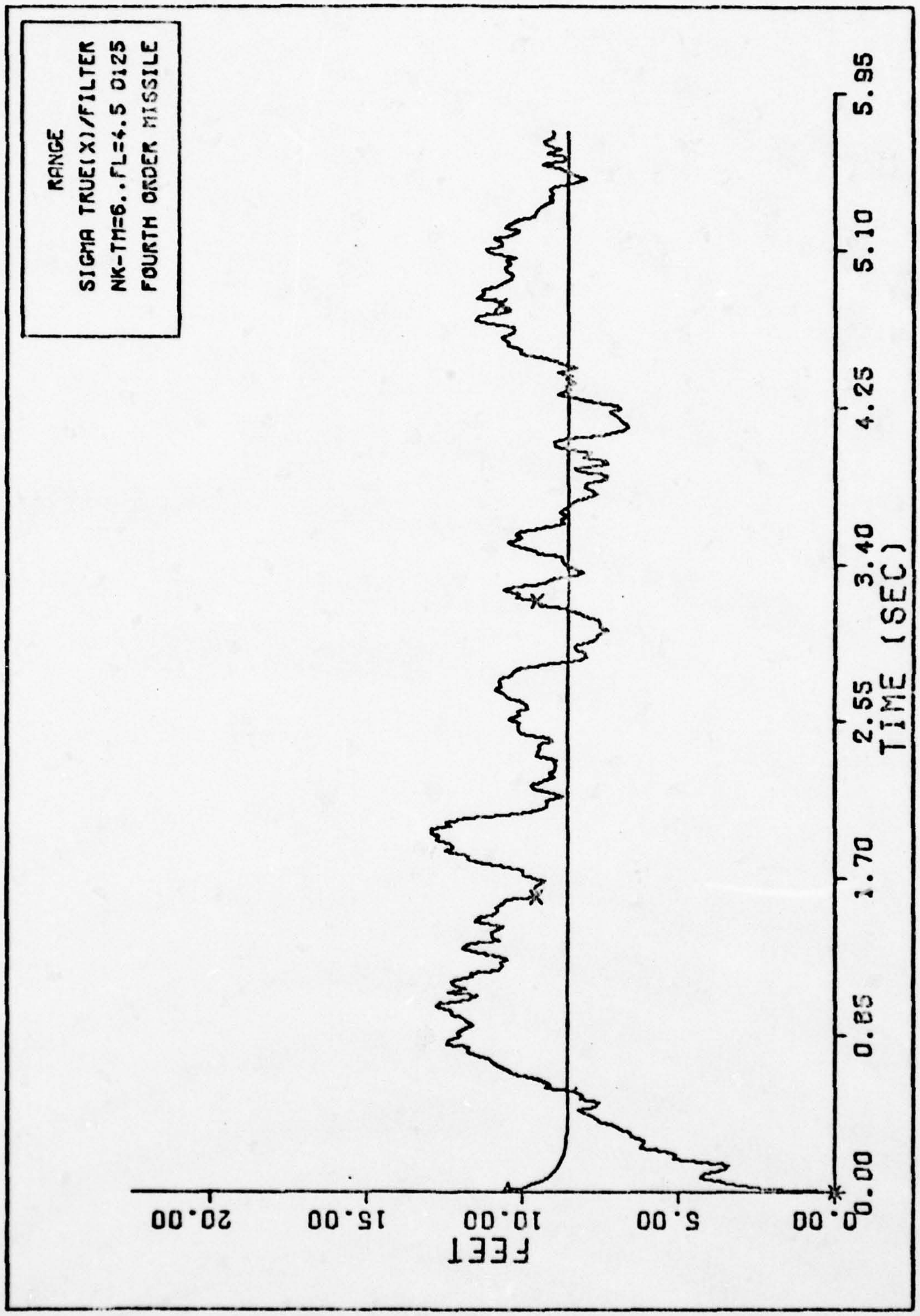

Fig. 87. RANGE SIGMAS FOURTH ORDER

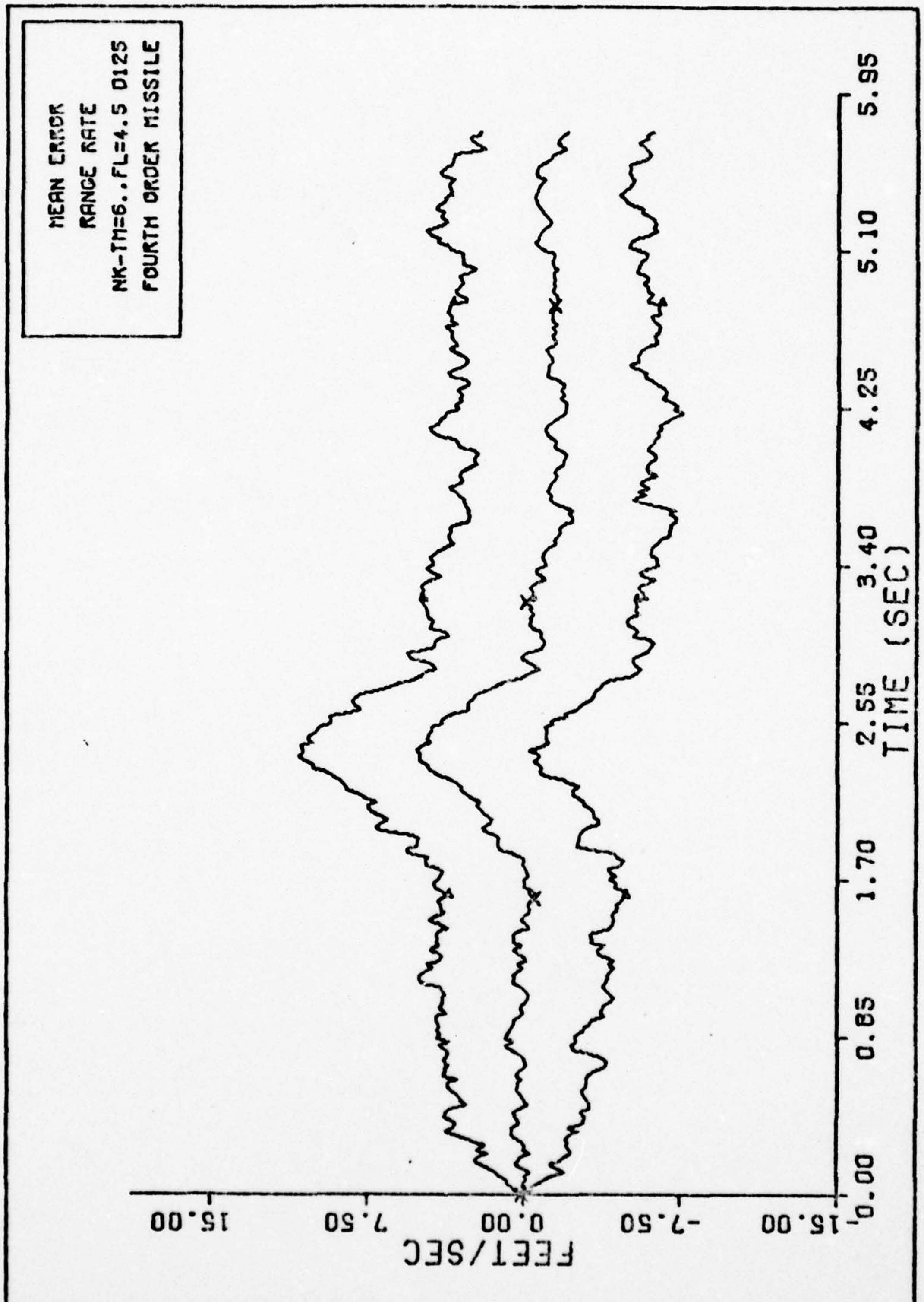

Fig. 88. RANGE RATE FOURTH ORDER MISSILE

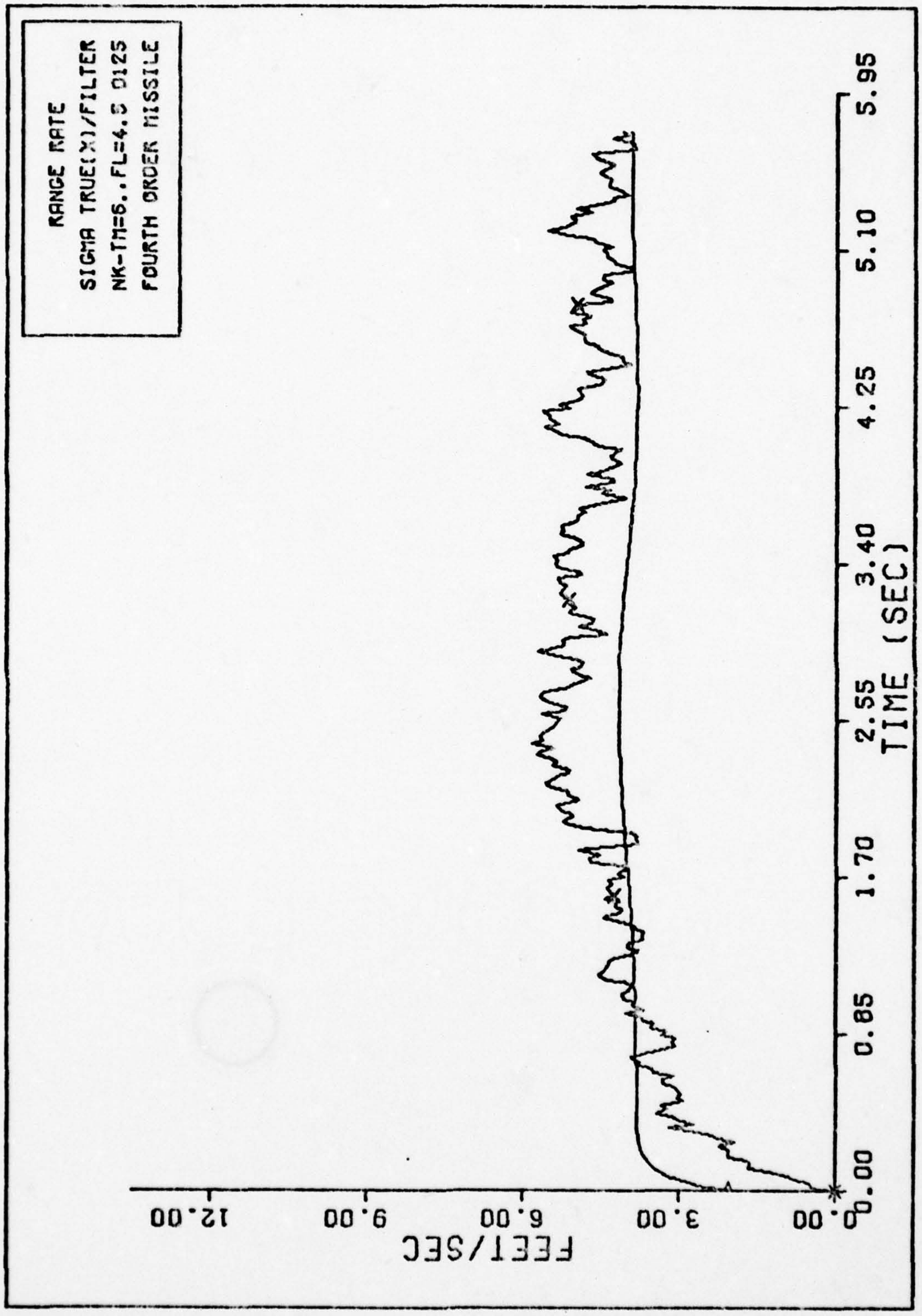

Fig. 89. RANGE RATE SIGMAS FOURTH ORDER

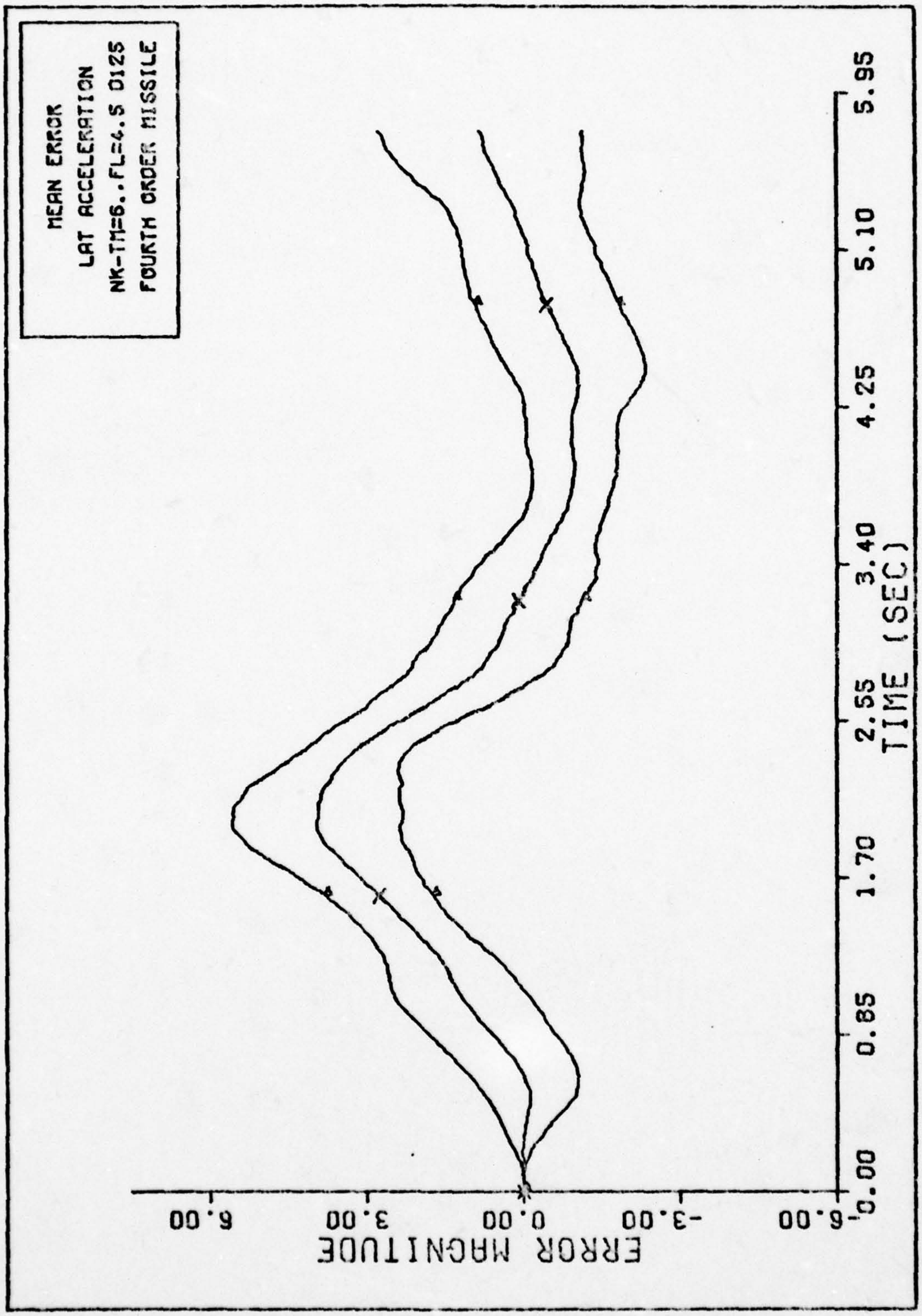

Fig. 90. LAT ACCELERATION FOURTH ORDER MISSILE

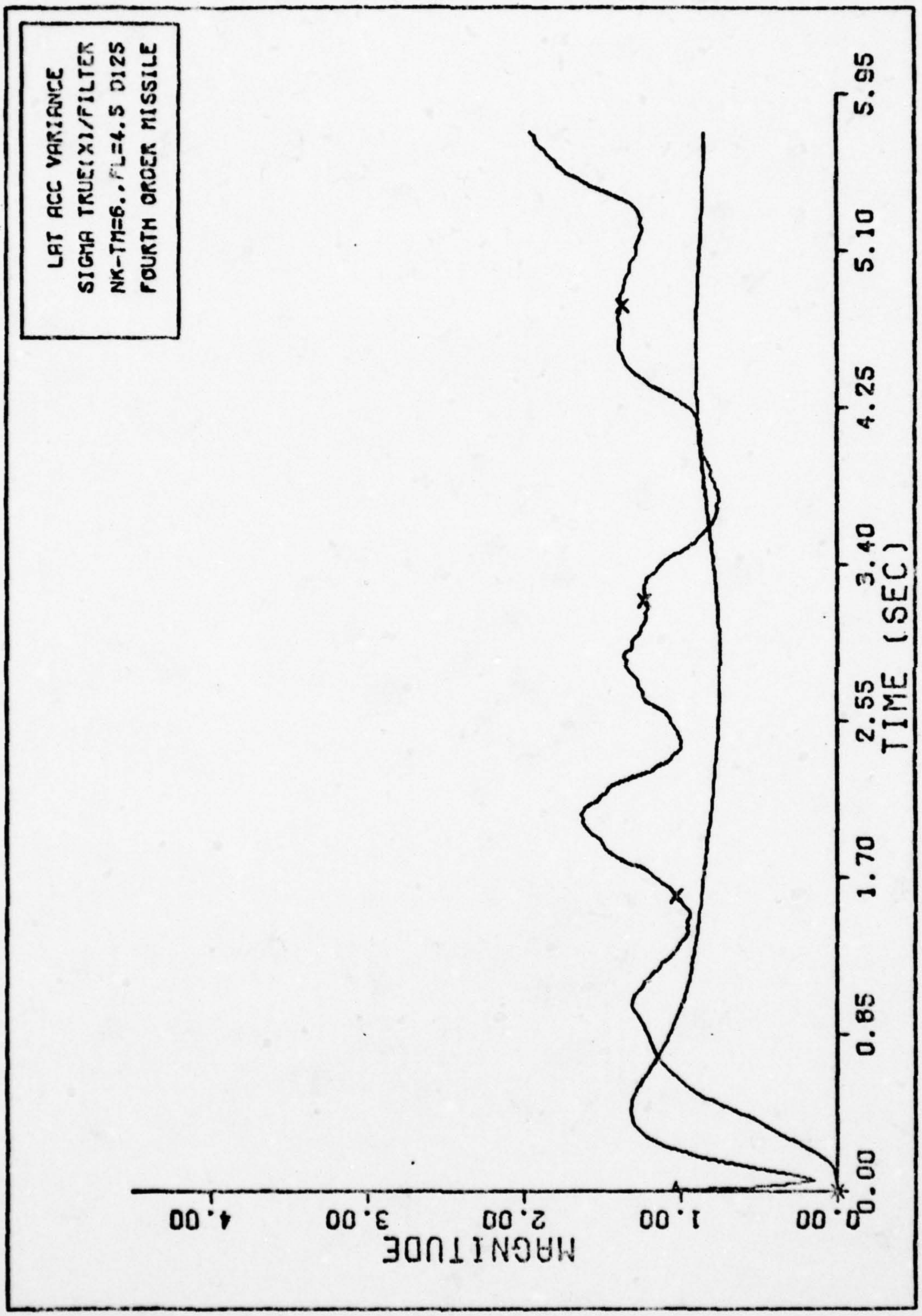

Fig. 91. LAT ACCELERATION SIGMAS FOURTH ORDER

Sensitivity Analysis ($n = 3.$)

The initial state estimates and the tuning parameters for this case are

$$
\begin{aligned}
V_{mx}^{I}(0) &= 1225.7 \text{ fps} \\
\dot{\theta}_{T}(0) &= 4.363345 \text{ radians} \\
R(0) &= 10000. \text{ feet} \\
\dot{R}(0) &= -2122. \text{ fps} \\
a_{L}(0) &= 0. \\
n(0) &= 4.5 \\
\tau_{f}(0) &= \text{N/A} \\
M/S(0) &= 29.197 \text{ slugs/ft}^2
\end{aligned}
$$

$$
\underline{R} = \begin{bmatrix} 4.E-5 & 0. & 0. \\ 0. & 500. & 0. \\ 0. & 0. & 100. \end{bmatrix}
$$

$$
\underline{P}_0 = \begin{bmatrix}
100. & 0. & 0. & 0. & 0. & 0. & 0. & 0. \\
0. & 1.E-8 & 0. & 0. & 0. & 0. & 0. & 0. \\
0. & 0. & 101. & 0. & 0. & 0. & 0. & 0. \\
0. & 0. & 0. & 4. & 0. & 0. & 0. & 0. \\
0. & 0. & 0. & 0. & 1. & 0. & 0. & 0. \\
0. & 0. & 0. & 0. & 0. & 0. & 0. & 0. \\
0. & 0. & 0. & 0. & 0. & 0. & 0. & 0. \\
0. & 0. & 0. & 0. & 0. & 0. & 0. & 0.
\end{bmatrix}
$$

$$
\underline{Q} = \begin{bmatrix}
101. & 0. & 0. & 0. & 0. & 0. & 0. & 0. \\
0. & 1.E-6 & 0. & 0. & 0. & 0. & 0. & 0. \\
0. & 0. & 500. & 0. & 0. & 0. & 0. & 0. \\
0. & 0. & 0. & 100. & 0. & 0. & 0. & 0. \\
0. & 0. & 0. & 0. & 5. & 0. & 0. & 0. \\
0. & 0. & 0. & 0. & 0. & 0. & 0. & 0. \\
0. & 0. & 0. & 0. & 0. & 0. & 0. & 0. \\
0. & 0. & 0. & 0. & 0. & 0. & 0. & 0.
\end{bmatrix}
$$

This set of plots was generated by setting the proportional navigation constant, n, to 3 in the truth model. The fourth order filter was used with n set to 4.5 in the filter. Only the dynamic states of the missile model were estimated by the filter.

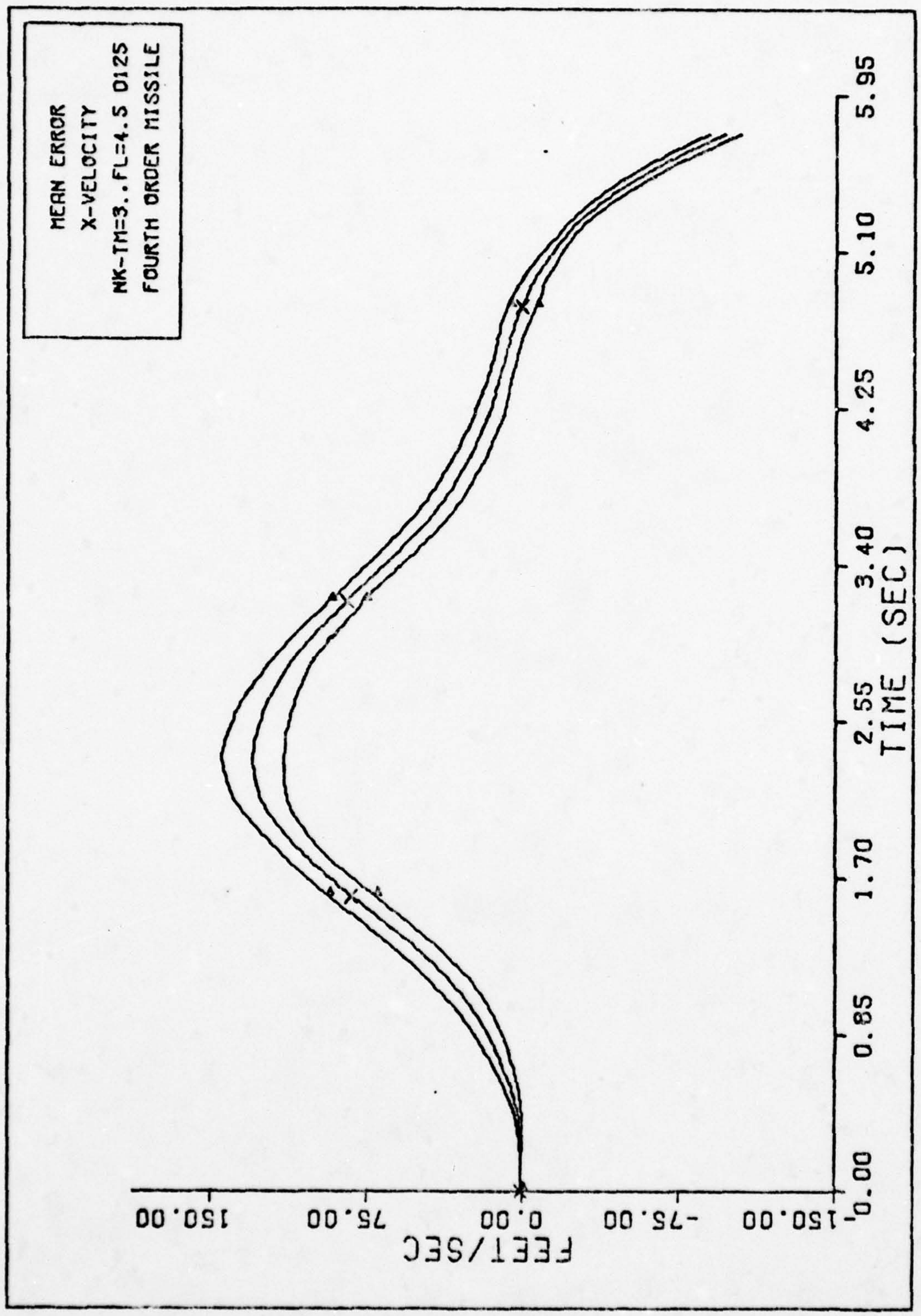

Fig. 92. X-VELOCITY FOURTH ORDER MISSILE

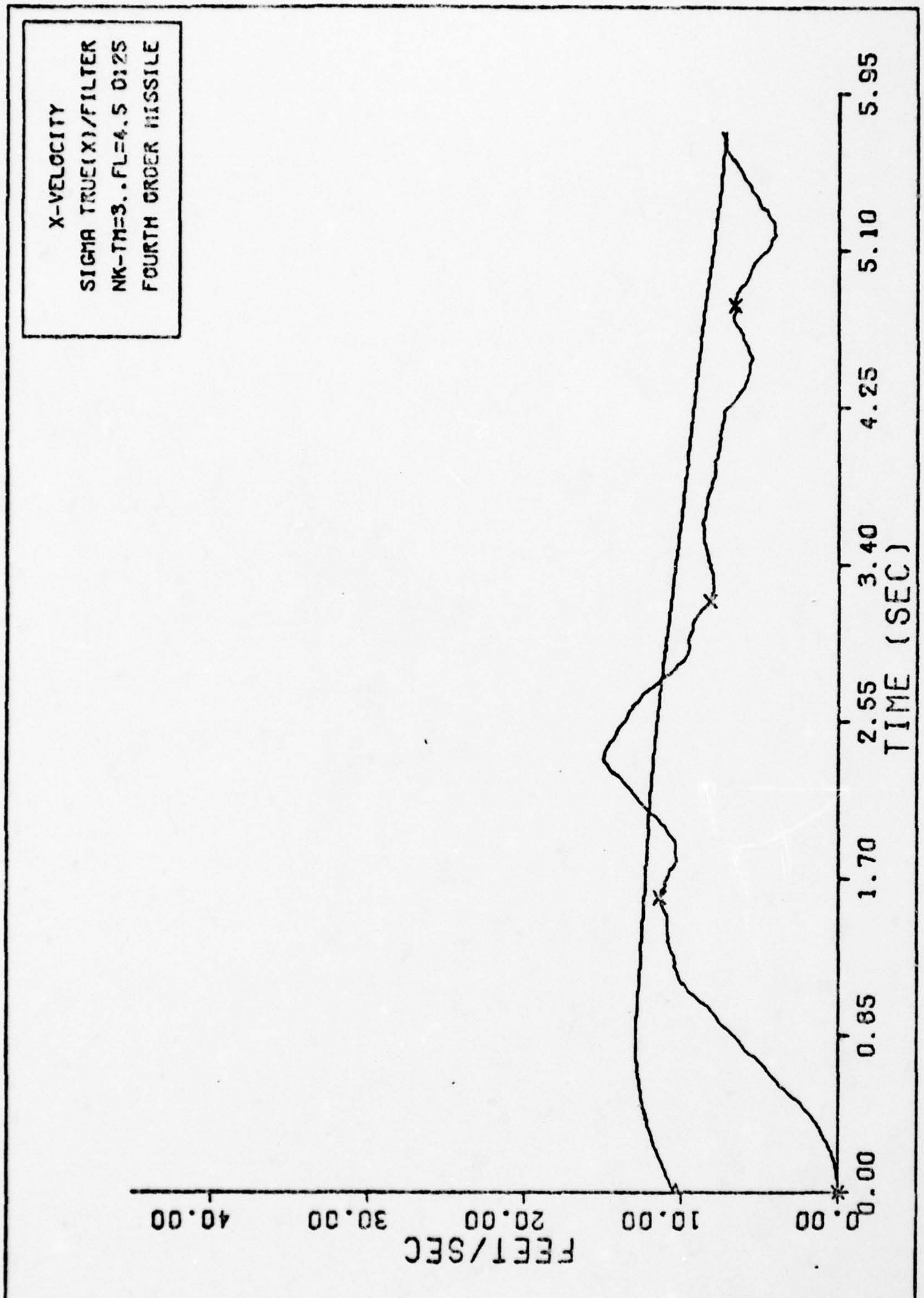

Fig. 93. X-VELOCITY SIGMAS FOURTH ORDER

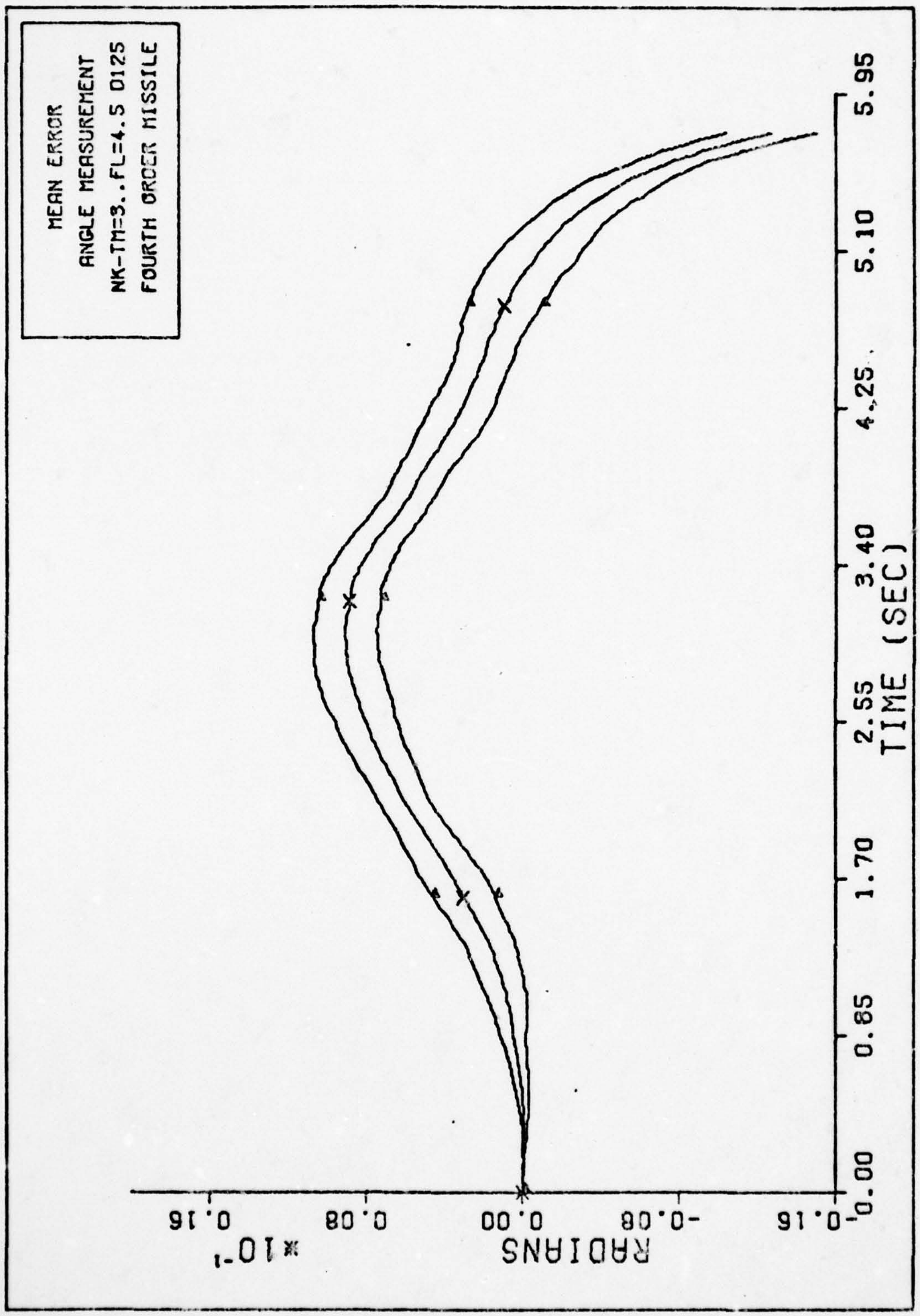

Fig. 94. ANGLE MEASUREMENT FOURTH ORDER MISSILE

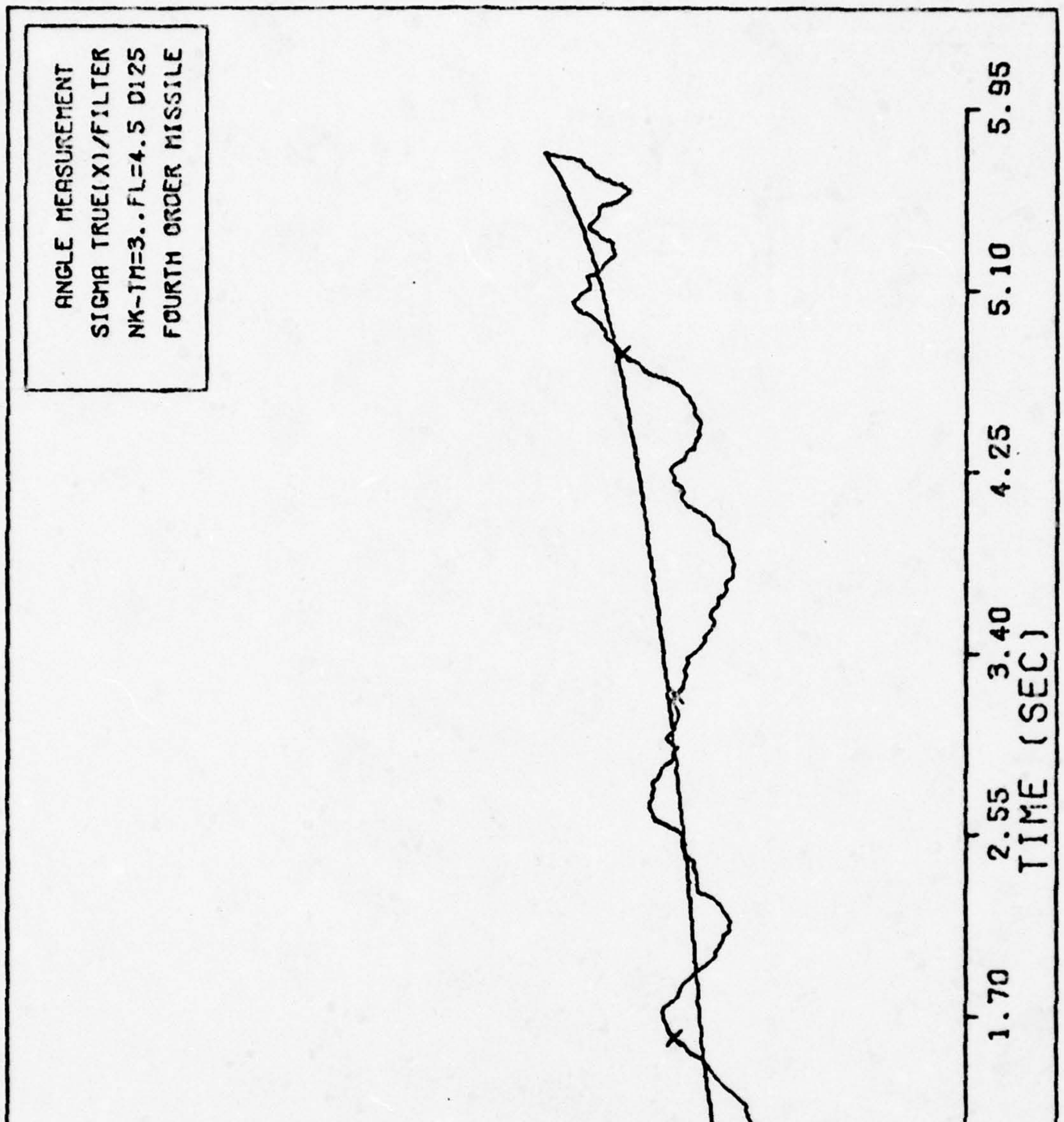

Fig. 95. ANGLE MEASUREMENT SIGMAS FOURTH ORDER

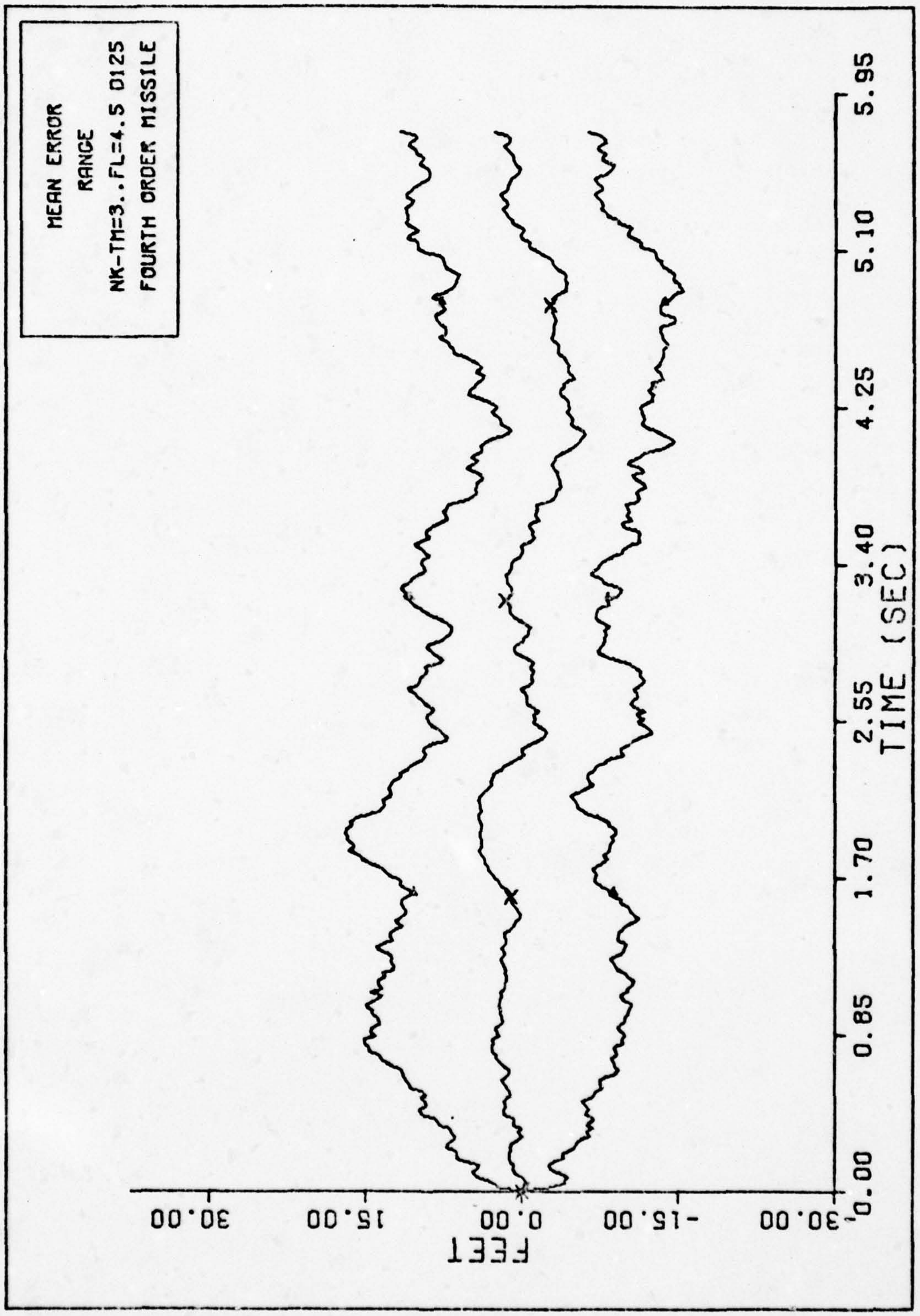

Fig. 96. RANGE FOURTH ORDER MISSILE

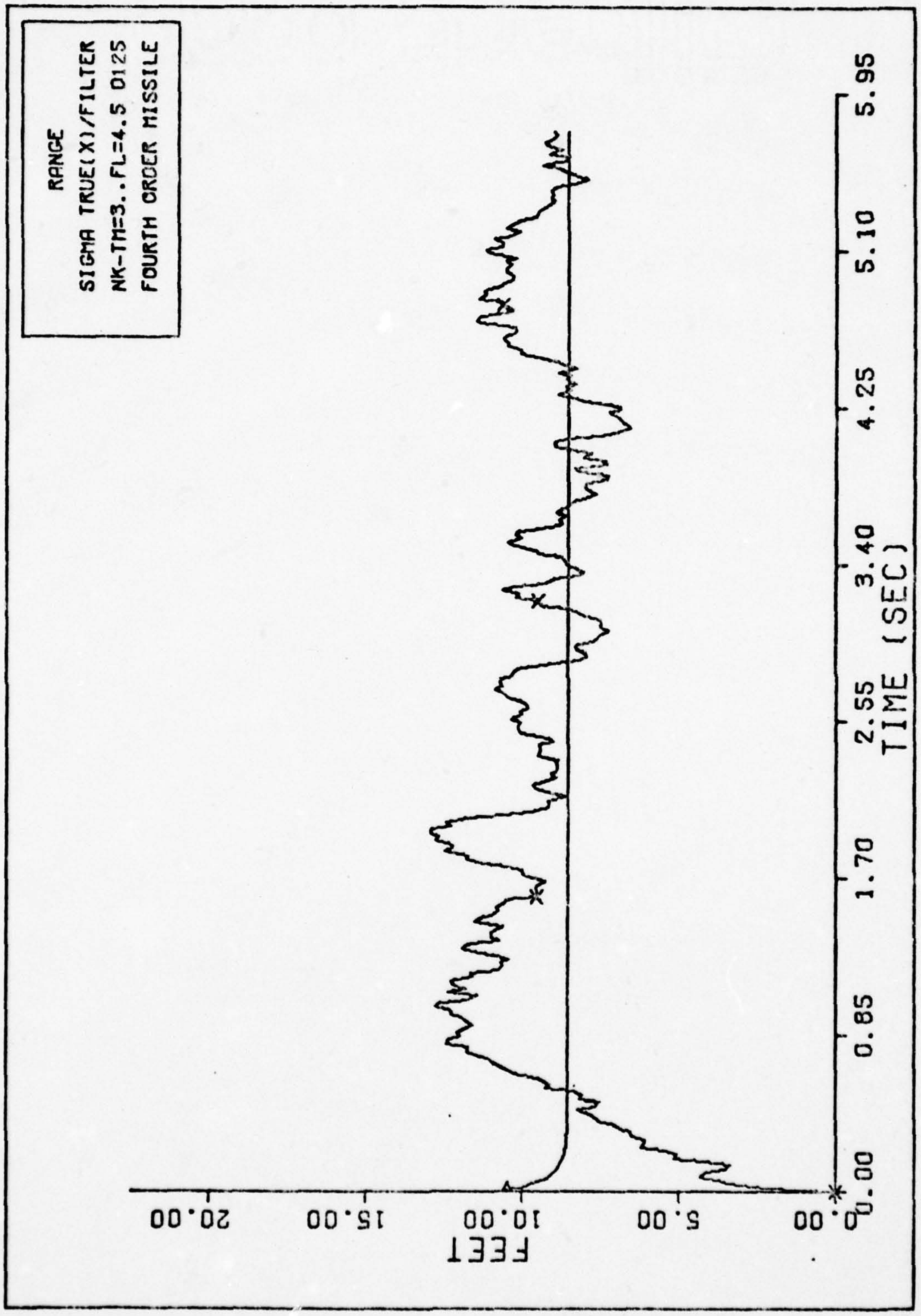

Fig. 97. RANGE SIGMAS FOURTH ORDER

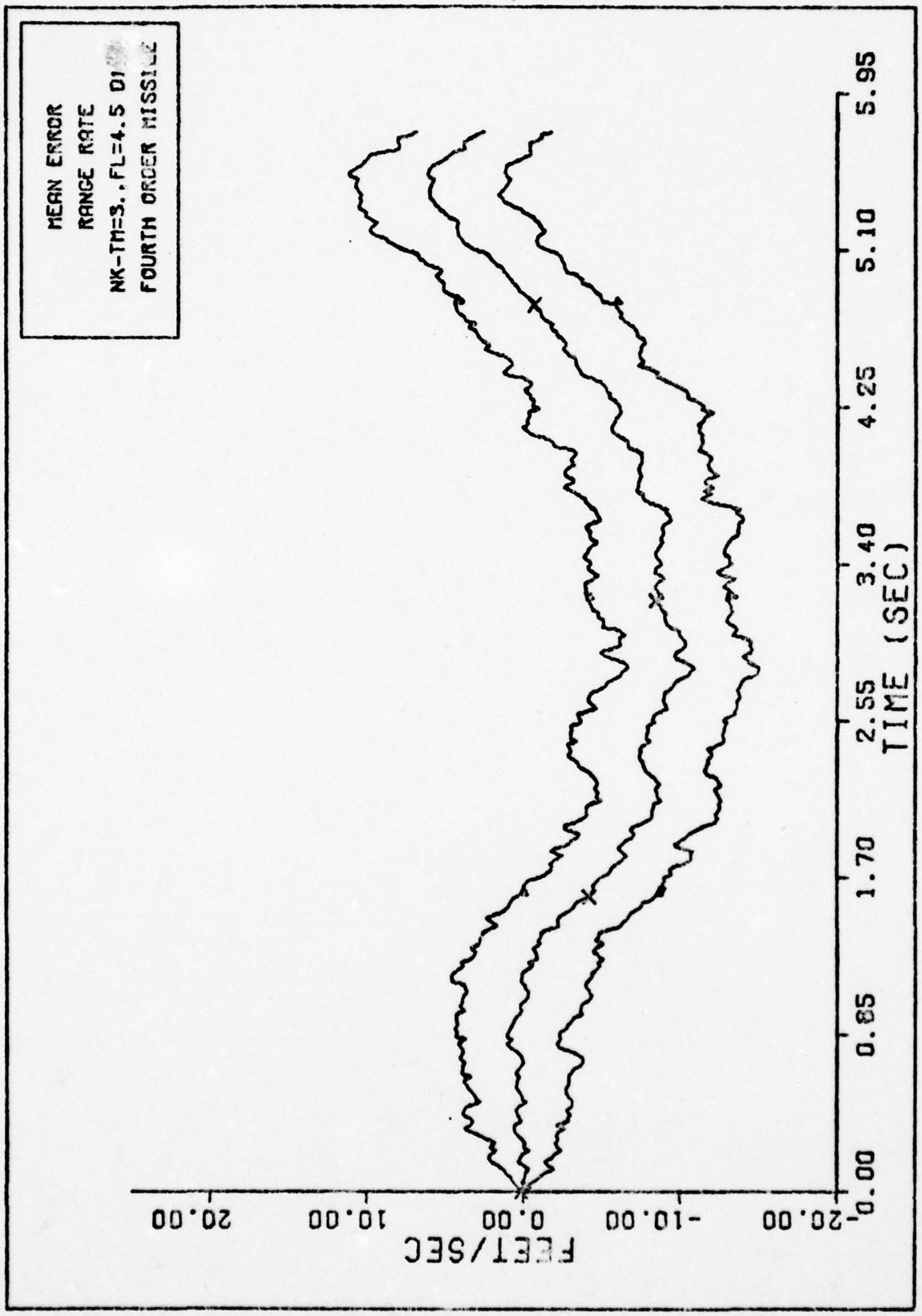

Fig. 98. RANGE RATE FOURTH ORDER MISSILE

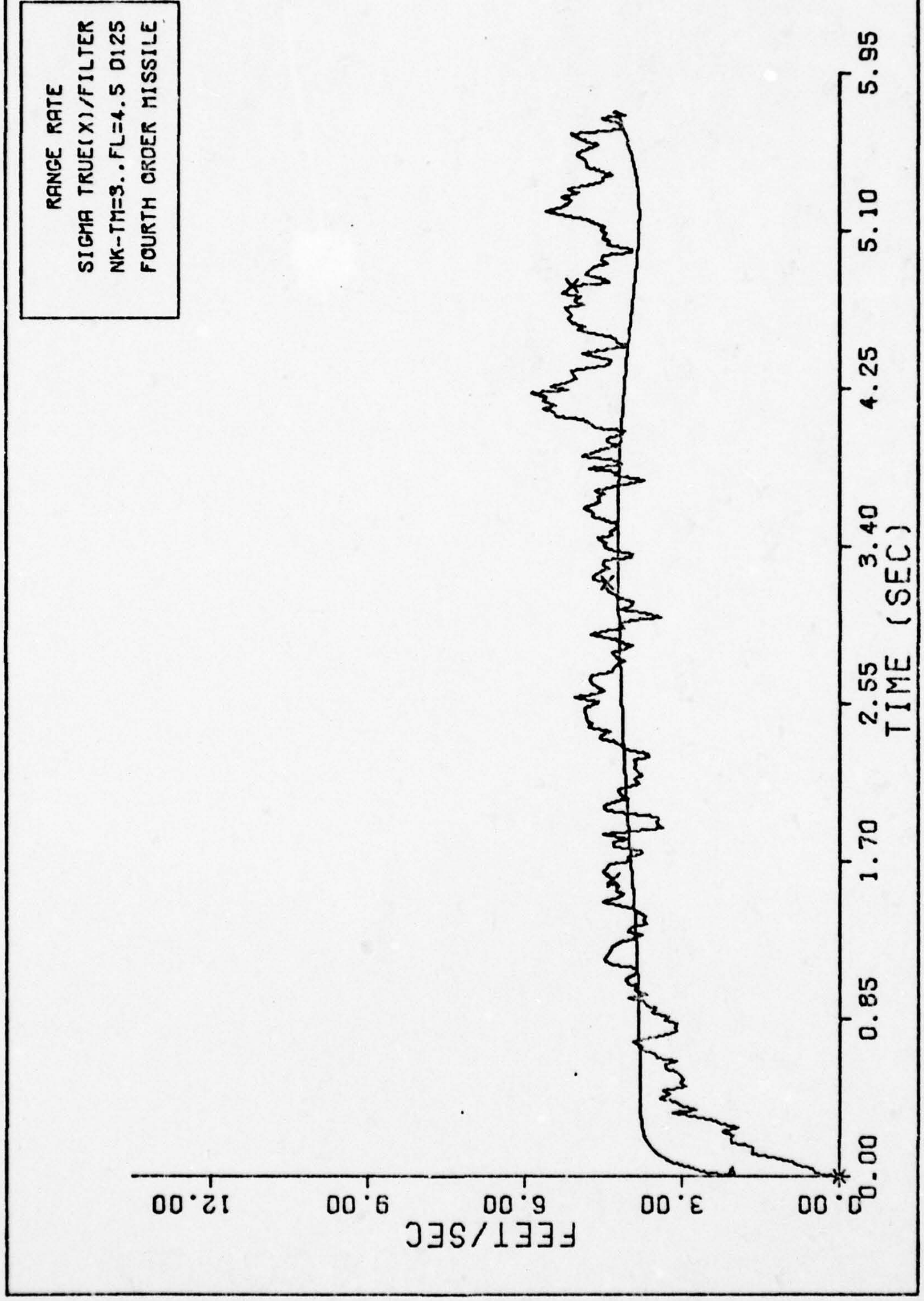

Fig. 99. RANGE RATE SIGMAS FOURTH ORDER

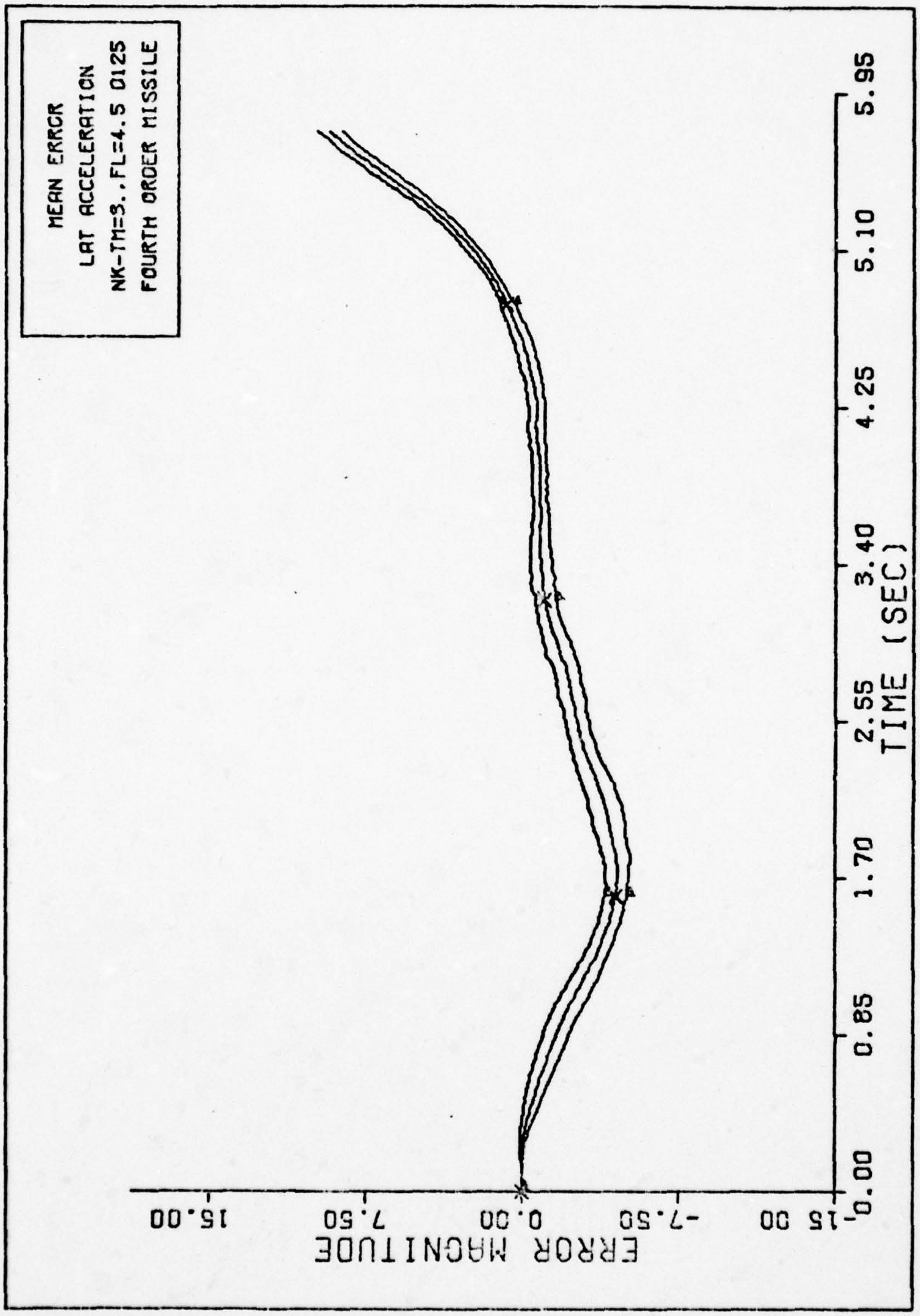

Fig. 100. LAT ACCELERATION FOURTH ORDER MISSILE

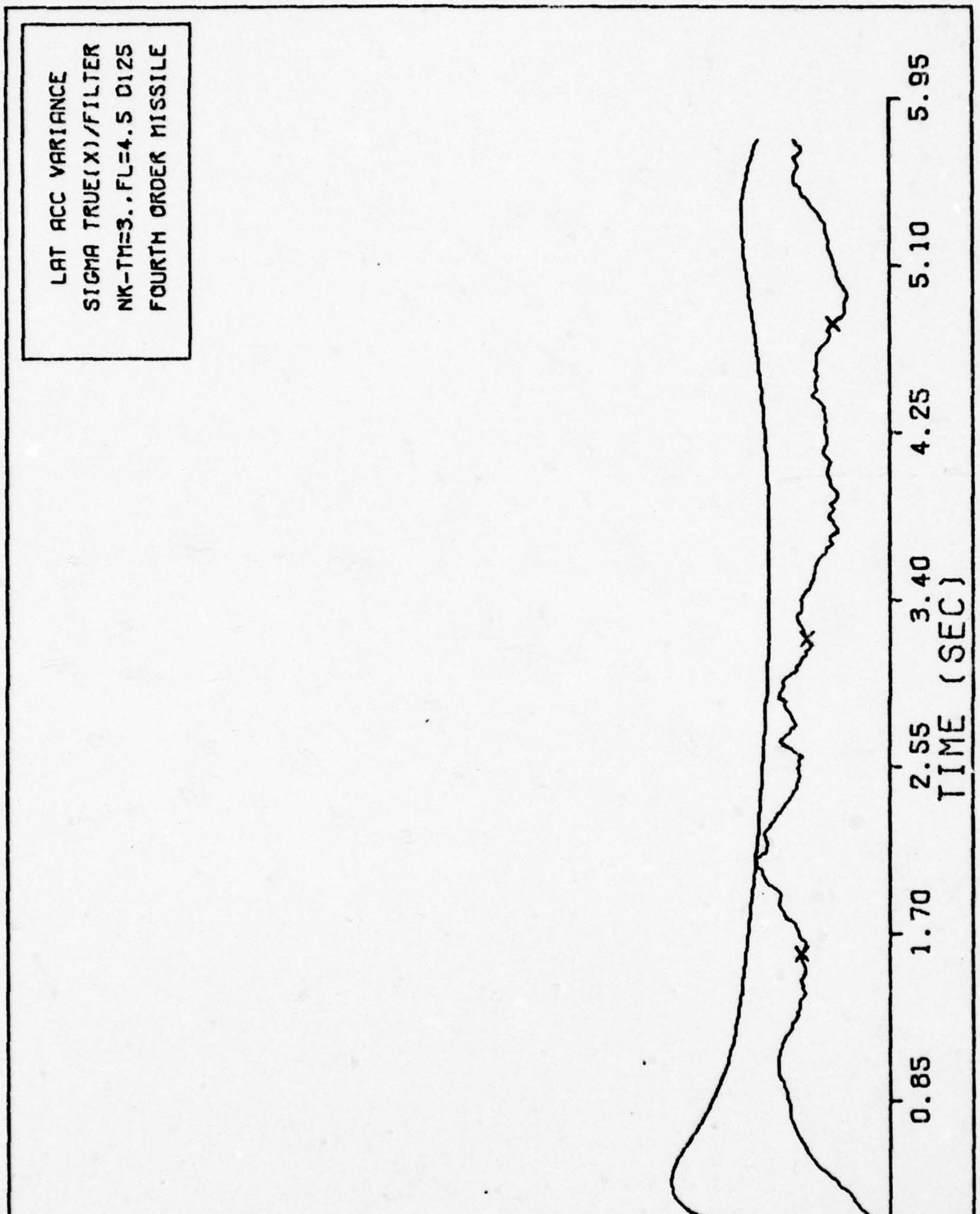

Fig. 101. LAT ACCELERATION SIGMAS FOURTH ORDER

Sensitivity Analysis ($\tau_2 = .8$)

The initial state estimates and the tuning parameters for this case are

$$V^I_{mx}(0) = 1225.7 \text{ fps}$$
$$\dot{\theta}(0) = 4.363345 \text{ radians}$$
$$R(0) = 10000. \text{ feet}$$
$$\dot{R}(0) = -2122. \text{ fps}$$
$$a_L(0) = 0.$$
$$n(0) = 4.5$$
$$\tau_f(0) = \text{N/A}$$
$$M/S(0) = 29.197 \text{ slugs/ft}^2$$

$$\underline{R} = \begin{bmatrix} 4.E-5 & 0. & 0. \\ 0. & 500. & 0. \\ 0. & 0. & 100. \end{bmatrix}$$

$$\underline{P}_0 = \begin{bmatrix} 100. & 0. & 0. & 0. & 0. & 0. & 0. & 0. \\ 0. & 1.E-8 & 0. & 0. & 0. & 0. & 0. & 0. \\ 0. & 0. & 101. & 0. & 0. & 0. & 0. & 0. \\ 0. & 0. & 0. & 4. & 0. & 0. & 0. & 0. \\ 0. & 0. & 0. & 0. & 1. & 0. & 0. & 0. \\ 0. & 0. & 0. & 0. & 0. & 0. & 0. & 0. \\ 0. & 0. & 0. & 0. & 0. & 0. & 0. & 0. \\ 0. & 0. & 0. & 0. & 0. & 0. & 0. & 0. \end{bmatrix}$$

$$\underline{Q} = \begin{bmatrix} 101. & 0. & 0. & 0. & 0. & 0. & 0. & 0. \\ 0. & 1.E-6 & 0. & 0. & 0. & 0. & 0. & 0. \\ 0. & 0. & 500. & 0. & 0. & 0. & 0. & 0. \\ 0. & 0. & 0. & 100. & 0. & 0. & 0. & 0. \\ 0. & 0. & 0. & 0. & 5. & 0. & 0. & 0. \\ 0. & 0. & 0. & 0. & 0. & 0. & 0. & 0. \\ 0. & 0. & 0. & 0. & 0. & 0. & 0. & 0. \\ 0. & 0. & 0. & 0. & 0. & 0. & 0. & 0. \end{bmatrix}$$

This set of plots was generated by setting the time constant of the guidance system, τ_2 to .8 seconds in the truth model. τ_2 in the filter was set to 0.3 seconds. The fourth order filter was used and only the dynamic states of the missile model were estimated.

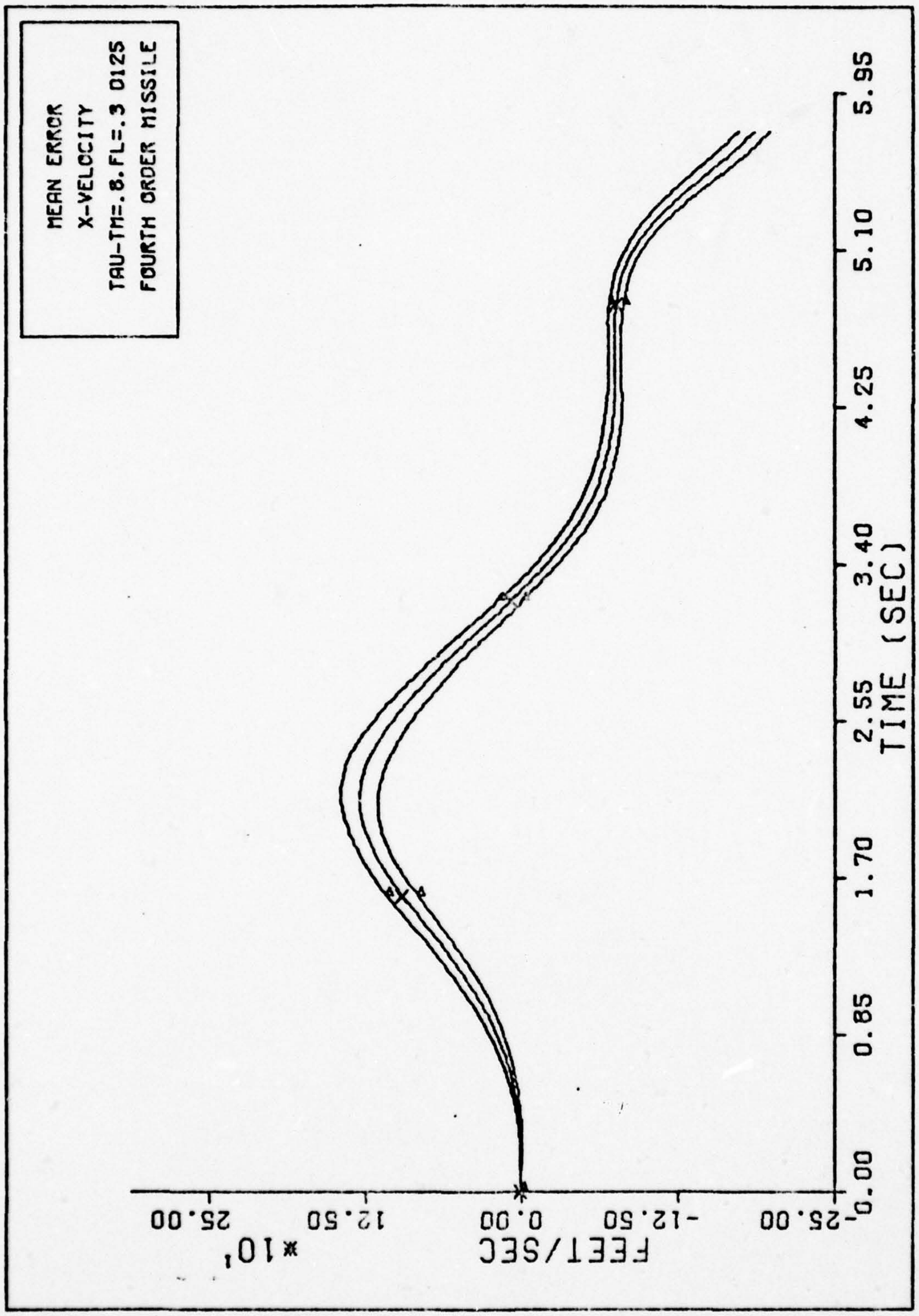

Fig. 102. X-VELOCITY FOURTH ORDER MISSILE

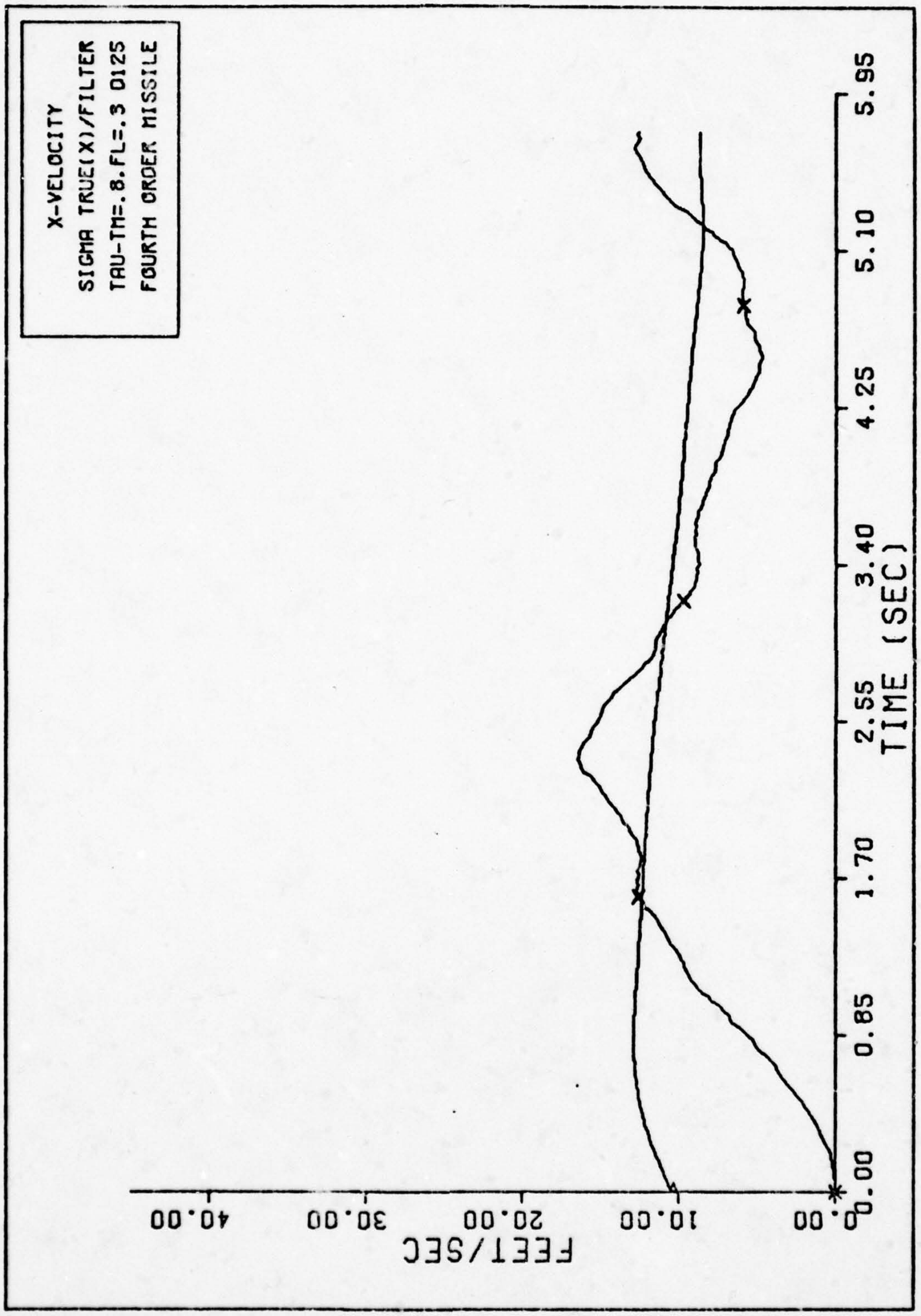

Fig. 103. X-VELOCITY SIGMAS FOURTH ORDER

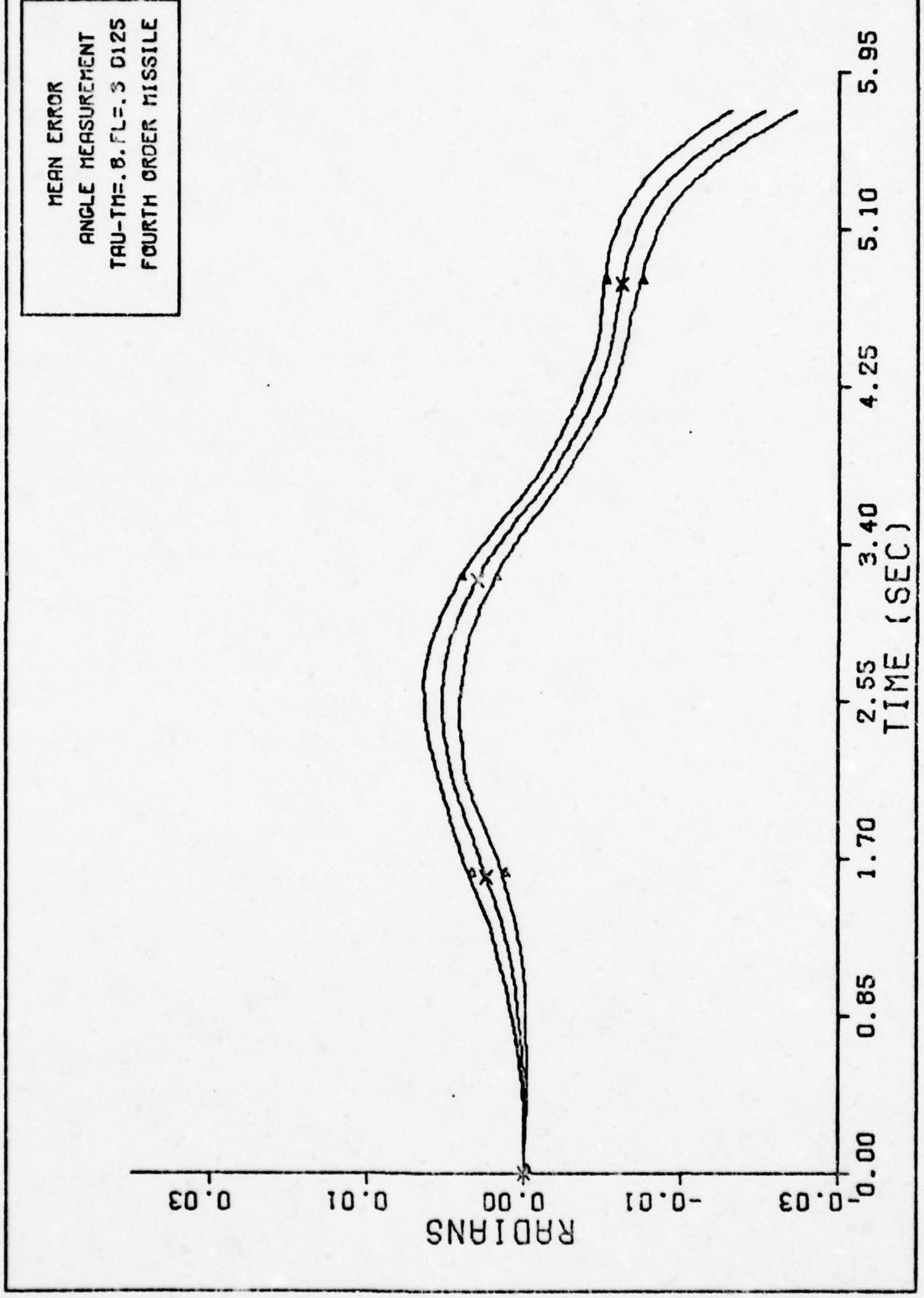

Fig. 104. ANGLE MEASUREMENT FOURTH ORDER MISSILE

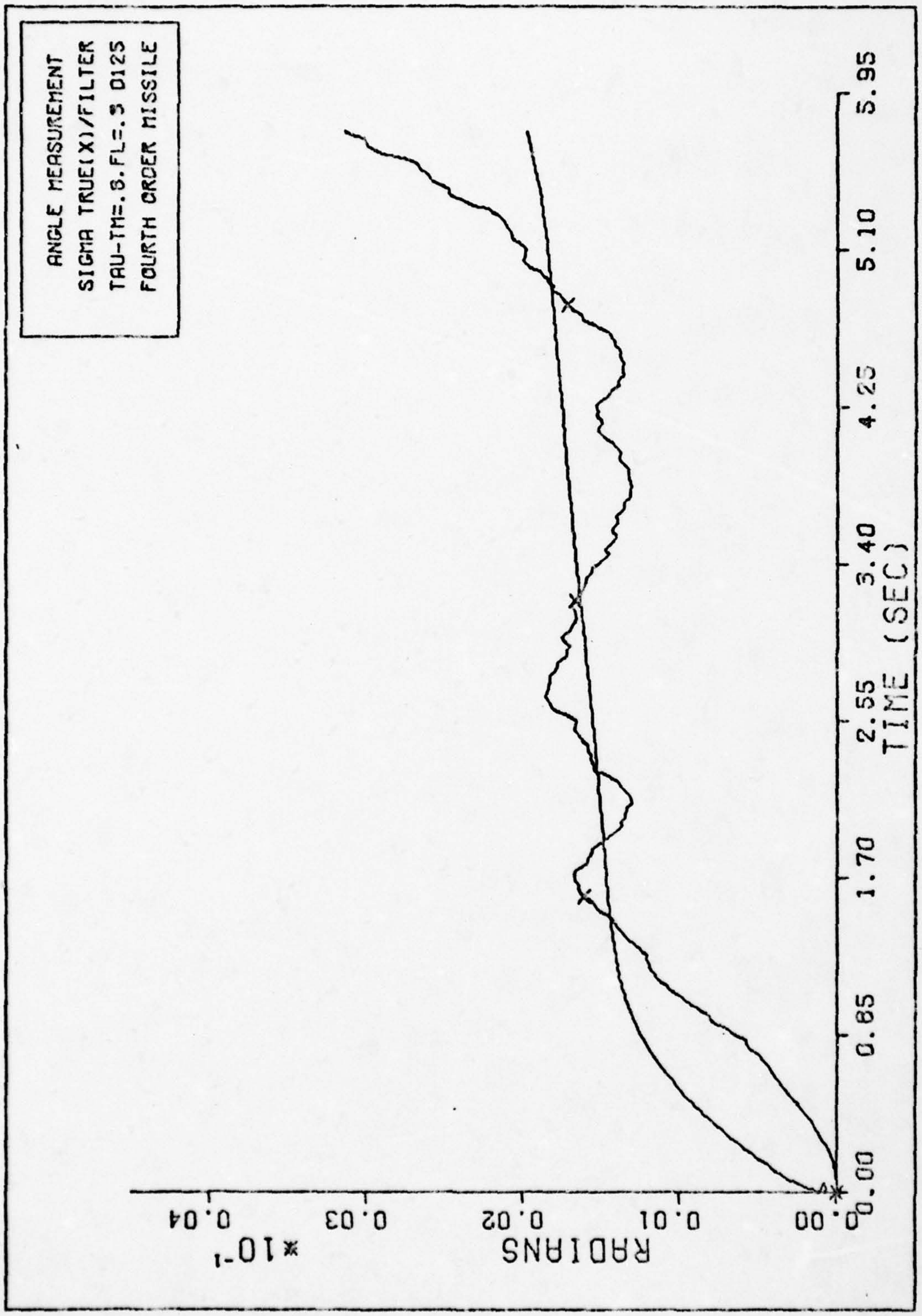

Fig. 105. ANGLE MEASUREMENT SIGMAS FOURTH ORDER

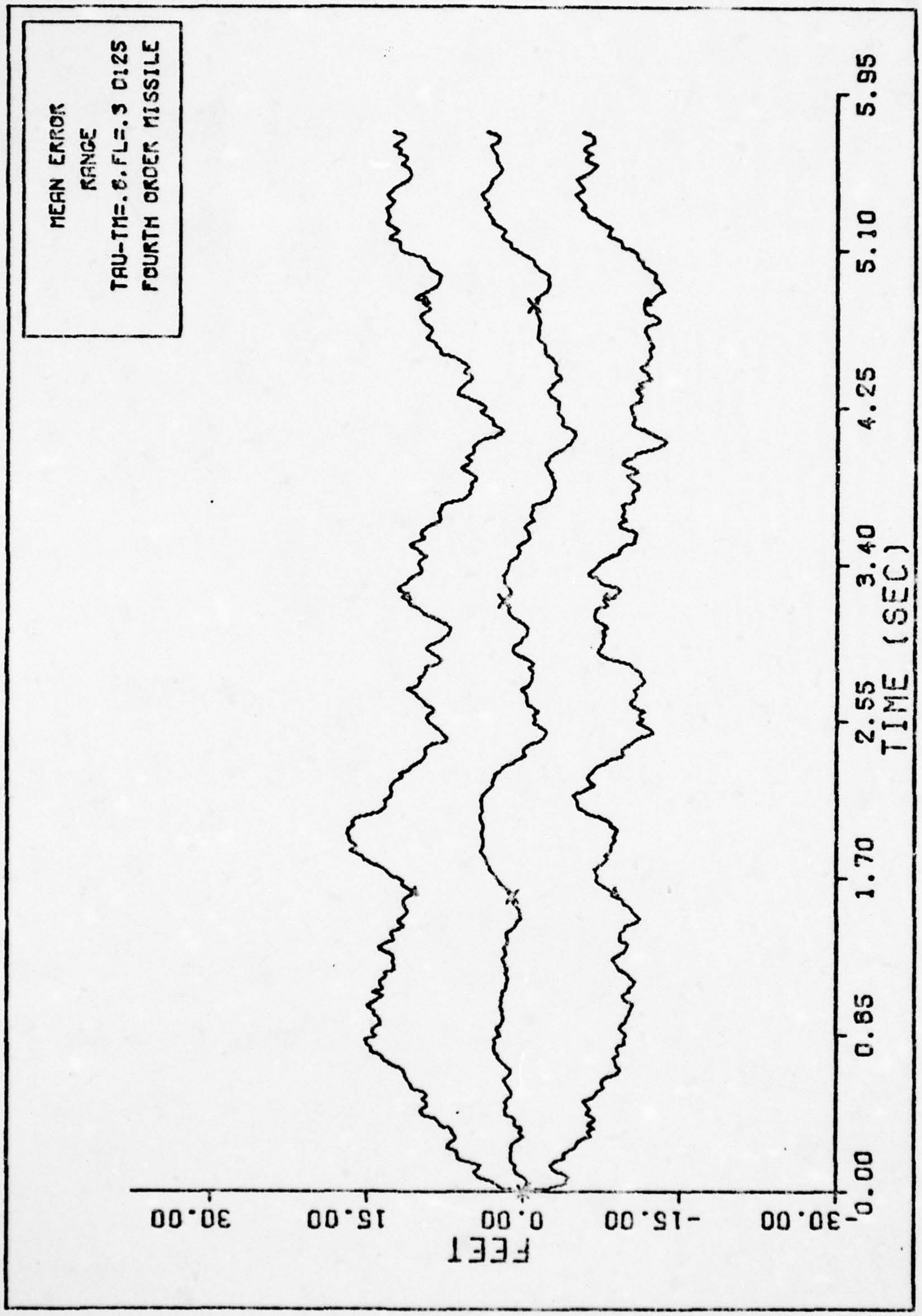

Fig. 106. RANGE FOURTH ORDER MISSILE

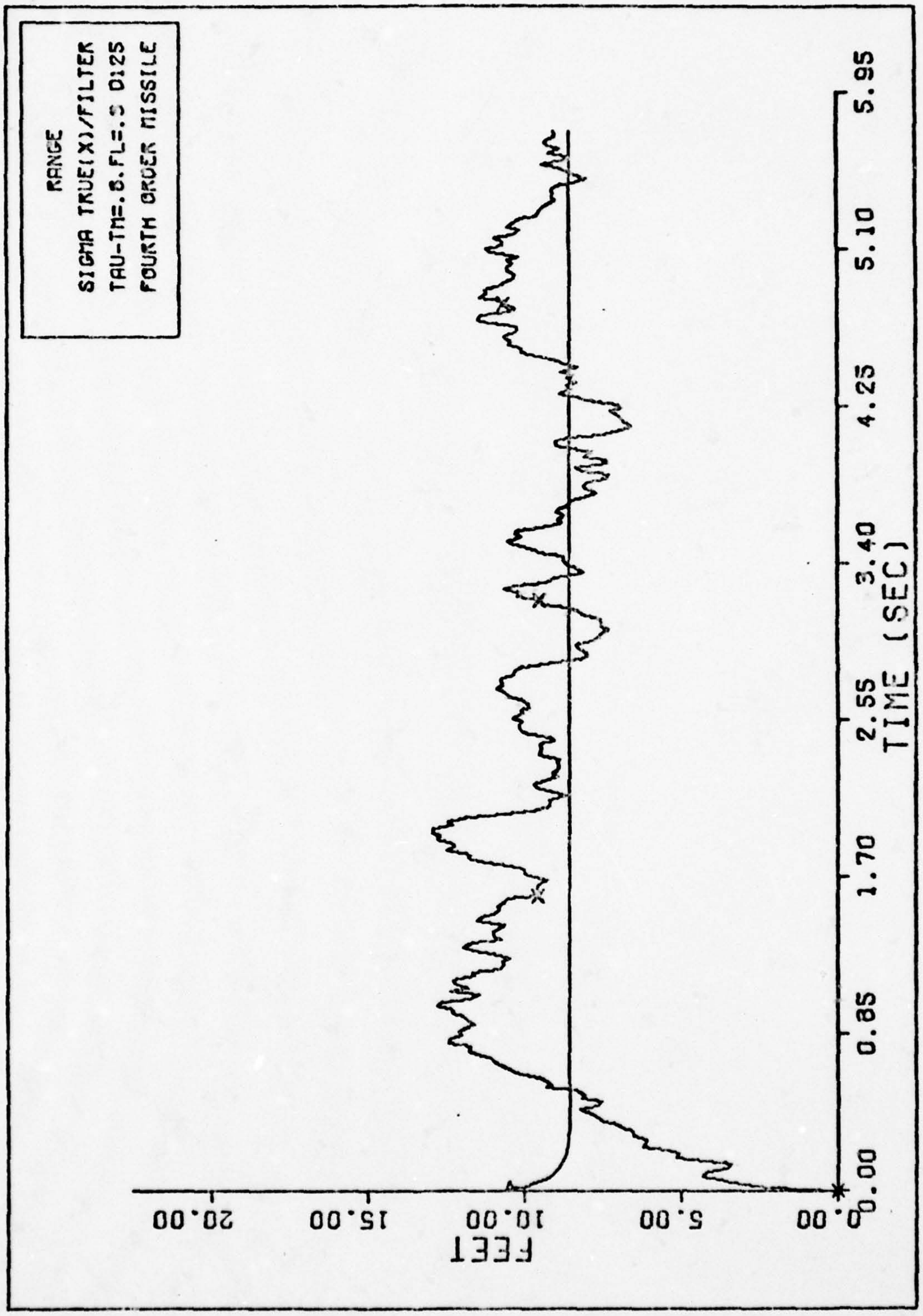

Fig. 107. RANGE SIGMAS FOURTH ORDER

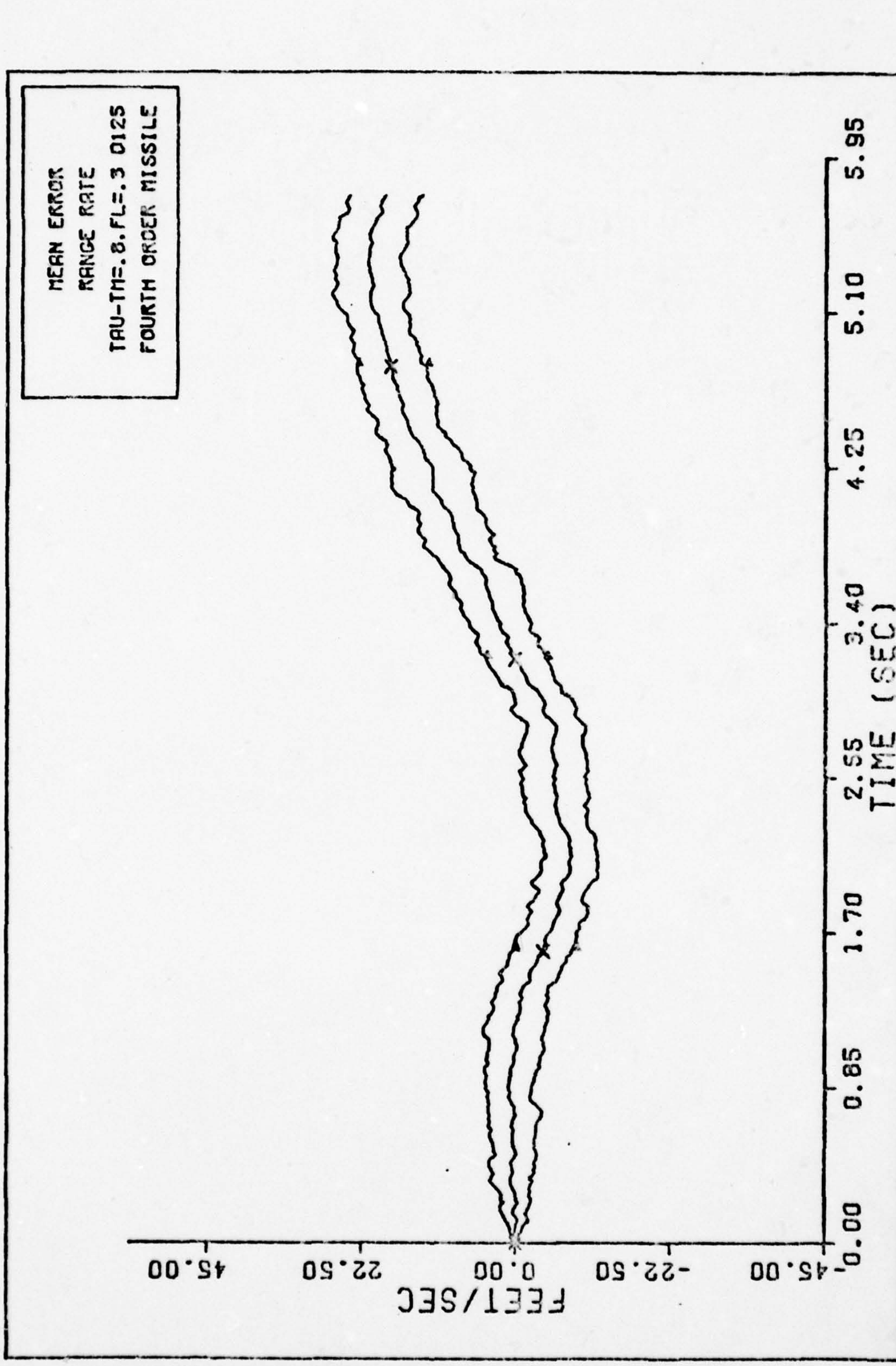

Fig. 108. RANGE RATE FOURTH ORDER MISSILE

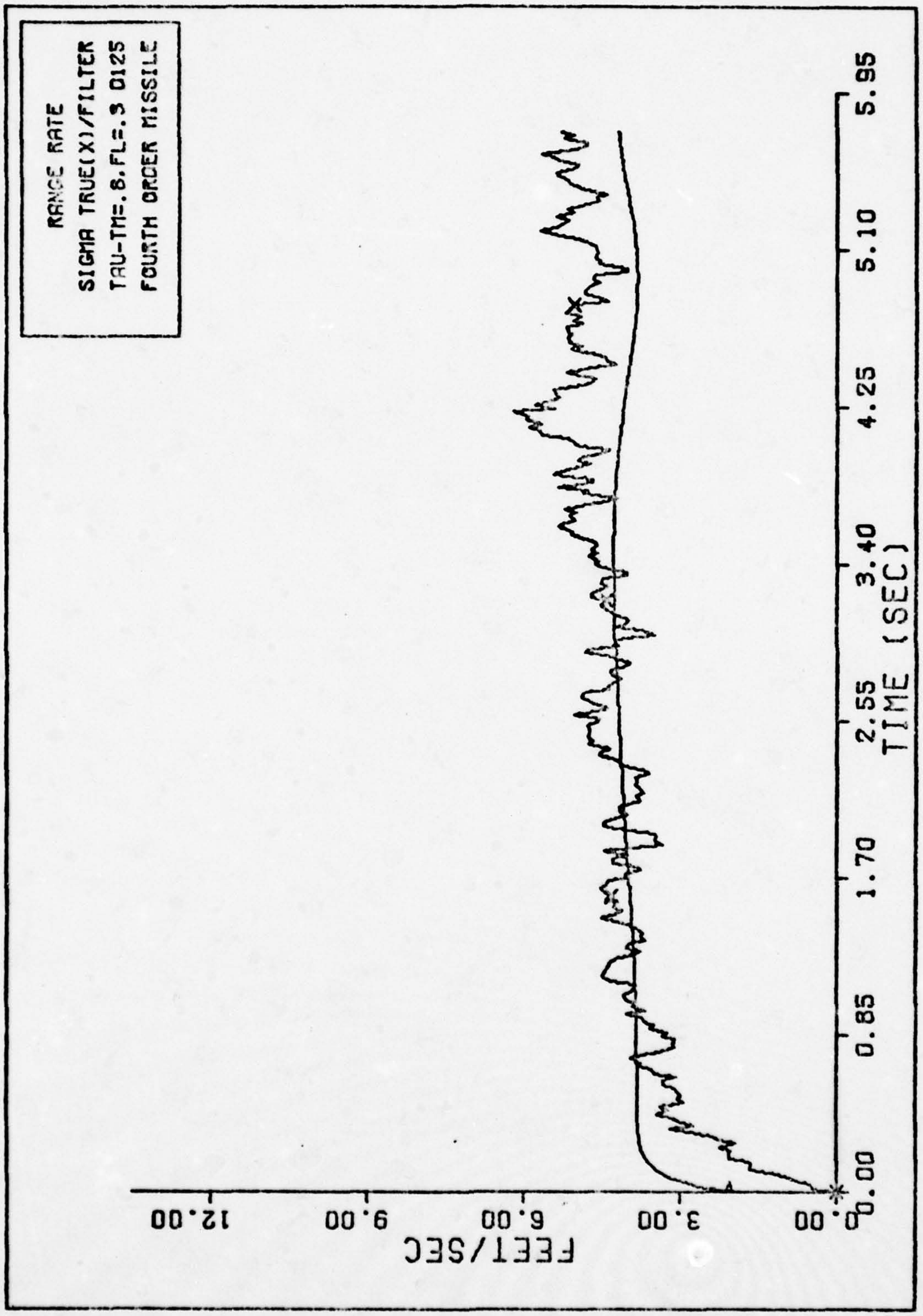

Fig. 109. RANGE RATE SIGMAS FOURTH ORDER

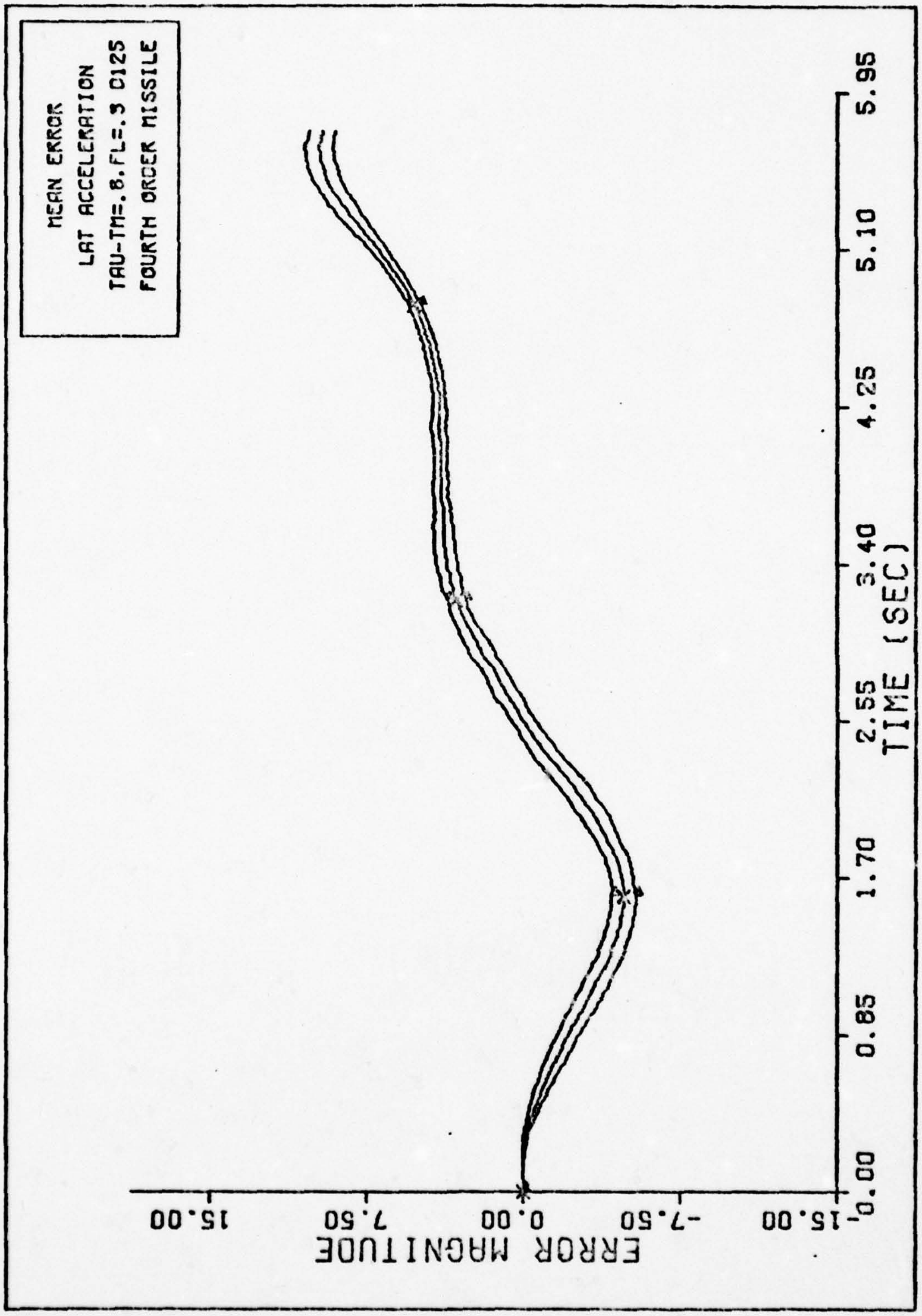

Fig. 110. LAT ACCELERATION FOURTH ORDER MISSILE

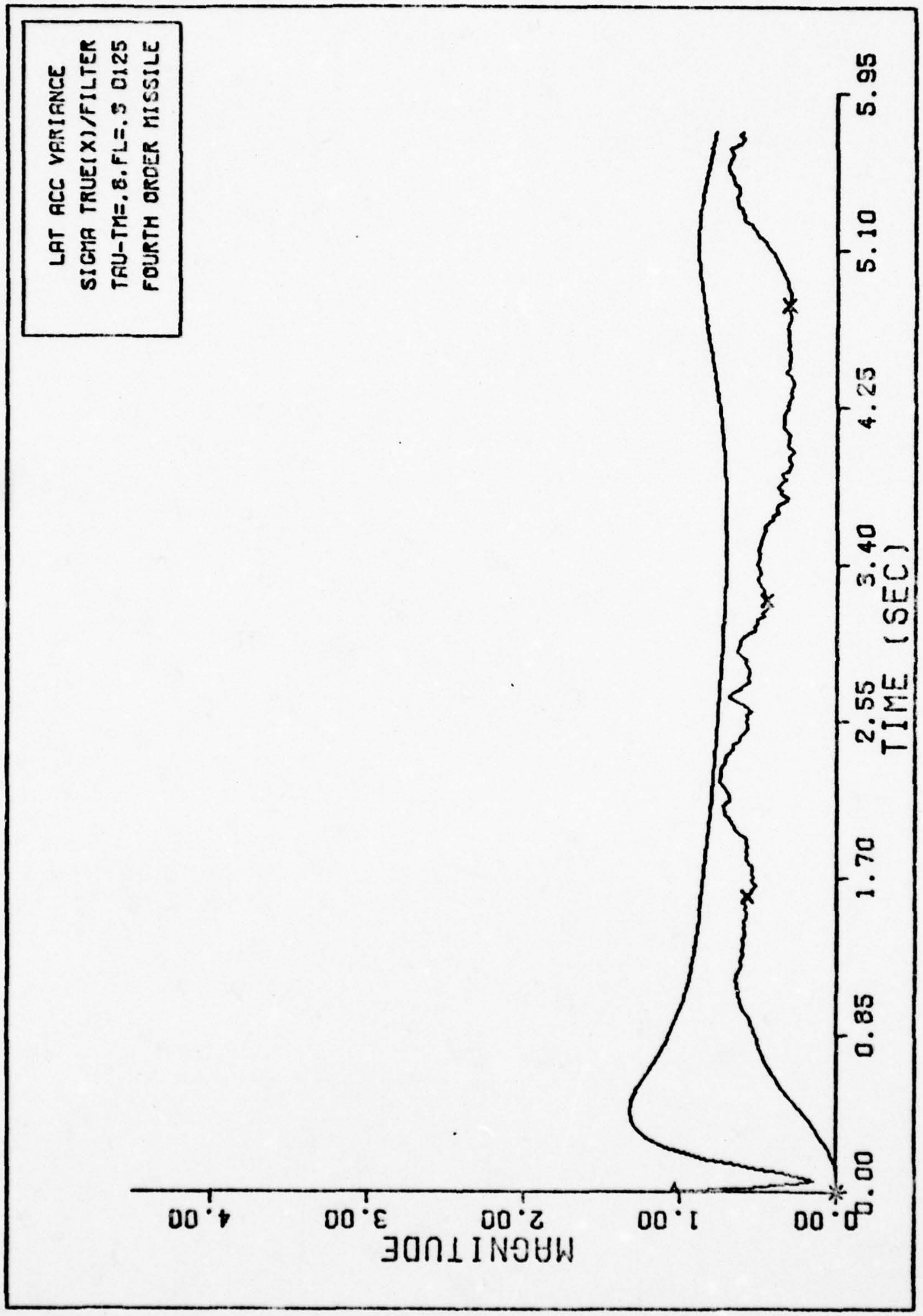

Fig. 111. LAT ACCELERATION SIGMAS FOURTH ORDER

Sensitivity Analysis ($\tau_2 = .1$)

The initial state estimates and the tuning parameters for this case are

$$V^I_{mx}(0) = 1225.7 \text{ fps}$$
$$\dot{\theta}_T(0) = 4.363345 \text{ radians}$$
$$R(0) = 10000. \text{ feet}$$
$$\dot{R}(0) = -2122. \text{ fps}$$
$$a_L(0) = 0.$$
$$n(0) = 4.5$$
$$\tau_f(0) = \text{N/A}$$
$$M/S(0) = 29.197 \text{ slugs/ft}^2$$

$$\underline{R} = \begin{bmatrix} 4.E{-}5 & 0. & 0. \\ 0. & 500. & 0. \\ 0. & 0. & 100. \end{bmatrix}$$

$$\underline{P}_0 = \begin{bmatrix} 100. & 0. & 0. & 0. & 0. & 0. & 0. & 0. \\ 0. & 1.E{-}8 & 0. & 0. & 0. & 0. & 0. & 0. \\ 0. & 0. & 101. & 0. & 0. & 0. & 0. & 0. \\ 0. & 0. & 0. & 4. & 0. & 0. & 0. & 0. \\ 0. & 0. & 0. & 0. & 1. & 0. & 0. & 0. \\ 0. & 0. & 0. & 0. & 0. & 0. & 0. & 0. \\ 0. & 0. & 0. & 0. & 0. & 0. & 0. & 0. \\ 0. & 0. & 0. & 0. & 0. & 0. & 0. & 0. \end{bmatrix}$$

$$\underline{Q} = \begin{bmatrix} 101. & 0. & 0. & 0. & 0. & 0. & 0. & 0. \\ 0. & 1.E-6 & 0. & 0. & 0. & 0. & 0. & 0. \\ 0. & 0. & 500. & 0. & 0. & 0. & 0. & 0. \\ 0. & 0. & 0. & 100. & 0. & 0. & 0. & 0. \\ 0. & 0. & 0. & 0. & 5. & 0. & 0. & 0. \\ 0. & 0. & 0. & 0. & 0. & 0. & 0. & 0. \\ 0. & 0. & 0. & 0. & 0. & 0. & 0. & 0. \\ 0. & 0. & 0. & 0. & 0. & 0. & 0. & 0. \end{bmatrix}$$

This set of plots was generated by setting the time constant of the guidance system, τ_2, to .1 seconds in the truth model. τ_2 in the filter was set to 0.3 seconds. The fourth order filter was used and only the dynamic states of the missile model were estimated.

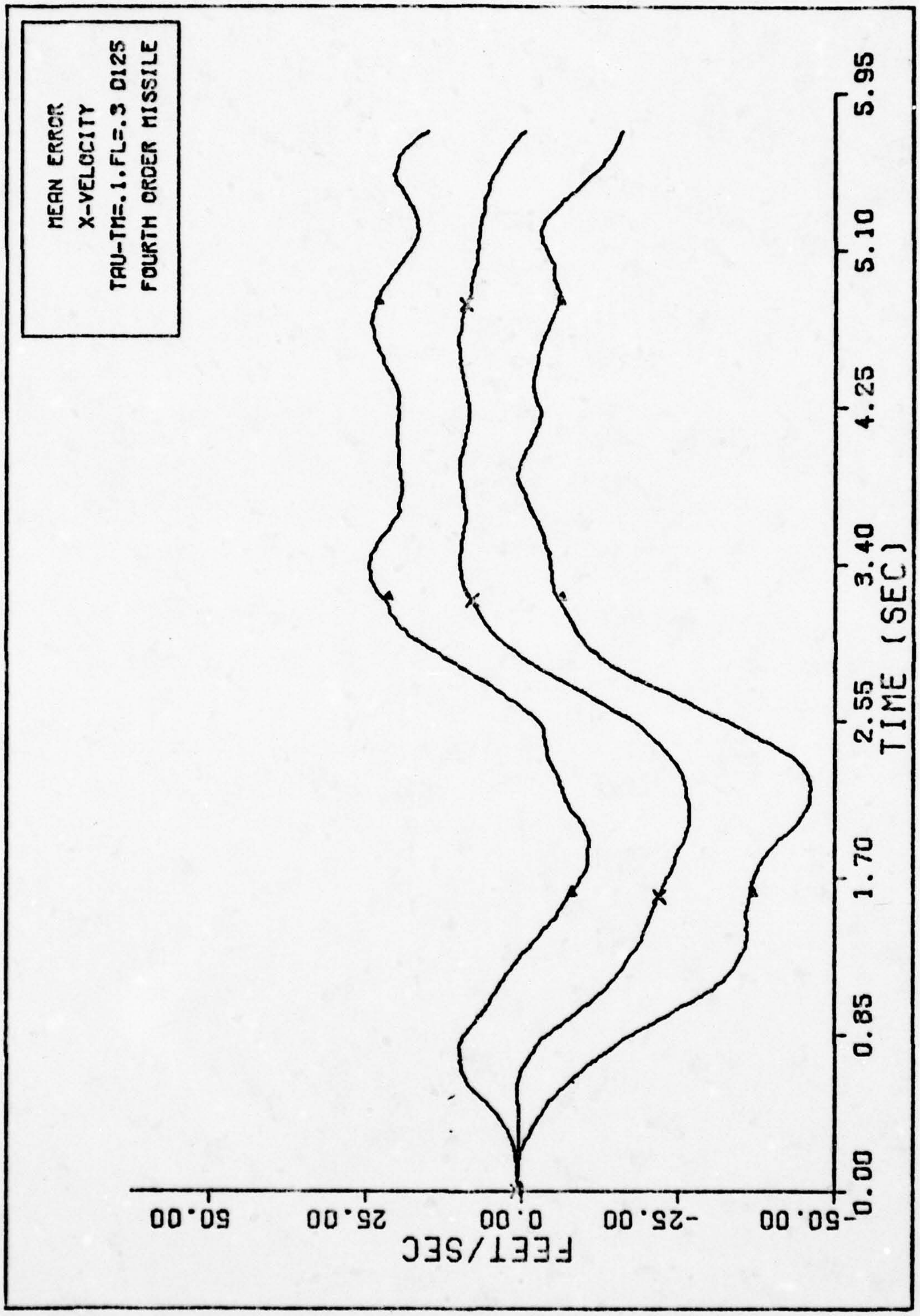

Fig. 112. X-VELOCITY FOURTH ORDER MISSILE

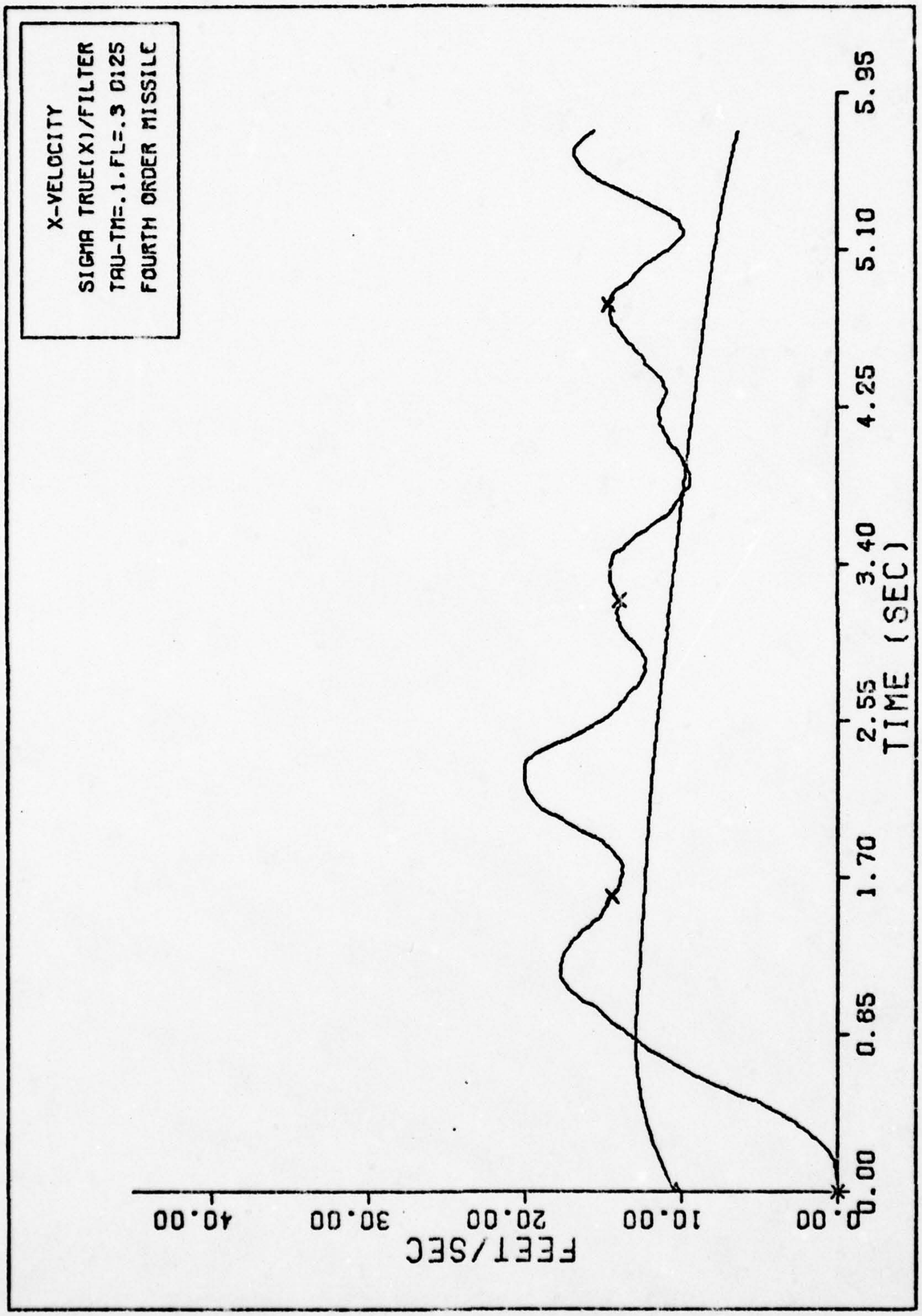

Fig. 113. X-VELOCITY SIGMAS FOURTH ORDER

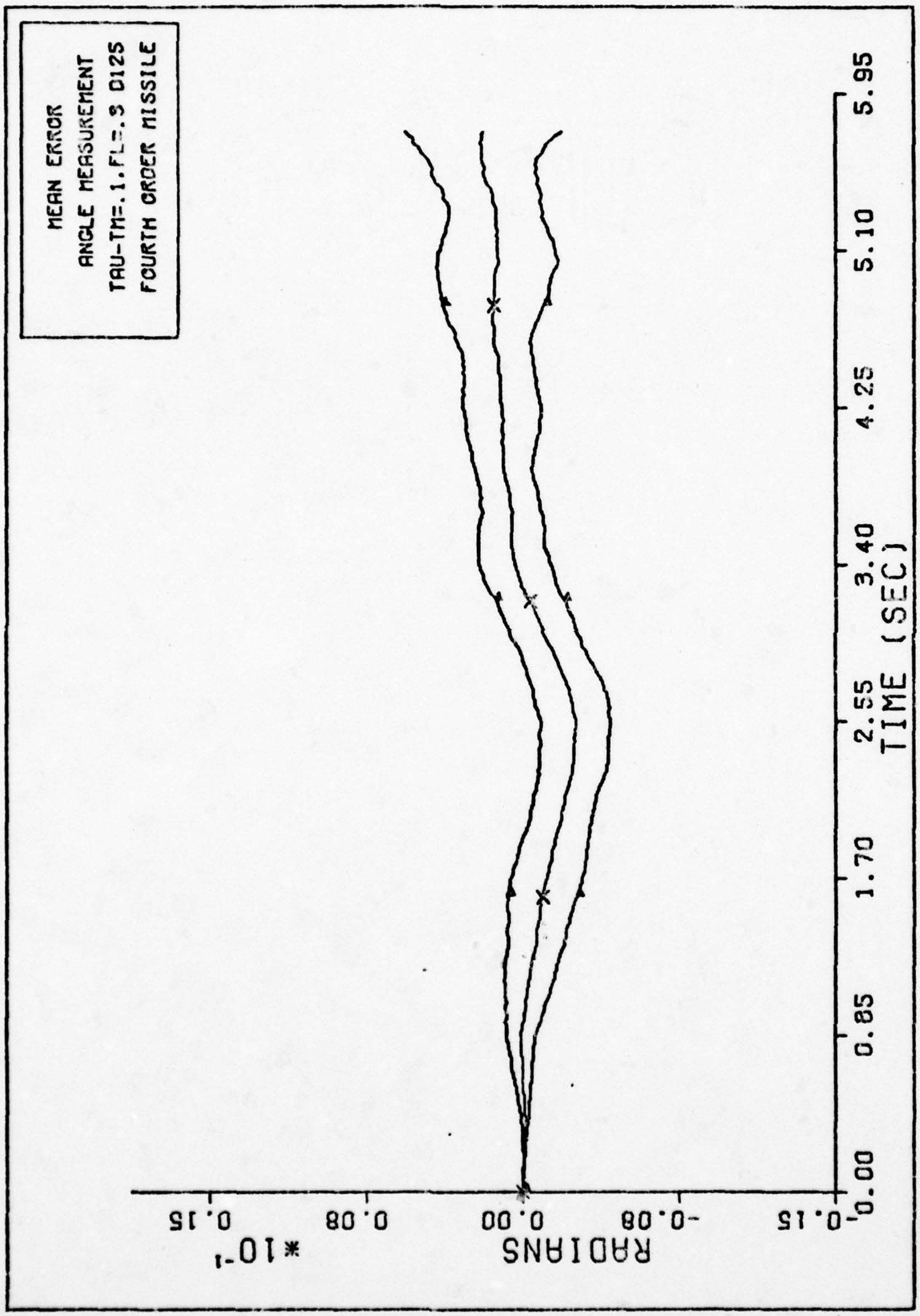

Fig. 114. ANGLE MEASUREMENT FOURTH ORDER MISSILE

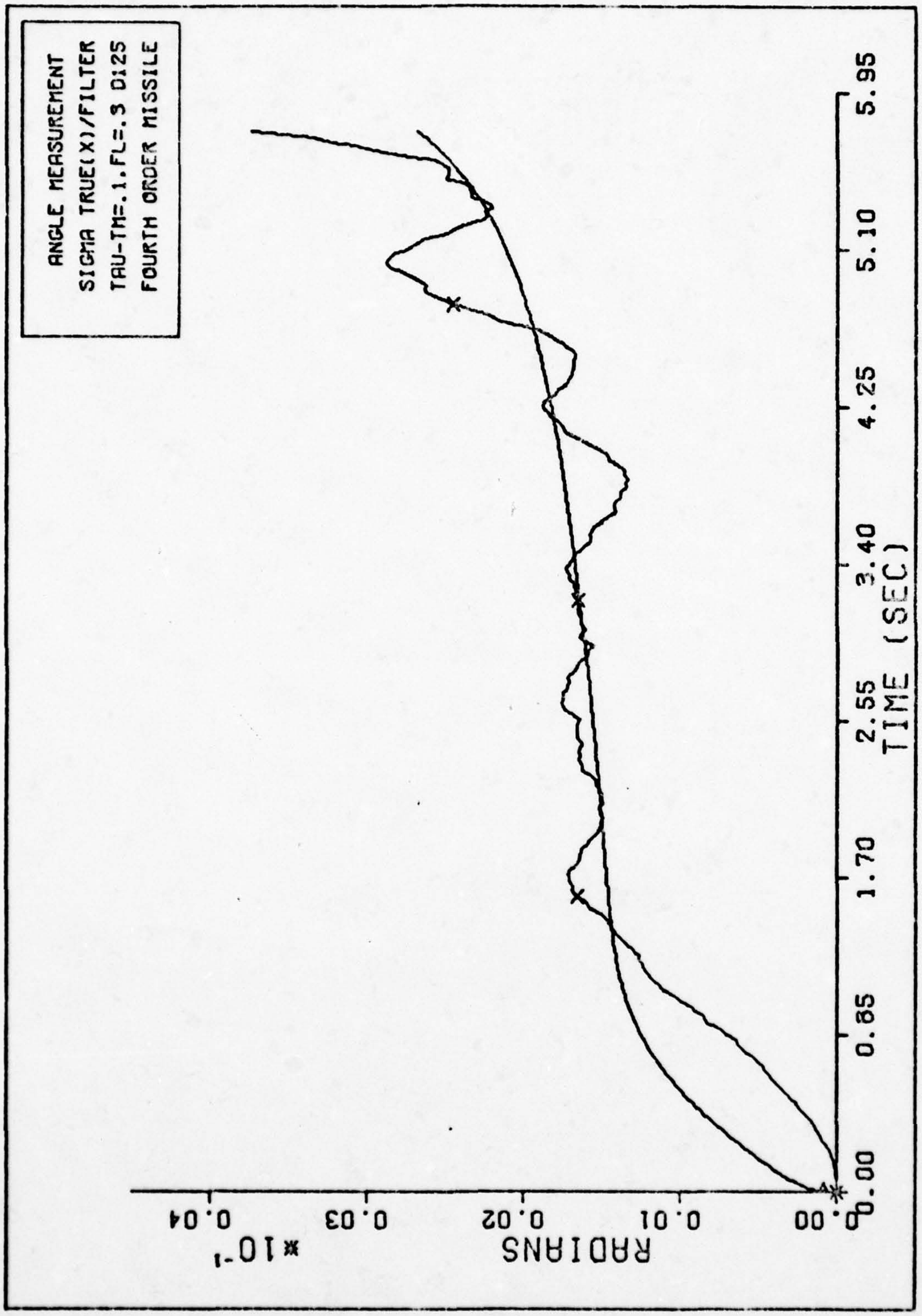

Fig. 115. ANGLE MEASUREMENT SIGMAS FOURTH ORDER

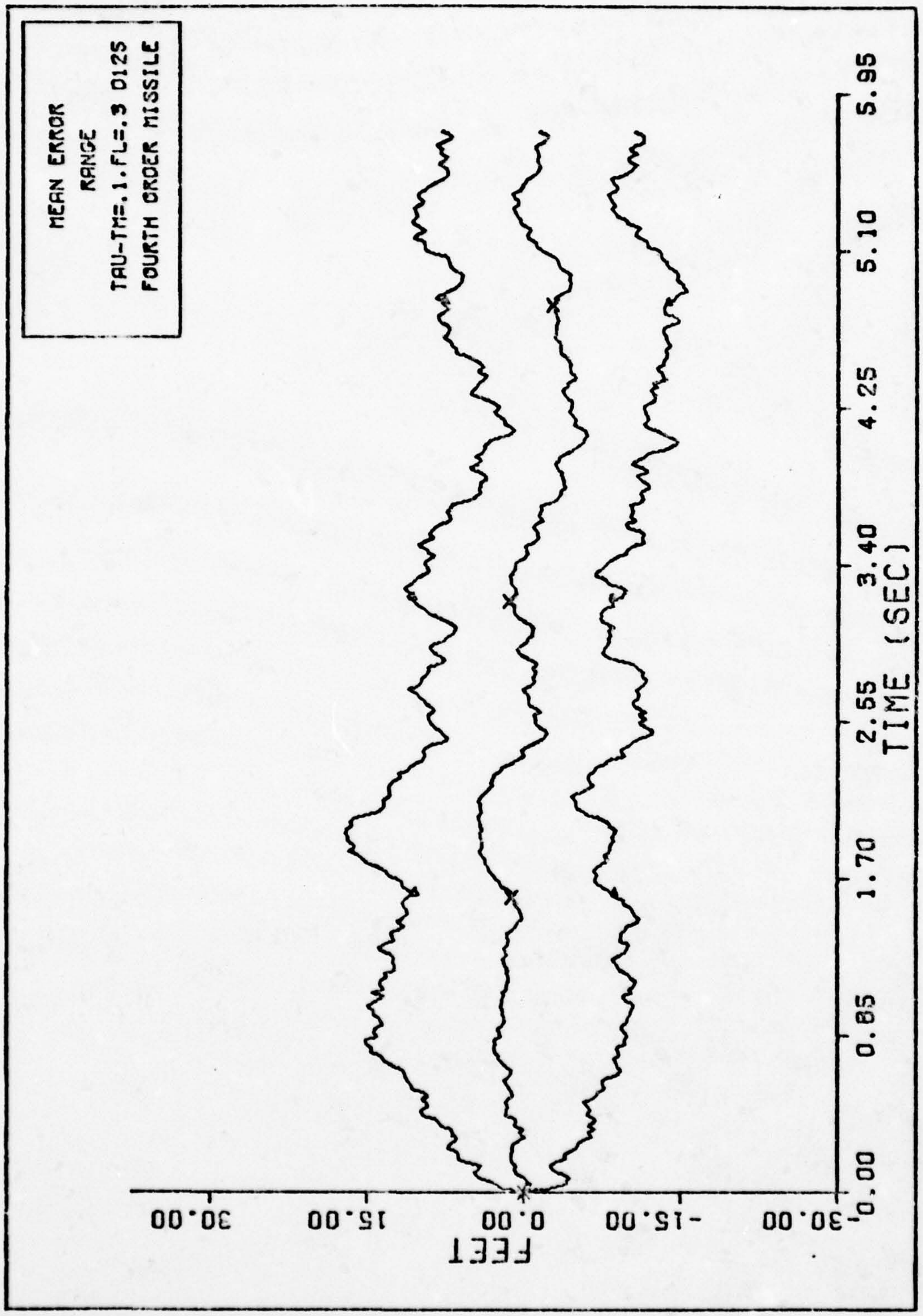

Fig. 116. RANGE FOURTH ORDER MISSILE

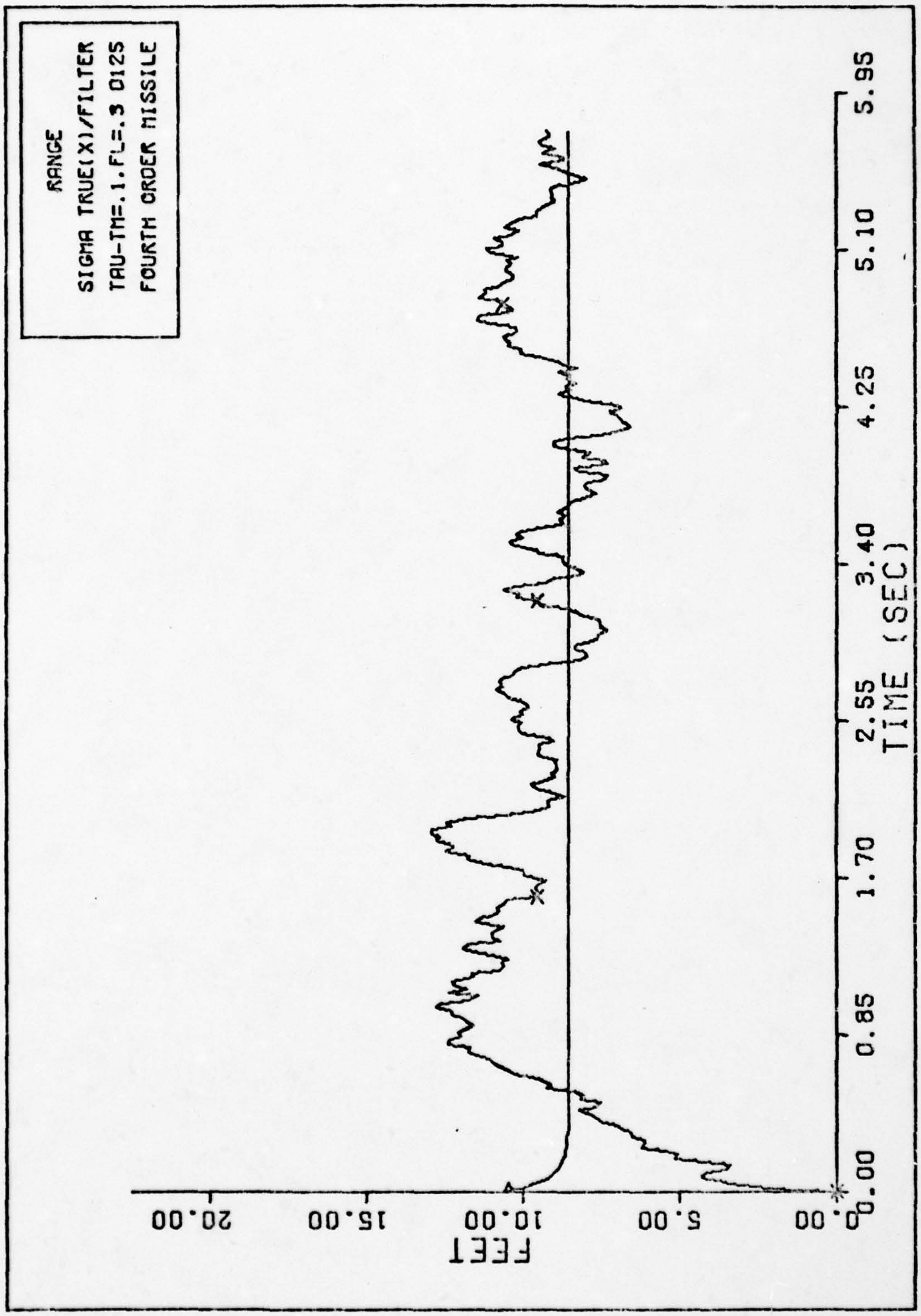

Fig. 117. RANGE SIGMAS FOURTH ORDER

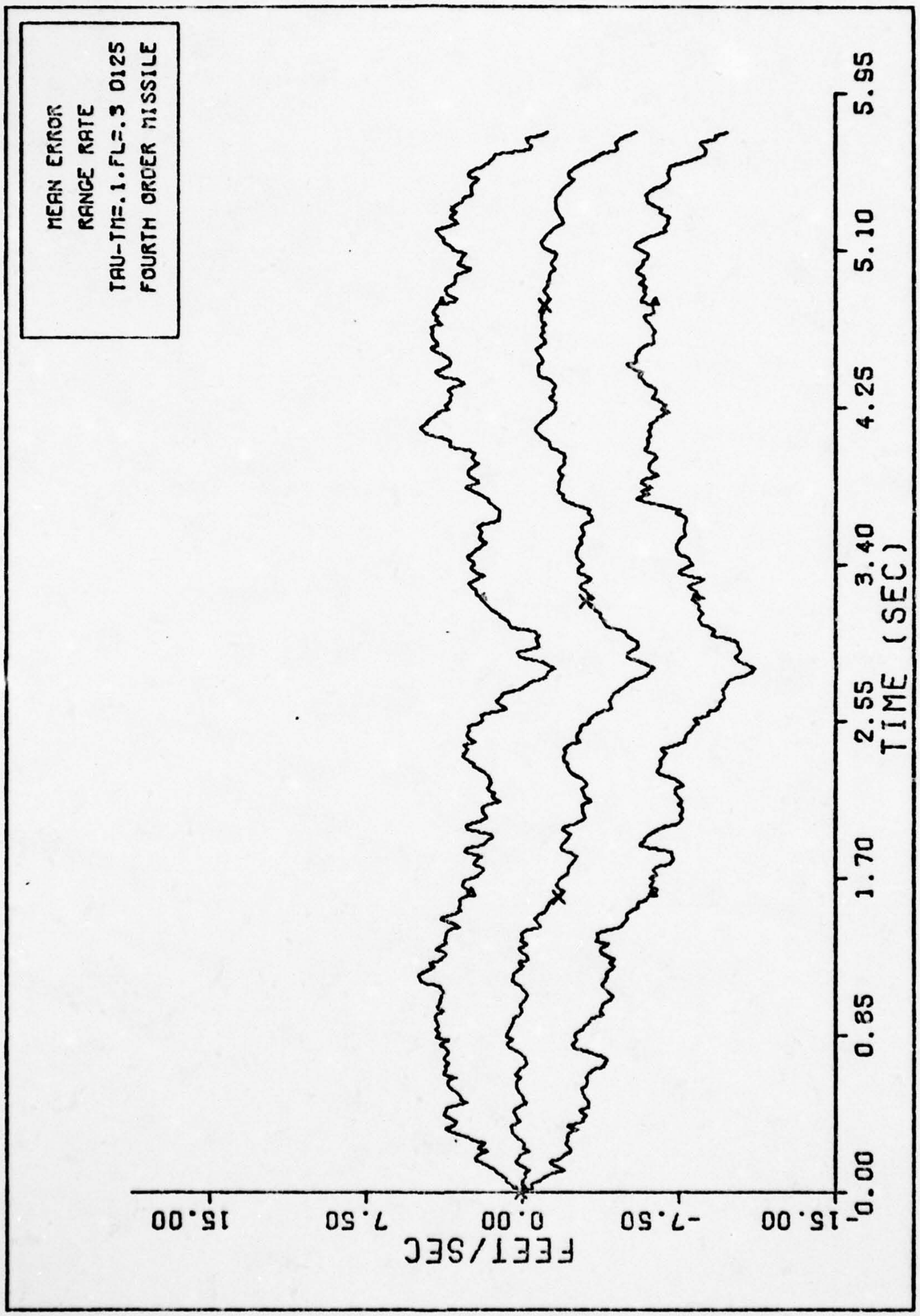

Fig. 118. RANGE RATE FOURTH ORDER MISSILE

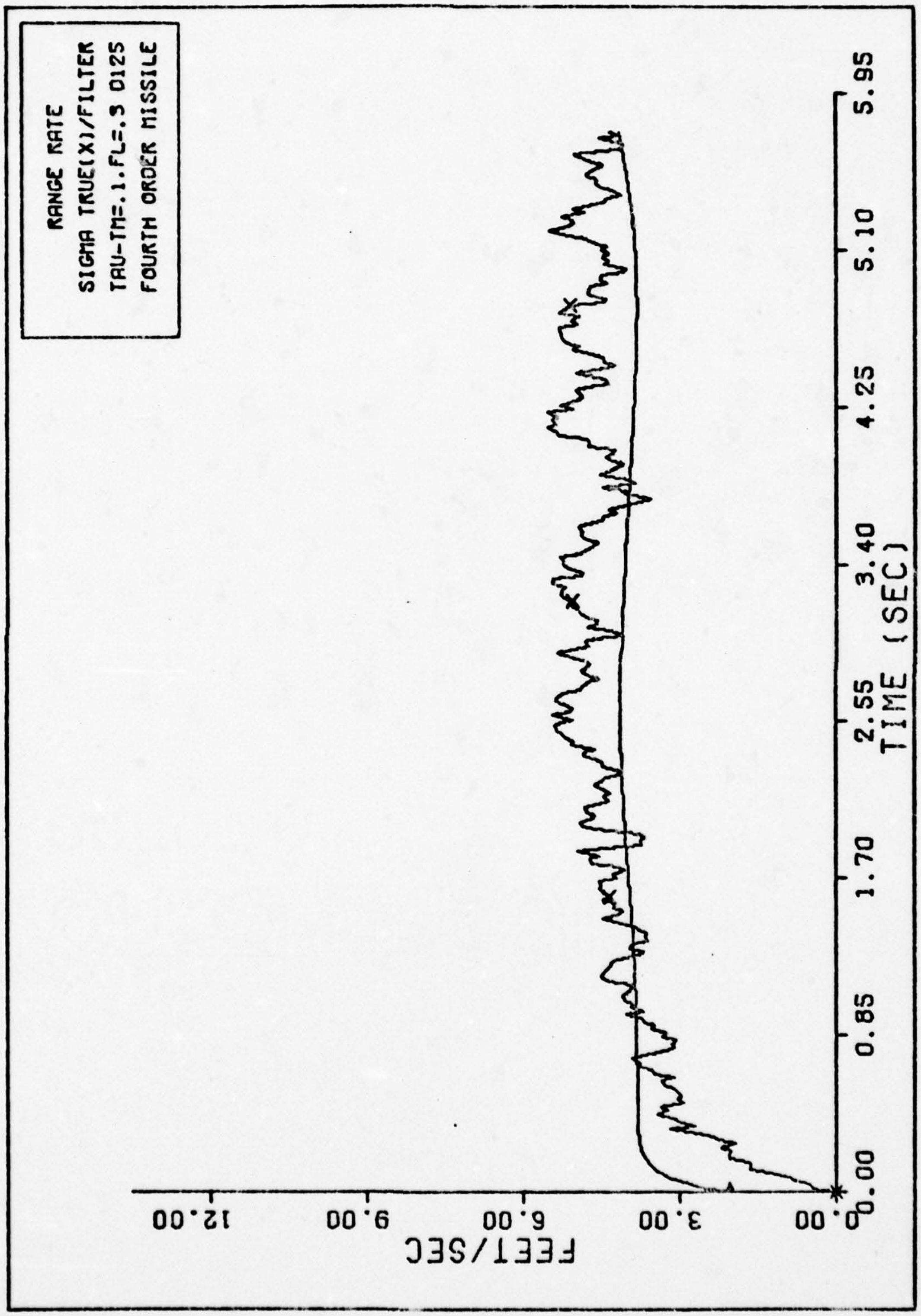

Fig. 119. RANGE RATE SIGMAS FOURTH ORDER

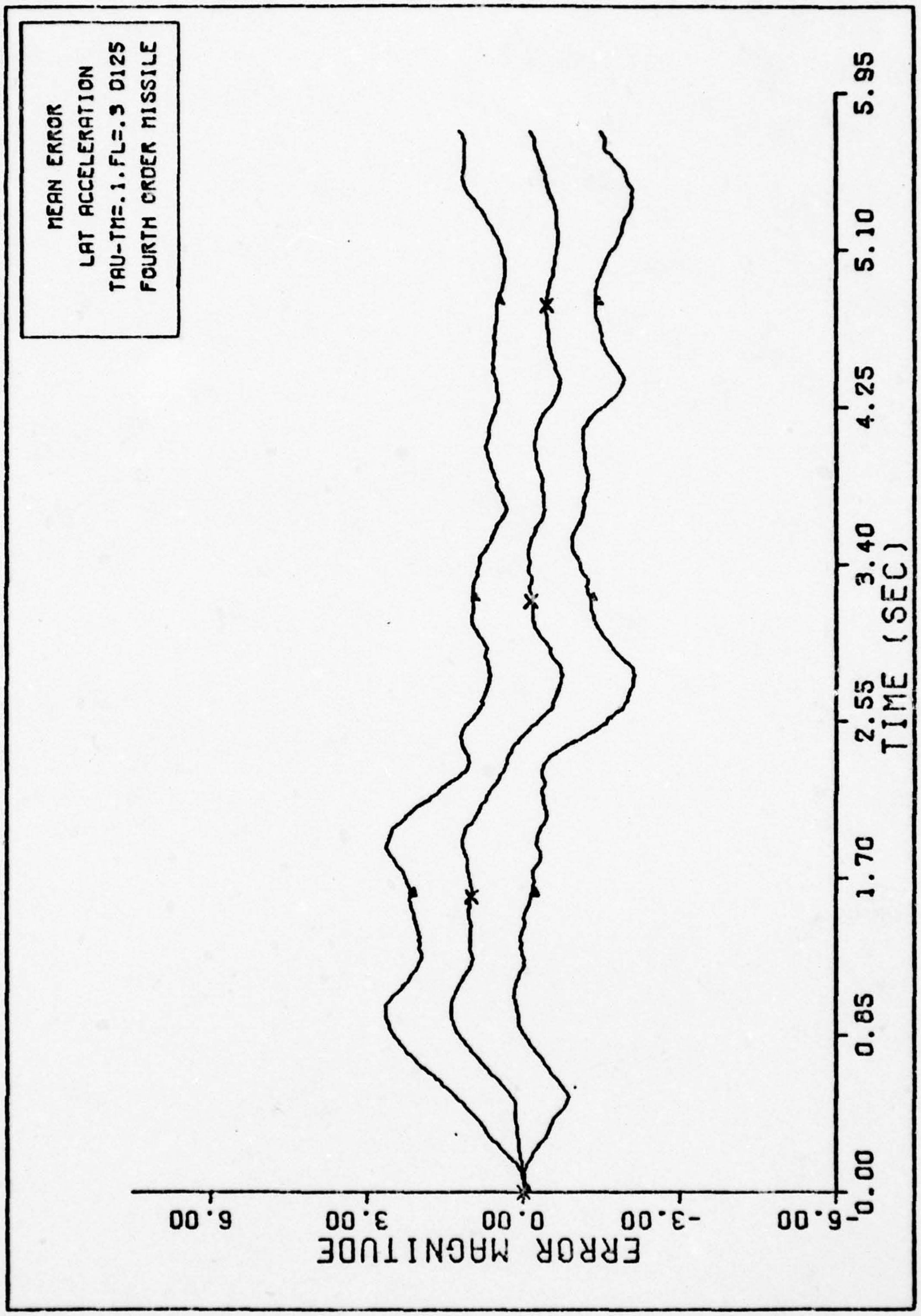

Fig. 120. LAT ACCELERATION FOURTH ORDER MISSILE

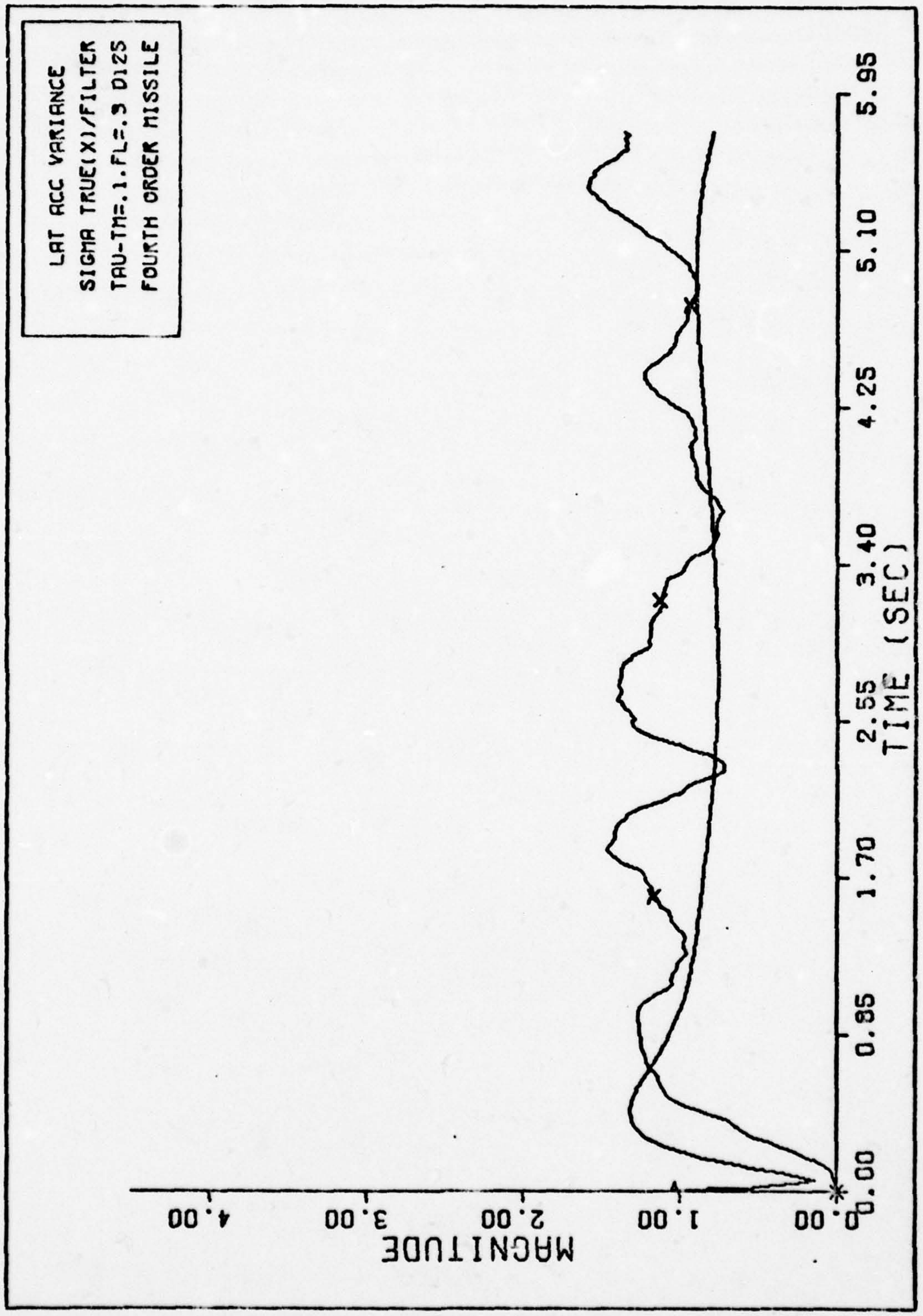

Fig. 121. LAT ACCELERATION SIGMAS FOURTH ORDER

Sensitivity Analysis ($M = 2.$)

The initial state estimates and the tuning parameters for this case are

$$V^I_{mx}(0) = 1225.7 \text{ fps}$$
$$\dot{\theta}_T(0) = 4.363345 \text{ radians}$$
$$R(0) = 10000. \text{ feet}$$
$$\dot{R}(0) = -2122. \text{ fps}$$
$$a_L(0) = 0.$$
$$n(0) = 4.5$$
$$\tau_f(0) = \text{N/A}$$
$$M/S(0) = 29.197 \text{ slugs/ft}^2$$

$$\underline{R} = \begin{bmatrix} 4.E-5 & 0. & 0. \\ 0. & 500. & 0. \\ 0. & 0. & 100. \end{bmatrix}$$

$$\underline{P}_0 = \begin{bmatrix} 100. & 0. & 0. & 0. & 0. & 0. & 0. & 0. \\ 0. & 1.E-8 & 0. & 0. & 0. & 0. & 0. & 0. \\ 0. & 0. & 101. & 0. & 0. & 0. & 0. & 0. \\ 0. & 0. & 0. & 4. & 0. & 0. & 0. & 0. \\ 0. & 0. & 0. & 0. & 1. & 0. & 0. & 0. \\ 0. & 0. & 0. & 0. & 0. & 0. & 0. & 0. \\ 0. & 0. & 0. & 0. & 0. & 0. & 0. & 0. \\ 0. & 0. & 0. & 0. & 0. & 0. & 0. & 0. \end{bmatrix}$$

$$\underline{Q} = \begin{bmatrix} 101. & 0. & 0. & 0. & 0. & 0. & 0. & 0. \\ 0. & 1.E-6 & 0. & 0. & 0. & 0. & 0. & 0. \\ 0. & 0. & 500. & 0. & 0. & 0. & 0. & 0. \\ 0. & 0. & 0. & 100. & 0. & 0. & 0. & 0. \\ 0. & 0. & 0. & 0. & 5. & 0. & 0. & 0. \\ 0. & 0. & 0. & 0. & 0. & 0. & 0. & 0. \\ 0. & 0. & 0. & 0. & 0. & 0. & 0. & 0. \\ 0. & 0. & 0. & 0. & 0. & 0. & 0. & 0. \end{bmatrix}$$

This set of plots was generated by setting the mass in the truth model to 2 slugs. The fourth order filter was used with the mass of the missile in its model set at 4. Both, filter and truth model used an S (for M/S) of .137 ft^2. Only the dynamic states of the missile model were estimated.

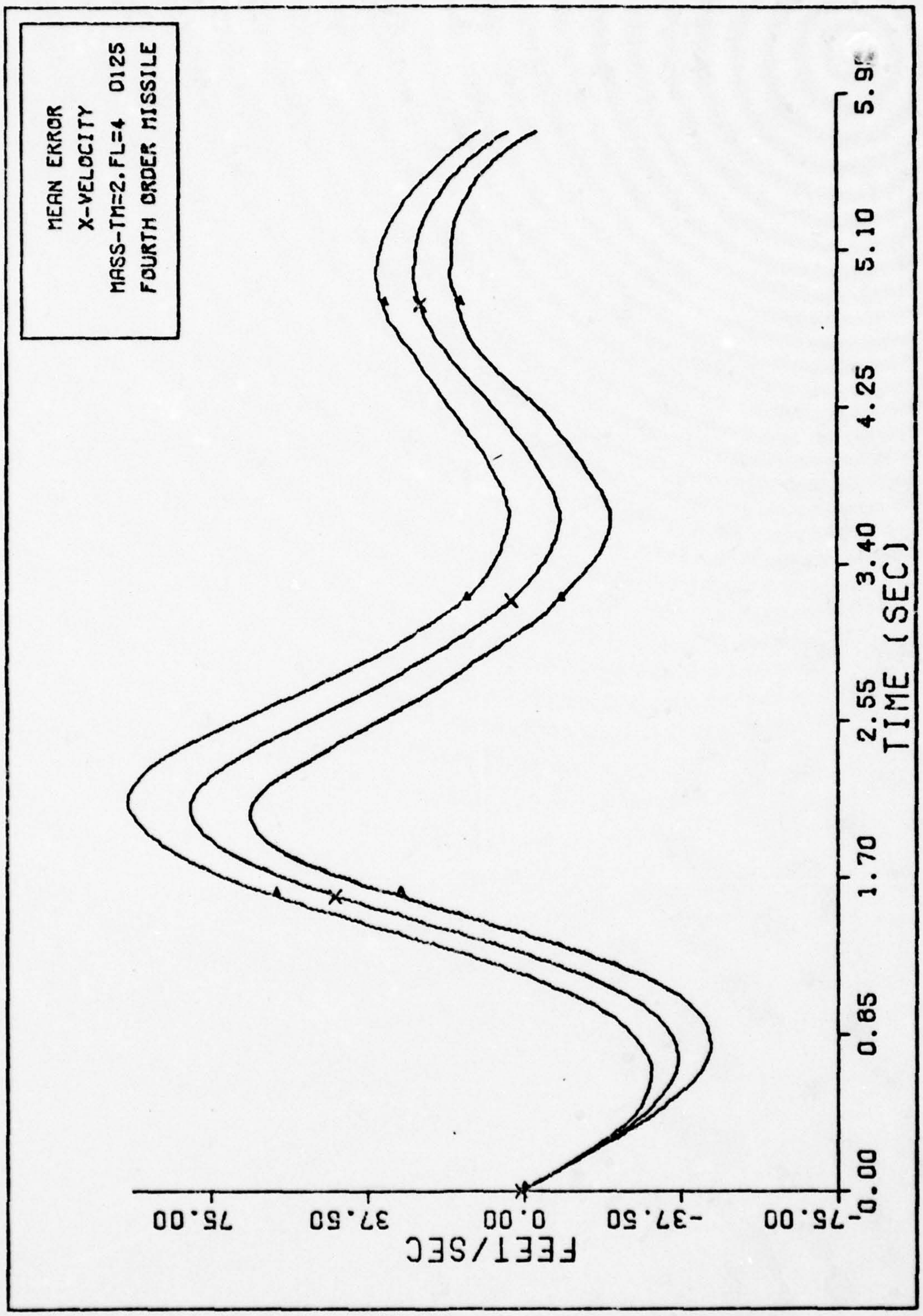

Fig. 122. X-VELOCITY FOURTH ORDER MISSILE

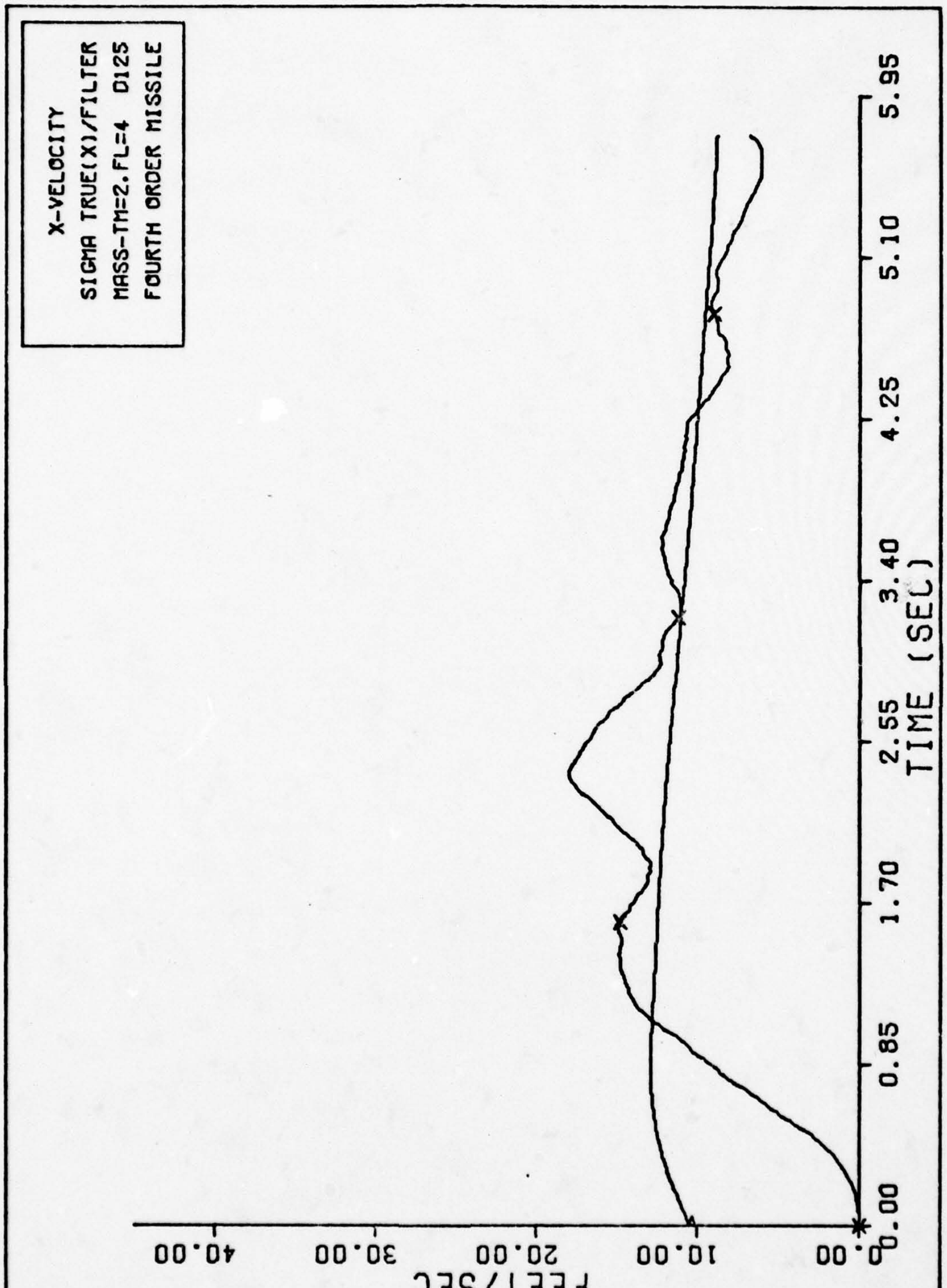

Fig. 123. X-VELOCITY SIGMAS FOURTH ORDER

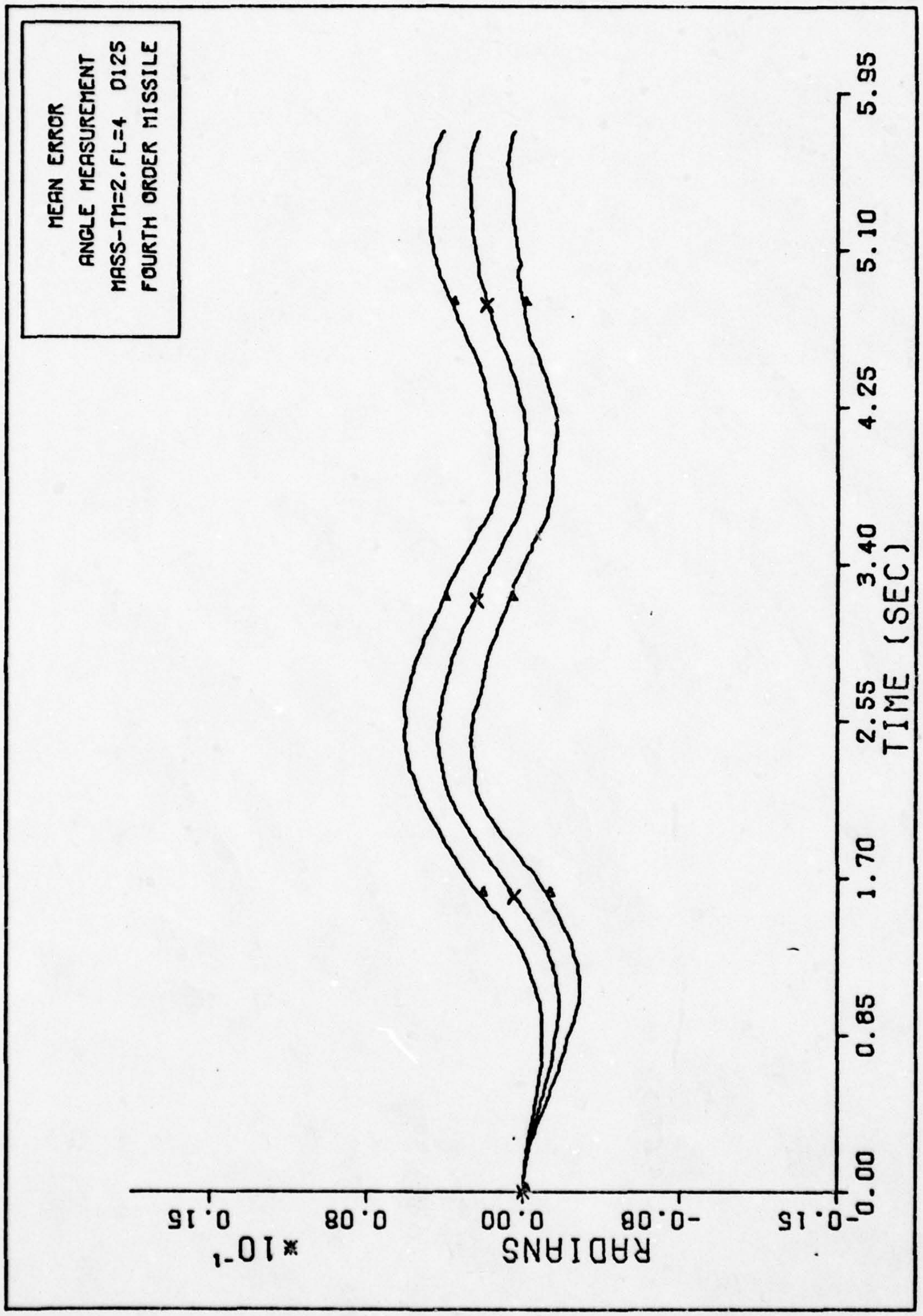

Fig. 124. ANGLE MEASUREMENT FOURTH ORDER MISSILE

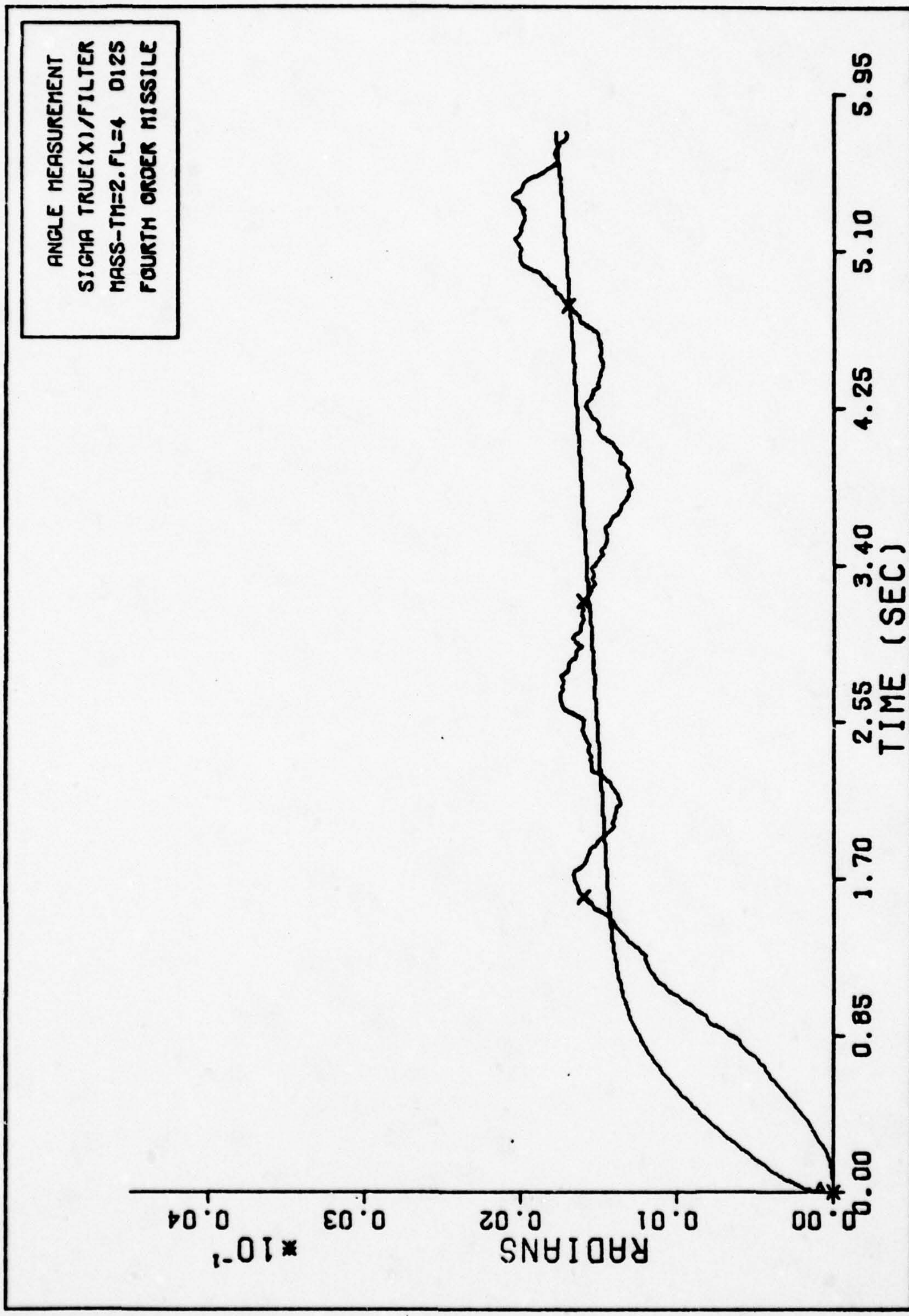

Fig. 125. ANGLE MEASUREMENT SIGMAS FOURTH ORDER

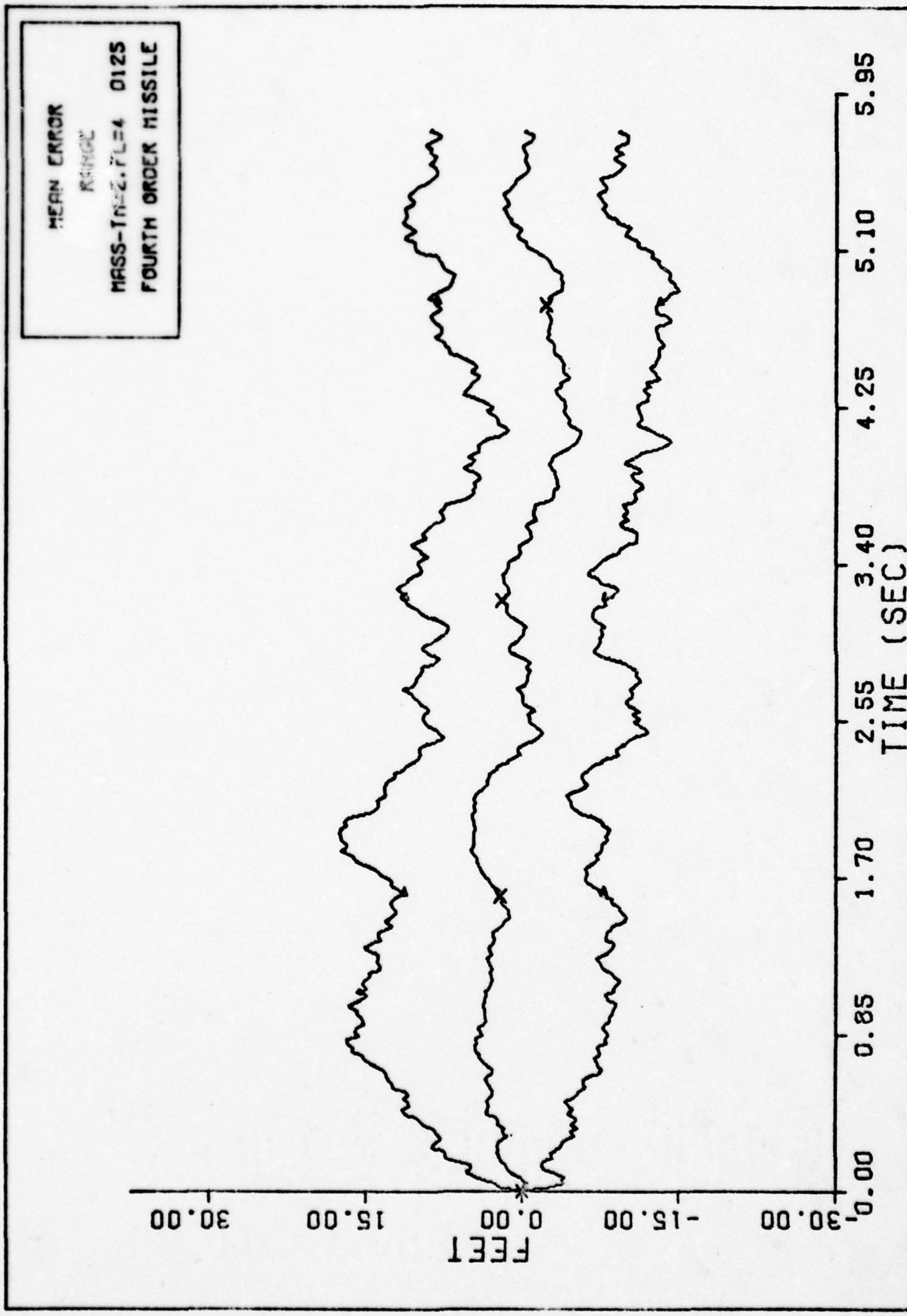

Fig. 126. RANGE FOURTH ORDER MISSILE

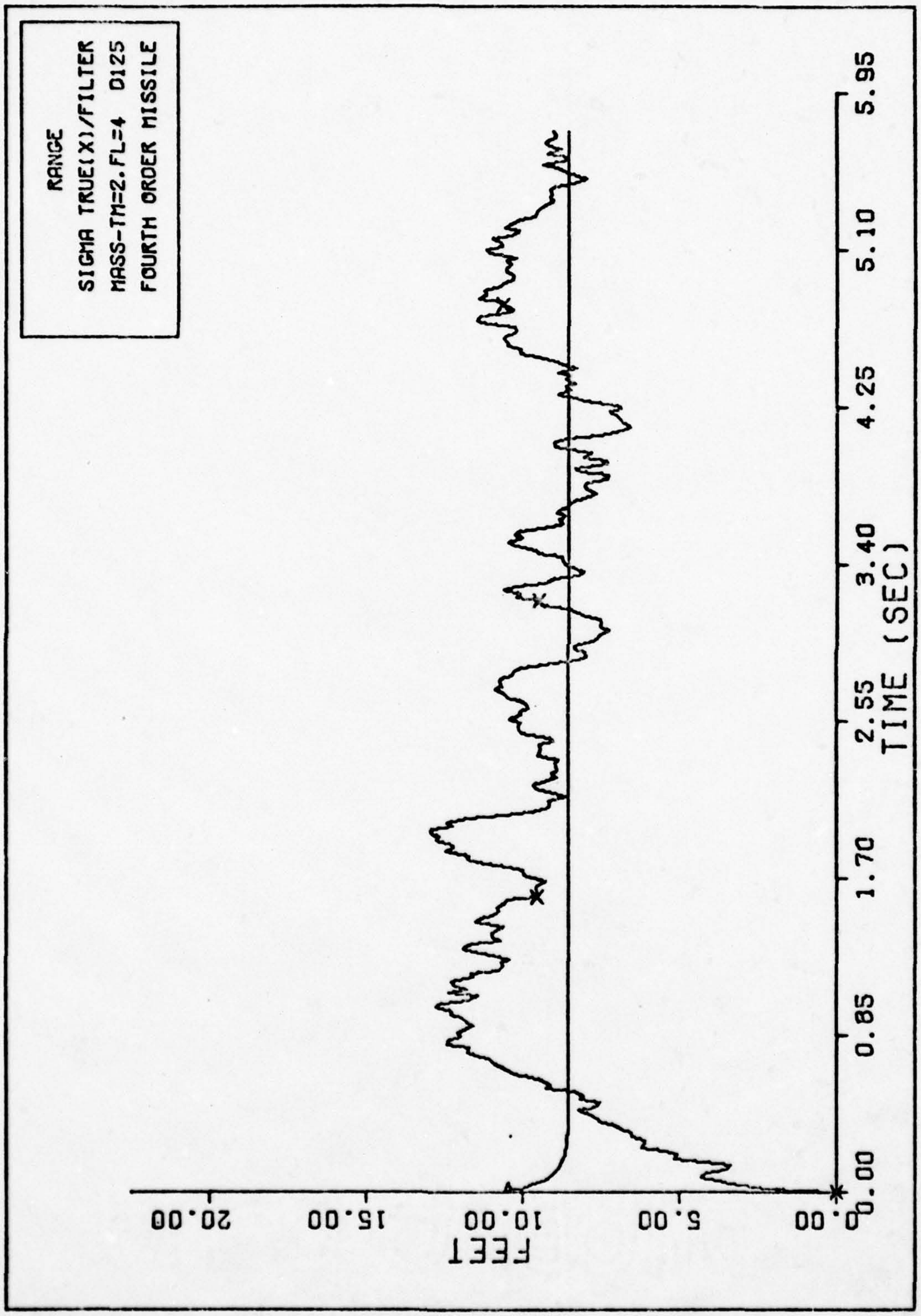

Fig. 127. RANGE SIGMAS FOURTH ORDER

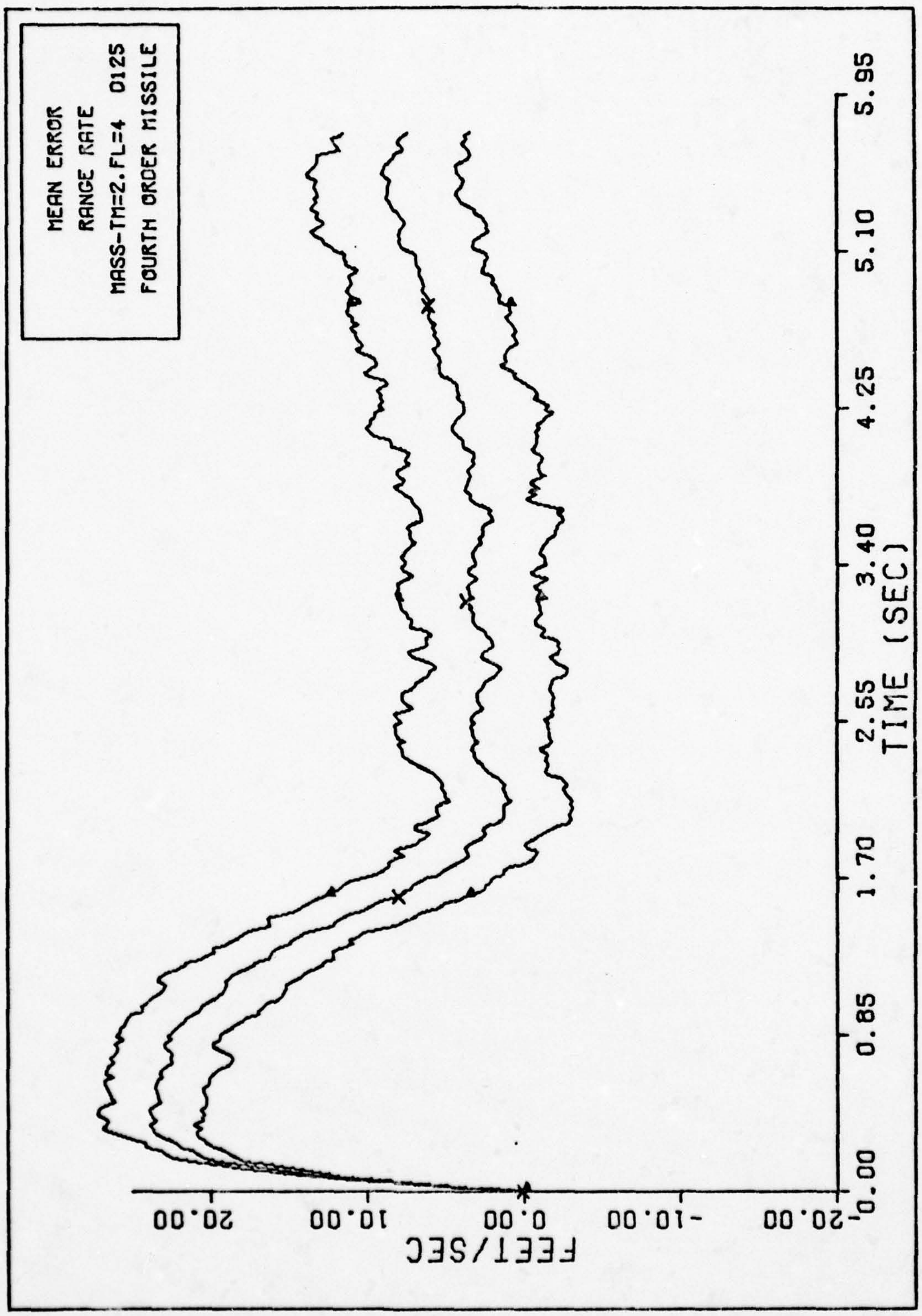

Fig. 128. RANGE RATE FOURTH ORDER MISSILE

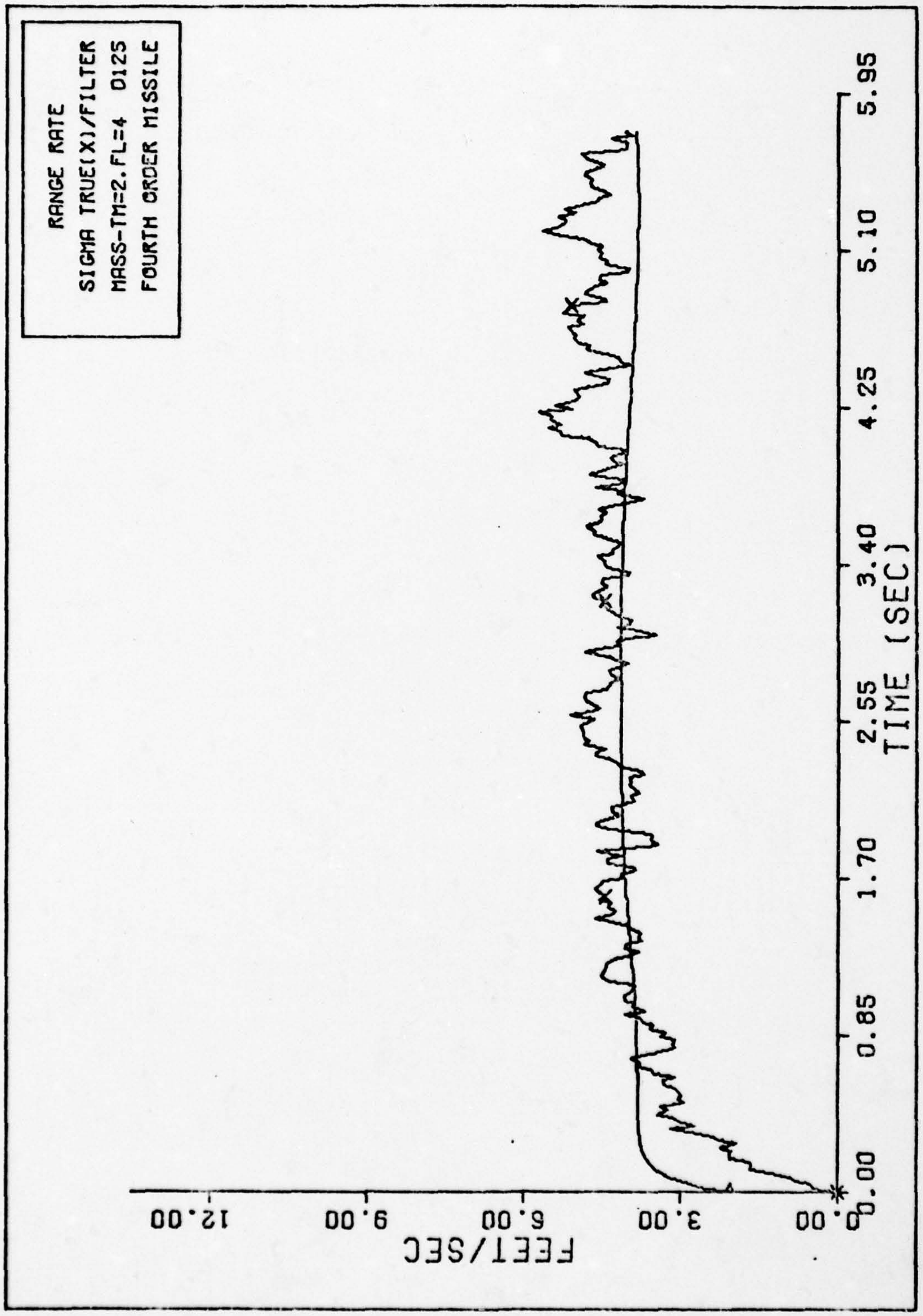

Fig. 129. RANGE RATE SIGMAS FOURTH ORDER

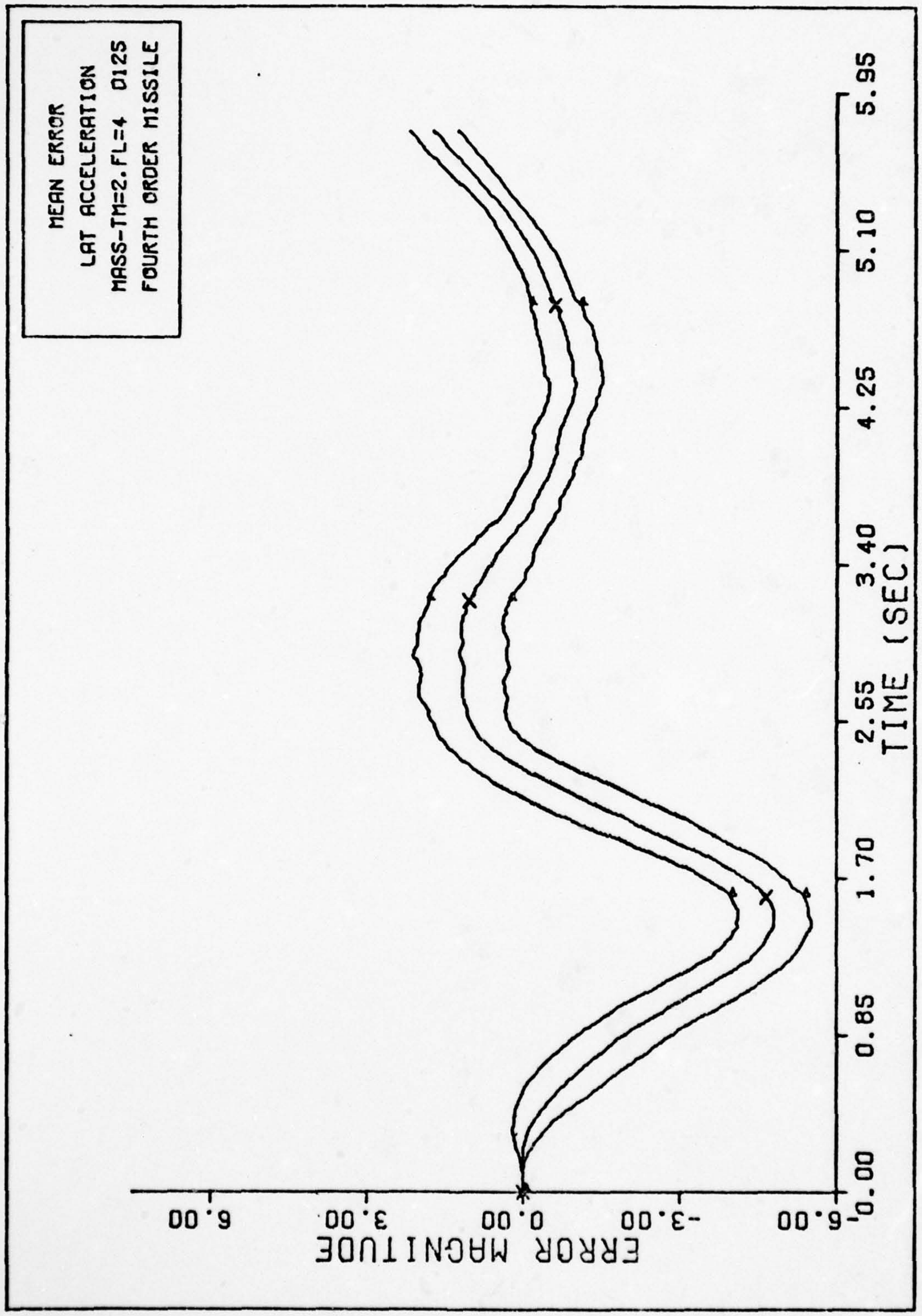

Fig. 130. LAT ACCELERATION FOURTH ORDER MISSILE

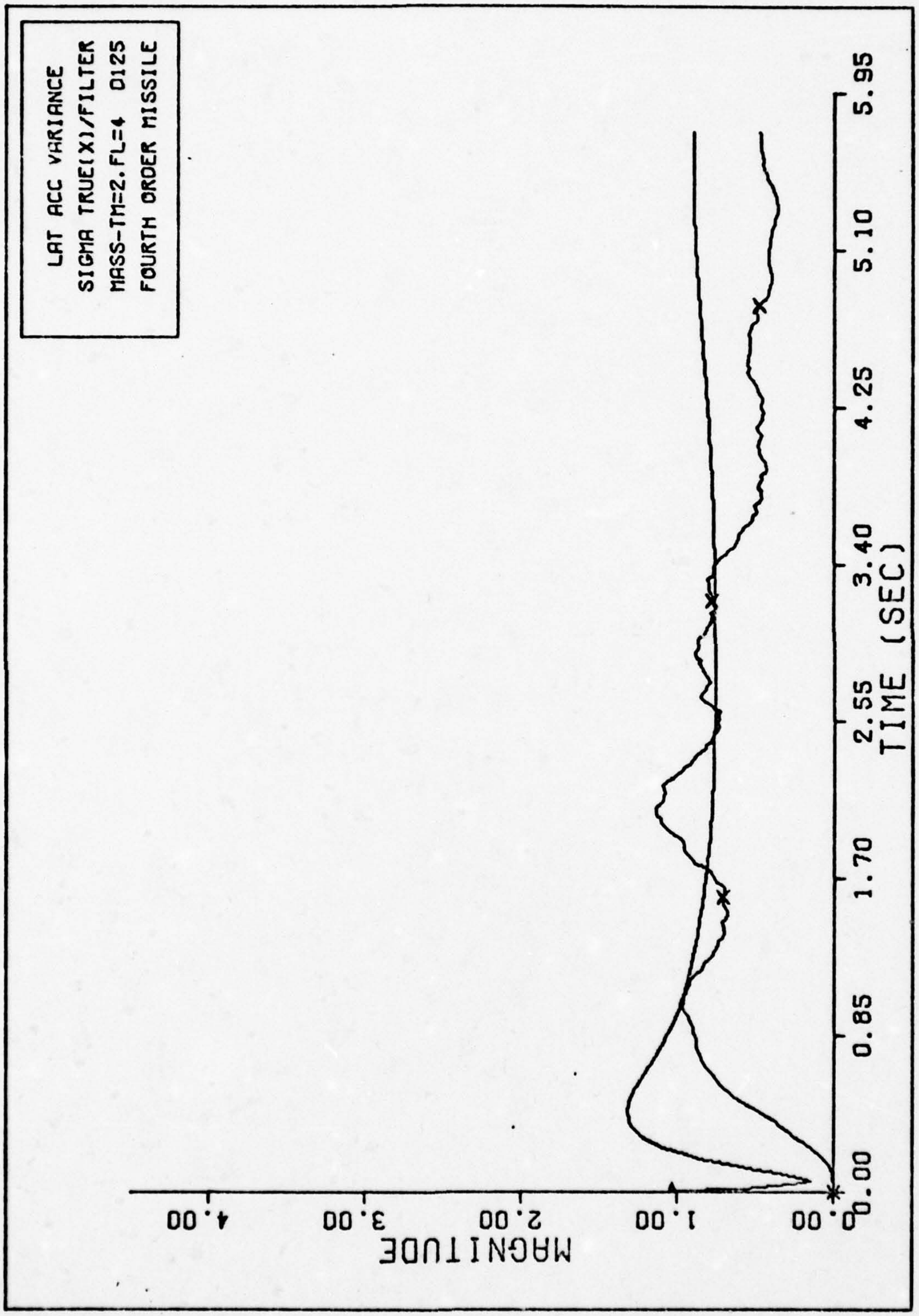

Fig. 131. LAT ACCELERATION SIGMAS FOURTH ORDER

Sensitivity Analysis ($M = 8.$)

The initial state estimates and the tuning parameters for this case are

$$
\begin{aligned}
V^I_{mx}(0) &= 1225.7 \text{ fps} \\
\dot{\theta}_T(0) &= 4.363345 \text{ radians} \\
R(0) &= 10000. \text{ feet} \\
\dot{R}(0) &= -2122. \text{ fps} \\
a_L(0) &= 0. \\
n(0) &= 4.5 \\
\tau_f(0) &= \text{N/A} \\
M/S(0) &= 29.197 \text{ slugs/ft}^2
\end{aligned}
$$

$$
\underline{R} = \begin{bmatrix} 4.E{-5} & 0. & 0. \\ 0. & 500. & 0. \\ 0. & 0. & 100. \end{bmatrix}
$$

$$
\underline{P}_0 = \begin{bmatrix}
100. & 0. & 0. & 0. & 0. & 0. & 0. & 0. \\
0. & 1.E{-8} & 0. & 0. & 0. & 0. & 0. & 0. \\
0. & 0. & 101. & 0. & 0. & 0. & 0. & 0. \\
0. & 0. & 0. & 4. & 0. & 0. & 0. & 0. \\
0. & 0. & 0. & 0. & 1. & 0. & 0. & 0. \\
0. & 0. & 0. & 0. & 0. & 0. & 0. & 0. \\
0. & 0. & 0. & 0. & 0. & 0. & 0. & 0. \\
0. & 0. & 0. & 0. & 0. & 0. & 0. & 0.
\end{bmatrix}
$$

$$
\underset{\sim}{Q} = \begin{bmatrix}
101. & 0. & 0. & 0. & 0. & 0. & 0. & 0. \\
0. & 1.E-6 & 0. & 0. & 0. & 0. & 0. & 0. \\
0. & 0. & 500. & 0. & 0. & 0. & 0. & 0. \\
0. & 0. & 0. & 100. & 0. & 0. & 0. & 0. \\
0. & 0. & 0. & 0. & 5. & 0. & 0. & 0. \\
0. & 0. & 0. & 0. & 0. & 0. & 0. & 0. \\
0. & 0. & 0. & 0. & 0. & 0. & 0. & 0. \\
0. & 0. & 0. & 0. & 0. & 0. & 0. & 0.
\end{bmatrix}
$$

This set of plots was generated by setting the mass in the truth model to 8 slugs. The fourth order filter was used with the mass of the missile in its model set at 4. Both, filter and truth model used an S (for M/S) of .137 ft^2. Only the dynamic states of the missile model were estimated.

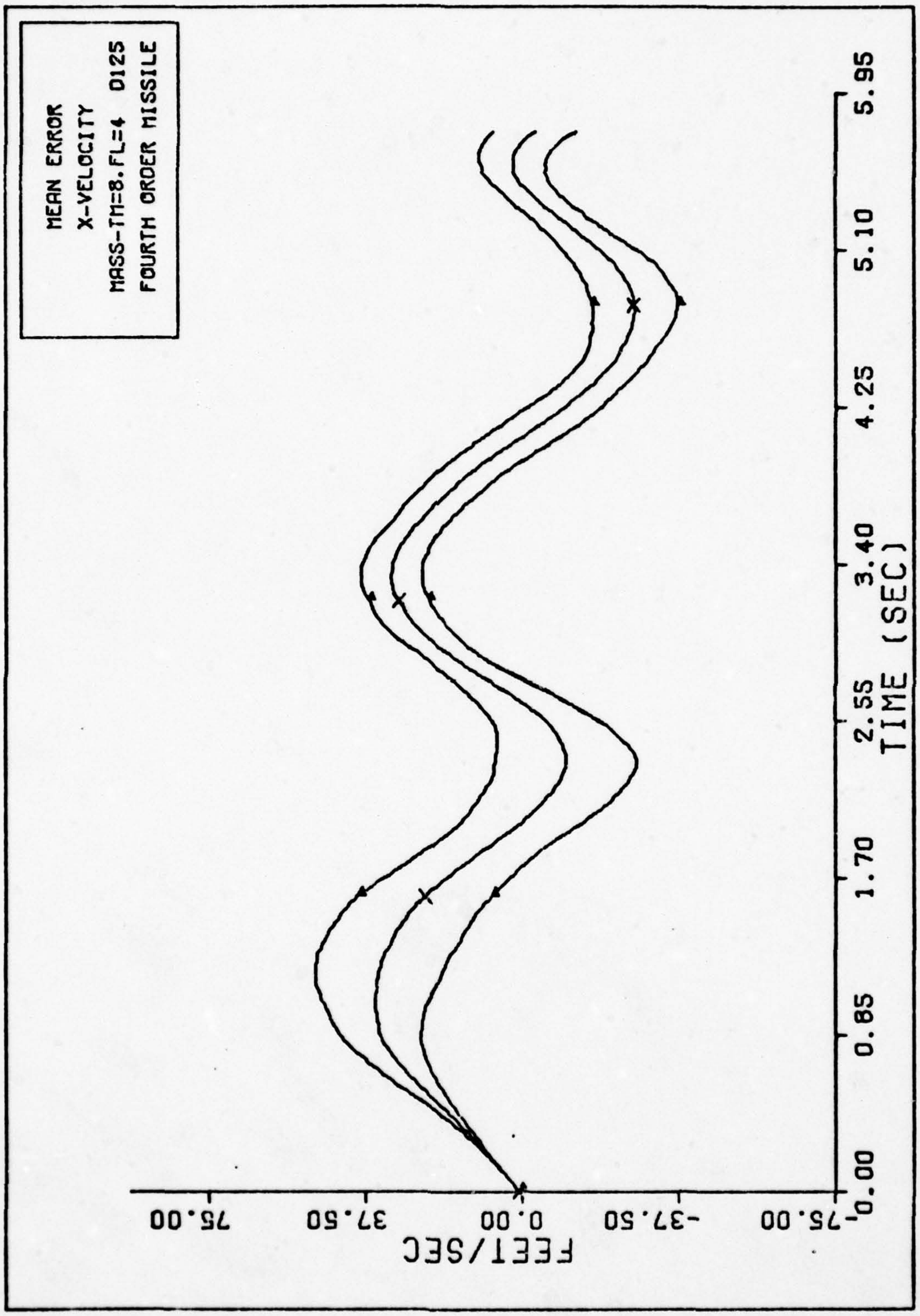

Fig. 132. X-VELOCITY FOURTH ORDER MISSILE

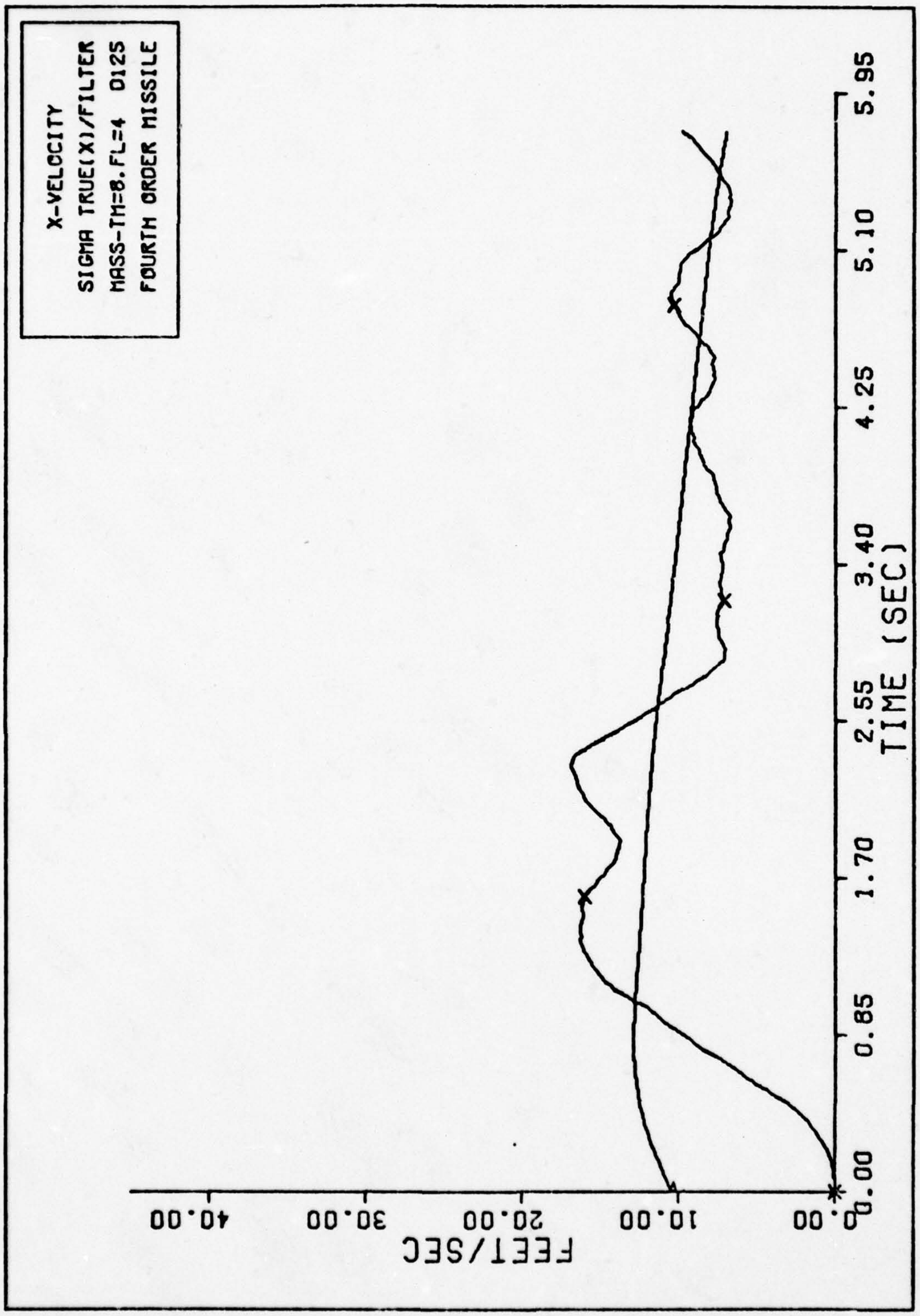

Fig. 133. X-VELOCITY SIGMAS FOURTH ORDER

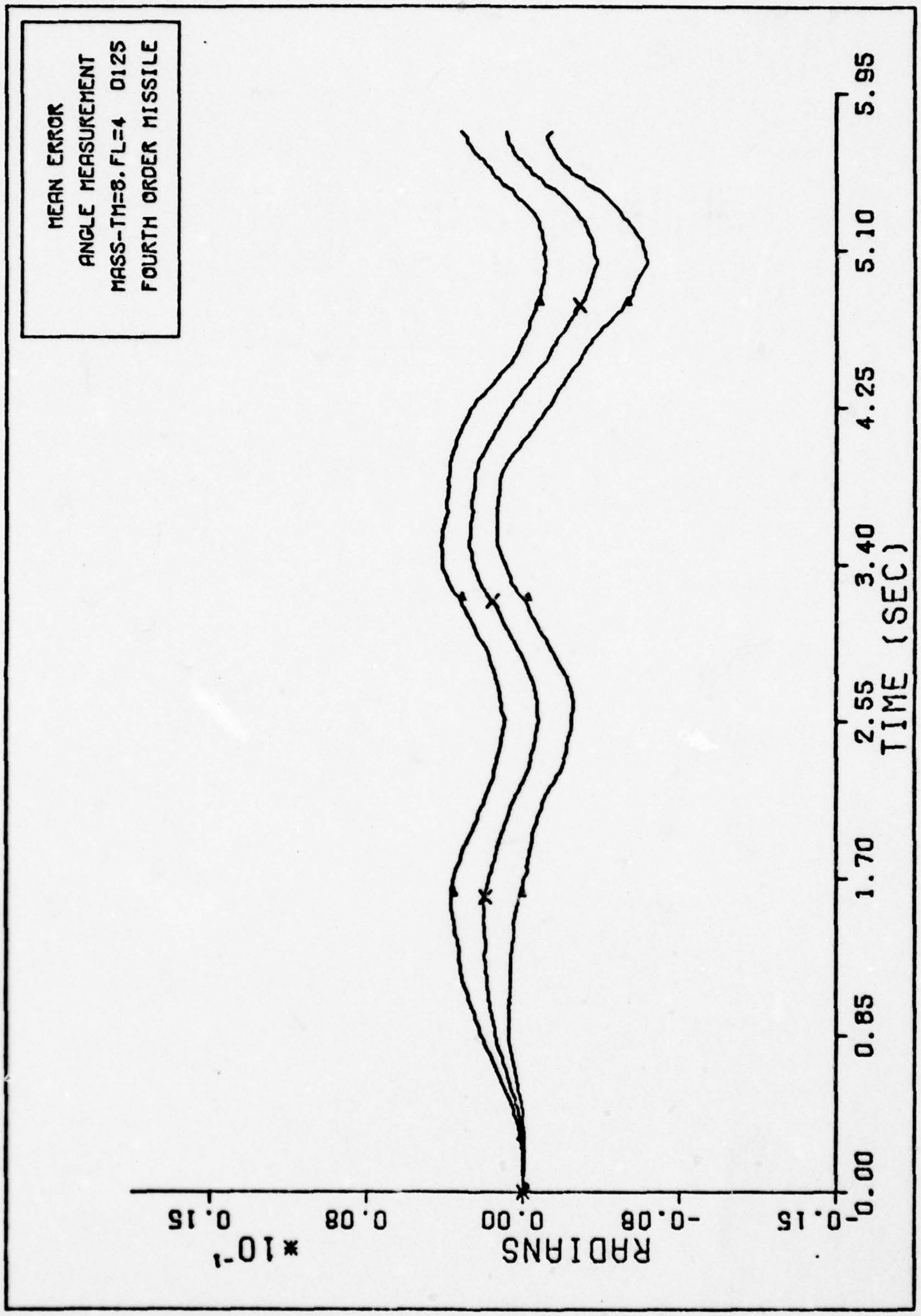

Fig. 134. ANGLE MEASUREMENT FOURTH ORDER MISSILE

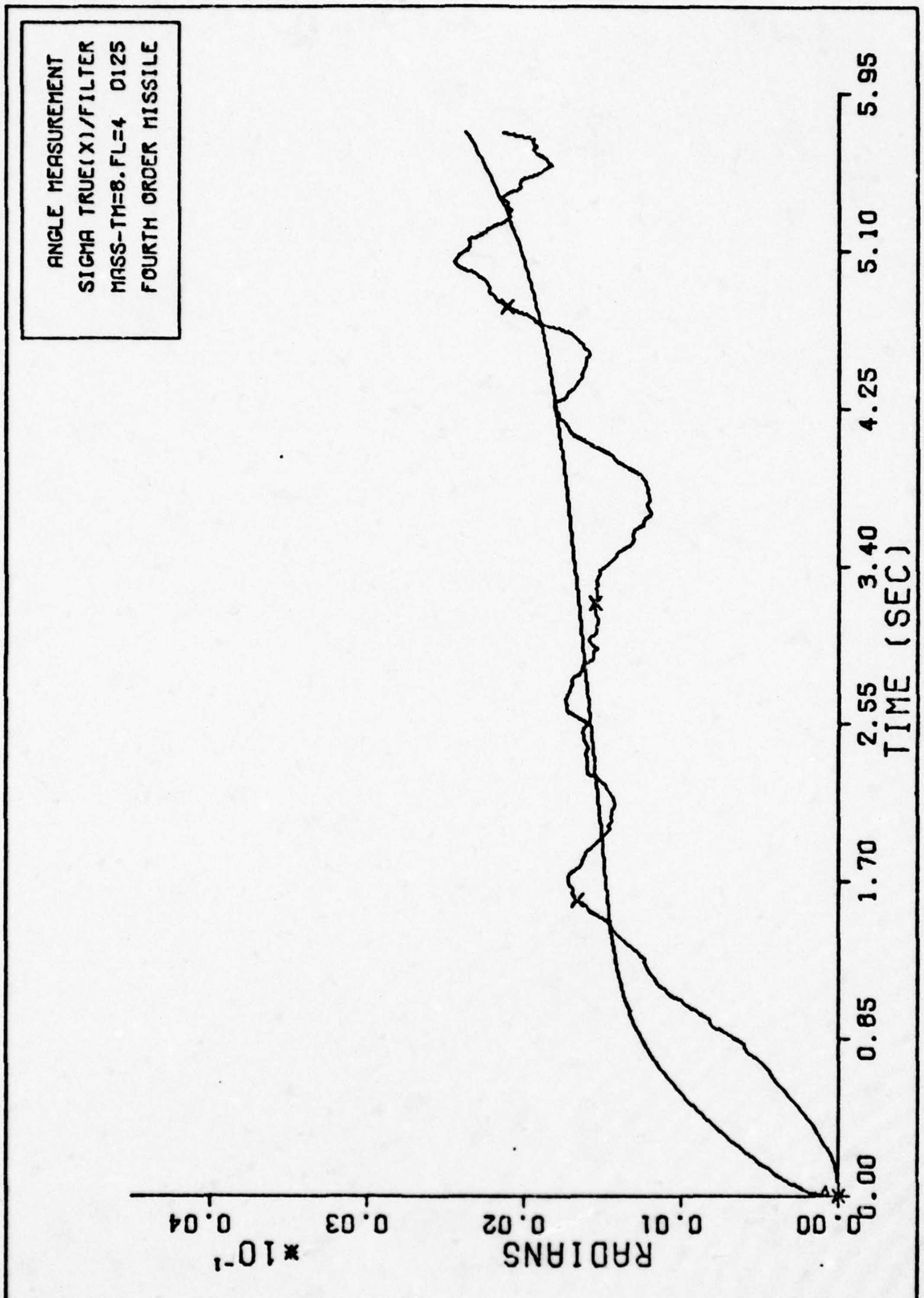

Fig. 135. ANGLE MEASUREMENT SIGMAS FOURTH ORDER

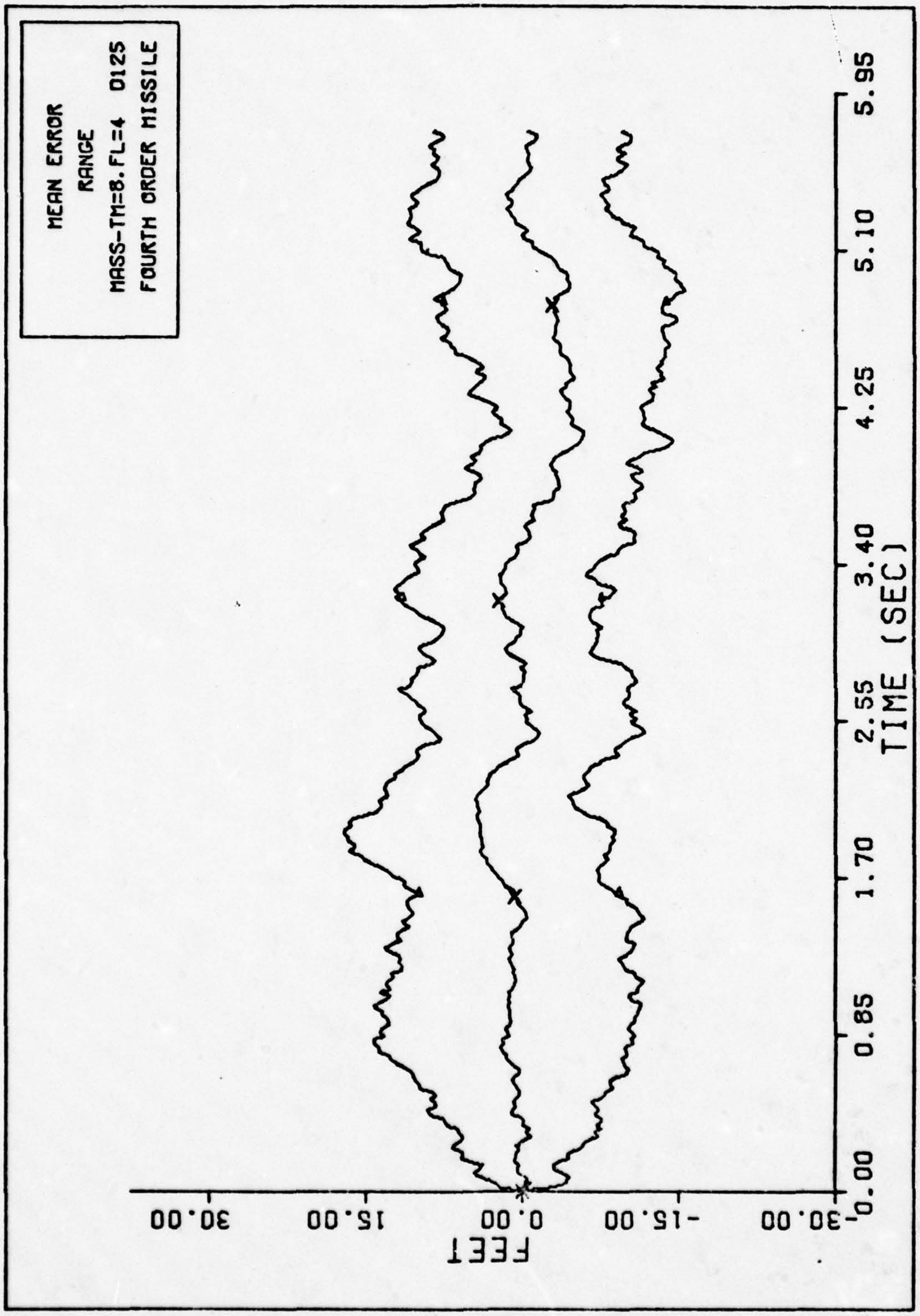

Fig. 136. RANGE FOURTH ORDER MISSILE

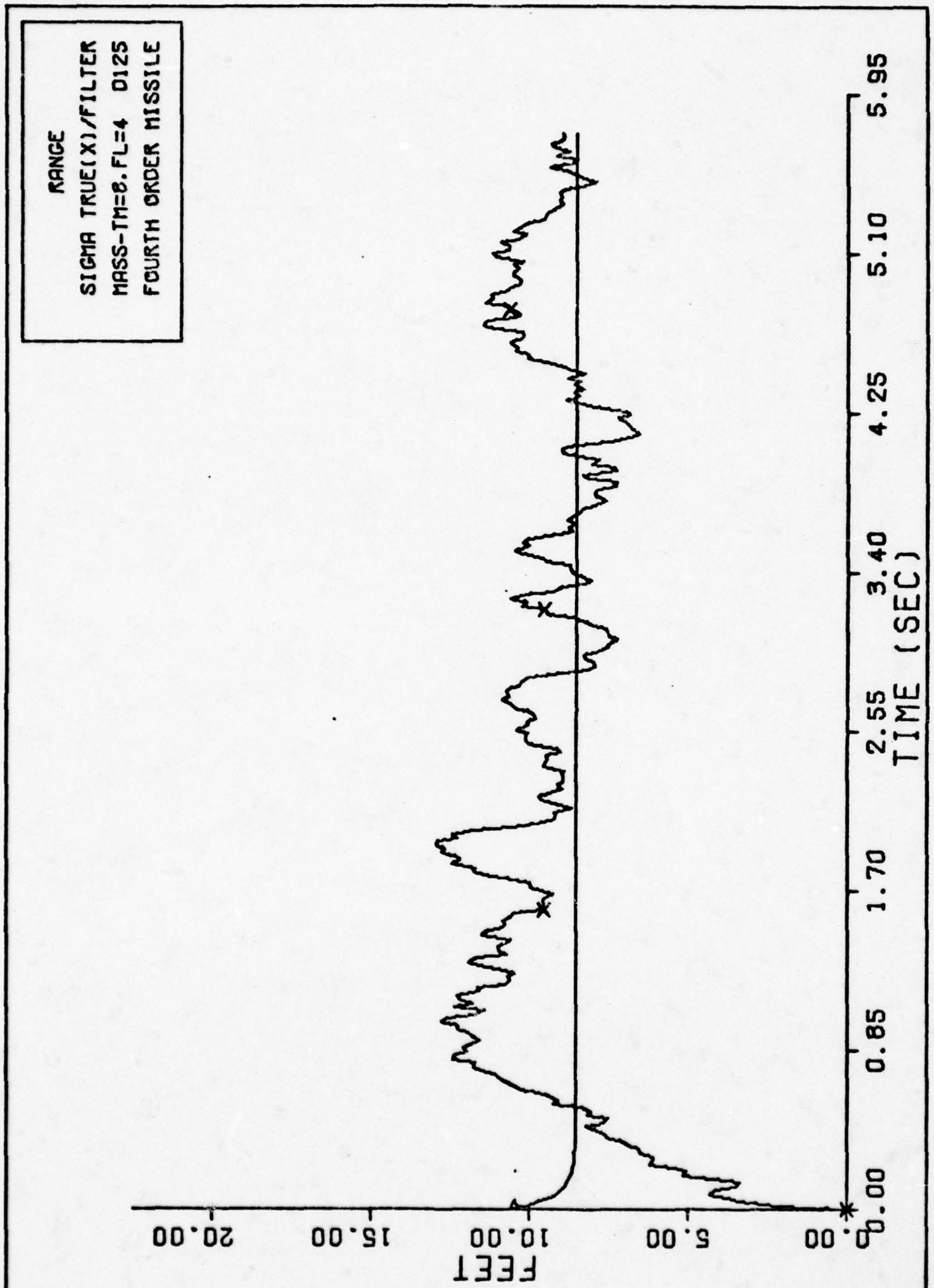

Fig. 137. RANGE SIGMAS FOURTH ORDER

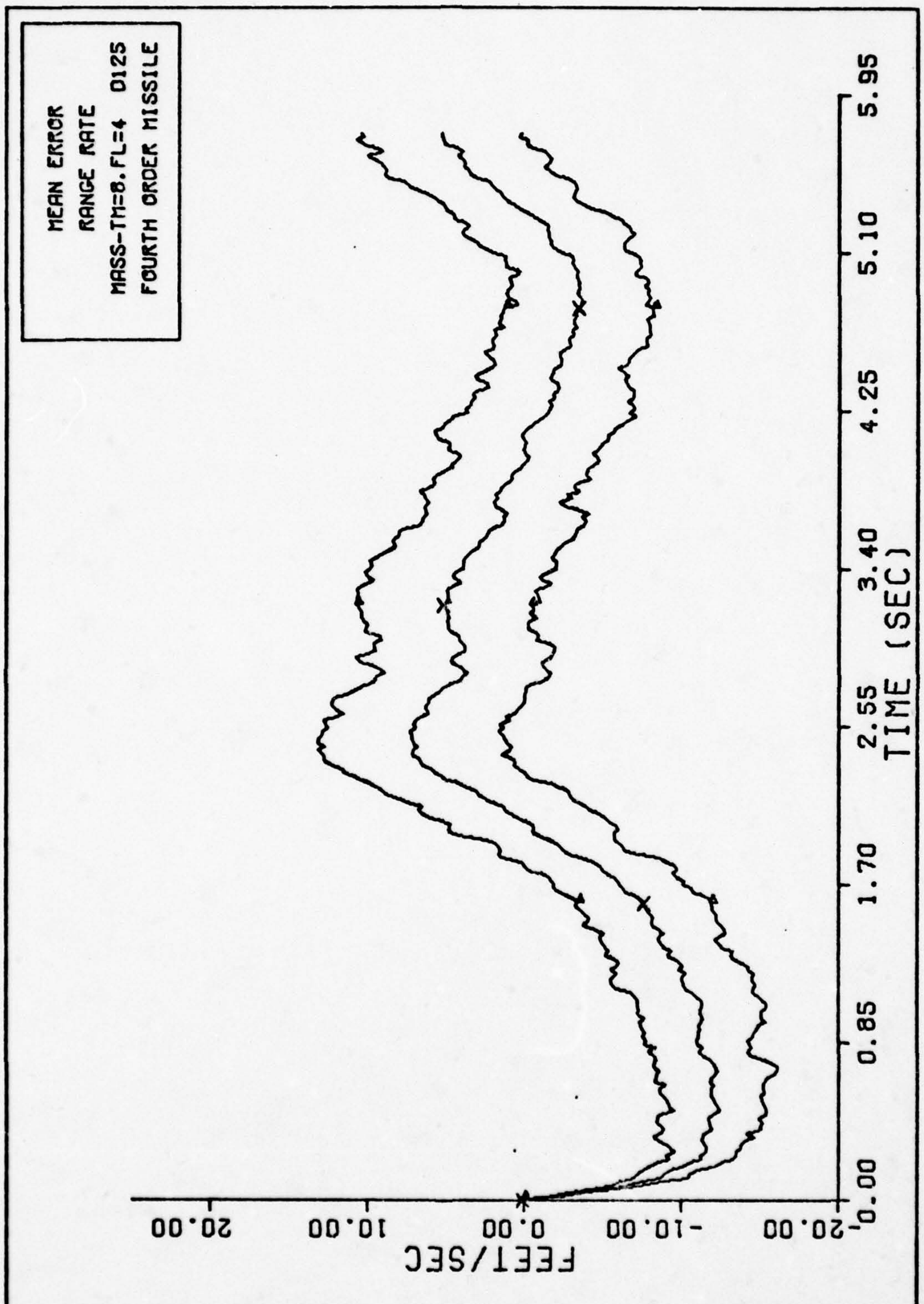

Fig. 138. RANGE RATE FOURTH ORDER MISSILE

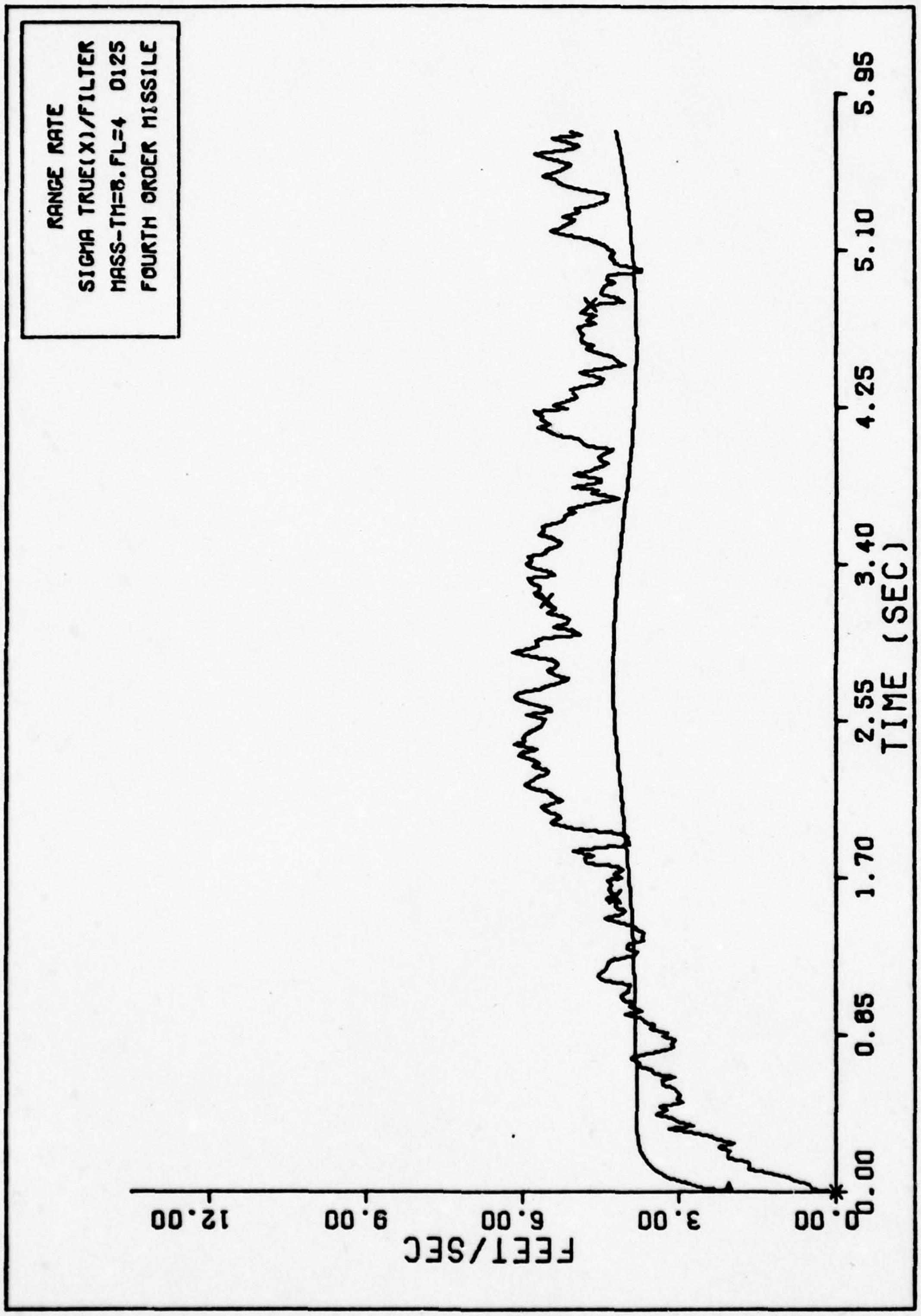

Fig. 139. RANGE RATE SIGMAS FOURTH ORDER

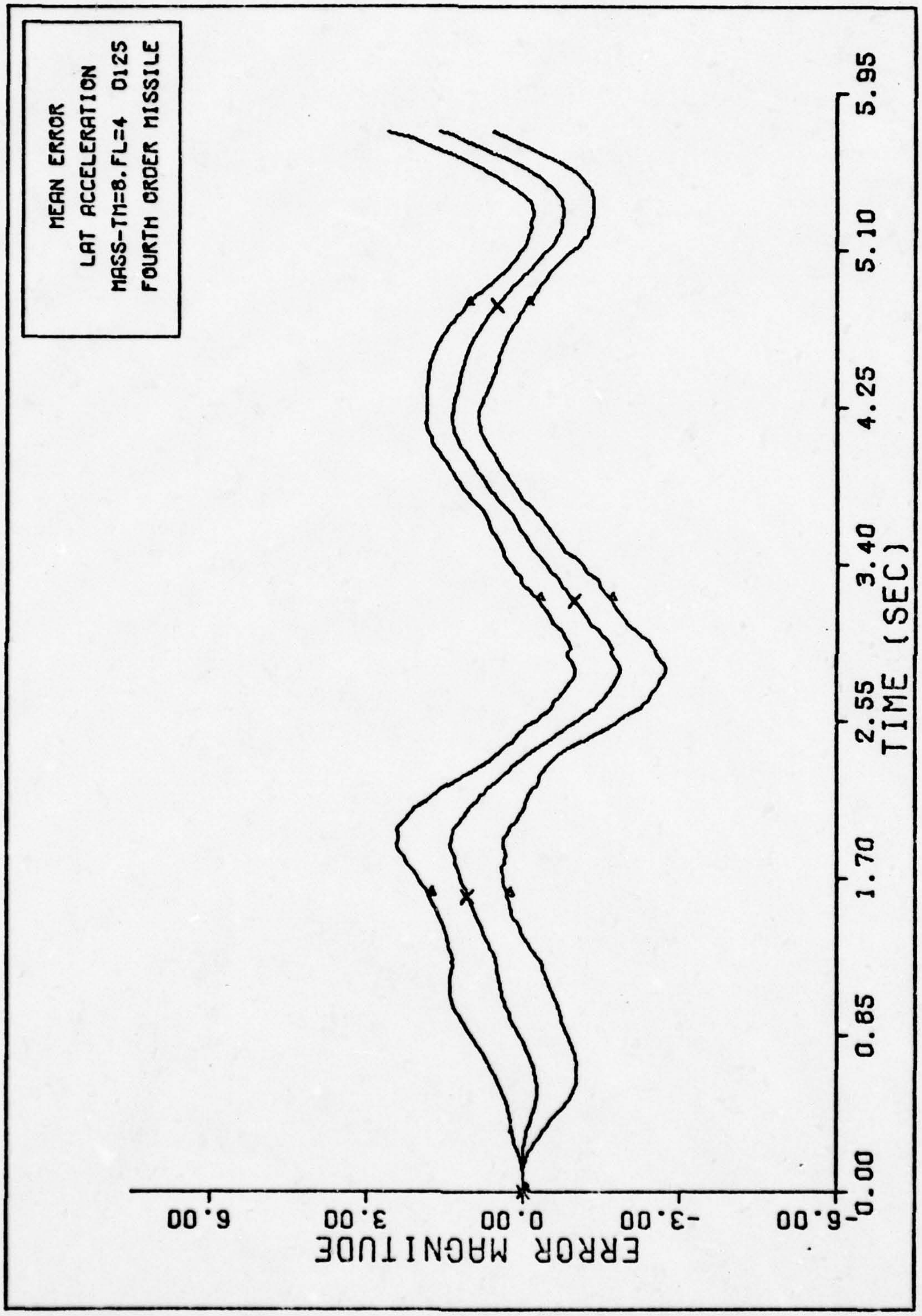

Fig. 140. LAT ACCELERATION FOURTH ORDER MISSILE

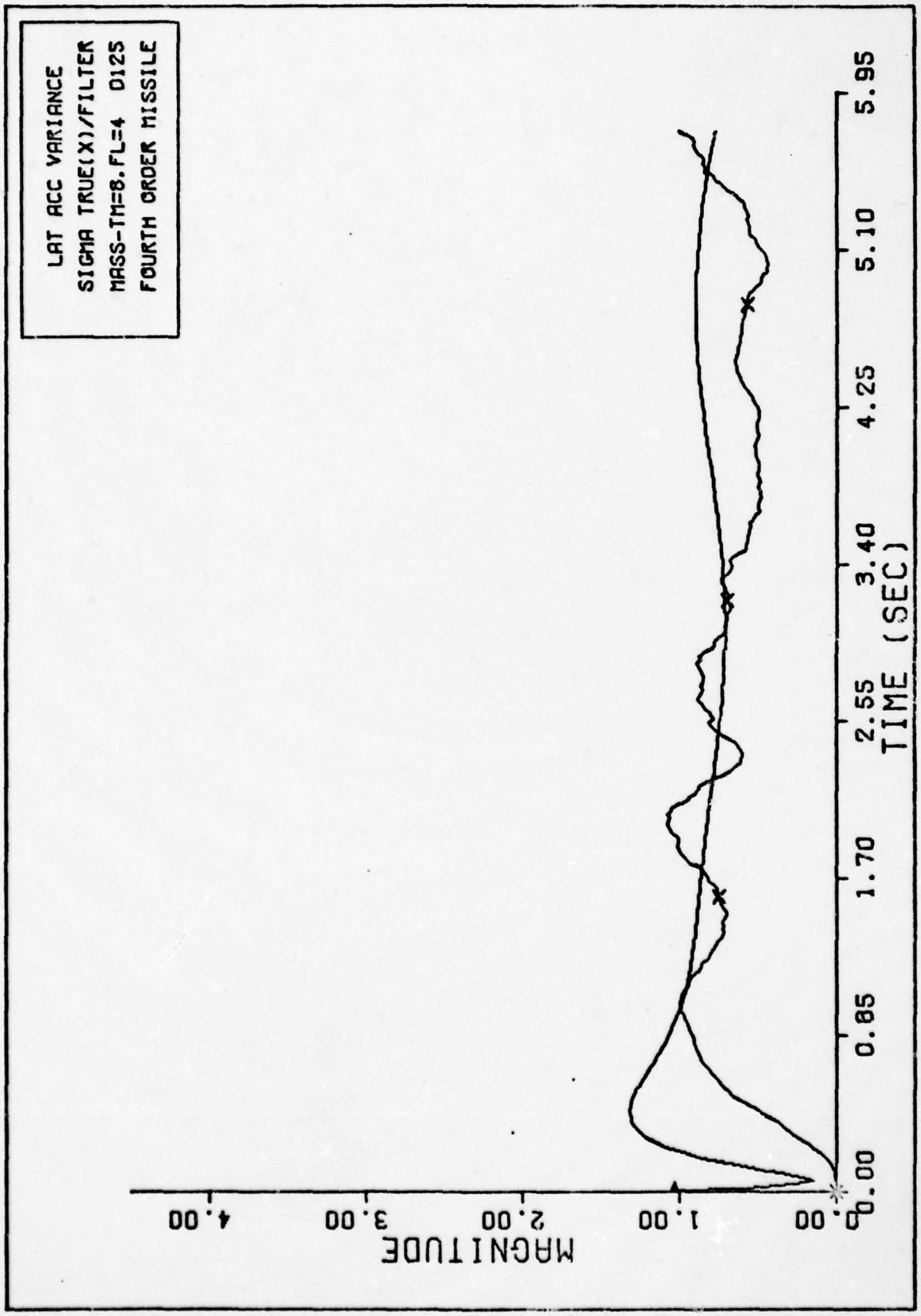

Fig. 141. LAT ACCELERATION SIGMAS FOURTH ORDER

First Order Missile Filter (τ_f set equal to .85)

The initial state estimates and the tuning parameters for this case are

$$
\begin{aligned}
V_{mx}^{I}(0) &= 1225.7 \text{ fps} \\
\dot{\theta}_T(0) &= 4.363345 \text{ radians} \\
R(0) &= 10000. \text{ feet} \\
\dot{R}(0) &= -2122. \text{ fps} \\
a_L(0) &= 0. \\
n(0) &= 4.5 \\
\tau_f(0) &= .85 \text{ seconds} \\
M/S(0) &= 29.197 \text{ slugs/ft}^2
\end{aligned}
$$

$$
\underline{R} = \begin{bmatrix} 3.E-5 & 0. & 0. \\ 0. & 500. & 0. \\ 0. & 0. & 100. \end{bmatrix}
$$

$$
\underline{P}_0 = \begin{bmatrix}
100. & 0. & 0. & 0. & 0. & 0. & 0. & 0. \\
0. & 1.E-8 & 0. & 0. & 0. & 0. & 0. & 0. \\
0. & 0. & 101. & 0. & 0. & 0. & 0. & 0. \\
0. & 0. & 0. & 4. & 0. & 0. & 0. & 0. \\
0. & 0. & 0. & 0. & 1. & 0. & 0. & 0. \\
0. & 0. & 0. & 0. & 0. & 0. & 0. & 0. \\
0. & 0. & 0. & 0. & 0. & 0. & 0. & 0. \\
0. & 0. & 0. & 0. & 0. & 0. & 0. & 0.
\end{bmatrix}
$$

$$\underline{Q} = \begin{bmatrix} 250. & 0. & 0. & 0. & 0. & 0. & 0. & 0. \\ 0. & 1.E-6 & 0. & 0. & 0. & 0. & 0. & 0. \\ 0. & 0. & 500. & 0. & 0. & 0. & 0. & 0. \\ 0. & 0. & 0. & 200. & 0. & 0. & 0. & 0. \\ 0. & 0. & 0. & 0. & 1. & 0. & 0. & 0. \\ 0. & 0. & 0. & 0. & 0. & 0. & 0. & 0. \\ 0. & 0. & 0. & 0. & 0. & 0. & 0. & 0. \\ 0. & 0. & 0. & 0. & 0. & 0. & 0. & 0. \end{bmatrix}$$

These plots were generated by the first order filter with a time constant of .85 seconds. The value of τ_f was found from an iterative process by comparing filter performance for various values of τ_f. .85 seconds was found to produce the least error in the dynamic states of the missile model. Only the dynamic states were estimated in this case.

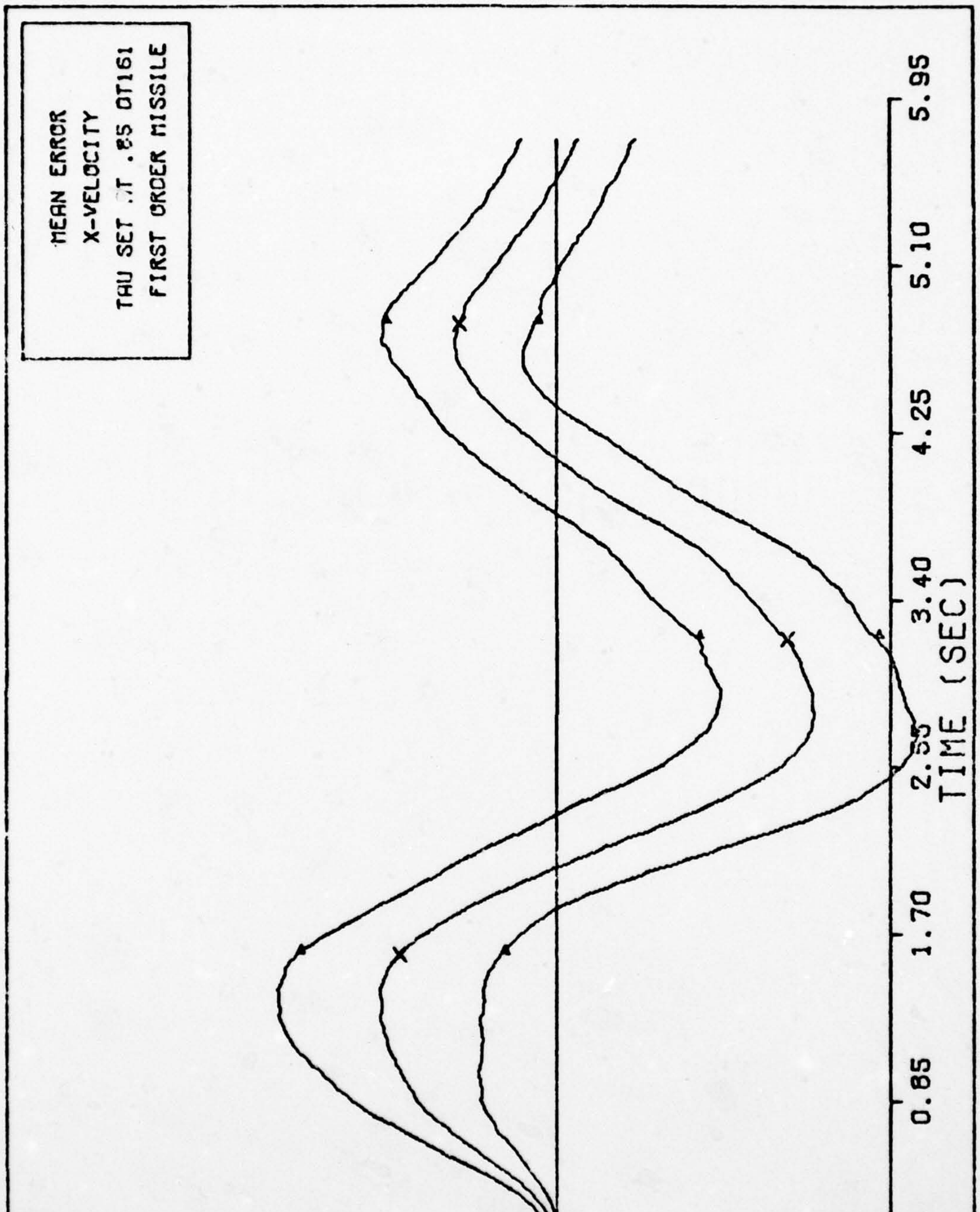

Fig. 142. X-VELOCITY FIRST ORDER MISSILE

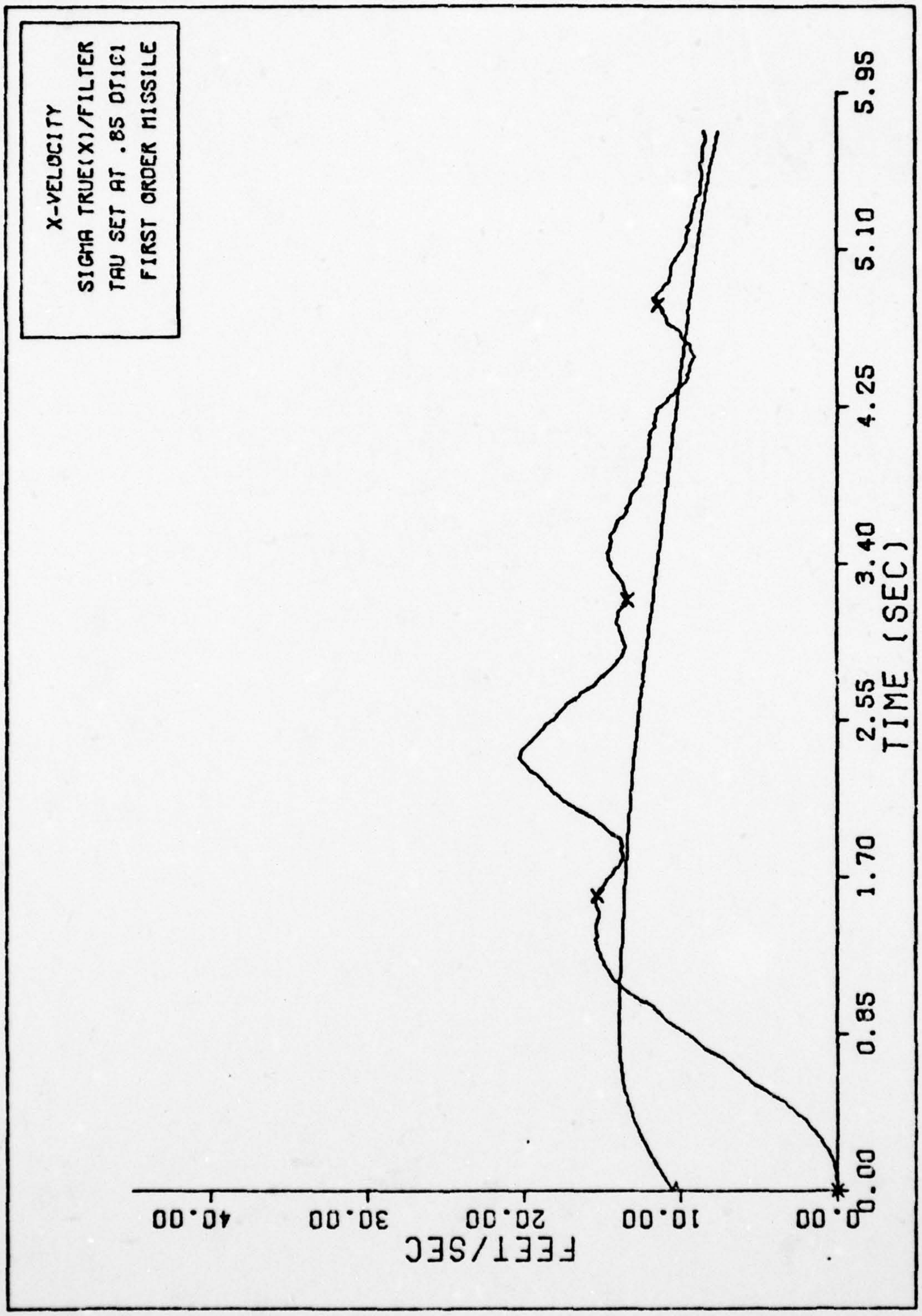

Fig. 143. X-VELOCITY SIGMAS FIRST ORDER

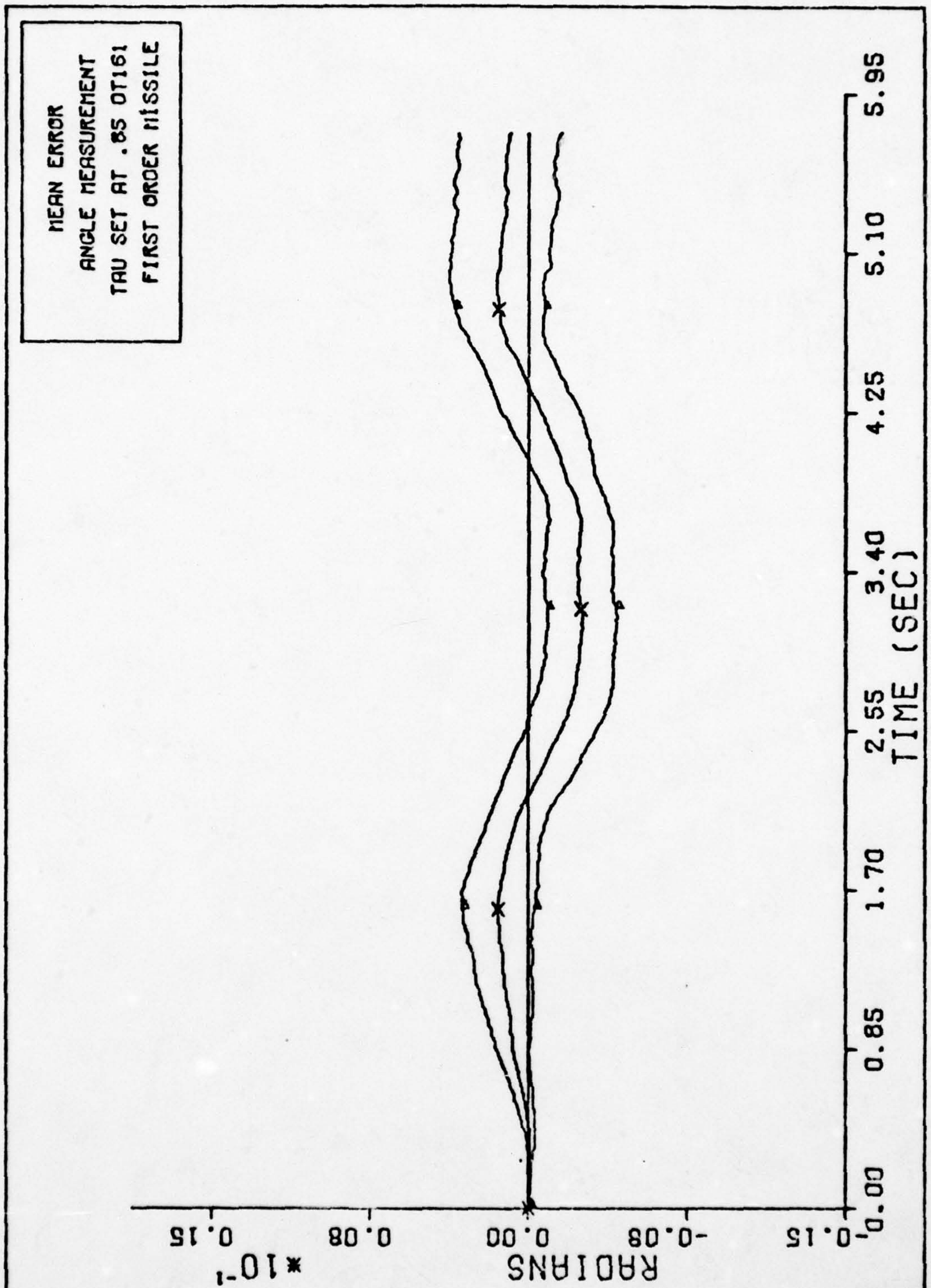

Fig. 144. ANGLE MEASUREMENT FIRST ORDER MISSILE

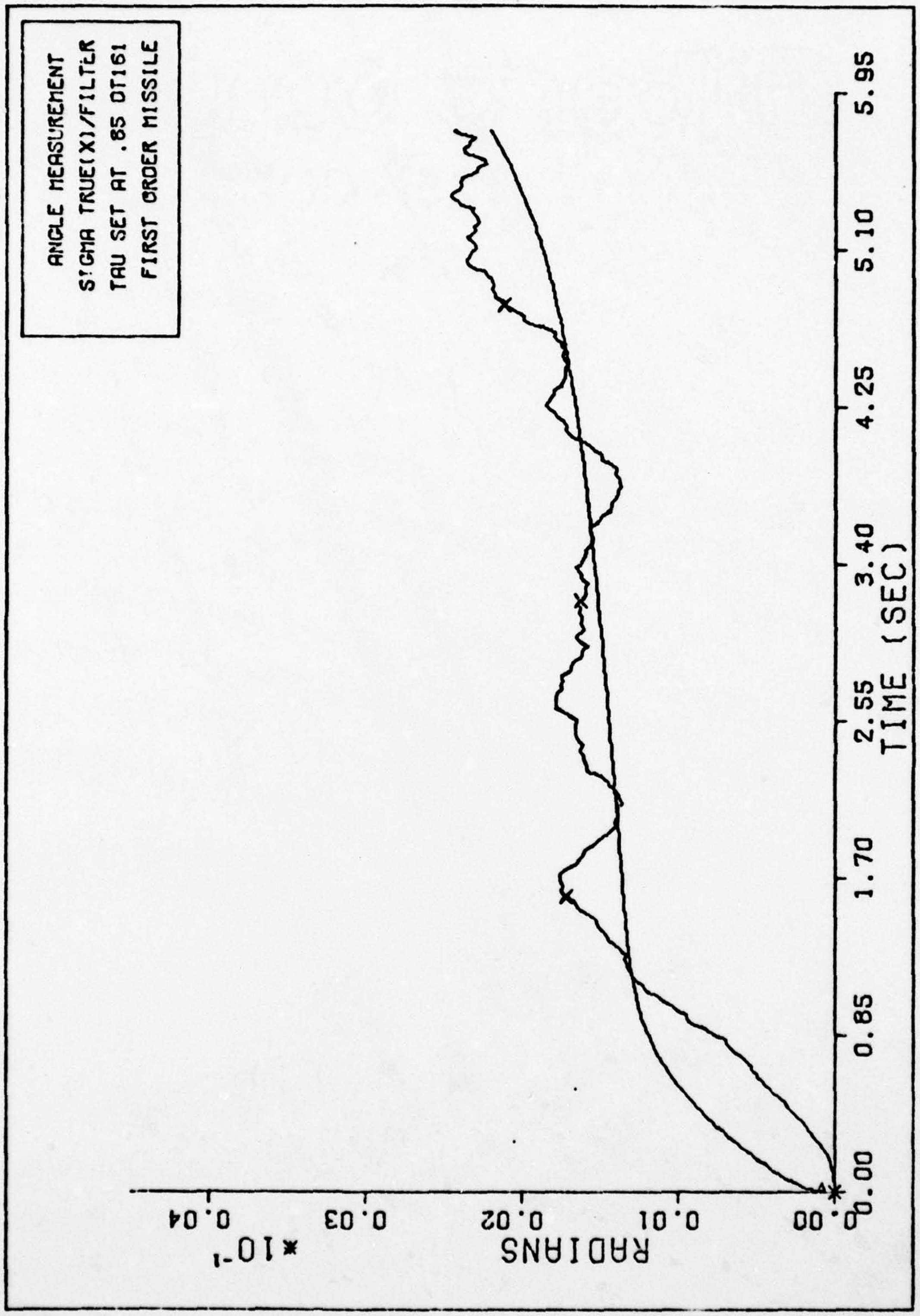

Fig. 145. ANGLE MEASUREMENT SIGMAS FIRST ORDER

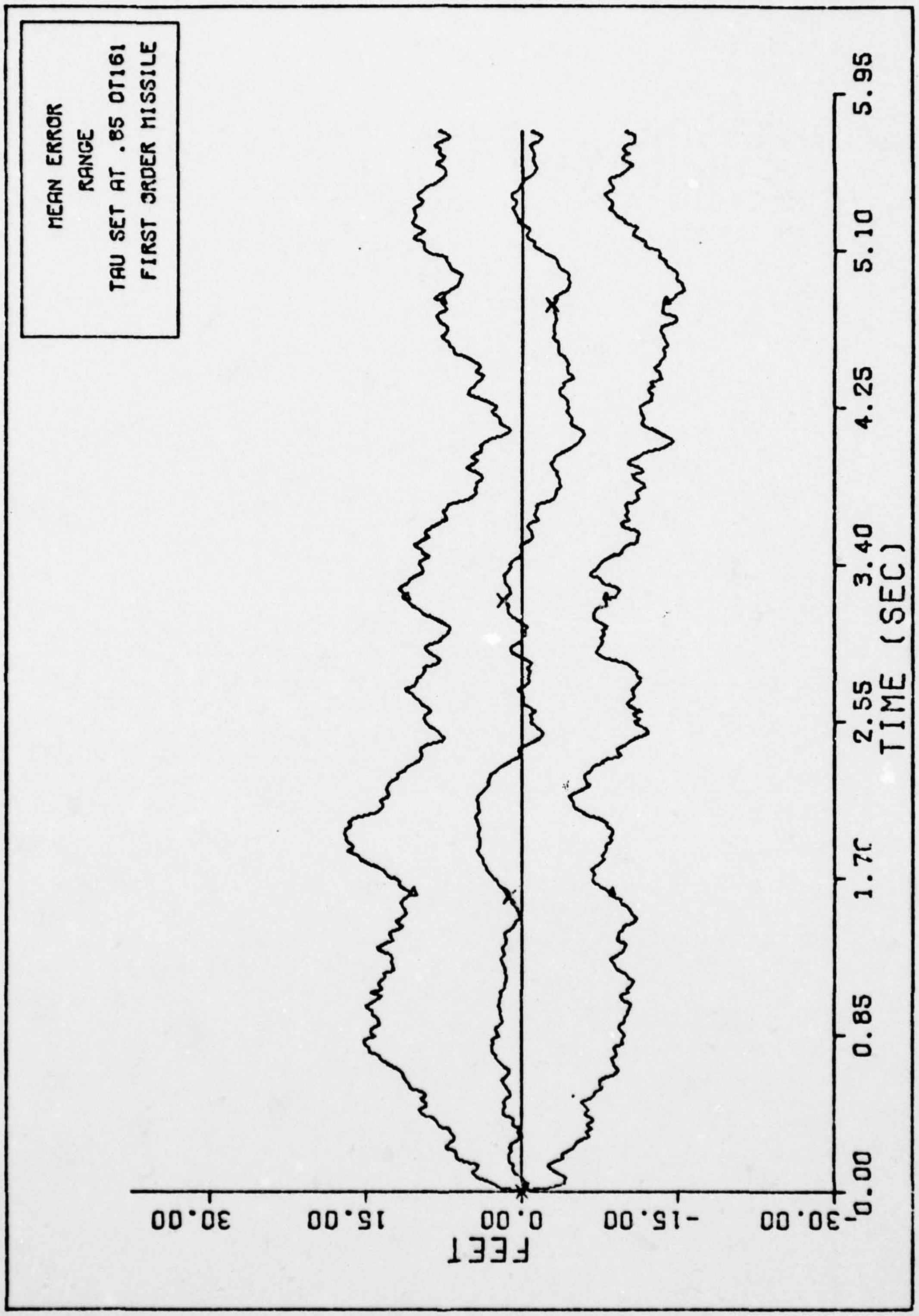

Fig. 146. RANGE rIRST ORDER MISSILE

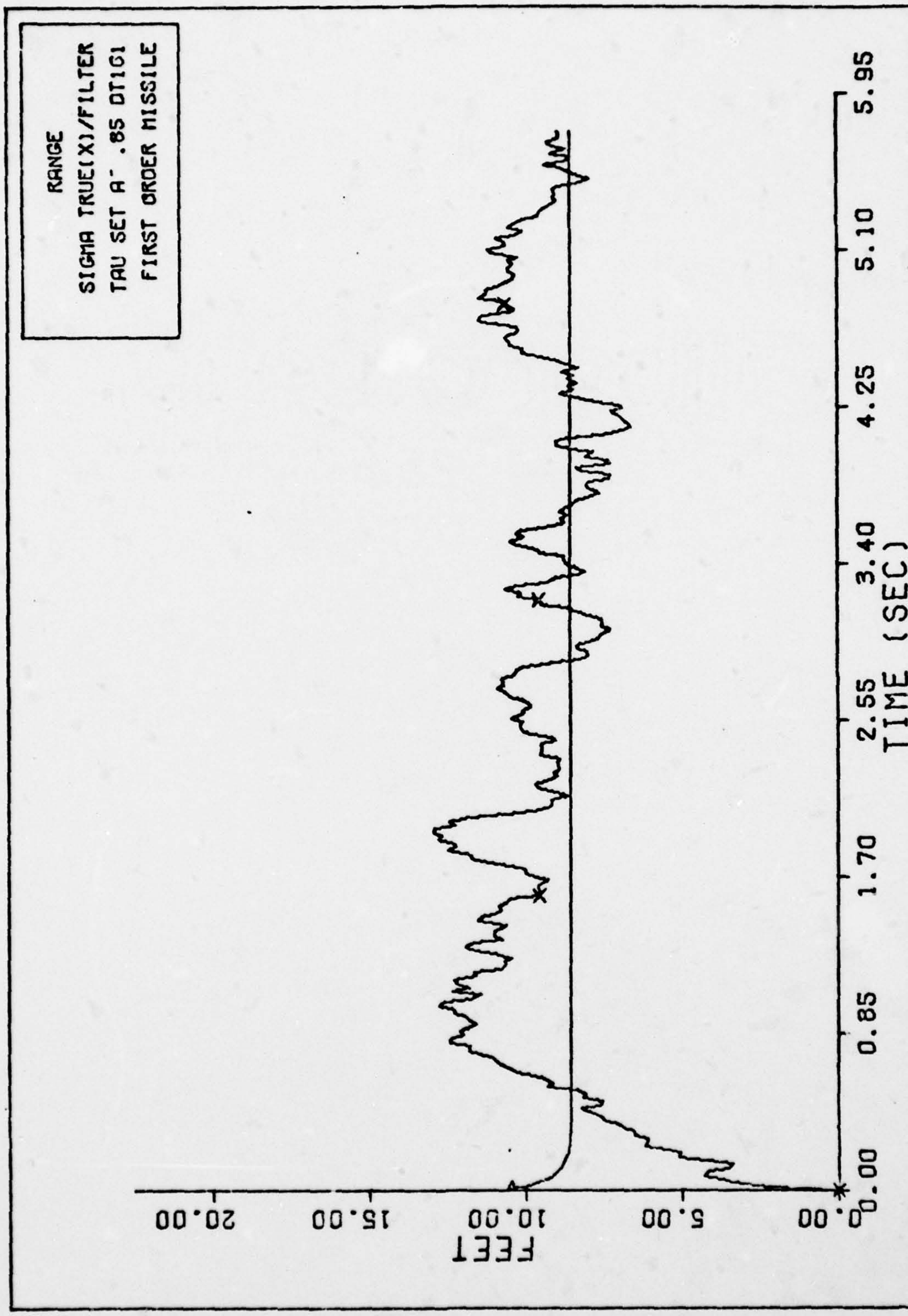

Fig. 147. RANGE SIGMAS FIRST ORDER

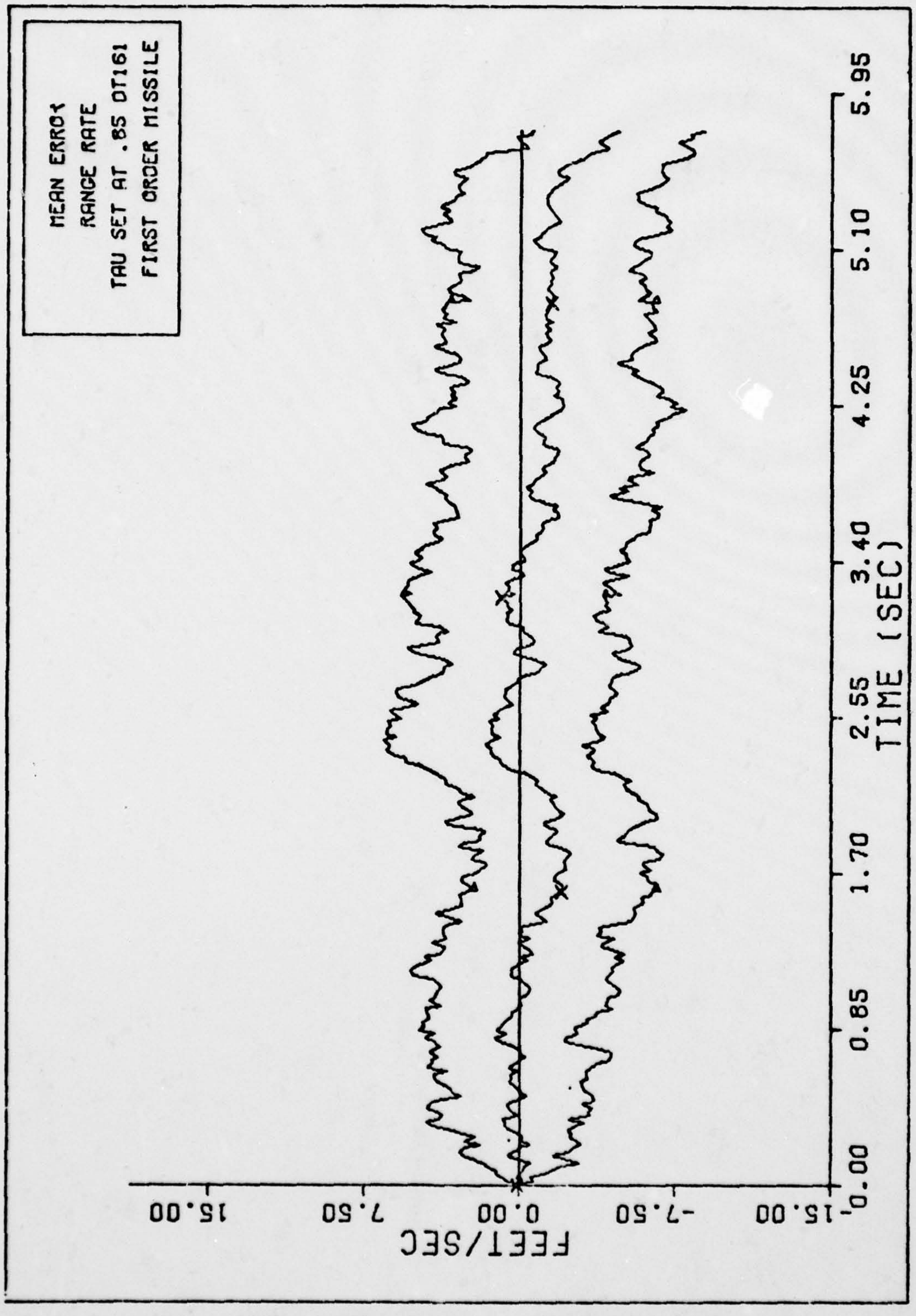

Fig. 148. RANGE RATE FIRST ORDER MISSILE

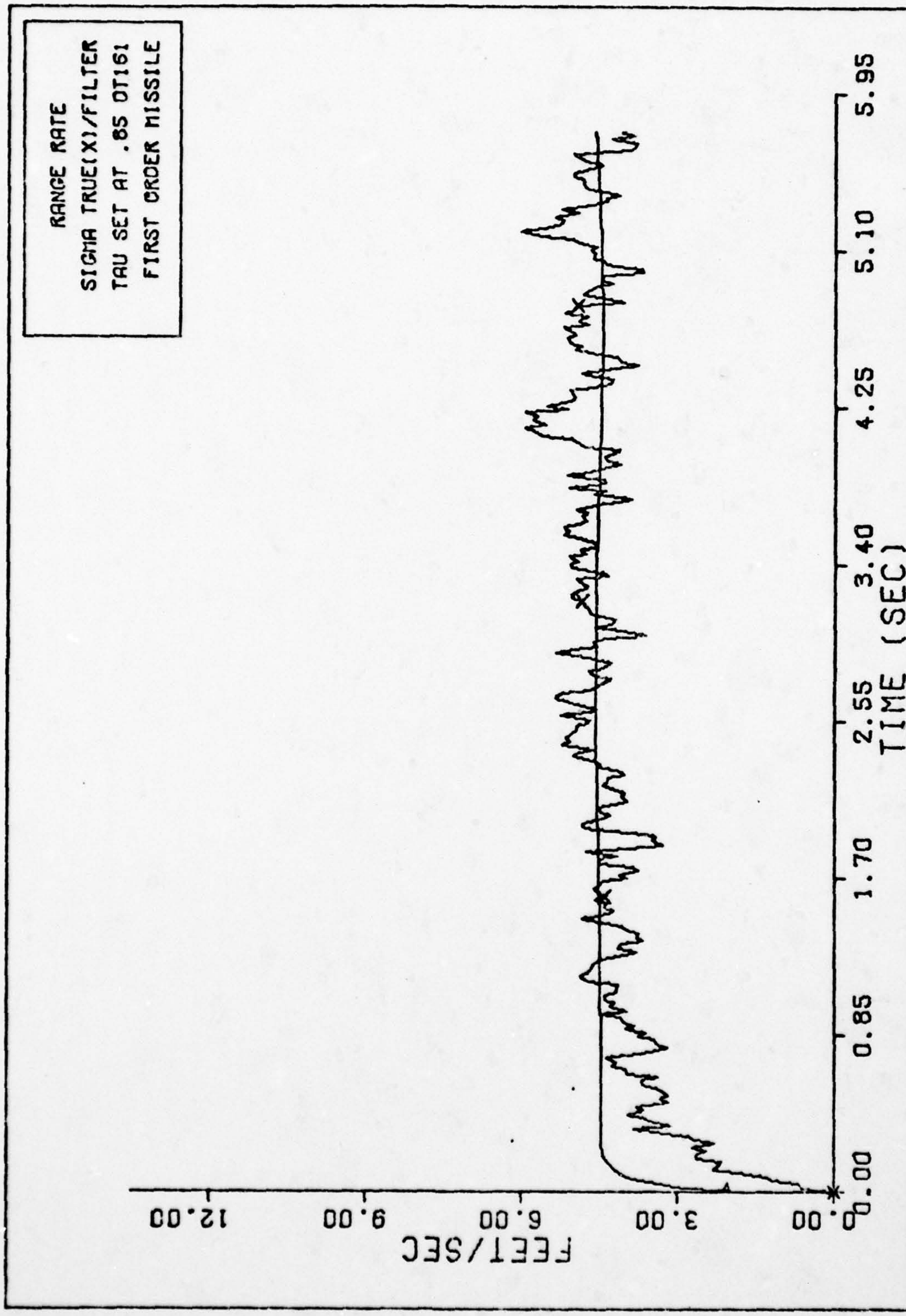

Fig. 149. RANGE RATE SIGMAS FIRST ORDER

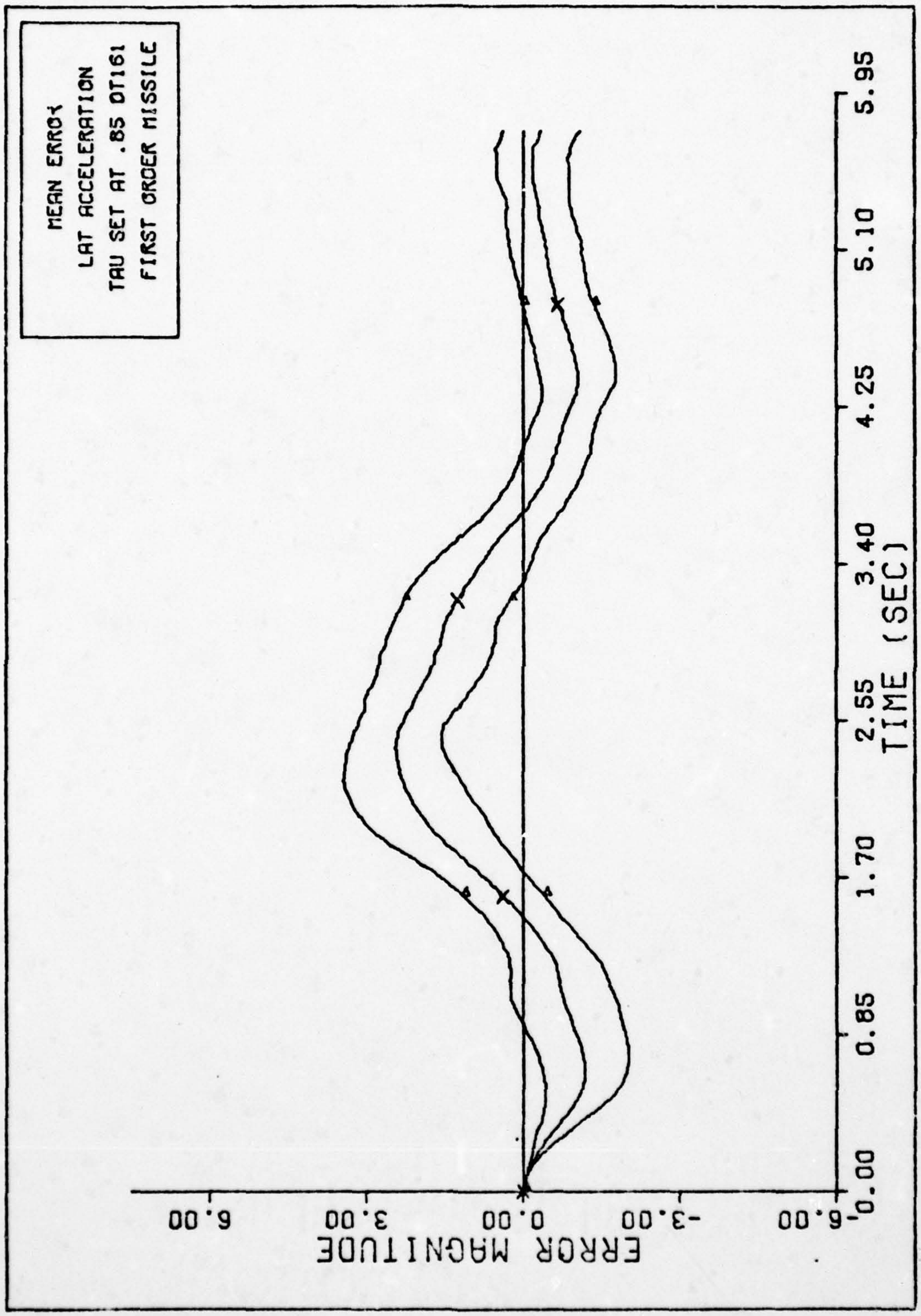

Fig. 150. LAT ACCELERATION FIRST ORDER MISSILE

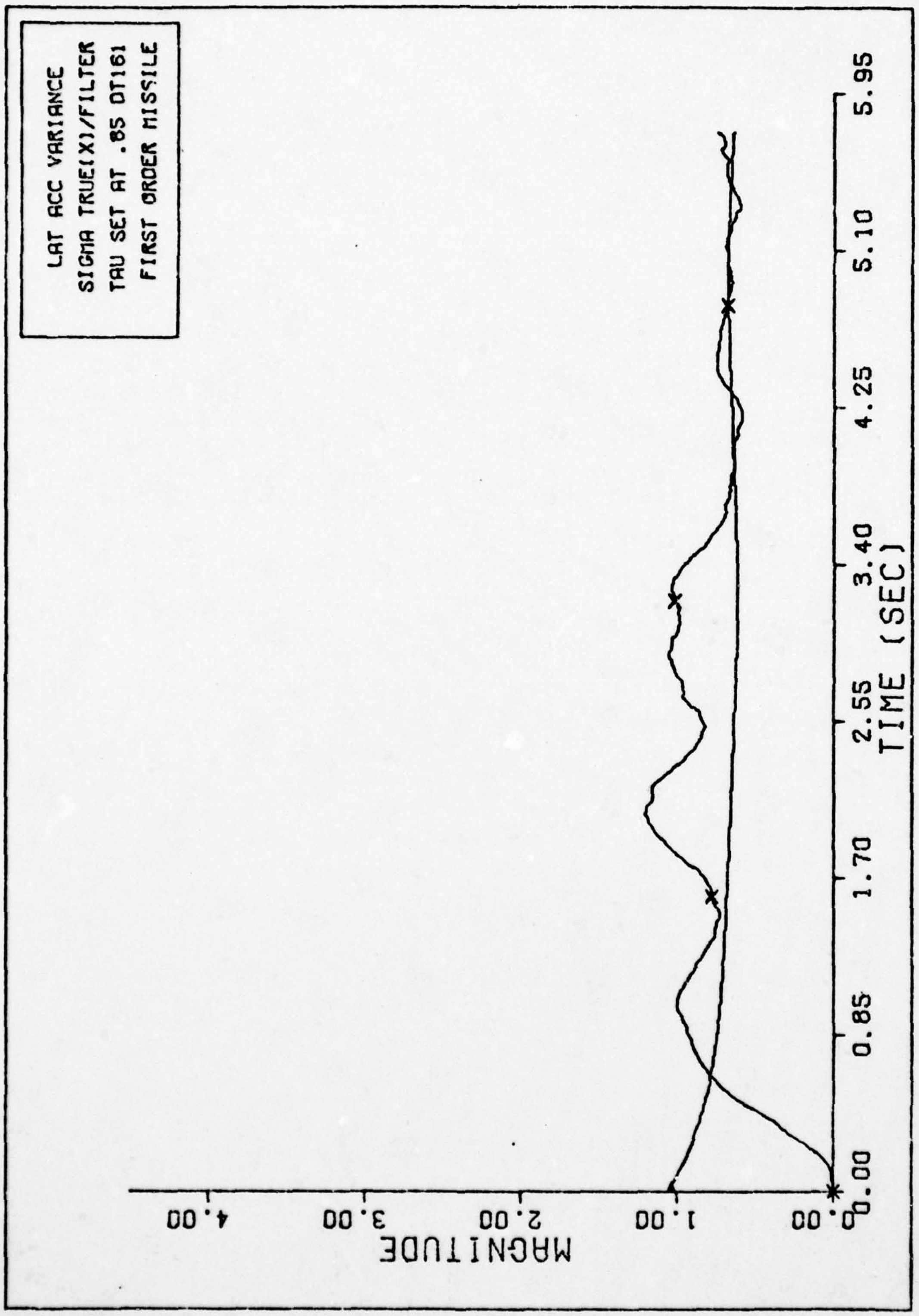

Fig. 151. LAT ACCELERATION SIGMAS FIRST ORDER

$\underline{n}$ Estimation - $\underline{n}$ Initialized at 3.

The initial state estimates and the tuning parameters for this case are

$$
\begin{aligned}
V^I_{mx}(0) &= 1225.7 \text{ fps} \\
\dot{\theta}_T(0) &= 4.363345 \text{ radians} \\
R(0) &= 10000. \text{ feet} \\
\dot{R}(0) &= -2122. \text{ fps} \\
a_L(0) &= 0. \\
n(0) &= 3. \\
\tau_f(0) &= .85 \text{ seconds} \\
M/S(0) &= 29.197 \text{ slugs/ft}^2
\end{aligned}
$$

$$
\underline{R} = \begin{bmatrix} 3.E{-5} & 0. & 0. \\ 0. & 500. & 0. \\ 0. & 0. & 100. \end{bmatrix}
$$

$$
\underline{P}_0 = \begin{bmatrix}
100. & 0. & 0. & 0. & 0. & 0. & 0. & 0. \\
0. & 1.E{-8} & 0. & 0. & 0. & 0. & 0. & 0. \\
0. & 0. & 101. & 0. & 0. & 0. & 0. & 0. \\
0. & 0. & 0. & 4. & 0. & 0. & 0. & 0. \\
0. & 0. & 0. & 0. & 1. & 0. & 0. & 0. \\
0. & 0. & 0. & 0. & 0. & 5. & 0. & 0. \\
0. & 0. & 0. & 0. & 0. & 0. & 0. & 0. \\
0. & 0. & 0. & 0. & 0. & 0. & 0. & 0.
\end{bmatrix}
$$

$$
\underline{Q} = \begin{bmatrix}
150. & 0. & 0. & 0. & 0. & 0. & 0. & 0. \\
0. & 1.E-6 & 0. & 0. & 0. & 0. & 0. & 0. \\
0. & 0. & 500. & 0. & 0. & 0. & 0. & 0. \\
0. & 0. & 0. & 200. & 0. & 0. & 0. & 0. \\
0. & 0. & 0. & 0. & 1. & 0. & 0. & 0. \\
0. & 0. & 0. & 0. & 0. & .01 & 0. & 0. \\
0. & 0. & 0. & 0. & 0. & 0. & 0. & 0. \\
0. & 0. & 0. & 0. & 0. & 0. & 0. & 0.
\end{bmatrix}
$$

This set of plots was generated by the first order filter when estimating n, which was initialized at 3 in the filter. The true value of n in the truth model was 4.5. The other parameters in the filter model were not estimated.

AD-A055 637 AIR FORCE INST OF TECH WRIGHT-PATTERSON AFB OHIO SCH--ETC F/G 19/5
AN EXTENDED KALMAN FILTER FIRE CONTROL SYSTEM AGAINST AIR-TO-AI--ETC(U)
DEC 77 S J CUSUMANO, M DE PONTE

UNCLASSIFIED AFIT/GE/EE/77-13-VOL-2 NL

3 OF 4
ADA
055637

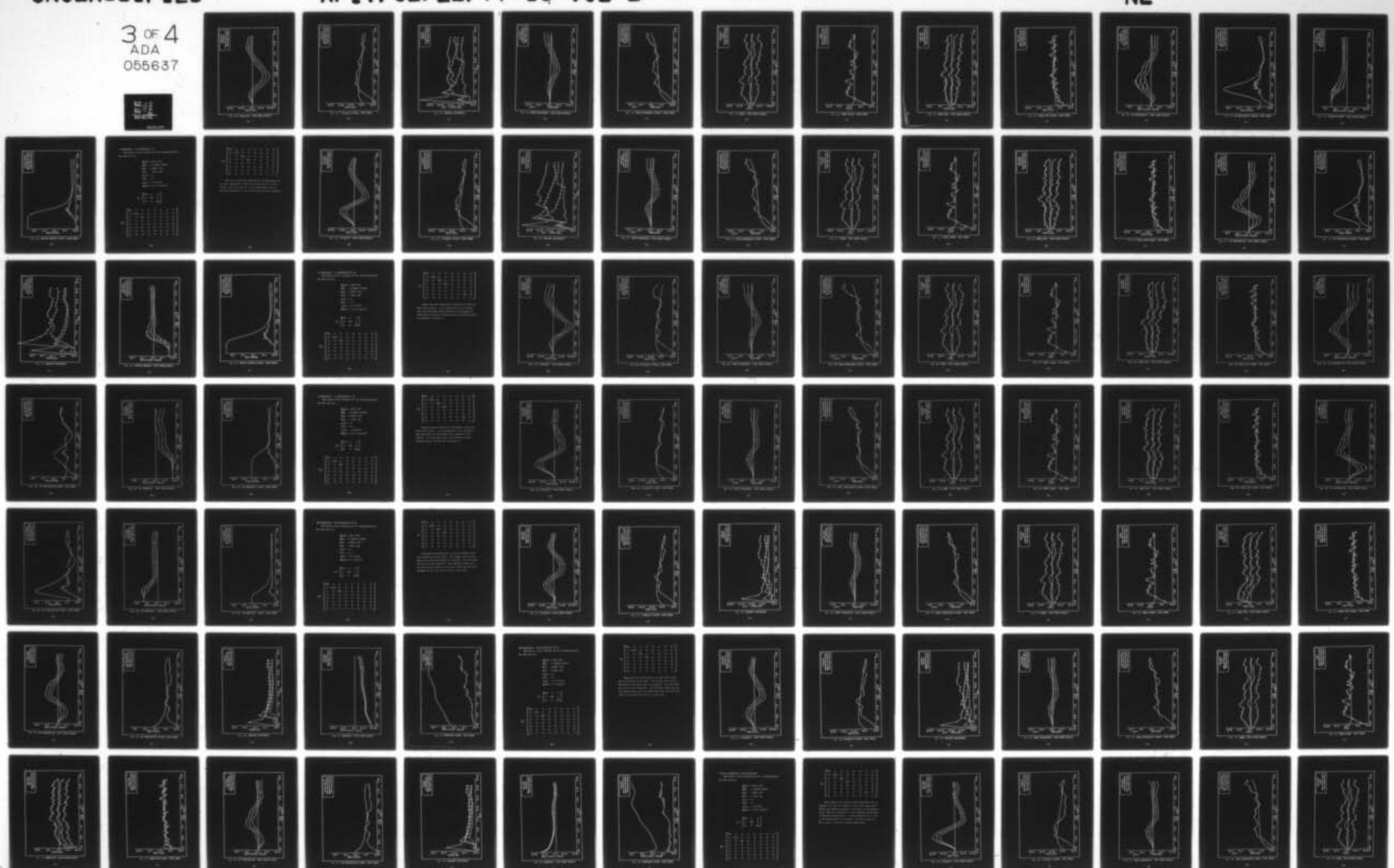

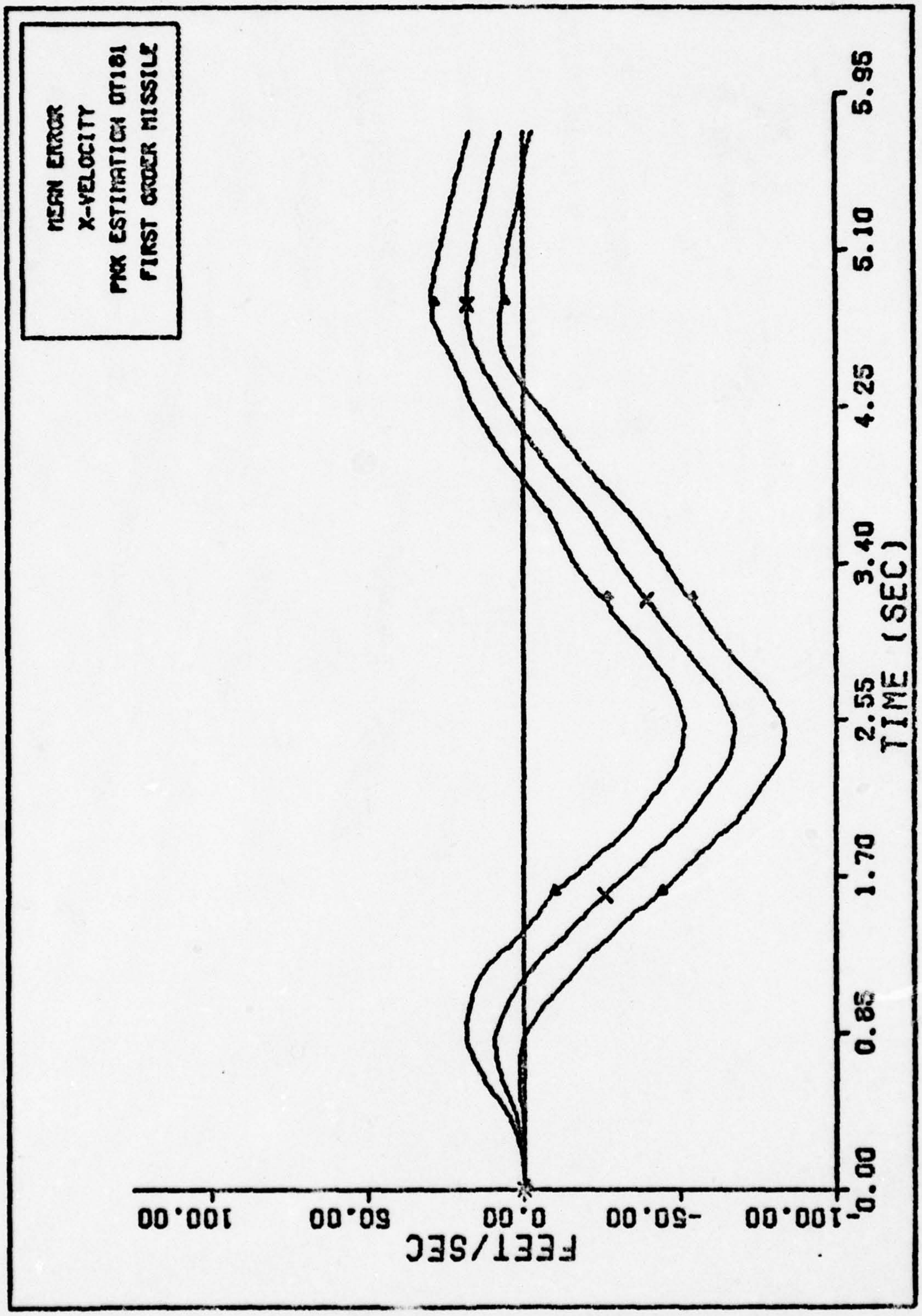

Fig. 152. X-VELOCITY FIRST ORDER MISSILE

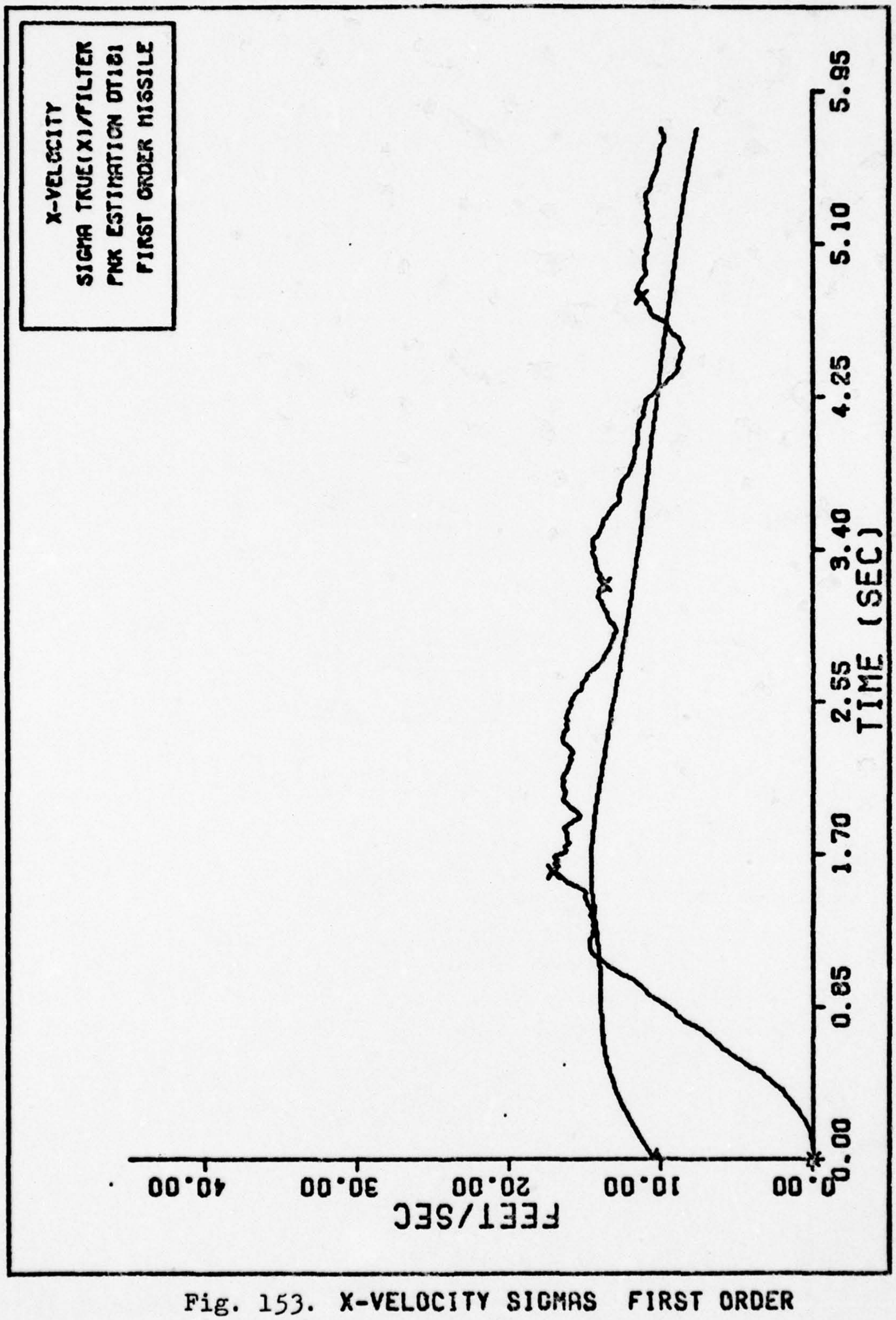

Fig. 153. X-VELOCITY SIGMAS FIRST ORDER

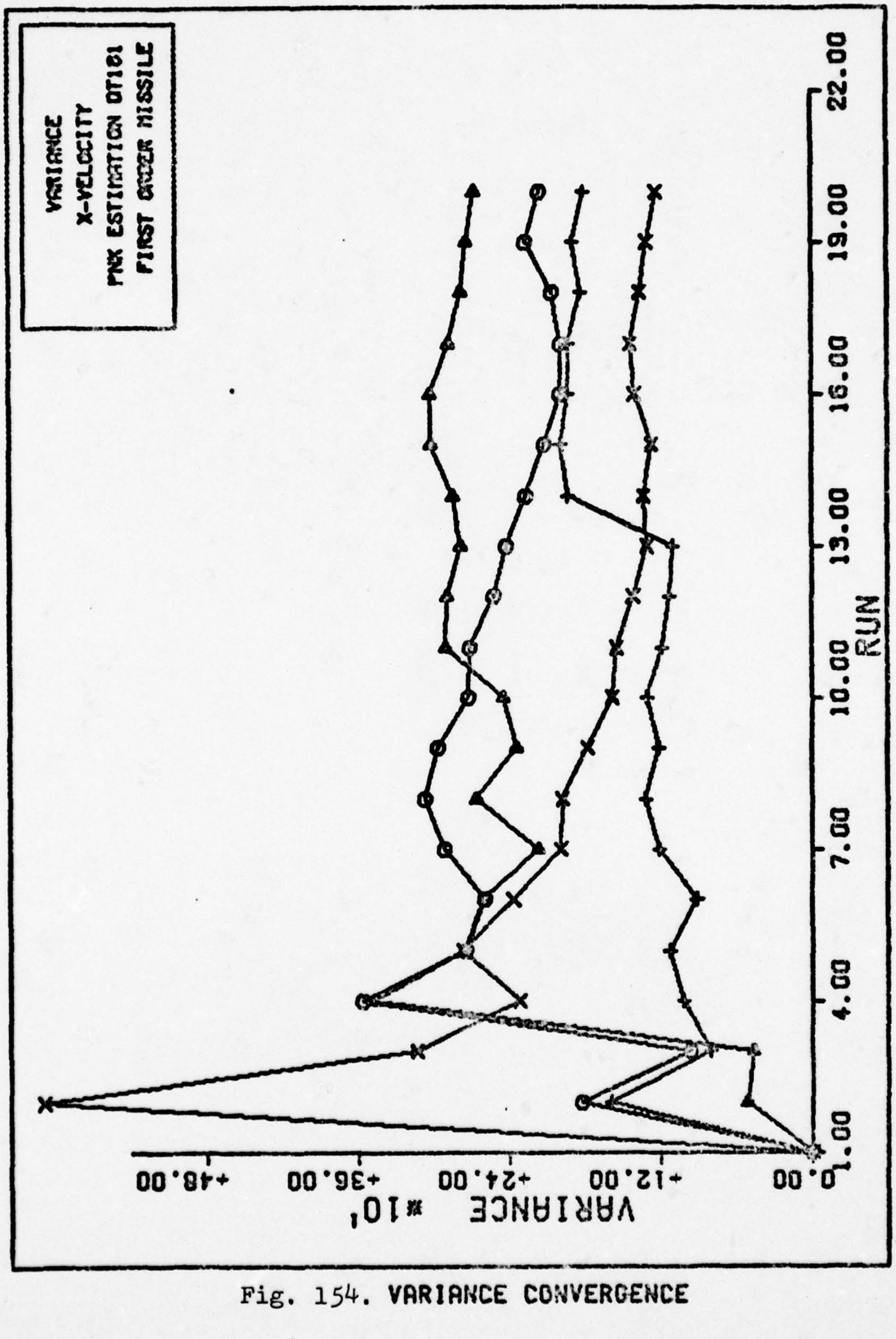

Fig. 154. VARIANCE CONVERGENCE

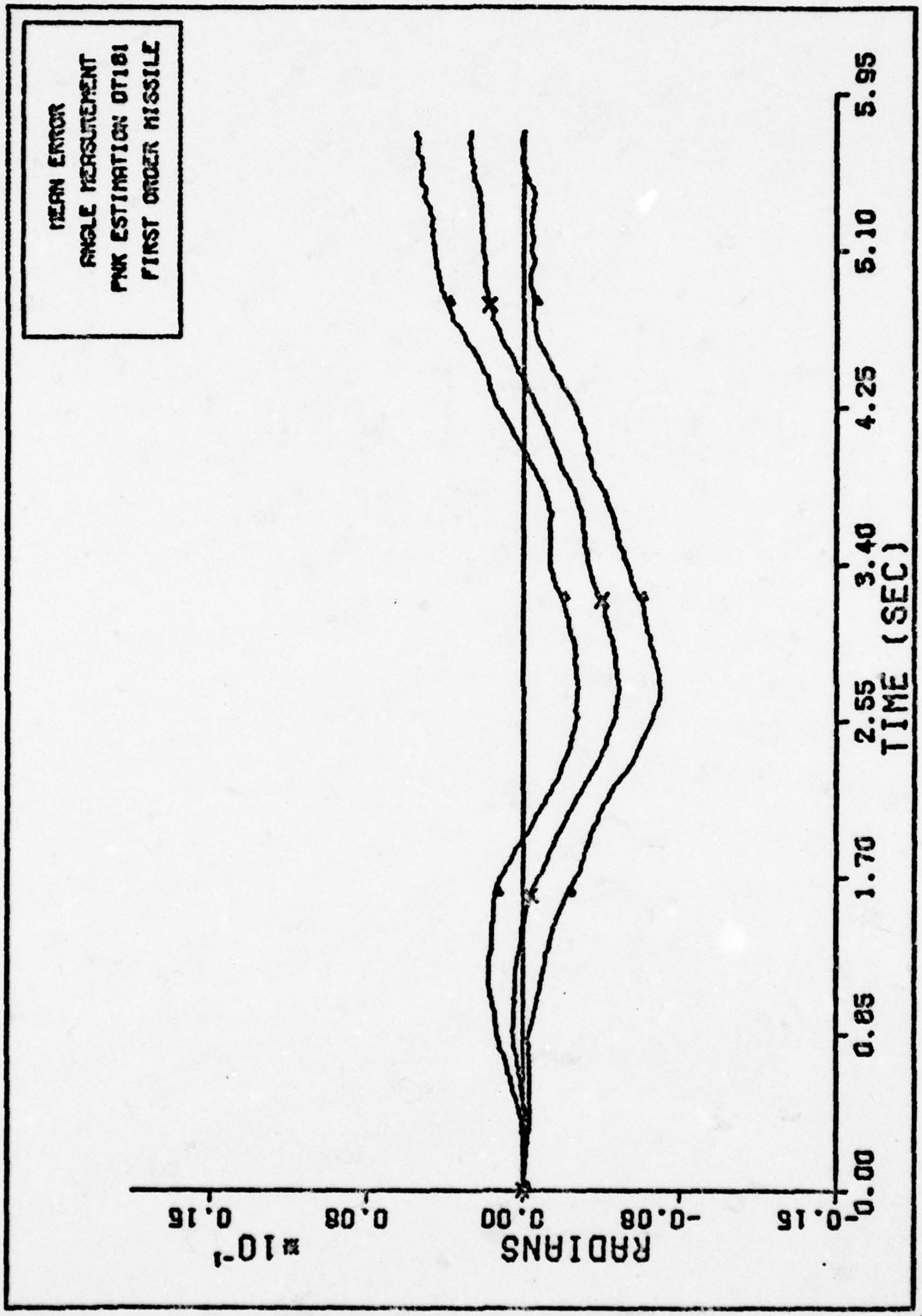

Fig. 155. ANGLE MEASUREMENT FIRST ORDER MISSILE

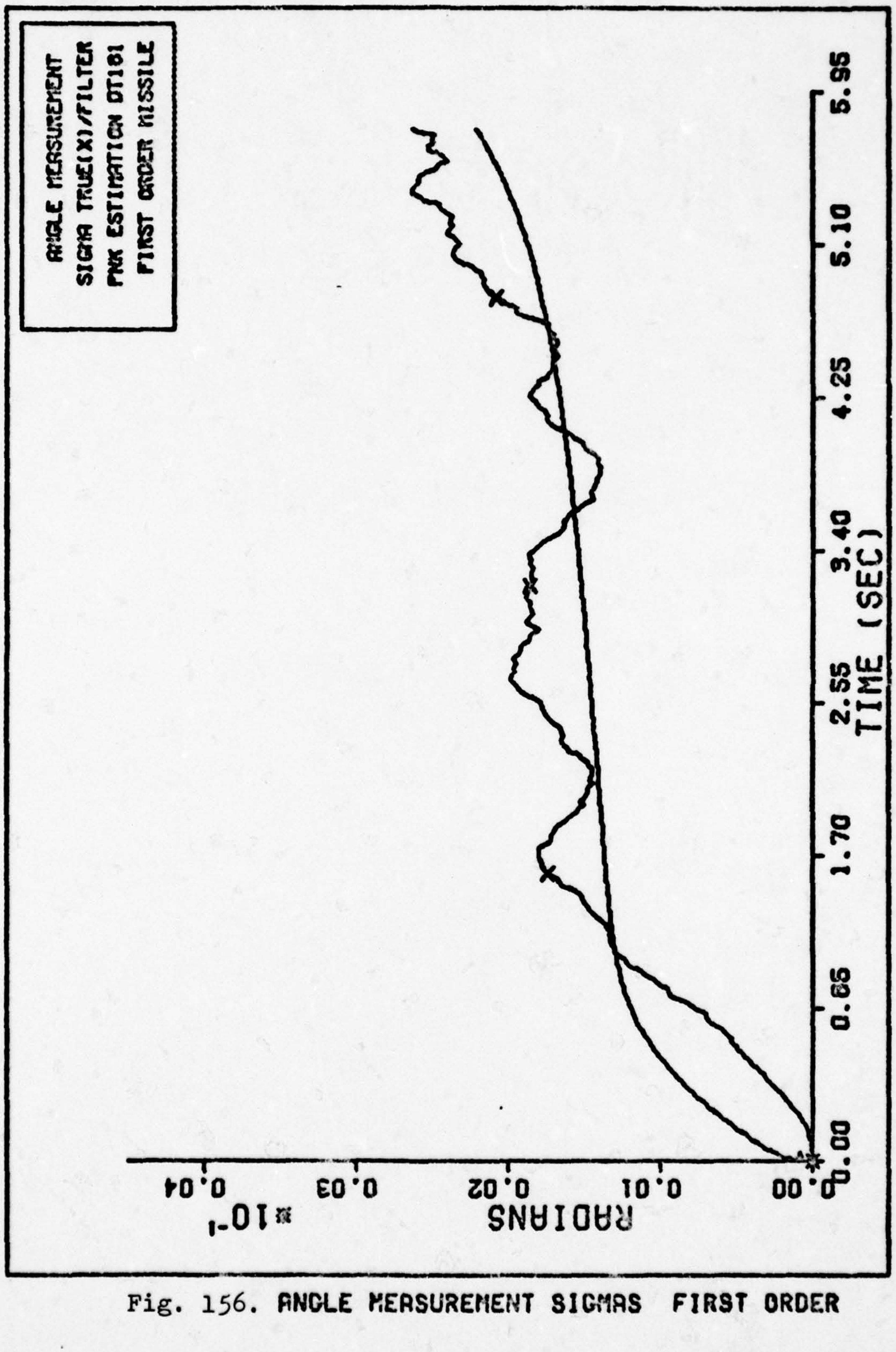

Fig. 156. ANGLE MEASUREMENT SIGMAS FIRST ORDER

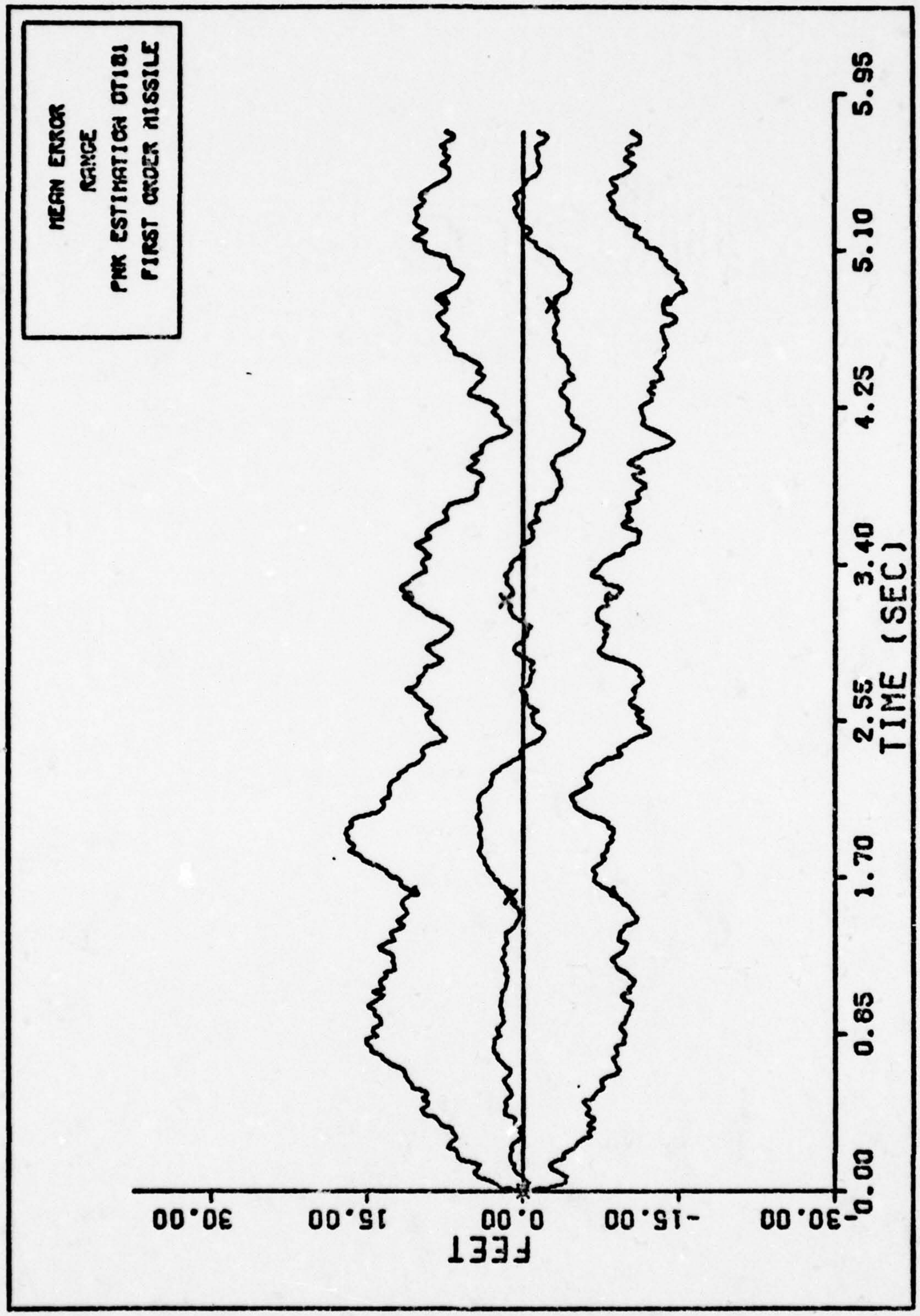

Fig. 157. RANGE FIRST ORDER MISSILE

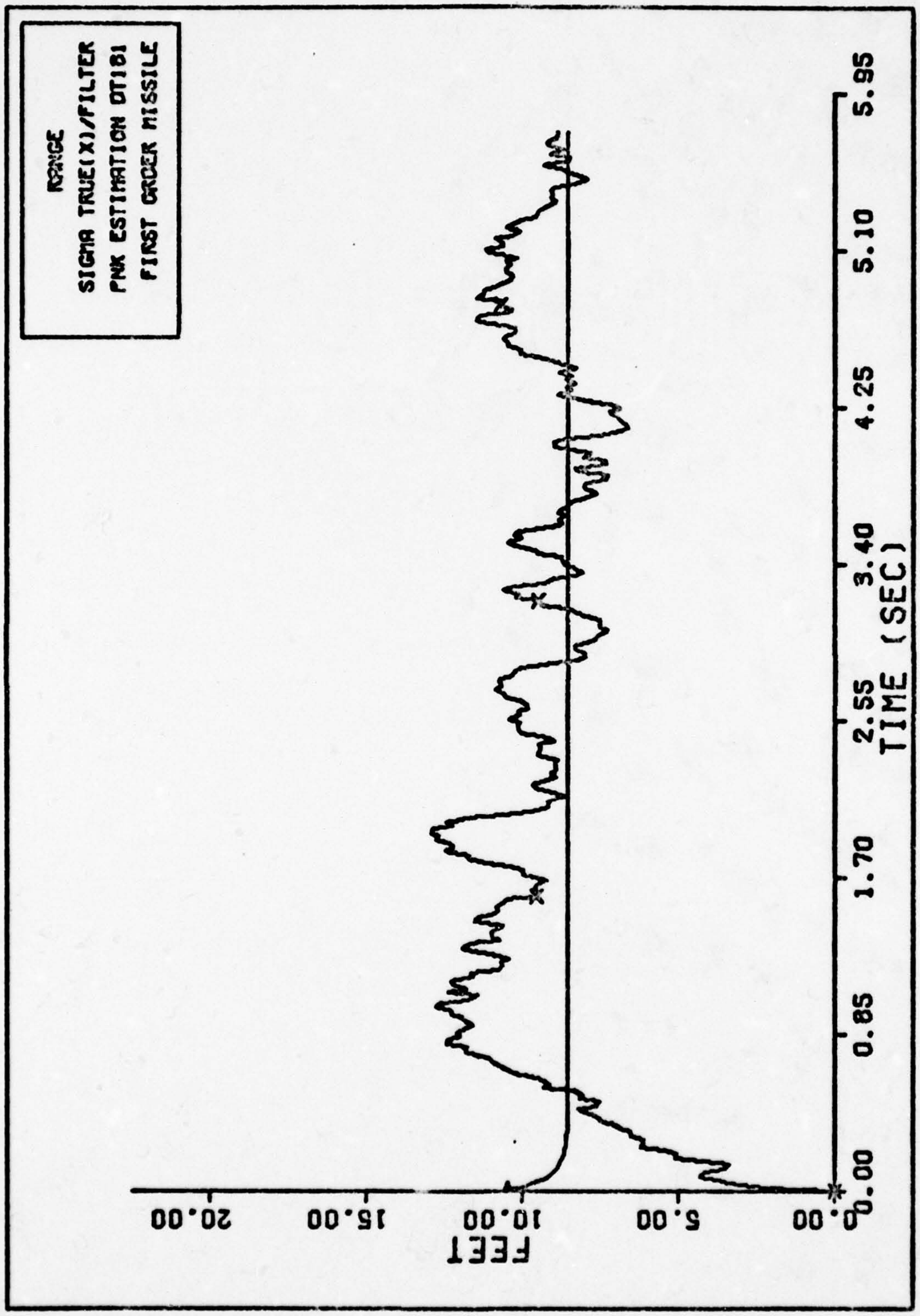

Fig. 158. RANGE SIGMAS FIRST ORDER

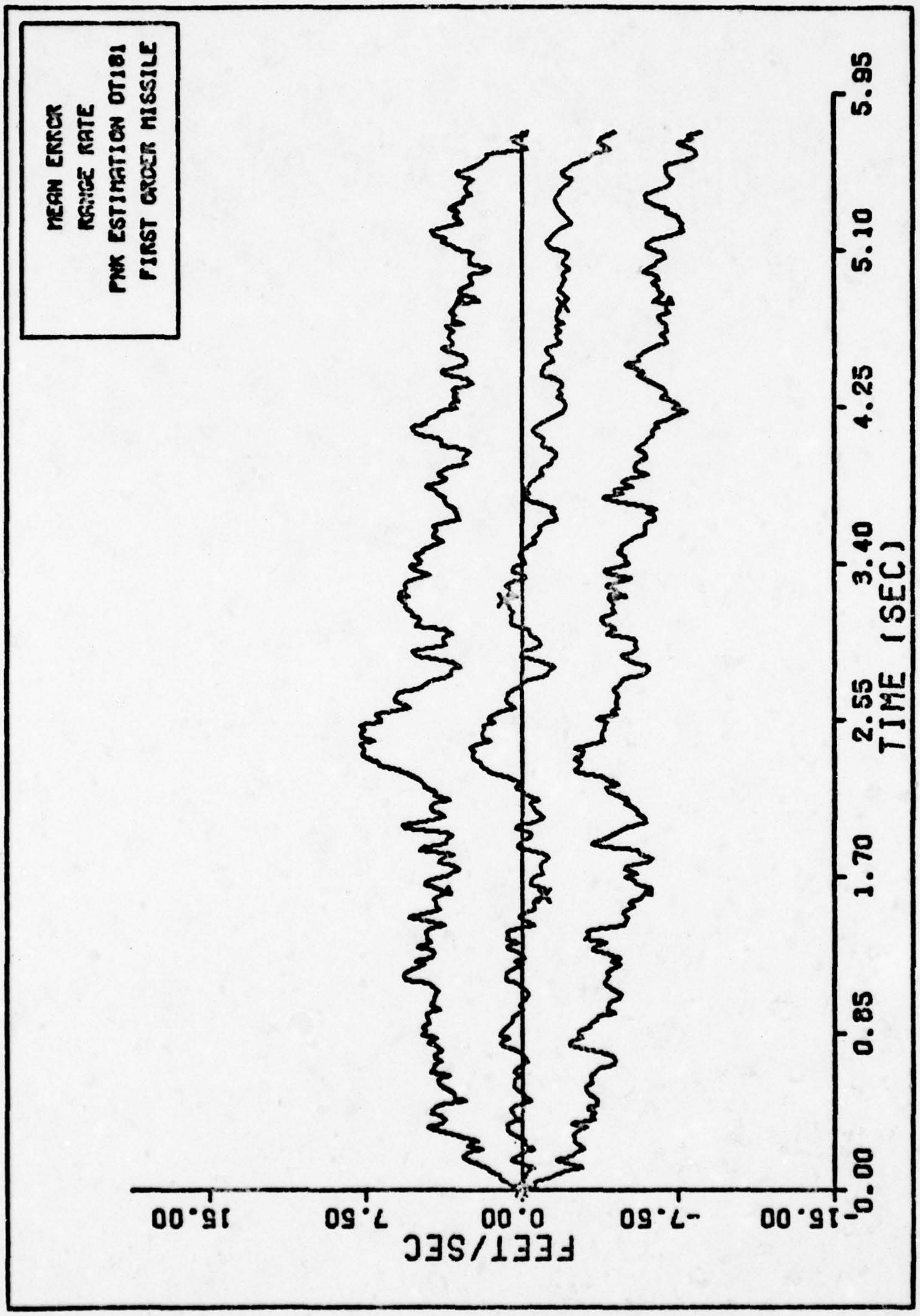

Fig. 159. RANGE RATE FIRST ORDER MISSILE

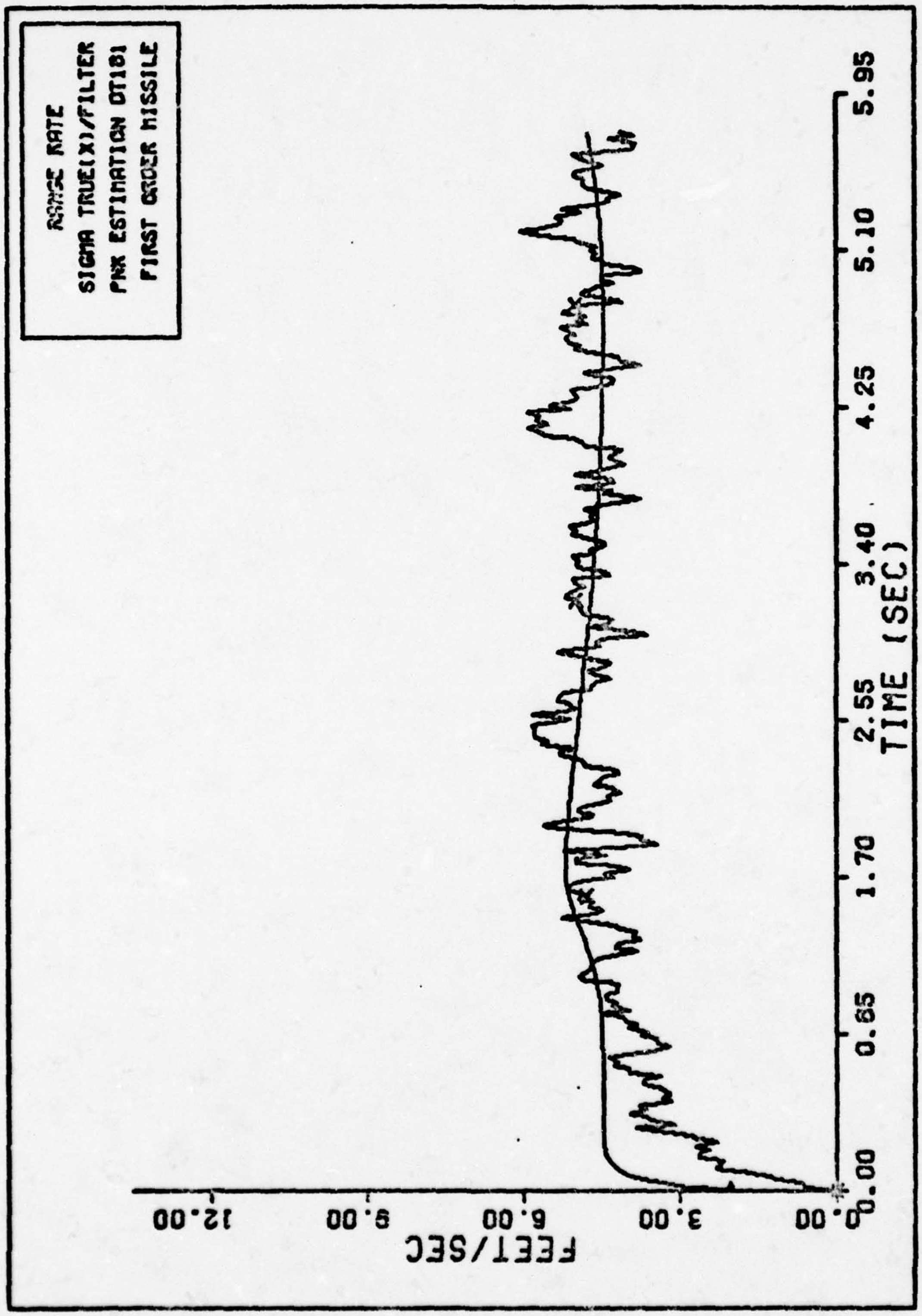

Fig. 160. RANGE RATE SIGMAS FIRST ORDER

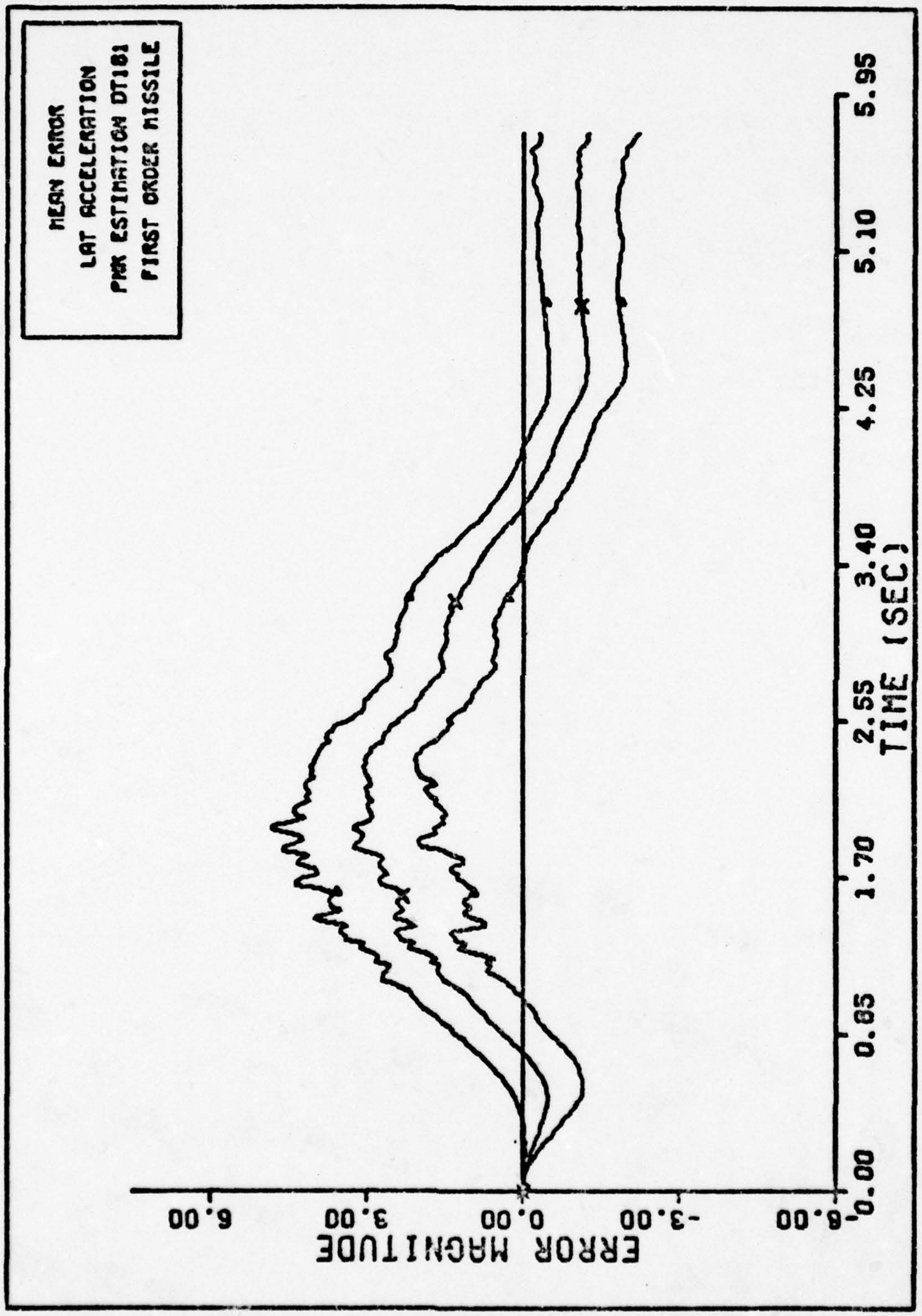

Fig. 161. LAT ACCELERATION FIRST ORDER MISSILE

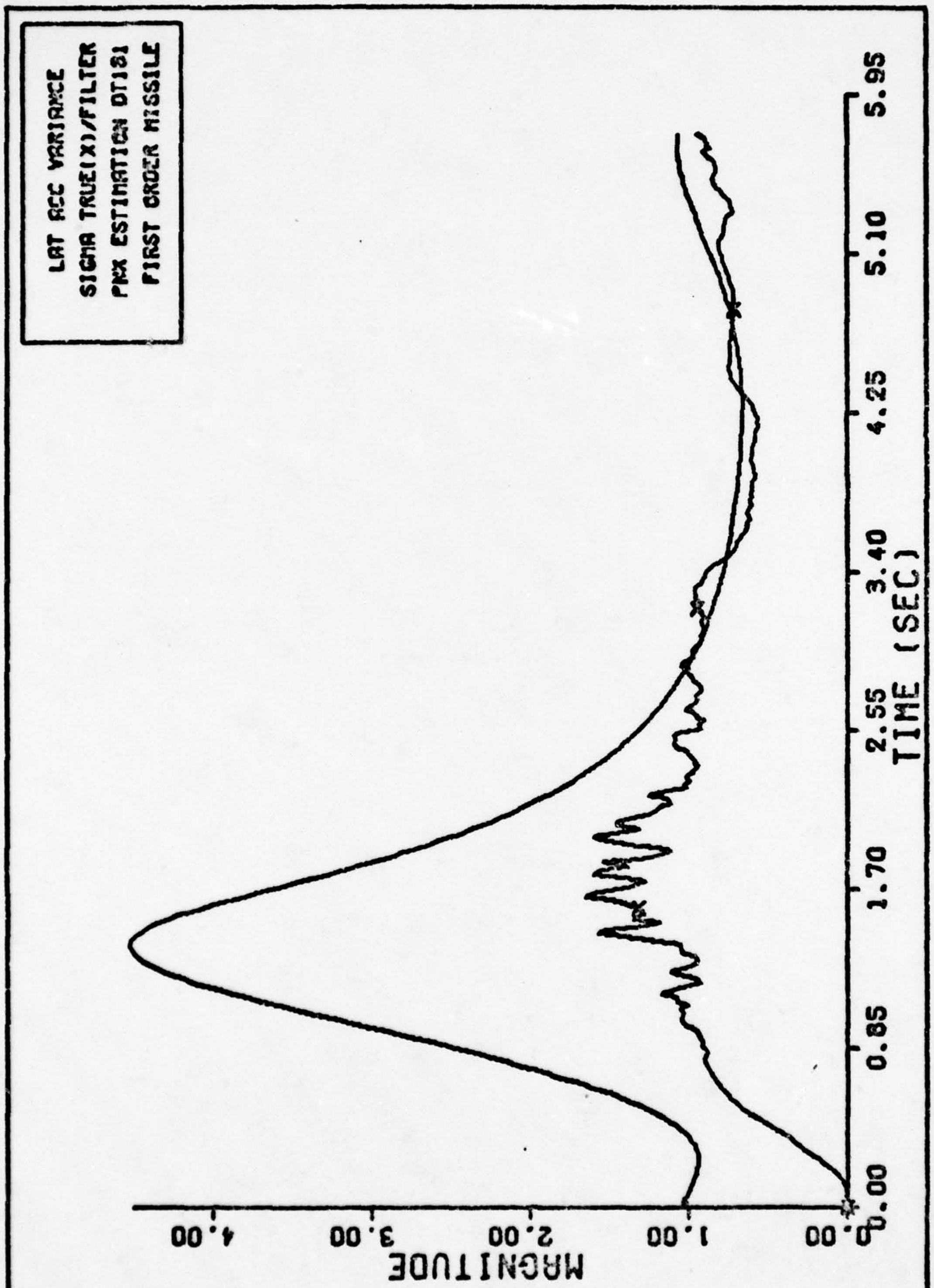

Fig. 162. LAT ACCELERATION SIGMAS FIRST ORDER

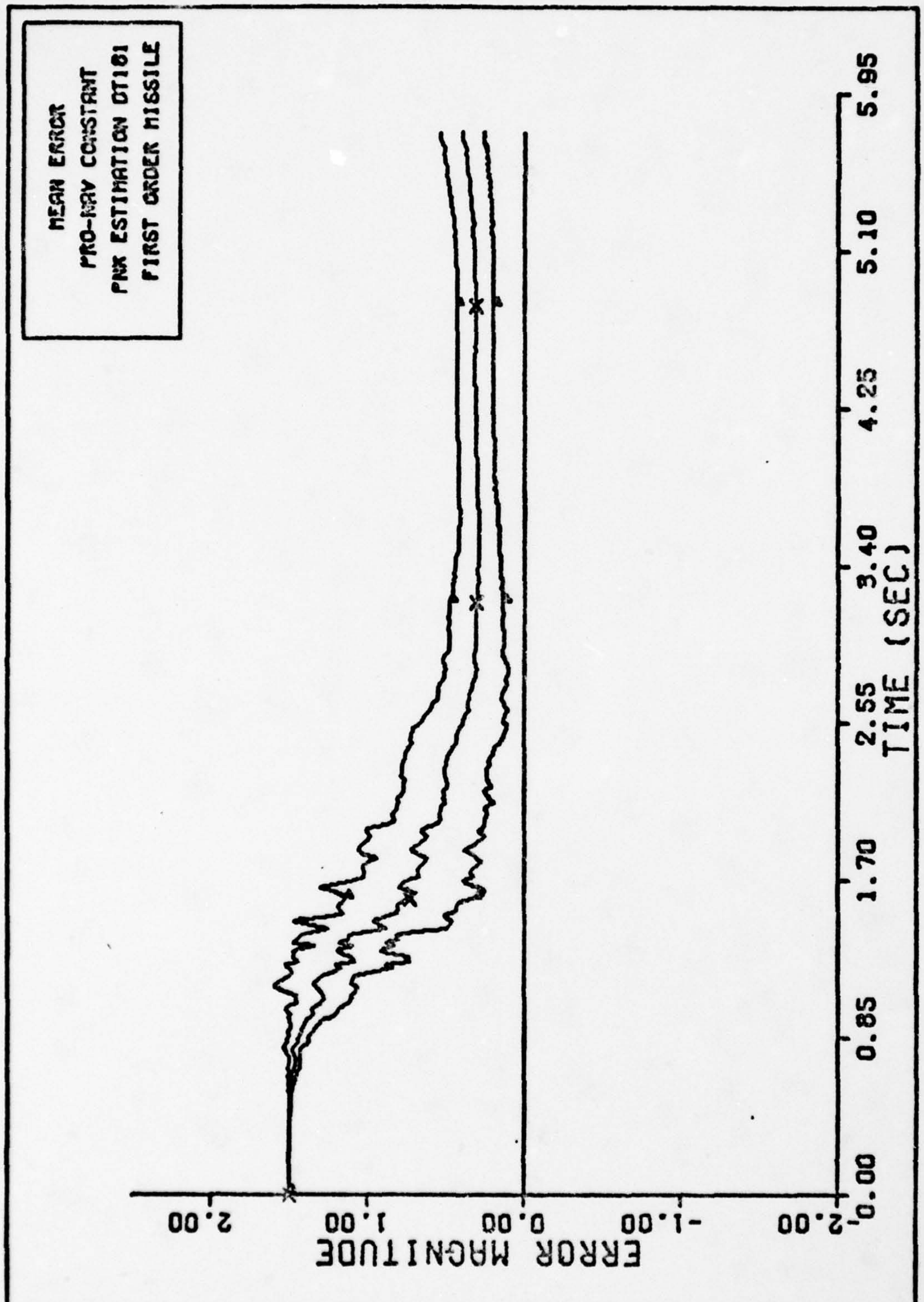

Fig. 163. PRO-NAV CONSTANT FIRST ORDER MISSILE

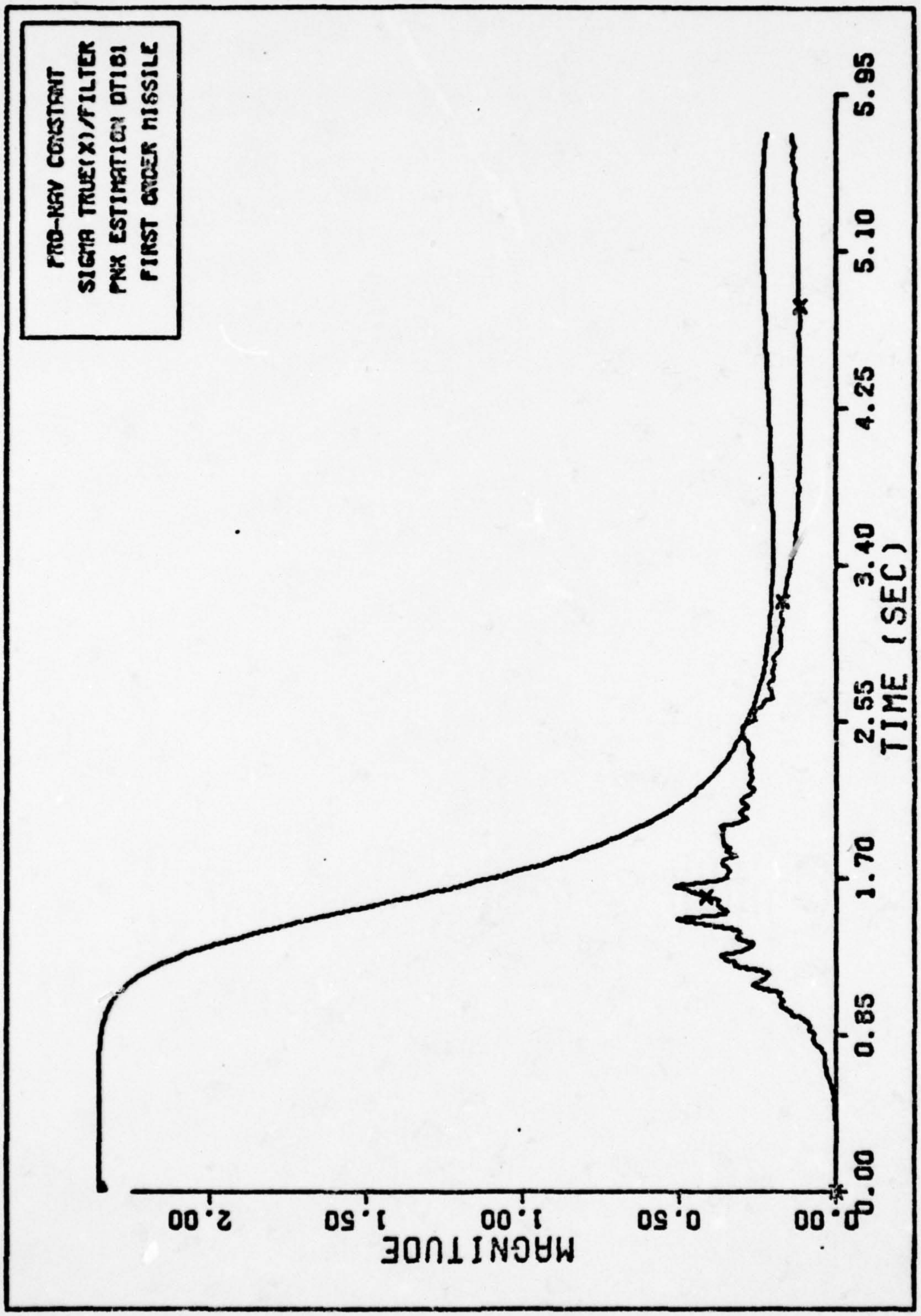

Fig. 164. PRO-NAV CONSTANT SIGMAS FIRST ORDER

n Estimation - n Initialized at 6.

The initial state estimates and the tuning parameters for this case are

$$V_{mx}^{I}(0) = 1225.7 \text{ fps}$$

$$\dot{\theta}_T(0) = 4.363345 \text{ radians}$$

$$R(0) = 10000. \text{ feet}$$

$$\dot{R}(0) = -2122. \text{ fps}$$

$$a_L(0) = 0.$$

$$n(0) = 6.$$

$$\tau_f(0) = .85 \text{ seconds}$$

$$M/S(0) = 29.197 \text{ slugs/ft}^2$$

$$\underline{R} = \begin{bmatrix} 3.E-5 & 0. & 0. \\ 0. & 500. & 0. \\ 0. & 0. & 100. \end{bmatrix}$$

$$\underline{P}_0 = \begin{bmatrix} 100. & 0. & 0. & 0. & 0. & 0. & 0. & 0. \\ 0. & 1.E-8 & 0. & 0. & 0. & 0. & 0. & 0. \\ 0. & 0. & 101. & 0. & 0. & 0. & 0. & 0. \\ 0. & 0. & 0. & 4. & 0. & 0. & 0. & 0. \\ 0. & 0. & 0. & 0. & 1. & 0. & 0. & 0. \\ 0. & 0. & 0. & 0. & 0. & 5. & 0. & 0. \\ 0. & 0. & 0. & 0. & 0. & 0. & 0. & 0. \\ 0. & 0. & 0. & 0. & 0. & 0. & 0. & 0. \end{bmatrix}$$

$$\underline{Q} = \begin{bmatrix} 150. & 0. & 0. & 0. & 0. & 0. & 0. & 0. \\ 0. & 1.E-6 & 0. & 0. & 0. & 0. & 0. & 0. \\ 0. & 0. & 500. & 0. & 0. & 0. & 0. & 0. \\ 0. & 0. & 0. & 200. & 0. & 0. & 0. & 0. \\ 0. & 0. & 0. & 0. & 1. & 0. & 0. & 0. \\ 0. & 0. & 0. & 0. & 0. & .01 & 0. & 0. \\ 0. & 0. & 0. & 0. & 0. & 0. & 0. & 0. \\ 0. & 0. & 0. & 0. & 0. & 0. & 0. & 0. \end{bmatrix}$$

This set of plots was generated by the first order filter when estimating n, which was initialized at 6 in the filter. The true value of n in the truth model was 4.5. The other parameters in the filter model were not estimated.

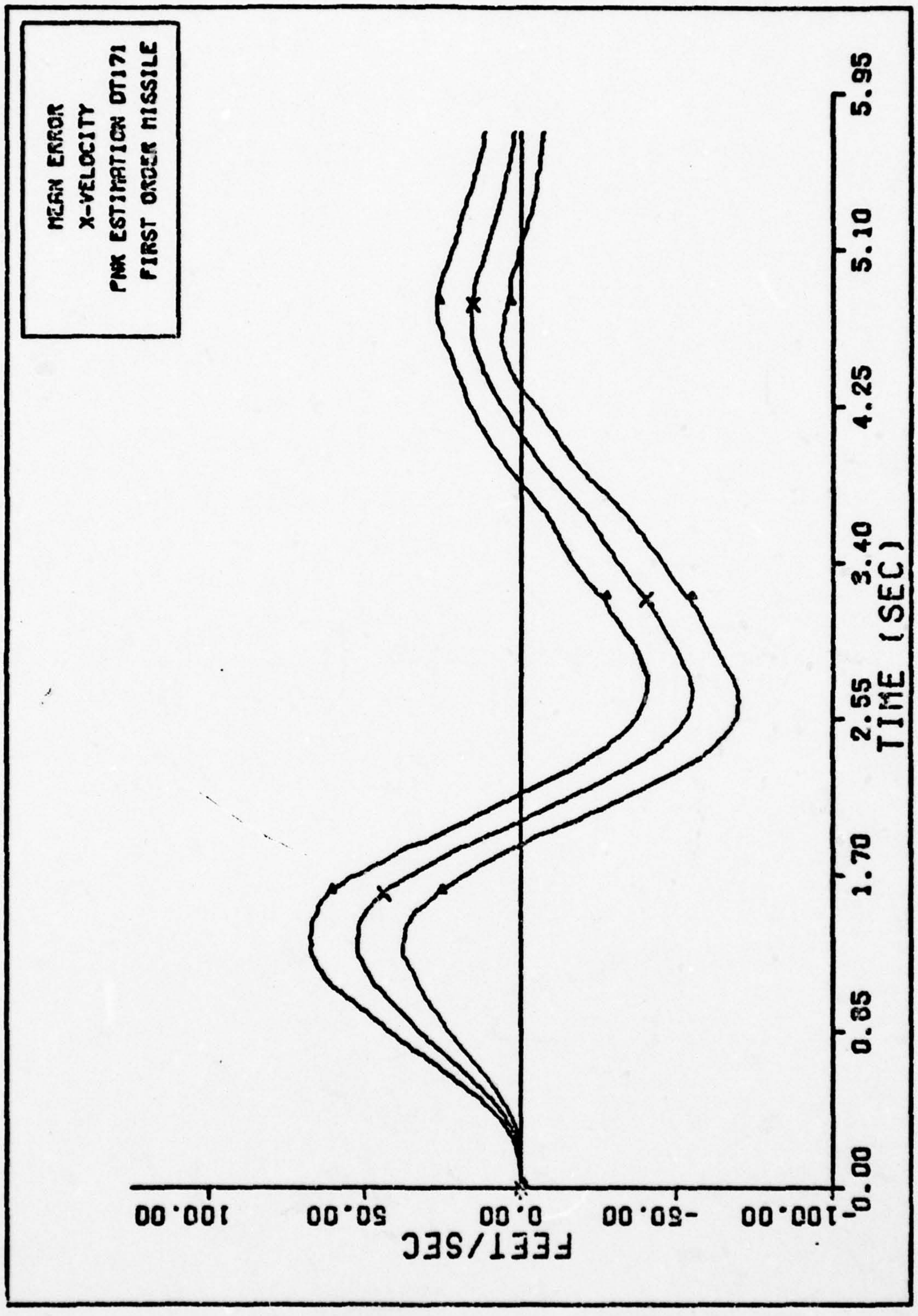

Fig. 165. X-VELOCITY FIRST ORDER MISSILE

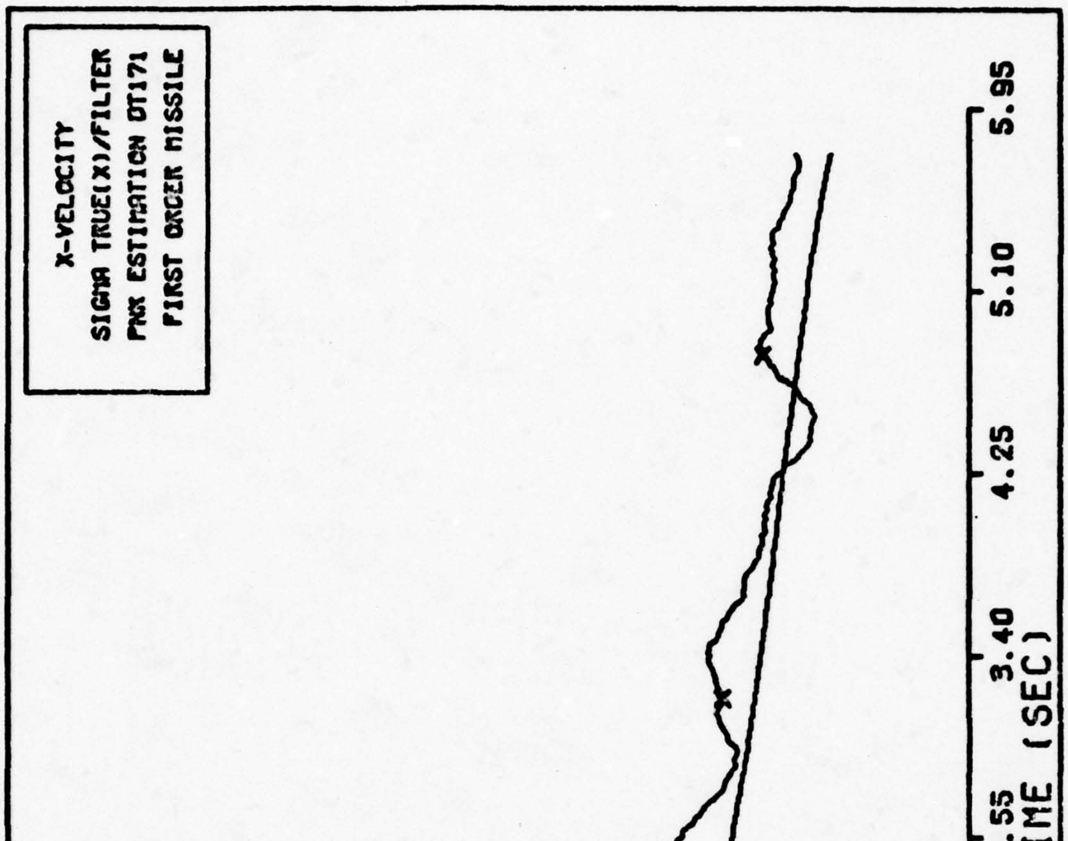

Fig. 166. X-VELOCITY SIGMAS FIRST ORDER

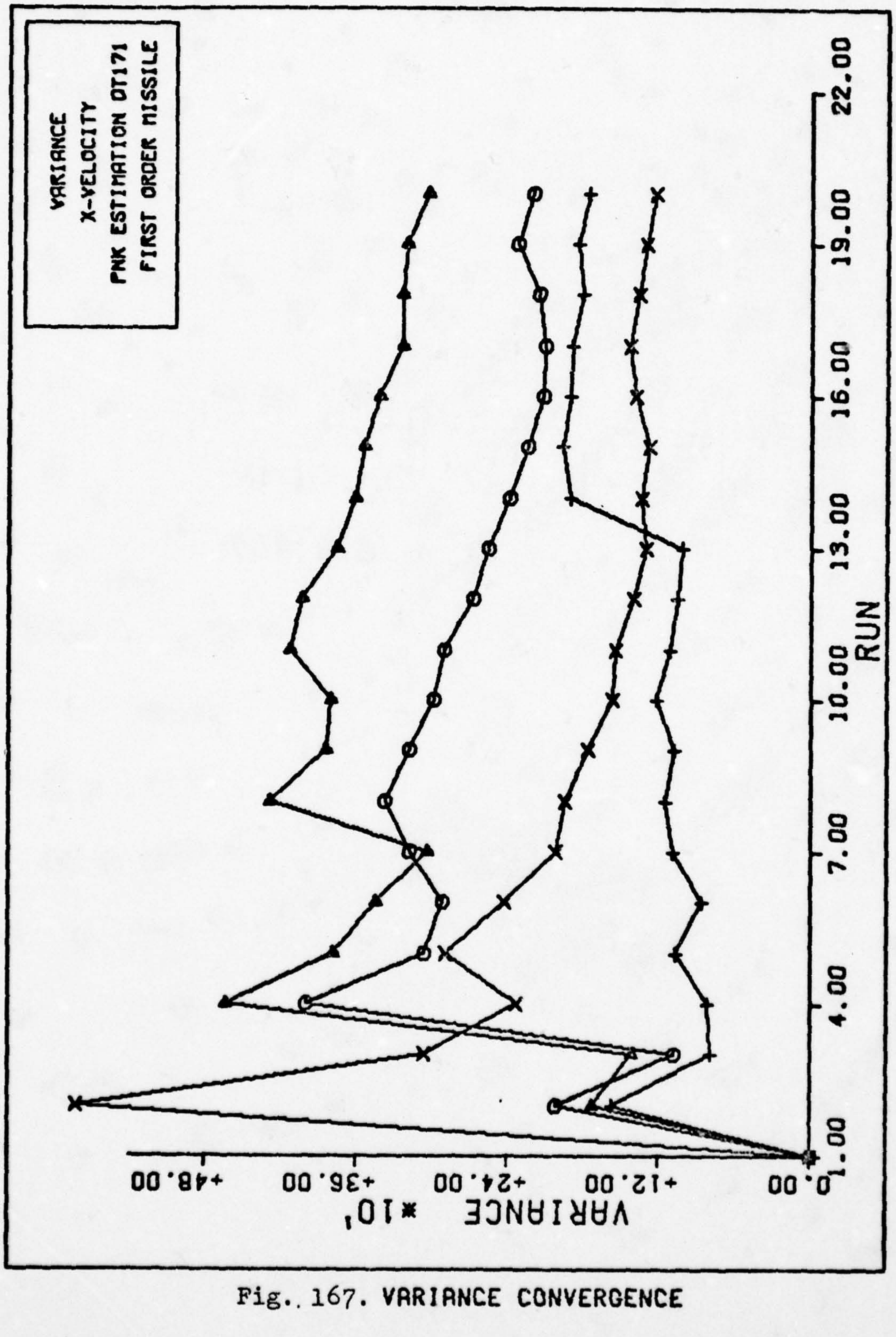

Fig. 167. VARIANCE CONVERGENCE

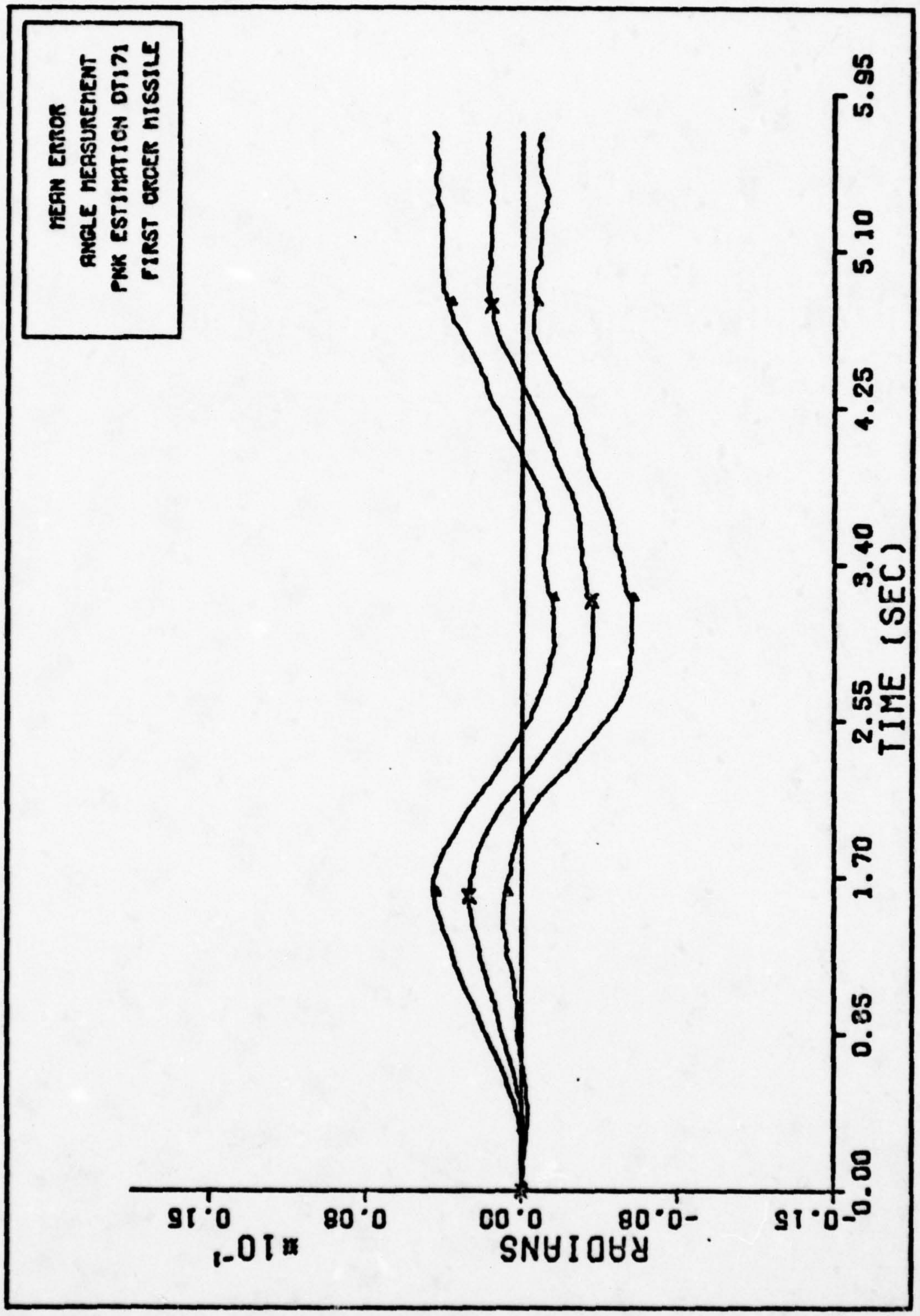

Fig. 168. ANGLE MEASUREMENT FIRST ORDER MISSILE

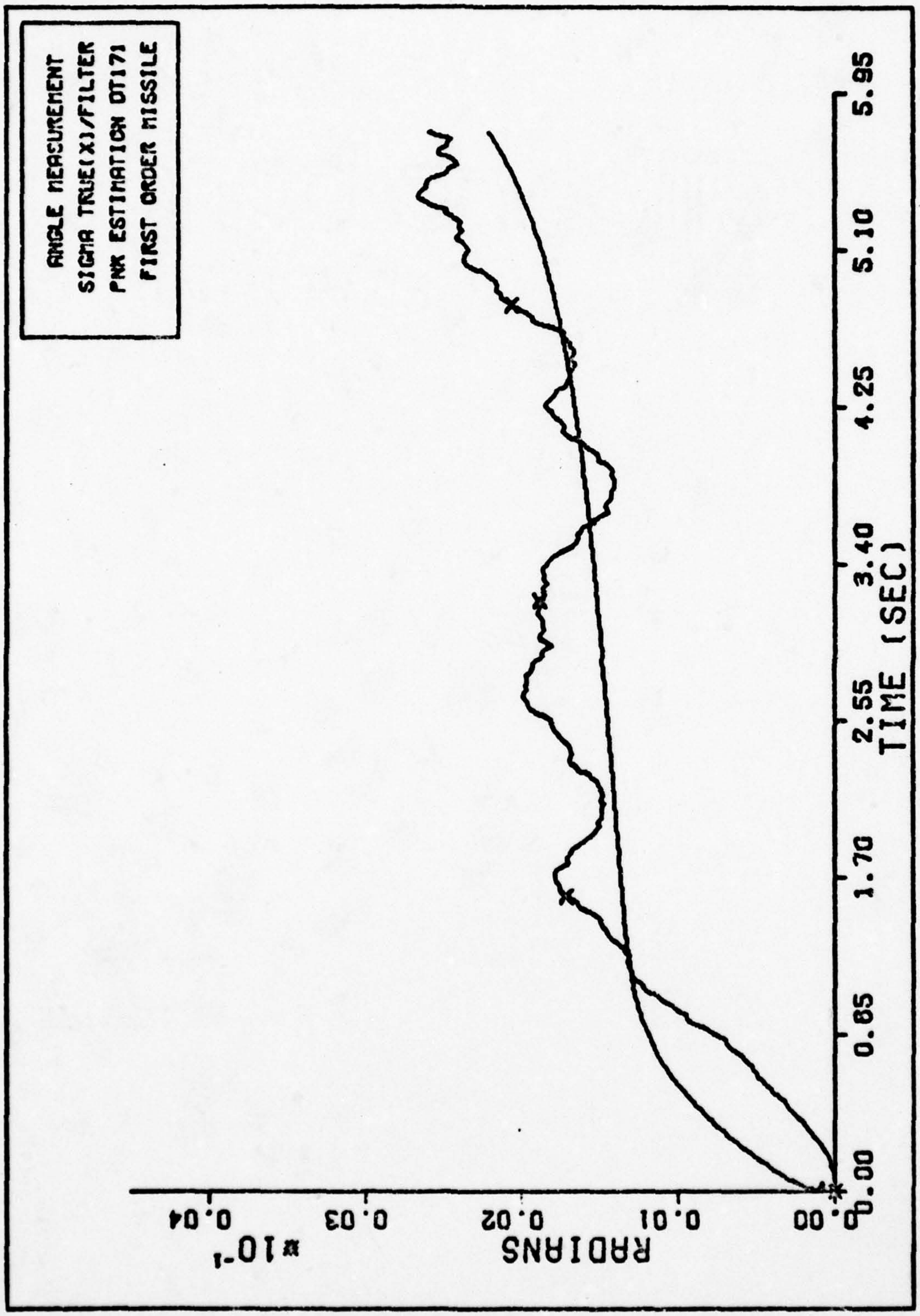

Fig. 169. ANGLE MEASUREMENT SIGMAS FIRST ORDER

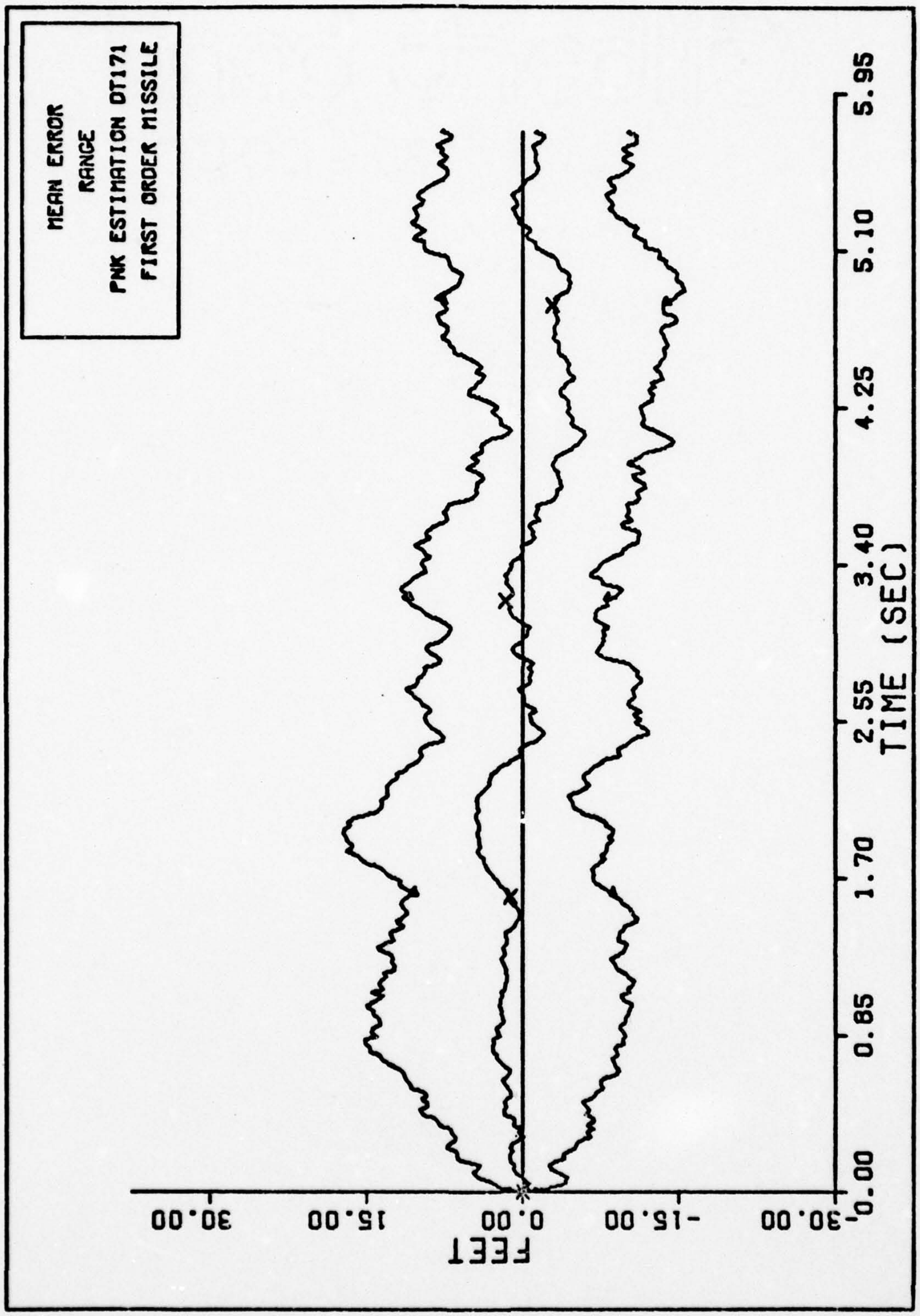

Fig. 170. RANGE FIRST ORDER MISSILE

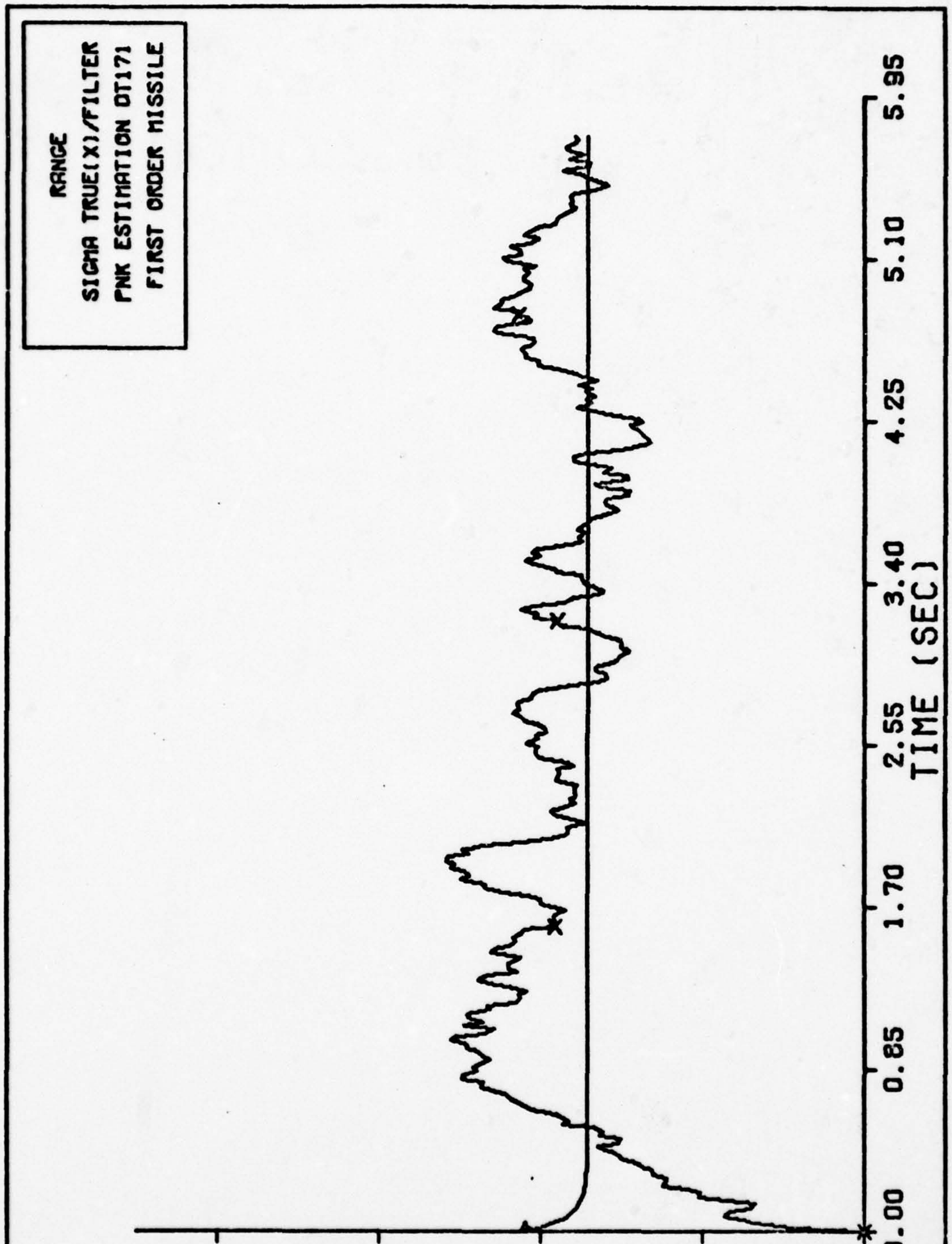

Fig. 171. RANGE SIGMAS FIRST ORDER

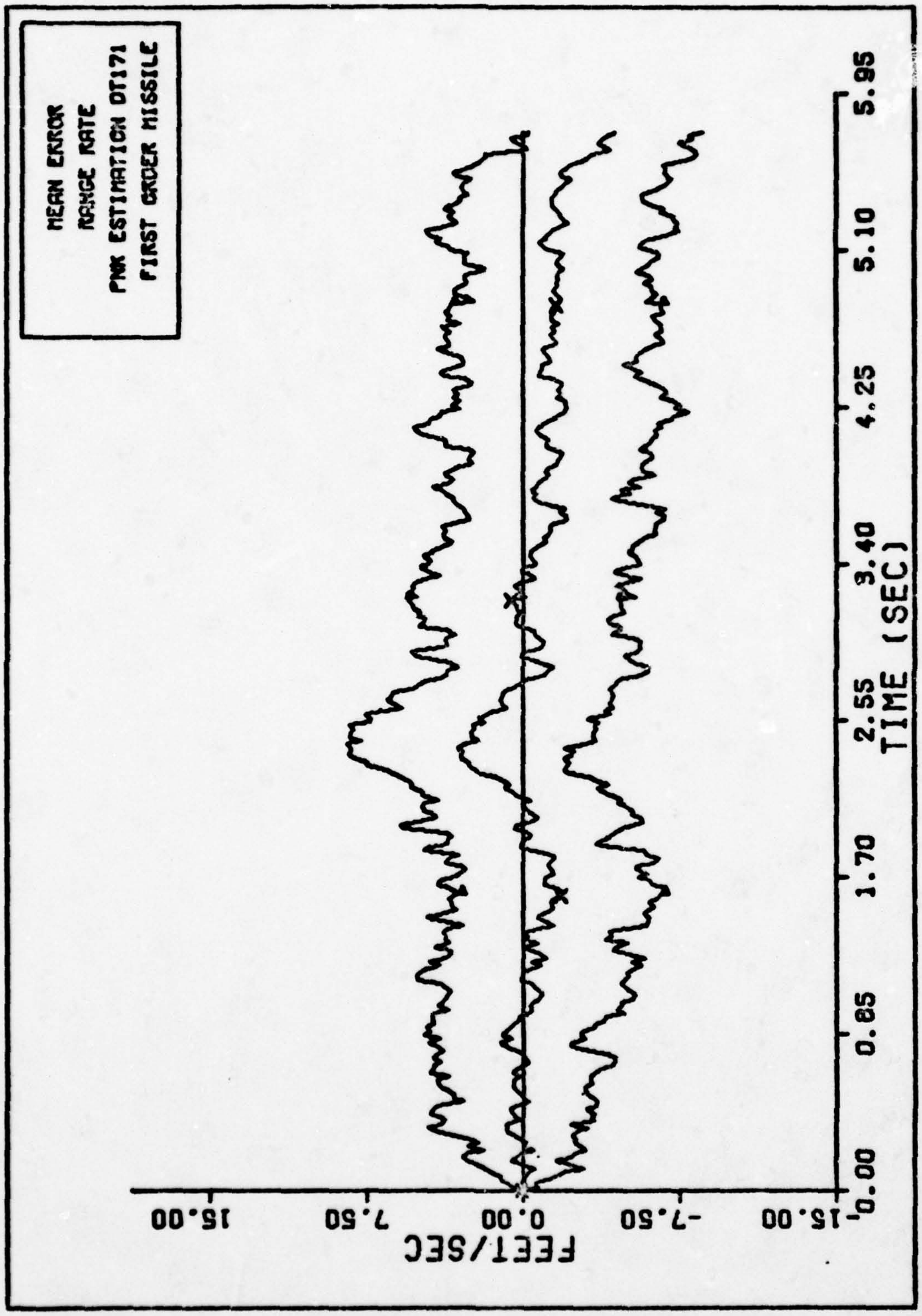

Fig. 172. RANGE RATE FIRST ORDER MISSILE

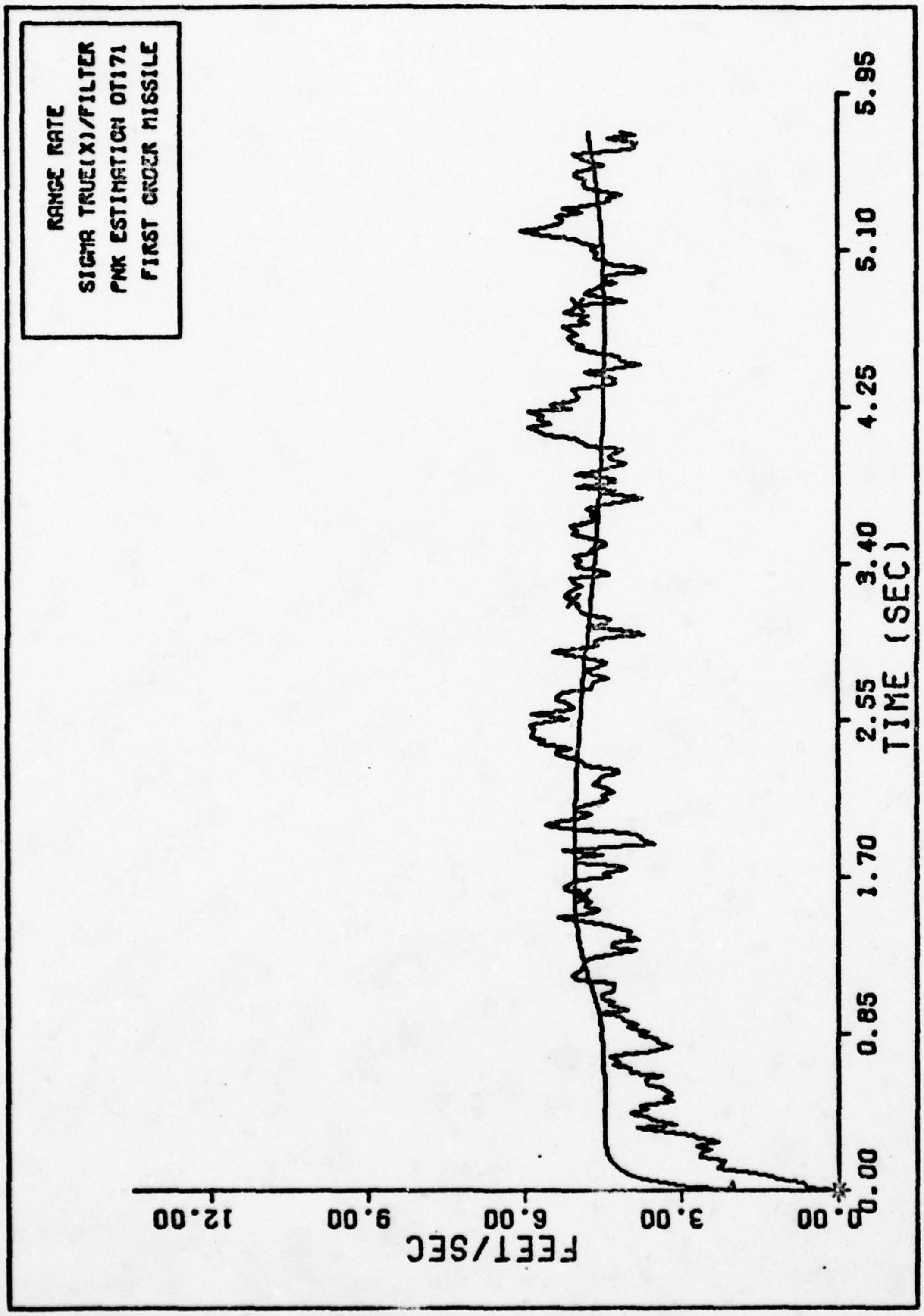

Fig. 173. RANGE RATE SIGMAS FIRST ORDER

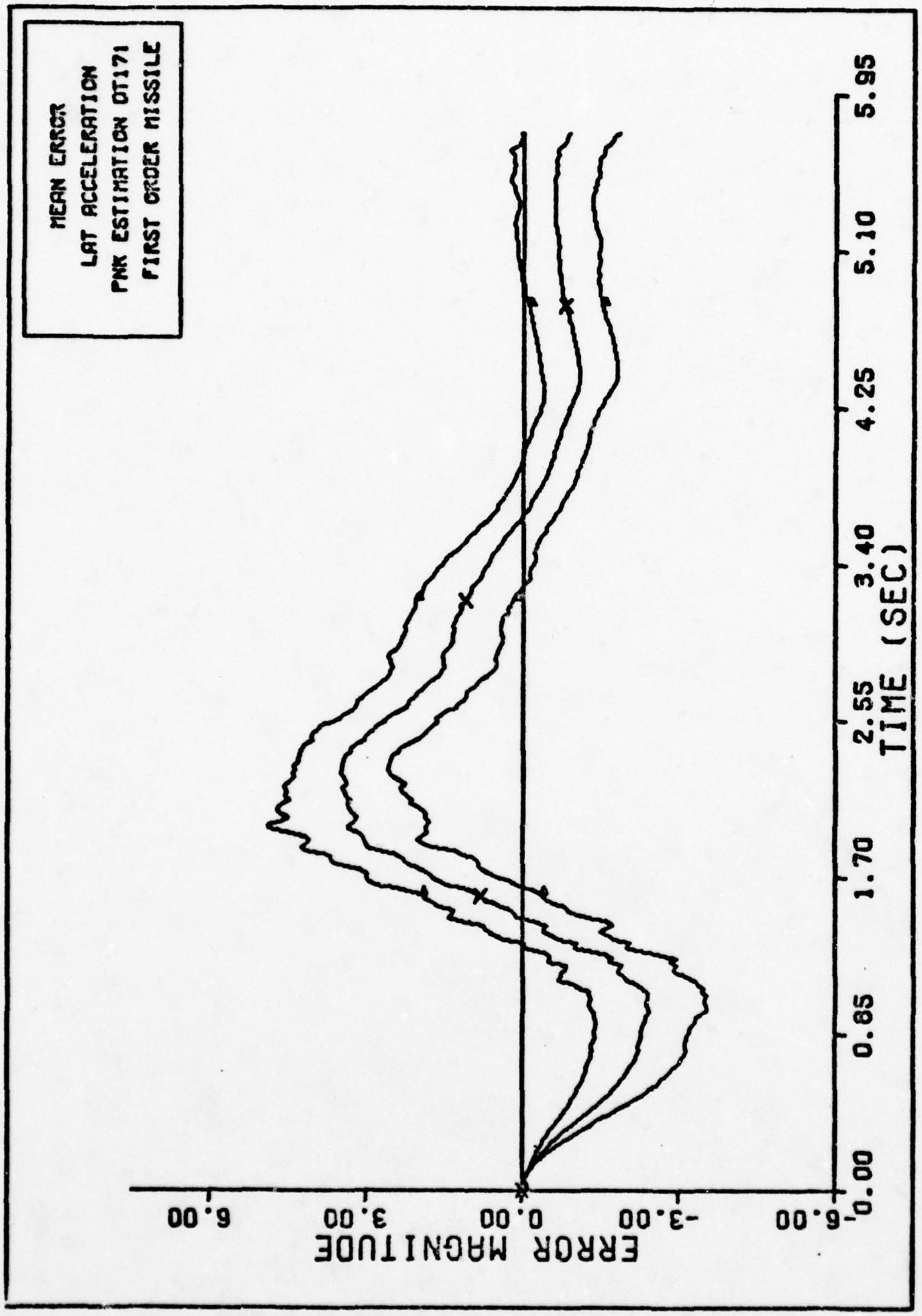

Fig. 174. LAT ACCELERATION FIRST ORDER MISSILE

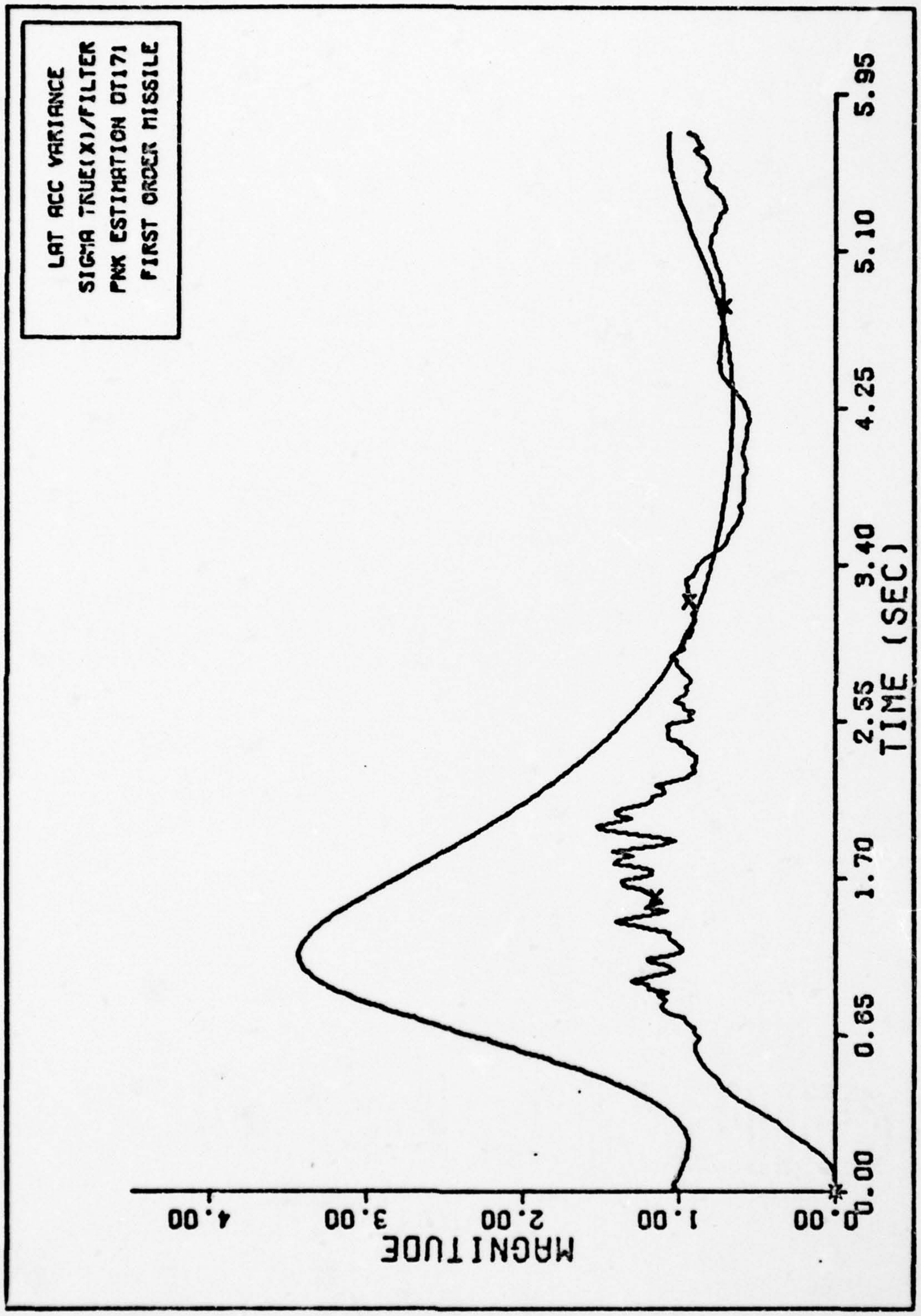

Fig. 175. LAT ACCELERATION SIGMAS FIRST ORDER

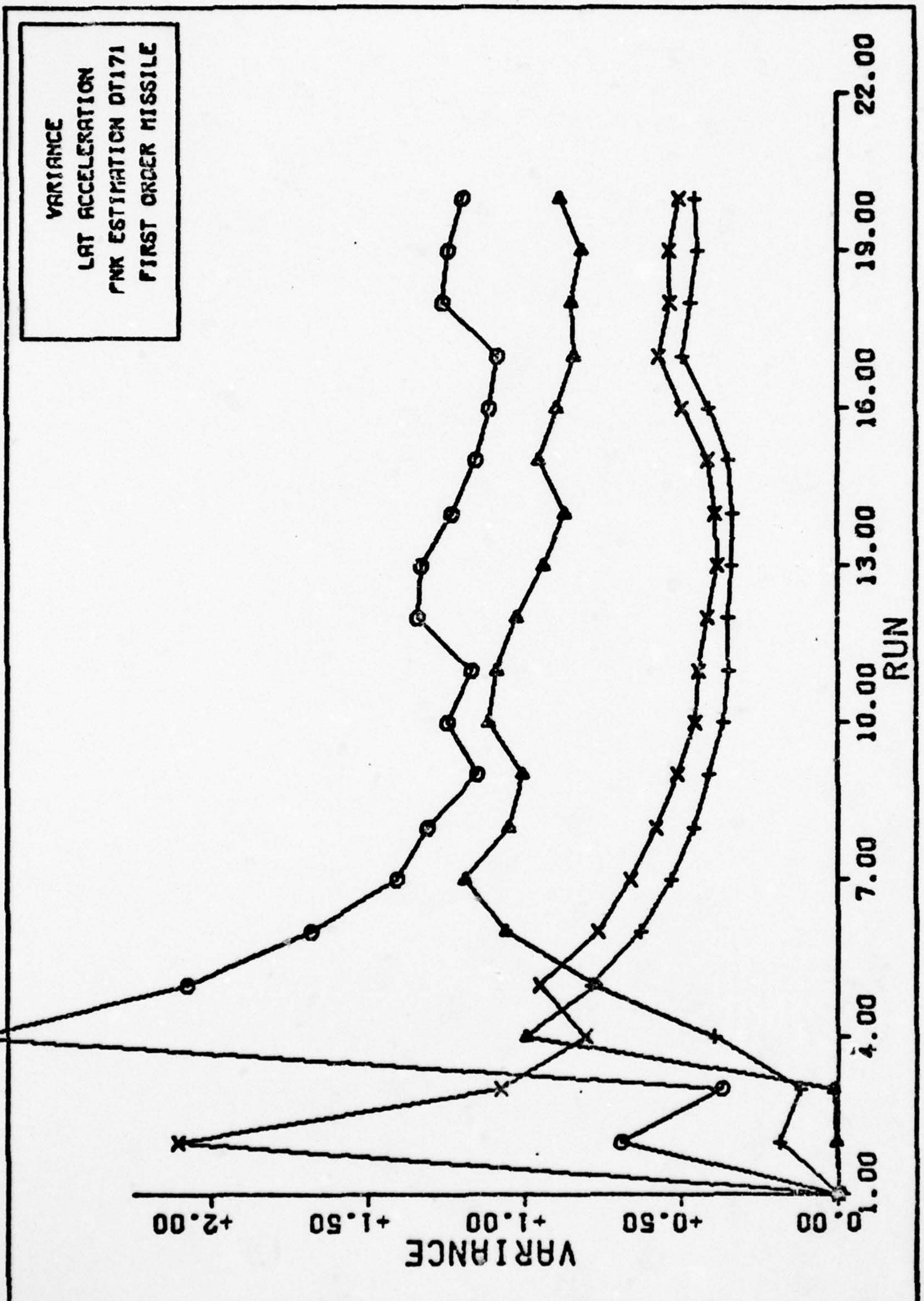

Fig. 176. VARIANCE CONVERGENCE

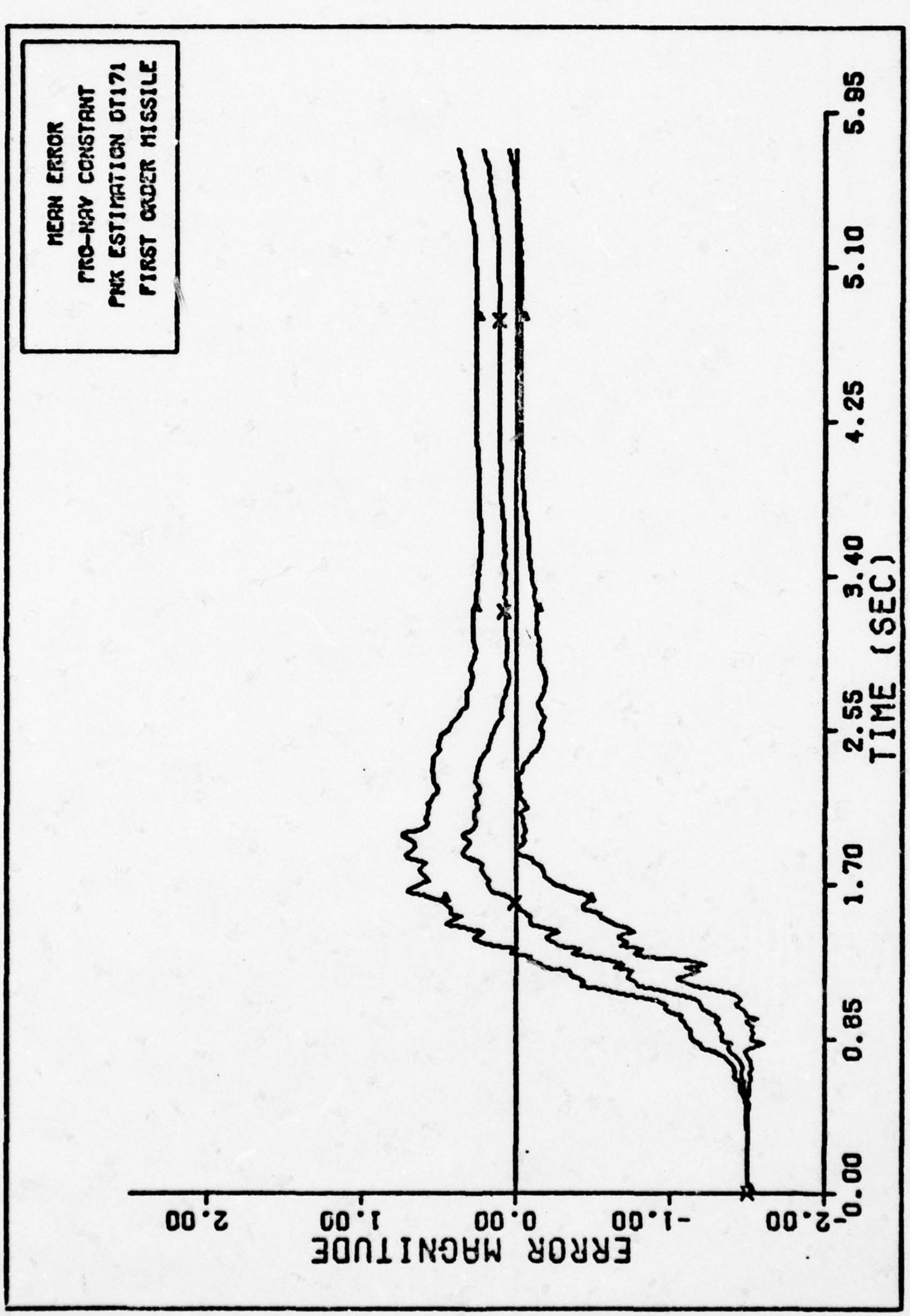

Fig. 177. PRO-NAV CONSTANT FIRST ORDER MISSILE

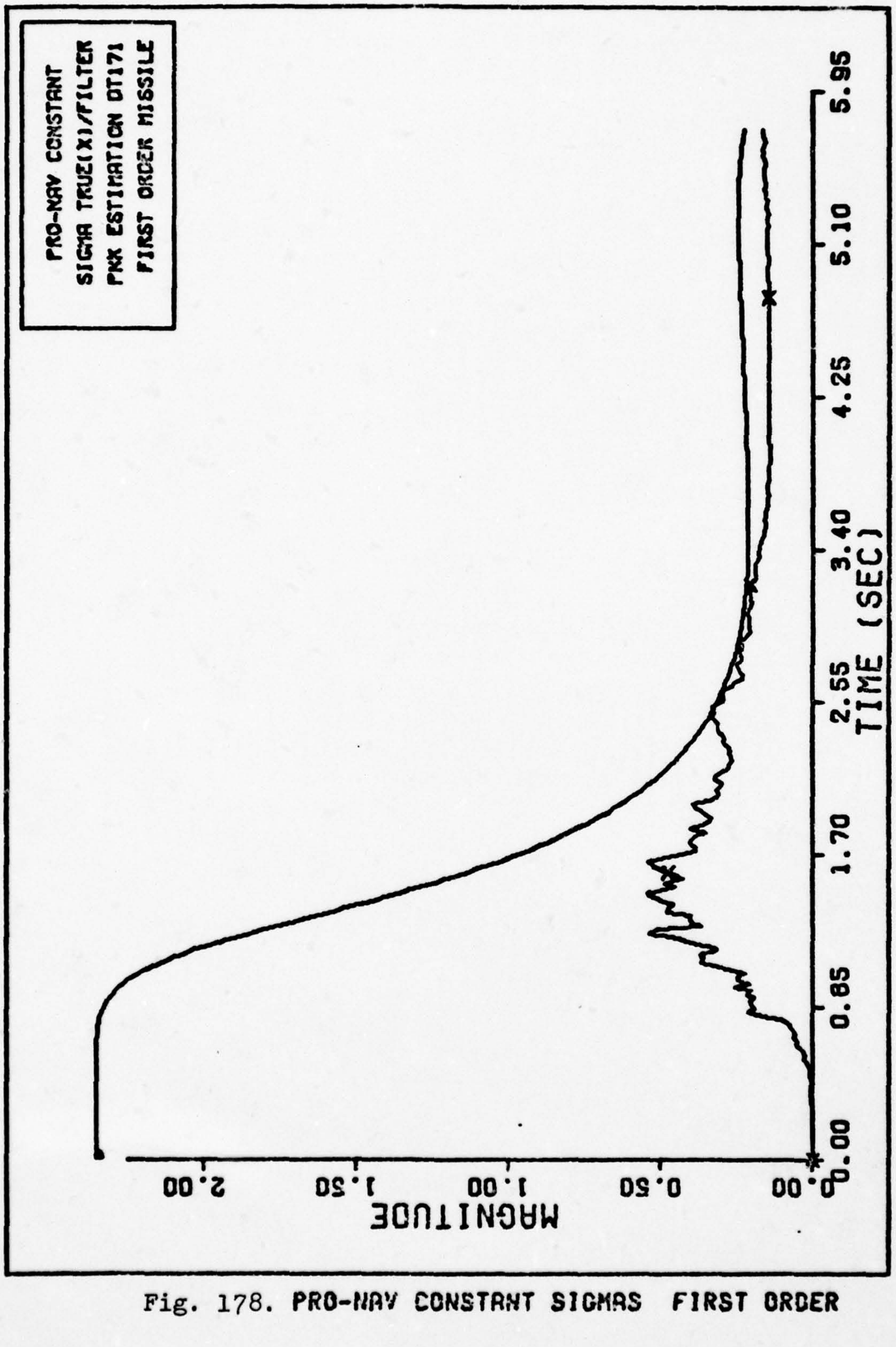

Fig. 178. PRO-NAV CONSTANT SIGMAS FIRST ORDER

τ_f Estimation - τ_f initialized at 1.5

The initial state estimates and the tuning parameters for this case are

$$
\begin{aligned}
V^I_{mx}(0) &= 1225.7 \text{ fps} \\
\dot{\theta}_T(0) &= 4.363345 \text{ radians} \\
R(0) &= 10000. \text{ feet} \\
\dot{R}(0) &= -2122. \text{ fps} \\
a_L(0) &= 0. \\
n(0) &= 4.5 \\
\tau_f(0) &= 1.5 \text{ seconds} \\
M/S(0) &= 29.197 \text{ slugs/ft}^2
\end{aligned}
$$

$$
\underline{R} = \begin{bmatrix} 3.E-5 & 0. & 0. \\ 0. & 500. & 0. \\ 0. & 0. & 100. \end{bmatrix}
$$

$$
\underline{P}_0 = \begin{bmatrix}
100. & 0. & 0. & 0. & 0. & 0. & 0. & 0. \\
0. & 1.E-8 & 0. & 0. & 0. & 0. & 0. & 0. \\
0. & 0. & 101. & 0. & 0. & 0. & 0. & 0. \\
0. & 0. & 0. & 4. & 0. & 0. & 0. & 0. \\
0. & 0. & 0. & 0. & 1. & 0. & 0. & 0. \\
0. & 0. & 0. & 0. & 0. & 0. & 0. & 0. \\
0. & 0. & 0. & 0. & 0. & 0. & .2 & 0. \\
0. & 0. & 0. & 0. & 0. & 0. & 0. & 0.
\end{bmatrix}
$$

$$\underline{Q} = \begin{bmatrix} 250. & 0. & 0. & 0. & 0. & 0. & 0. & 0. \\ 0. & 1.E-6 & 0. & 0. & 0. & 0. & 0. & 0. \\ 0. & 0. & 500. & 0. & 0. & 0. & 0. & 0. \\ 0. & 0. & 0. & 200. & 0. & 0. & 0. & 0. \\ 0. & 0. & 0. & 0. & .1 & 0. & 0. & 0. \\ 0. & 0. & 0. & 0. & 0. & 0. & 0. & 0. \\ 0. & 0. & 0. & 0. & 0. & 0. & .001 & 0. \\ 0. & 0. & 0. & 0. & 0. & 0. & 0. & 0. \end{bmatrix}$$

These plots were generated by estimating τ_f with the first order filter. τ_f was initialized at 1.5 seconds with its truth model value defined as 0.85 seconds The truth model value was determined from an interative search as described in Chapter IV.

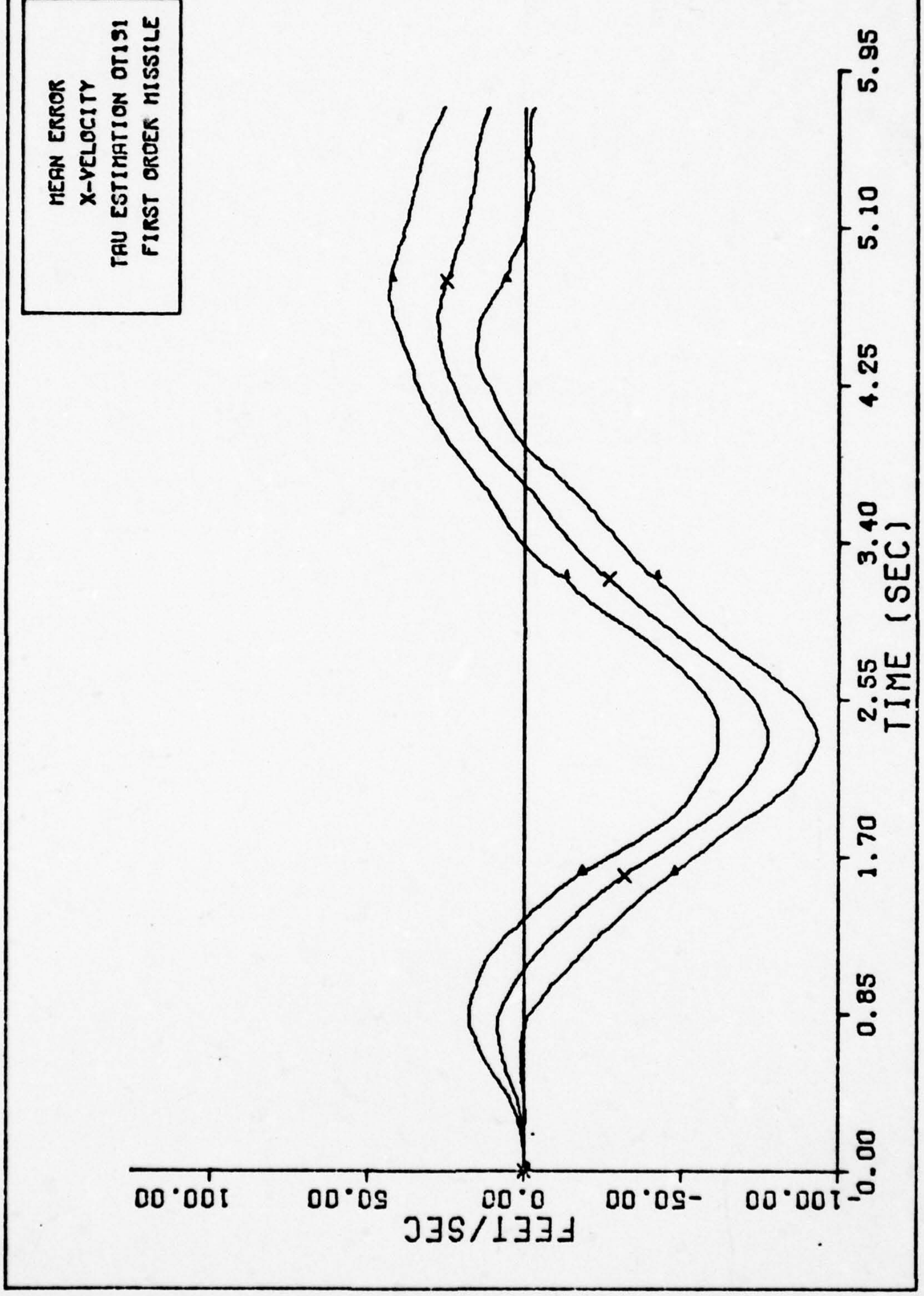

Fig. 179. X-VELOCITY FIRST ORDER MISSILE

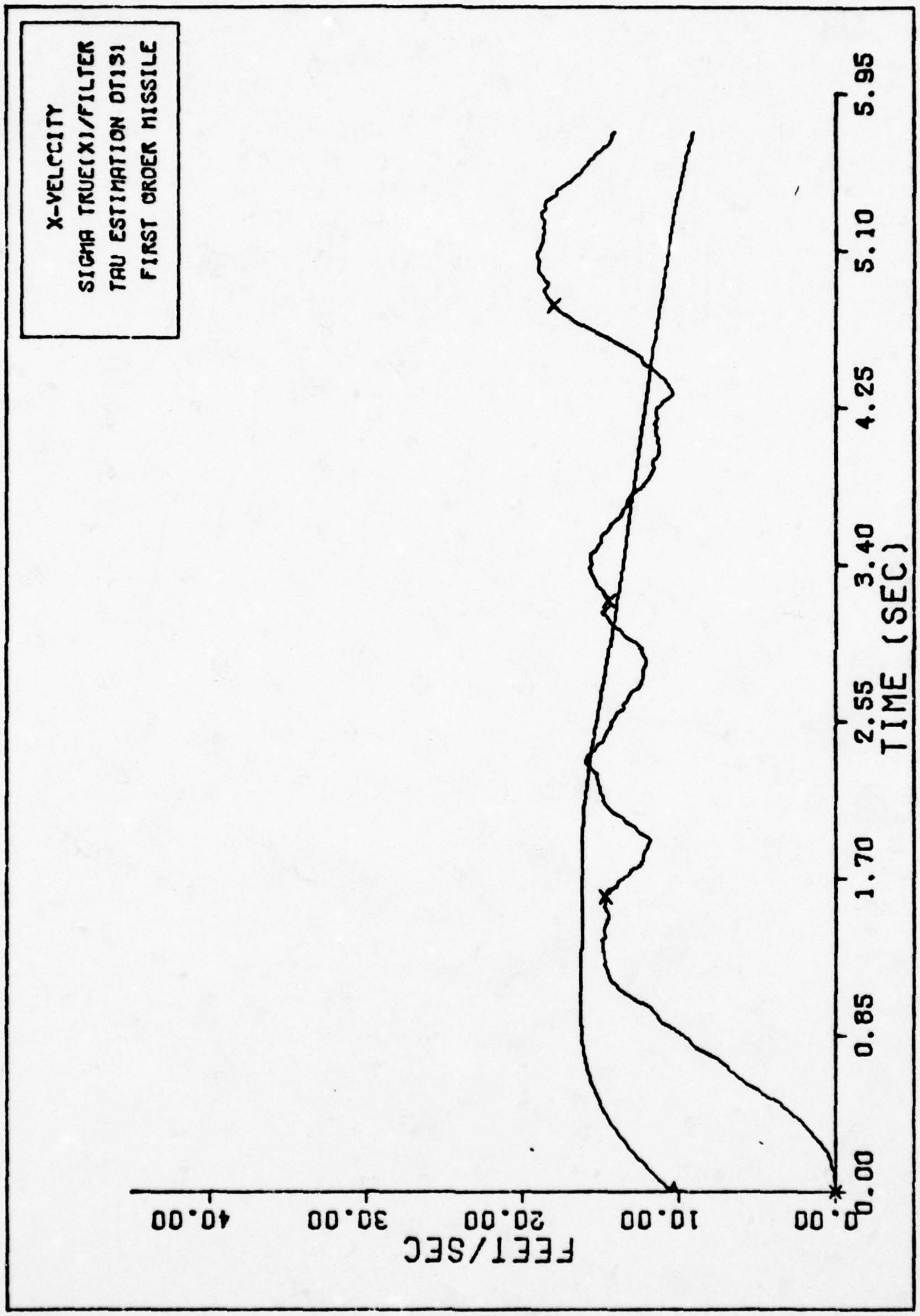

Fig. 180. X-VELOCITY SIGMAS FIRST ORDER

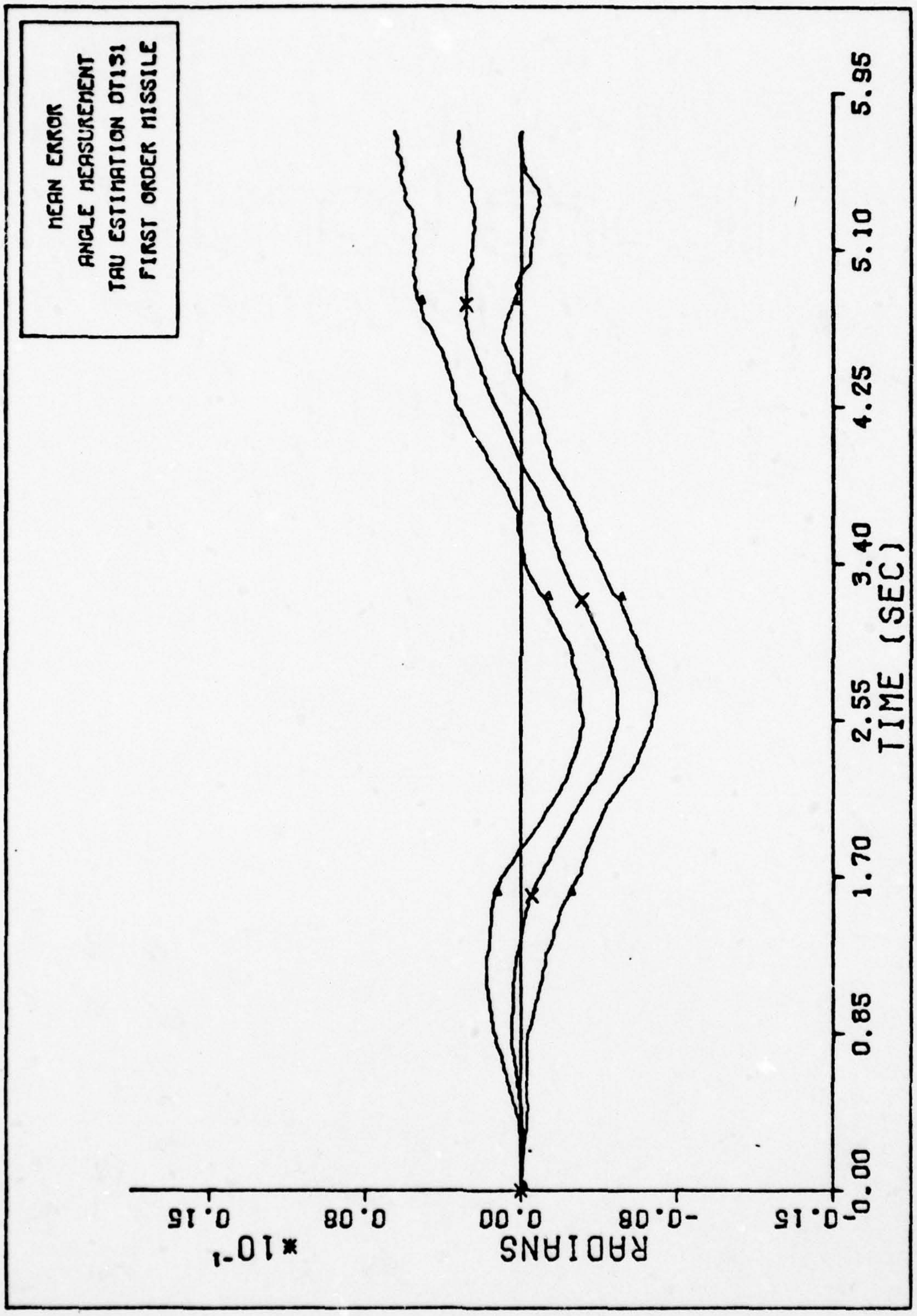

Fig. 181. ANGLE MEASUREMENT FIRST ORDER MISSILE

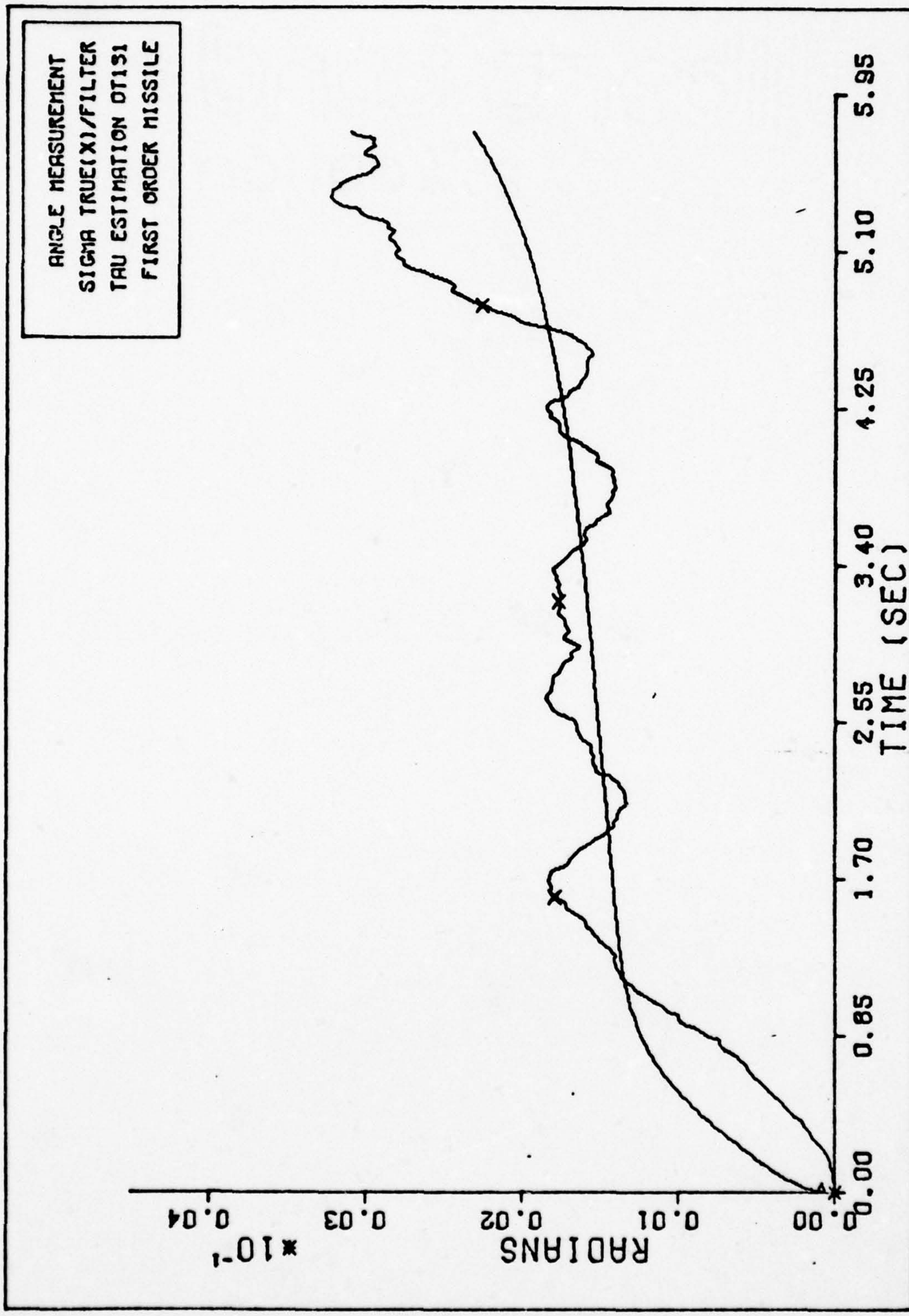

Fig. 182. ANGLE MEASUREMENT SIGMAS FIRST ORDER

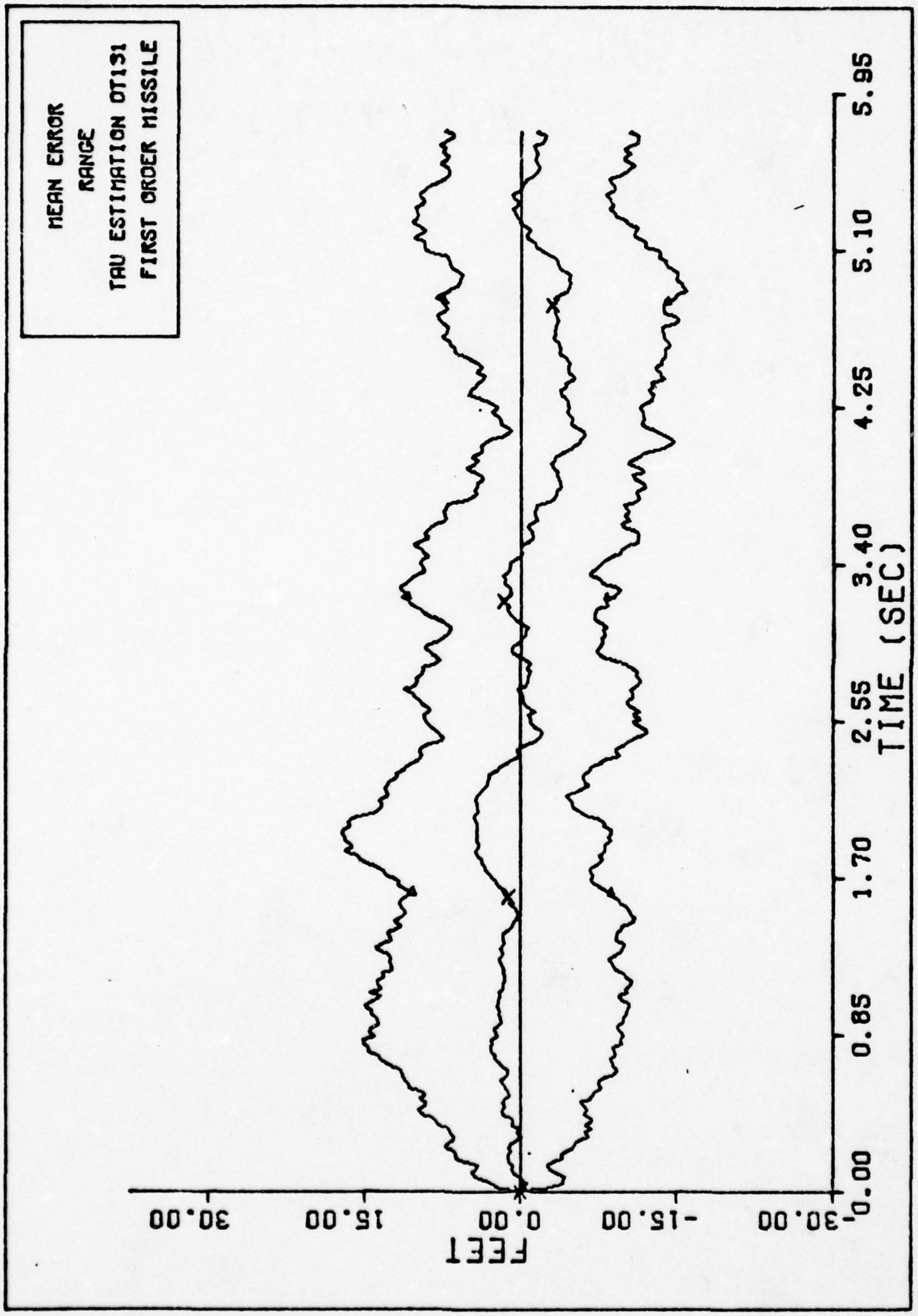

Fig. 183. RANGE FIRST ORDER MISSILE

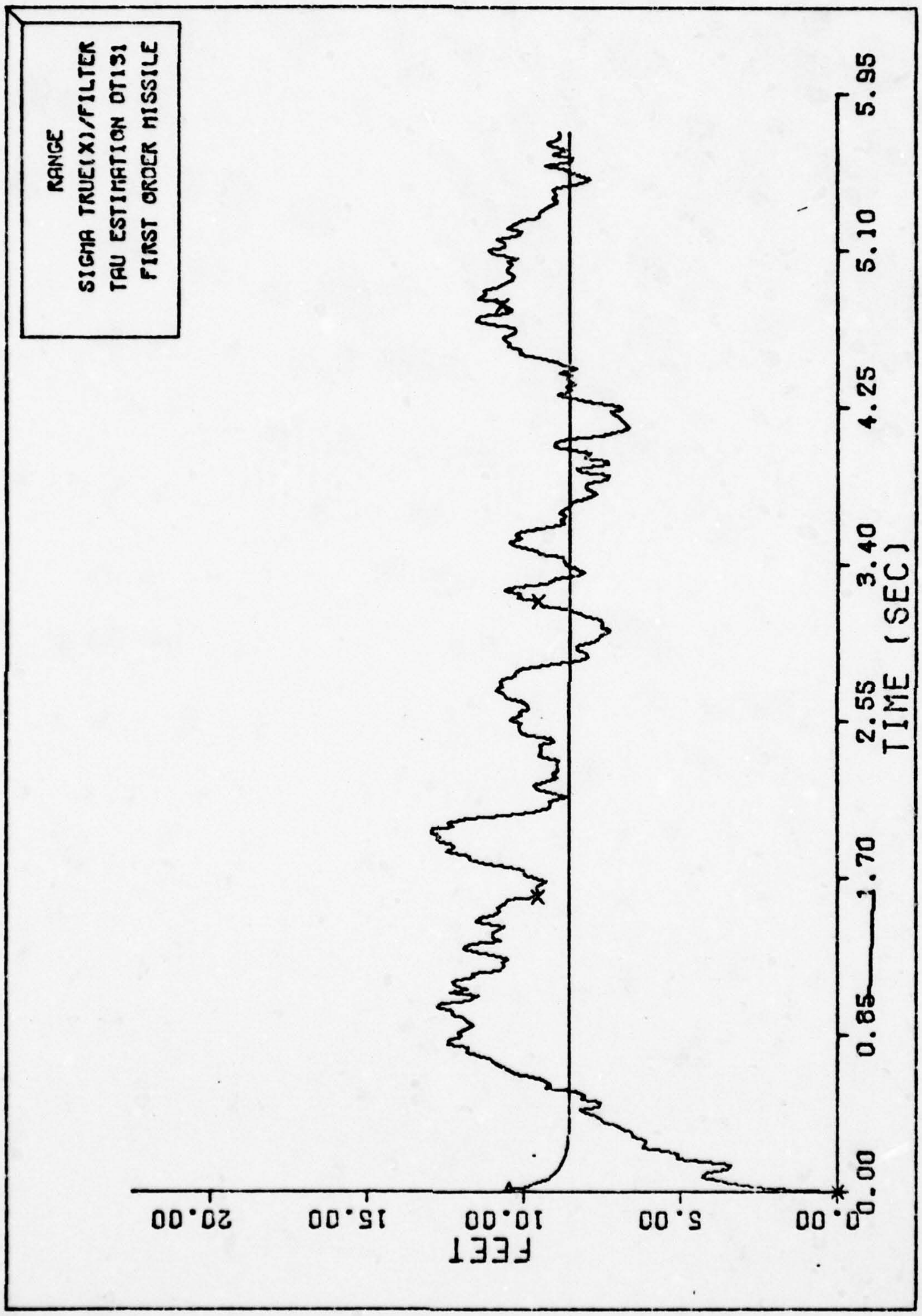

Fig. 184. RANGE SIGMAS FIRST ORDER

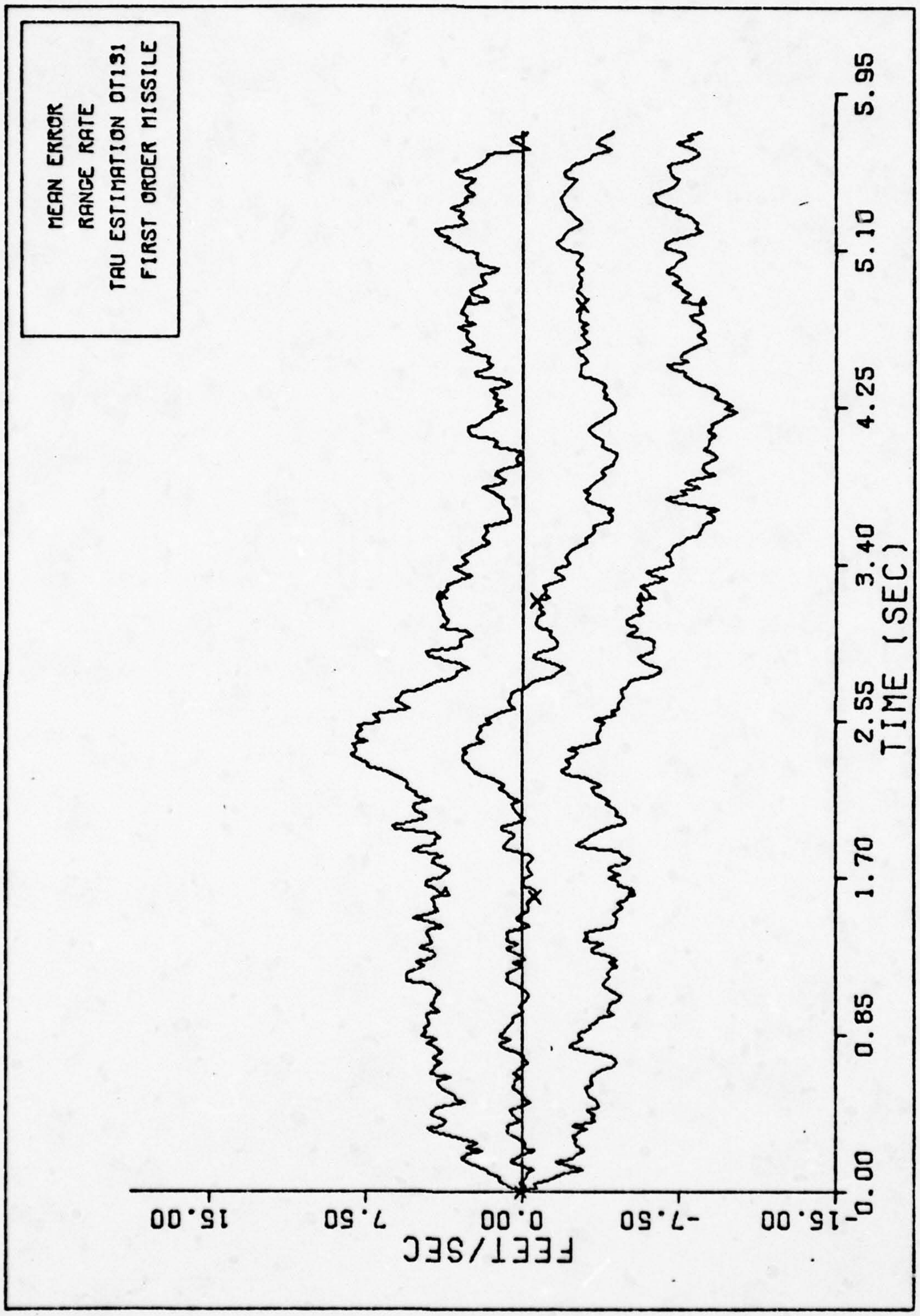

Fig. 185. RANGE RATE FIRST ORDER MISSILE

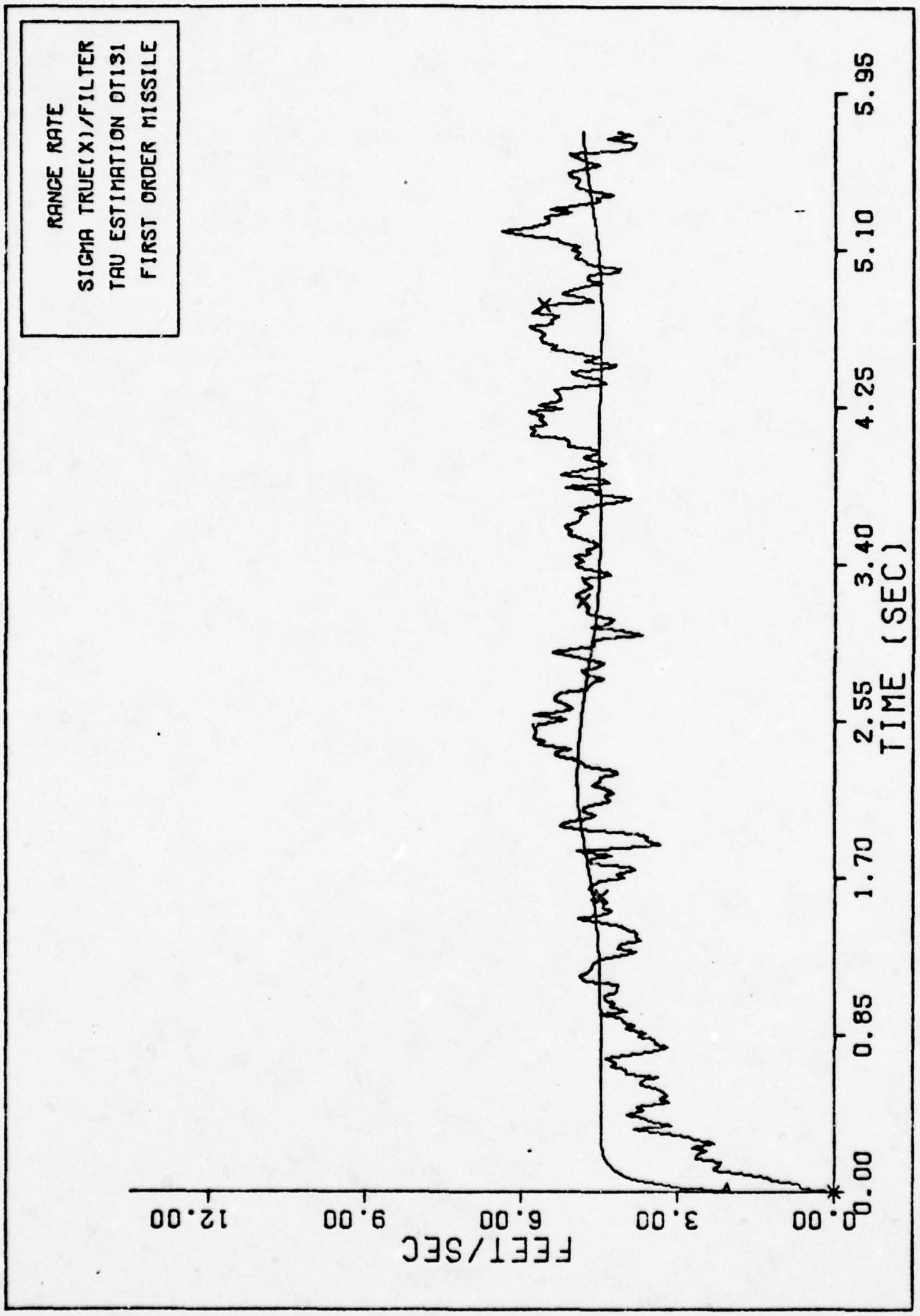

Fig. 186. RANGE RATE SIGMAS FIRST ORDER

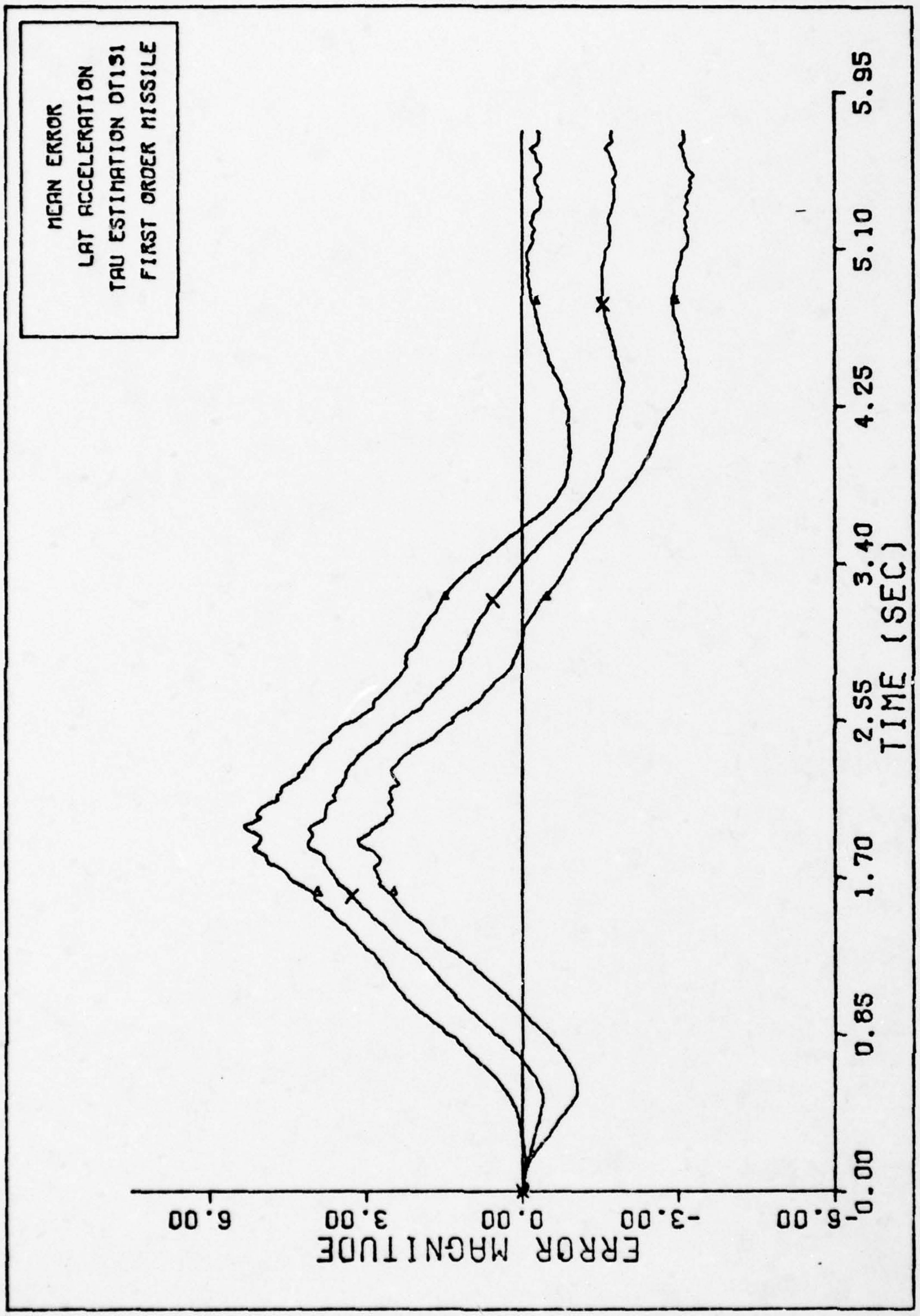

Fig. 187. LAT ACCELERATION FIRST ORDER MISSILE

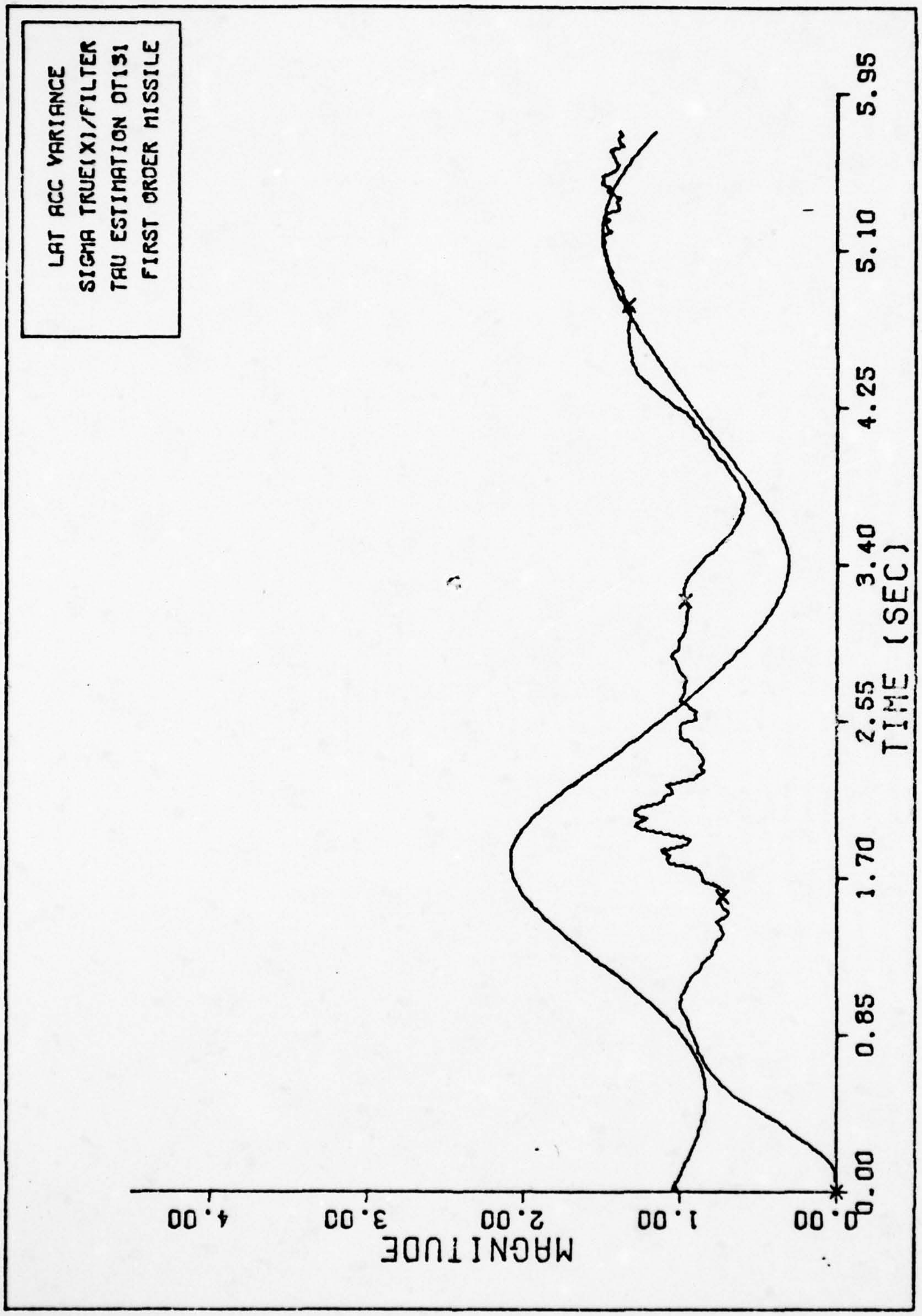

Fig. 188. LAT ACCELERATION SIGMAS FIRST ORDER

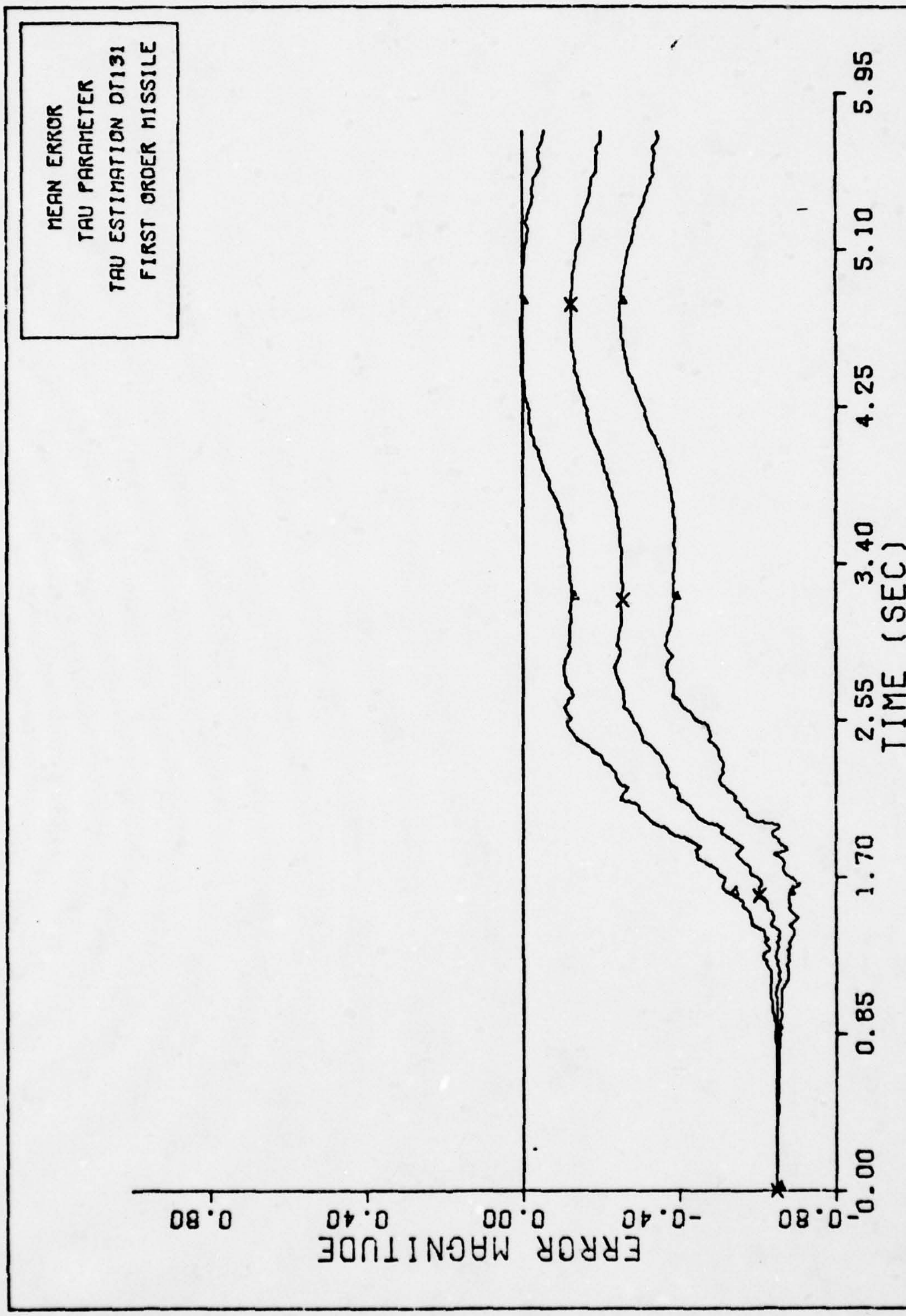

Fig. 189. TAU PARAMETER FIRST ORDER MISSILE

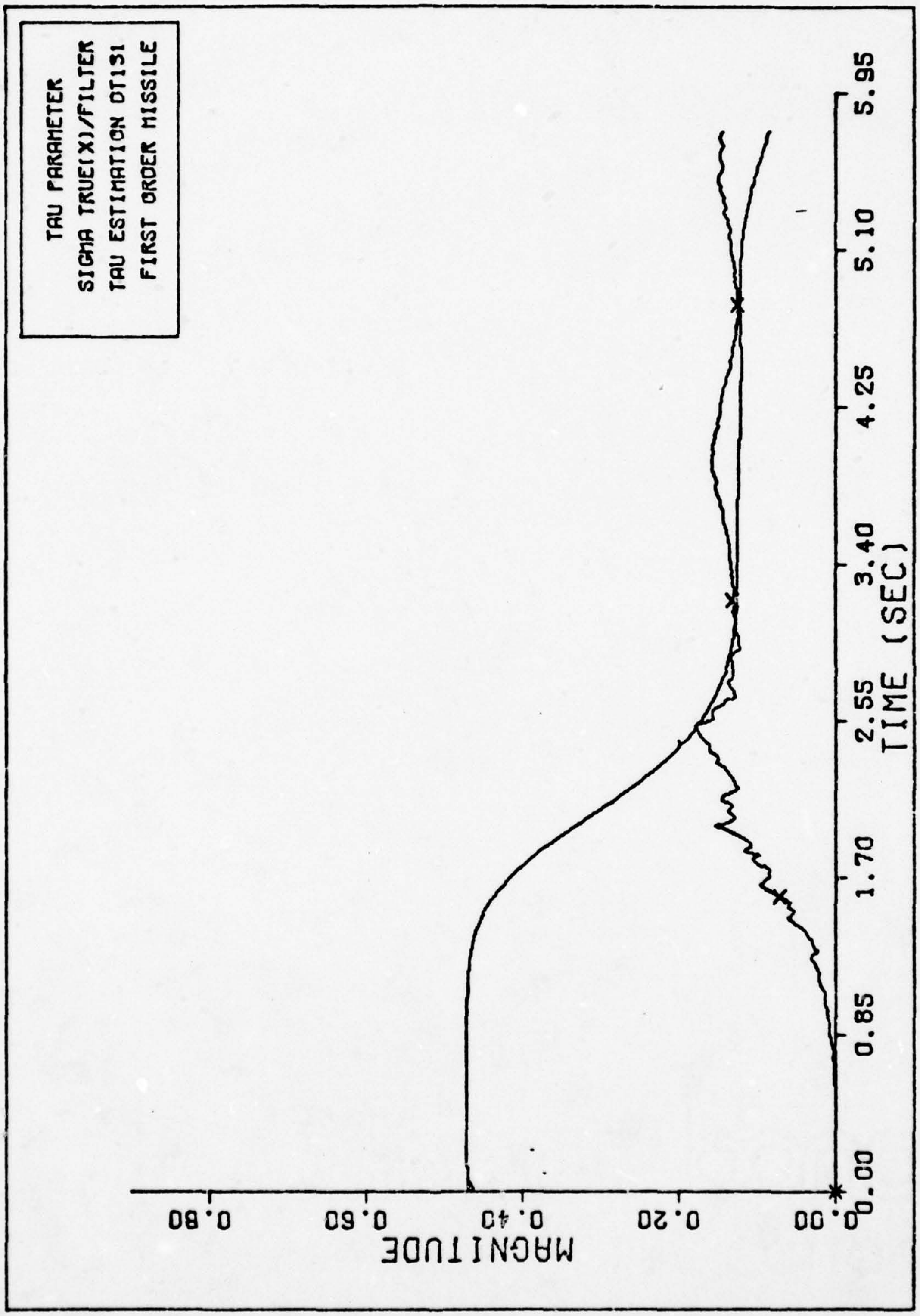

Fig. 190. TAU PARAMETER SIGMAS FIRST ORDER

τ_f Estimation - τ_f Initialized at .3

The initial state estimates and the tuning parameters for this case are

$$V^I_{mx}(0) = 1225.7 \text{ fps}$$
$$\dot{\theta}_T(0) = 4.363345 \text{ radians}$$
$$R(0) = 10000. \text{ feet}$$
$$\dot{R}(0) = -2122. \text{ fps}$$
$$a_L(0) = 0.$$
$$n(0) = 4.5$$
$$\tau_f(0) = .3 \text{ seconds}$$
$$M/S(0) = 29.197 \text{ slugs/ft}^2$$

$$\underline{R} = \begin{bmatrix} 3.E-5 & 0. & 0. \\ 0. & 500. & 0. \\ 0. & 0. & 100. \end{bmatrix}$$

$$\underline{P}_0 = \begin{bmatrix} 100. & 0. & 0. & 0. & 0. & 0. & 0. & 0. \\ 0. & 1.E-8 & 0. & 0. & 0. & 0. & 0. & 0. \\ 0. & 0. & 101. & 0. & 0. & 0. & 0. & 0. \\ 0. & 0. & 0. & 4. & 0. & 0. & 0. & 0. \\ 0. & 0. & 0. & 0. & 1. & 0. & 0. & 0. \\ 0. & 0. & 0. & 0. & 0. & 0. & 0. & 0. \\ 0. & 0. & 0. & 0. & 0. & 0. & .2 & 0. \\ 0. & 0. & 0. & 0. & 0. & 0. & 0. & 0. \end{bmatrix}$$

$$
\underline{Q} = \begin{bmatrix}
250. & 0. & 0. & 0. & 0. & 0. & 0. & 0. \\
0. & 1.E-6 & 0. & 0. & 0. & 0. & 0. & 0. \\
0. & 0. & 500. & 0. & 0. & 0. & 0. & 0. \\
0. & 0. & 0. & 200. & 0. & 0. & 0. & 0. \\
0. & 0. & 0. & 0. & .1 & 0. & 0. & 0. \\
0. & 0. & 0. & 0. & 0. & 0. & 0. & 0. \\
0. & 0. & 0. & 0. & 0. & 0. & .001 & 0. \\
0. & 0. & 0. & 0. & 0. & 0. & 0. & 0.
\end{bmatrix}
$$

These plots were generated by estimating τ_f with the first order filter. τ_f was initialized at 0.3 seconds in the filter with its truth model value defined as 0.85 seconds. The truth model value was determined from an iterative search as described in Chapter IV.

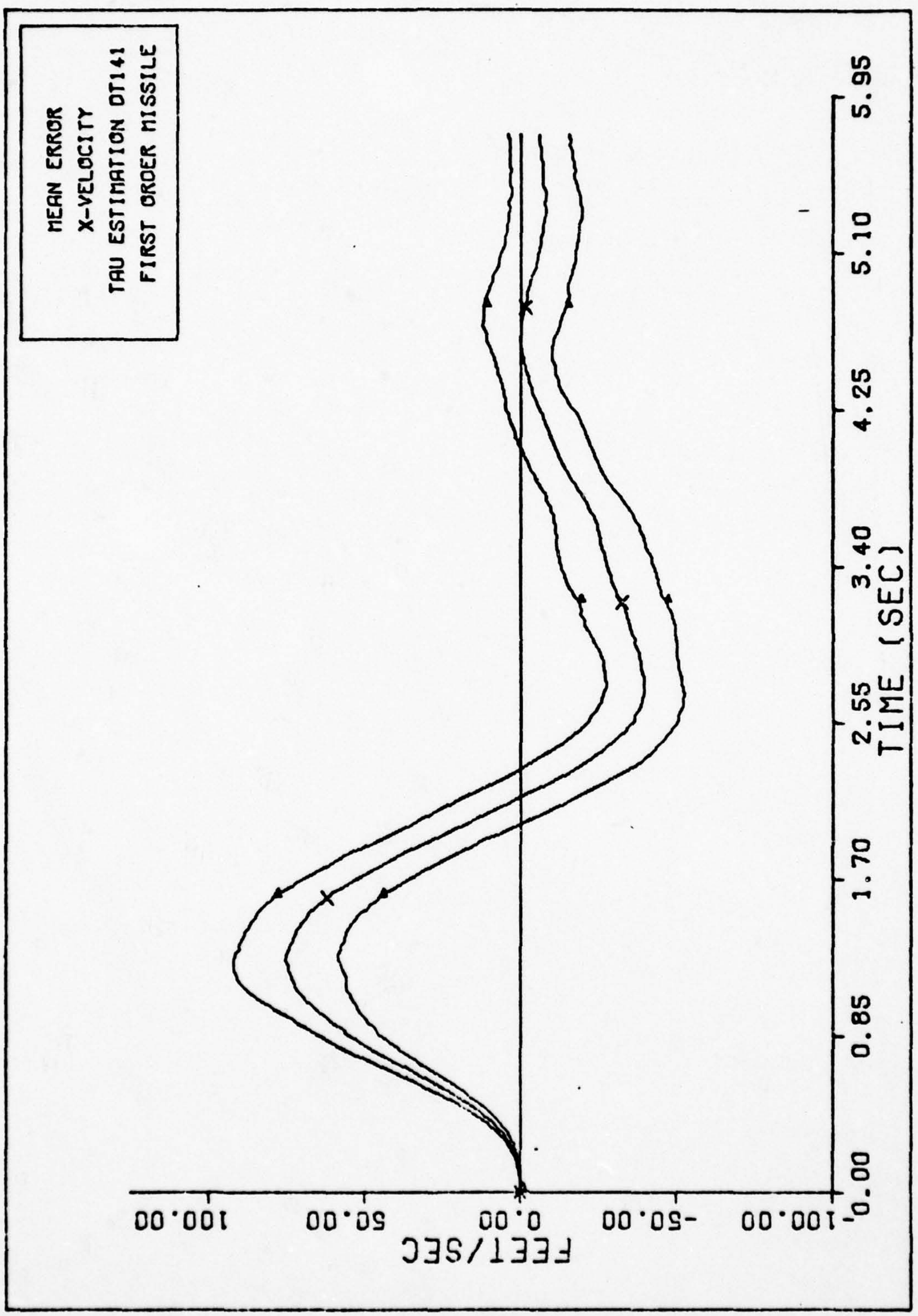

Fig. 191. X-VELOCITY FIRST ORDER MISSILE

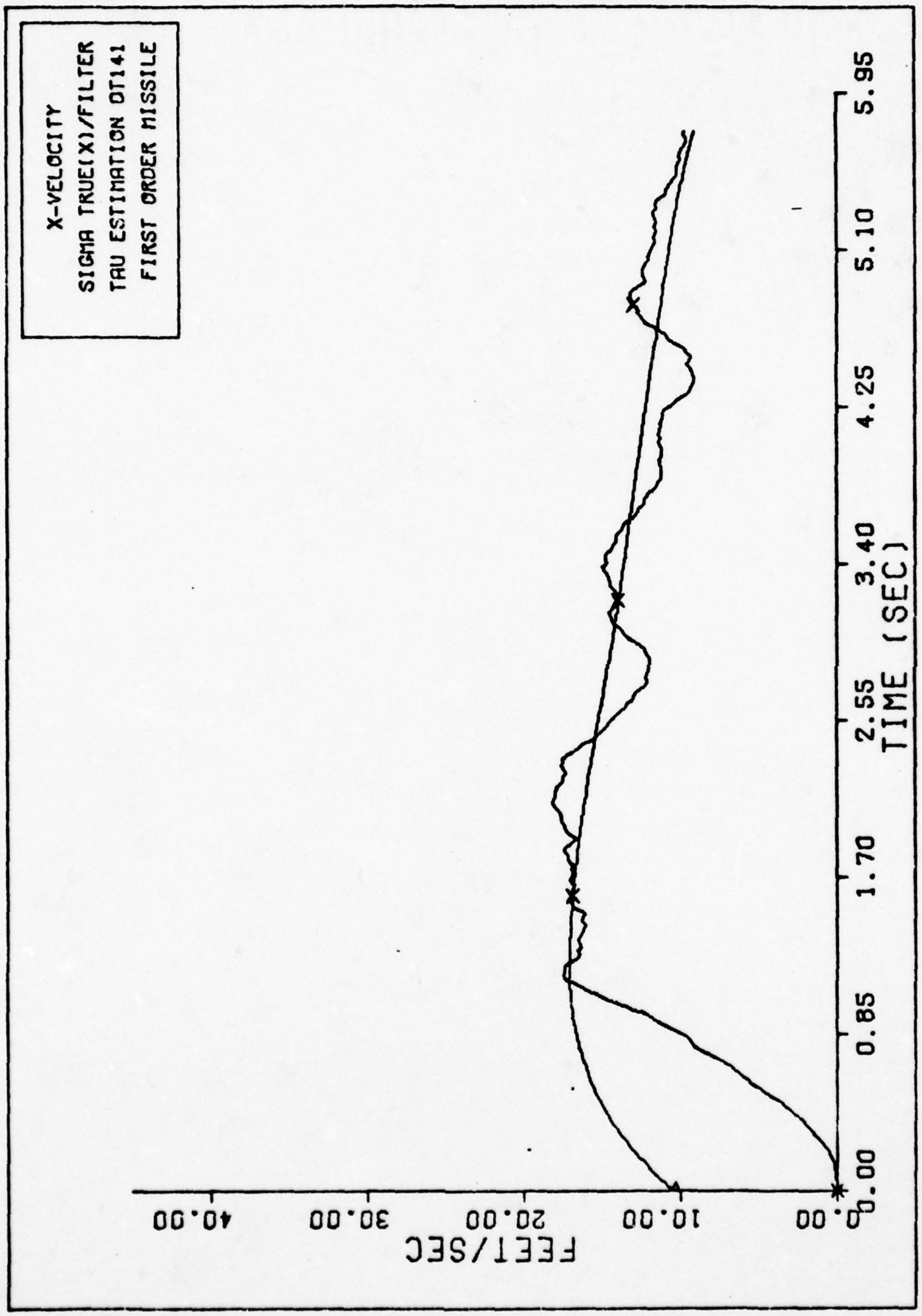

Fig. 192. X-VELOCITY SIGMAS FIRST ORDER

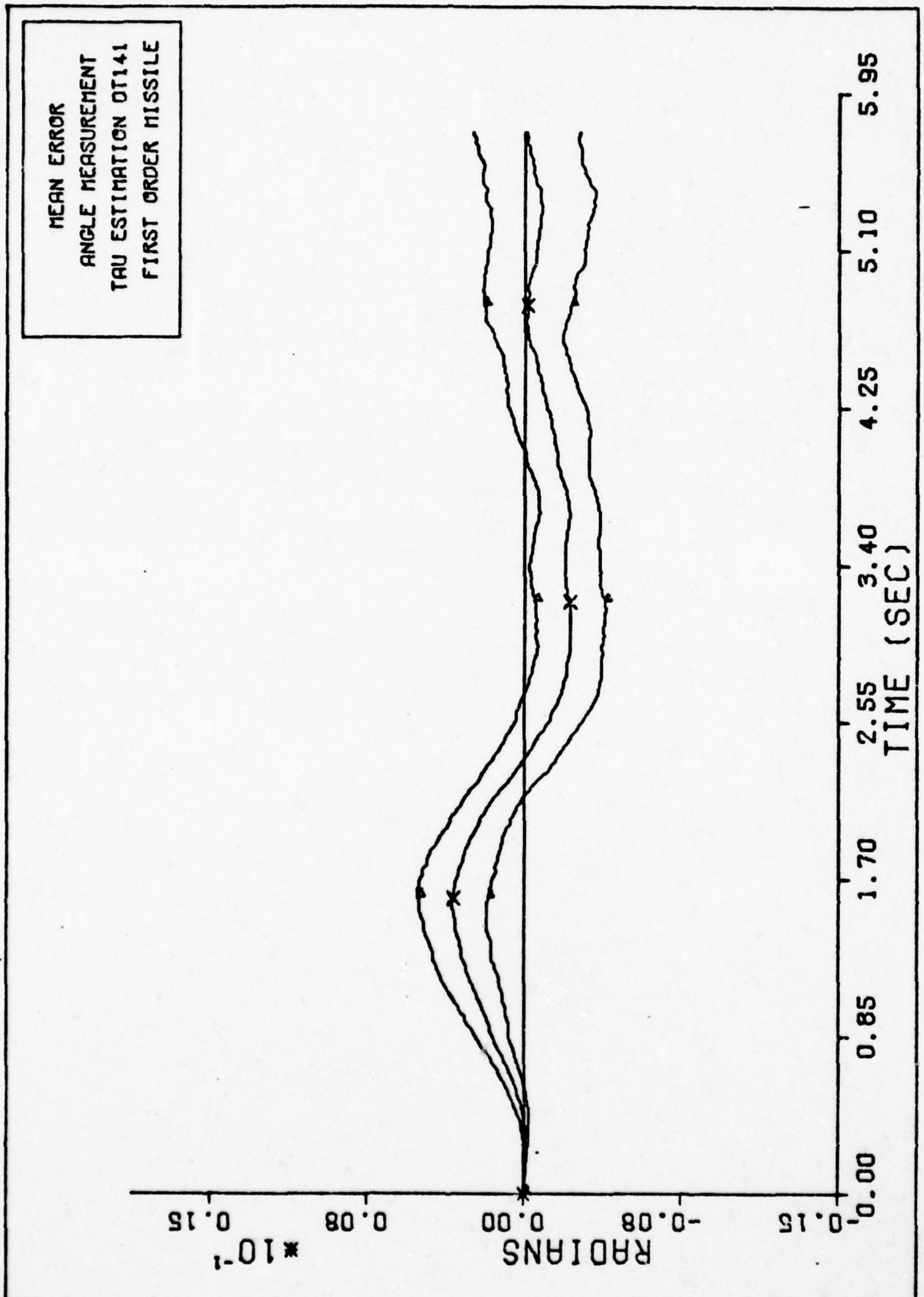

Fig. 193. ANGLE MEASUREMENT FIRST ORDER MISSILE

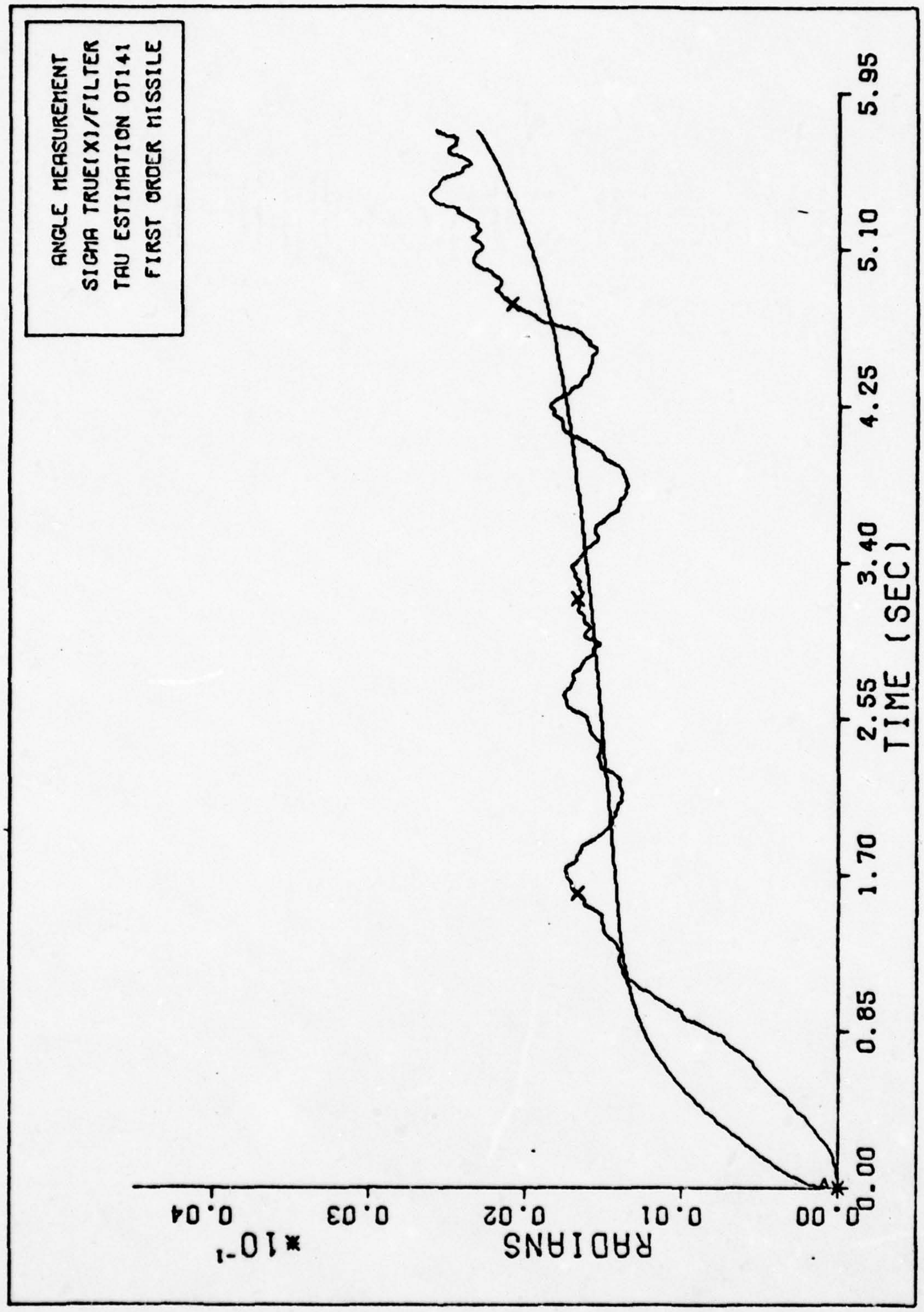

Fig. 194. ANGLE MEASUREMENT SIGMAS FIRST ORDER

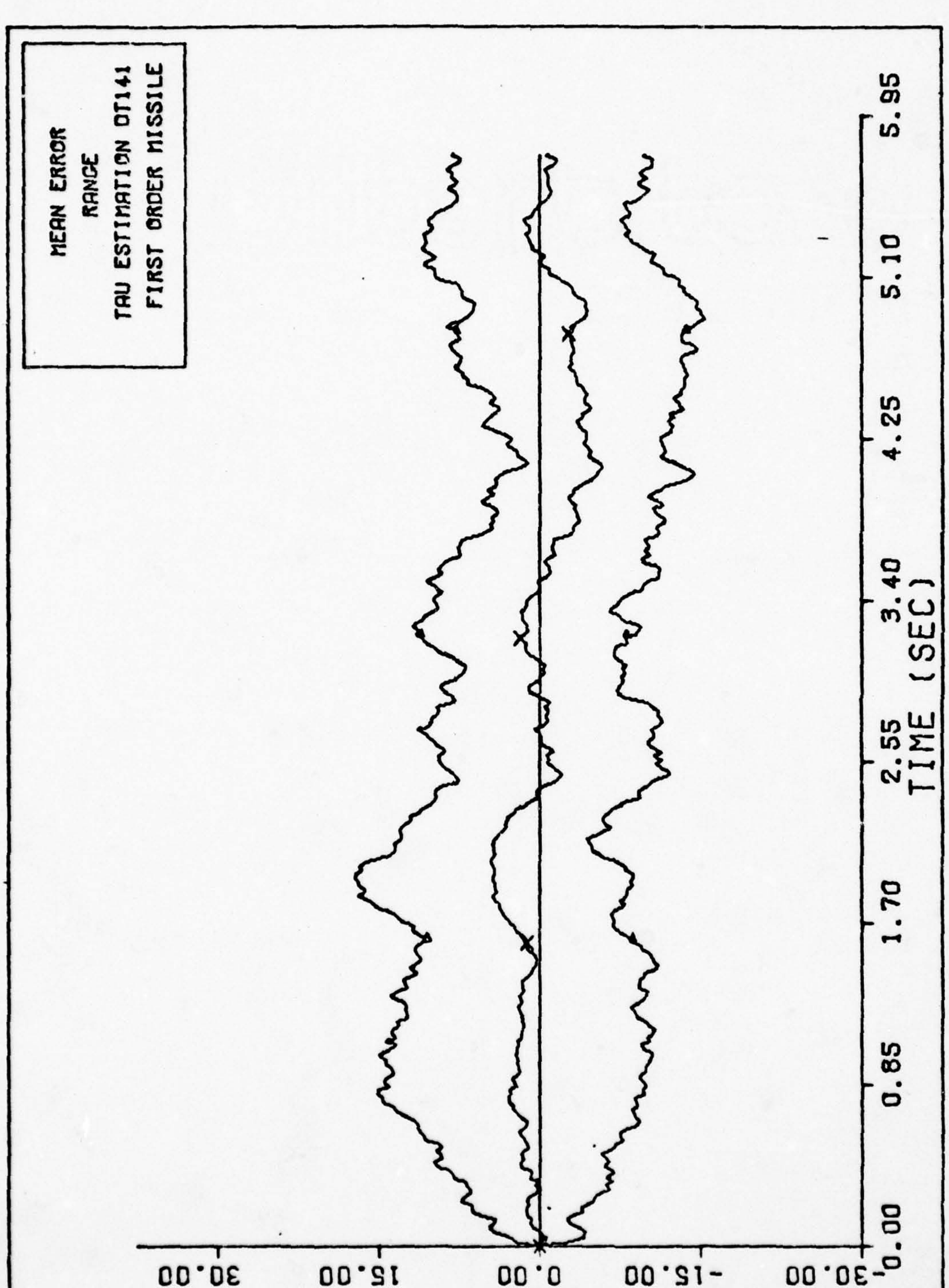

Fig. 195. RANGE FIRST ORDER MISSILE

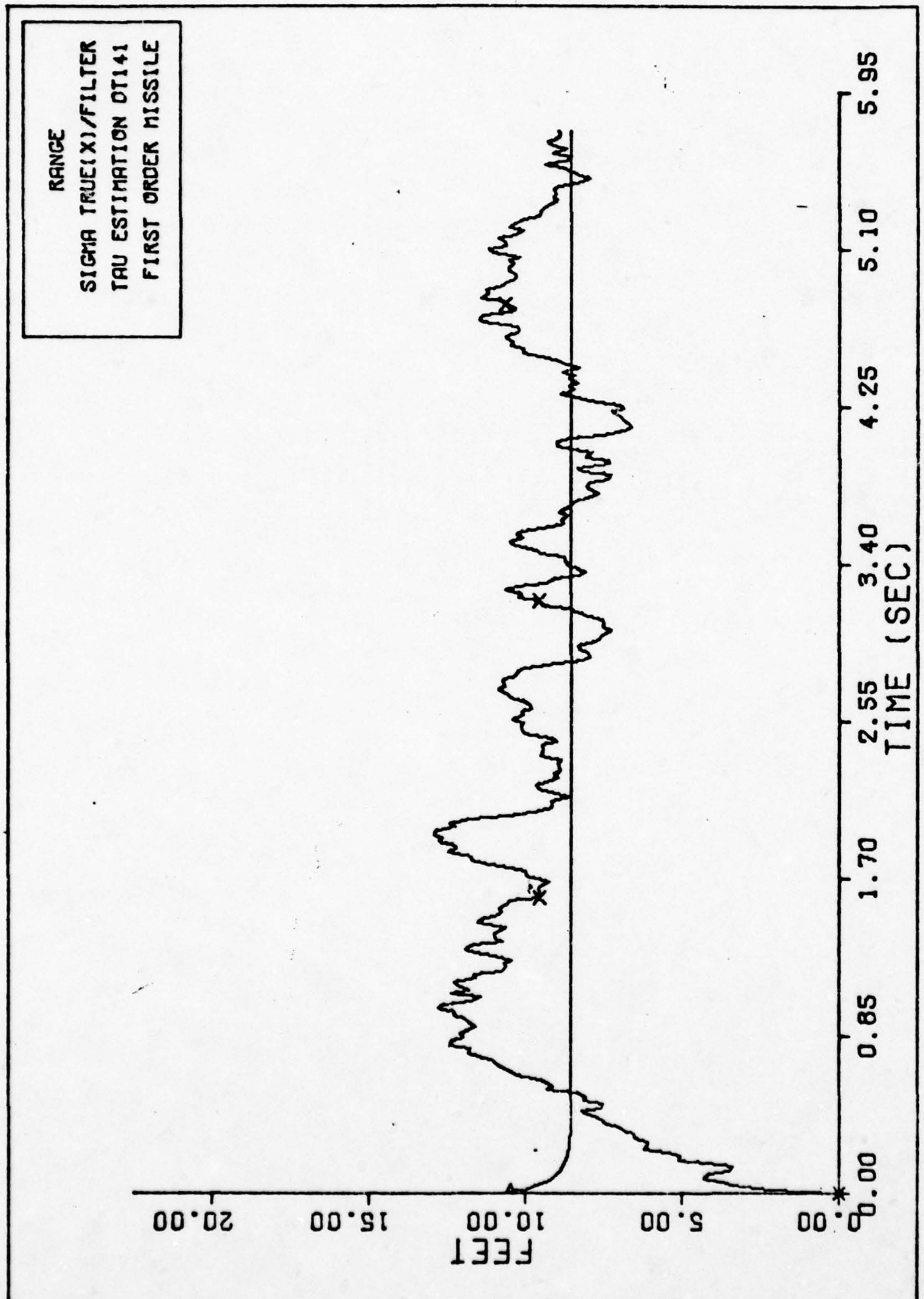

Fig. 196. RANGE SIGMAS FIRST ORDER

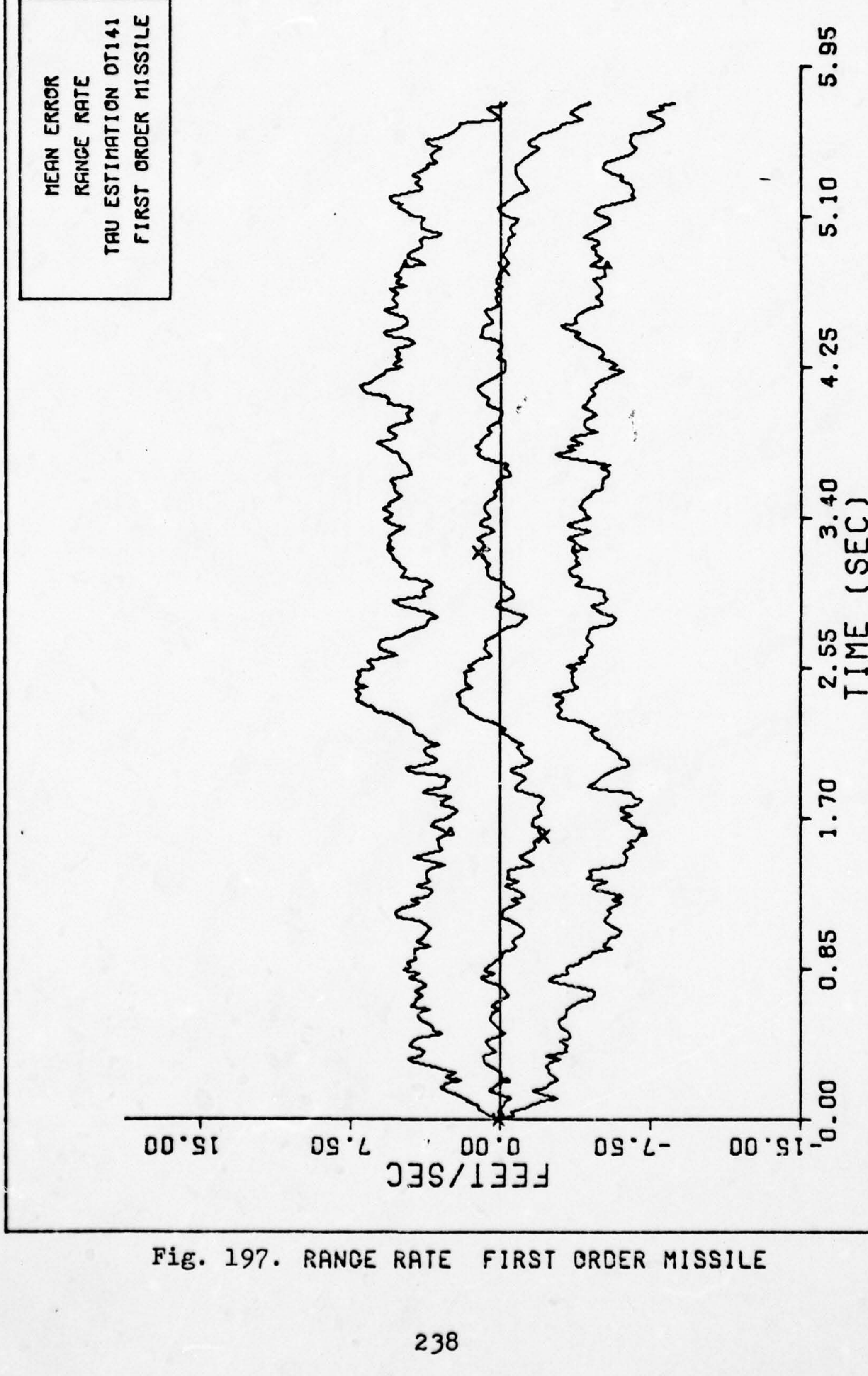

Fig. 197. RANGE RATE FIRST ORDER MISSILE

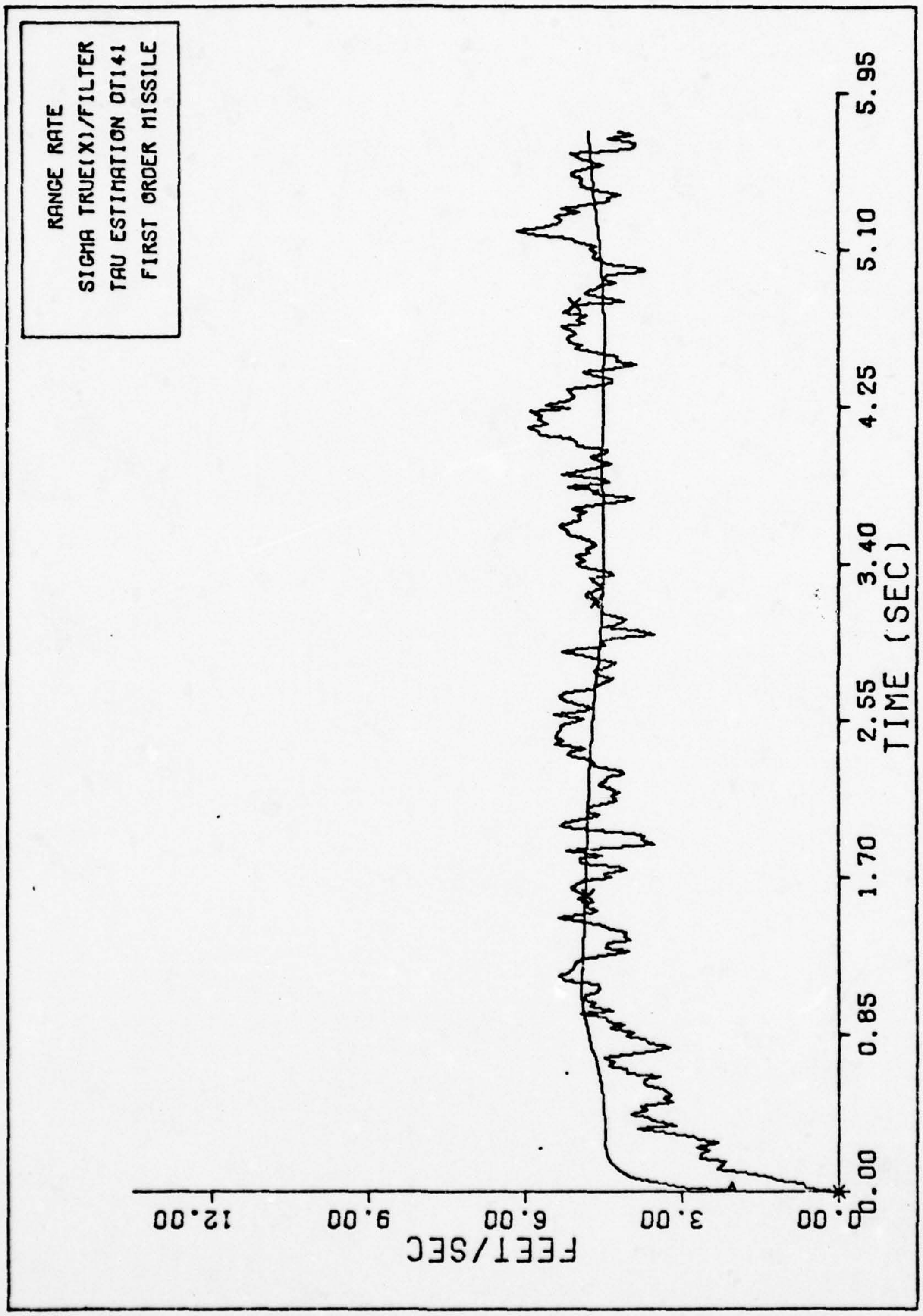

Fig. 198. RANGE RATE SIGMAS FIRST ORDER

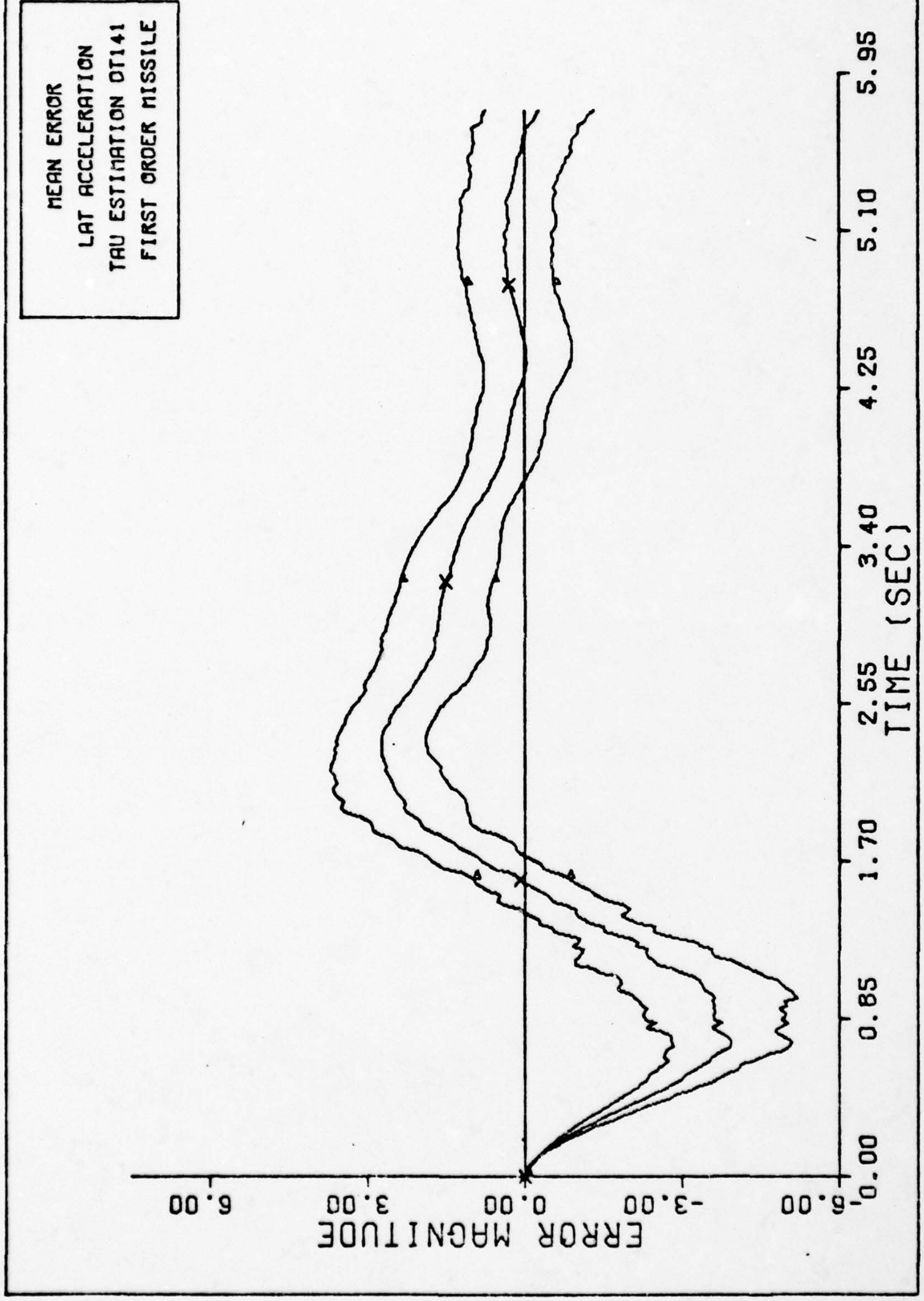

Fig. 199. LAT ACCELERATION FIRST ORDER MISSILE

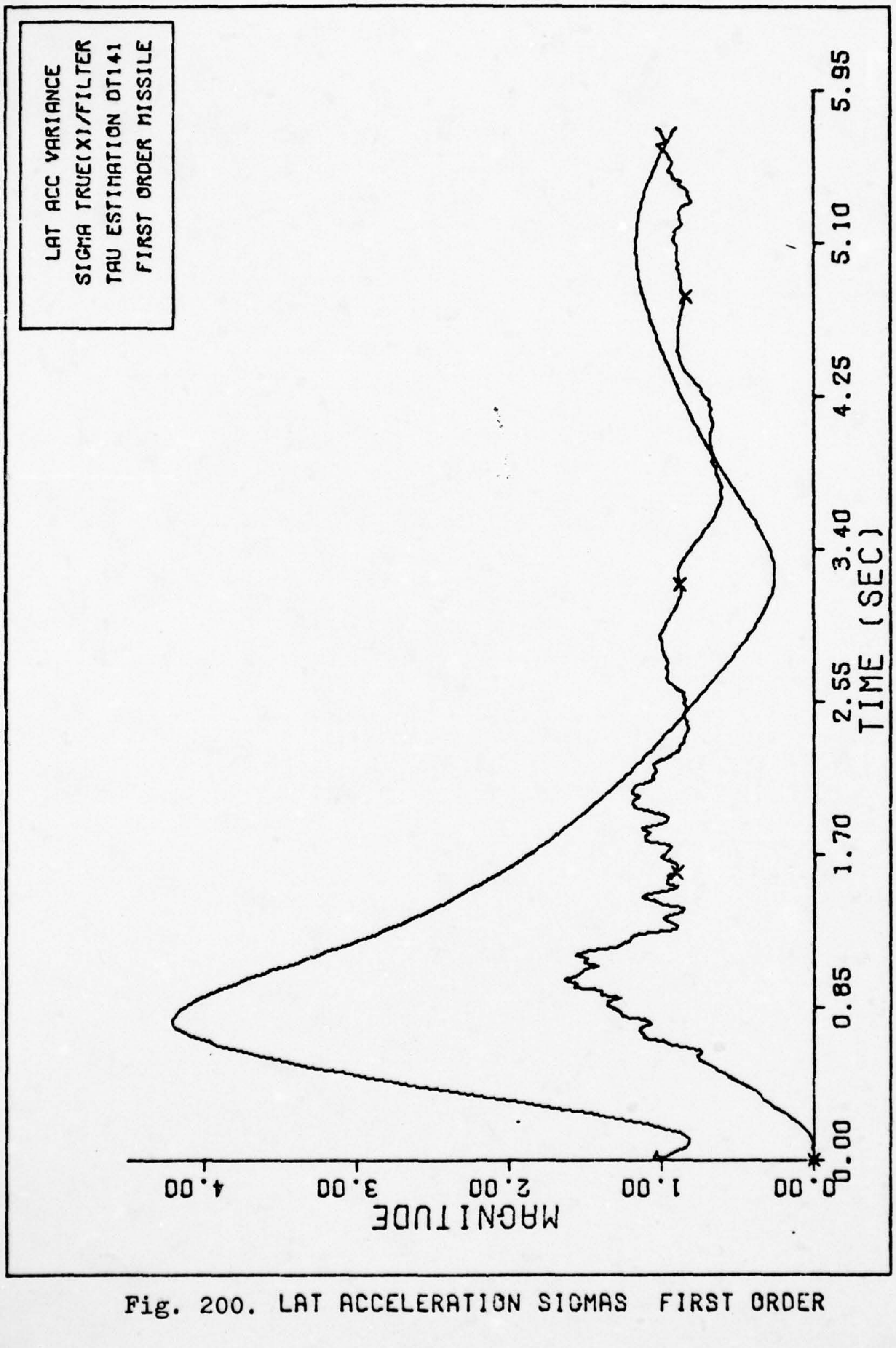

Fig. 200. LAT ACCELERATION SIGMAS FIRST ORDER

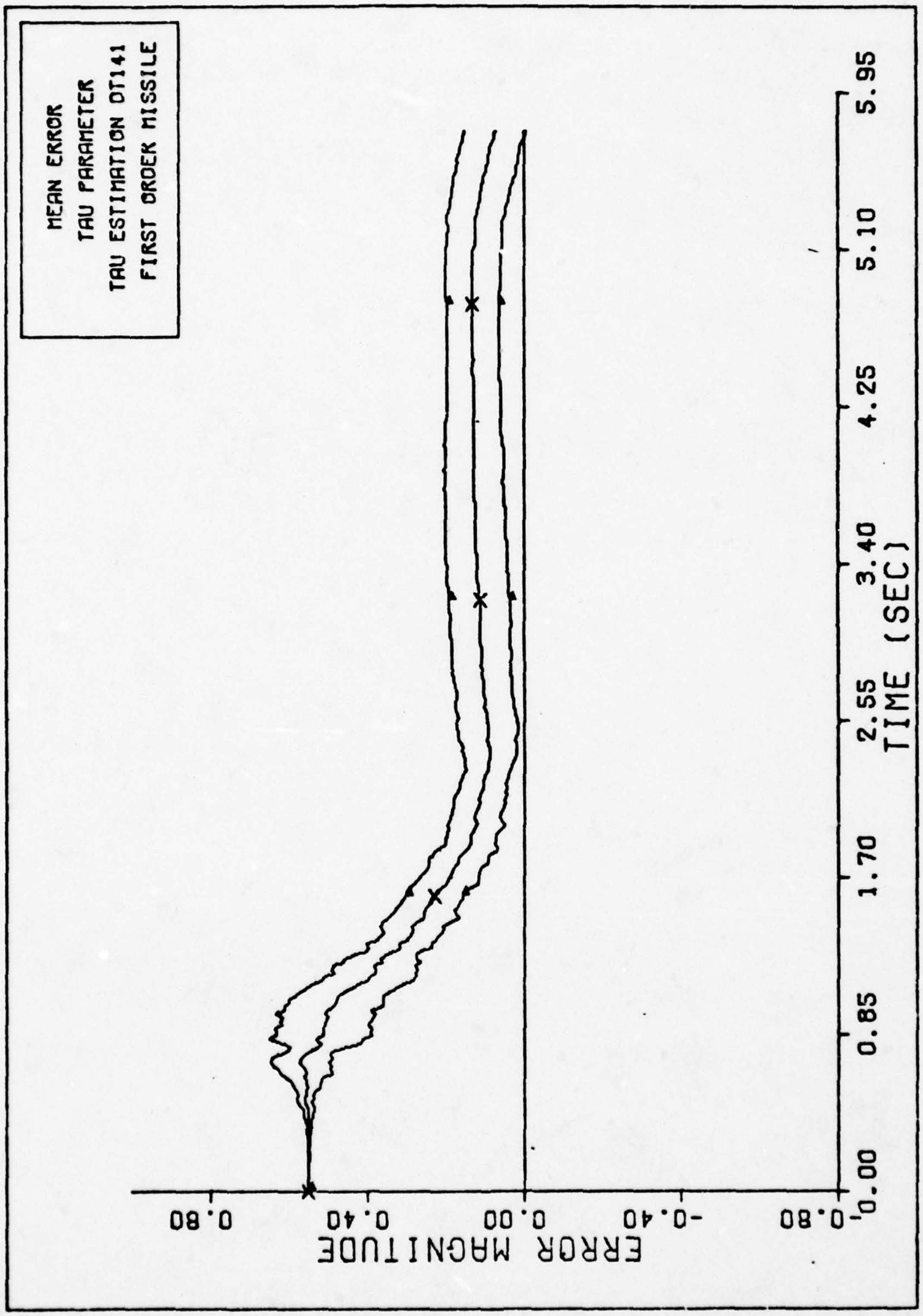

Fig. 201. TAU PARAMETER FIRST ORDER MISSILE

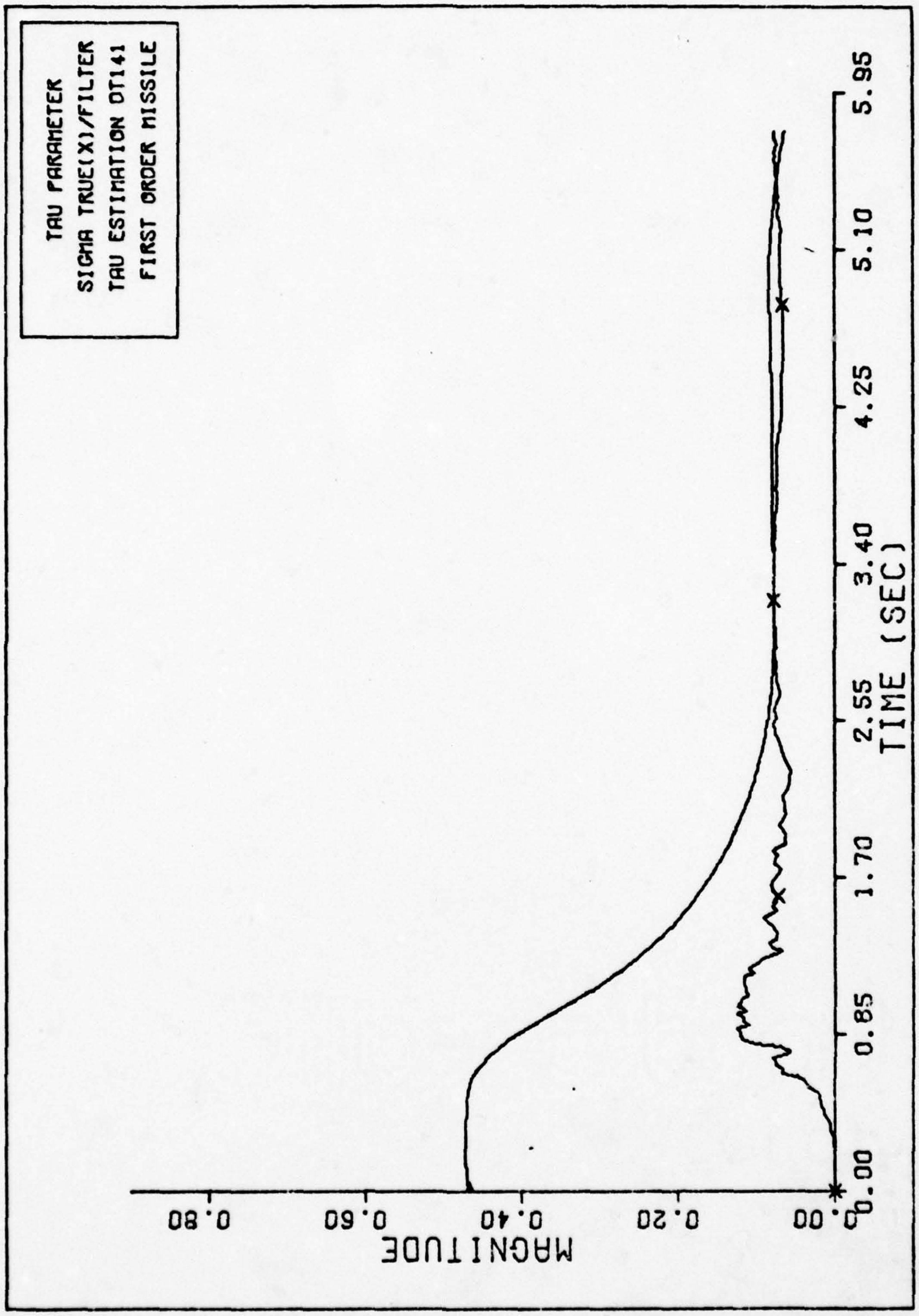

Fig. 202. TAU PARAMETER SIGMAS FIRST ORDER

M/S Estimation - M/S Initialized at 45.

The initial state estimates and the tuning parameters for this case are

$$V^I_{mx}(0) = 1225.7 \text{ fps}$$
$$\dot{\theta}_T(0) = 4.363345 \text{ radians}$$
$$R(0) = 10000. \text{ feet}$$
$$\dot{R}(0) = -2122. \text{ fps}$$
$$a_L(0) = 0.$$
$$n(0) = 4.5$$
$$\tau_f(0) = .85 \text{ seconds}$$
$$M/S(0) = 45. \text{ slugs/ft}^2$$

$$\underline{R} = \begin{bmatrix} 3.E-5 & 0. & 0. \\ 0. & 500. & 0. \\ 0. & 0. & 100. \end{bmatrix}$$

$$\underline{P}_0 = \begin{bmatrix} 100. & 0. & 0. & 0. & 0. & 0. & 0. & 0. \\ 0. & 1.E-8 & 0. & 0. & 0. & 0. & 0. & 0. \\ 0. & 0. & 101. & 0. & 0. & 0. & 0. & 0. \\ 0. & 0. & 0. & 4. & 0. & 0. & 0. & 0. \\ 0. & 0. & 0. & 0. & 5. & 0. & 0. & 0. \\ 0. & 0. & 0. & 0. & 0. & 0. & 0. & 0. \\ 0. & 0. & 0. & 0. & 0. & 0. & 0. & 0. \\ 0. & 0. & 0. & 0. & 0. & 0. & 0. & 5. \end{bmatrix}$$

$$\underline{Q} = \begin{bmatrix} 250. & 0. & 0. & 0. & 0. & 0. & 0. & 0. \\ 0. & 1.E-6 & 0. & 0. & 0. & 0. & 0. & 0. \\ 0. & 0. & 500. & 0. & 0. & 0. & 0. & 0. \\ 0. & 0. & 0. & 200. & 0. & 0. & 0. & 0. \\ 0. & 0. & 0. & 0. & 3. & 0. & 0. & 0. \\ 0. & 0. & 0. & 0. & 0. & 0. & 0. & 0. \\ 0. & 0. & 0. & 0. & 0. & 0. & 0. & 0. \\ 0. & 0. & 0. & 0. & 0. & 0. & 0. & 5. \end{bmatrix}$$

These plots were generated by the first order filter when estimating the M/S ratio. The initial value of this ratio set in the filter was 45.0 slugs/ft^2. The true value was set at 29.197 slugs/ft^2. This parameter along with the five dynamic states of the missile model were the only estimates of the first order filter in this case.

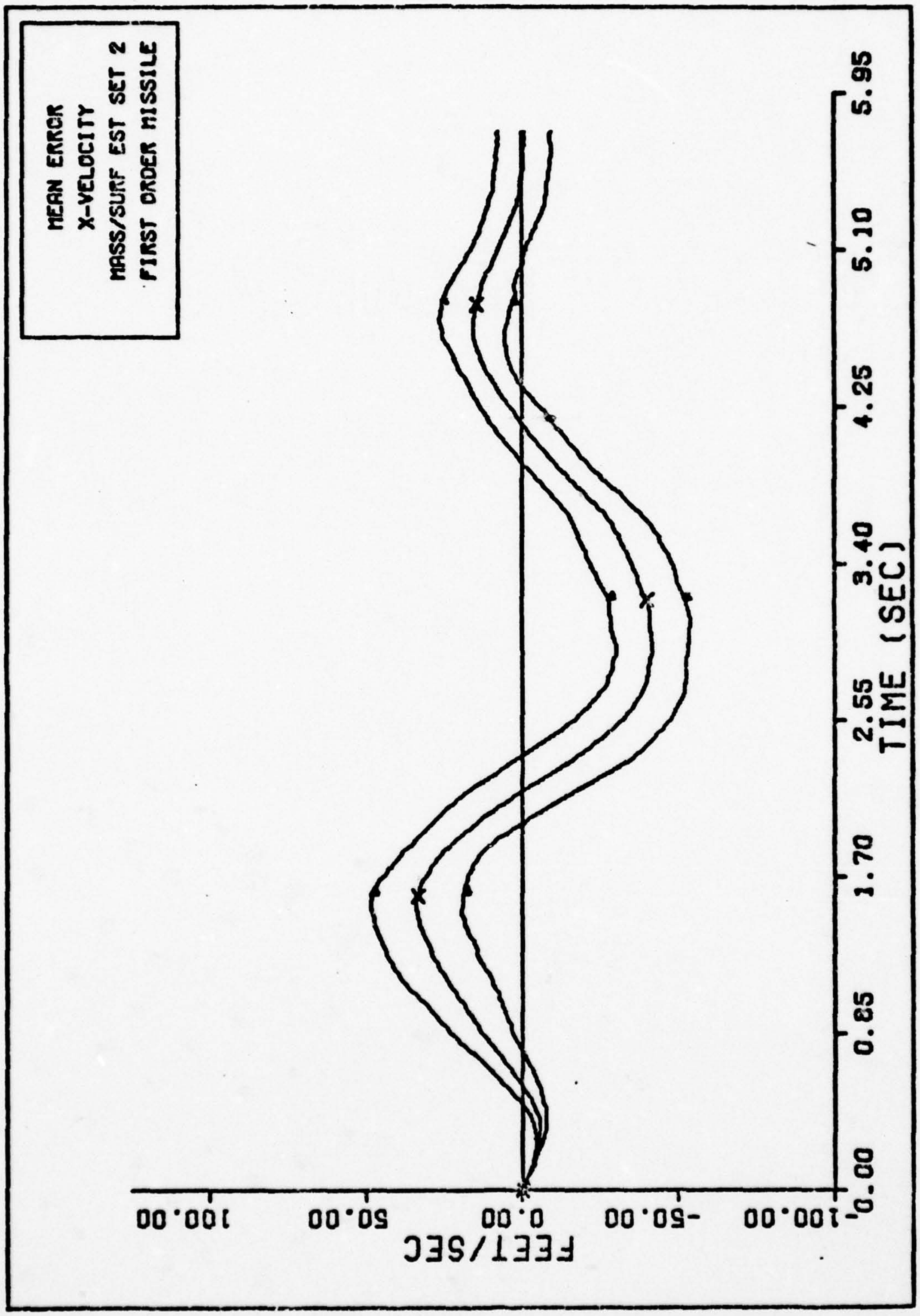

Fig. 203. X-VELOCITY FIRST ORDER MISSILE

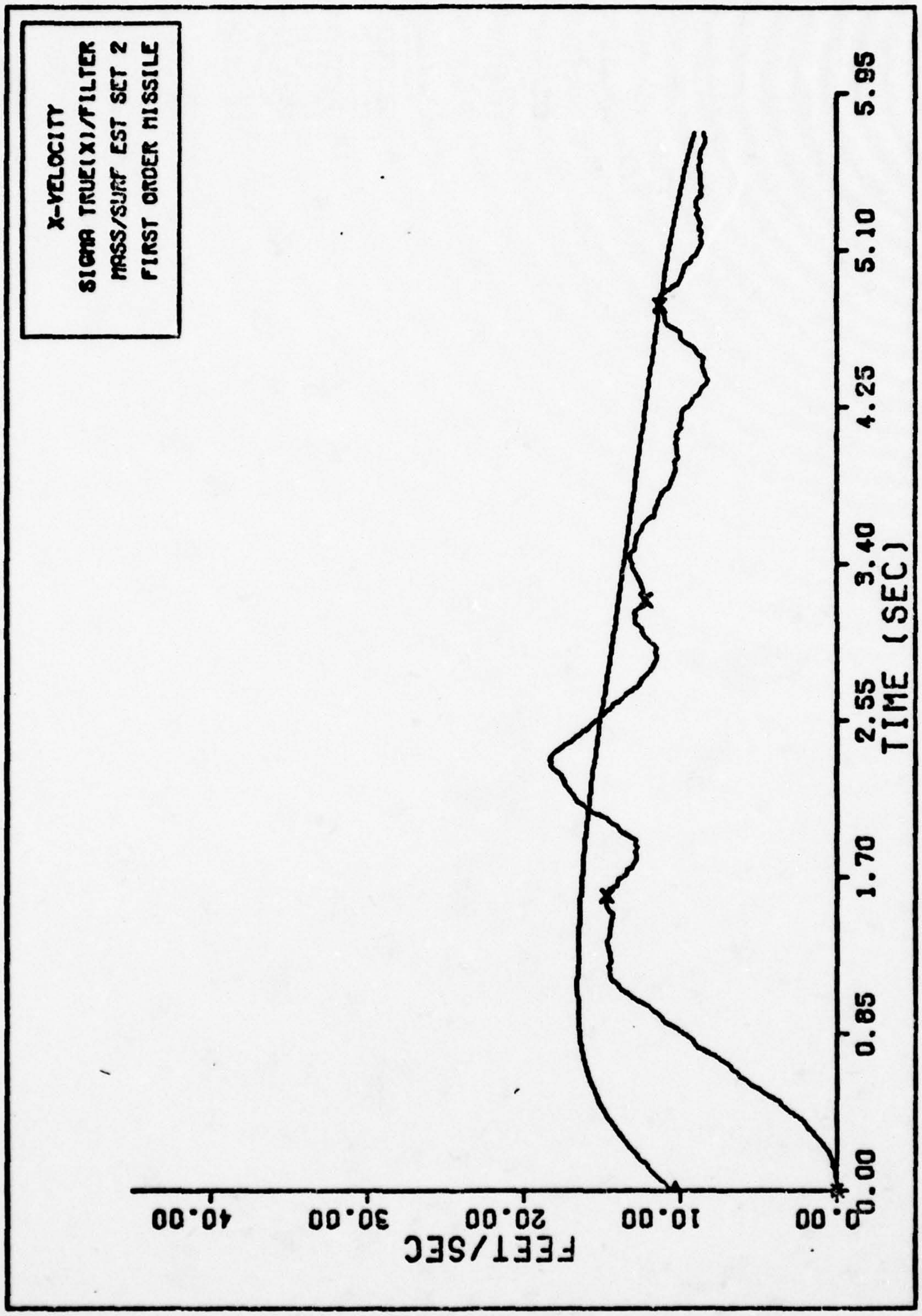

Fig. 204. X-VELOCITY SIGMAS FIRST ORDER

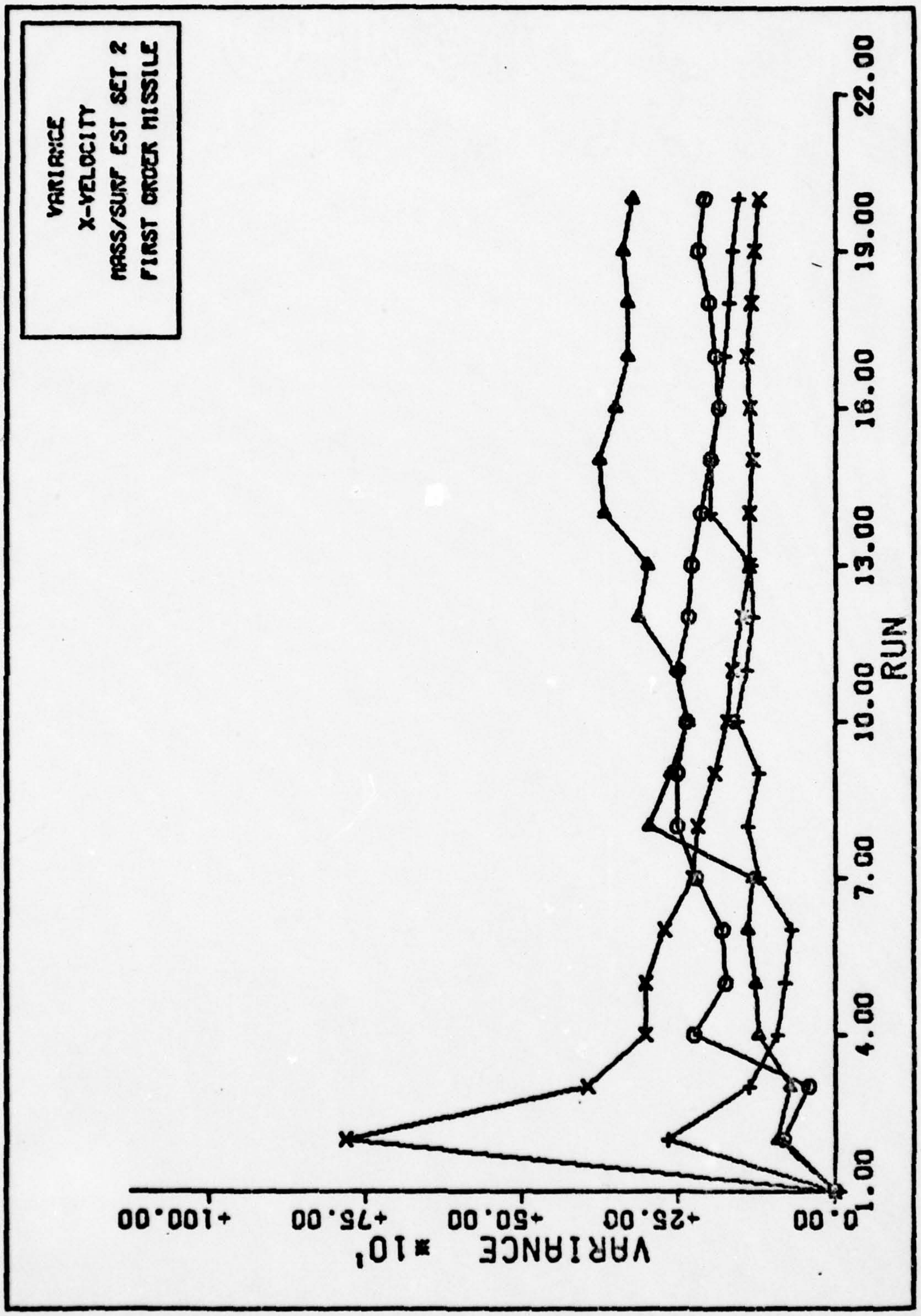

Fig. 205. VARIANCE CONVERGENCE

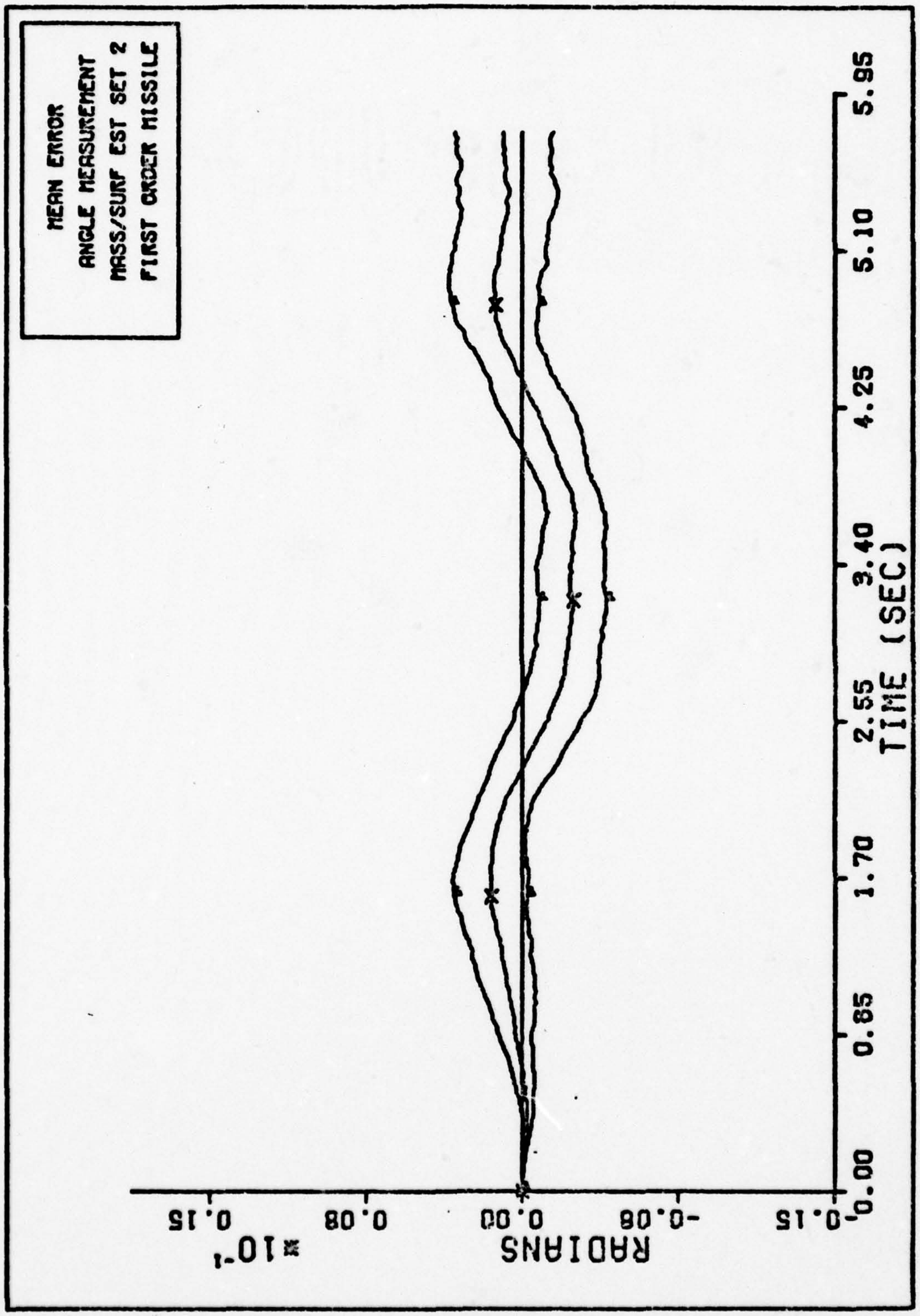

Fig. 206. ANGLE MEASUREMENT FIRST ORDER MISSILE

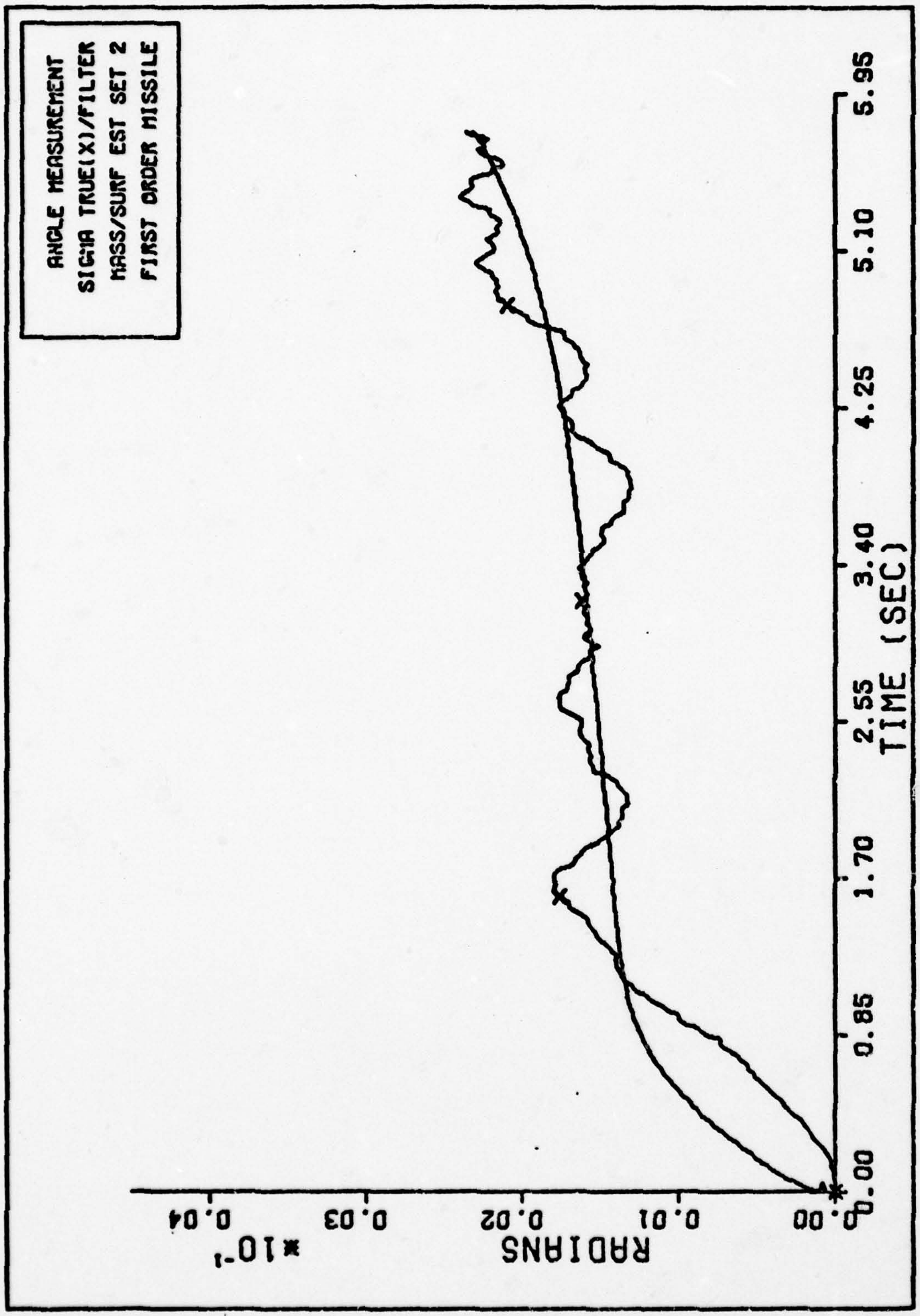

Fig. 207. ANGLE MEASUREMENT SIGMAS FIRST ORDER

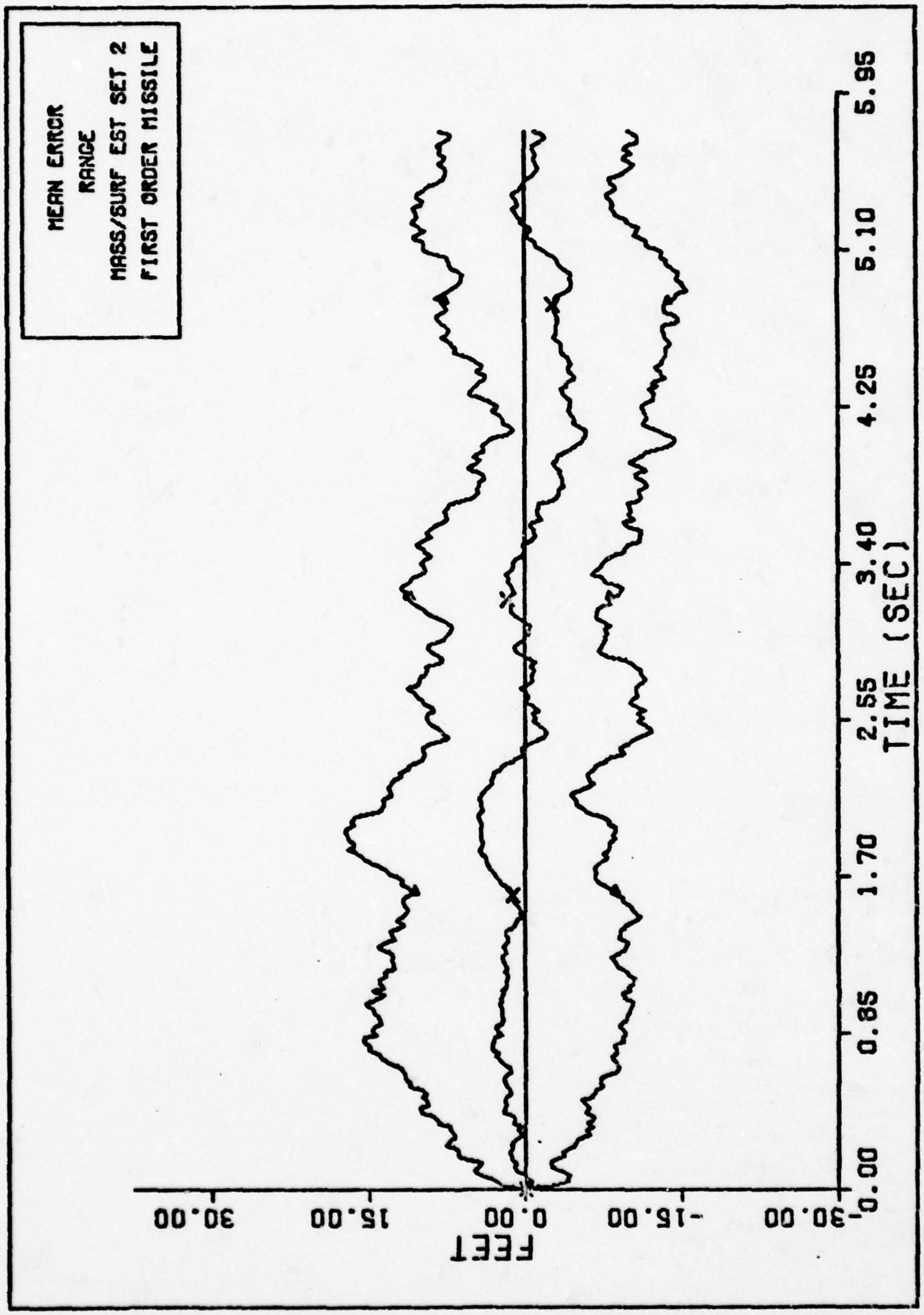

Fig. 208. RANGE FIRST ORDER MISSILE

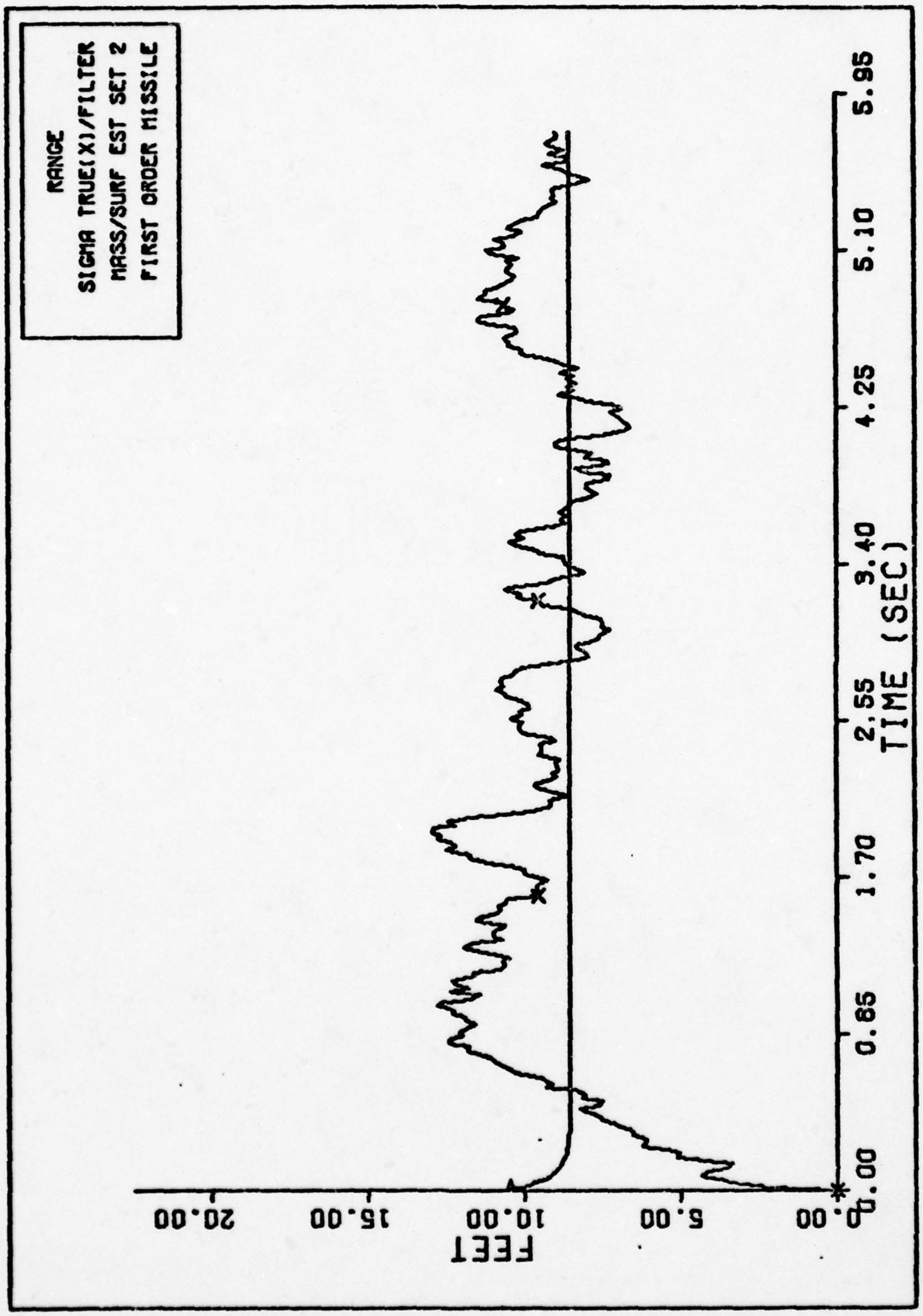

Fig. 209. RANGE SIGMAS FIRST ORDER

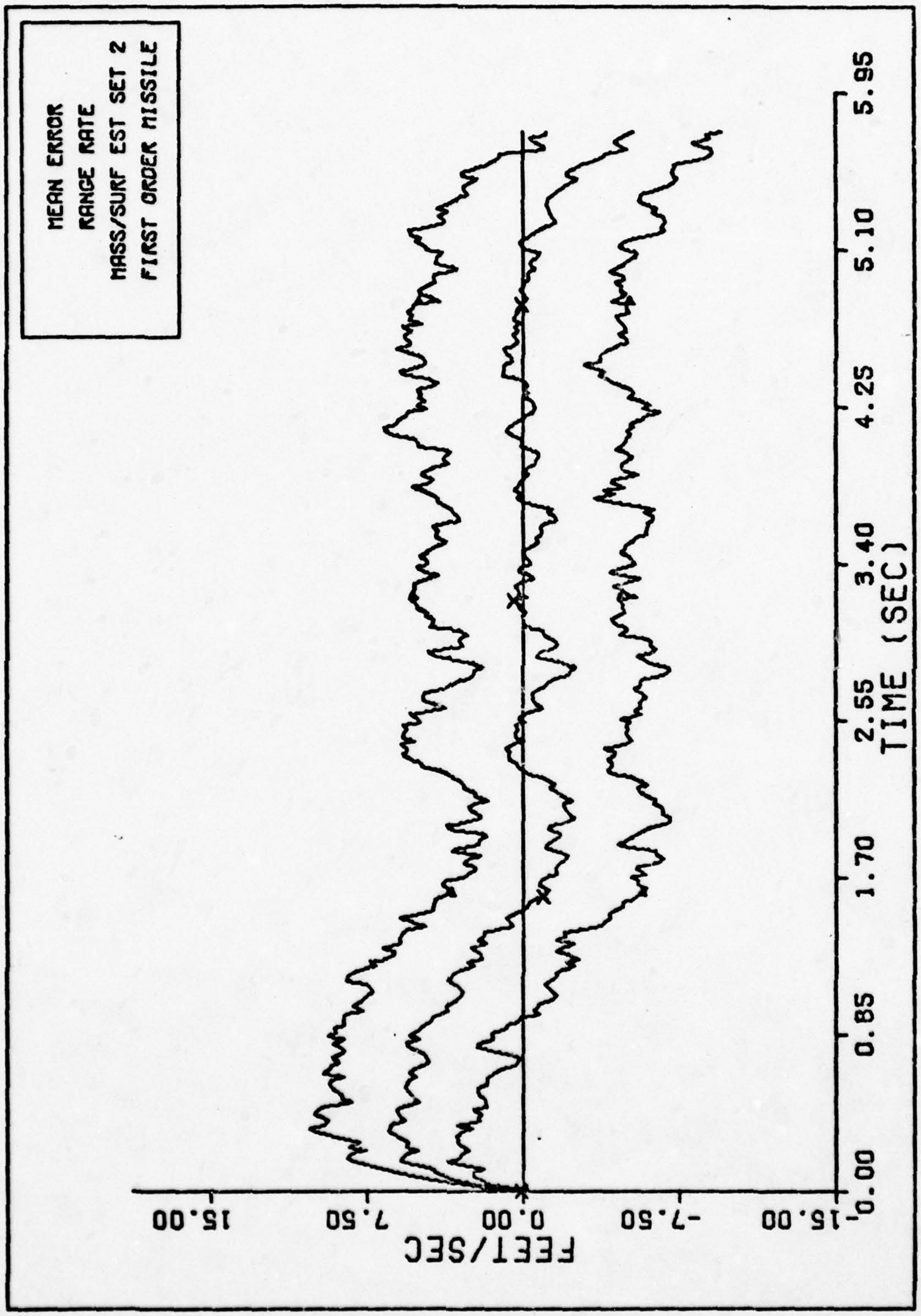

Fig. 210. RANGE RATE FIRST ORDER MISSILE

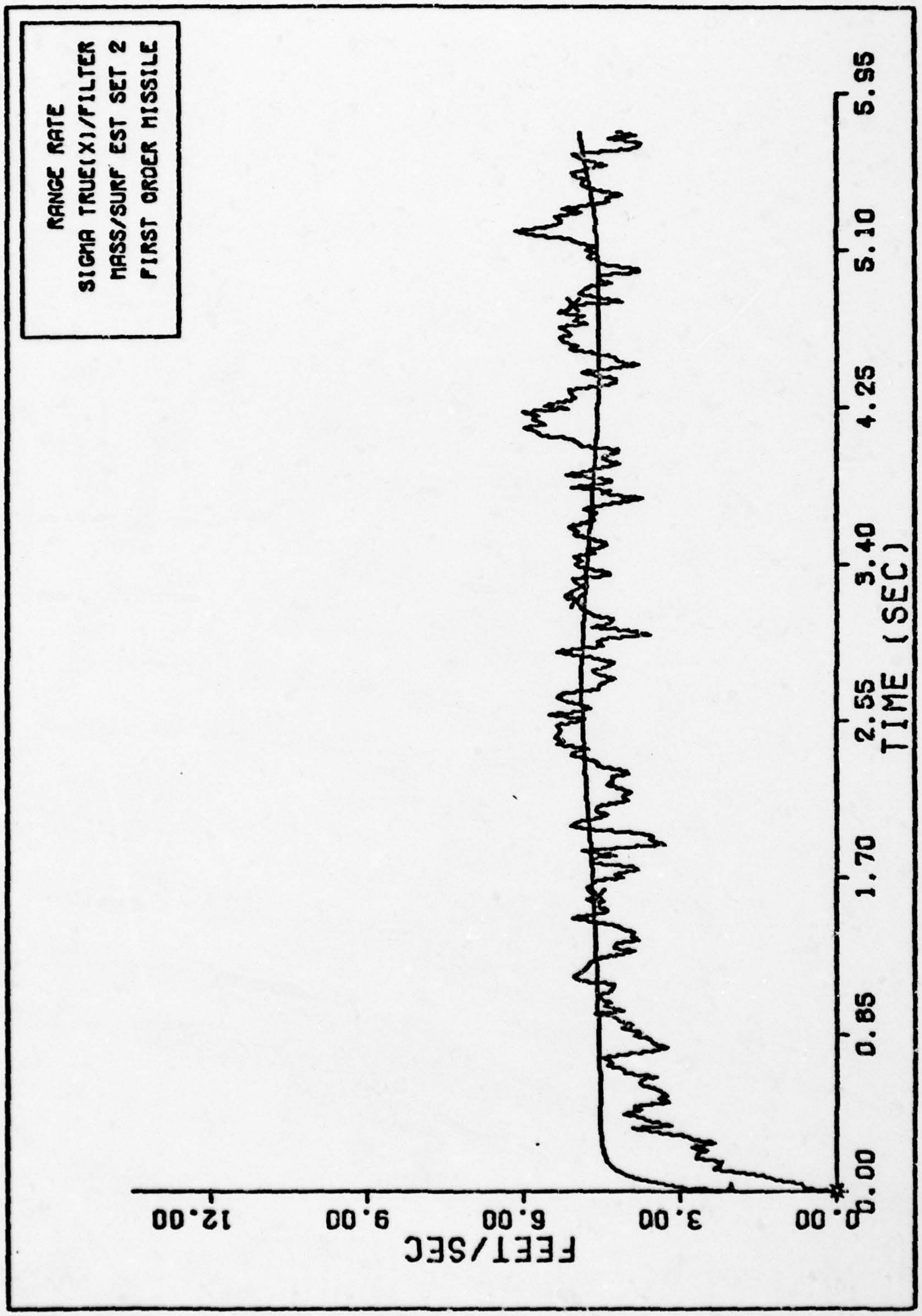

Fig. 211. RANGE RATE SIGMAS FIRST ORDER

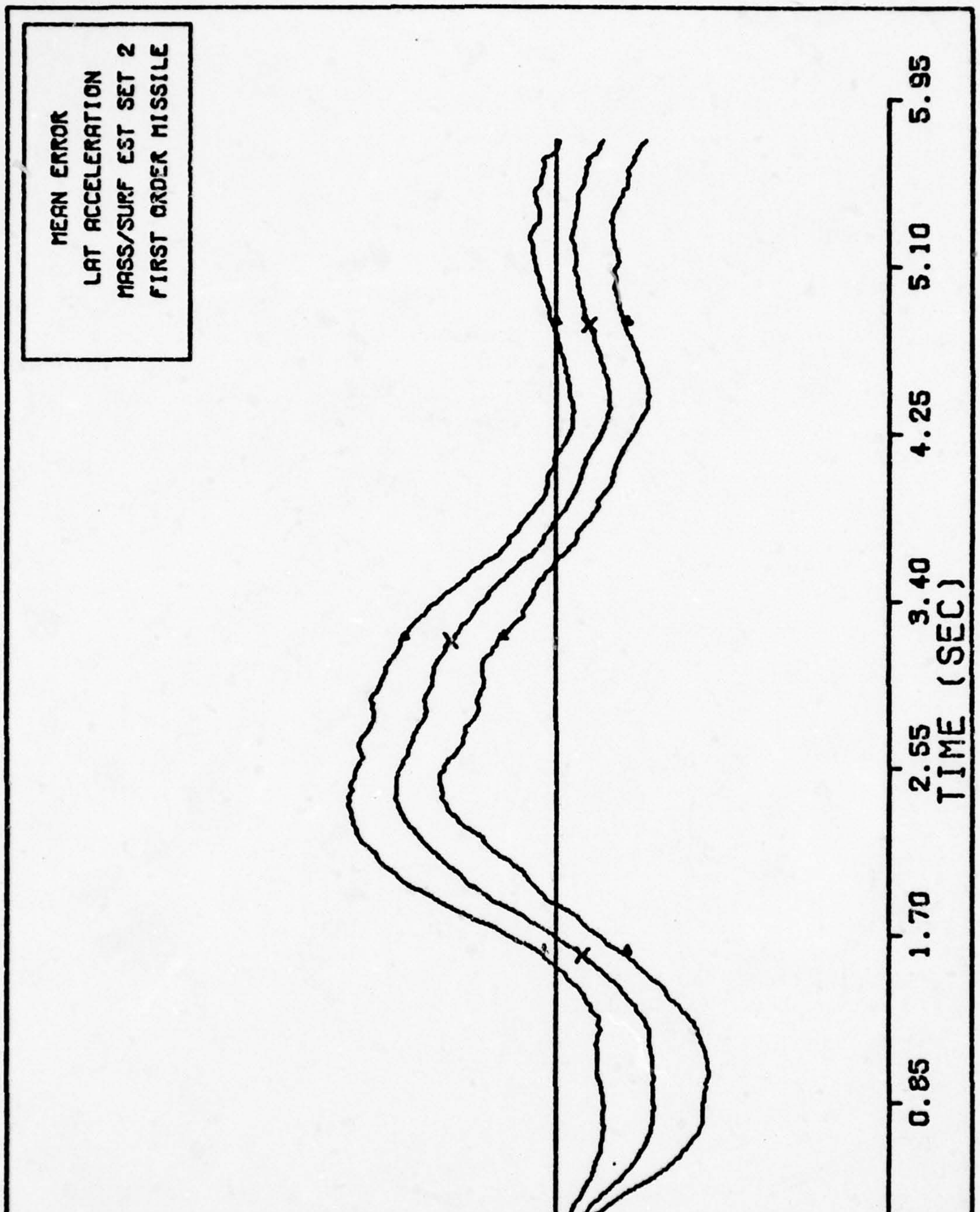

Fig. 212. LAT ACCELERATION FIRST ORDER MISSILE

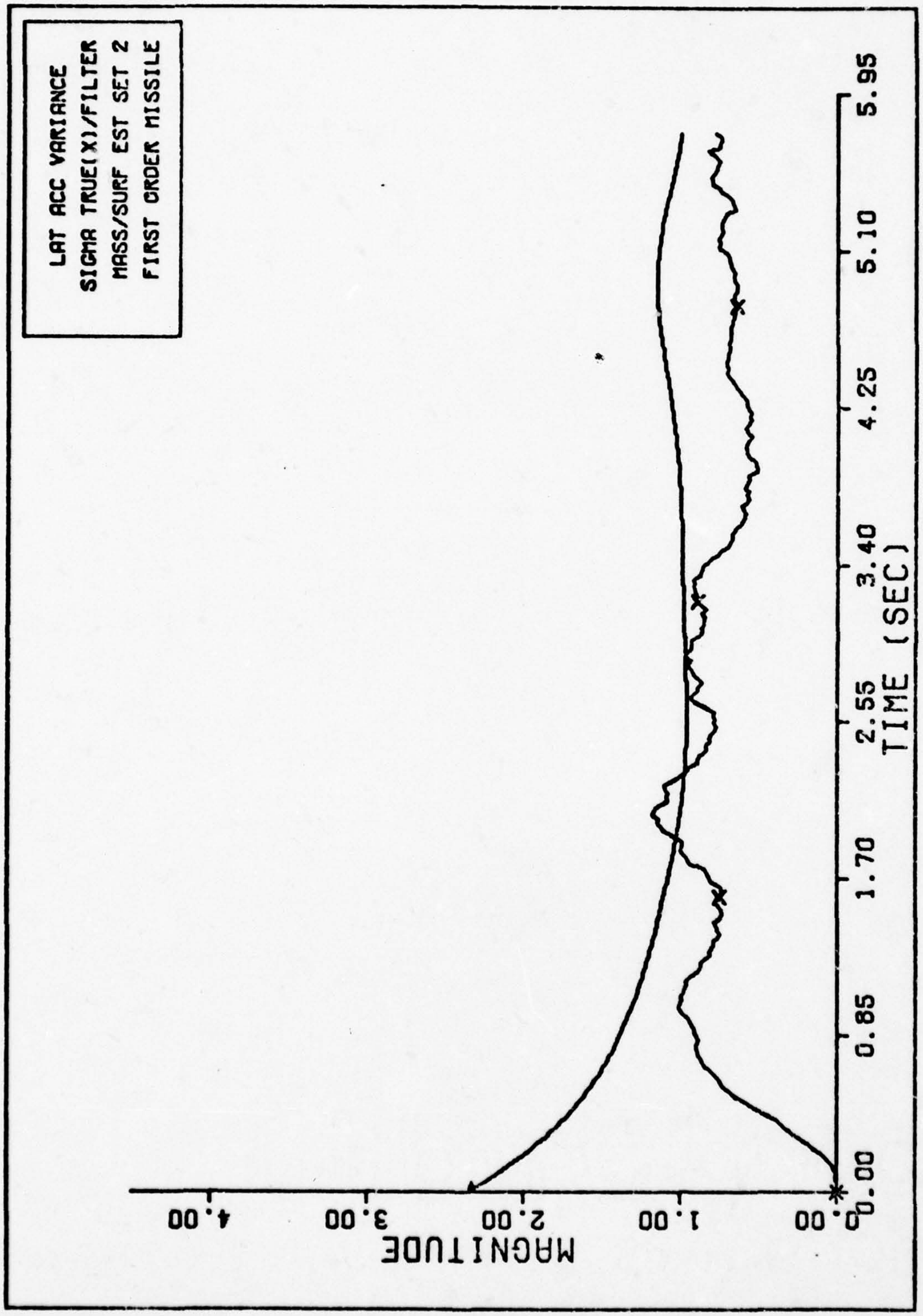

Fig. 213. LAT ACCELERATION SIGMAS FIRST ORDER

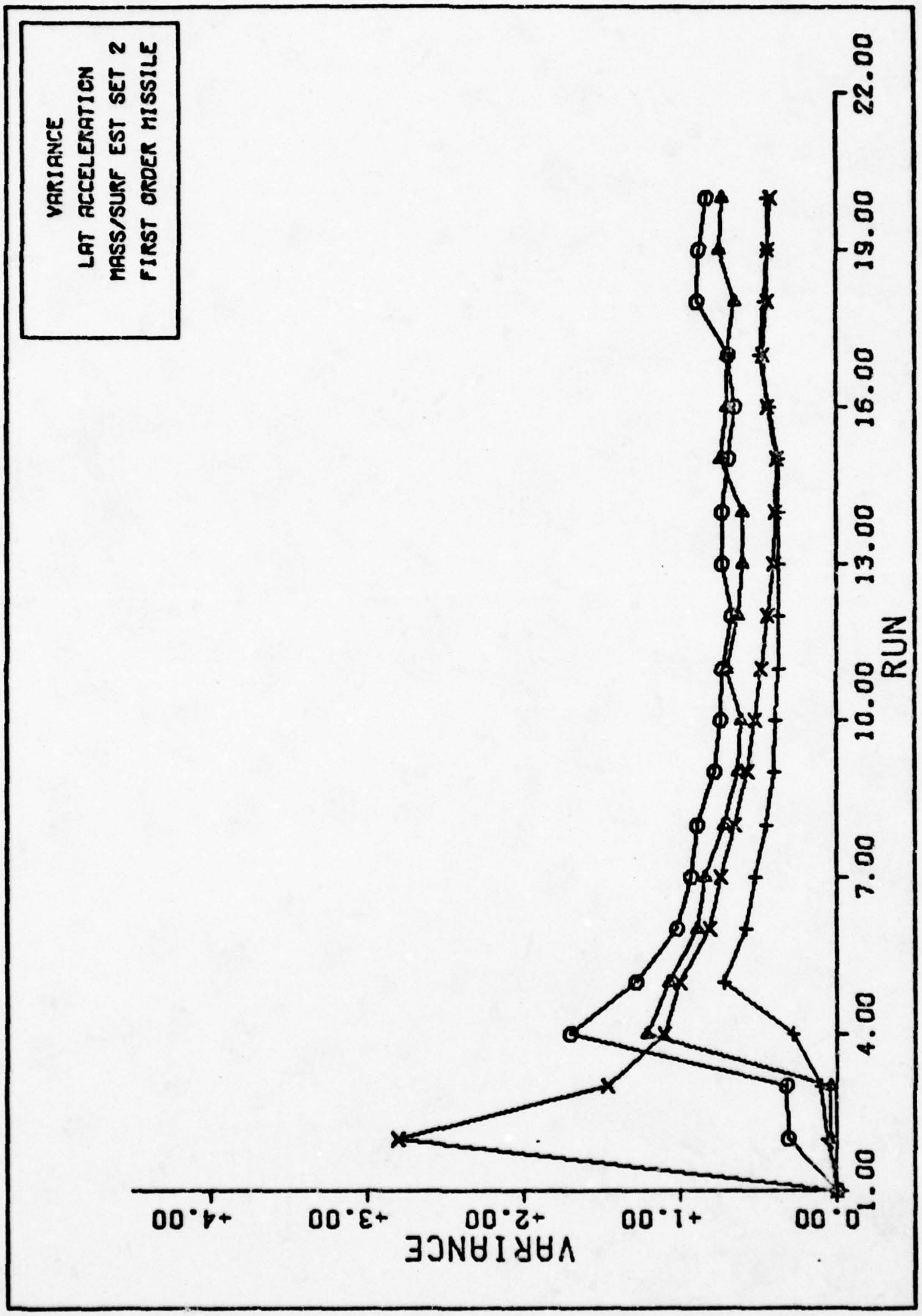

Fig. 214. VARIANCE CONVERGENCE

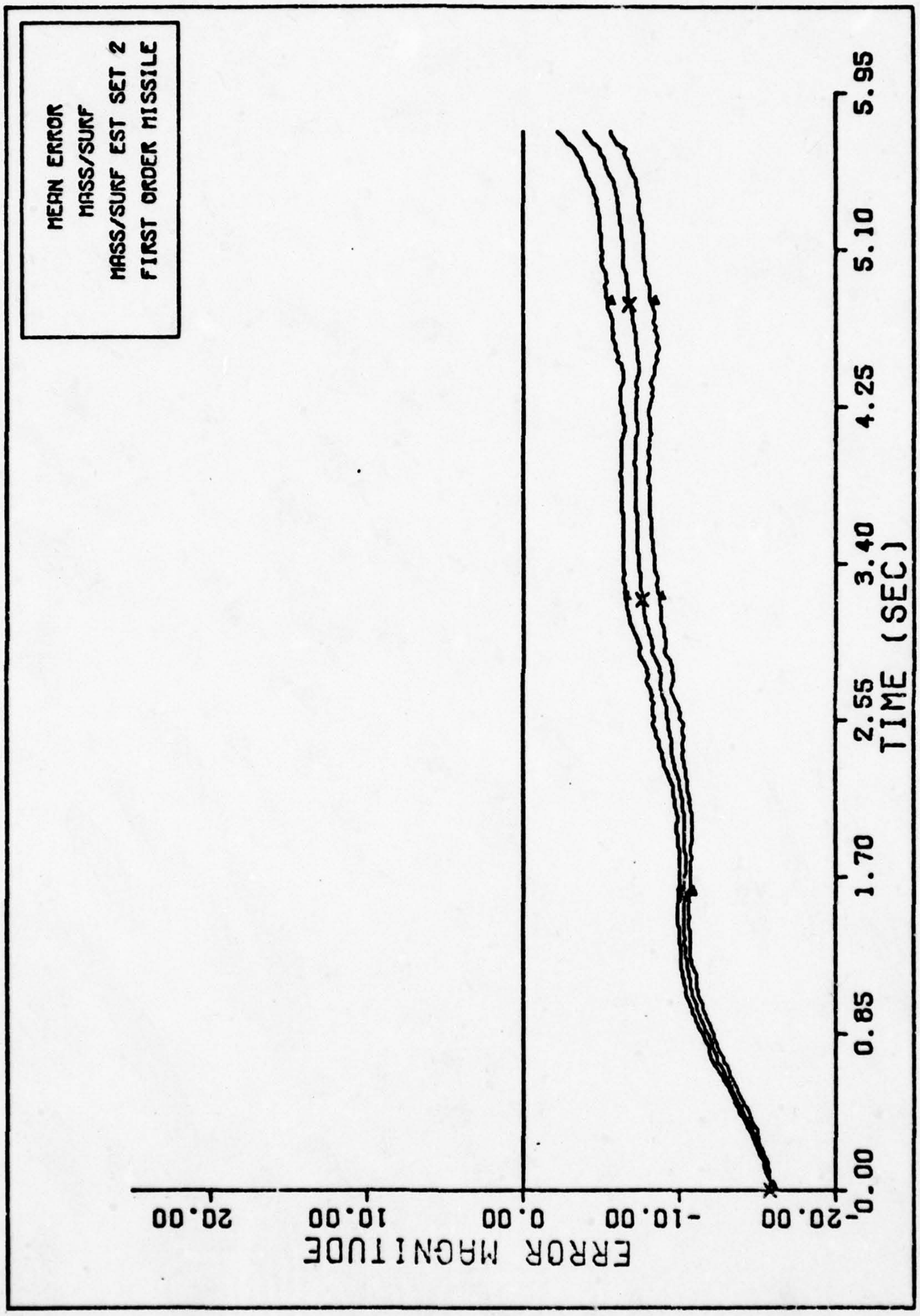

Fig. 215. MASS/SURF FIRST ORDER MISSILE

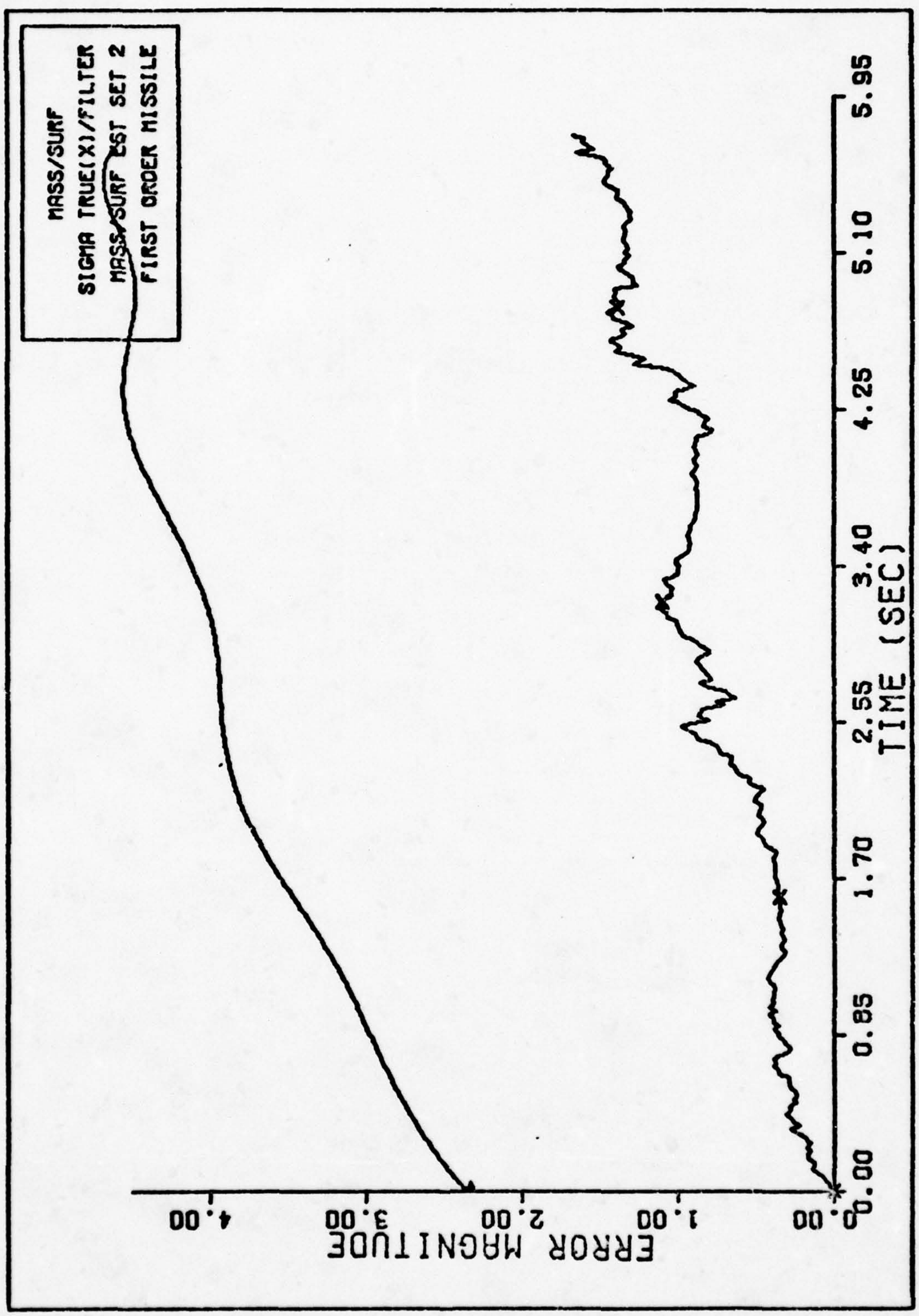

Fig. 216. MASS/SURF SIGMAS FIRST ORDER

M/S Estimation - M/S Initialized at 15.

The initial state estimates and the tuning parameters for this case are

$$
\begin{aligned}
V^I_{mx}(0) &= 1225.7 \text{ fps} \\
\dot{\theta}_T(0) &= 4.363345 \text{ radians} \\
R(0) &= 10000. \text{ feet} \\
\dot{R}(0) &= -2122. \text{ fps} \\
a_L(0) &= 0. \\
n(0) &= 4.5 \\
\tau_f(0) &= .85 \text{ seconds} \\
M/S(0) &= 15 \text{ slugs/ft}^2
\end{aligned}
$$

$$
\underline{R} = \begin{bmatrix} 3.E-5 & 0. & 0. \\ 0. & 500. & 0. \\ 0. & 0. & 100. \end{bmatrix}
$$

$$
\underline{P}_0 = \begin{bmatrix}
100. & 0. & 0. & 0. & 0. & 0. & 0. & 0. \\
0. & 1.E-8 & 0. & 0. & 0. & 0. & 0. & 0. \\
0. & 0. & 101. & 0. & 0. & 0. & 0. & 0. \\
0. & 0. & 0. & 4. & 0. & 0. & 0. & 0. \\
0. & 0. & 0. & 0. & 5. & 0. & 0. & 0. \\
0. & 0. & 0. & 0. & 0. & 0. & 0. & 0. \\
0. & 0. & 0. & 0. & 0. & 0. & 0. & 0. \\
0. & 0. & 0. & 0. & 0. & 0. & 0. & 5.
\end{bmatrix}
$$

$$
\underline{Q} = \begin{bmatrix}
250. & 0. & 0. & 0. & 0. & 0. & 0. & 0. \\
0. & 1.E-6 & 0. & 0. & 0. & 0. & 0. & 0. \\
0. & 0. & 500. & 0. & 0. & 0. & 0. & 0. \\
0. & 0. & 0. & 200. & 0. & 0. & 0. & 0. \\
0. & 0. & 0. & 0. & 3. & 0. & 0. & 0. \\
0. & 0. & 0. & 0. & 0. & 0. & 0. & 0. \\
0. & 0. & 0. & 0. & 0. & 0. & 0. & 0. \\
0. & 0. & 0. & 0. & 0. & 0. & 0. & 5.
\end{bmatrix}
$$

These plots were generated by the first order filter when estimating the M/S ratio. The initial value of this ratio set in the filter was 15.0 slugs/ft^2. The true value was set at 29.197 slugs/ft^2. This parameter along with the five dynamic states of the missile model were the only estimates of the first order filter in this case.

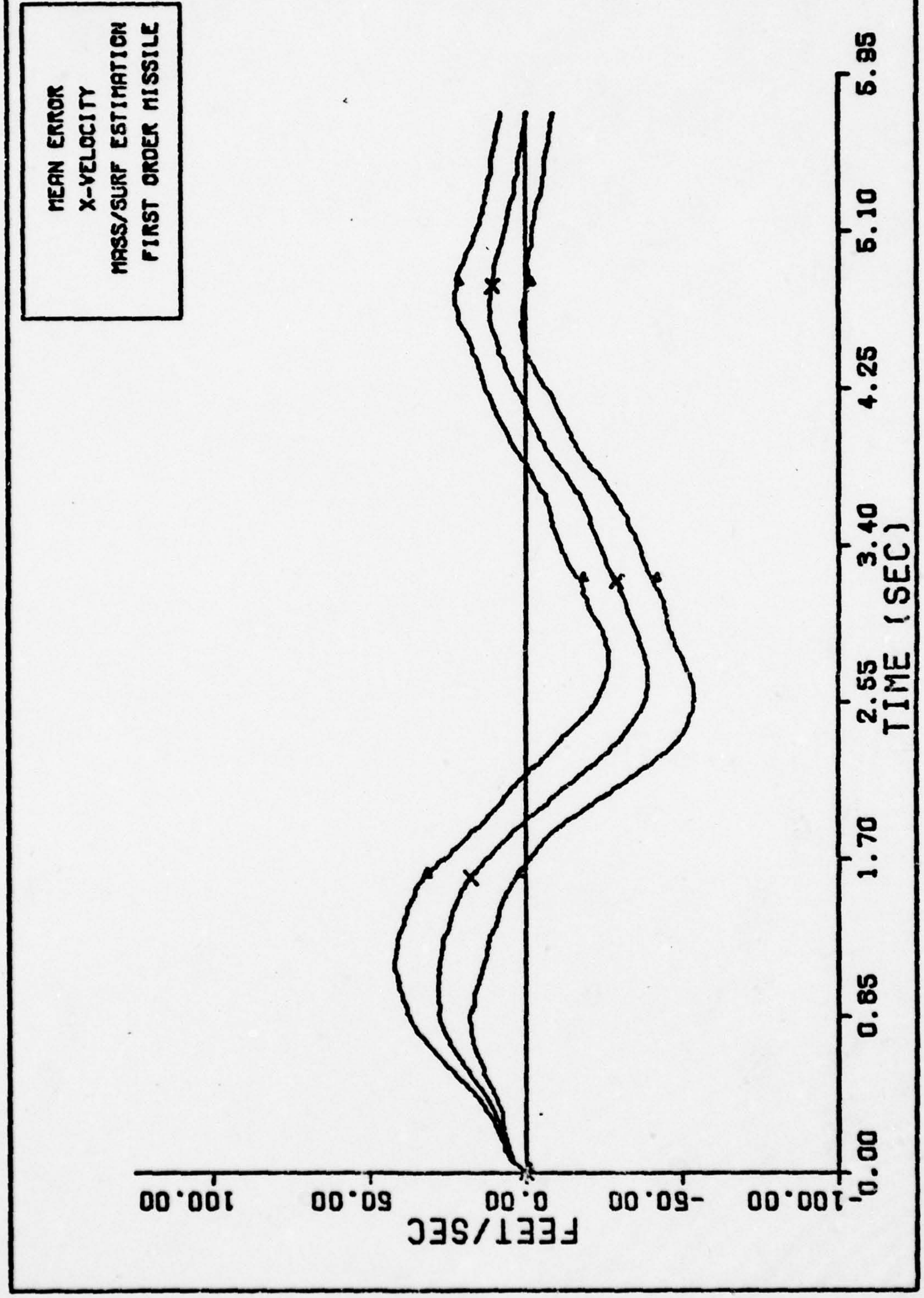

Fig. 217. X-VELOCITY FIRST ORDER MISSILE

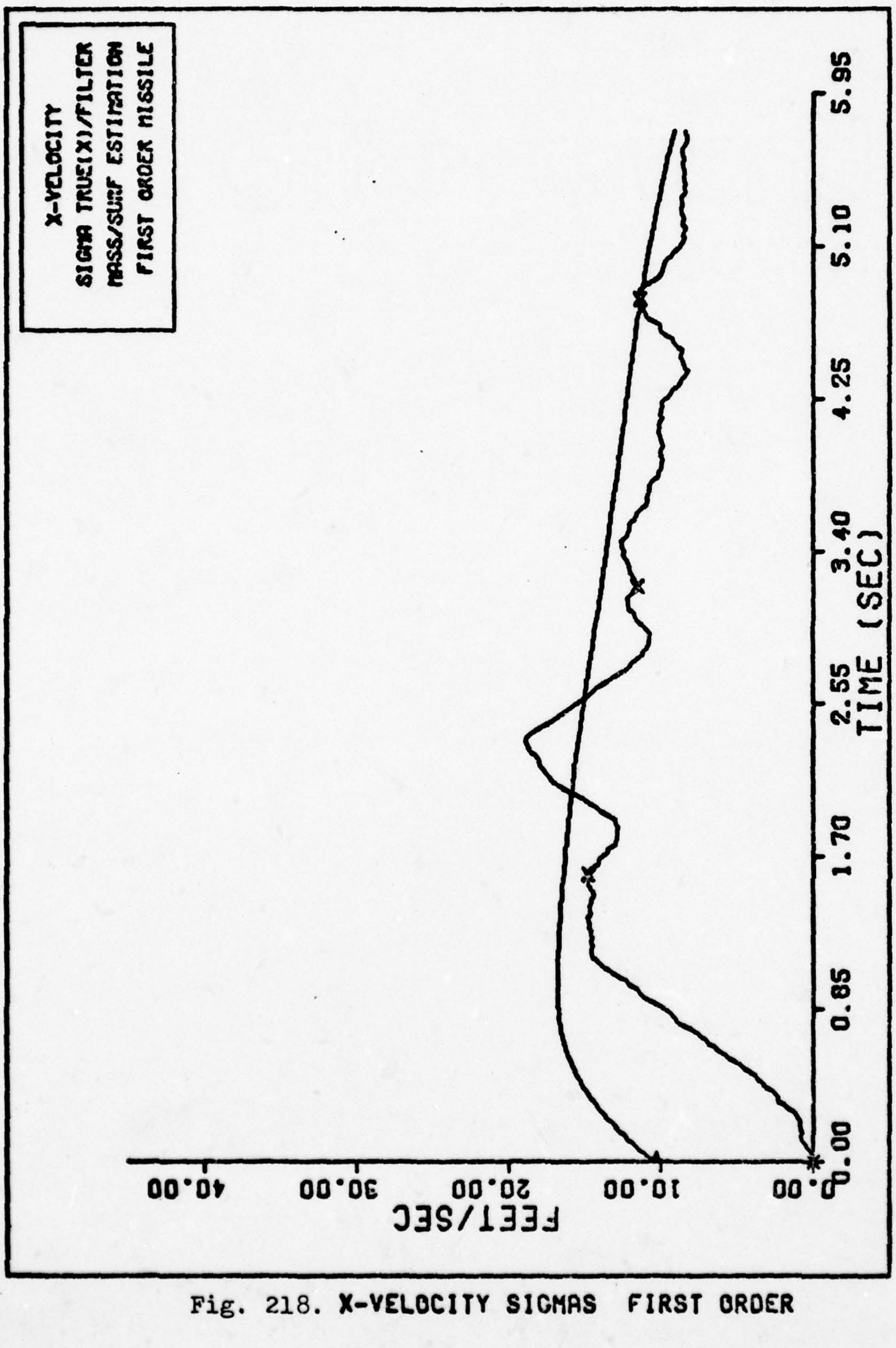

Fig. 218. X-VELOCITY SIGMAS FIRST ORDER

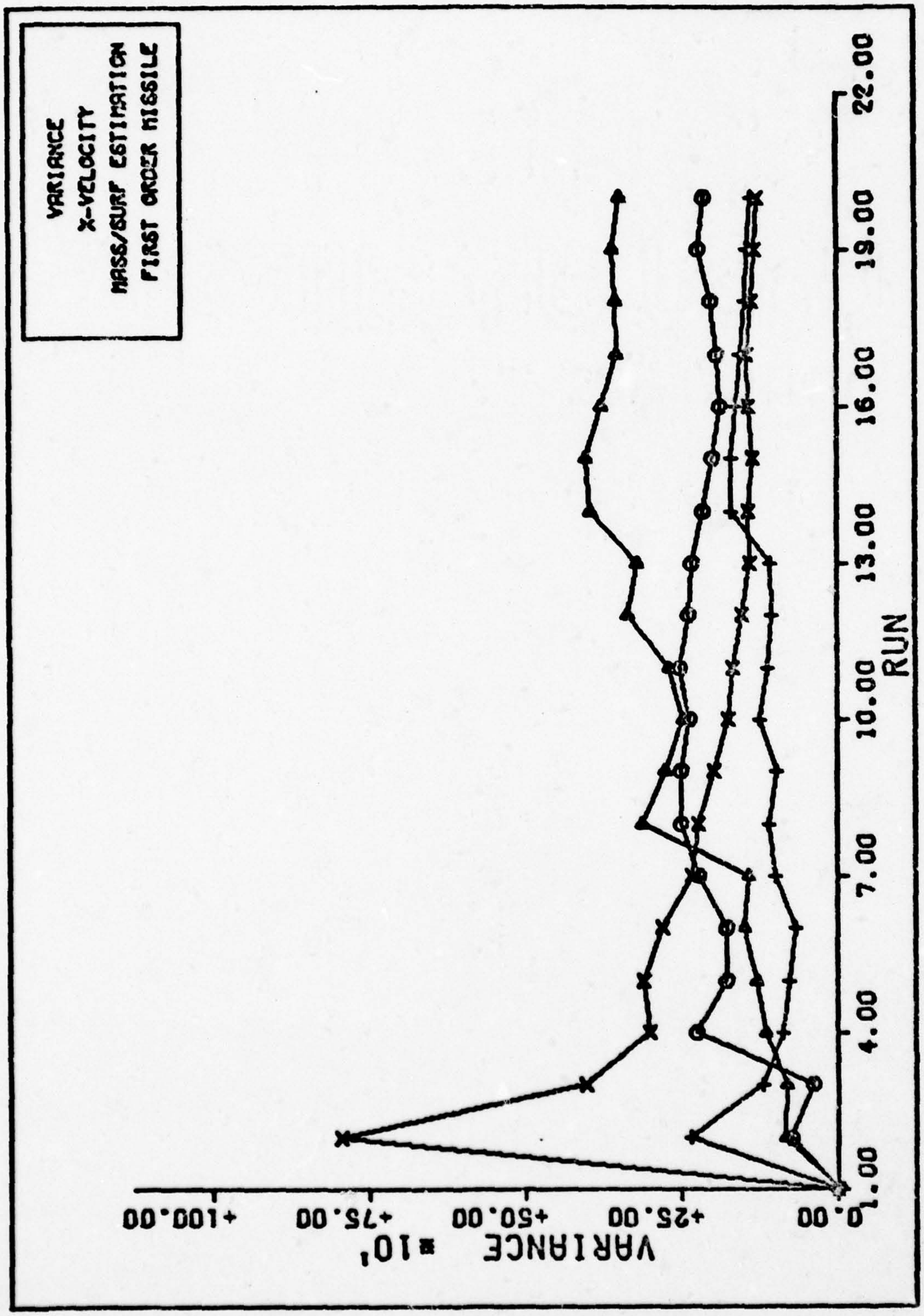

Fig. 219. VARIANCE CONVERGENCE

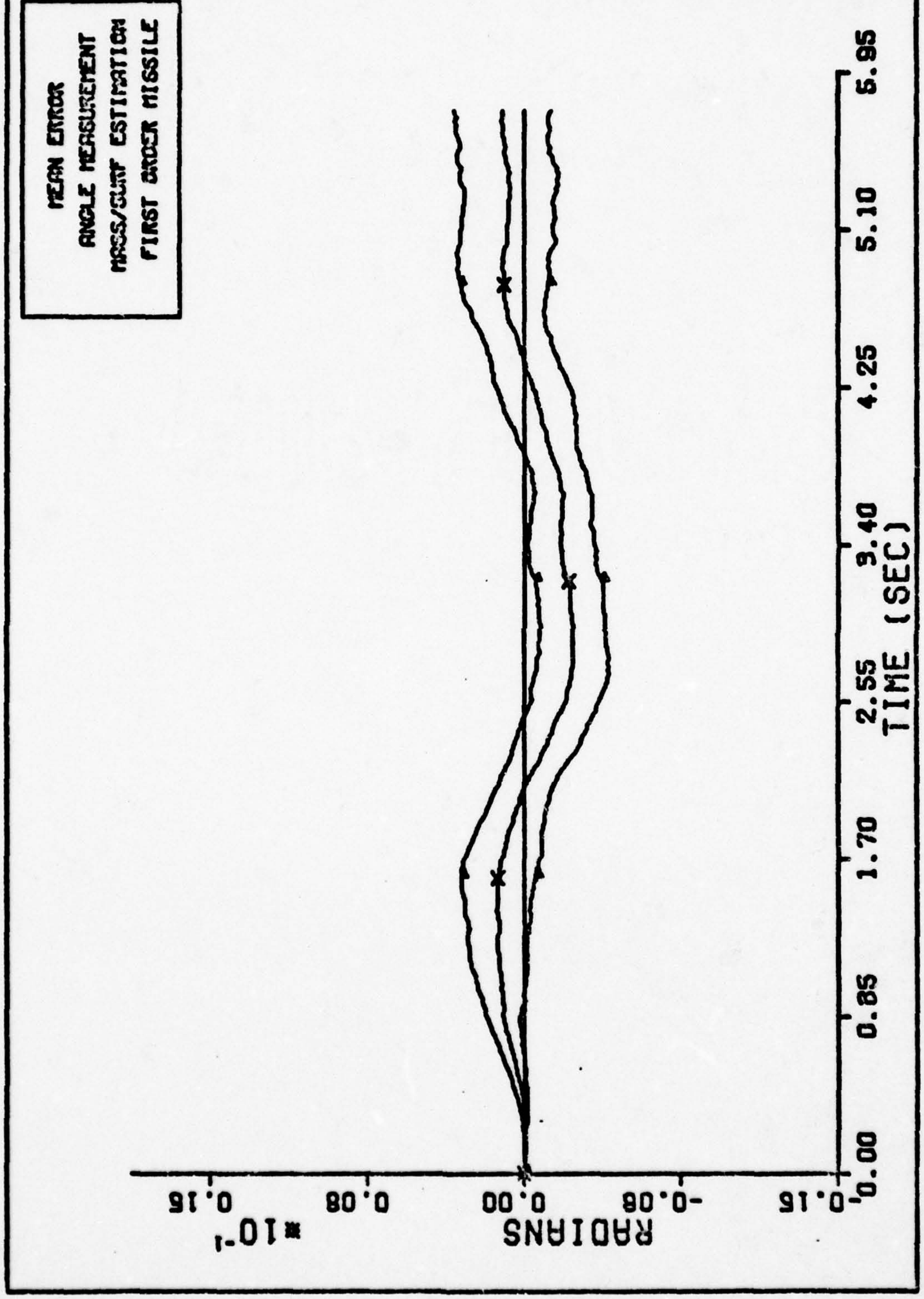

Fig. 220. ANGLE MEASUREMENT FIRST ORDER MISSILE

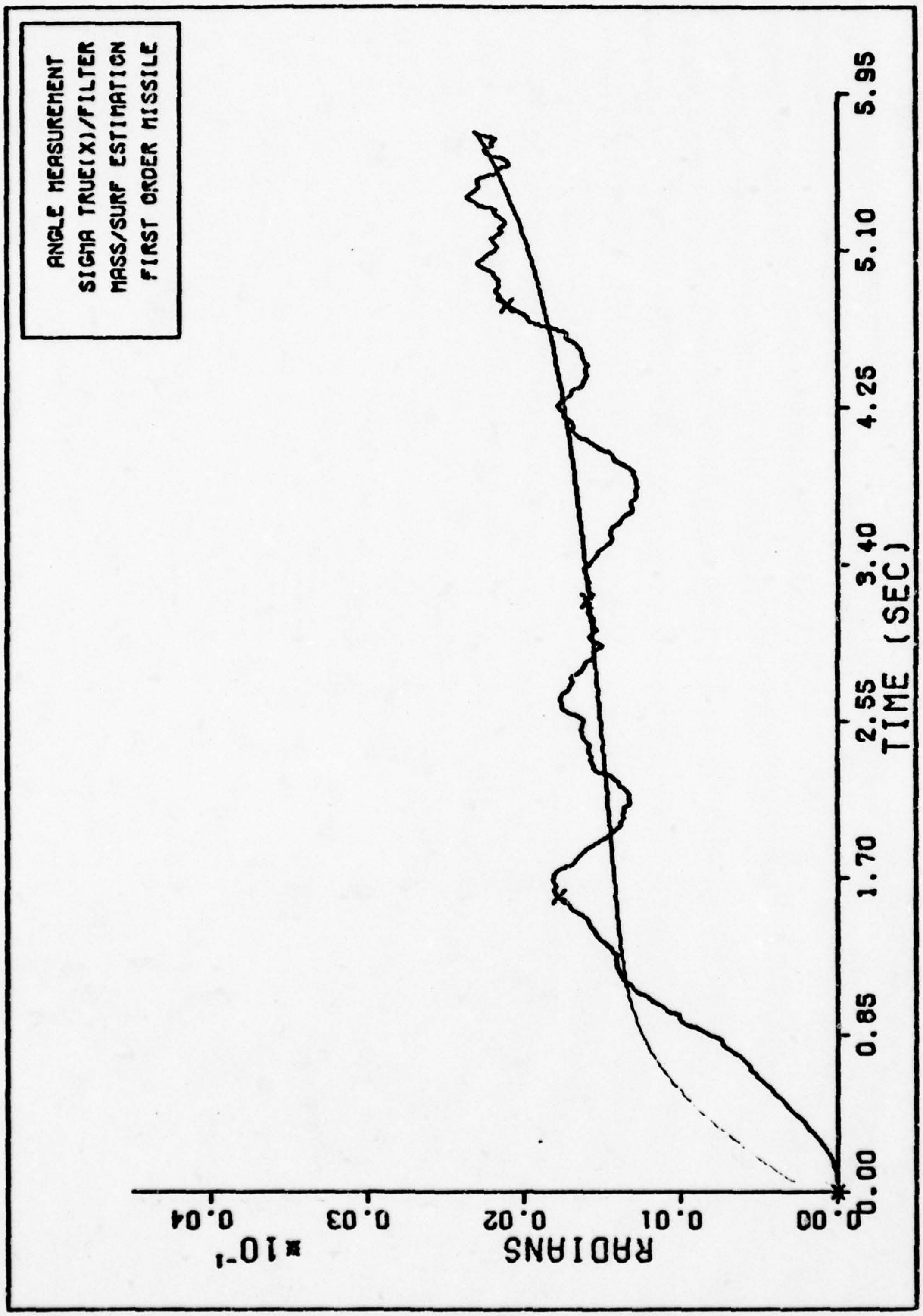

Fig. 221. ANGLE MEASUREMENT SIGMAS FIRST ORDER

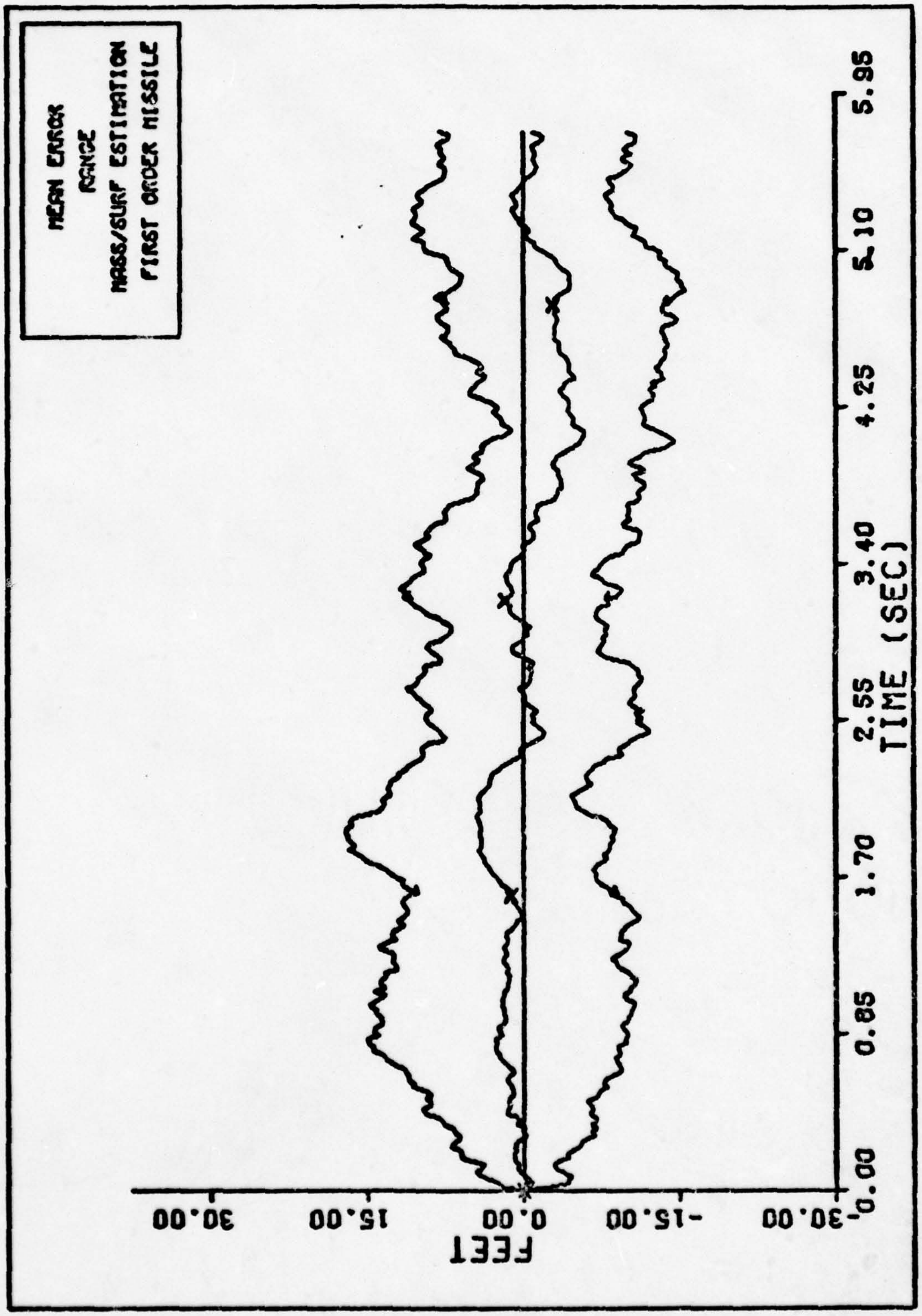

Fig. 222. RANGE FIRST ORDER MISSILE

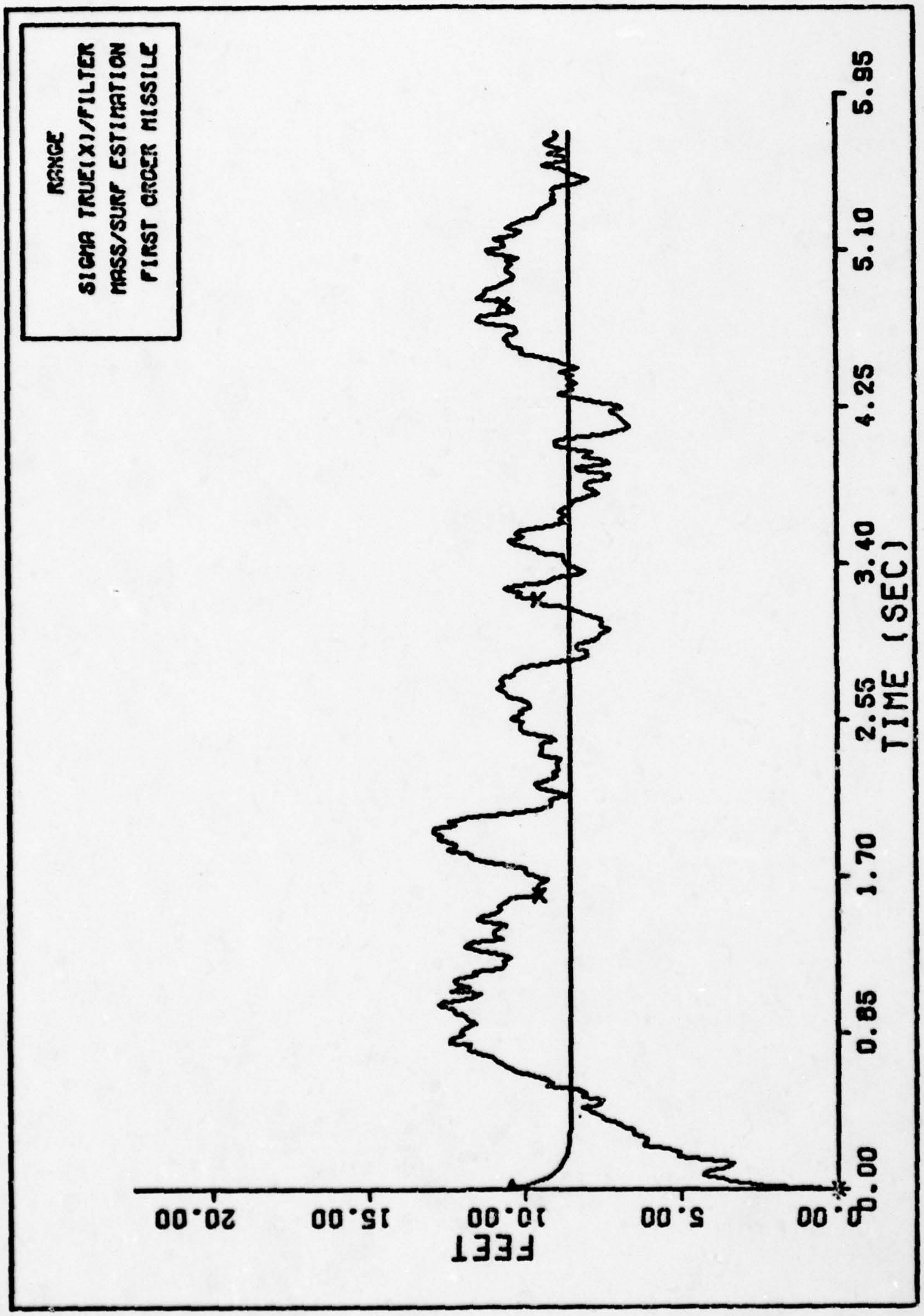

Fig. 223. RANGE SIGMAS FIRST ORDER

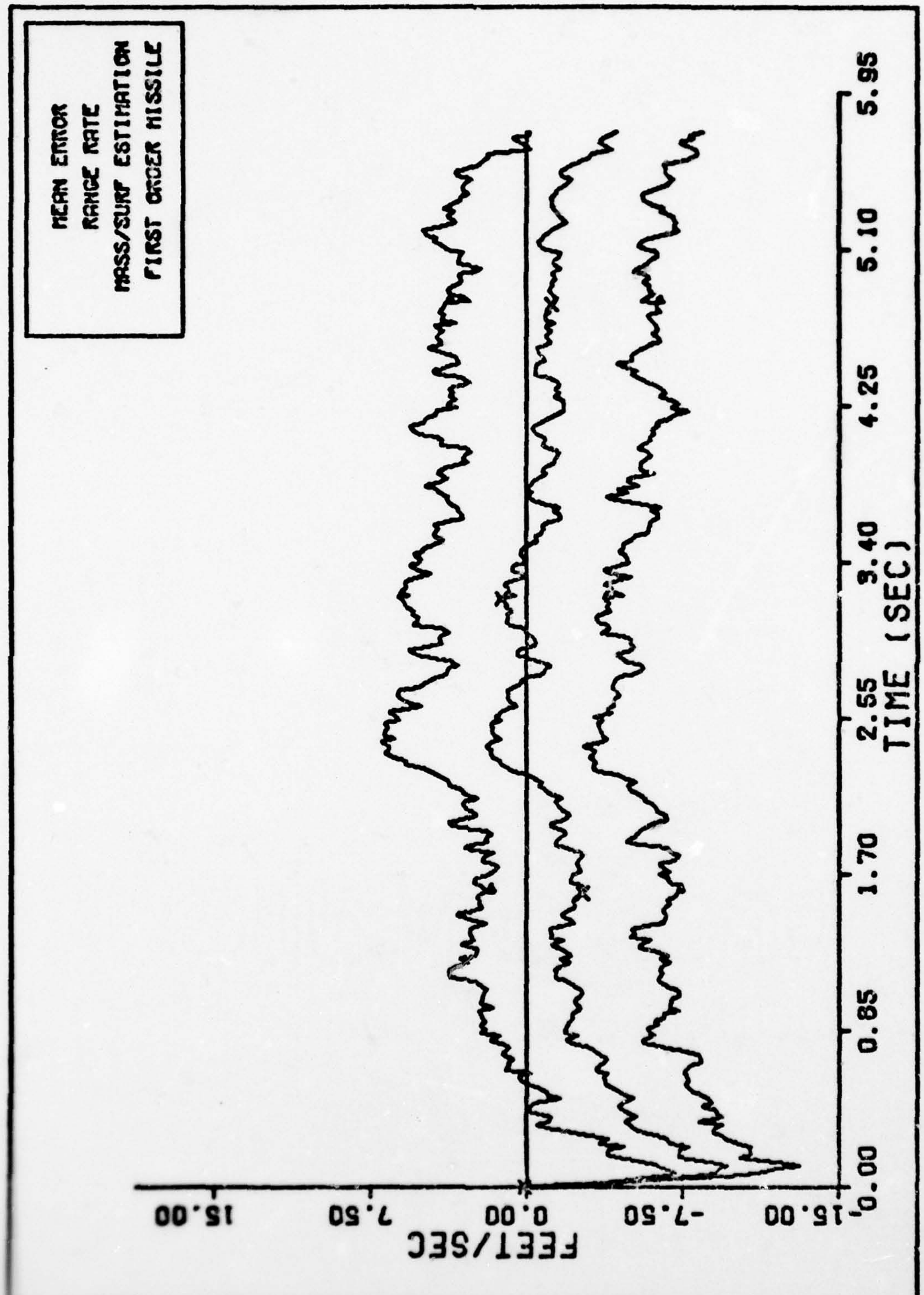

Fig. 224. RANGE RATE FIRST ORDER MISSILE

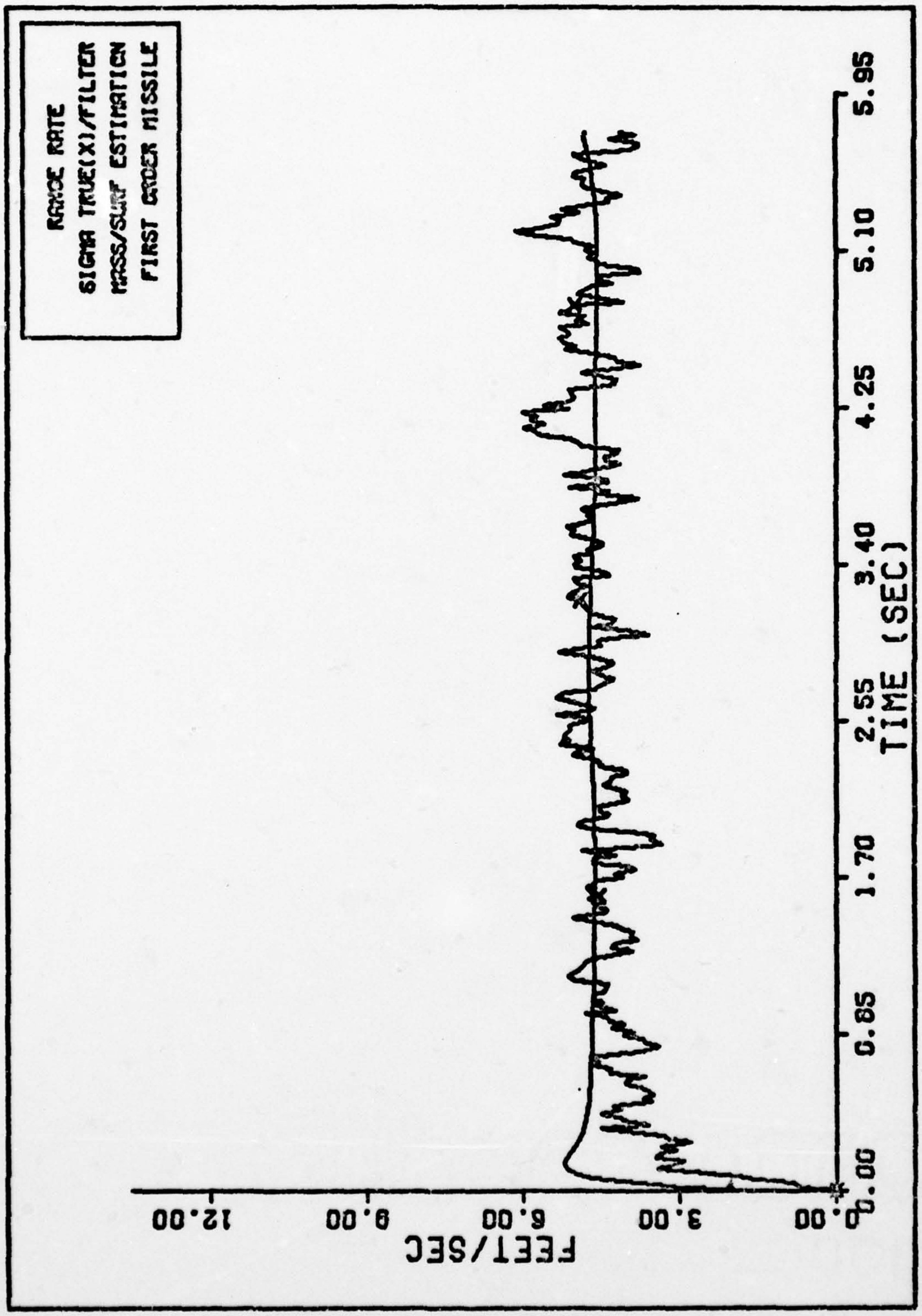

Fig. 225. RANGE RATE SIGMAS FIRST ORDER

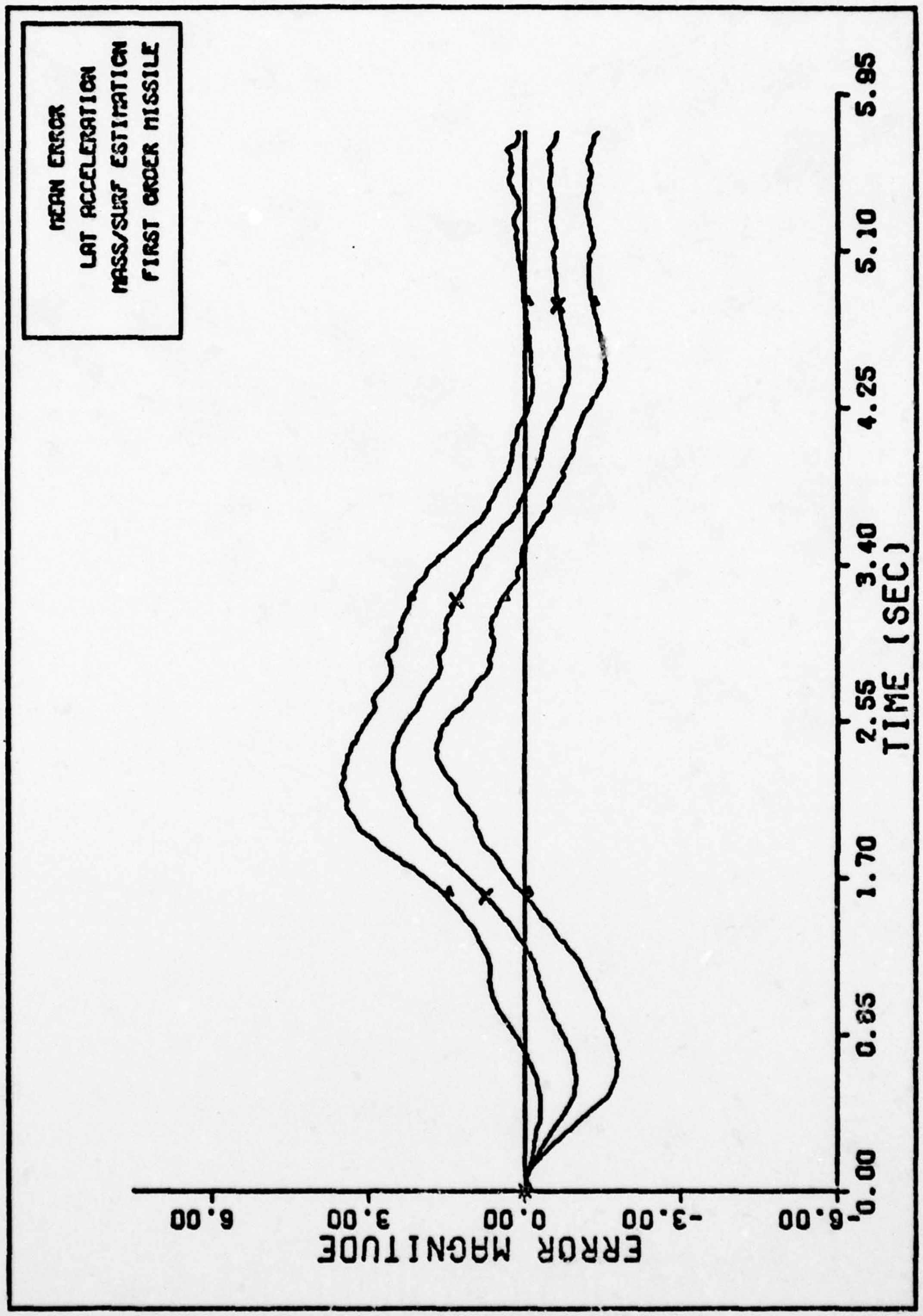

Fig. 226. LAT ACCELERATION FIRST ORDER MISSILE

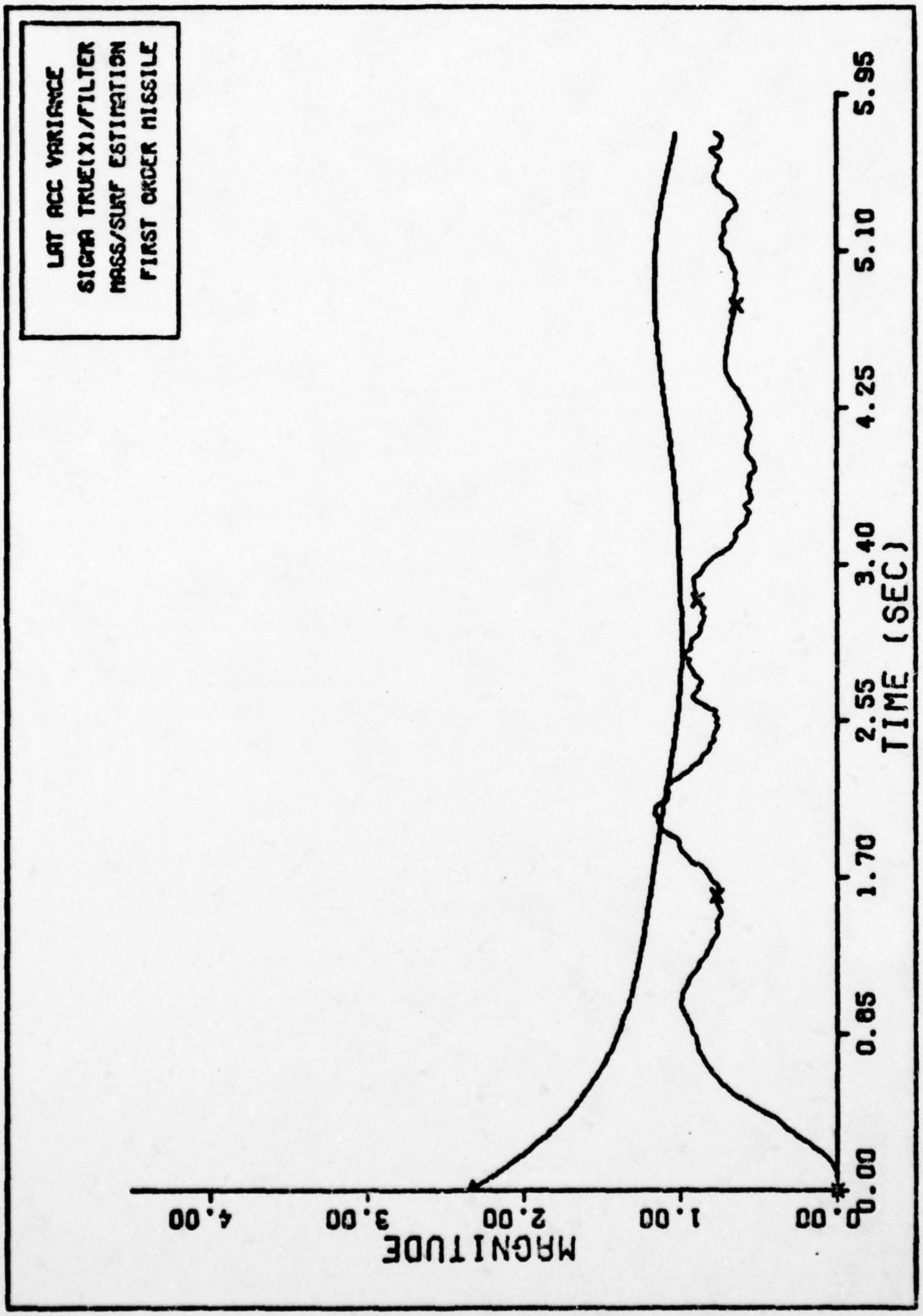

Fig. 227. LAT ACCELERATION SIGMAS FIRST ORDER

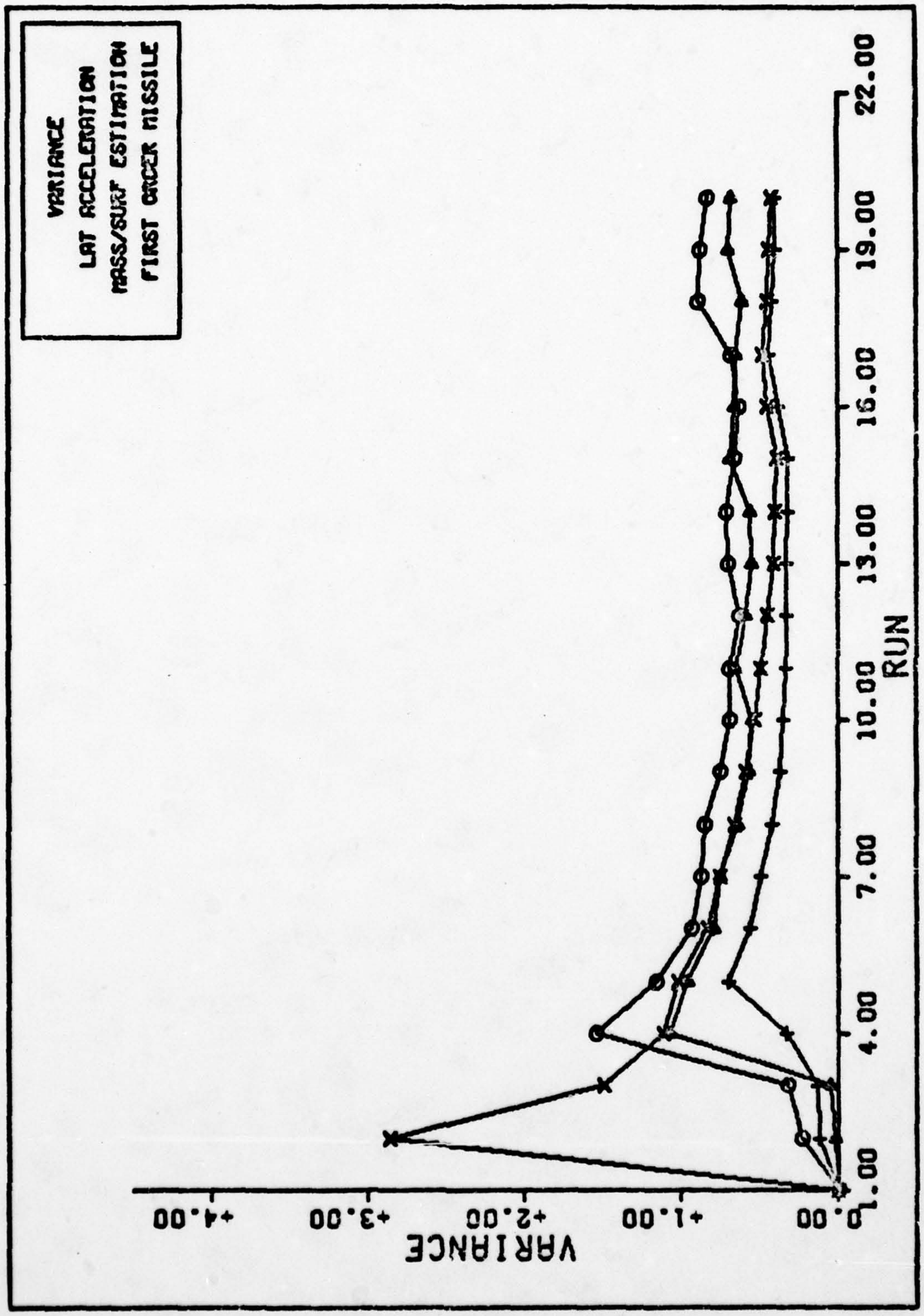

Fig. 228. VARIANCE CONVERGENCE

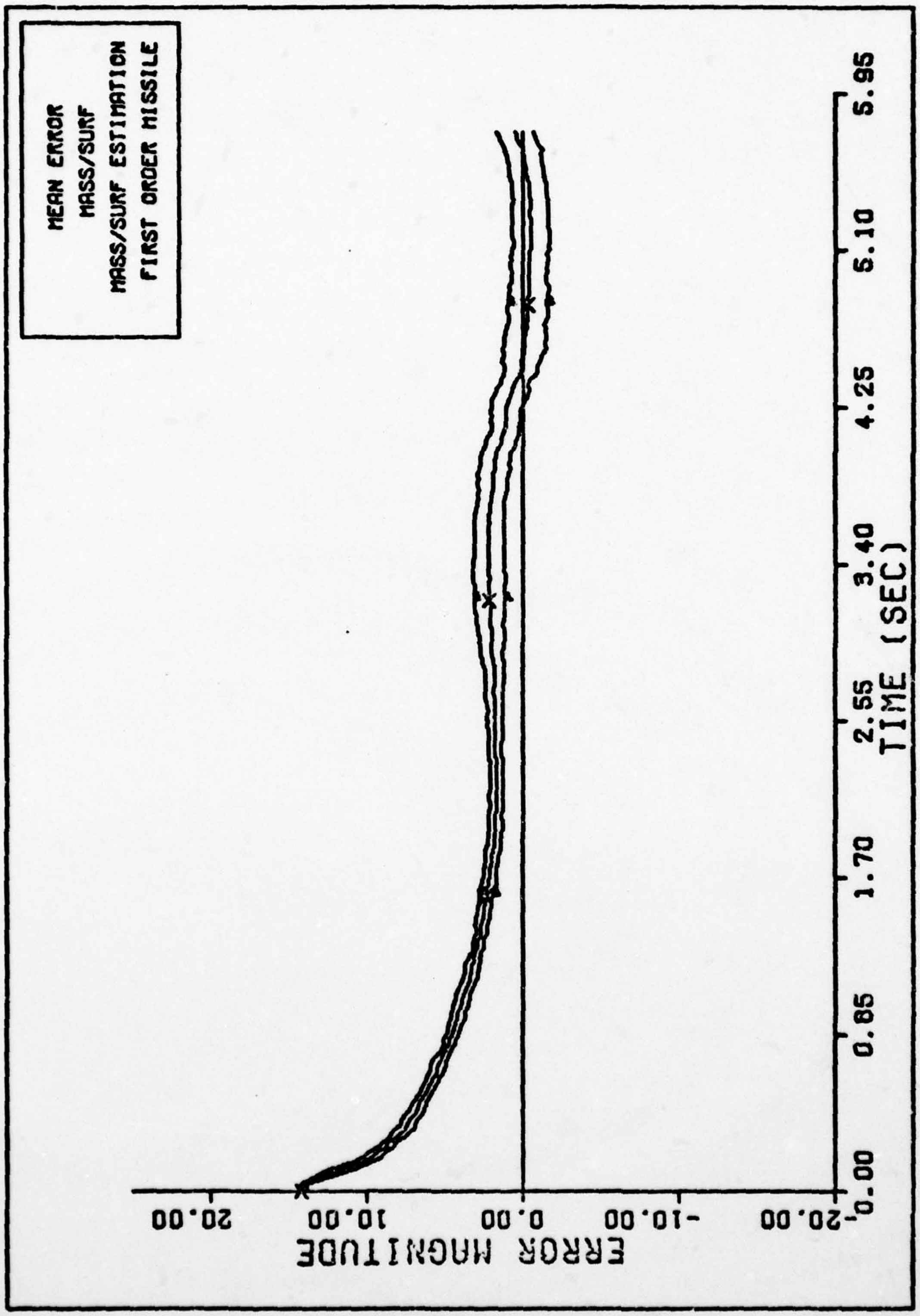

Fig. 229. MASS/SURF FIRST ORDER MISSILE

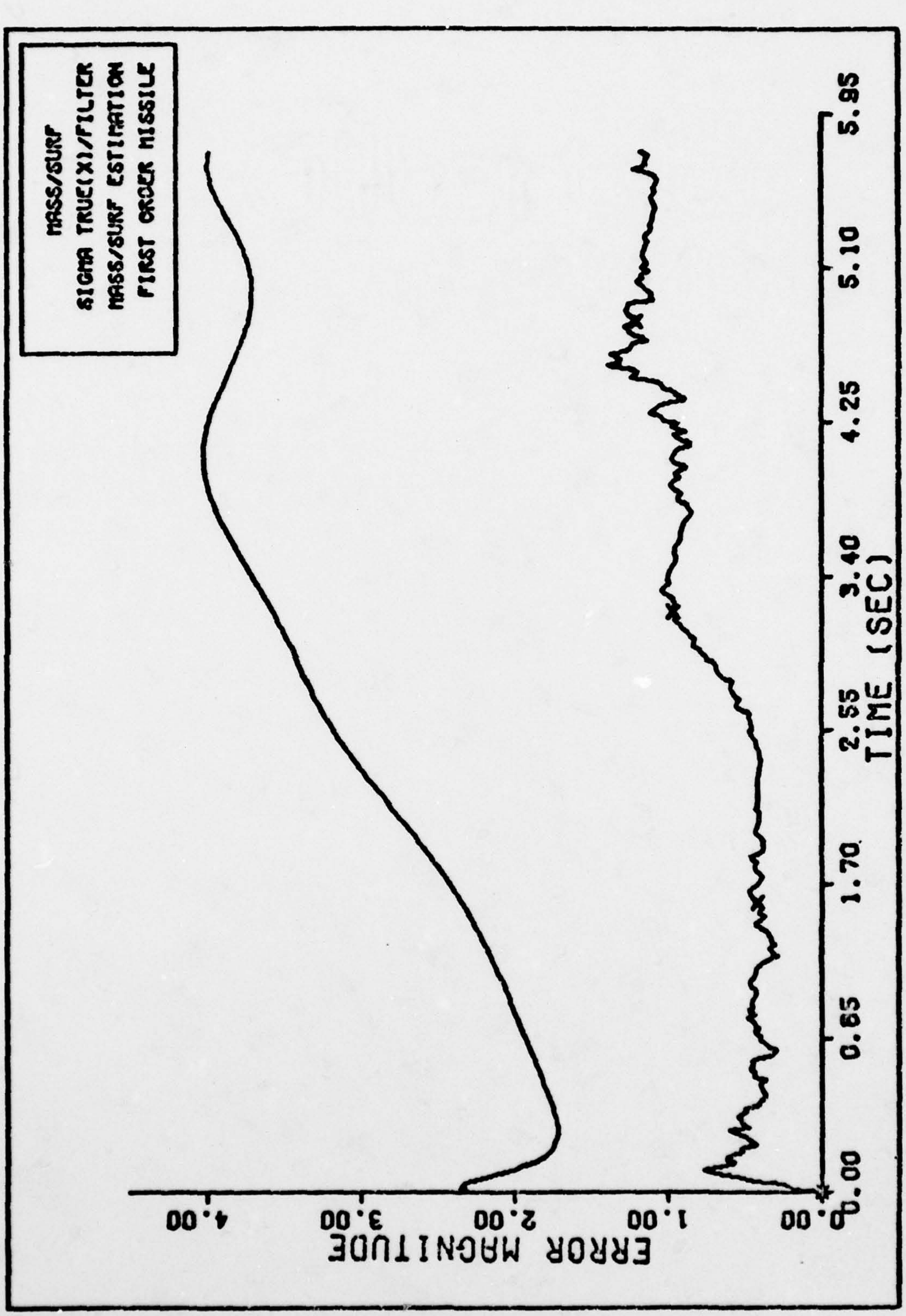

Fig. 230. MASS/SURF SIGMAS FIRST ORDER

<u>n and τ_f Estimation (high-g scenario)</u>

The initial state estimates and the tuning parameters for this case are

$$
\begin{aligned}
V^I_{mx}(0) &= 1225.7 \text{ fps} \\
\dot{\theta}_T(0) &= 4.363345 \text{ radians} \\
R(0) &= 10000. \text{ feet} \\
\dot{R}(0) &= -2122. \text{ fps} \\
a_L(0) &= 0. \\
n(0) &= 6. \\
\tau_f(0) &= .3 \text{ seconds} \\
M/S(0) &= 29.197 \text{ slugs/ft}^2
\end{aligned}
$$

$$
\underline{R} = \begin{bmatrix} 3.E-5 & 0. & 0. \\ 0. & 500. & 0. \\ 0. & 0. & 100. \end{bmatrix}
$$

$$
\underline{P}_0 = \begin{bmatrix}
100. & 0. & 0. & 0. & 0. & 0. & 0. & 0. \\
0. & 1.E-8 & 0. & 0. & 0. & 0. & 0. & 0. \\
0. & 0. & 101. & 0. & 0. & 0. & 0. & 0. \\
0. & 0. & 0. & 4. & 0. & 0. & 0. & 0. \\
0. & 0. & 0. & 0. & 5. & 0. & 0. & 0. \\
0. & 0. & 0. & 0. & 0. & 5. & 0. & 0. \\
0. & 0. & 0. & 0. & 0. & 0. & .2 & 0. \\
0. & 0. & 0. & 0. & 0. & 0. & 0. & 0.
\end{bmatrix}
$$

$$
\underline{Q} = \begin{bmatrix}
250. & 0. & 0. & 0. & 0. & 0. & 0. & 0. \\
0. & 1.E-6 & 0. & 0. & 0. & 0. & 0. & 0. \\
0. & 0. & 500. & 0. & 0. & 0. & 0. & 0. \\
0. & 0. & 0. & 200. & 0. & 0. & 0. & 0. \\
0. & 0. & 0. & 0. & 10. & 0. & 0. & 0. \\
0. & 0. & 0. & 0. & 0. & .01 & 0. & 0. \\
0. & 0. & 0. & 0. & 0. & 0. & .001 & 0. \\
0. & 0. & 0. & 0. & 0. & 0. & 0. & 0.
\end{bmatrix}
$$

These results were produced when estimating n and τ_f together with the five dynamic states. Since these parameters only appeared together in the model of the guidance strip, they were considered the most difficult combination to estimate simultaneously. n was initialized at 6., and τ_f was initialized at 0.3 seconds. The true values of n and τ_f were 4.5 and 0.85 seconds respectively.

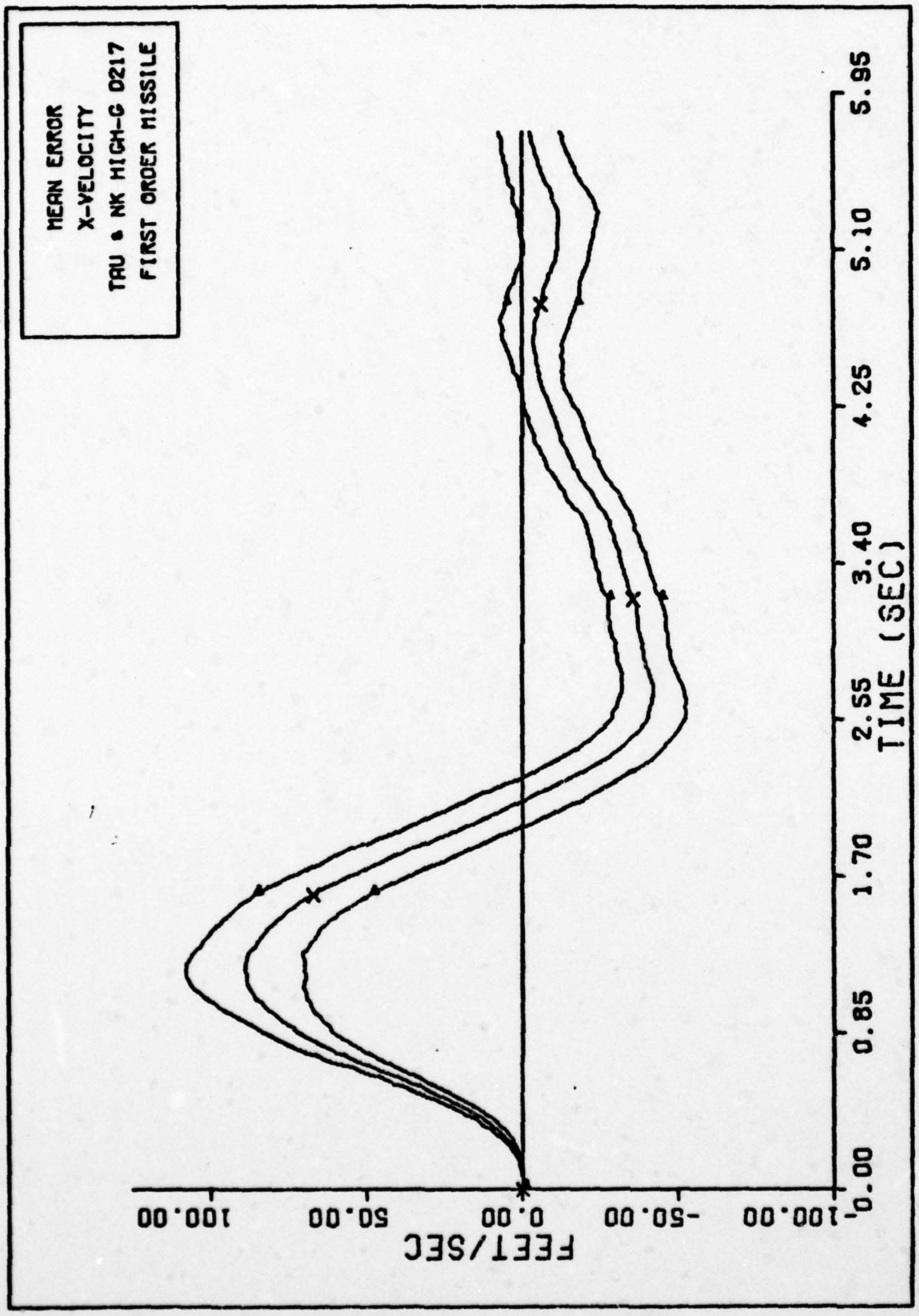

Fig. 231. X-VELOCITY FIRST ORDER MISSILE

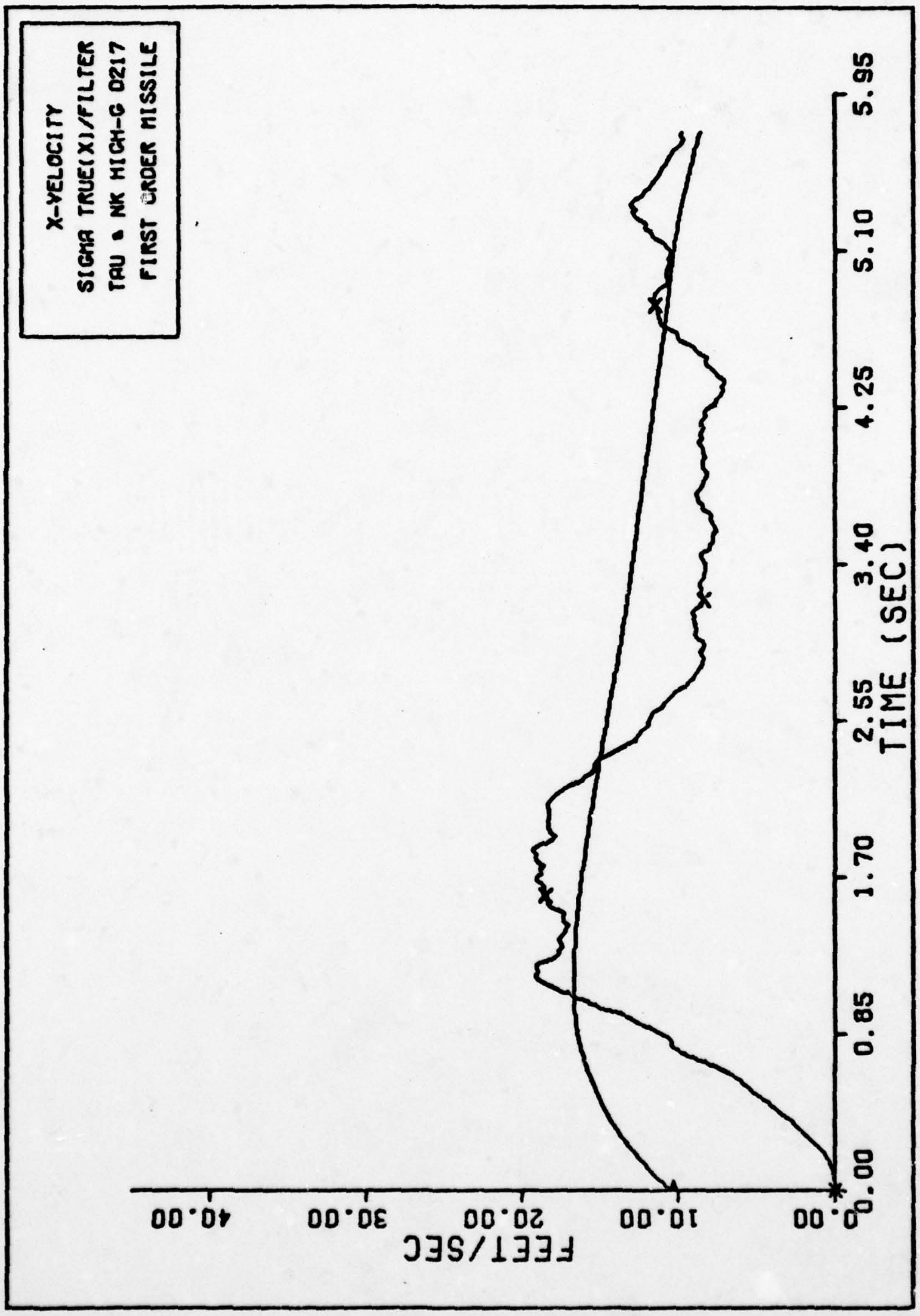

Fig. 232. X-VELOCITY SIGMAS FIRST ORDER

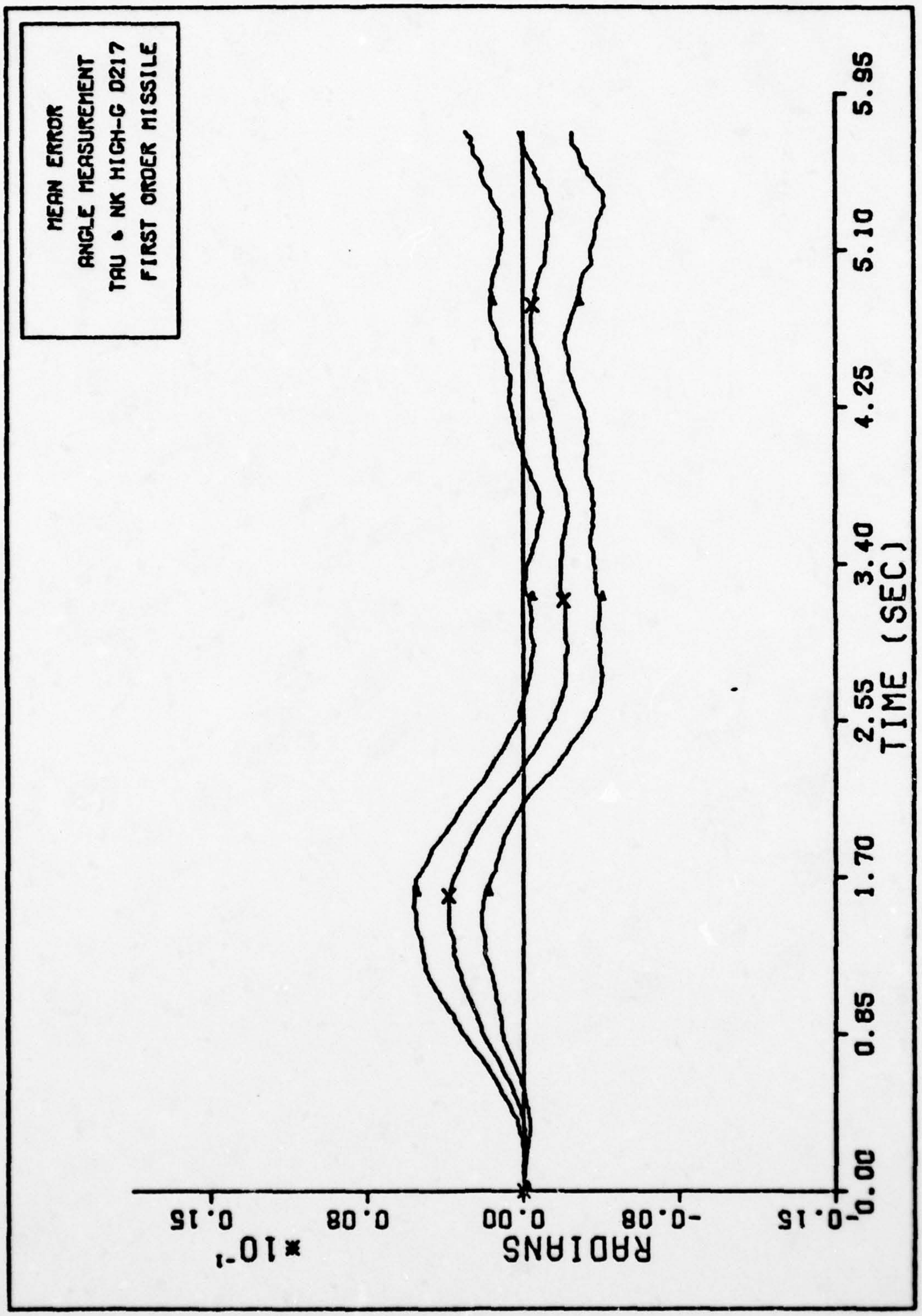

Fig. 233. ANGLE MEASUREMENT FIRST ORDER MISSILE

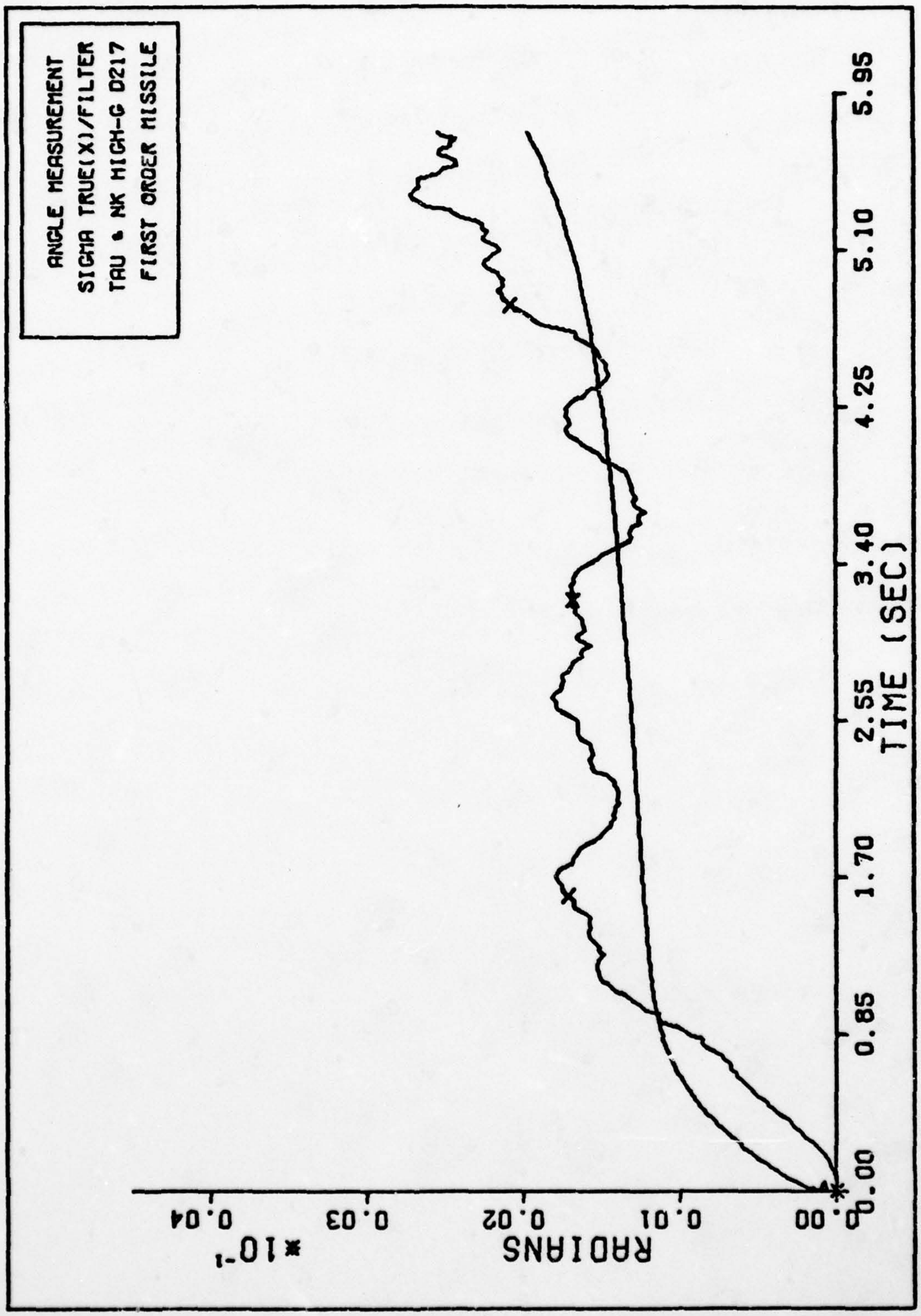

Fig. 234. ANGLE MEASUREMENT SIGMAS FIRST ORDER

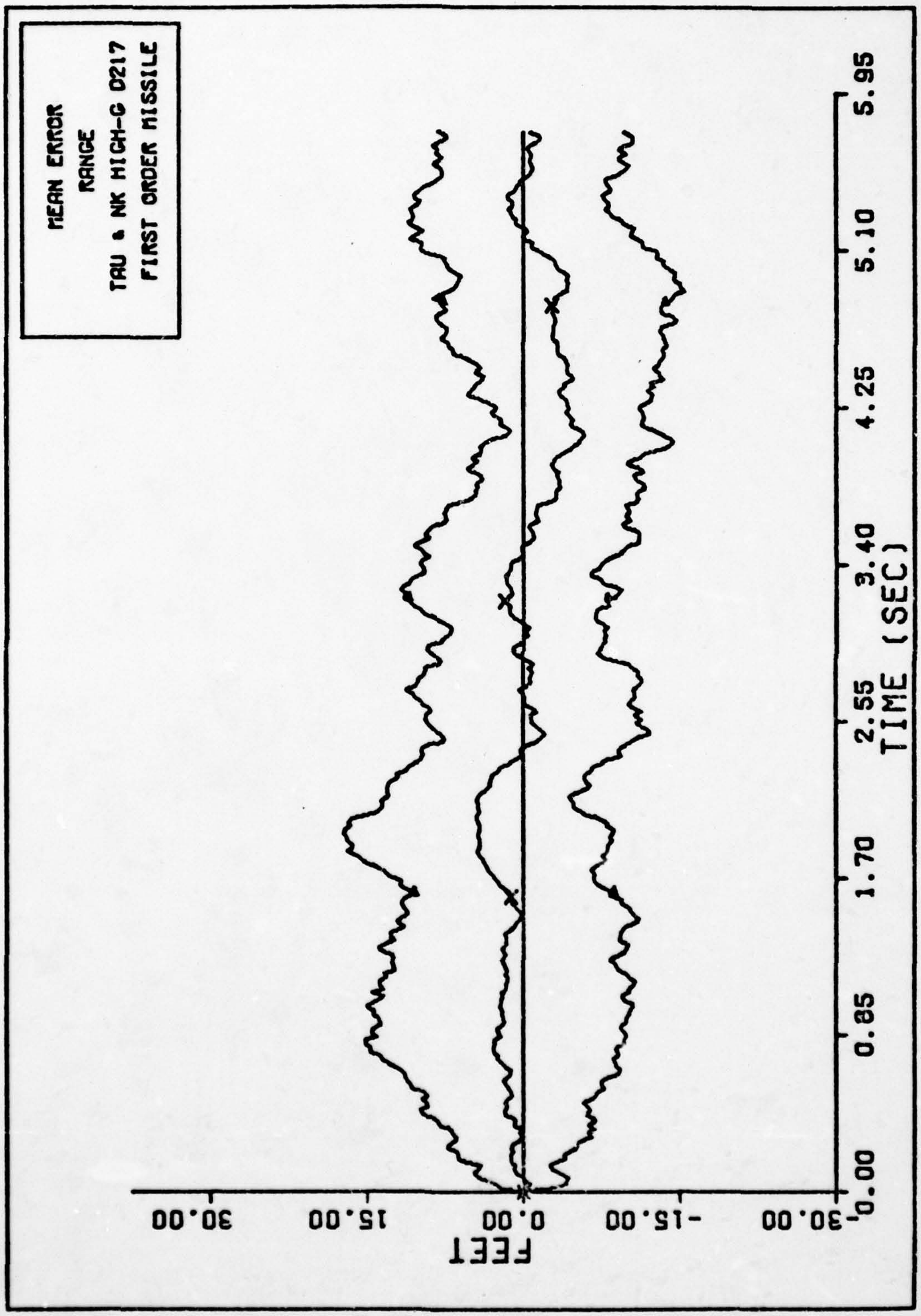

Fig. 235. RANGE FIRST ORDER MISSILE

AD-A055 637 AIR FORCE INST OF TECH WRIGHT-PATTERSON AFB OHIO SCH--ETC F/G 19/5
AN EXTENDED KALMAN FILTER FIRE CONTROL SYSTEM AGAINST AIR-TO-AI--ETC(U)
DEC 77 S J CUSUMANO, M DE PONTE
UNCLASSIFIED AFIT/GE/EE/77-13-VOL-2 NL

4 OF 4
ADA
055637

END
DATE
FILMED
8-78
DDC

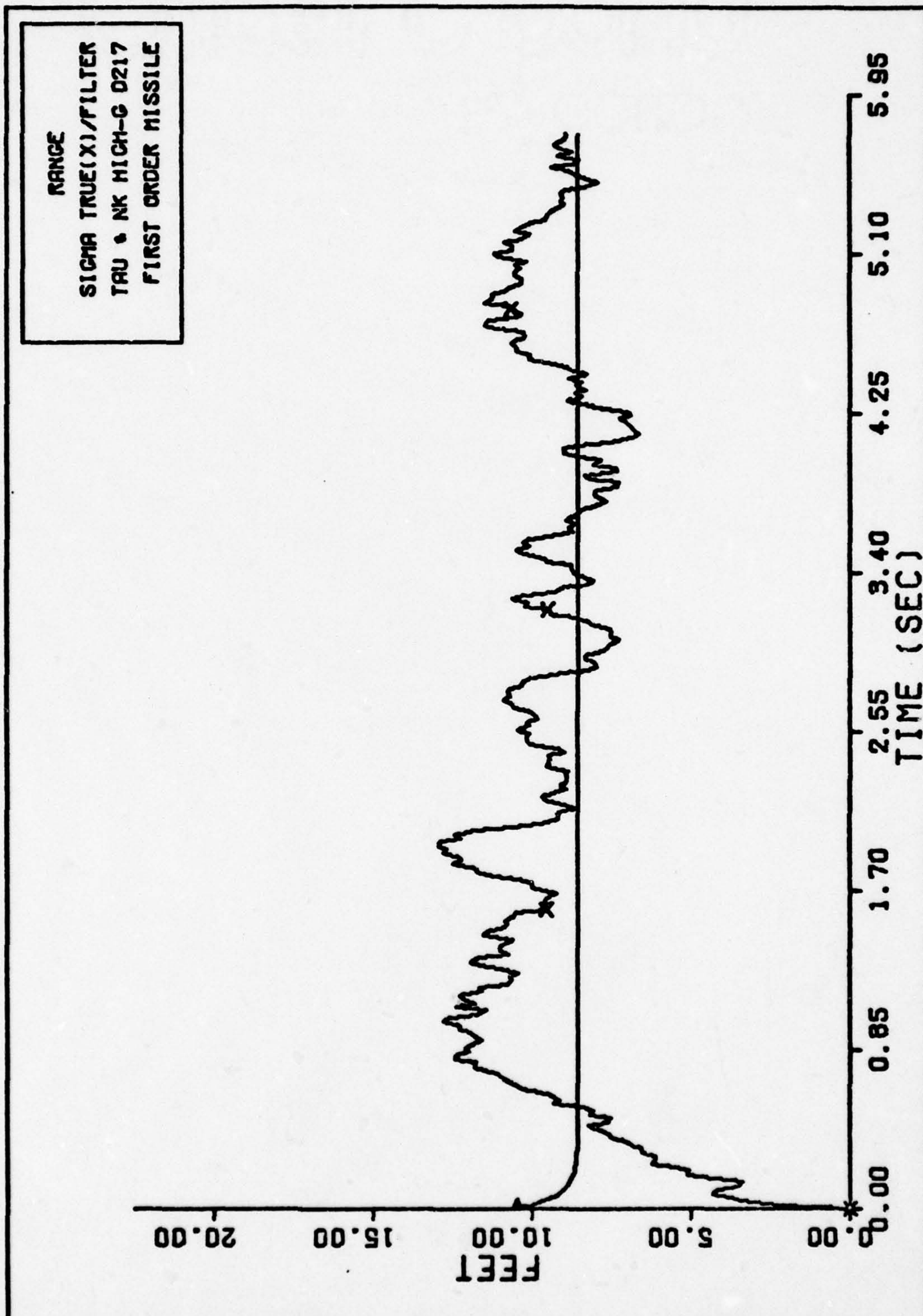

Fig. 236. RANGE SIGMAS FIRST ORDER

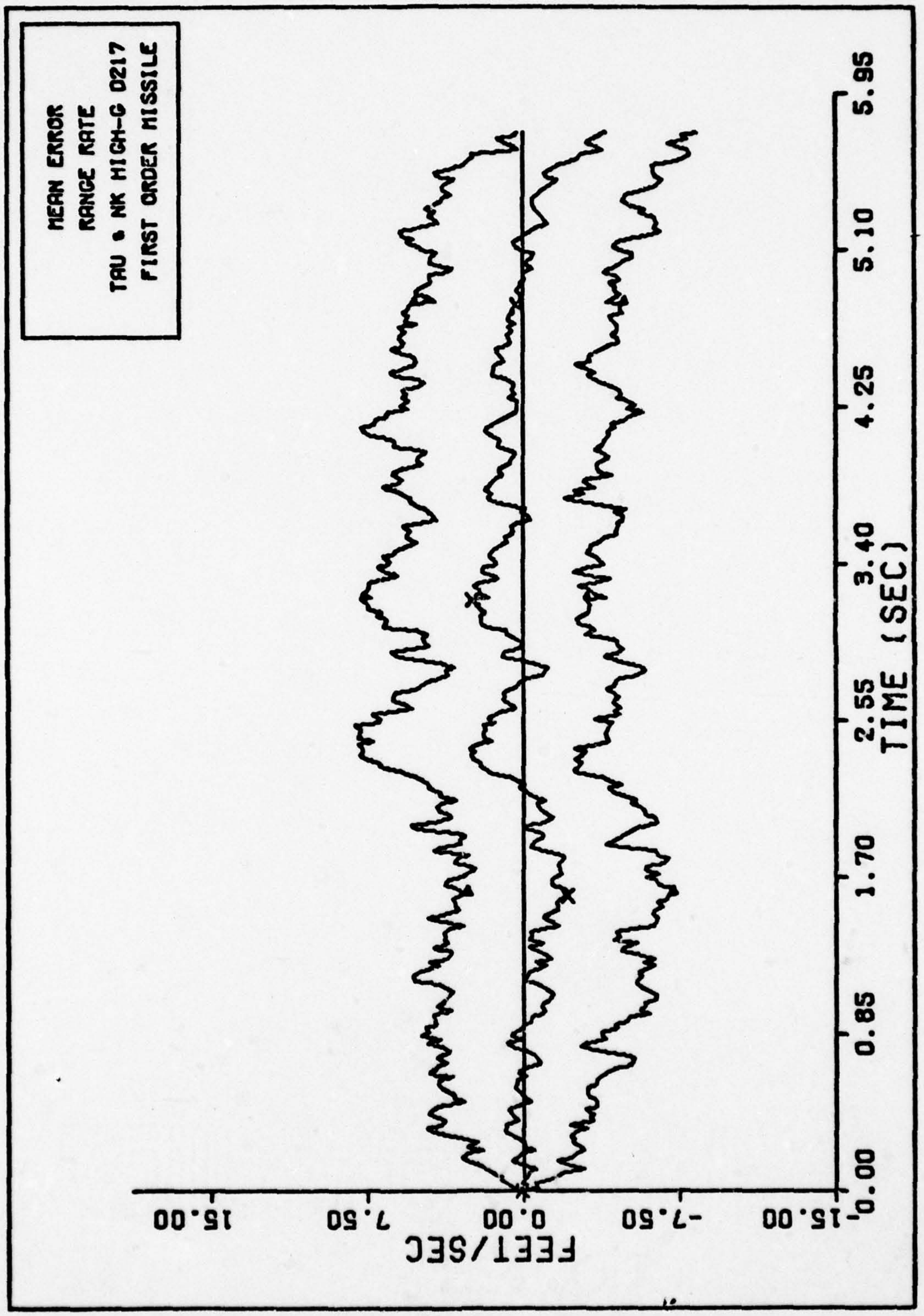

Fig. 237. RANGE RATE FIRST ORDER MISSILE

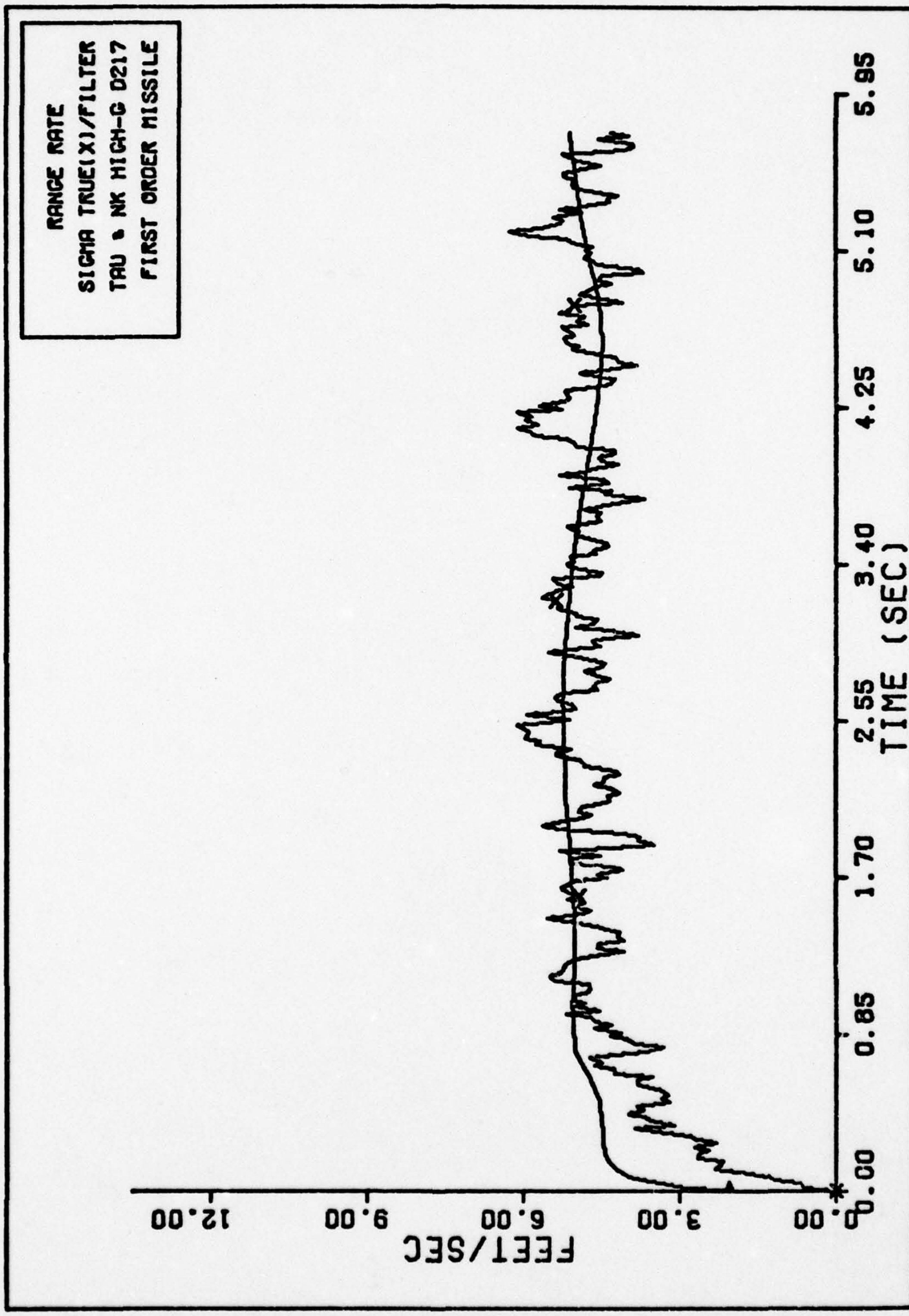

Fig. 238. RANGE RATE SIGMAS FIRST ORDER

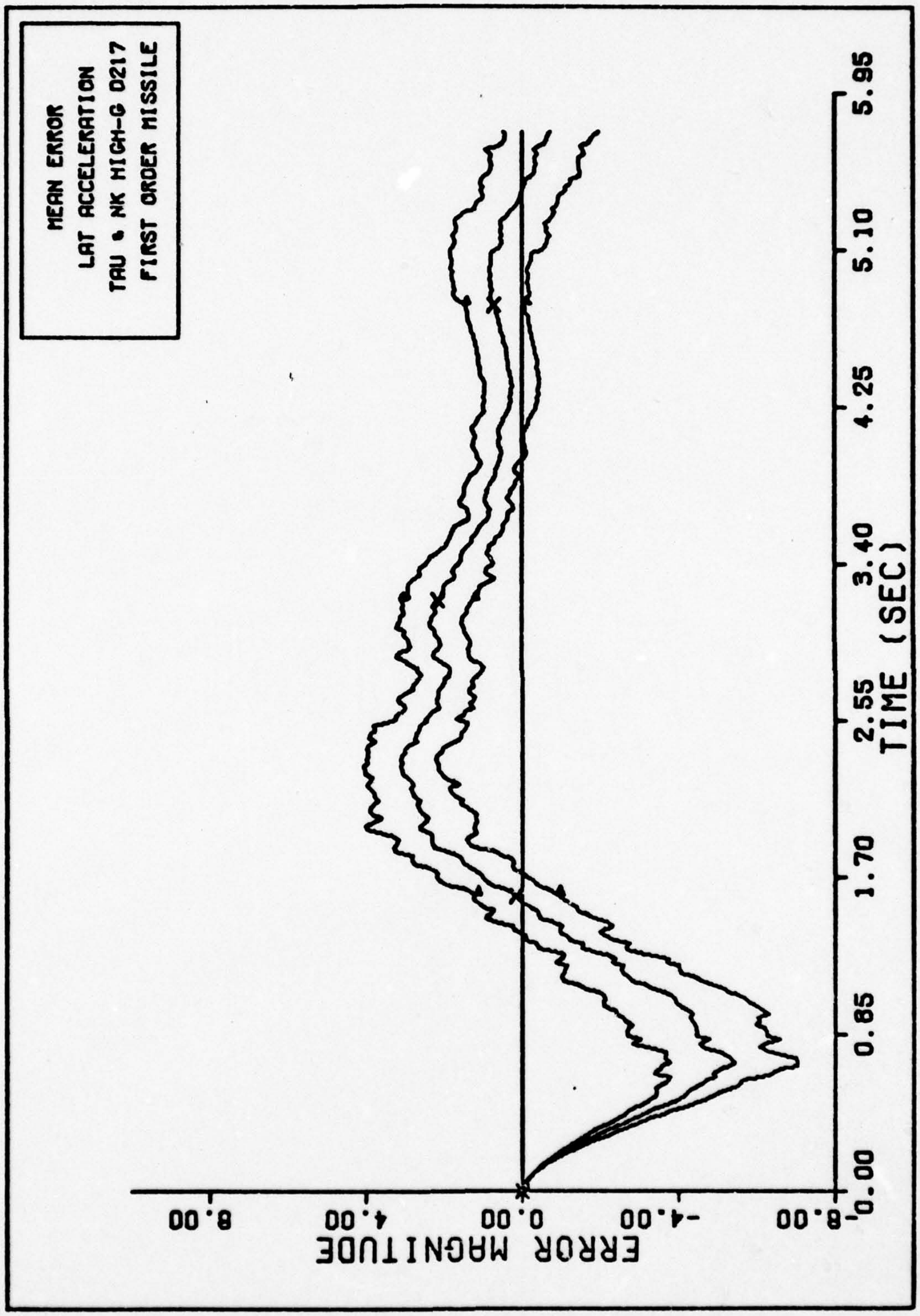

Fig. 239. LAT ACCELERATION FIRST ORDER MISSILE

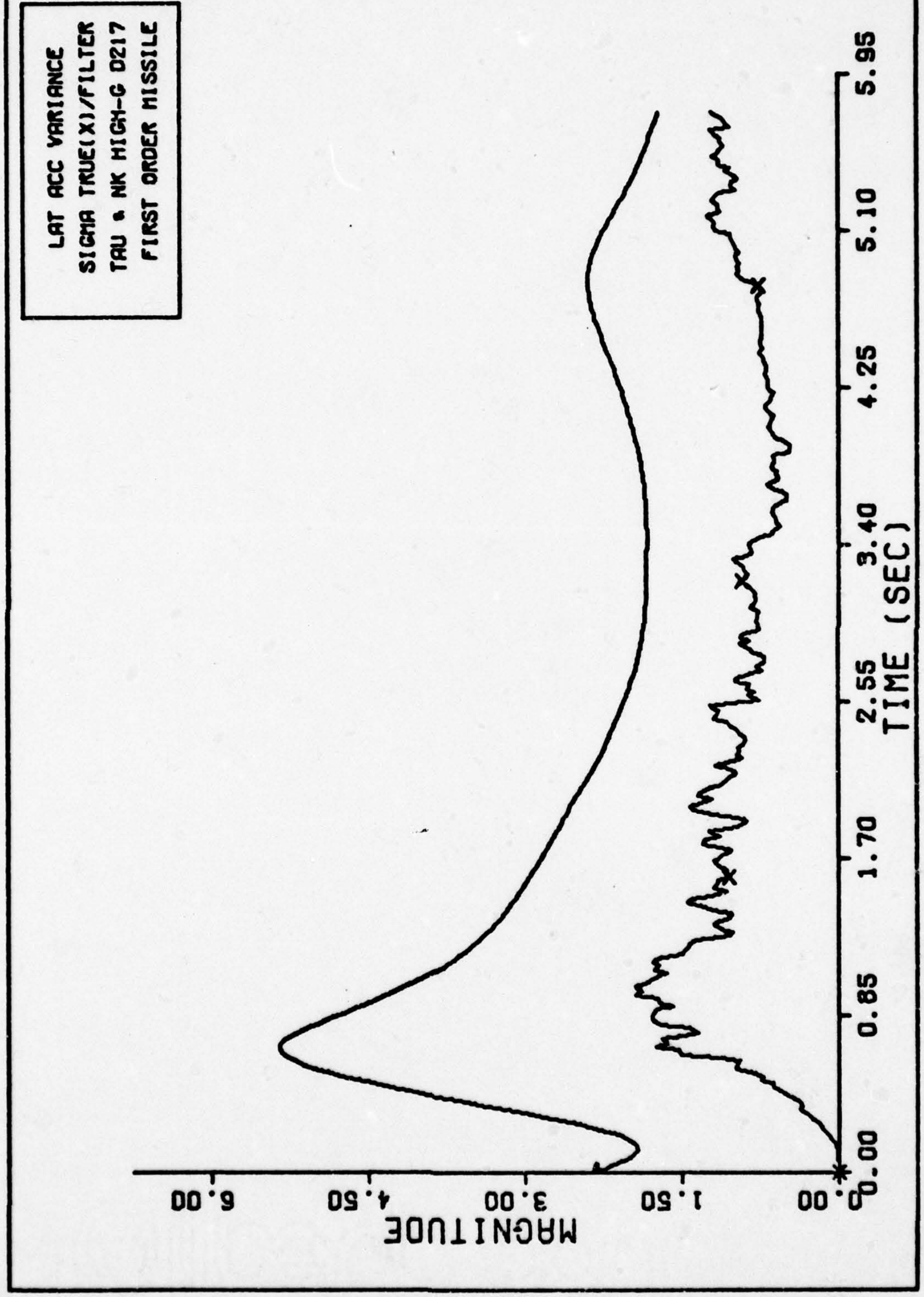

Fig. 240. LAT ACCELERATION SIGMAS FIRST ORDER

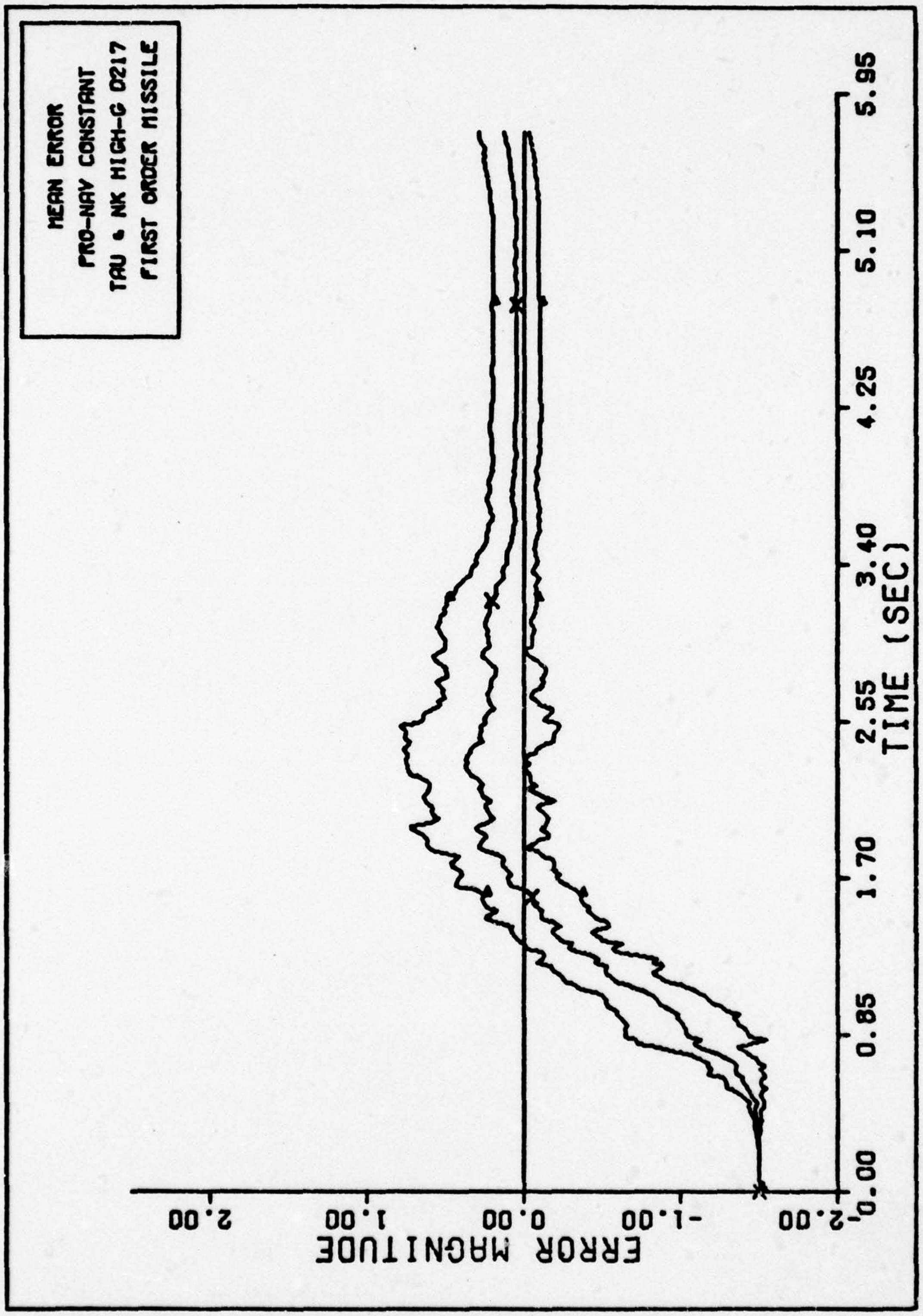

Fig. 241. PRO-NAV CONSTANT FIRST ORDER MISSILE

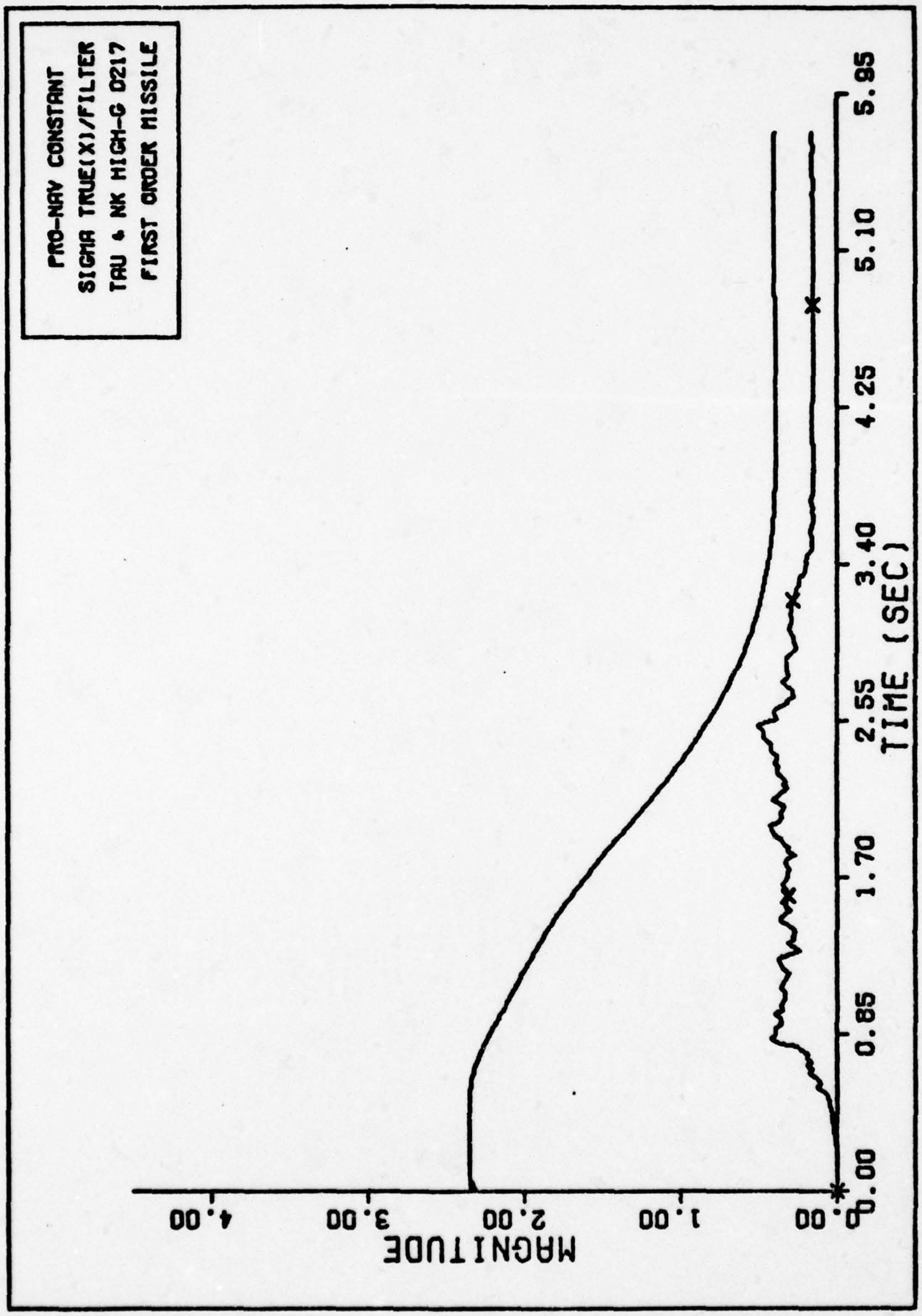

Fig. 242. PRO-NAV CONSTANT SIGMAS FIRST ORDER

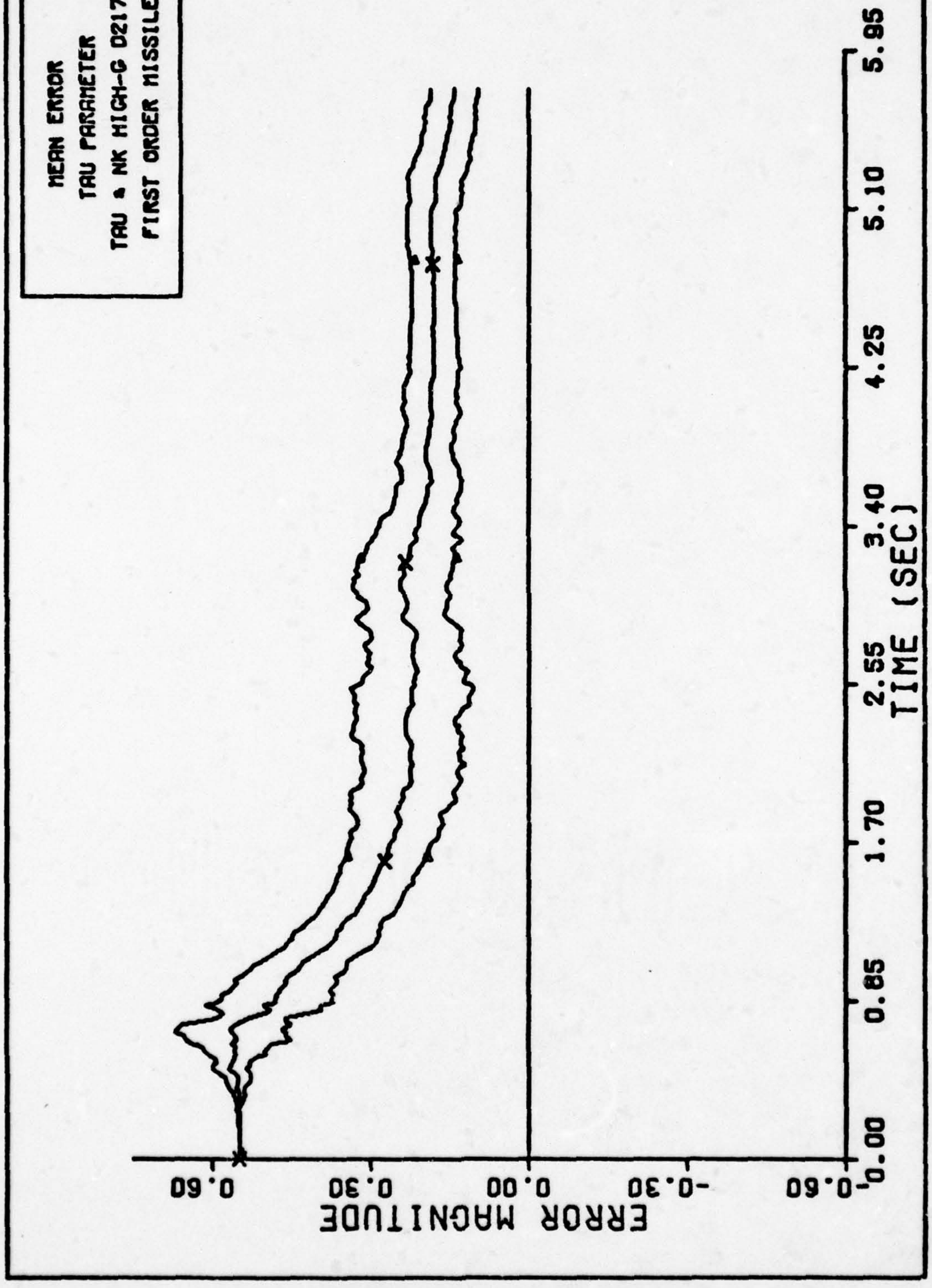

Fig. 243. TAU PARAMETER FIRST ORDER MISSILE

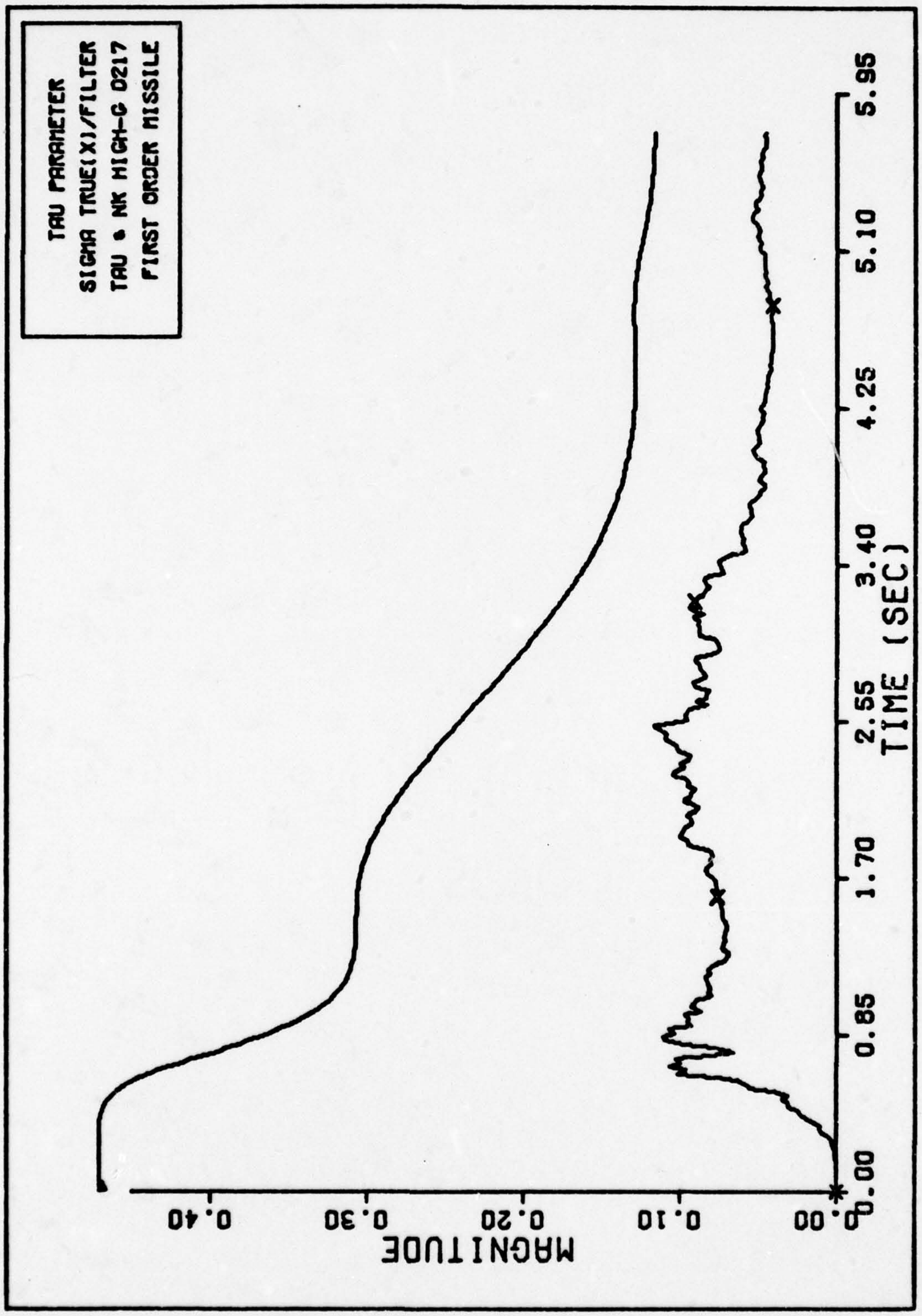

Fig. 244. TAU PARAMETER SIGMAS FIRST ORDER

$\underline{n}$ **and** $\underline{\tau_f}$ **Estimation** (low-g scenario)

The initial state estimates and the tuning parameters for this case are

$$V^{I}_{mx}(0) = 1225.7 \text{ fps}$$

$$\dot{\theta}_T(0) = 4.363345 \text{ radians}$$

$$R(0) = 10000. \text{ feet}$$

$$\dot{R}(0) = -2122. \text{ fps}$$

$$a_L(0) = 0.$$

$$n(0) = 3.$$

$$\tau_f(0) = 1.5 \text{ seconds}$$

$$M/S(0) = 29.197 \text{ slugs/ft}^2$$

$$\underline{R} = \begin{bmatrix} 3.E\text{-}5 & 0. & 0. \\ 0. & 500. & 0. \\ 0. & 0. & 100. \end{bmatrix}$$

$$\underline{P}_0 = \begin{bmatrix} 100. & 0. & 0. & 0. & 0. & 0. & 0. & 0. \\ 0. & 1.E\text{-}8 & 0. & 0. & 0. & 0. & 0. & 0. \\ 0. & 0. & 101. & 0. & 0. & 0. & 0. & 0. \\ 0. & 0. & 0. & 4. & 0. & 0. & 0. & 0. \\ 0. & 0. & 0. & 0. & 5. & 0. & 0. & 0. \\ 0. & 0. & 0. & 0. & 0. & 5. & 0. & 0. \\ 0. & 0. & 0. & 0. & 0. & 0. & .2 & 0. \\ 0. & 0. & 0. & 0. & 0. & 0. & 0. & 0. \end{bmatrix}$$

$$
\mathbf{Q} = \begin{bmatrix}
250. & 0. & 0. & 0. & 0. & 0. & 0. & 0. \\
0. & 1.E-6 & 0. & 0. & 0. & 0. & 0. & 0. \\
0. & 0. & 500. & 0. & 0. & 0. & 0. & 0. \\
0. & 0. & 0. & 200. & 0. & 0. & 0. & 0. \\
0. & 0. & 0. & 0. & 10. & 0. & 0. & 0. \\
0. & 0. & 0. & 0. & 0. & .01 & 0. & 0. \\
0. & 0. & 0. & 0. & 0. & 0. & .001 & 0. \\
0. & 0. & 0. & 0. & 0. & 0. & 0. & 0.
\end{bmatrix}
$$

These plots were generated as a test case to determine if the parameters could be estimated for a low-g scenario. Only n and τ_f were estimated along with the five dynamic states of the missile model. These plots can be compared with Figures 231 through 244 which were generated using the high-g scenario. The n and τ_f in the filter, for this set, were initialized at 3.0 and 1.5 seconds respectively. The true n was 4.5 and thr true value for τ_f was defined as 0.85 seconds.

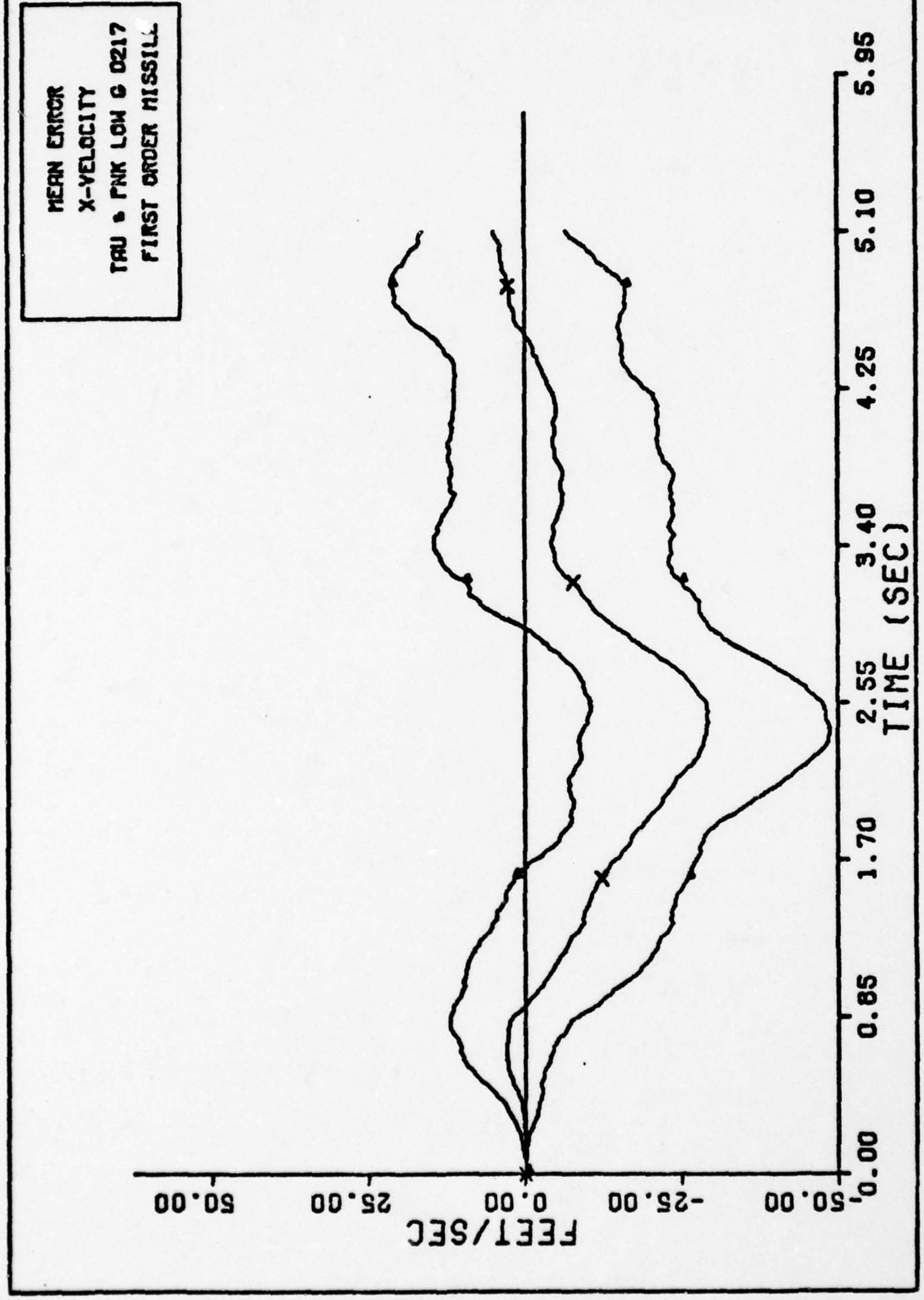

Fig. 245. X-VELOCITY FIRST ORDER MISSILE

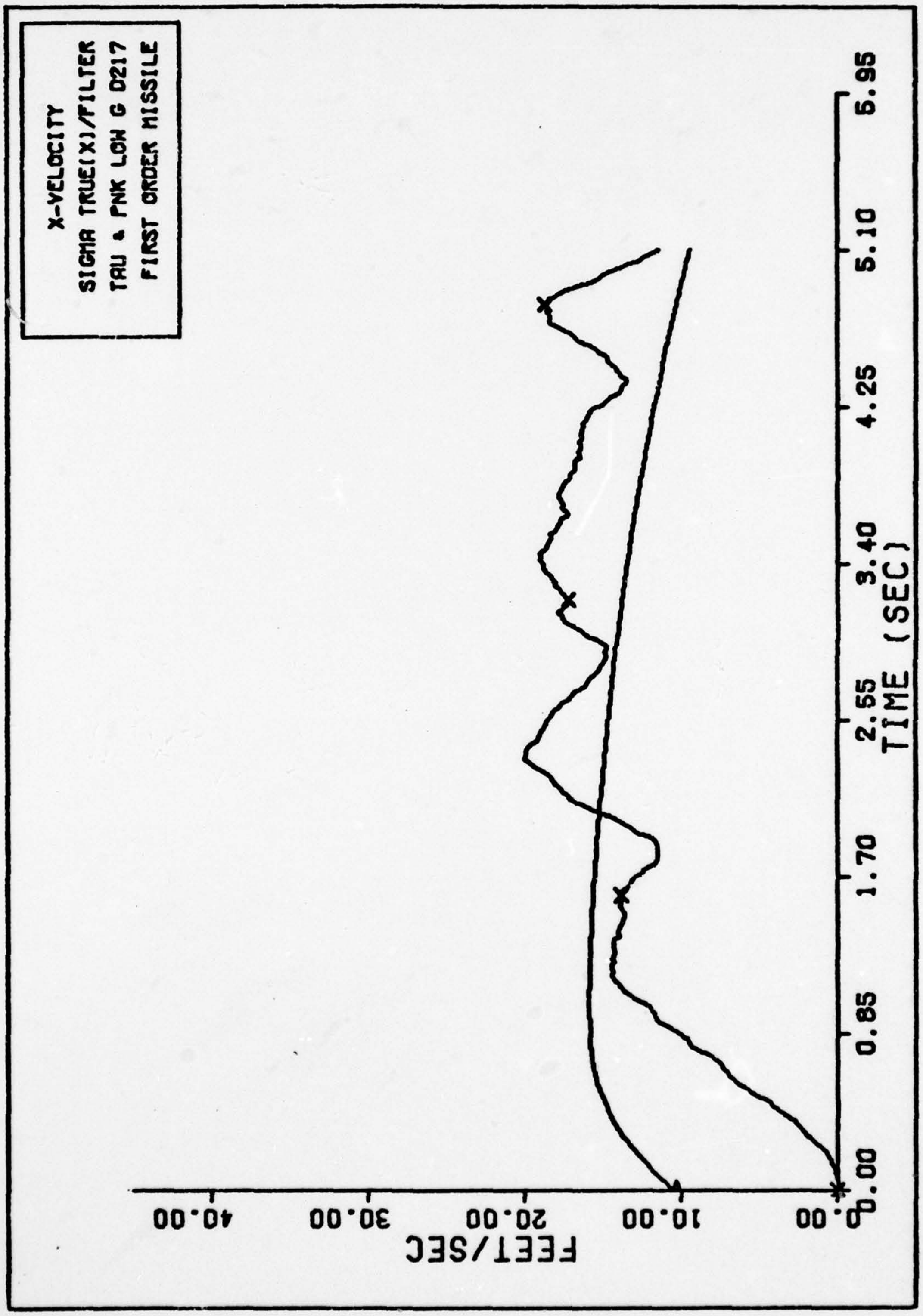

Fig. 246. X-VELOCITY SIGMAS FIRST ORDER

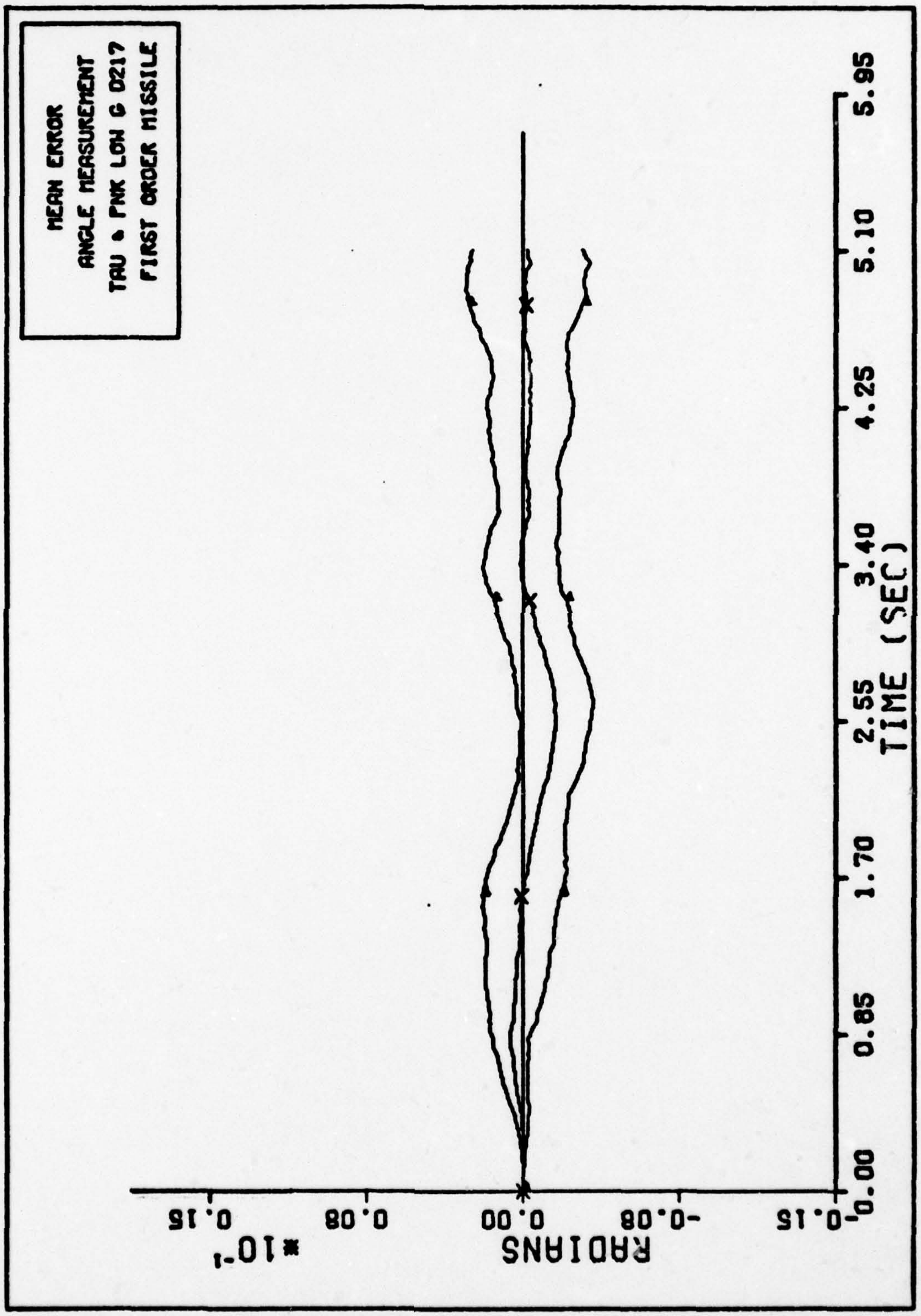

Fig. 247. ANGLE MEASUREMENT FIRST ORDER MISSILE

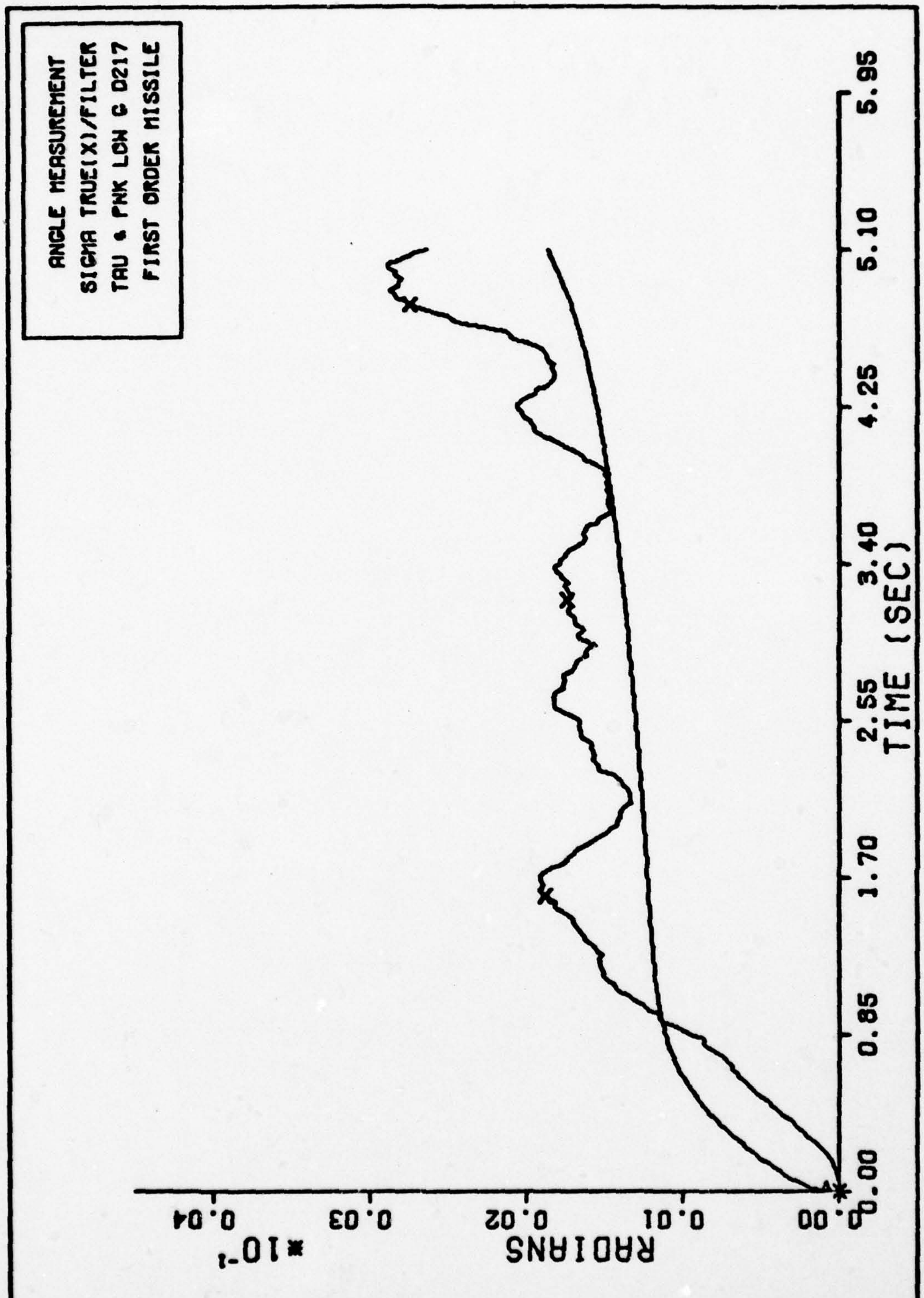

Fig. 248. ANGLE MEASUREMENT SIGMAS FIRST ORDER

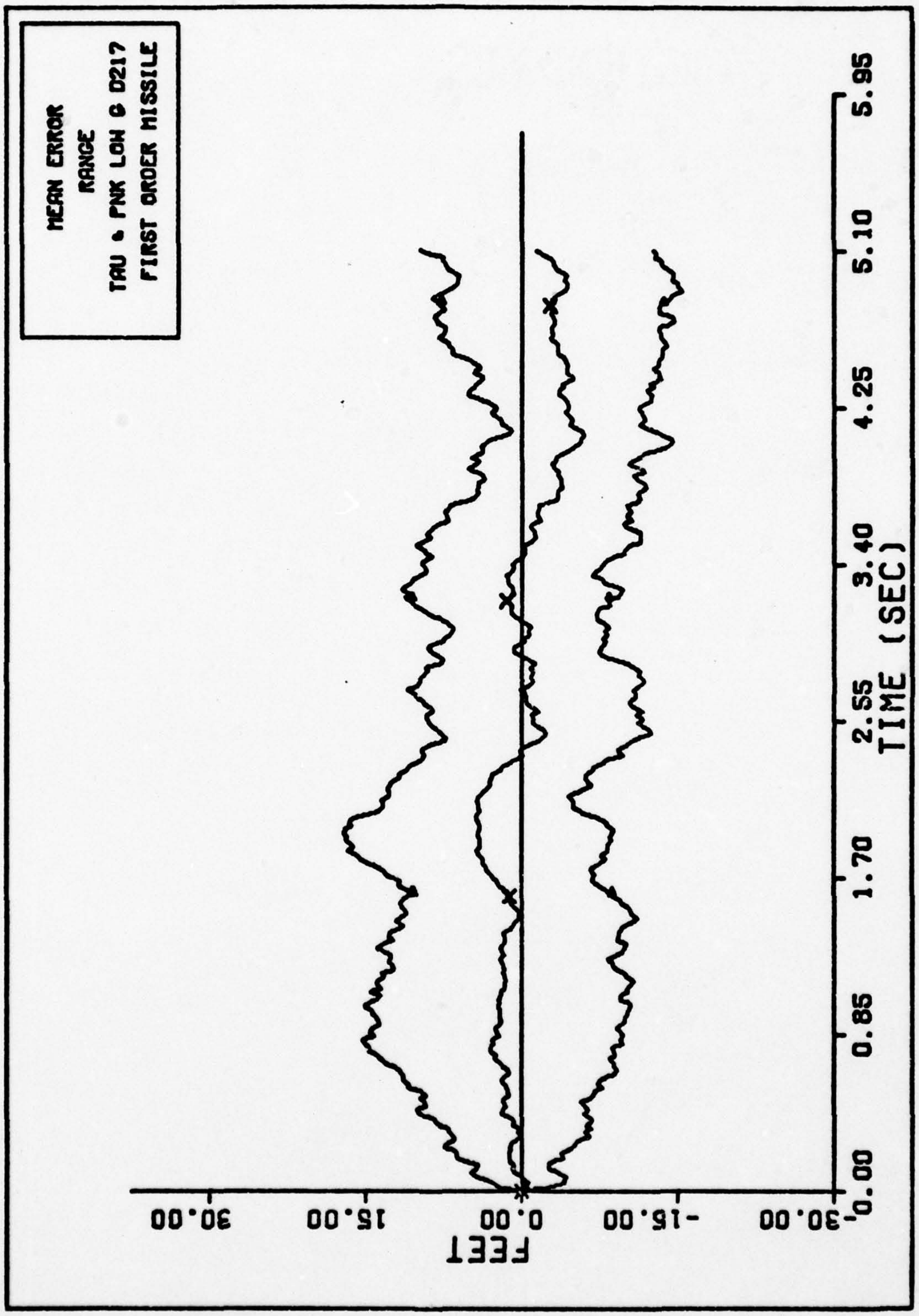

Fig. 249. RANGE FIRST ORDER MISSILE

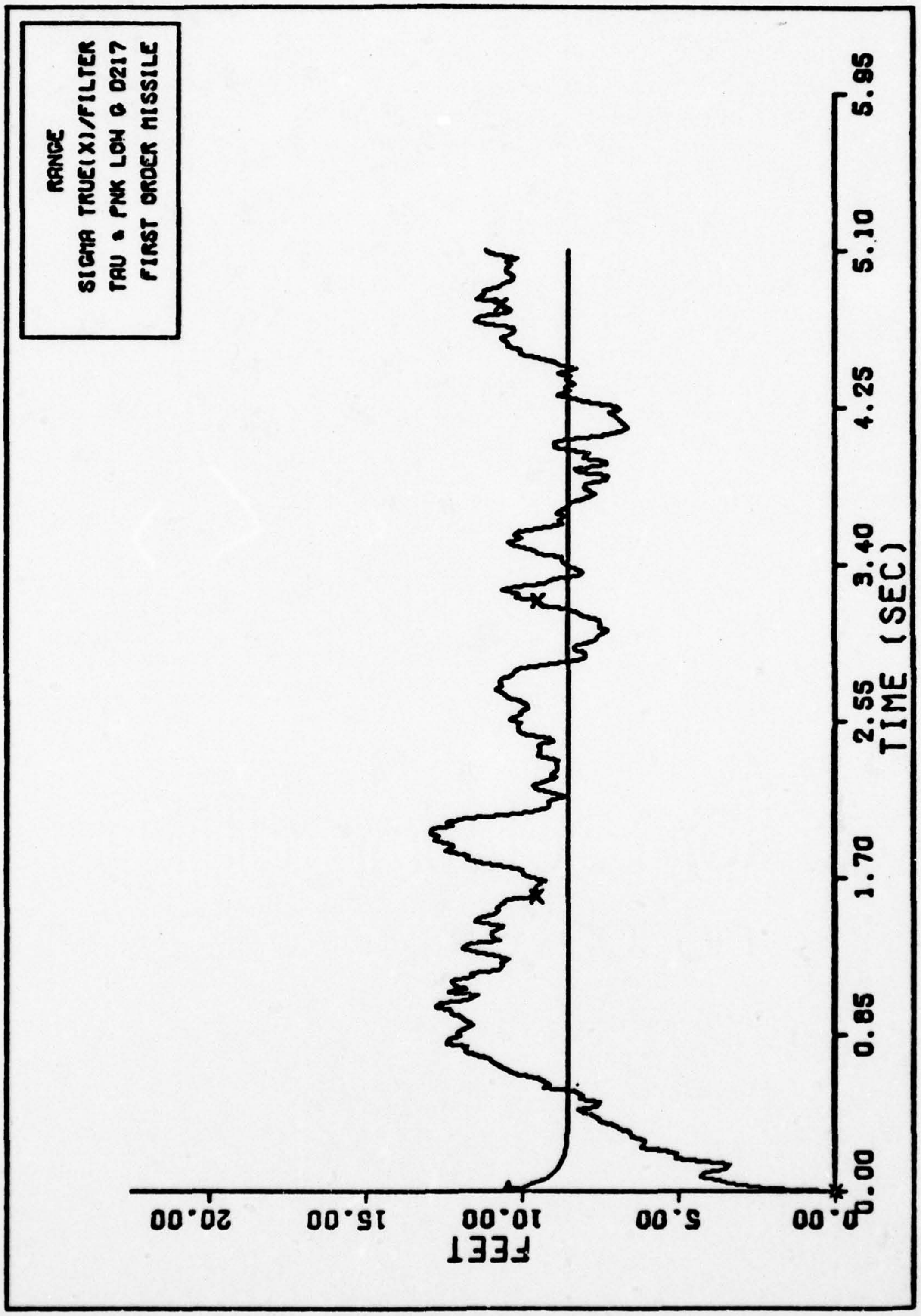

Fig. 250. RANGE SIGMAS FIRST ORDER

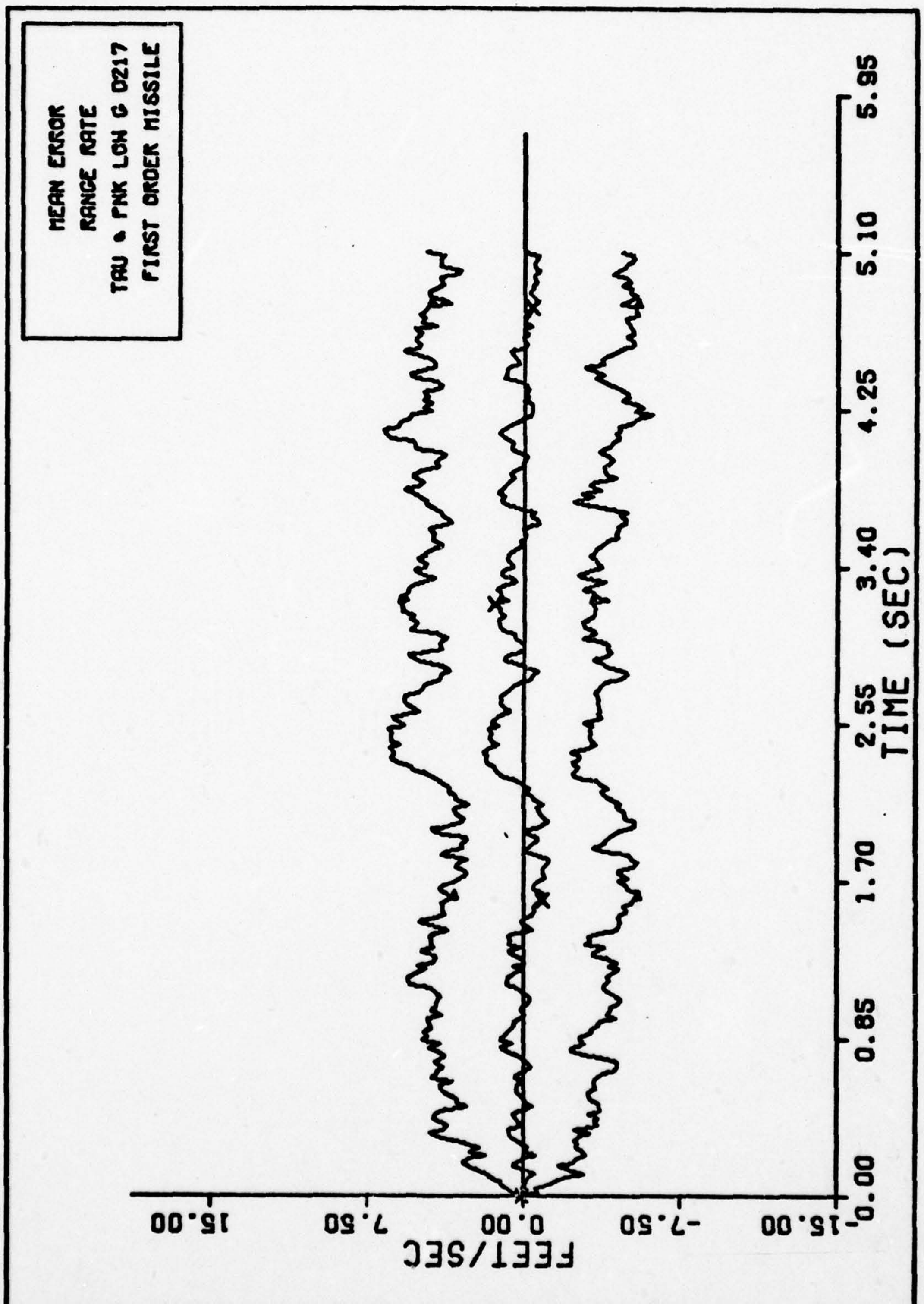

Fig. 251. RANGE RATE FIRST ORDER MISSILE

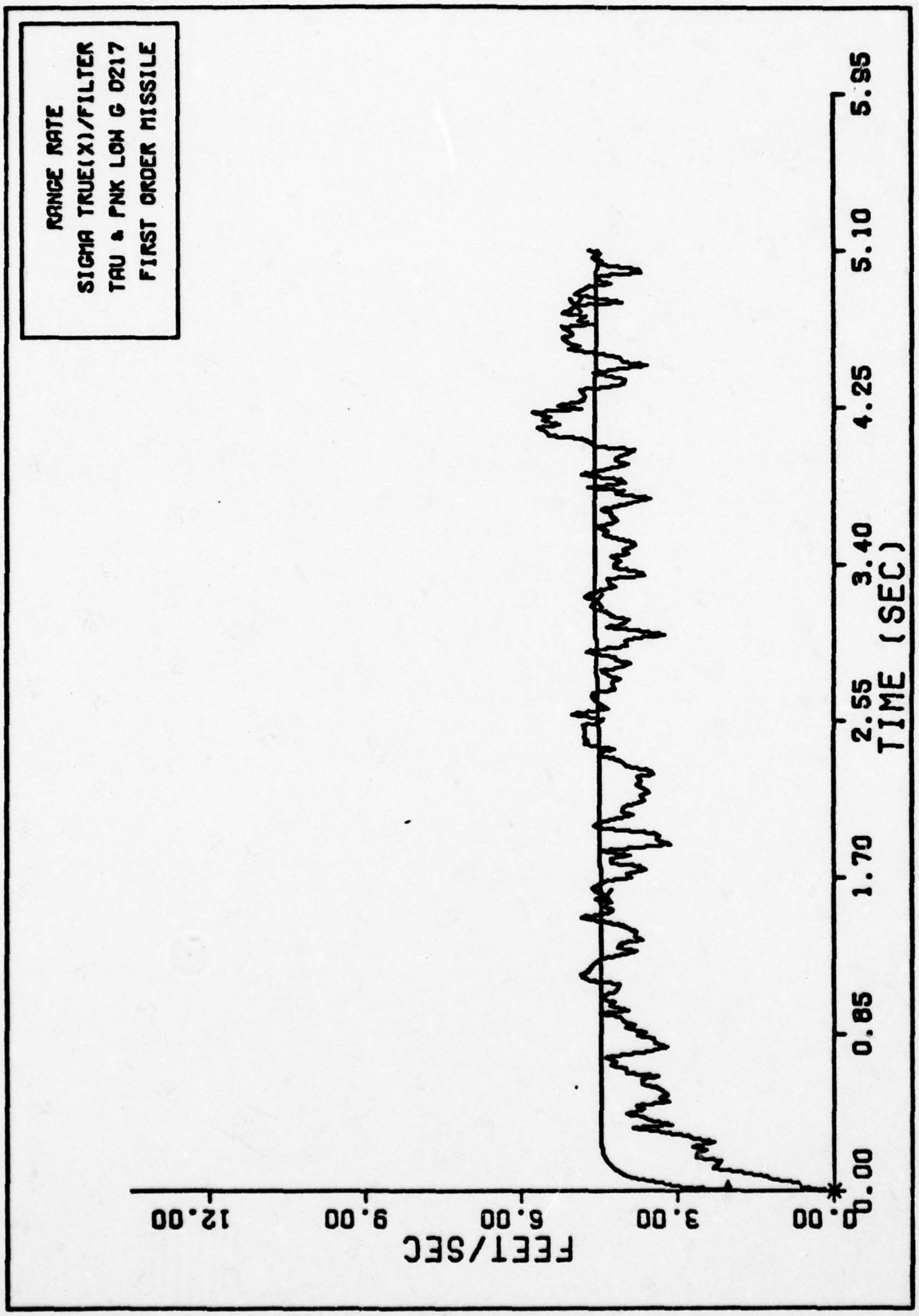

Fig. 252. RANGE RATE SIGMAS FIRST ORDER

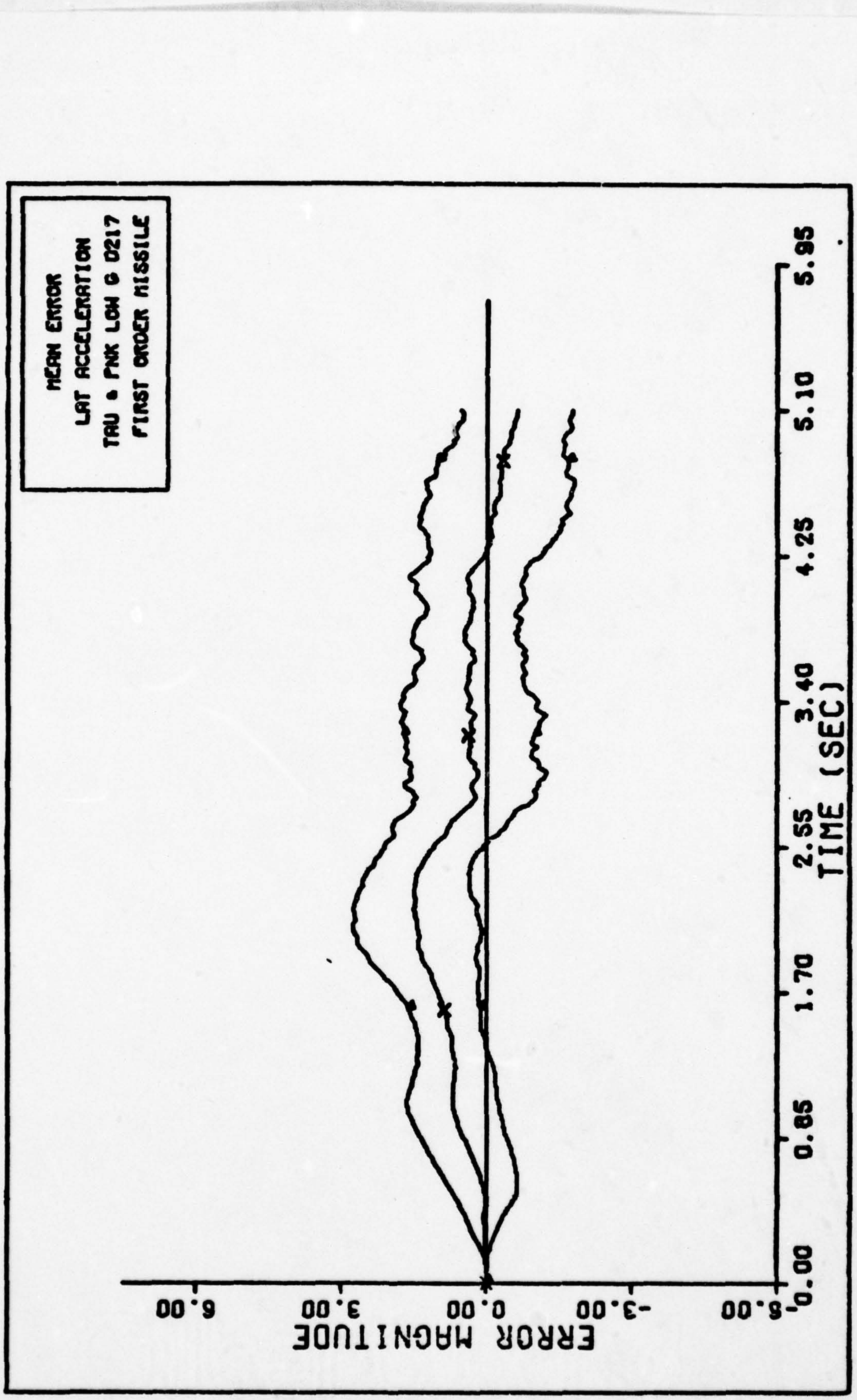

Fig. 253. LAT ACCELERATION FIRST ORDER MISSILE

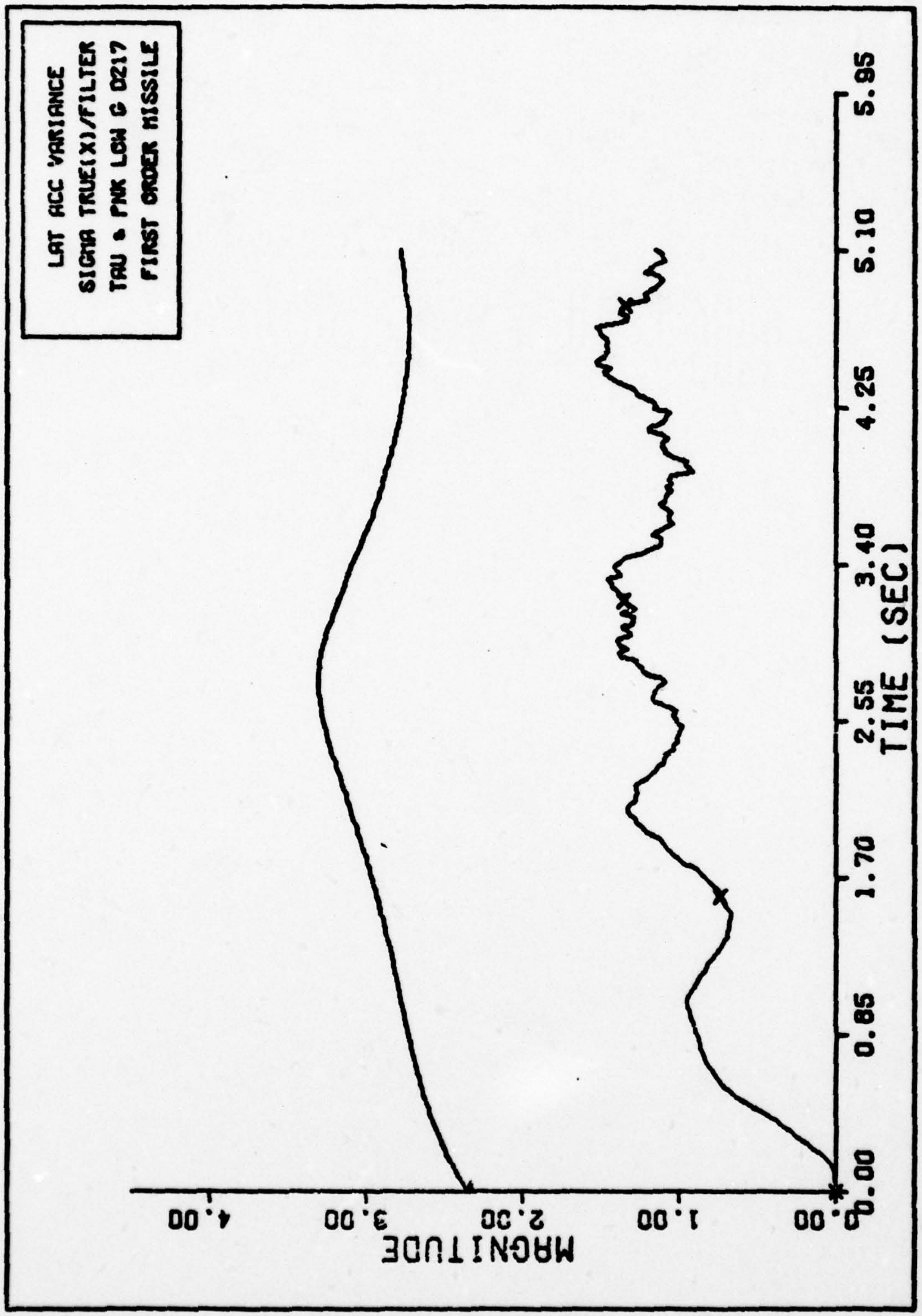

Fig. 254. LAT ACCELERATION SIGMAS FIRST ORDER

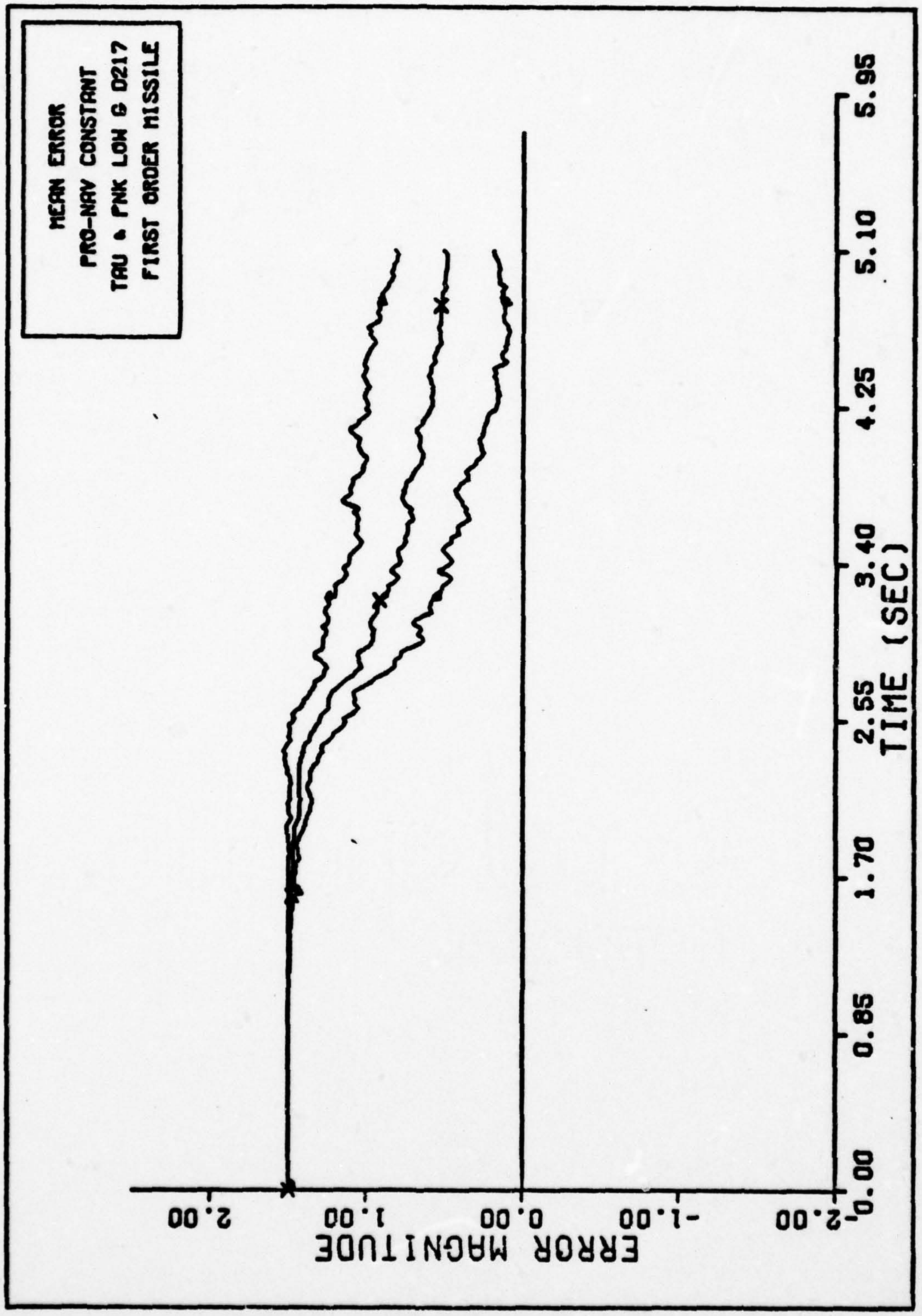

Fig. 255. PRO-NAV CONSTANT FIRST ORDER MISSILE

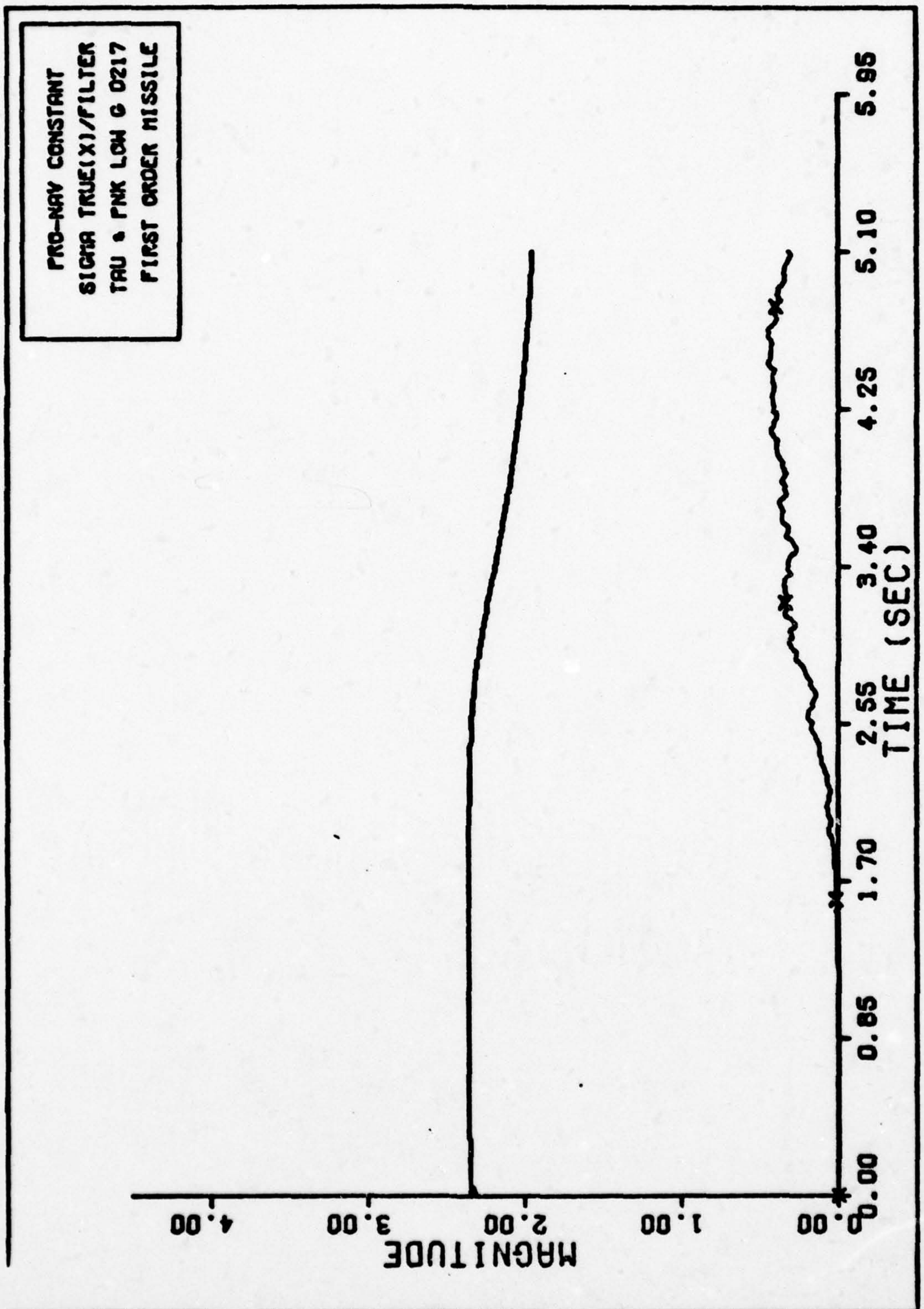

Fig. 256. -RO-NAV CONSTANT SIGMAS FIRST ORDER

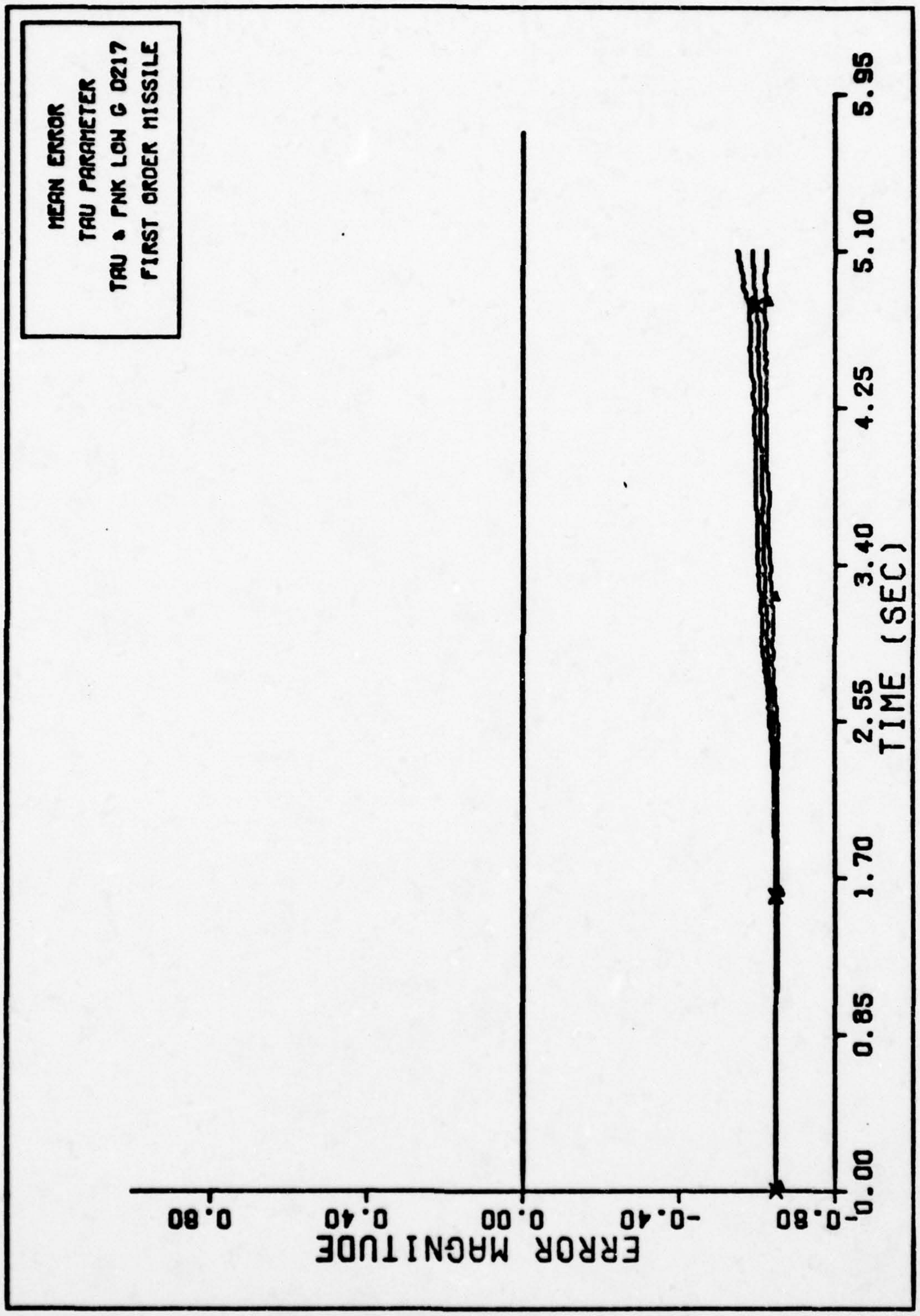

Fig. 257. TAU PARAMETER FIRST ORDER MISSILE

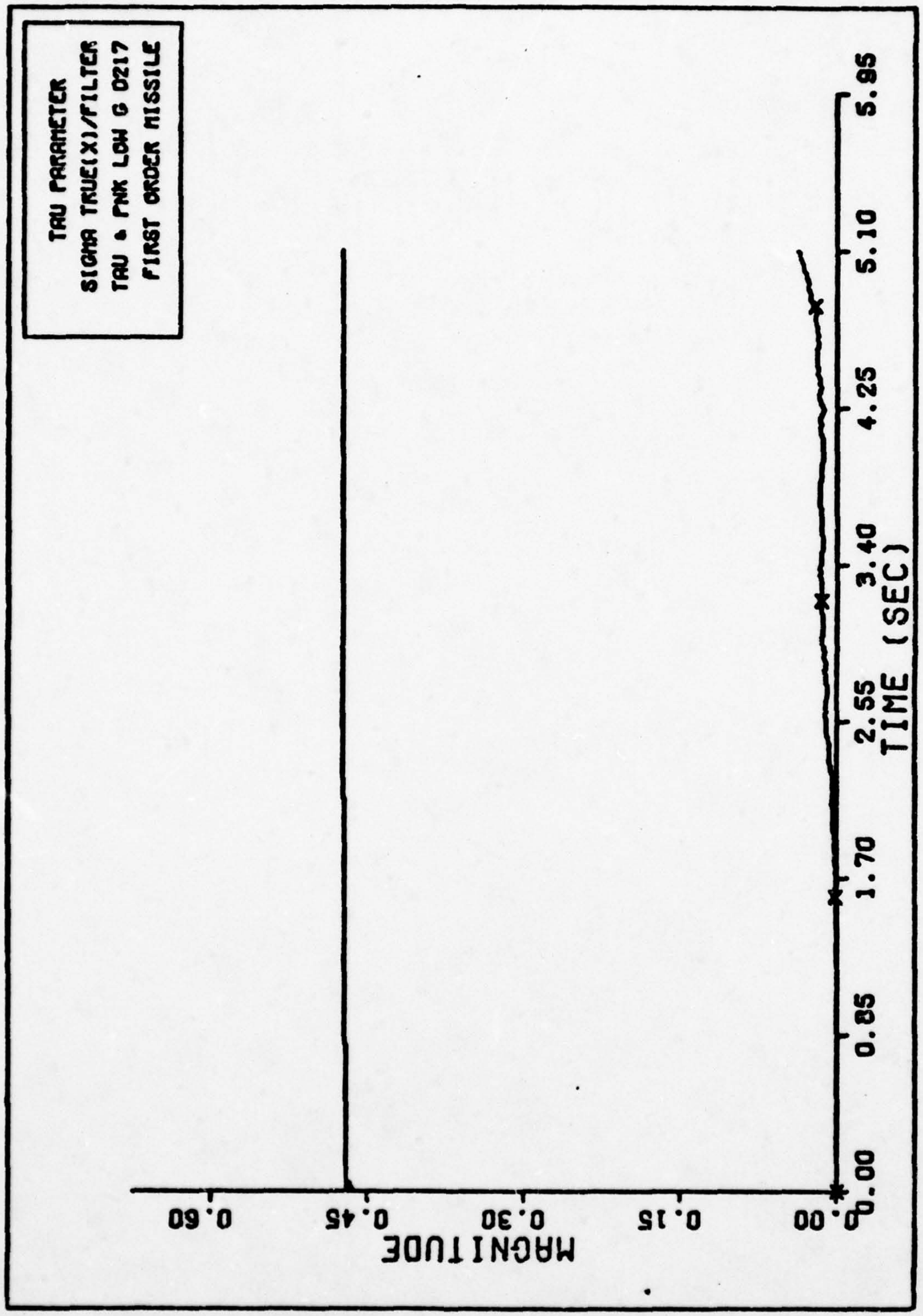

Fig. 258. TAU PARAMETER SIGMAS FIRST ORDER

$\underline{n}$, $\underline{\tau_f}$, and M/S Estimation

The initial state estimates and the tuning parameters for this case are

$$
\begin{aligned}
V^I_{mx}(0) &= 1225.7 \text{ fps} \\
\dot{\theta}_T(0) &= 4.363345 \text{ radians} \\
R(0) &= 10000. \text{ feet} \\
\dot{R}(0) &= -2122. \text{ fps} \\
a_L(0) &= 0. \\
n(0) &= 6. \\
\tau_f(0) &= .3 \text{ seconds} \\
M/S(0) &= 15. \text{ slugs/ft}^2
\end{aligned}
$$

$$
\underline{R} = \begin{bmatrix} 2.E-5 & 0. & 0. \\ 0. & 500. & 0. \\ 0. & 0. & 100. \end{bmatrix}
$$

$$
\underline{P}_0 = \begin{bmatrix}
100. & 0. & 0. & 0. & 0. & 0. & 0. & 0. \\
0. & 1.E-8 & 0. & 0. & 0. & 0. & 0. & 0. \\
0. & 0. & 101. & 0. & 0. & 0. & 0. & 0. \\
0. & 0. & 0. & 4. & 0. & 0. & 0. & 0. \\
0. & 0. & 0. & 0. & 5. & 0. & 0. & 0. \\
0. & 0. & 0. & 0. & 0. & 5. & 0. & 0. \\
0. & 0. & 0. & 0. & 0. & 0. & .2 & 0. \\
0. & 0. & 0. & 0. & 0. & 0. & 0. & 5.
\end{bmatrix}
$$

$$
\underline{Q} = \begin{bmatrix}
250. & 0. & 0. & 0. & 0. & 0. & 0. & 0. \\
0. & 1.E\text{-}6 & 0. & 0. & 0. & 0. & 0. & 0. \\
0. & 0. & 500. & 0. & 0. & 0. & 0. & 0. \\
0. & 0. & 0. & 200. & 0. & 0. & 0. & 0. \\
0. & 0. & 0. & 0. & 5. & 0. & 0. & 0. \\
0. & 0. & 0. & 0. & 0. & .01 & 0. & 0. \\
0. & 0. & 0. & 0. & 0. & 0. & .001 & 0. \\
0. & 0. & 0. & 0. & 0. & 0. & 0. & 3.
\end{bmatrix}
$$

These plots were generated to demonstrate the first order filter's ability to estimate all three parameters and all five dynamic states simultaneously. The states were not initialized with any error. The parameter were initialized in the filter as follows

$$n(0) = 6.0 \quad , \text{ true value } = 4.5$$

$$\tau_f(0) = 0.3 \text{ seconds} \quad , \text{ true value } = .85 \text{ seconds}$$

$$M/S(0) = 15. \text{ slugs/ft}^2 \quad , \text{ true value } = 29.197 \text{ slugs/ft}^2$$

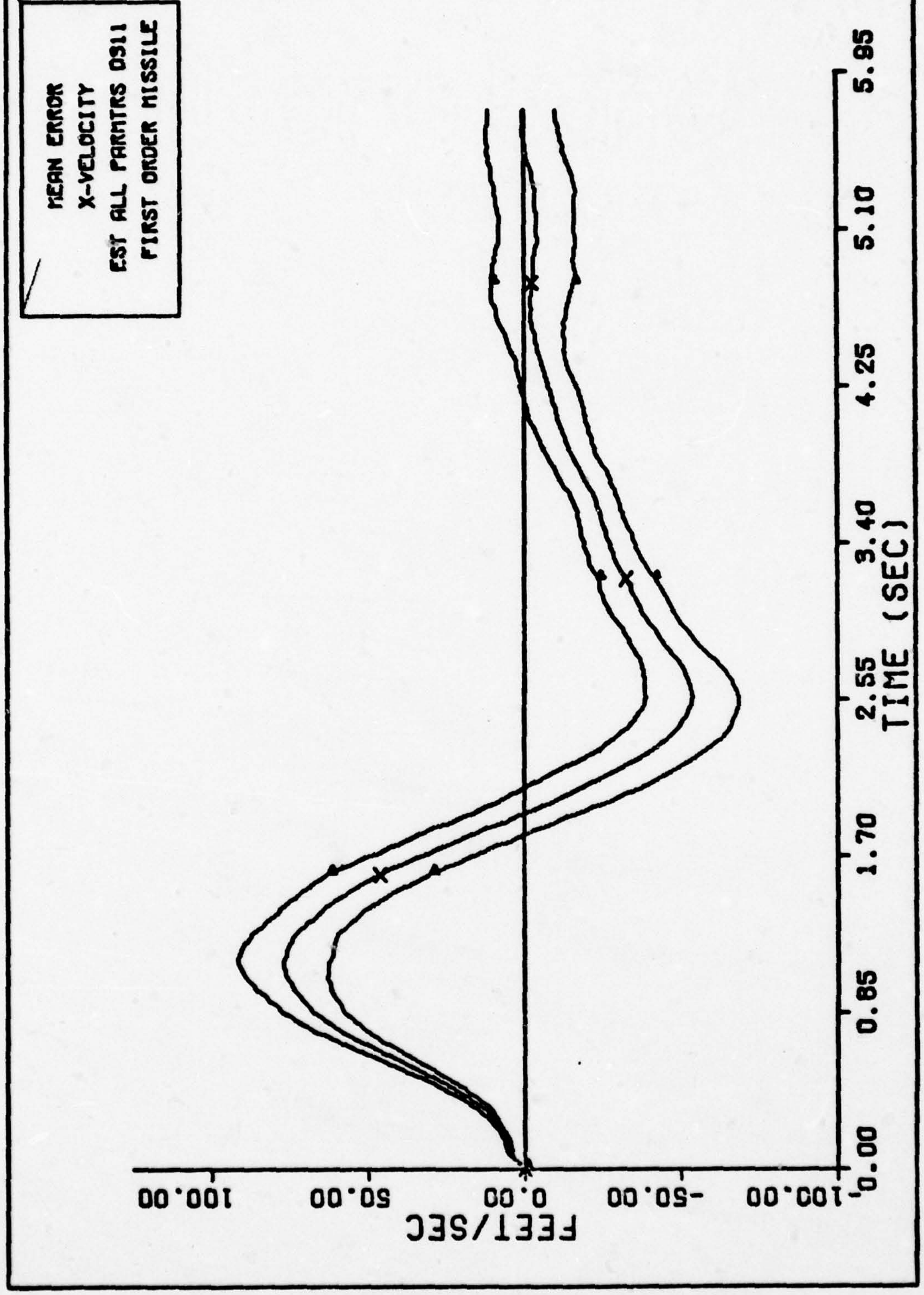

Fig. 259. X-VELOCITY FIRST ORDER MISSILE

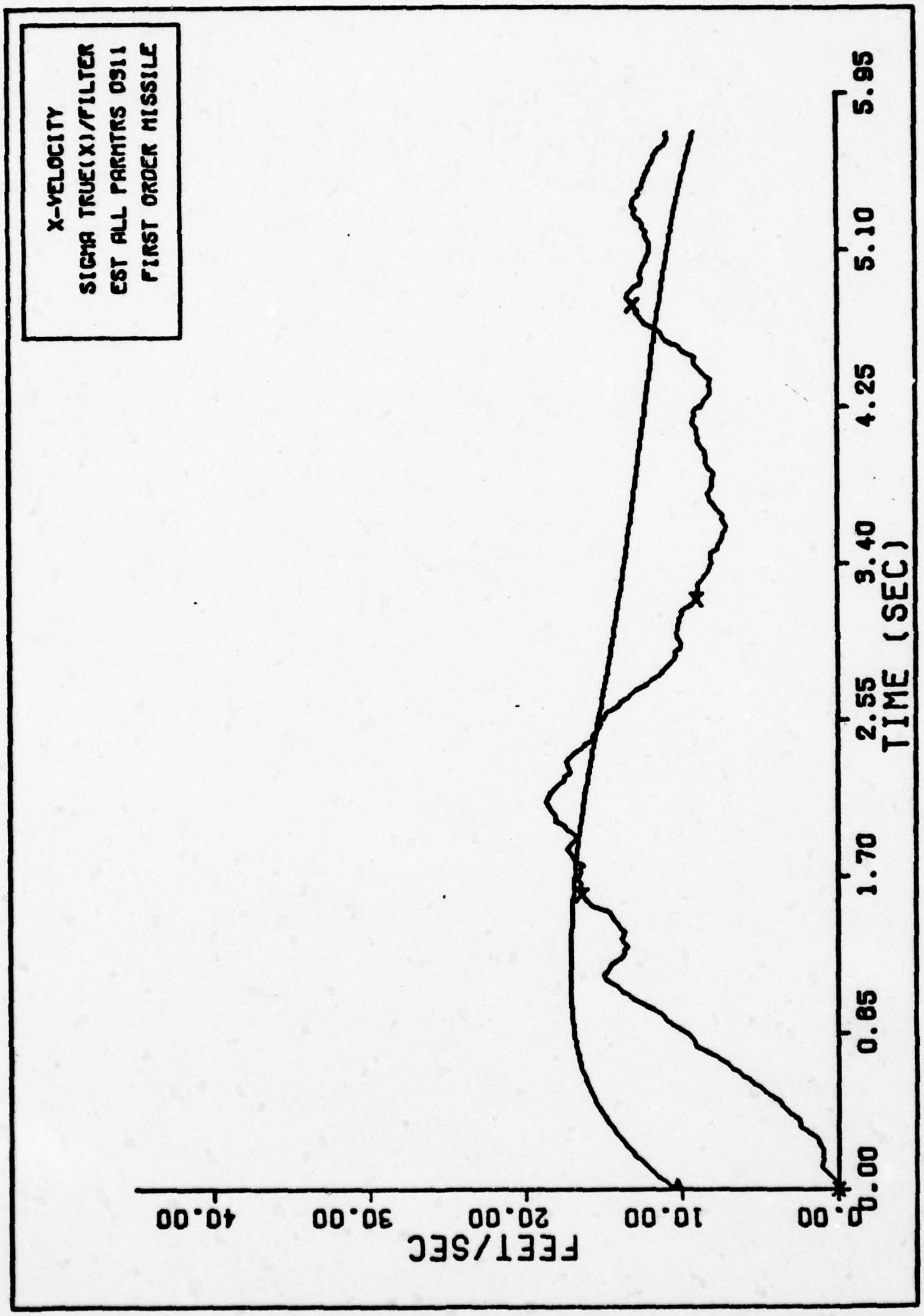

Fig. 260. X-VELOCITY SIGMAS FIRST ORDER

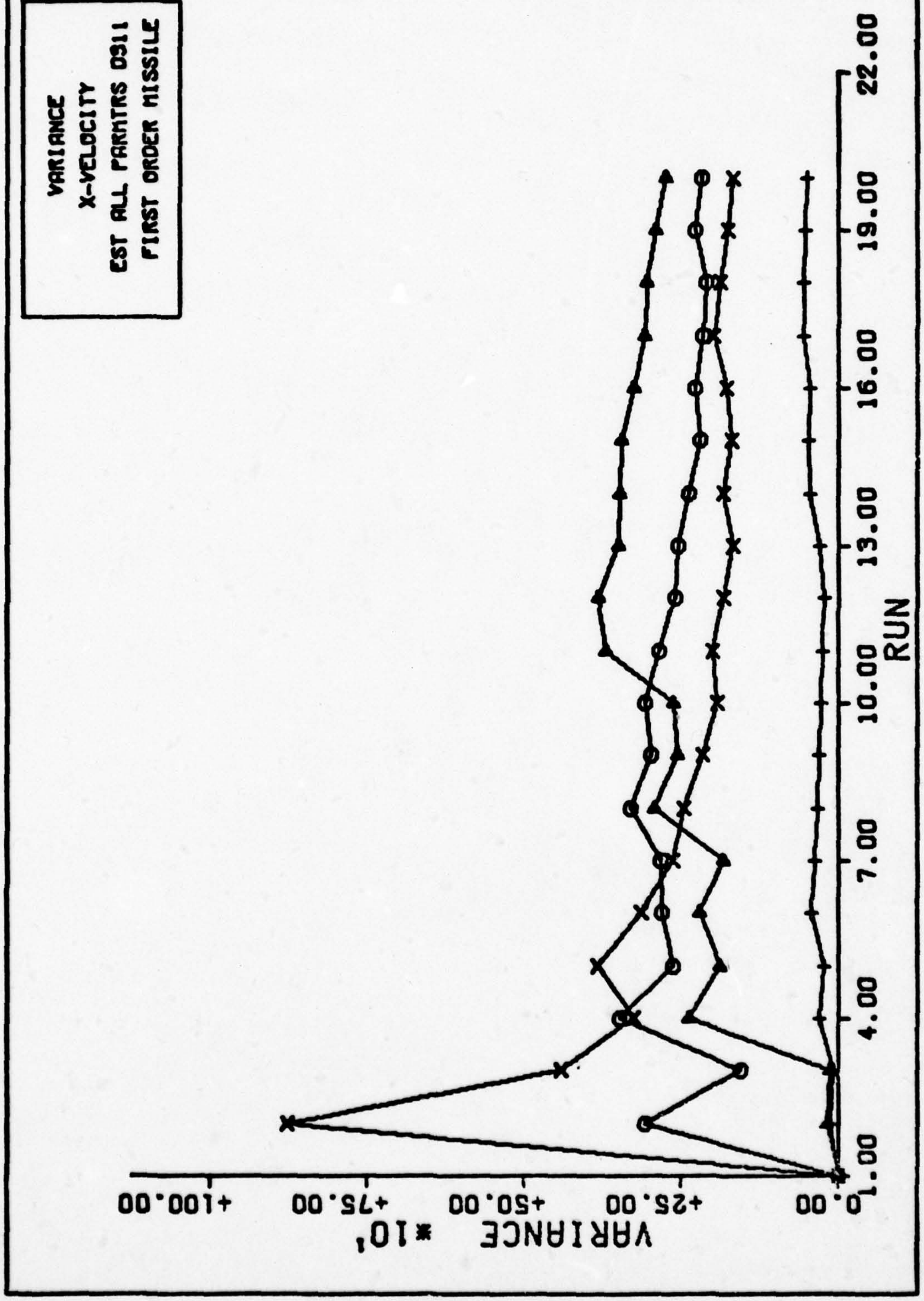

Fig. 261. VARIANCE CONVERGENCE

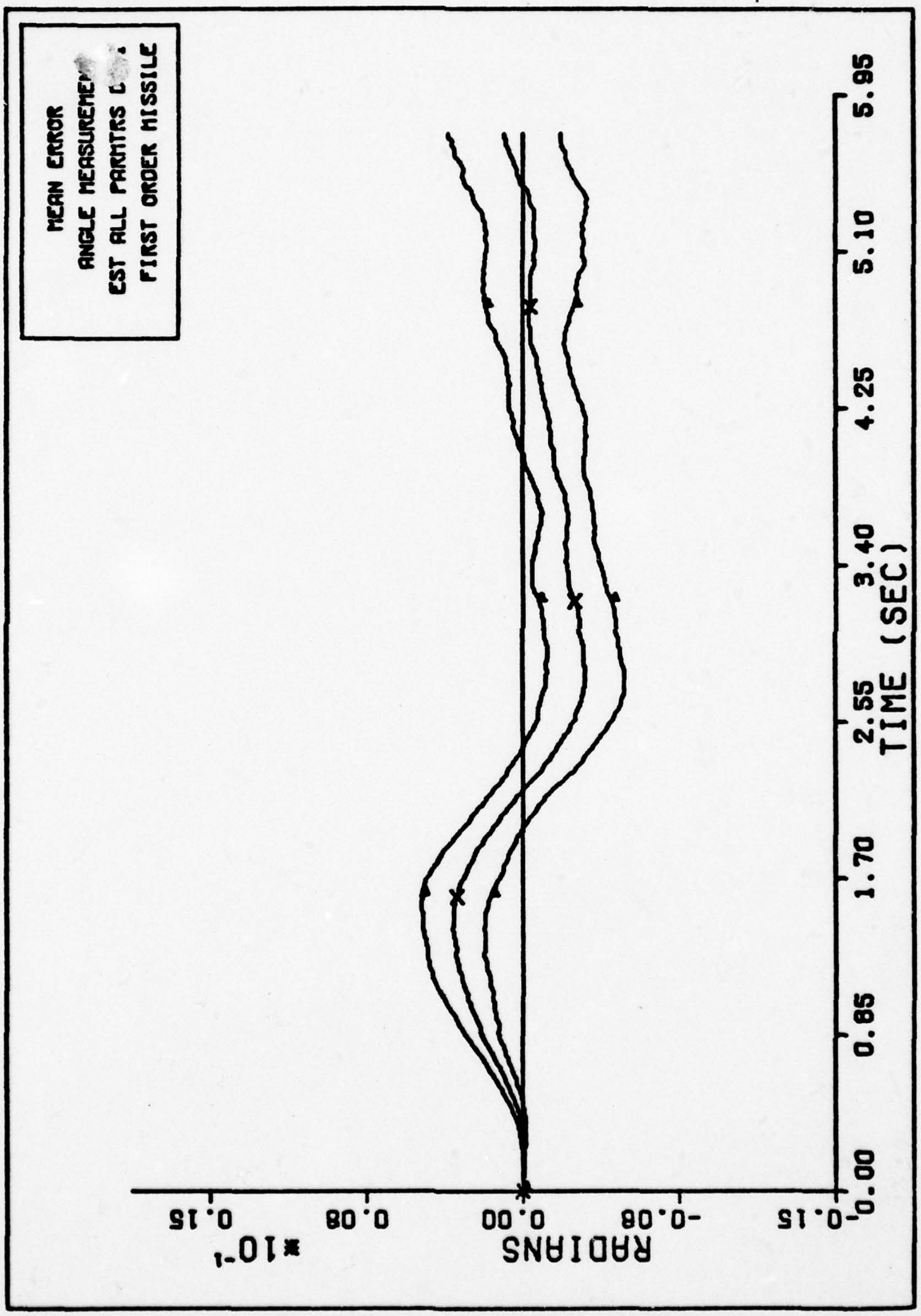

Fig. 262. ANGLE MEASUREMENT FIRST ORDER MISSILE

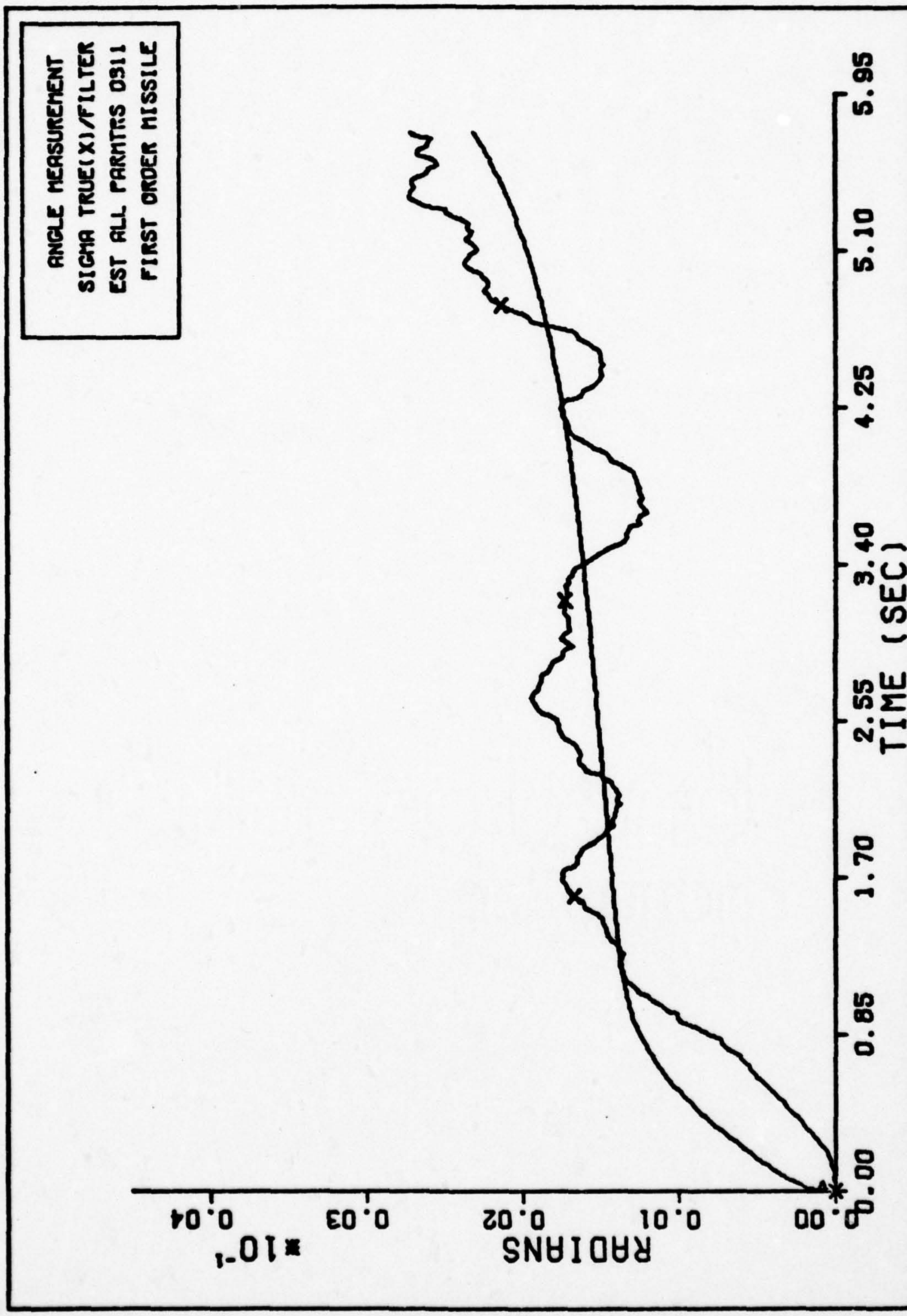

Fig. 263. ANGLE MEASUREMENT SIGMAS FIRST ORDER

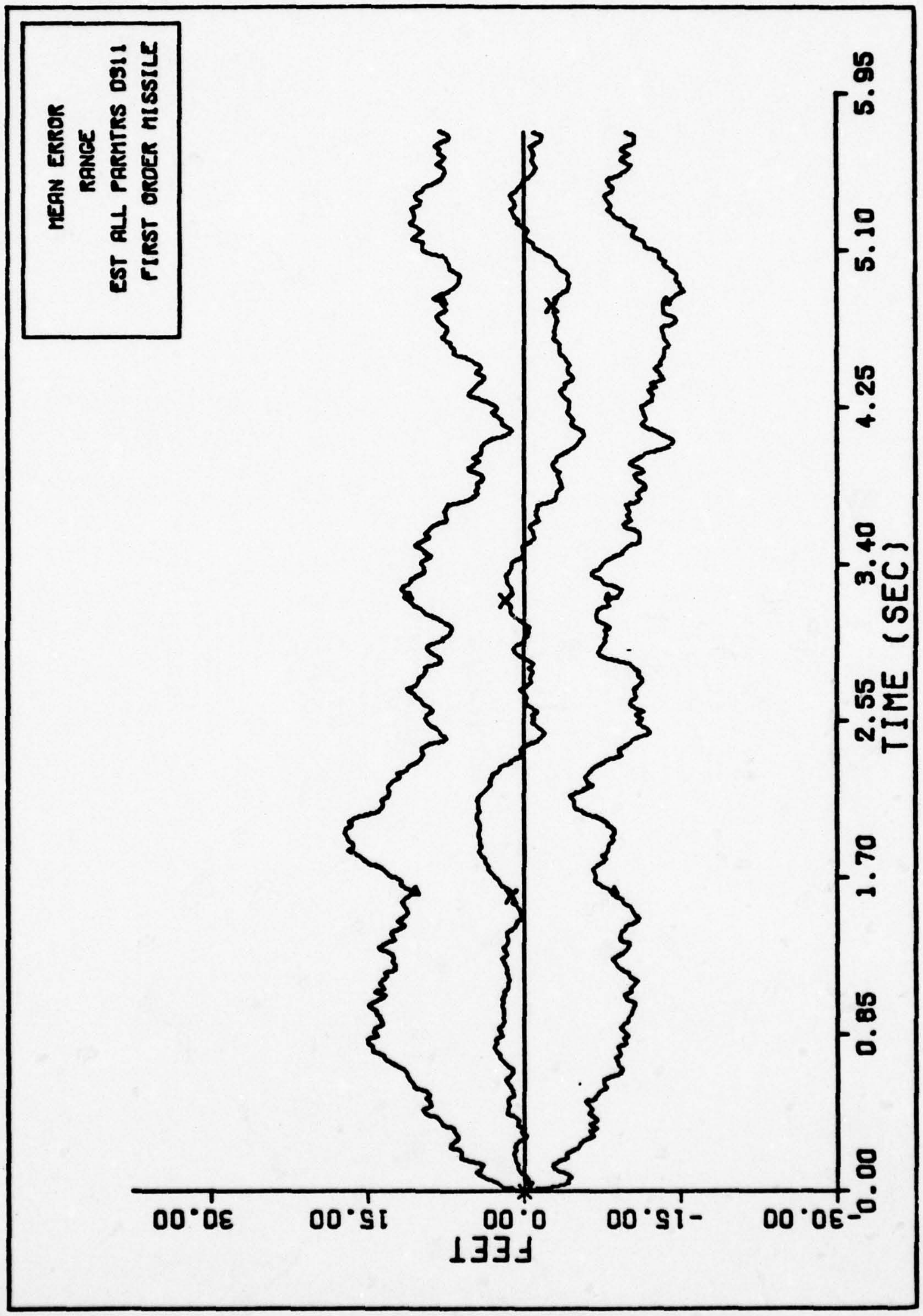

Fig. 264. RANGE FIRST ORDER MISSILE

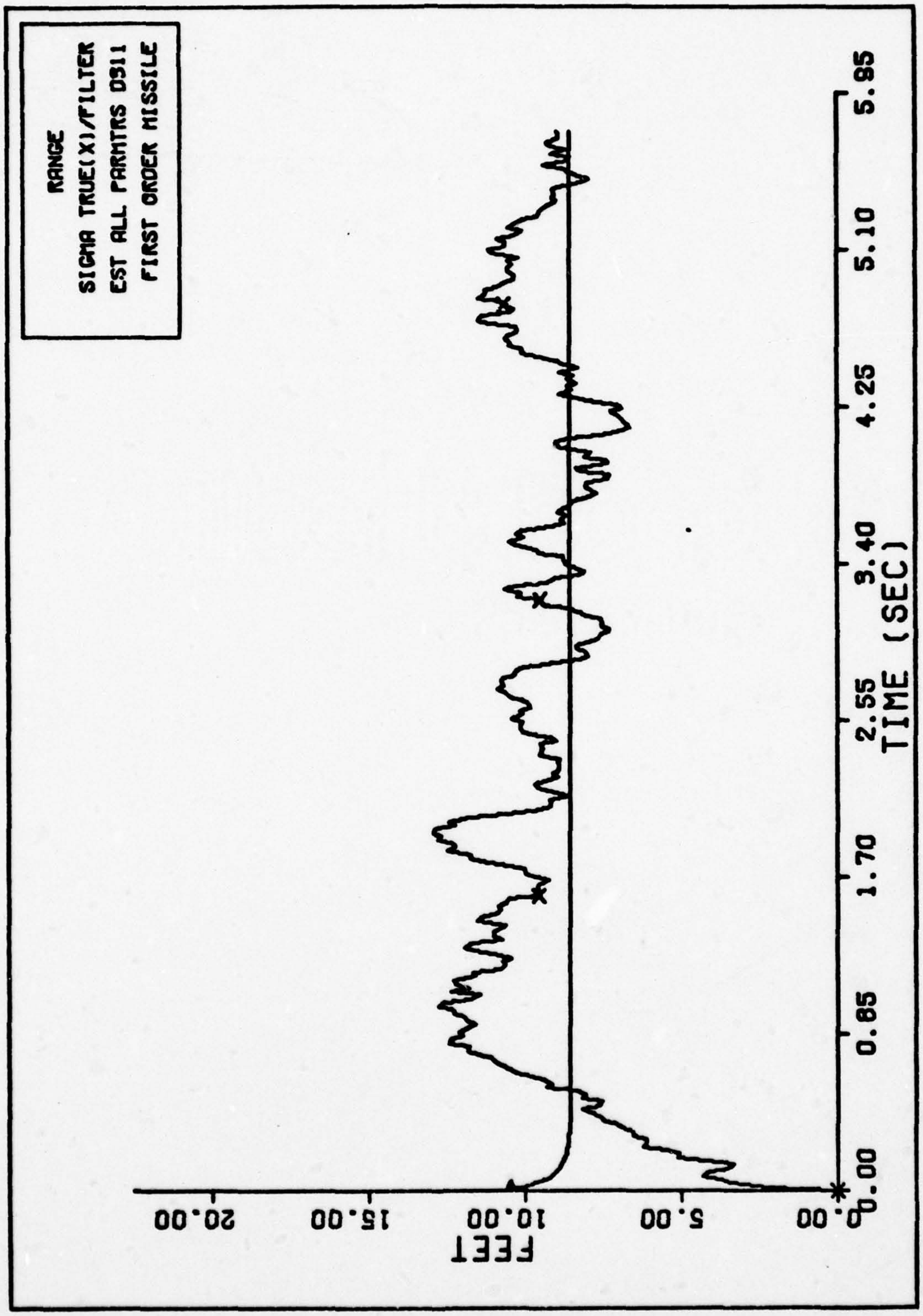

Fig. 265. RANGE SIGMAS FIRST ORDER

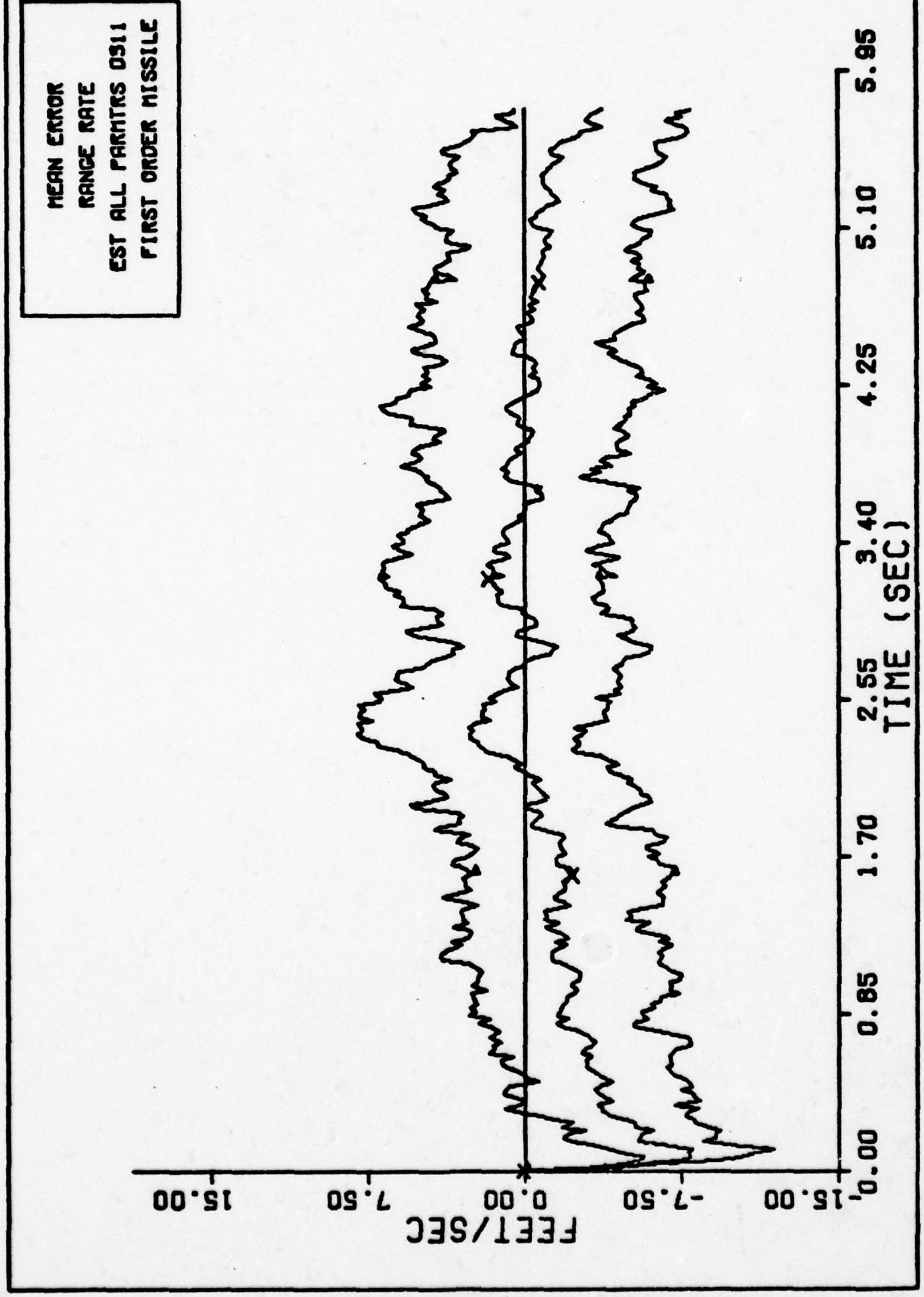

Fig. 266. RANGE RATE FIRST ORDER MISSILE

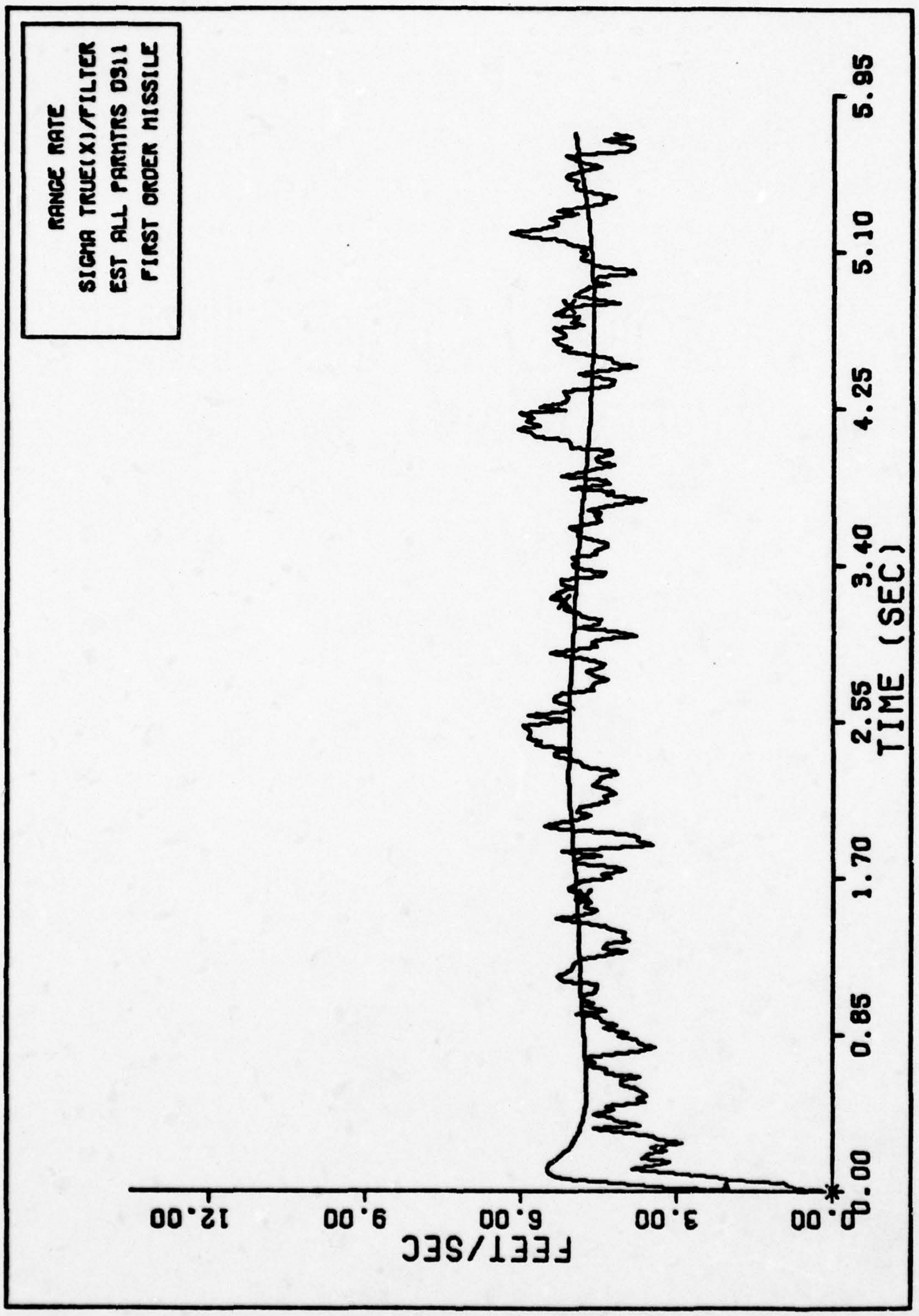

Fig. 267. RANGE RATE SIGMAS FIRST ORDER

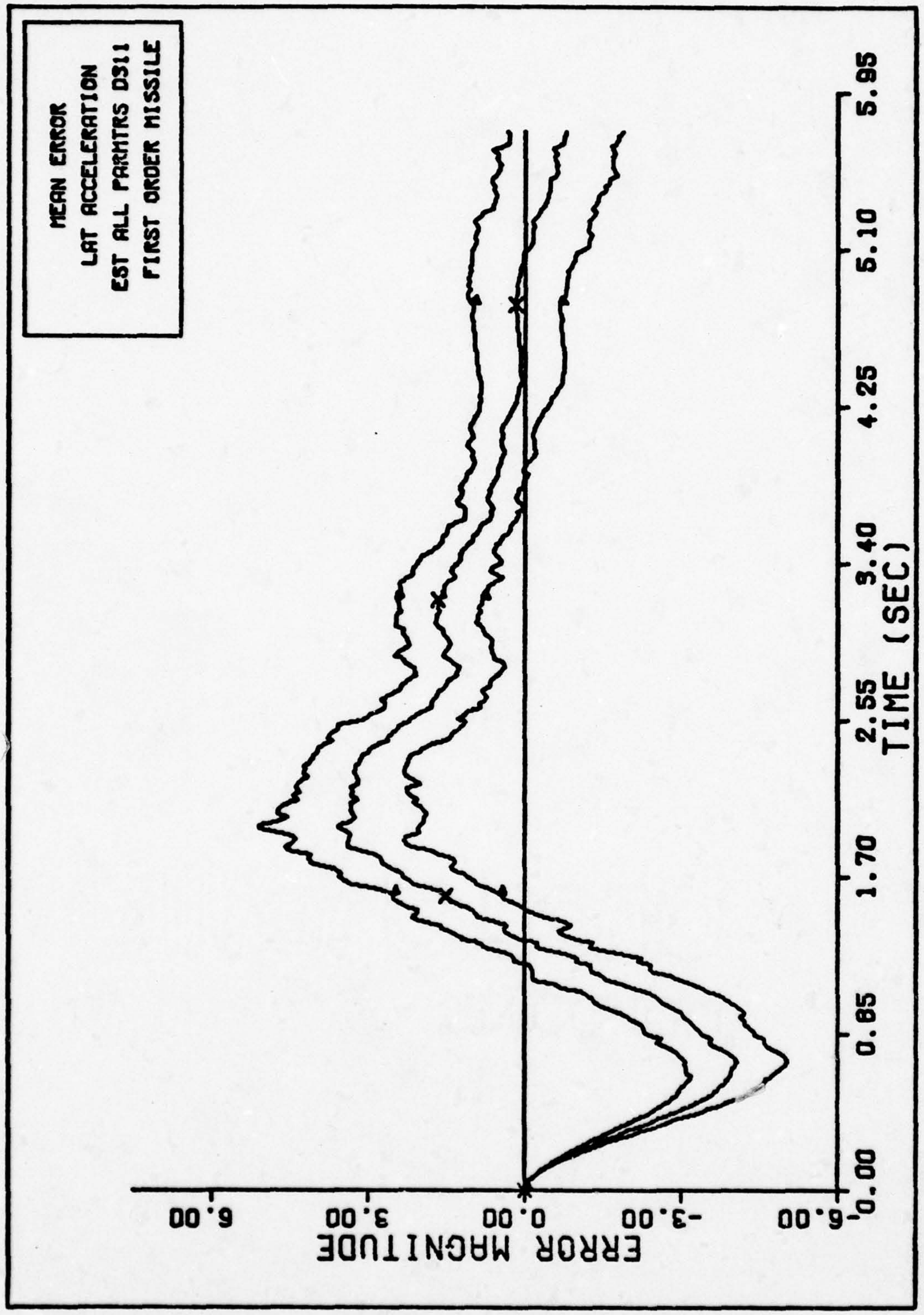

Fig. 268. LAT ACCELERATION FIRST ORDER MISSILE

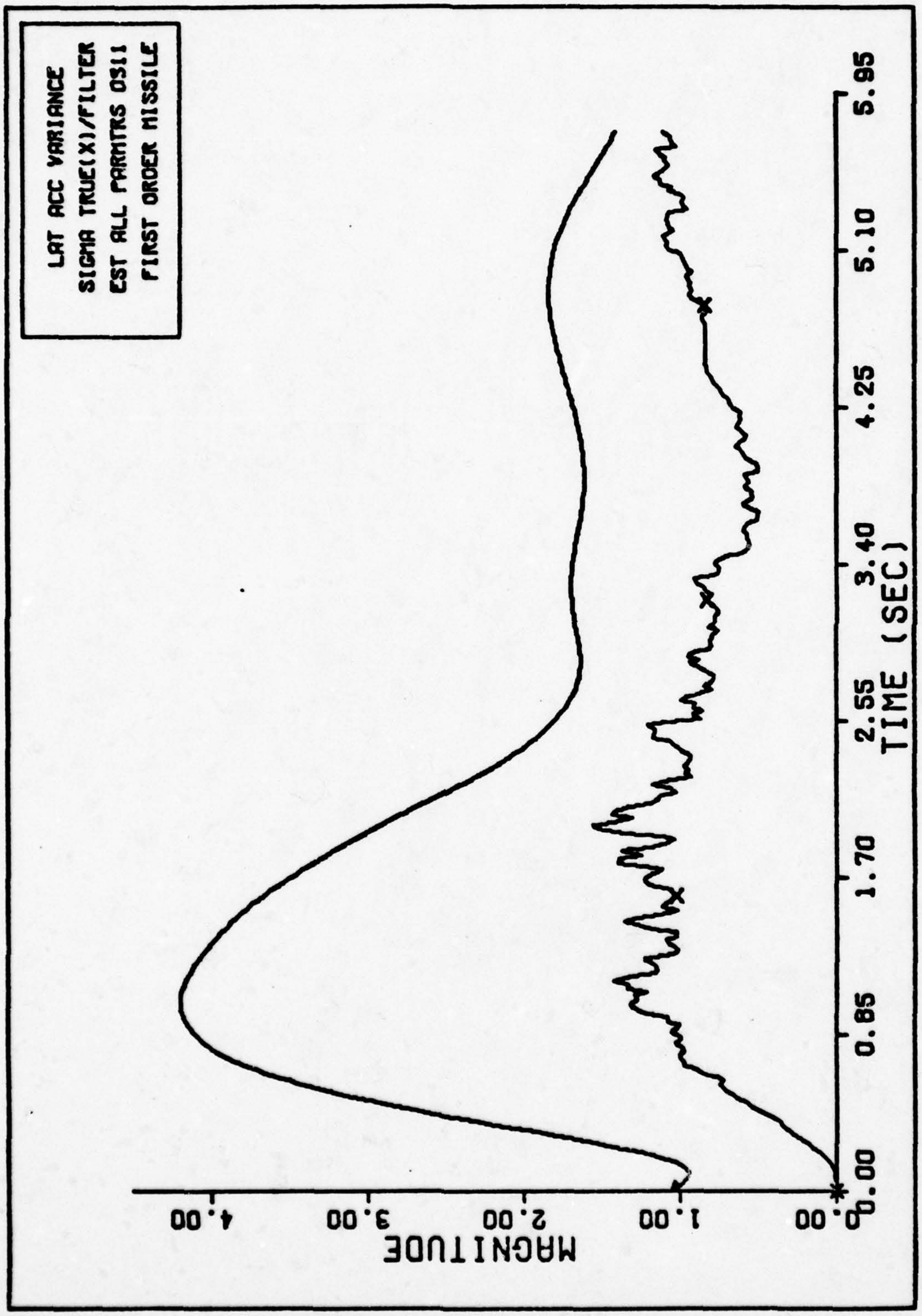

Fig. 269. LAT ACCELERATION SIGMAS FIRST ORDER

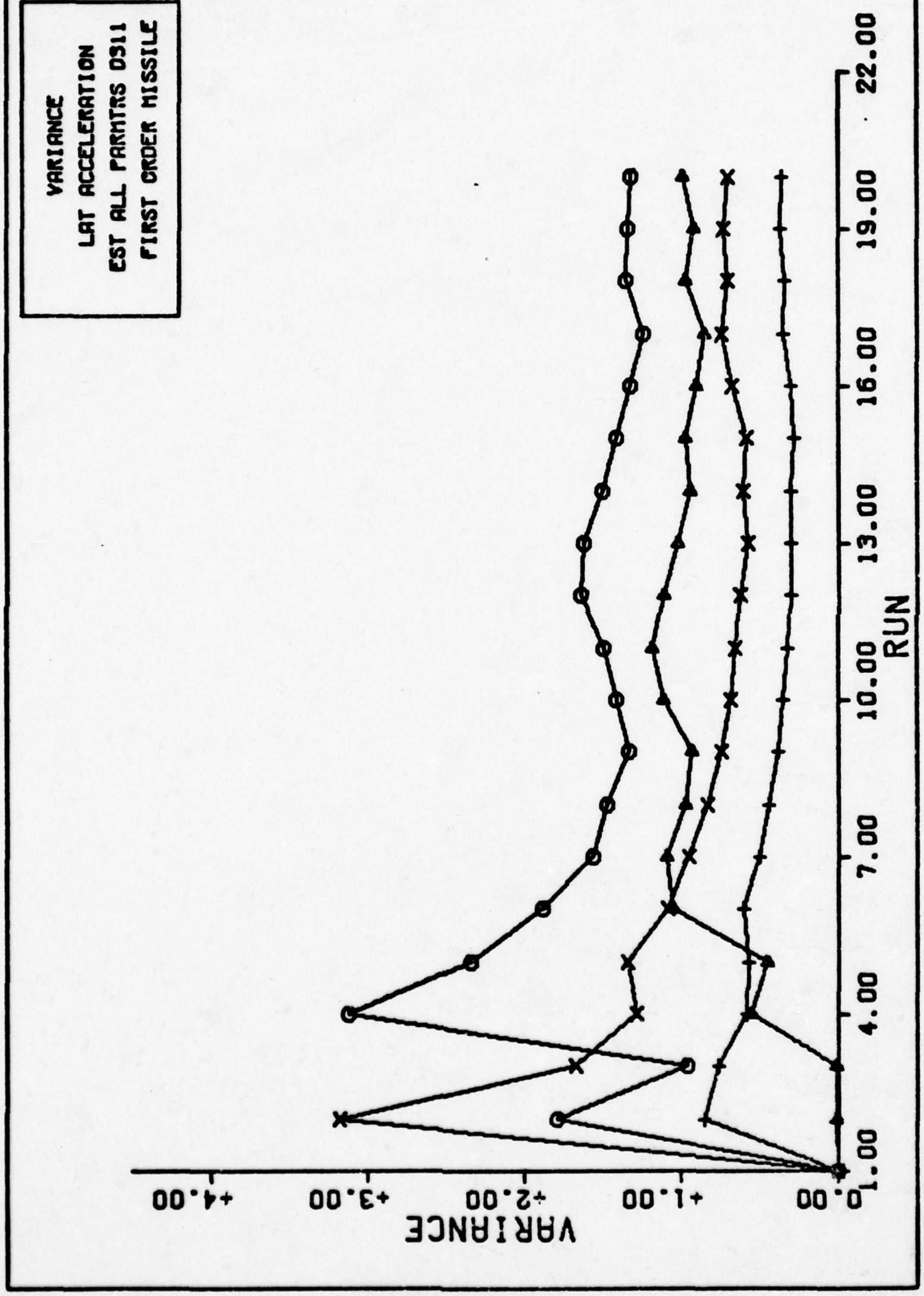

Fig. 270. VARIANCE CONVERGENCE

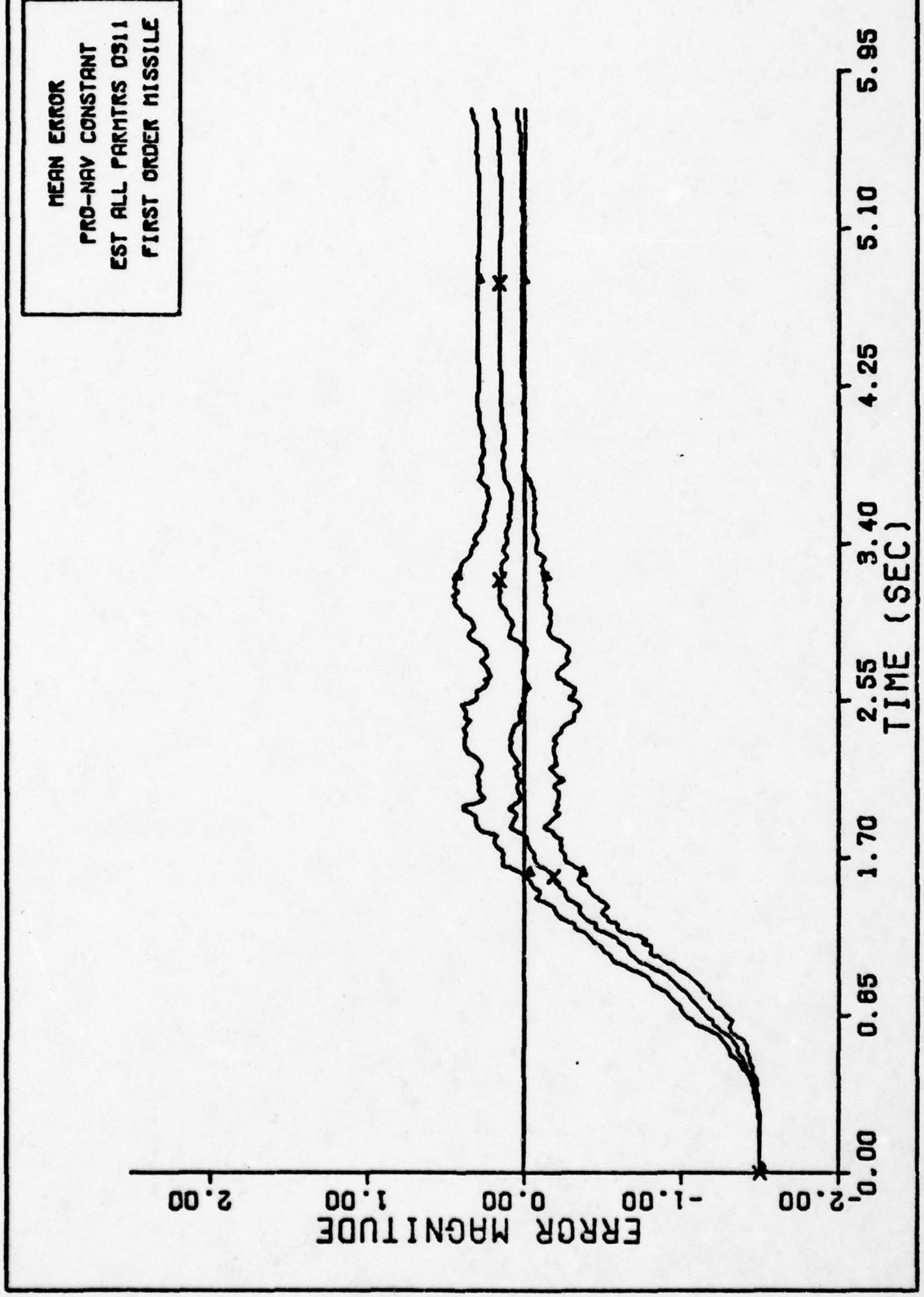

Fig. 271. PRO-NAV CONSTANT FIRST ORDER MISSILE

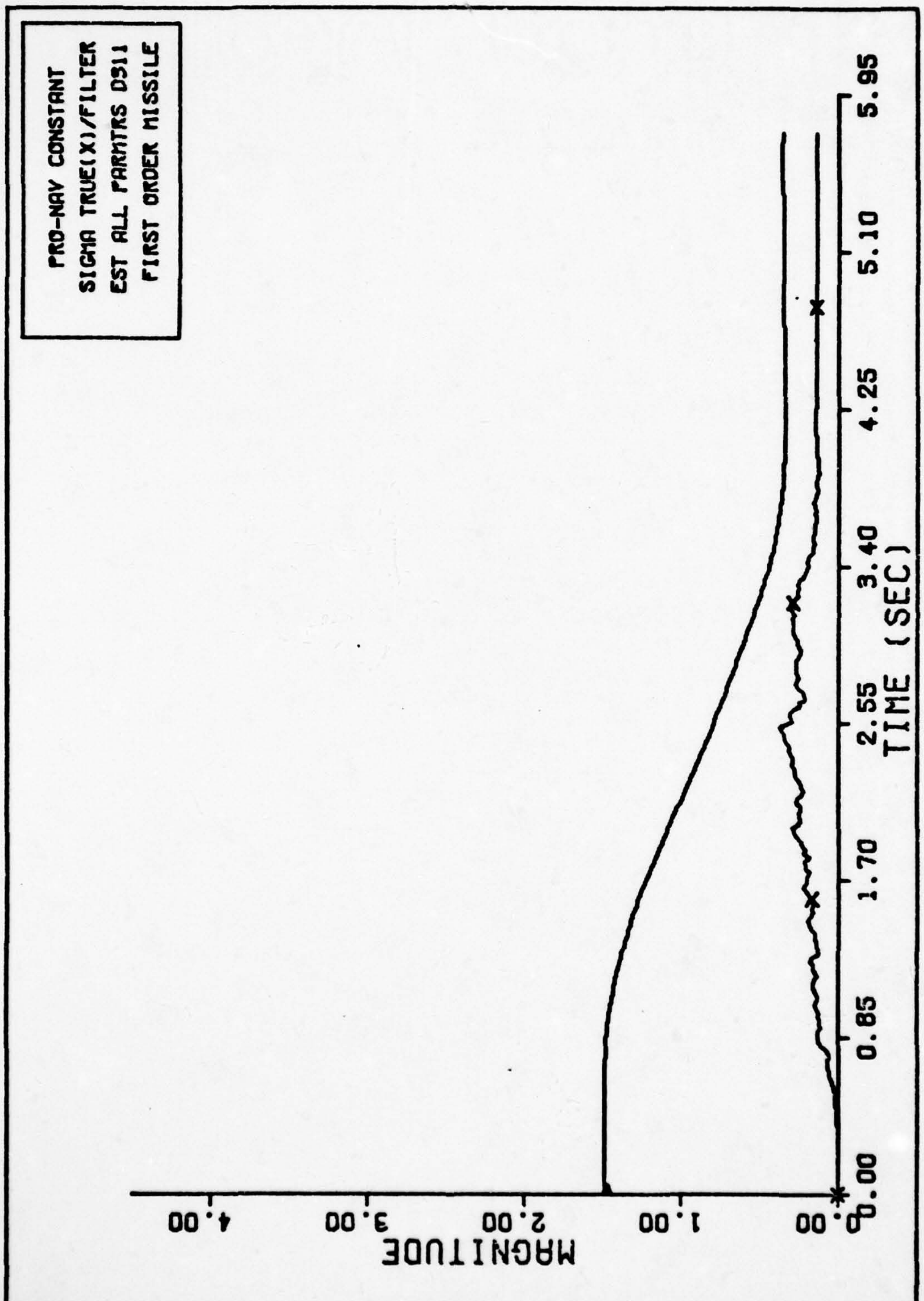

Fig. 272. PRO-NAV CONSTANT SIGMAS FIRST ORDER

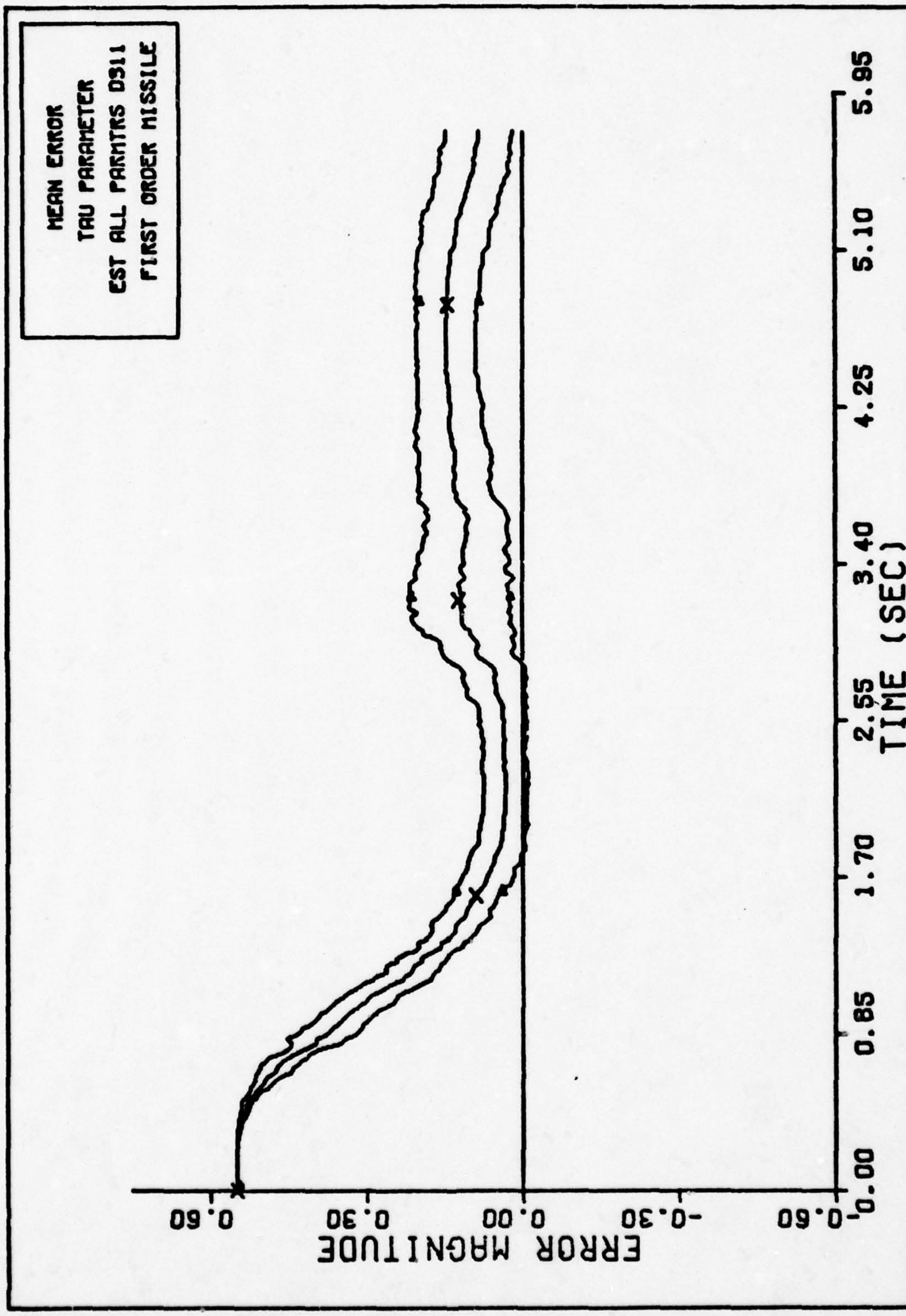

Fig. 273. TAU PARAMETER FIRST ORDER MISSILE

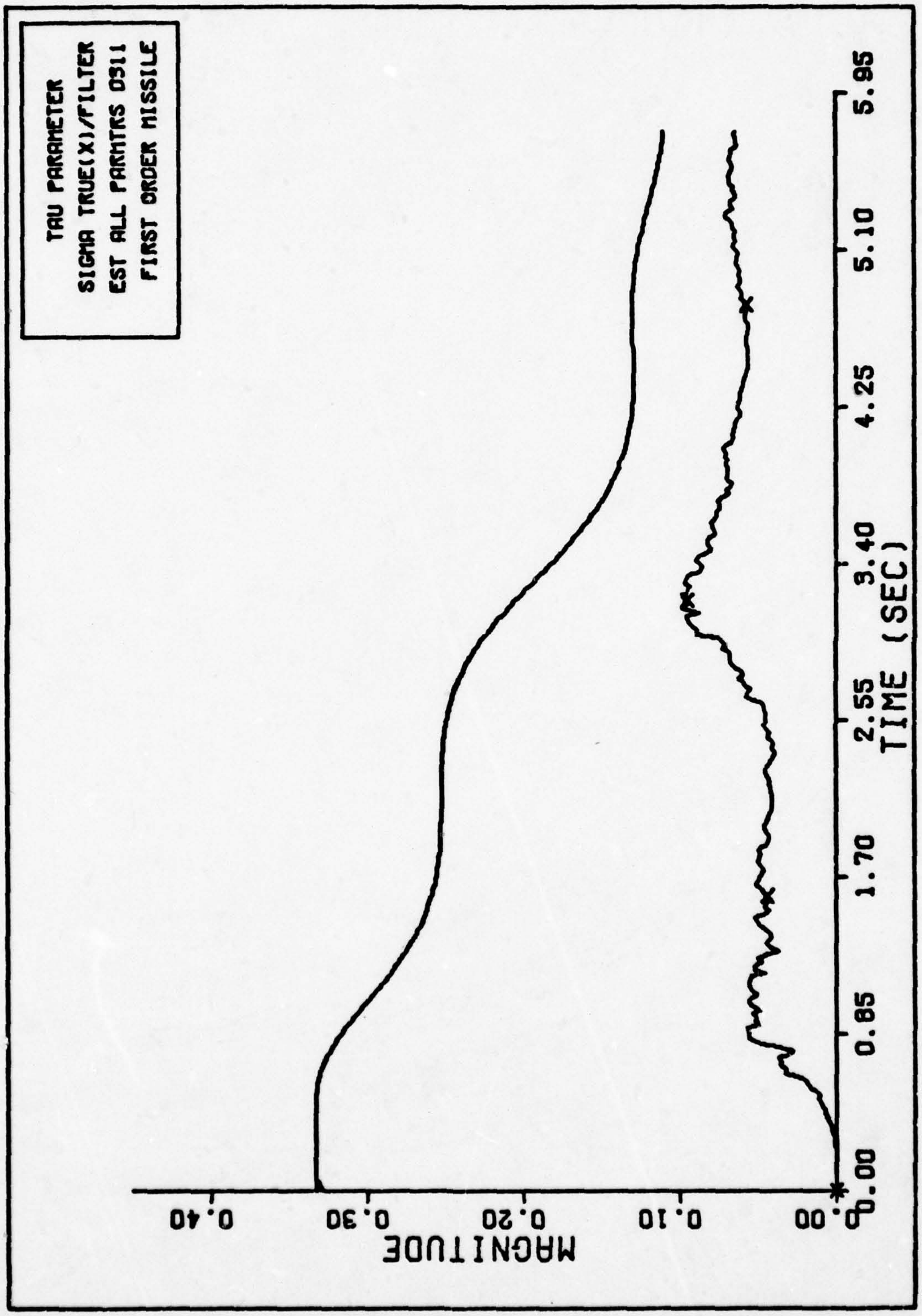

Fig. 274. TAU PARAMETER SIGMAS FIRST ORDER

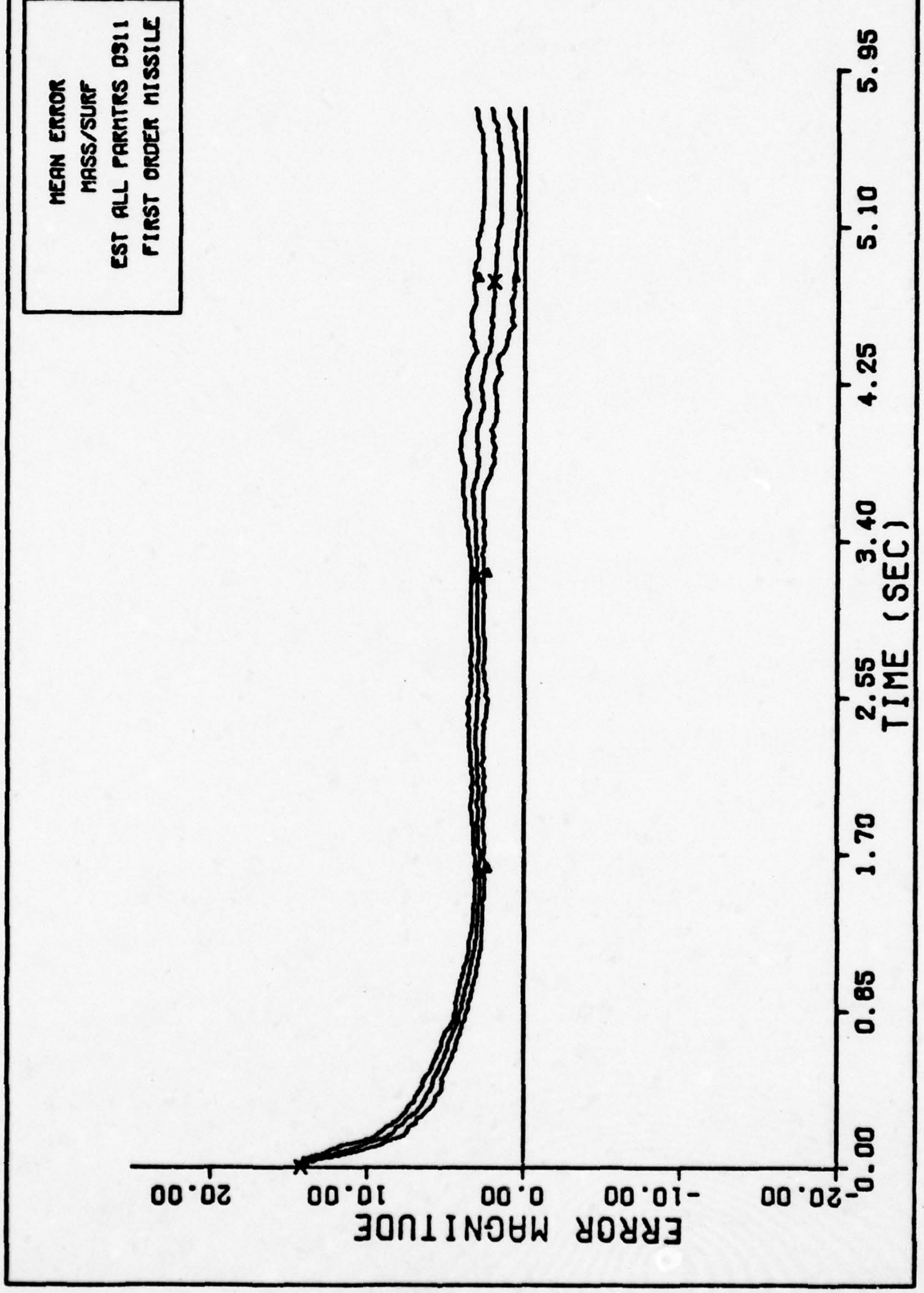

Fig. 275. MASS/SURF FIRST ORDER MISSILE

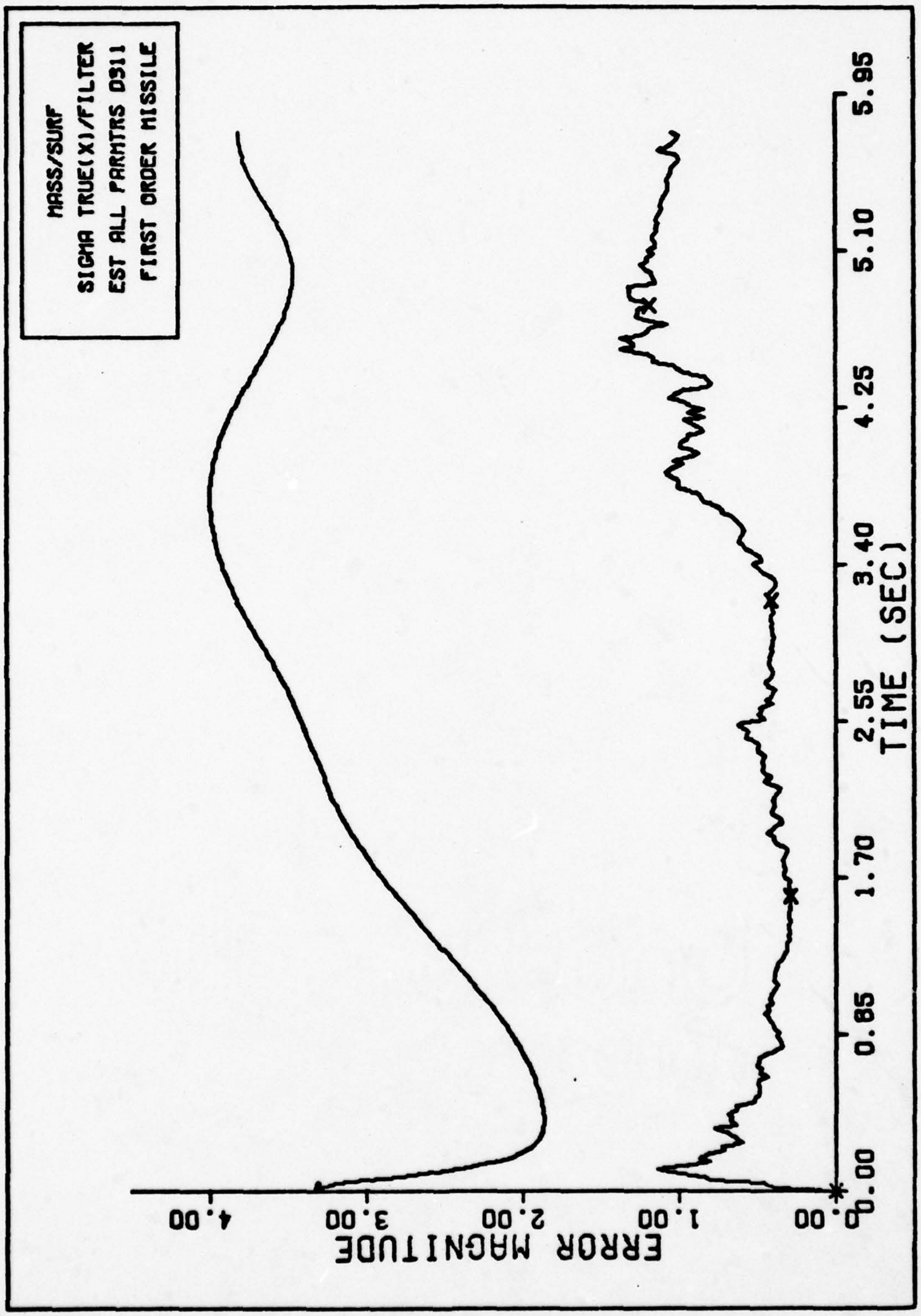

Fig. 276. MASS/SURF SIGMAS FIRST ORDER

$\underline{n}$, $\underline{\tau_f}$, and M/S Estimation with Initial State Errors

The initial state estimates and the tuning parameters for this case are

$$
\begin{aligned}
V^I_{mx}(0) &= 1000.\ \text{fps} \\
\dot{\theta}_T(0) &= 4.343345\ \text{radians} \\
R(0) &= 9000.\ \text{feet} \\
\dot{R}(0) &= -1900.\ \text{fps} \\
a_L(0) &= 15.\ \text{g's} \\
n(0) &= 6. \\
\tau_f(0) &= .3\ \text{seconds} \\
M/S(0) &= 15.\ \text{slugs/ft}^2
\end{aligned}
$$

$$
\underline{R} = \begin{bmatrix} 3.E-5 & 0. & 0. \\ 0. & 500. & 0. \\ 0. & 0. & 100. \end{bmatrix}
$$

$$
\underline{P}_0 = \begin{bmatrix}
100. & 0. & 0. & 0. & 0. & 0. & 0. & 0. \\
0. & 1.E-8 & 0. & 0. & 0. & 0. & 0. & 0. \\
0. & 0. & 101. & 0. & 0. & 0. & 0. & 0. \\
0. & 0. & 0. & 4. & 0. & 0. & 0. & 0. \\
0. & 0. & 0. & 0. & 1. & 0. & 0. & 0. \\
0. & 0. & 0. & 0. & 0. & .4 & 0. & 0. \\
0. & 0. & 0. & 0. & 0. & 0. & .009 & 0. \\
0. & 0. & 0. & 0. & 0. & 0. & 0. & 5.
\end{bmatrix}
$$

$$
\underline{Q} = \begin{bmatrix}
250. & 0. & 0. & 0. & 0. & 0. & 0. & 0. \\
0. & 1.E-6 & 0. & 0. & 0. & 0. & 0. & 0. \\
0. & 0. & 500. & 0. & 0. & 0. & 0. & 0. \\
0. & 0. & 0. & 200. & 0. & 0. & 0. & 0. \\
0. & 0. & 0. & 0. & 10. & 0. & 0. & 0. \\
0. & 0. & 0. & 0. & 0. & .5 & 0. & 0. \\
0. & 0. & 0. & 0. & 0. & 0. & .001 & 0. \\
0. & 0. & 0. & 0. & 0. & 0. & 0. & .009
\end{bmatrix}
$$

This was the final evaluation of the first order filter. The states and parameters were both initialized with large errors. The initial values of the filter's states are given on the previous page. The true values for each are listed below.

$$
\begin{aligned}
V_{mx}^{I}(0) &= 1225.6 \text{ fps} \\
\dot{\theta}_T(0) &= 4.363345 \text{ radians} \\
R(0) &= 10000. \text{ feet} \\
\dot{R}(0) &= -2122. \text{ fps} \\
a_L(0) &= 0. \\
n(0) &= 4.5 \\
\tau_f(0) &= .85 \text{ seconds} \\
M/S(0) &= 29.197 \text{ slugs/ft}^2
\end{aligned}
$$

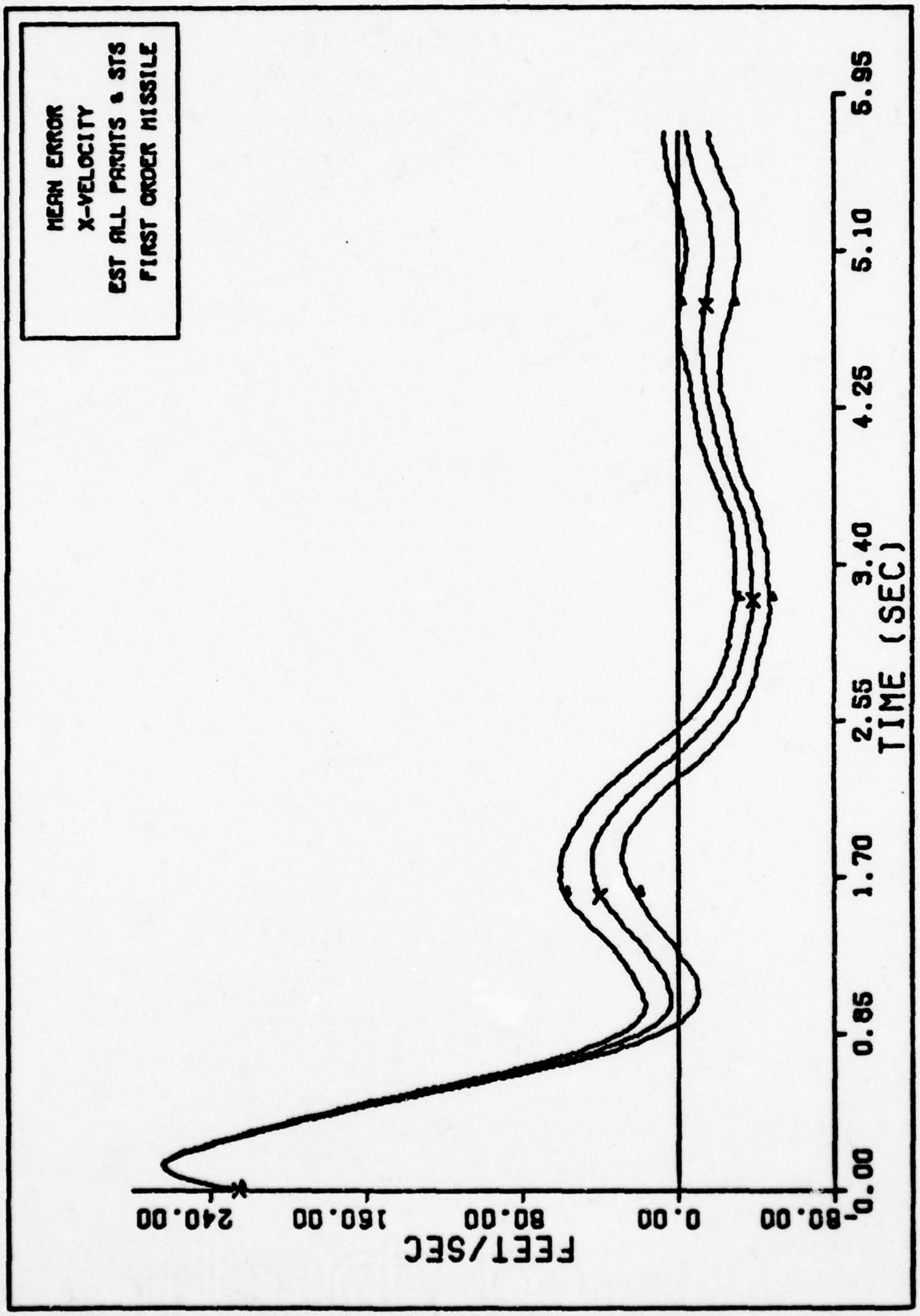

Fig. 277. X-VELOCITY FIRST ORDER MISSILE

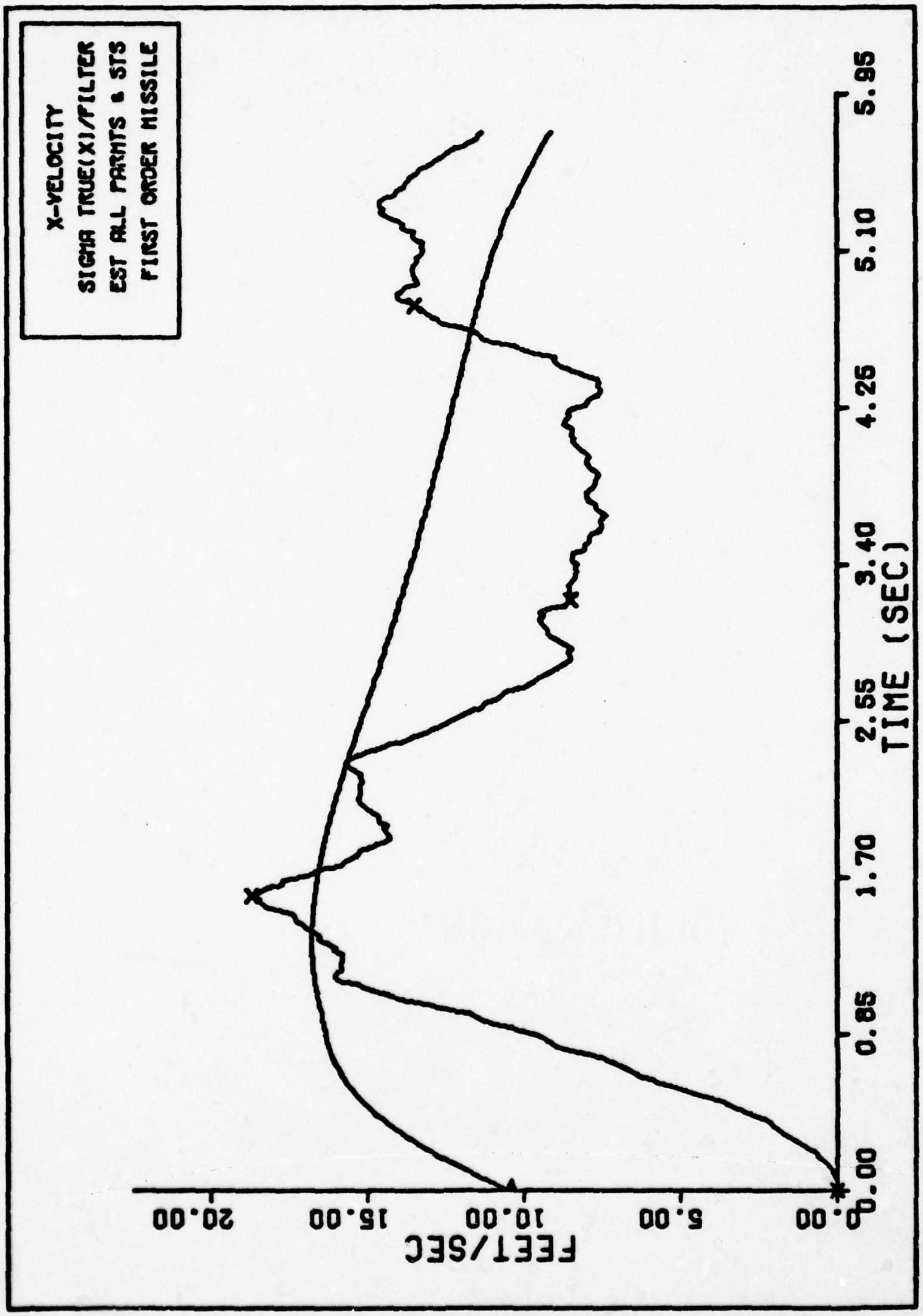

Fig. 278. X-VELOCITY SIGMAS FIRST ORDER

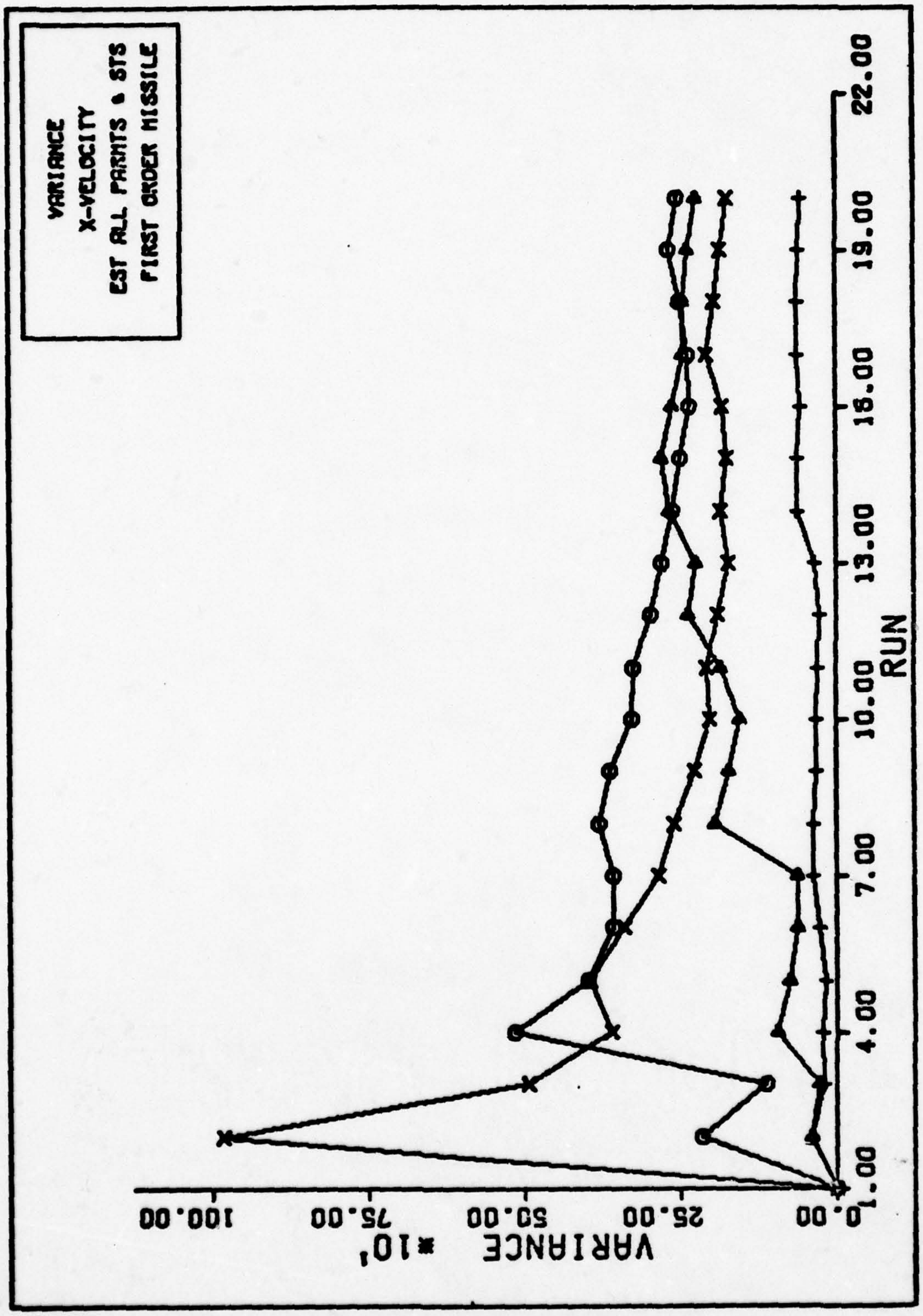

Fig. 279. VARIANCE CONVERGENCE

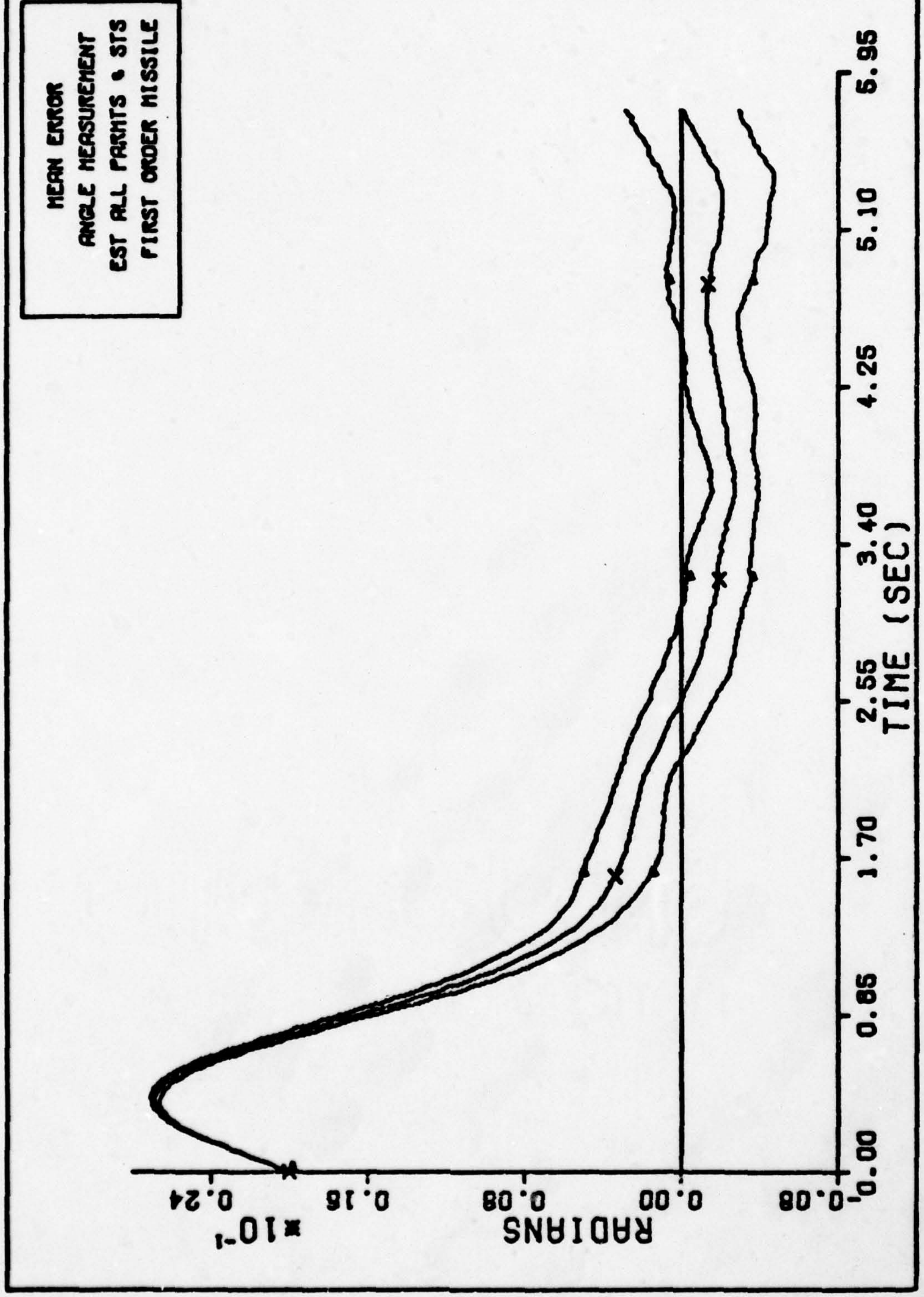

Fig. 280. ANGLE MEASUREMENT FIRST ORDER MISSILE

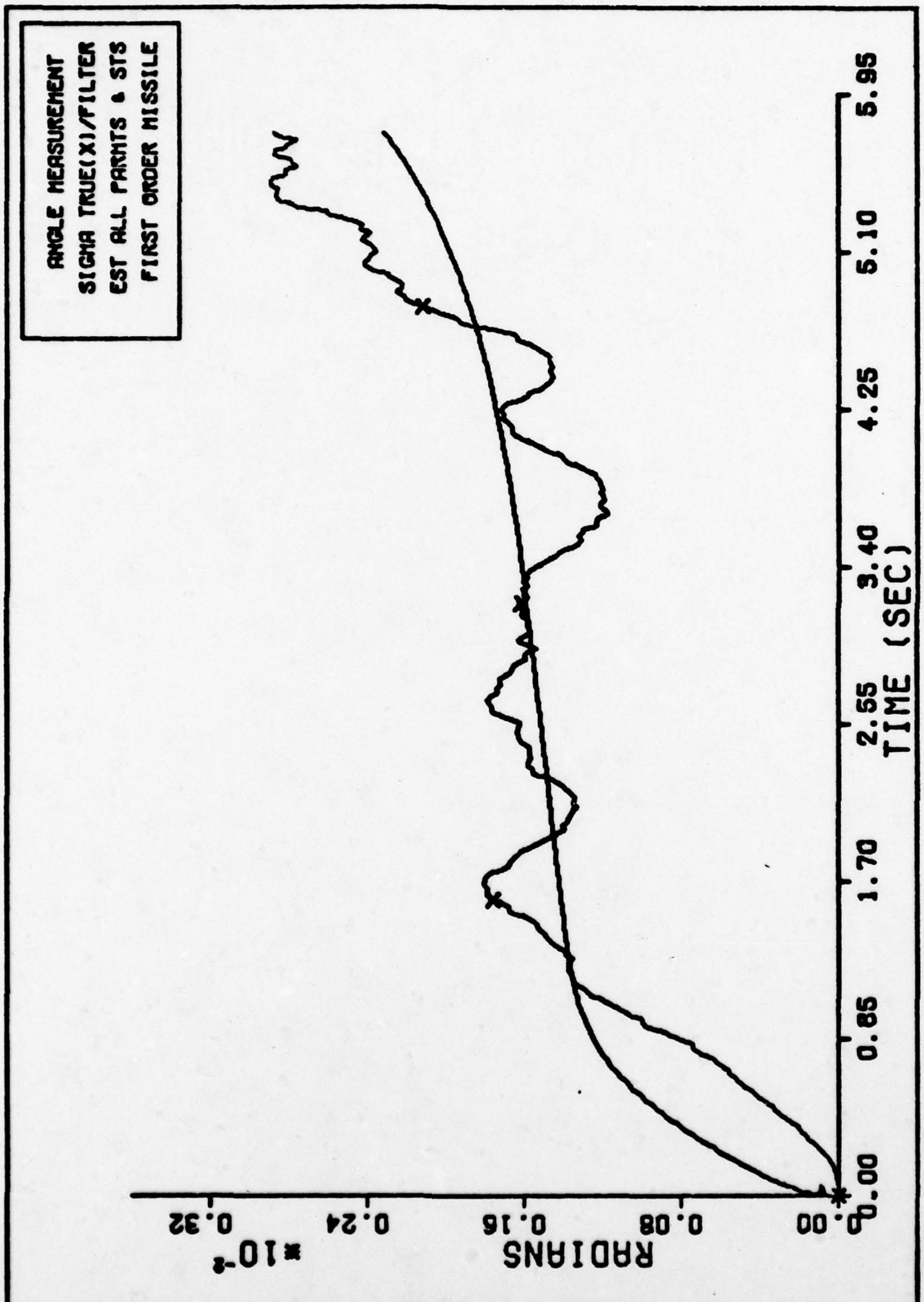

Fig. 281. ANGLE MEASUREMENT SIGMAS FIRST ORDER

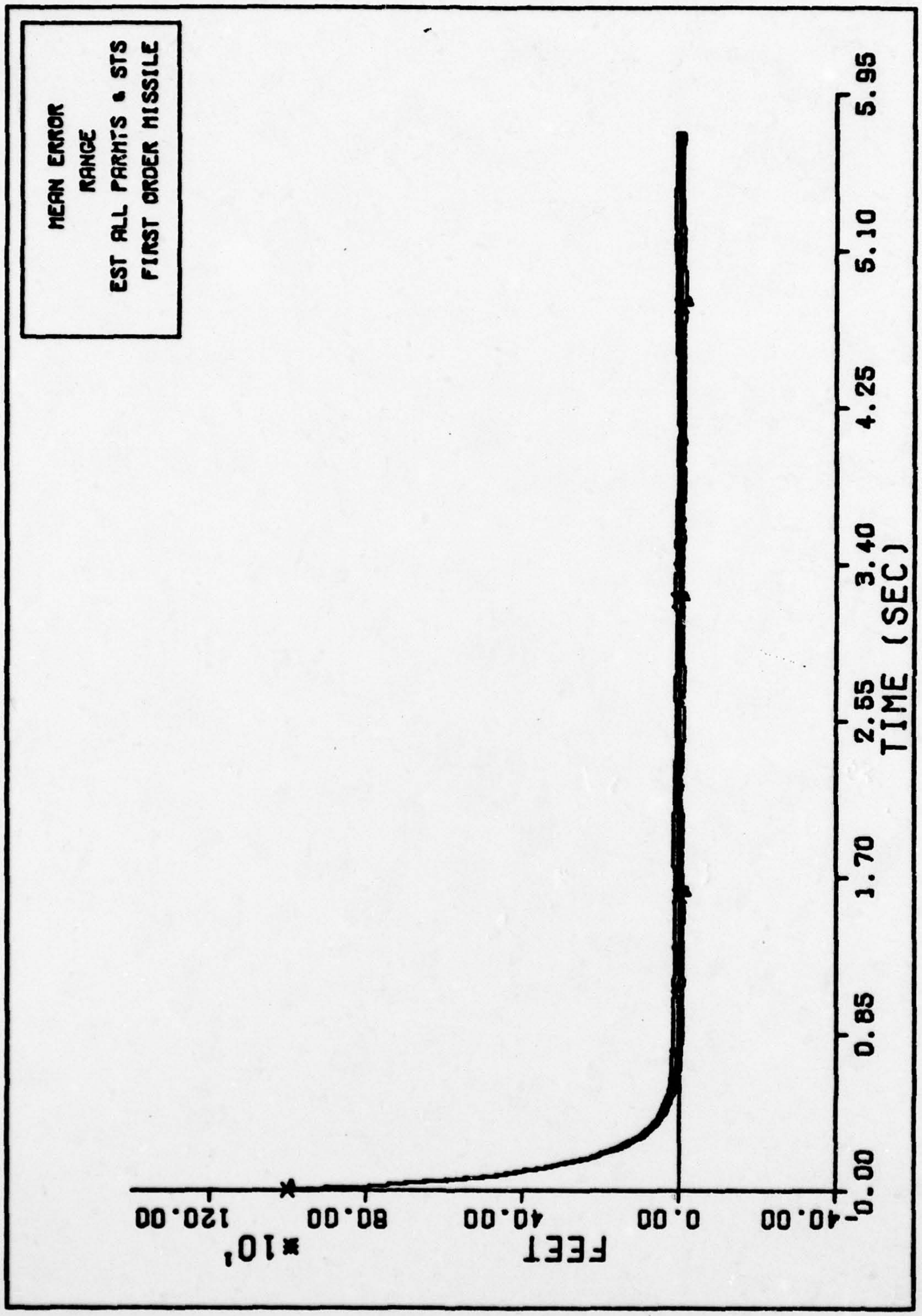

Fig. 282. RANGE FIRST ORDER MISSILE

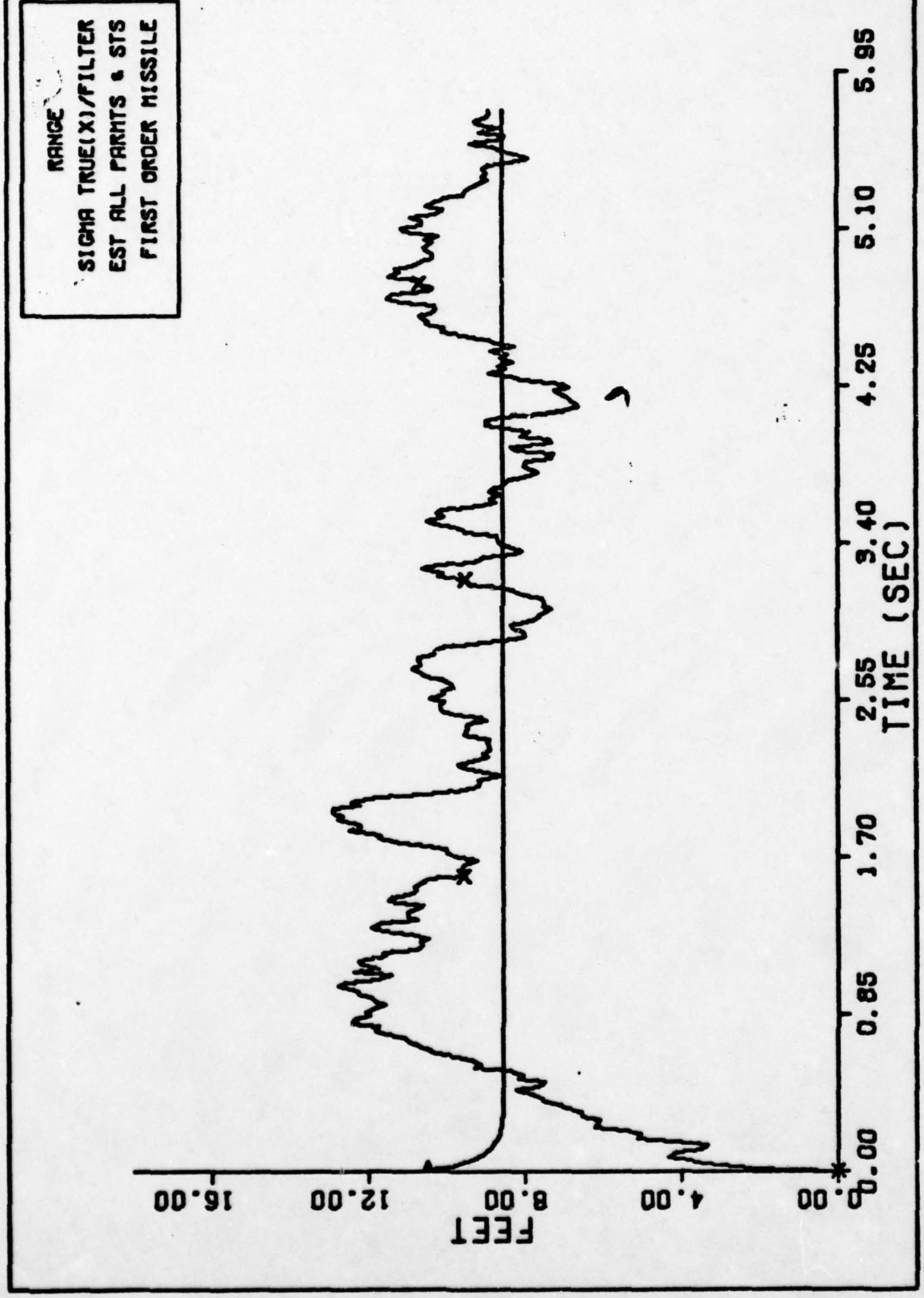

Fig. 283. RANGE SIGMAS FIRST ORDER

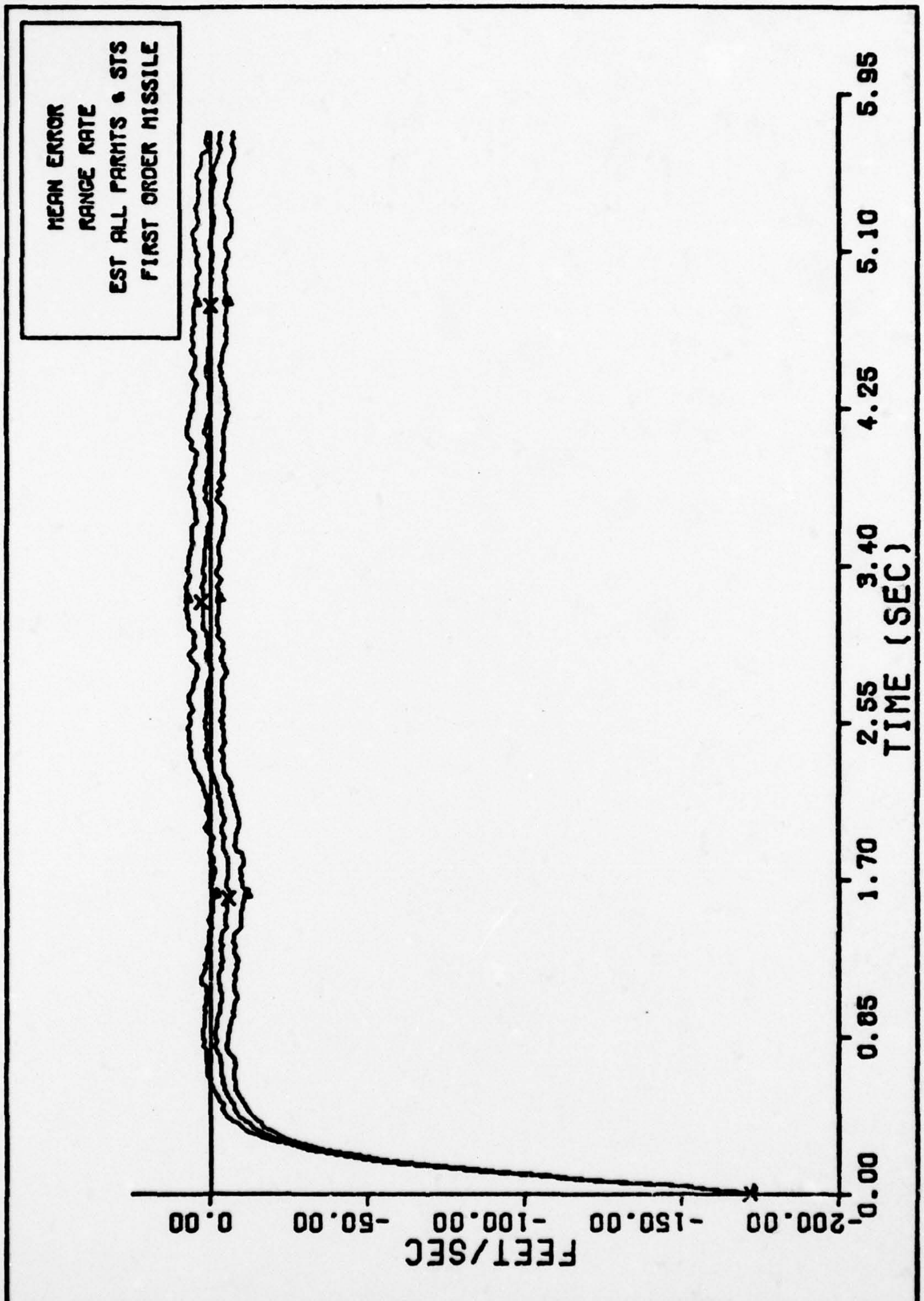

Fig. 284. RANGE RATE FIRST ORDER MISSILE

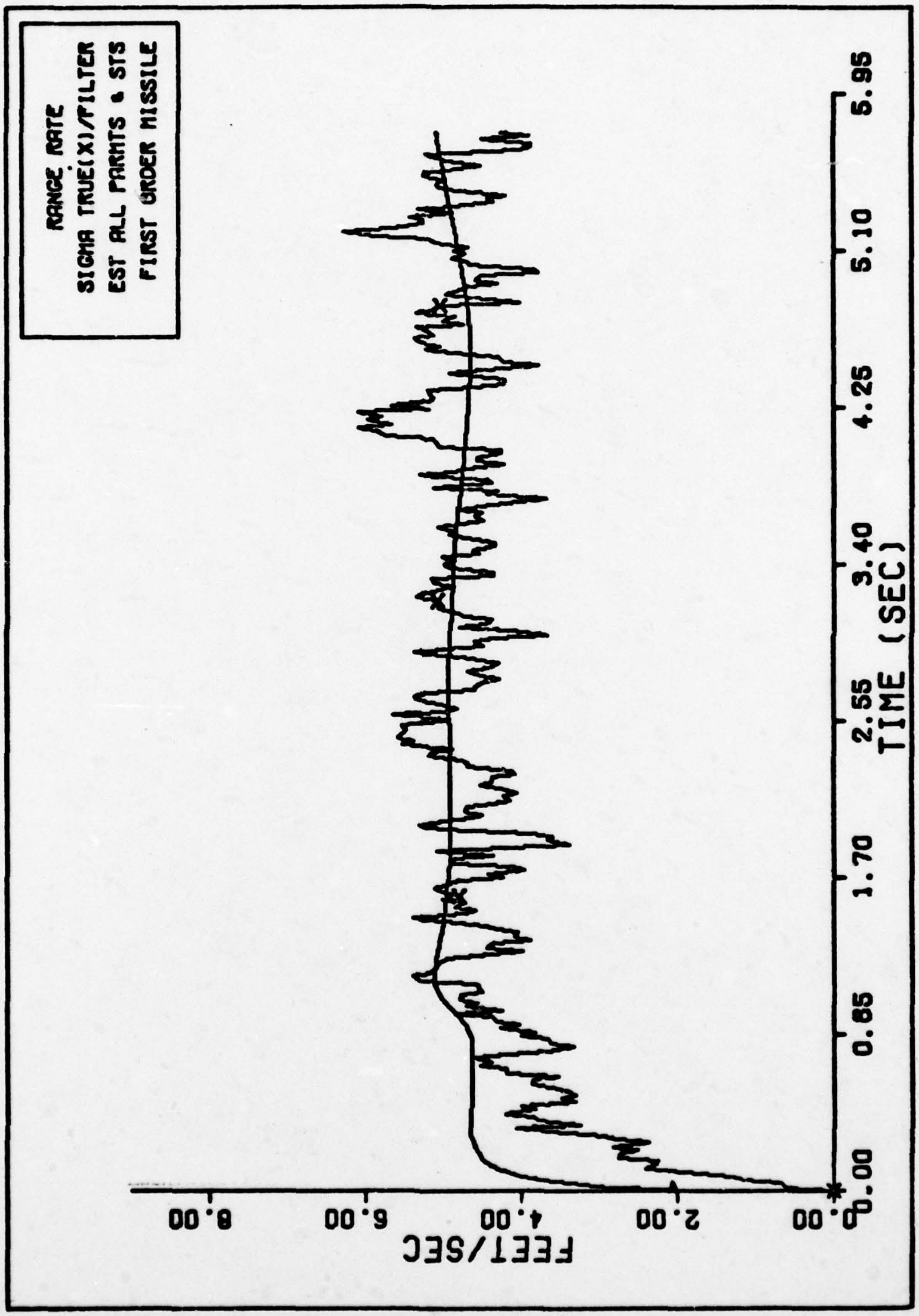

Fig. 285. RANGE RATE SIGMAS FIRST ORDER

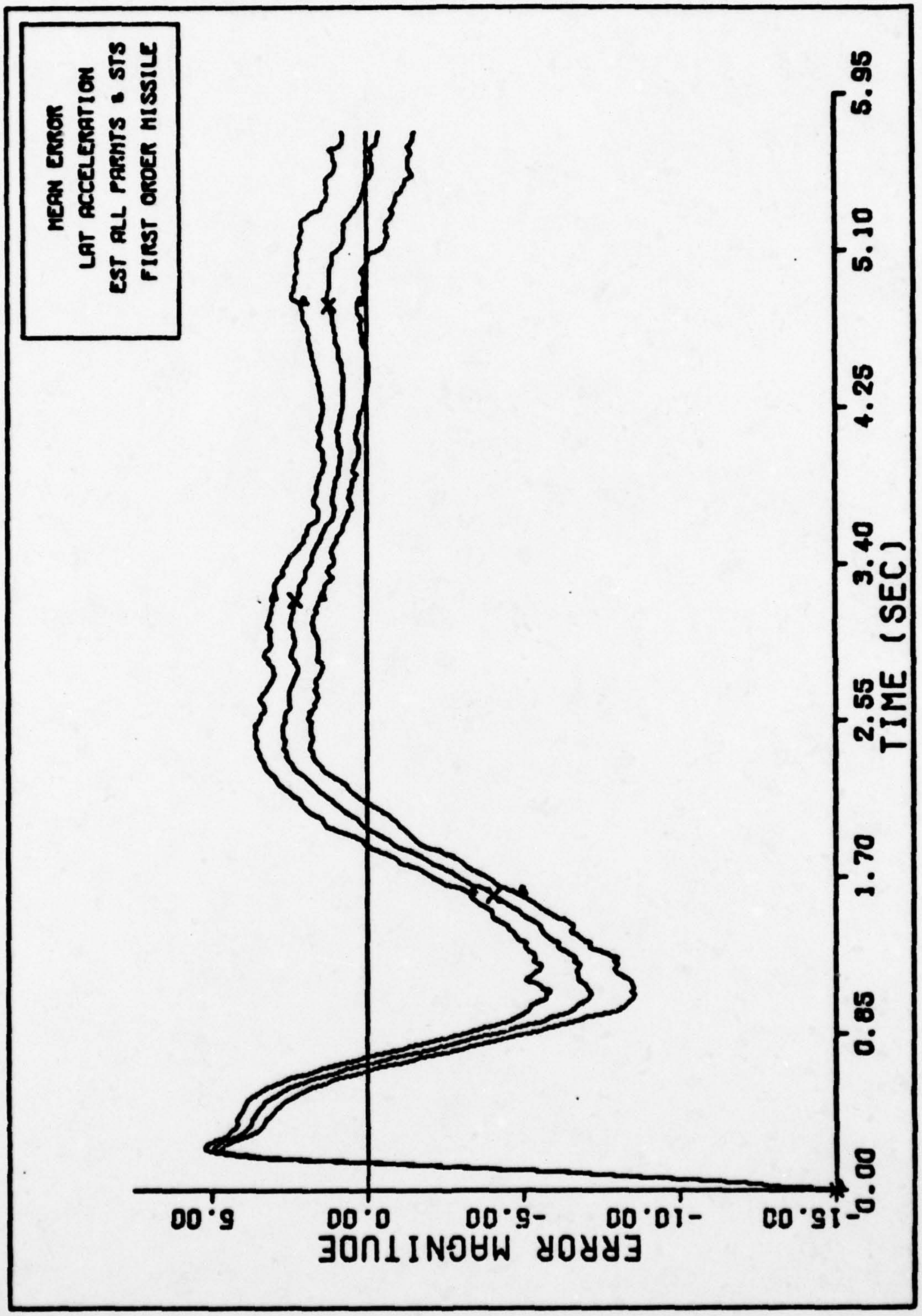

Fig. 286. LAT ACCELERATION FIRST ORDER MISSILE

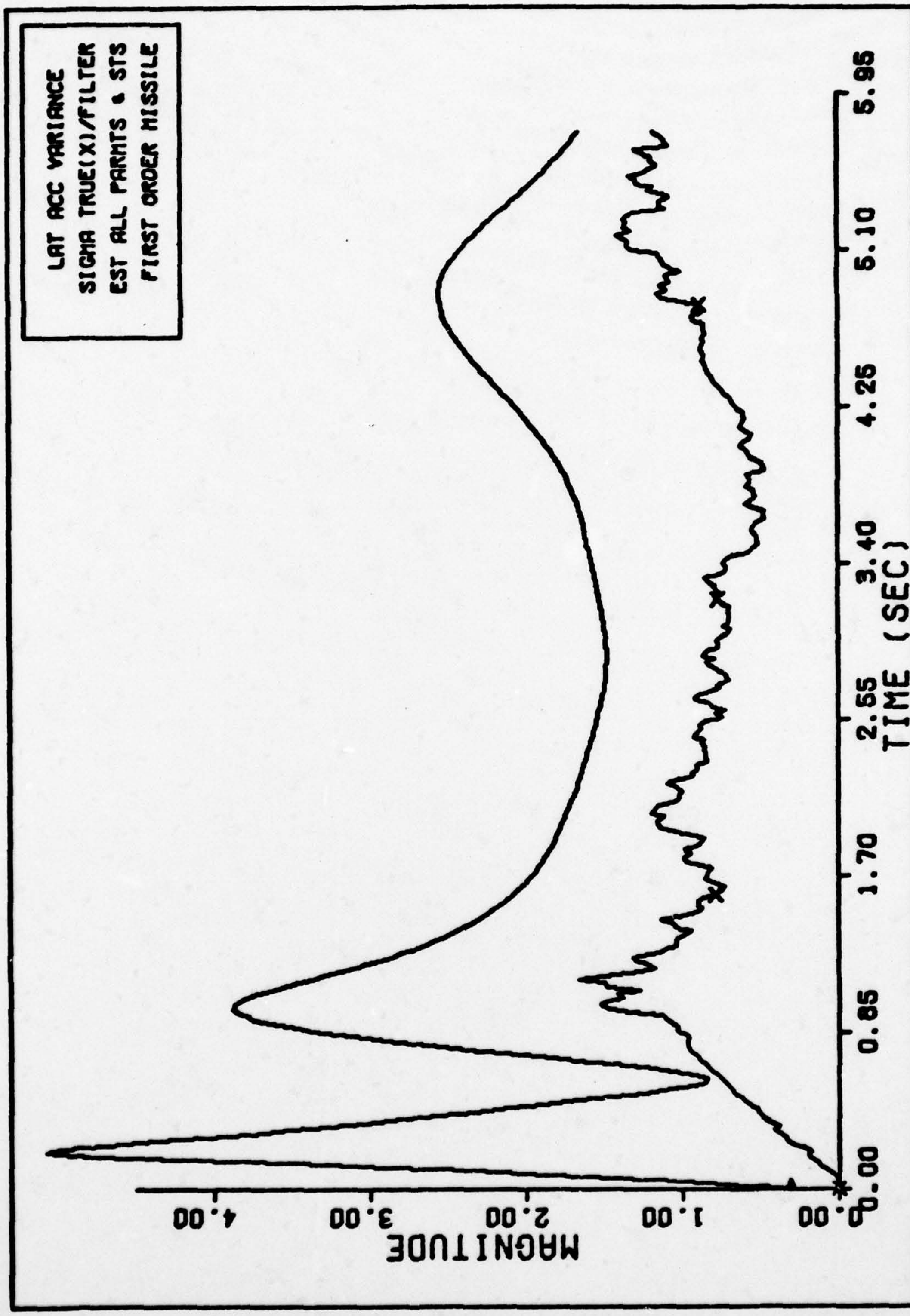

Fig. 287. LAT ACCELERATION SIGMAS FIRST ORDER

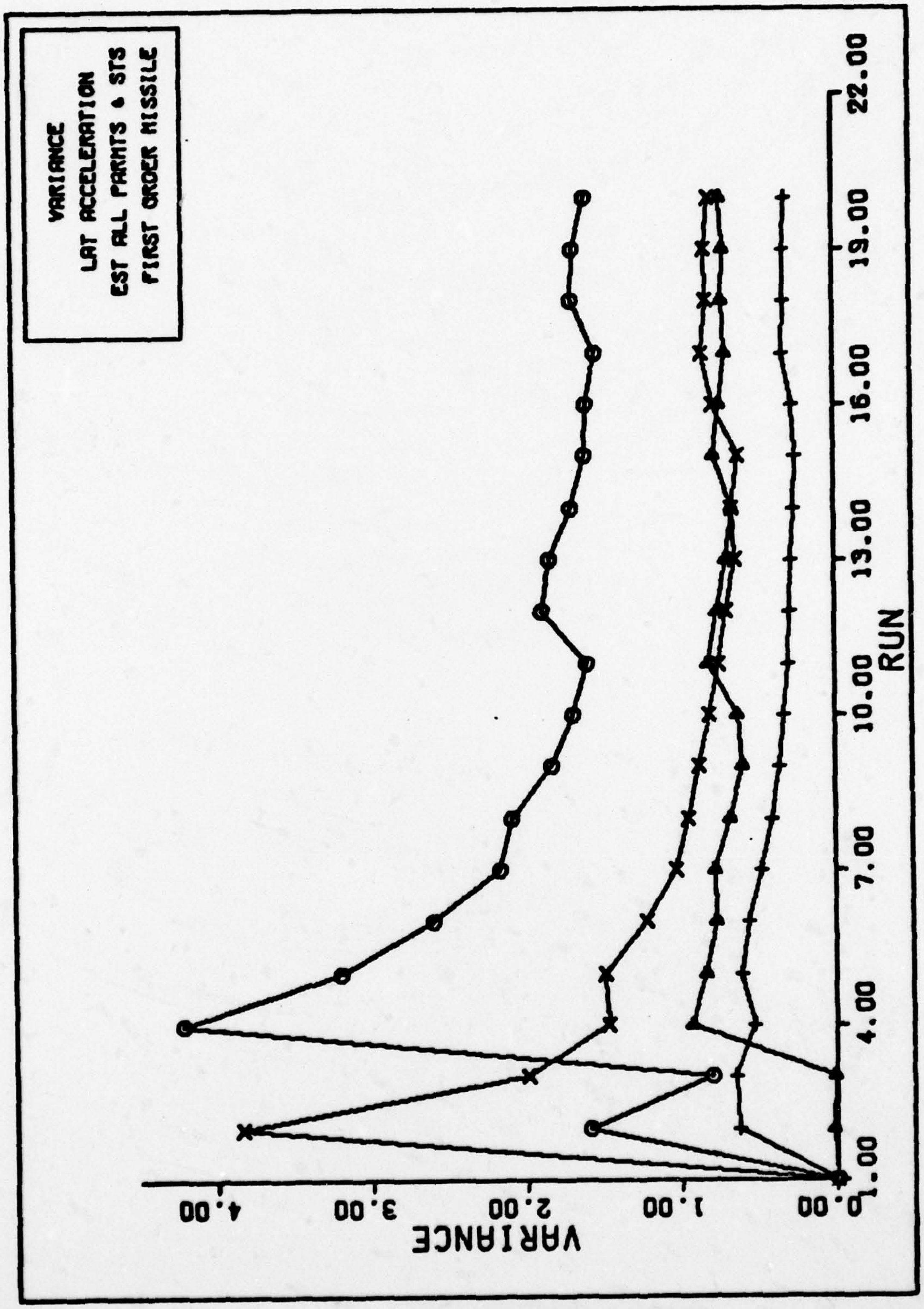

Fig. 288. VARIANCE CONVERGENCE

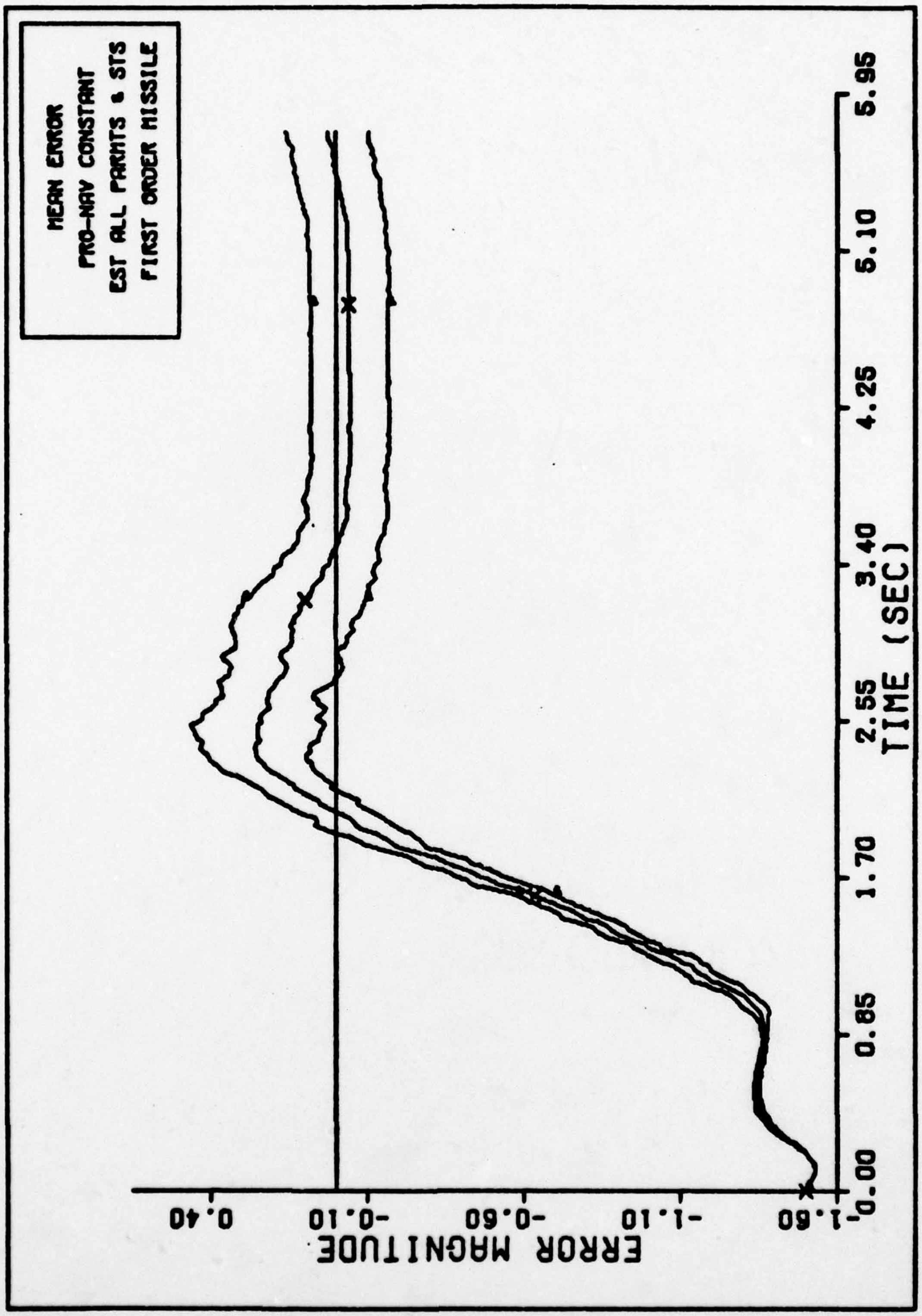

Fig. 289. PRO-NAV CONSTANT FIRST ORDER MISSILE

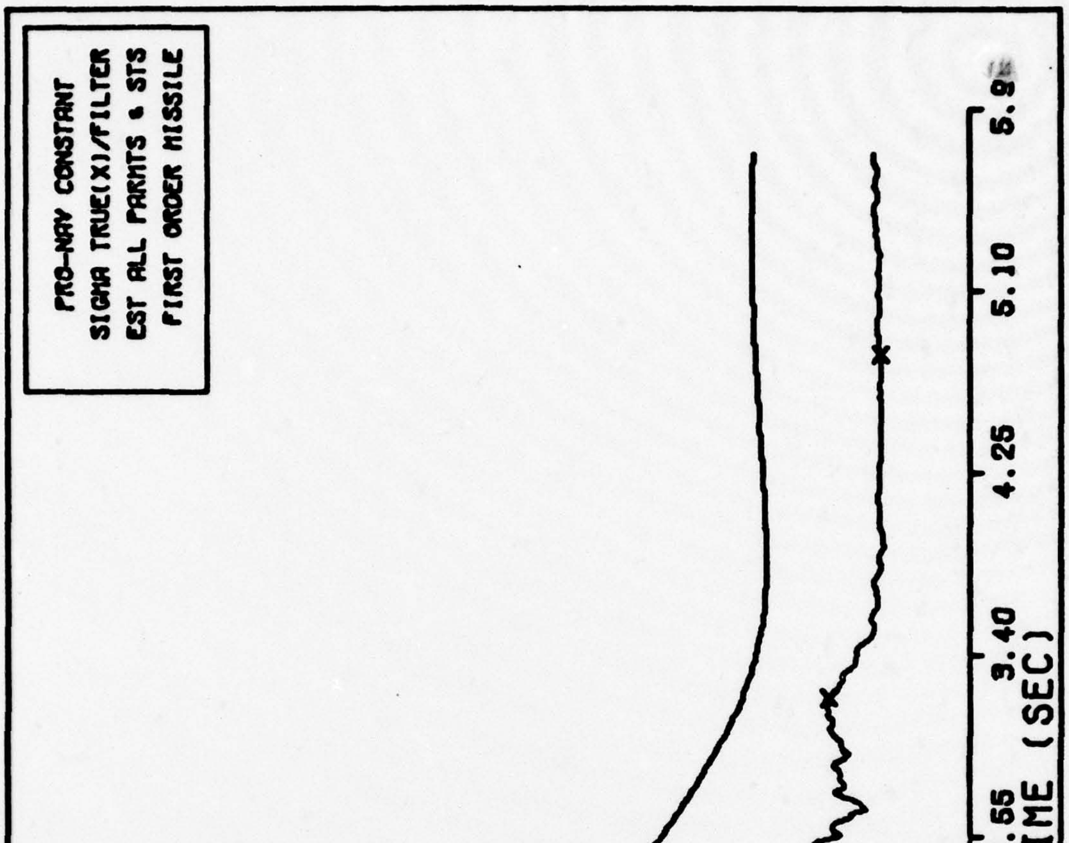

Fig. 290. PRO-NAV CONSTANT SIGMAS FIRST ORDER

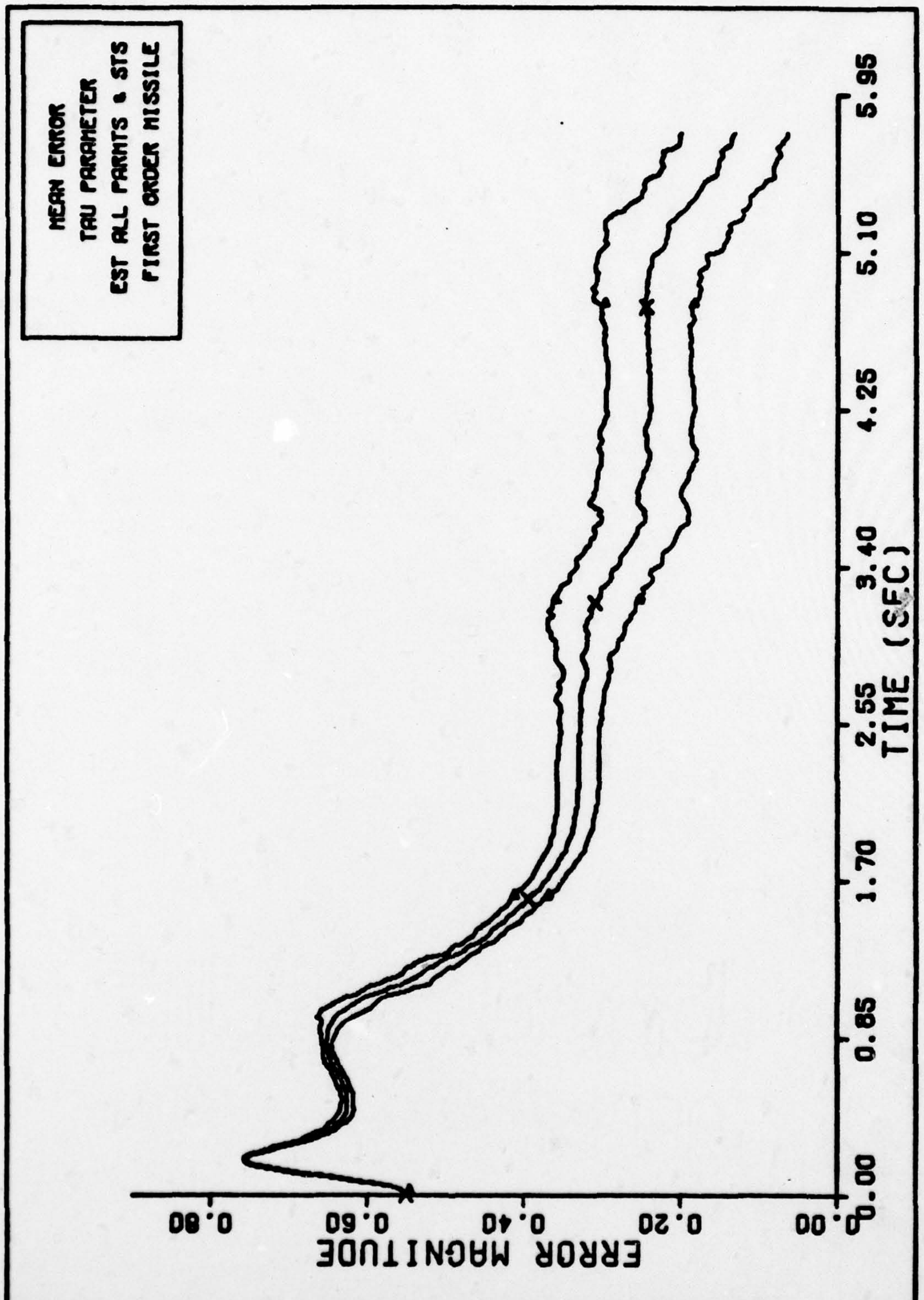

Fig. 291. TAU PARAMETER FIRST ORDER MISSILE

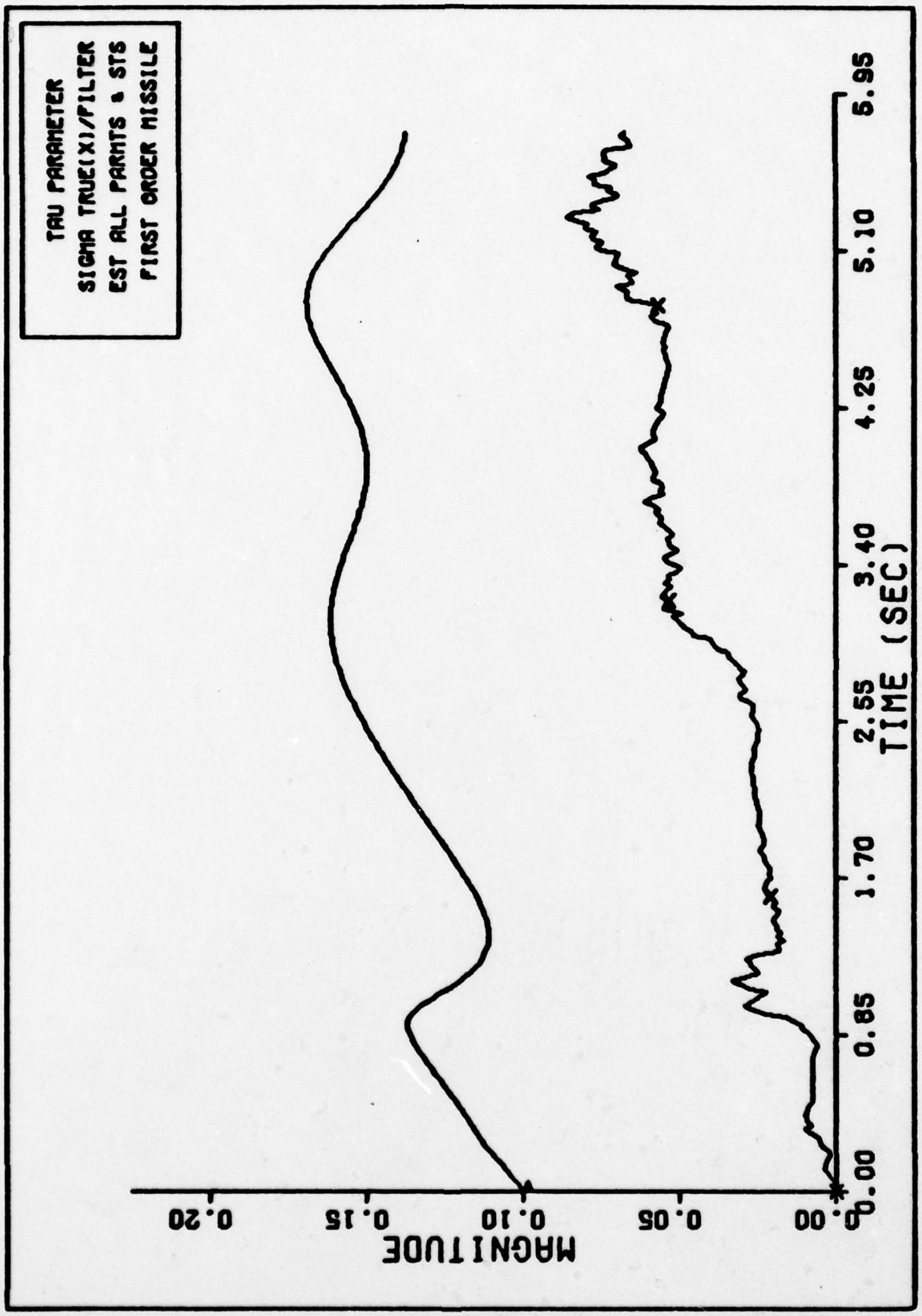

Fig. 292. TAU PARAMETER SIGMAS FIRST ORDER

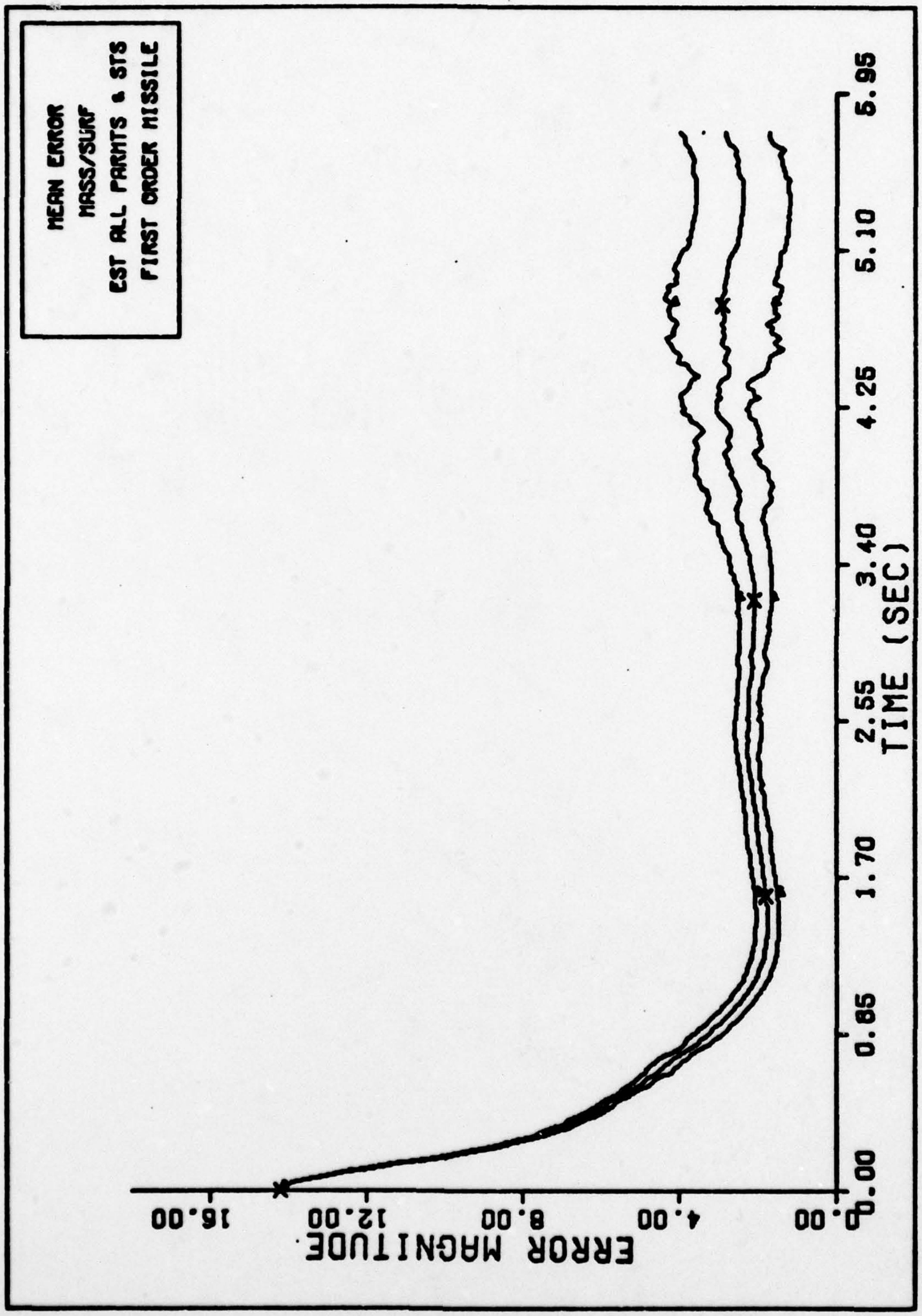

Fig. 293. MASS/SURF FIRST ORDER MISSILE

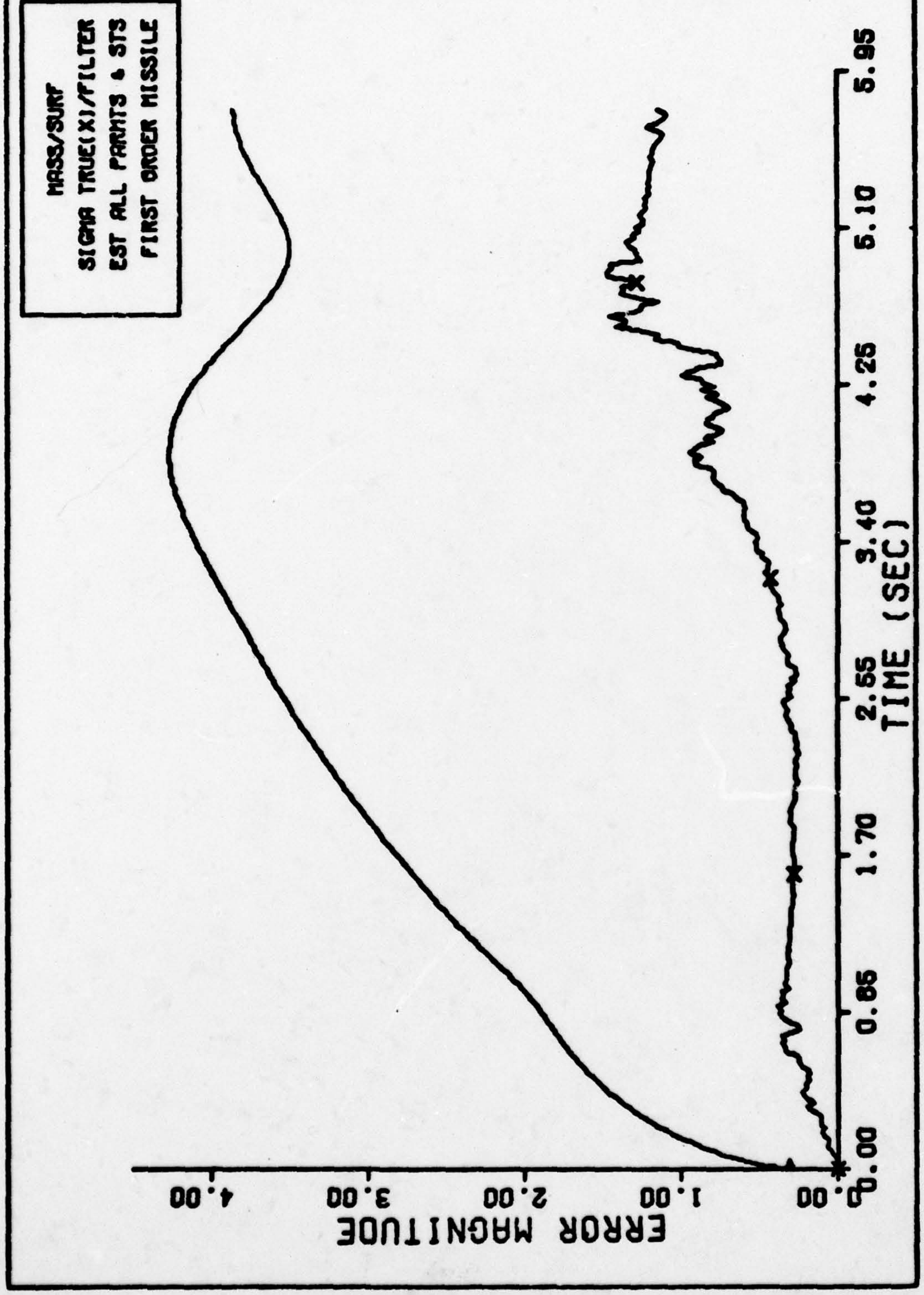

Fig. 294. MASS/SURF SIGMAS FIRST ORDER